BEILSTEIN JOURNAL OF ORGANIC CHEMISTRY

Hypervalent halogen chemistry

Edited by Tanja Gulder and Joanna Wencel-Delord

Imprint

Beilstein Journal of Organic Chemistry
www.bjoc.org
ISSN 1860-5397
Email: journals-support@beilstein-institut.de

The *Beilstein Journal of Organic Chemistry* is published by the Beilstein-Institut zur Förderung der Chemischen Wissenschaften.

Beilstein-Institut zur Förderung der Chemischen Wissenschaften
Trakehner Straße 7–9
60487 Frankfurt am Main
Germany
www.beilstein-institut.de

BEILSTEIN JOURNAL OF ORGANIC CHEMISTRY

SOMOphilic alkyne vs radical-polar crossover approaches: The full story of the azido-alkynylation of alkenes

Julien Borrel and Jerome Waser*

Commentary

Open Access

Address:
Laboratory of Catalysis and Organic Synthesis, Institute of Chemical Sciences and Engineering, Ecole Polytechnique Fédérale de Lausanne, EPFL SB ISIC LCSO, BCH 4306, 1015 Lausanne, Switzerland

Email:
Jerome Waser* - jerome.waser@epfl.ch

* Corresponding author

Keywords:
alkyne; azide; hypervalent iodine; photoredox; trifluoroborate salt

Beilstein J. Org. Chem. **2024,** *20,* 701–713.
https://doi.org/10.3762/bjoc.20.64

Received: 03 November 2023
Accepted: 21 March 2024
Published: 03 April 2024

This article is part of the thematic issue "Hypervalent halogen chemistry".

Guest Editor: T. Gulder

Abstract

We report the detailed background for the discovery and development of the synthesis of homopropargylic azides by the azido-alkynylation of alkenes. Initially, a strategy involving SOMOphilic alkynes was adopted, but only resulted in a 29% yield of the desired product. By switching to a radical-polar crossover approach and after optimization, a high yield (72%) of the homopropargylic azide was reached. Full insights are given about the factors that were essential for the success of the optimization process.

Introduction

Homopropargylic azides are important building blocks bearing two of the most versatile functional groups, allowing a rich panel of functionalization. They have been used as intermediates in numerous syntheses to access bioactive compounds [1-4] or materials [5-7]. In addition, azide reduction affords homopropargylic amines, which can be found in bioactive molecules and have been tested in structure–activity relationship studies (Scheme 1A) [8-10]. Moreover, transformations have been developed to exploit the two functional groups simultaneously, for example through their intramolecular cyclization to form pyrroles in the presence of transition metal catalysts [11-14].

Currently, this motif is synthesized by sequential introduction of the two functional groups [11-13]. Addition of a lithium acetylide to an epoxide affords the corresponding homopropargylic alcohol which can then undergo a sequence of mesylation and substitution with azide ions to produce the desired homopropargylic azide. However, this approach gives only access to products bearing the alkyne at the least substituted position. To the best of our knowledge, no general strategy has been employed to access the other regioisomer possessing a terminal azide, despite its implication in the synthesis of complex molecules [3,6]. Therefore, the development of a straightforward reaction to synthesize homopropargylic azides would be of general interest.

The azido-alkynylation of alkenes would allow to generate the desired motif in a single step, greatly increasing the molecular

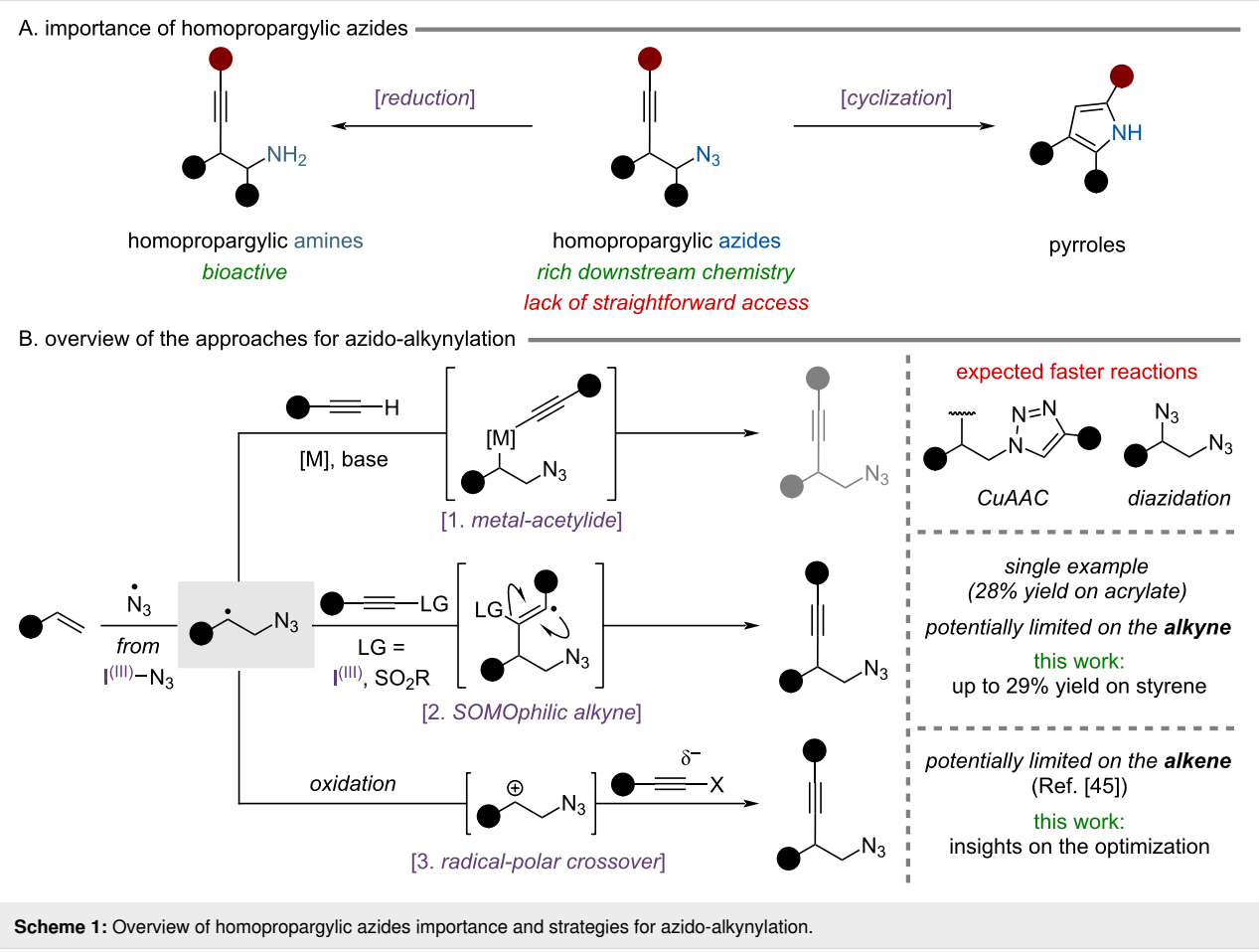

Scheme 1: Overview of homopropargylic azides importance and strategies for azido-alkynylation.

complexity of the starting substrate. Using radical chemistry would lead to a regioselective addition of azide radicals to the alkene, forming selectively the most stabilized C-centered radical. A prominent method for the generation of azide radicals relies on hypervalent iodine reagents [15,16]. Azidobenziodoxolone, also known as Zhdankin reagent, has often been used under thermal or photochemical conditions to generate the desired azide radical in a controlled fashion. However, recent safety issues arising from the shock and impact sensitivity of the compound led to the development of the azidobenziodazolone scaffold [17]. This class of derivative showed an improved safety profile while retaining the redox properties of the original reagent.

A single example of azido-alkynylation has been reported by Ramasastry and co-workers during a mechanistic study for an azido-hydration reaction [18]. The homopropargylic azide was obtained in only 28% yield using phenyl vinyl ketone. Based on reported aza-alkynylation reactions [19-23] and modern azidation methods using radical chemistry [17,24-26] three approaches could be envisaged. All of them would initially involve the addition of azide radicals to an alkene, generating a carbon-centered radical. Then, different trapping of this intermediate could be performed (Scheme 1B).

First, C-centered radicals are known to recombine with metal-acetylides, in particular copper [27]. Reductive elimination of the organometallic intermediate would lead to the desired product (Scheme 1B, reaction 1). Unfortunately, this approach will not be compatible in the case of azidation since the copper, azides and alkynes present in the mixture are expected to undergo alkyne–azide cycloaddition reactions [28]. Moreover, different azide sources are known to efficiently promote the diazidation of alkenes in the presence of a copper catalyst, often proceeding via a radical mechanism [24,29-31].

A second approach would involve SOMOphilic alkynes to trap the radical by a purely open-shell mechanism (Scheme 1B, reaction 2). Two classes of reagents are commonly used: ethynylbenziodoxolones (EBXs) [32,33] and alkynylsulfones [34]. A potential limitation of this method lies in the substitution of the transferred alkyne. The efficiency of the radical addition to those reagents is known to be highly dependent on the alkyne substituent. Arylalkynes are expected to perform well

but in multiple cases alkyl substituents were reported to afford low yields or no reaction [35-38].

Finally, a radical-polar crossover (RPC) approach could be envisaged [39,40]. Instead of attempting to trap the C-centered radical, further oxidation would generate the corresponding carbocation, which upon reaction with a nucleophilic alkyne would form the product (Scheme 1B, reaction 3). Based on precedence in the literature, this method should allow to transfer efficiently both aryl- and alkyl-substituted alkynes [41-44]. On the other hand, the nature of the alkene might be limited as it would strongly influence the oxidation potential of the carbon radical and the stability of the resulting carbocation. Recently, we reported the first successful application of an RPC strategy for the azido-alkynylation of styrenes [45].

Herein, we describe our initial effort towards developing an azido-alkynylation of alkenes using the SOMOphilic alkyne approach instead. Then, the optimization of the RPC strategy will be discussed in detail, giving insights into the different steps of the optimization, which were available only as raw data in our previous work [45].

Results and Discussion

SOMOphilic alkynes

We started to investigate the azido-alkynylation of styrene (**1a**) using EBX reagent **2** as SOMOphilic alkyne (Table 1). Tosyl-azidobenziodazolone (Ts-ABZ, **3**), previously developed by our group [17], was selected as an azide source. Upon light irradiation, it can release an azide radical by homolysis of the I–N_3 bond [46]. We were pleased to see that irradiation of a mixture of styrene (**1a**), Ph-EBX (**2**) and Ts-ABZ (**3**) afforded 17% isolated yield of the desired homopropargylic azide **4a** (Table 1, entry 1). Heating the reaction to 80 °C instead of using light to form the radical only afforded traces of the product (Table 1, entry 2). Changing the solvent to DCE slightly increased the yield (Table 1, entry 3). Blue light with an emission spectrum centered around 467 nm was initially selected since Ph-EBX is known to absorb light of lower wavelength, which is expected to cause degradation [47]. Indeed, when the reaction was carried out using 440 nm blue light a lower yield of 10% was obtained and full conversion of the EBX reagent was observed (Table 1, entry 4). Next, we wanted to test different additives in the transformation in an attempt to increase the yield. Addition of acetoxybenziodoxolone (AcOBX) has previously been re-

Table 1: Optimization of the azido-alkynylation using Ph-EBX.

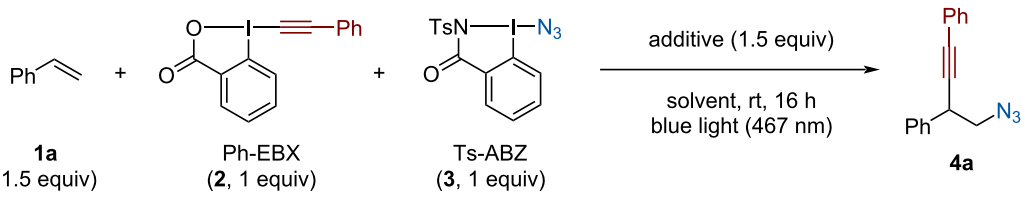

1a (1.5 equiv) | Ph-EBX (**2**, 1 equiv) | Ts-ABZ (**3**, 1 equiv) | **4a**

Entry	Solvent	Additive	Equiv variation	Yield **4a** (%)[a]
1	CH_3CN	–	–	(17)
2[b]	CH_3CN	–	–	<5
3	DCE	–	–	19
4[c]	DCE	–	–	10
5	DCE	AcOBX		18
6	DCE	$(TMS)_3SiH$	–	–
7	DCE	$(iPr)_2O$	–	16
8	DCE	L-ascorbic acid	–	16
9	DCE	Hantzsch ester	–	–
10	CH_3CN	HCOONa	–	8
11	DCE	DABCO, TBAI	additive (1.1 equiv)	–
12	DCE	AcOH, TFA, TFE	–	20
13	DCE	HFIP	–	24
14	DCE	HFIP	styrene (2 equiv)	24
15	DCE	HFIP	Ts-ABZ (1.5 equiv)	29

[a]NMR yield determined using CH_2Br_2 as internal standard, yield in parenthesis correspond to the isolated yield. [b]Reaction was heated to 80 °C without light irradiation. [c]Reaction carried out using blue light (440 nm).

ported to help initiating the degradation of Ts-ABZ (**3**) to the azidyl radical [46]. In our case, no difference in yield was observed (Table 1, entry 5). Currently, the reaction is expected to generate a large quantity of iodanyl radical from Ts-ABZ (**3**) homolysis and from the addition–elimination on Ph-EBX (**2**). Since no quencher is present in the mixture, we wondered if the accumulation of those radicals could be responsible for the low yields obtained. Addition of $(TMS)_3SiH$, a $H^\bullet$ donor, suppressed the reaction by reducing Ph-EBX (**2**) (Table 1, entry 6). Using diisopropyl ether as a milder donor had no effect on the reaction (Table 1, entry 7). Next, we tested reducing agents expected to react with the iodanyl radical. The addition of L-ascorbic acid led to no improvement of yield and Hantzsch ester suppressed the formation of the desired product (Table 1, entries 8 and 9). Carrying out the reaction in the presence of sodium formate, which can play a dual role of $H^\bullet$ donor and reductant [48,49], only led to a decreased of Ph-EBX (**2**) conversion, along with a diminished yield (Table 1, entry 10). The addition of DABCO [18] or TBAI [50], two additives known to activate azidobenziodoxolone (ABX), afforded complex mixtures with no trace of **4a** (Table 1, entry 11). Acids or fluorinated alcohols were tested to activate the different hypervalent iodine reagents. While AcOH, TFA and TFE had no impact on the reaction (Table 1, entry 12), the presence of 1.5 equivalents of HFIP slightly improved the yield (Table 1, entry 13). Increasing the amount of styrene in the reaction had no impact (Table 1, entry 14), highlighting that the issue might come from an inefficient trapping of the C-centered radical by Ph-EBX (**2**) and not from a sluggish addition of azide radicals to the double bond. We attempted to solve this issue by using Ts-ABZ (**3**) in excess, which should increase the overall quantity of carbon radicals formed, doing so slightly improved the yield of **4a** to 29% with no styrene remaining (Table 1, entry 15).

Styrene was initially selected as model substrate since the addition of azide radicals generated by ABX was well reported [24,29]. We wanted to explore different classes of alkenes as the double bond substitution would greatly impact both the azide radical addition and the reactivity of the C-centered radical with Ph-EBX (**2**). Aliphatic alkenes, enamides, enol ethers and acrylates were tested in the reaction but did not lead to formation of the desired products (Scheme S1, Supporting Information File 1). In almost all cases >70% of the EBX reagent was left after 16 hours of reaction.

Radical-polar crossover

Due to the disappointing results obtained with EBX reagents as SOMOphilic alkynes, we turned our attention to the development of a radical-polar crossover approach using photoredox catalysis. The final results obtained were described in our previous publication [45], but only the raw data for optimization was given in the form of tables in the Supporting Information. We now provide full insights into the different steps of the optimization process, highlighting the decisions taken and the unexpected results obtained.

Ts-ABZ (**3**) was kept as the azide radical source since it is known to be reduced by photocatalysts such as $Cu(dap)_2Cl$ [17]. This perfectly fits a catalytic cycle involving the reduction of Ts-ABZ (**3**) followed by oxidation of the carbon radical to form a carbocation and regenerate the ground state catalyst. Styrene (**1a**) was used as model substrate since the formation of a stabilized carbocation might be required for the reaction to occur. Xu [41] and Molander [42] previously reported the quenching of similar cationic species by alkynyl-BF_3K salts. Boronate **5a** was therefore selected as nucleophilic alkyne. Gratifyingly, using $Cu(dap)_2Cl$ in DCE under blue light irradiation afforded **4a** in 17% NMR yield (Table 2, entry 1). The major byproduct formed during the transformation was identified as diazide **6**. When a copper photocatalyst is involved, a lot of diazidation can be observed. We assumed it could be caused by the reaction of Ts-ABZ (**3**) with a non-complexed copper catalyst formed during the transformation [24,51]. When iridium-based photocatalysts were tested, no product formation or only traces were observed (Table 2, entries 2 and 3). Using $Ru(bpy)_3Cl_2{\cdot}6H_2O$ afforded 17% of **4a**, a similar yield as with $Cu(dap)_2Cl$ with a reduced formation of **6** (Table 2, entry 4). In contrast, $Ru(bpz)_3(PF_6)_2$ did not form the desired product probably due to its too high reduction potential compared to Ts-ABZ (**3**) (value reported for ABX: $E_{1/2}(ABX) = -0.43$ V vs SCE) [52] (Table 2, entry 5). In general, organic dyes could not catalyze the transformation except for 4ClDPAIPN which afforded 10% of yield of **4a** (Table 2, entries 6–10).

No correlation between the different redox potentials of the photocatalysts and the yield of the reaction could be established. $Ru(bpy)_3Cl_2{\cdot}6H_2O$ was selected as the optimal catalyst since it afforded the highest yield and minimized diazide formation.

Next, a solvent screening was performed as it can vastly influence reaction proceeding via a carbocation intermediate. Alkynyltrifluoroborates have a low solubility in chlorinated solvents but are well soluble in acetonitrile. Although this solvent has been used in similar transformation before [41,42,44], in our case only 9% of the desired product was obtained (Table 3, entry 2). A large quantity of product resulting from a Ritter-type reaction between acetonitrile and the carbocation intermediate could be observed by NMR [55]. Other highly polar solvents such as DMF and DMSO did not afford the homopropargylic azide (Table 3, entry 3). While alkynyl-BF_3K salts are usually well soluble in acetone, carrying the reaction in this solvent

Table 2: Photocatalyst screening.[a]

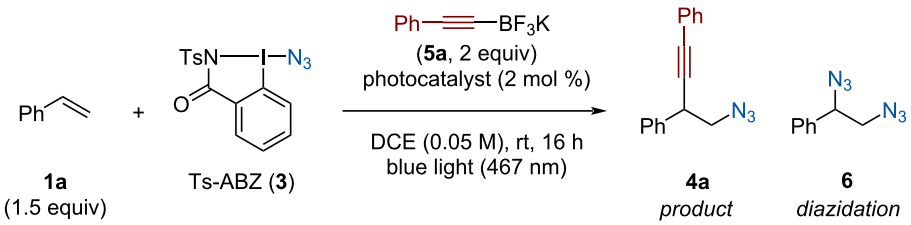

1a (1.5 equiv) | Ts-ABZ (**3**) | **4a** *product* | **6** *diazidation*

Entry	Photocatalyst	$E_{1/2}$ [PC*+/PC*] (V vs SCE)	Yield **4a** (%)[b]	Yield **6** (%)[b]
1	$Cu(dap)_2Cl$	−1.43[c]	17	14
2	$Ir(ppy)_3$	−1.88[c]	–	7
3	$[Ir(ppy)_2(dtbbpy)]PF_6$	−0.96[c]	<5	7
4	**$Ru(bpy)_3Cl_2·6H_2O$**	**−0.81[c]**	**17**	**6**
5	$Ru(bpz)_3(PF_6)_2$	−0.26[c]	–	<5
6	4*t*-BuCzIPN	−1.31[c]	–	<5
7	4DPAIPN	−1.52[d]	–	6
8	4ClDPAIPN	−1.30[d]	10	8
9	DPZ	−1.17[c]	<5	6
10	rose bengal	−0.68[c]	–	<5

[a]The data were already published in the supporting information of ref. [45] except for the yield of **6**. [b]NMR yield determined using CH_2Br_2 as internal standard. [c]Value taken from reference [53]. [d]Value taken from reference [54].

Table 3: Solvent screening.[a]

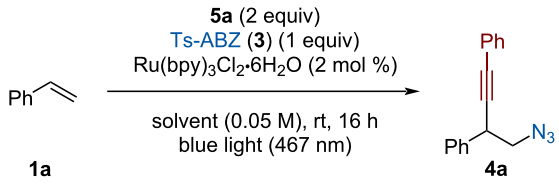

1a (1.5 equiv) | **4a**

Entry	Solvent	Yield **4a** (%)[b]
1	DCE	17
2	CH_3CN	9
3	DMF, DMSO	–
4	acetone	<5
5	EtOAc, dioxane, THF	8–15
6	**DME**	**36**
7	DME/HFIP (9:1)	39

[a]The data were already published in the supporting information of ref. [45]. [b]NMR yield determined using CH_2Br_2 as internal standard.

only afforded traces of the product (Table 3, entry 4). Ethyl acetate or ether solvents such as dioxane and THF led to similar or slightly reduced yields (Table 3, entry 5). We were pleased to see that running the reaction in DME afforded 36% of **4a** (Table 3, entry 6). A mixture of DME with HFIP, known to stabilize carbocationic intermediates [56], slightly increased the yield (Table 3, entry 7).

DME was selected for further optimization as the increased yield with the addition of HFIP was not significant enough to compensate the downside of having an expensive co-solvent. Next, the stoichiometry of the different reaction components was examined. When styrene (**1a**) was used as limiting reagent instead of Ts-ABZ (**3**), a slightly higher yield was observed (Table 4, entries 1 and 2). Increasing the excess of Ts-ABZ (**3**) from 1.25 to 1.5 equivalents had no impact on the reaction (Table 4, entry 3). Reducing the equivalents of **5a** to 1.25 only slightly diminished the yield while using 3 equivalents increased it to 44% (Table 4, entries 4 and 5). Surprisingly, **5a** could be used as limiting reagent without impacting the reaction (Table 4, entry 6). Carrying out the azido-alkynylation at low or high photocatalyst loading had no impact (Table 4, entry 7).

Considering the robustness of the reaction to fluctuation in stoichiometry, conditions using styrene (**1a**) as limiting reagent, slight excess of Ts-ABZ (**3**) and 2 equivalents of **5a** were selected, while keeping in mind that further fine-tuning can be done (Table 4, entry 2). They offered the best compromise of yield, waste of materials and reproducibility at this scale. So far, the reactions were carried out for 16 hours as it is typical for

Table 4: Equivalent screening.[a]

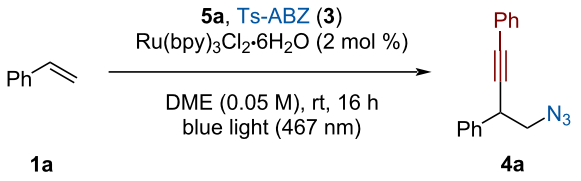

1a 4a

Entry	Ts-ABZ/**1a**/**5a** (equiv)	Yield **4a** (%)[b]
1	1/1.5/2	36
2	**1.25/1/2**	**42**
3	1.5/1/2	41
4	1.25/1/1.25	39
5	1.25/1/3	44
6	1.5/1.5/1	43
7[c]	1.25/1/2	39–40

[a]The data were already published in the supporting information of ref. [45]. [b]NMR yield determined using CH_2Br_2 as internal standard. [c]1 or 5 mol % of photocatalyst were used.

photocatalyzed reaction to be slow. We realized that full conversion of the alkene was reached very rapidly. In fact, the reaction could be carried out for 1.5 h with no difference in yield (Table 5, entries 1 and 2). It is only below this reaction time that a difference was observed, 21% of product was still formed after 10 min of reaction (Table 5, entries 3 and 4).

We then turned our attention to the light source used to irradiate the reaction. Initially, a homemade set-up using blue LED strips was used. When it was replaced by a commercially available Kessil lamp of the same wavelength and intensity we observed a similar yield (Table 5, entry 5). Reducing the strength of the irradiation from 44 to 22 W had no impact, similarly using a more energetic wavelength afforded the same yield (Table 5, entries 6 and 7). When lower energy light source such as green LEDs or a compact fluorescent lamp (CFL) were used only a small decrease in yield could be observed, although 4 hours of irradiation were needed to reach full conversion using CFL (Table 5, entries 8 and 9). The concentration, a factor expected to play an important role in a three-component reaction, had surprisingly little influence on the transformation. At lower concentration only a slight decrease of yield was observed, whereas higher concentration led to a similar yield (Table 5, entries 10 and 11).

The source of nucleophilic alkyne was evaluated, changing the counter ion from potassium to tetrabutylammonium (**7**) reduced the yield to 14% (Scheme 2A). When TMS-alkyne **8** was used, no product formation occurred. In this case, we observed that the initial reaction mixture before light irradiation was colorless. This was surprising, as in all the previous experiments a yellow/orange mixture was obtained due to the presence of the photocatalyst. Further investigation revealed that $Ru(bpy)_3Cl_2{\cdot}6H_2O$ is not soluble in DME (Scheme 2B). In

Table 5: Reaction time, light source and concentration screening.[a]

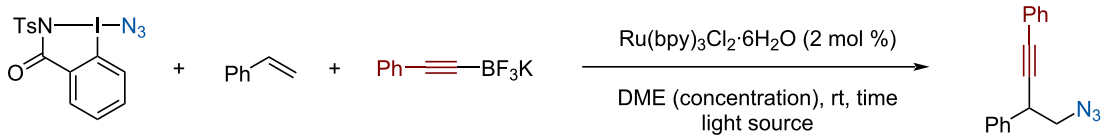

Ts-ABZ (**3**, 1.25 equiv) **1a** **5a** (2 equiv) **4a**

Entry	Time (h)	Light source	*c* (M)	Yield **4a** (%)[b]
1	16	blue LEDs 467 nm (40 W)	0.05	42
2	**1.5**	**blue LEDs 467 nm (40 W)**	**0.05**	**42**
3	1	blue LEDs 467 nm (40 W)	0.05	39
4	0.17	blue LEDs 467 nm (40 W)	0.05	21
5	1.5	Kessil 467 nm (44 W)	0.05	42
6	**1.5**	**Kessil 467 nm (22 W)**	**0.05**	**42**
7	1.5	Kessil 440 nm (45 W)	0.05	41
8	1.5	green LEDs 525 nm (40 W)	0.05	35
9	4	CFL (8 W)	0.05	38
10	1.5	blue LEDs 467 nm (40 W)	0.025	36
11	1.5	blue LEDs 467 nm (40 W)	0.1-0.2	41

[a]Blue/green LEDs refers to LED strips attached to a crystallization flask. The data were already published in the supporting information of ref. [45]. [b]NMR yield determined using CH_2Br_2 as internal standard.

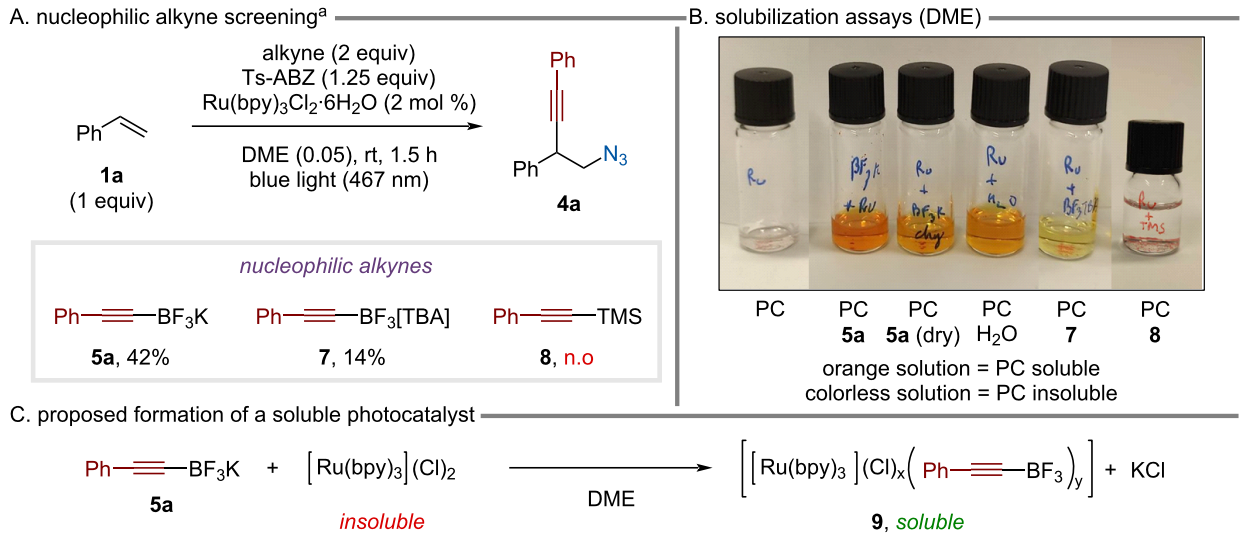

Scheme 2: Screening of nucleophilic alkynes and investigation of the photocatalyst solubility. n.o = not observed, PC = photocatalyst. [a]The data were already published in the supporting information of ref. [45].

contrast, when it is in the presence of alkynyl-BF_3K it readily dissolves. The addition of a couple of water drops to a suspension of photocatalyst in DME also allowed solubilization. The solubilization due to residual water coming from the alkynyl-BF_3K was ruled out by careful drying of **5a**. We postulated that an ion exchange between $Ru(bpy)_3Cl_2$ and **5a** can occur to afford a more soluble photocatalyst with the general formula **9** (Scheme 2C). Interestingly, when the solubilization experiment was carried out with the tetrabutylammonium salt **7** only moderate solubilization occurred (Scheme 2B), which could explain the lower yield previously observed (Scheme 2A). Neutral TMS-alkyne **8** cannot be involved in ion exchange and therefore this could be one of the reasons why no reaction occurred.

Next, we turned our attention to the temperature of the reaction, a factor rarely explored in photocatalyzed reaction due to the lack of available set-ups allowing an efficient light irradiation in addition to a proper temperature control. In our case, since the reaction previously showed to be very tolerant to different light intensity we could attempt to cool the reaction. Carrying out the transformation with the reaction vessel placed in an EtOAc bath cooled to 0 °C by an immersion cooler allowed to increase the yield to 50% (Table 6, entries 1 and 2). Decreasing the temperature to −20 °C slightly improved the yield and the mass balance of the reaction (Table 6, entry 3). At −41 °C the reaction time had to be increased to reach full conversion of styrene (**1a**), and the yield slightly decreased (Table 6, entry 4). As full conversion is still reached rapidly at −20 °C, we were interested to use a more convenient cooling bath made from ice and salt rather than the immersion cooler. We were pleased to see that running the reaction with this method of cooling afforded similar yield (Table 6, entry 5) even with a significantly more opaque bath mixture.

Having already modified most of the reaction parameters available we decided to explore the effect of different additives. In most reactions, **10** resulting from water addition was observed to some extent (4–8%), the presence of 4 Å molecular sieves effectively suppressed the formation of **10** (Table 7, entries 1 and 2). Unfortunately, the yield did not increase and only a slightly worse mass balance was observed. Multiple reagents are known to abstract fluorine from trifluoroborate salts to form the corresponding difluoroborate species [57-60]. This approach has previously been successful to increase the yield of different transformations. Using fluoride scavenger such as TMSCl, TFAA or $TMS_2(O)$ led to similar or lower yields (Table 7, entries 3–5). We were pleased to see that in the presence of $BF_3{\cdot}Et_2O$, **4a** was obtained in 75% yield (Table 7, entry 6). Addition of a less acidic boron Lewis acid $B(OTFE)_3$ had a detrimental effect (Table 7, entry 7). Increasing the stoichiometry of BF_3 to 2 equivalents lowered the yield significantly (Table 7, entry 8). In contrast, the loading could be reduced to 30 mol % without impacting the formation of **4a** (Table 7, entries 9 and 10).

Finally, a fine-tuning of the reaction conditions was performed. Increasing the concentration to 0.1 M afforded a comparable yield (Table 8, entries 1 and 2). Similarly, the equivalents of alkynyl-BF_3K **5a** could be reduced to 1.5, a further decrease started to impact the yield (Table 8, entries 3 and 4). Carrying out the reaction in degassed solvent is not mandatory but

Table 6: Temperature screening.[a]

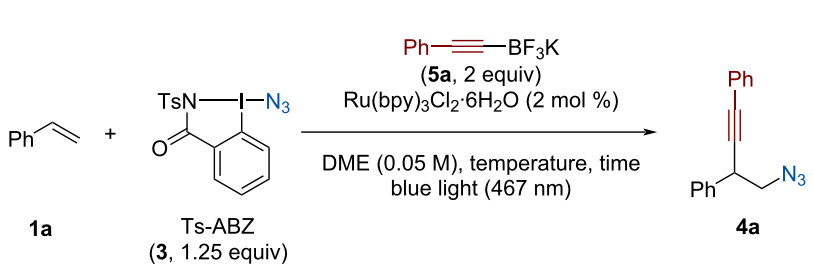

set-up with ice/NaCl bath

Entry	*T* (°C)	Method of cooling	Yield **4a** (%)[b]	Mass balance (%)[c]
1	rt	–	42	54
2	0	immersion cooler	50	64
3	–20	immersion cooler	52	71
4[d]	–41	immersion cooler	46	71
5	**–20**	**ice and NaCl bath**	**53**	**69**

[a]In all experiment the Kessil lamp was pointed diagonally towards the reaction vessel immersed in a cooling bath contained in a Dewar. An immersion cooler was placed in an EtOAc bath. The data were already published in the supporting information of ref. [45] except for the mass balance. The photo is a cropped version taken from ref. [45]. [b]NMR yield determined using CH_2Br_2 as internal standard. [c]The mass balance corresponds to the quantity of product + byproducts that could be determined by NMR integration. [d]Reaction was carried out for 3 h.

Table 7: Additive screening.

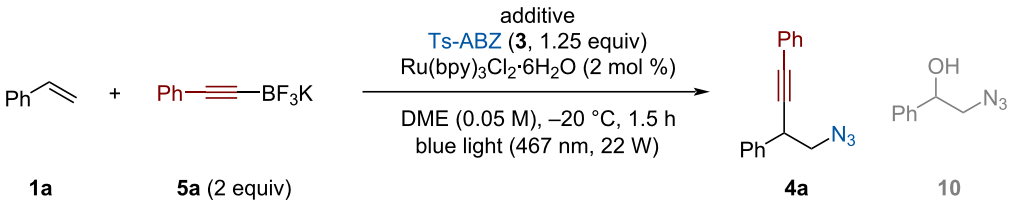

Entry	Additive	Equivalent	Yield **4a** (%)[b]	Yield **10** (%)[b]
1	–	–	53	8
2	MS 4 Å	50 mg/0.1 mmol	51	<5
3	TMSCl	1 equiv	40	–
4	TFAA	1 equiv	54	–
5	$(TMS)_2O$	1 equiv	48	13
6	$BF_3{\cdot}Et_2O$	1 equiv	75	–
7	$B(OTFE)_3$	1 equiv	53	10
8	$BF_3{\cdot}Et_2O$	2 equiv	37	n.d.
9	**$BF_3{\cdot}Et_2O$**	**0.3 equiv**	**72**	**9**
10	$BF_3{\cdot}Et_2O$	0.1 equiv	67	13

[a]The data were already published in the supporting information of Ref. [45] except for the yield of **10** and for entry 10. [b]NMR yield determined using CH_2Br_2 as internal standard. n.d. = not determined.

affords a better result (Table 8, entry 5). The photocatalyst could be changed to $Ru(bpy)_3(PF_6)_2$ without impacting the reaction (Table 8, entry 6). This photocatalyst was ultimately chosen since we observed a sharp decrease in yield when $Ru(bpy)_3Cl_2{\cdot}6H_2O$ was used with alkyl-substituted alkynyl-BF_3K, probably due to the poor solubilization of the catalyst. Finally, control experiments in the absence of photocatalyst or light only afforded traces of product (Table 8, entry 7).

Table 8: Fine-tuning of the reaction conditions.

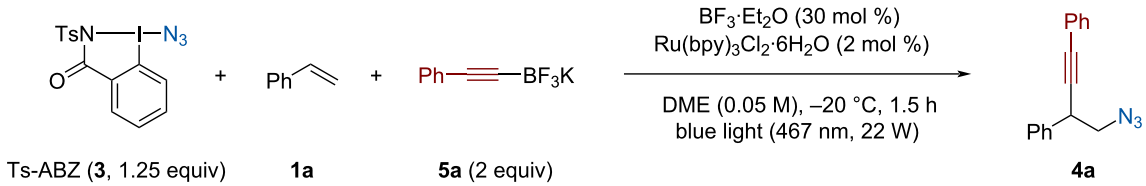

Ts-ABZ (**3**, 1.25 equiv) **1a** **5a** (2 equiv) **4a**

Entry	Change from standard conditions	Yield **4a** (%)[b]
1	none	72
2	*c* = 0.1 M	75
3	*c* = 0.1 M, **5a** (1.5 equiv)	74
4	*c* = 0.1 M, **5a** (1.25 equiv)	71
5	*c* = 0.1 M, **5a** (1.5 equiv), no degassing	65
6	***c* = 0.1 M, 5a (1.5 equiv), Ru(bpy)$_3$(PF$_6$)$_2$ (2 mol %)**	**74**
7	no photocatalyst or light, 16 h	<5

[a]The data were already published in the supporting information of ref. [45]. [b]NMR yield determined using CH_2Br_2 as internal standard.

The successful scope of the reaction was already described in our previous work [45], and will be only shortly described in a summarized form (Scheme 3). Styrene substituted with a *tert*-butyl at the *para* position afforded **4b** in 78% yield. Using a styrene bearing a sterically hindered aryl afforded **4c** in a similar yield. Homopropargylic azides possessing oxygen substitu-

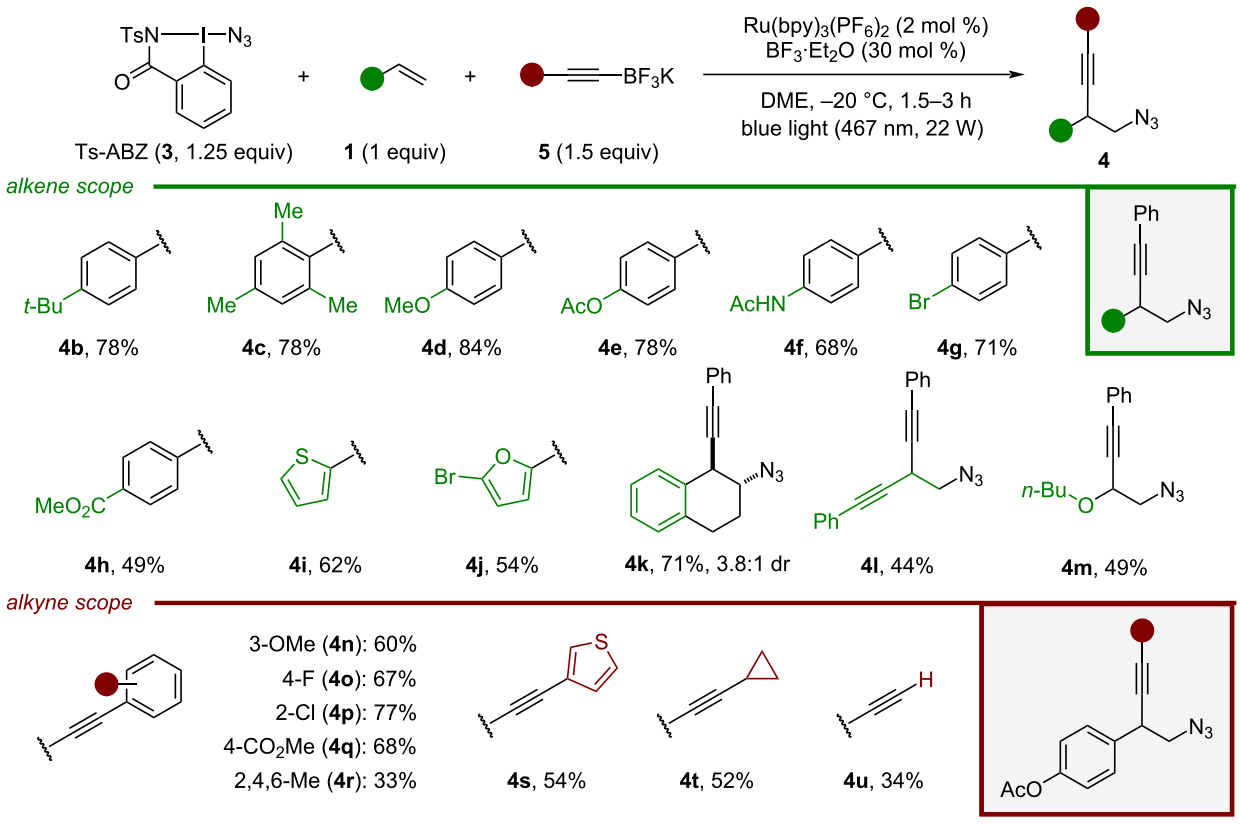

Scheme 3: Selected scope entries of the azido-alkynylation. The data were already published in ref. [45].

ents such as **4d** and **4e** could be obtained in 84% and 78% yield, respectively. We were pleased to see that the presence of an acetamide did not shut down the reaction, the corresponding product **4f** was obtained in 68%. The amide could have competed with the alkynyl-trifluoroborate for the carbocation trapping. An halogen-substituted styrene could be azido-alkynylated to afford **4g** in 71% yield. Electron-poor aryls are expected to destabilize the carbocation intermediate formed during the reaction. Nevertheless, **4h** possessing a *para* ester could be obtained, albeit with a decreased yield. Homopropargylic azides substituted with heteroaryls such as thiophene (**4i**) or a bromofuran (**4j**) were obtained in 62% and 54% yield, respectively. When the azido-alkynylation was carried out on 1,2-dihydronaphthalene, **4k** could be obtained in 71% yield and 3.8:1 dr. As expected, the configuration of the major diasteroisomer was determined to be *trans*. Diyne **4l** could be accessed in 44% yield from the exclusive 1,2-functionalization of the corresponding ene-yne. Crude NMR of the reaction did not show the presence of an allene product which could have been formed by a 1,4-functionalization. Enol ether could also be involved in the reaction, affording **4m** in 49% yield.

Next, we explored the variety of nucleophilic alkynes that could be introduced using *p*-acetoxystyrene as model substrate. Alkynyl-trifluoroborates bearing an electron-donating group (OMe) or electron-withdrawing groups (F, Cl, CO_2Me) on the aryl ring worked well in the transformation, affording homopropargylic azides **4n–q** in 60–77% yield. The reaction appears to be sensitive to the steric hindrance of the nucleophile: addition of a mesitylalkyne only formed 33% of **4r**. Pleasingly, heteroaryl substituents were tolerated, **4s** bearing a thiophene was obtained in 54% yield. The reaction could be extended to alkyl-substituted alkynes with little difference in yields. An homopropargylic azides possessing a cyclopropyl (**4t**) was formed in 52% yield. Finally, starting from potassium ethynyltrifluoroborate the free alkyne **4u** could be accessed in 34% yield with potential for further modification by cross-coupling. The full scope of the transformation can be found in Supporting Information File 1, Schemes S2 and S3 [45].

Concerning scope limitations, the azido-alkynylation of vinylpyridine **1b** was unsuccessful and thiazole **1c** only afforded 18% of the desired product, which proved to be unstable during purification (Scheme 4). Homopropargylic azides containing electron-rich nitrogen heterocycles could not be obtained. No product was observed by using vinylindole **1d** probably due its high tendency to polymerize. Although a slight amount of homopropargylic azide was formed using pyrrole **1e** it could not be isolated due to its instability. No conversion was observed when the transformation was attempted directly on the indole scaffold **1f**.

Only a small amount of product was formed using styrene **1g** bearing an extra α-phenyl substituent. A slightly higher yield

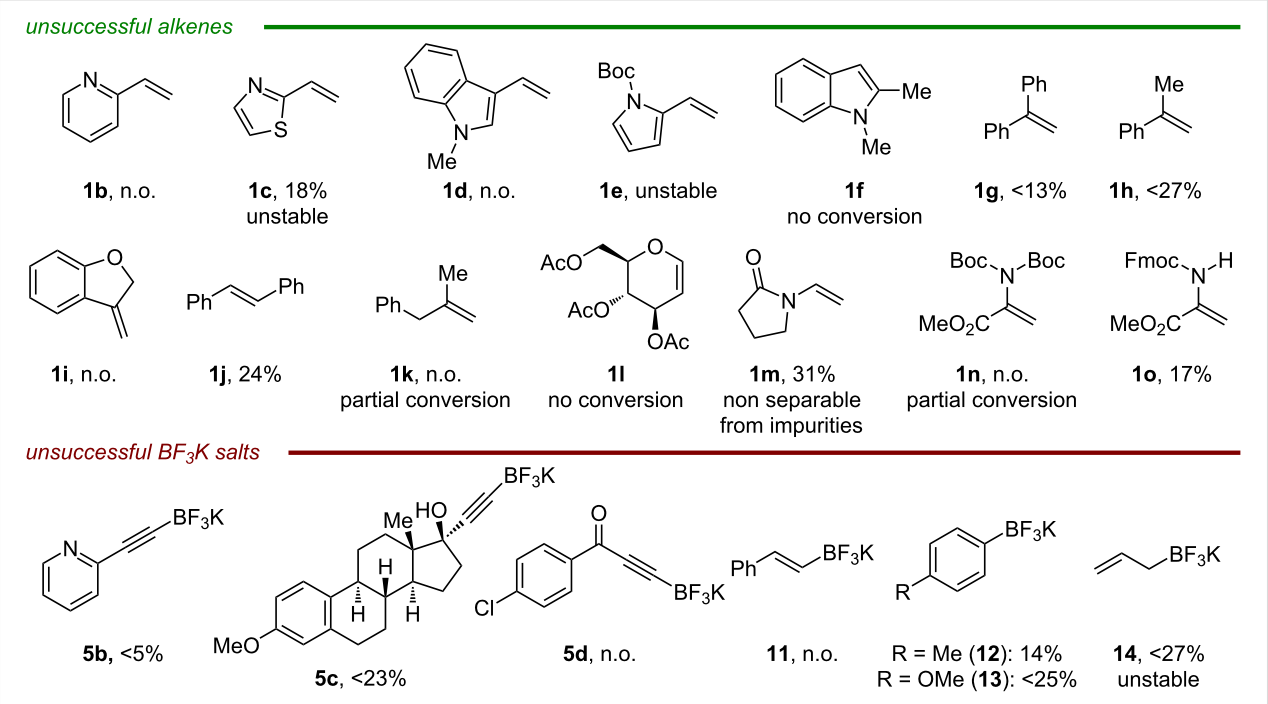

Scheme 4: Unsuccessful examples. The conditions used are the same as in Scheme 3. The yields reported were determined by NMR on crude mixtures. n.o. = not observed.

was observed when α-methylstyrene (**1h**) was used instead but it remained low (<27%). In general, when the reaction performed poorly (<30%) a large number of byproducts are formed, making the separation of the desired compound from the impurities impossible. Attempting the reaction on the cyclic substrate **1i** did not afford the desired product. Although β-substitution on the alkene is tolerated, using *trans*-stilbene only afforded 24% yield. Unfortunately, aliphatic alkenes are not tolerated in the reaction. When **1k** was used no product was formed and only partial conversion was observed. As a simple enol ether was reactive in the transformation, we attempted to use glucal **1l** but no conversion was observed. Enamide **1m** could be azido-alkynylated in low yield and the product was inseparable from impurities. When dehydroalanine **1n** was used in the reaction no product was formed and only partial conversion of the starting material was observed. We postulated that the presence of two Boc protecting groups on the nitrogen makes the oxidation of the C-centered radical challenging. By using **1o** only bearing one protecting group the desired product could be obtained, albeit in only 17% yield.

Pyridine-substituted alkynyl-BF_3K **5b** could not be transferred, and only traces of the product were observed. When **5c** derived from mestranol was involved in the reaction, the corresponding homopropargylic azide was obtained in <23% yield. We noticed that this particular alkynyltrifluoroborate salt has a low solubility in DME, which might cause the low yield observed. Ynonetrifluoroborate **5d** could not be introduced as nucleophile, probably due to its reduced reactivity caused by the electron-withdrawing acyl group. Unfortunately, although Molander previously reported the use of vinyl-trifluoroborate **11** to trap benzylic carbocation [42], in our case no product was observed. Since β-substituted styrenes can be involved in the transformation it is possible that the azide radicals can react either with the vinylic product formed in the reaction or with the starting vinyl-BF_3K. Simple aryl-BF_3K **12** only afforded 14% yield of the azido-arylated product, and using the more nucleophilic **13** only slightly improved the yield. Finally, a small amount of product resulting from the addition of allyl-BF_3K **14** could be observed but decomposed during purification.

Based on literature precedence [41,42,44] and experimental studies [45] a plausible photocatalytic cycle could be proposed (Scheme 5). Upon light irradiation, single-electron reduction of Ts-ABZ (**3**) ($E_{1/2}^{red}$ = −0.62 V vs SCE) [45] by the excited state photocatalyst ($E_{1/2}$ [Ru^{III}/Ru^{II}*] = −0.86 V vs SCE) [53] can occur to form an azide radical, which upon addition to styrene would generate intermediate **I-1**. Oxidation of the benzylic radical ($E_{1/2}^{ox}$ = +0.37 V vs SCE for the corresponding radical without the azide) [61] by the previously formed $Ru(bpy)^{3+}$ ($E_{1/2}$ [Ru^{III}/Ru^{II}] = +1.29 V vs SCE) [53] regenerates the ground state photocatalyst and forms carbocation **I-2**. Finally, nucleophilic addition of the alkynyl-trifluoroborate onto the benzylic carbocation would afford homopropargylic azide **4** [45].

Conclusion

In summary, an azido-alkynylation of styrenes to access homopropargylic azides was developed. The reaction was initially investigated using EBX reagents as SOMOphilic alkynes but this only afforded a 29% yield of the desired product. After switching to a radical-polar crossover approach the yield could be significantly improved. Key to the reaction optimization was the reduction of the temperature to −20 °C and the addition of $BF_3{\cdot}Et_2O$. A large variety of homopropargylic azides could be obtained in 30–84% yield using Ts-ABZ (**3**) as azide radical precursor and alkynyltrifluoroborates as nucleophilic alkyne source [62].

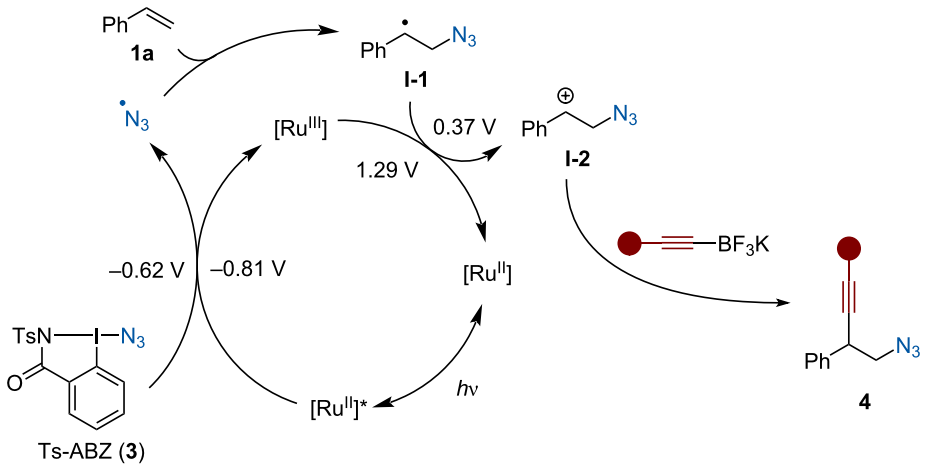

Scheme 5: Proposed mechanism.

Supporting Information

Supporting Information File 1

General methods, photochemistry set-up, reaction optimization, experimental procedures and compounds characterization.
[https://www.beilstein-journals.org/bjoc/content/supplementary/1860-5397-20-64-S1.pdf]

Funding

The authors thank the Ecole Polytechnique Fédérale de Lausanne for financial support. This publication was created as a part of NCCR Catalysis, a National Center of Competence in Research funded by the Swiss National Science Foundation (Grant No. 180544).

Author Contributions

Julien Borrel: conceptualization; data curation; investigation; validation; writing – original draft. Jerome Waser: conceptualization; funding acquisition; project administration; writing – review & editing.

ORCID® iDs

Julien Borrel - https://orcid.org/0000-0003-4045-5256
Jerome Waser - https://orcid.org/0000-0002-4570-914X

Data Availability Statement

All data that supports the findings of this study is available in the published article and/or the supporting information to this article.

References

1. Natchus, M. G.; Bookland, R. G.; Laufersweiler, M. J.; Pikul, S.; Almstead, N. G.; De, B.; Janusz, M. J.; Hsieh, L. C.; Gu, F.; Pokross, M. E.; Patel, V. S.; Garver, S. M.; Peng, S. X.; Branch, T. M.; King, S. L.; Baker, T. R.; Foltz, D. J.; Mieling, G. E. *J. Med. Chem.* **2001,** *44,* 1060–1071. doi:10.1021/jm000477l
2. Patel, M.; McHugh, R. J., Jr.; Cordova, B. C.; Klabe, R. M.; Bacheler, L. T.; Erickson-Viitanen, S.; Rodgers, J. D. *Bioorg. Med. Chem. Lett.* **2001,** *11,* 1943–1945. doi:10.1016/s0960-894x(01)00331-6
3. Miyazaki, T.; Yokoshima, S.; Simizu, S.; Osada, H.; Tokuyama, H.; Fukuyama, T. *Org. Lett.* **2007,** *9,* 4737–4740. doi:10.1021/ol702040y
4. Gahalawat, S.; Pandey, S. K. *Org. Biomol. Chem.* **2016,** *14,* 9287–9293. doi:10.1039/c6ob01775d
5. Montagnat, O. D.; Lessene, G.; Hughes, A. B. *J. Org. Chem.* **2010,** *75,* 390–398. doi:10.1021/jo9021887
6. Ito, M.; Mera, A.; Mashimo, T.; Seki, T.; Karanjit, S.; Ohashi, E.; Nakayama, A.; Kitamura, K.; Hamura, T.; Ito, H.; Namba, K. *Chem. – Eur. J.* **2018,** *24,* 17727–17733. doi:10.1002/chem.201804733
7. Nguyen, H. V.-T.; Jiang, Y.; Mohapatra, S.; Wang, W.; Barnes, J. C.; Oldenhuis, N. J.; Chen, K. K.; Axelrod, S.; Huang, Z.; Chen, Q.; Golder, M. R.; Young, K.; Suvlu, D.; Shen, Y.; Willard, A. P.; Hore, M. J. A.; Gómez-Bombarelli, R.; Johnson, J. A. *Nat. Chem.* **2022,** *14,* 85–93. doi:10.1038/s41557-021-00826-8
8. Kruse, L. I.; Kaiser, C.; DeWolf, W. E., Jr.; Chambers, P. A.; Goodhart, P. J.; Ezekiel, M.; Ohlstein, E. H. *J. Med. Chem.* **1988,** *31,* 704–706. doi:10.1021/jm00399a002
9. Shaw, A. N.; Dolle, R. E.; Kruse, L. I. *Tetrahedron Lett.* **1990,** *31,* 5081–5084. doi:10.1016/s0040-4039(00)97811-0
10. Tan, E. S.; Miyakawa, M.; Bunzow, J. R.; Grandy, D. K.; Scanlan, T. S. *J. Med. Chem.* **2007,** *50,* 2787–2798. doi:10.1021/jm0700417
11. Gorin, D. J.; Davis, N. R.; Toste, F. D. *J. Am. Chem. Soc.* **2005,** *127,* 11260–11261. doi:10.1021/ja053804t
12. Hiroya, K.; Matsumoto, S.; Ashikawa, M.; Ogiwara, K.; Sakamoto, T. *Org. Lett.* **2006,** *8,* 5349–5352. doi:10.1021/ol062249c
13. Wyrębek, P.; Sniady, A.; Bewick, N.; Li, Y.; Mikus, A.; Wheeler, K. A.; Dembinski, R. *Tetrahedron* **2009,** *65,* 1268–1275. doi:10.1016/j.tet.2008.11.094
14. Yamamoto, H.; Sasaki, I.; Mitsutake, M.; Karasudani, A.; Imagawa, H.; Nishizawa, M. *Synlett* **2011,** 2815–2818. doi:10.1055/s-0031-1289566
15. Mironova, I. A.; Kirsch, S. F.; Zhdankin, V. V.; Yoshimura, A.; Yusubov, M. S. *Eur. J. Org. Chem.* **2022,** e202200754. doi:10.1002/ejoc.202200754
16. Simonet-Davin, R.; Waser, J. *Synthesis* **2023,** *55,* 1652–1661. doi:10.1055/a-1966-4974
17. Alazet, S.; Preindl, J.; Simonet-Davin, R.; Nicolai, S.; Nanchen, A.; Meyer, T.; Waser, J. *J. Org. Chem.* **2018,** *83,* 12334–12356. doi:10.1021/acs.joc.8b02068
18. Shirke, R. P.; Ramasastry, S. S. V. *Org. Lett.* **2017,** *19,* 5482–5485. doi:10.1021/acs.orglett.7b02861
19. Davies, J.; Sheikh, N. S.; Leonori, D. *Angew. Chem., Int. Ed.* **2017,** *56,* 13361–13365. doi:10.1002/anie.201708497
20. Jia, J.; Ho, Y. A.; Bülow, R. F.; Rueping, M. *Chem. – Eur. J.* **2018,** *24,* 14054–14058. doi:10.1002/chem.201802907
21. Jiang, H.; Studer, A. *Chem. – Eur. J.* **2019,** *25,* 516–520. doi:10.1002/chem.201805490
22. Hu, Z.; Fu, L.; Chen, P.; Cao, W.; Liu, G. *Org. Lett.* **2021,** *23,* 129–134. doi:10.1021/acs.orglett.0c03826
23. Zhang, X.; Qi, D.; Jiao, C.; Zhang, Z.; Liu, X.; Zhang, G. *Org. Chem. Front.* **2021,** *8,* 6522–6529. doi:10.1039/d1qo01217g
24. Fumagalli, G.; Rabet, P. T. G.; Boyd, S.; Greaney, M. F. *Angew. Chem., Int. Ed.* **2015,** *54,* 11481–11484. doi:10.1002/anie.201502980
25. Alazet, S.; Le Vaillant, F.; Nicolai, S.; Courant, T.; Waser, J. *Chem. – Eur. J.* **2017,** *23,* 9501–9504. doi:10.1002/chem.201702599
26. Cong, F.; Wei, Y.; Tang, P. *Chem. Commun.* **2018,** *54,* 4473–4476. doi:10.1039/c8cc01096j
27. Zhang, Z.; Chen, P.; Liu, G. *Chem. Soc. Rev.* **2022,** *51,* 1640–1658. doi:10.1039/d1cs00727k
28. Meldal, M.; Tornøe, C. W. *Chem. Rev.* **2008,** *108,* 2952–3015. doi:10.1021/cr0783479
29. Lu, M.-Z.; Wang, C.-Q.; Loh, T.-P. *Org. Lett.* **2015,** *17,* 6110–6113. doi:10.1021/acs.orglett.5b03130
30. Zhou, H.; Jian, W.; Qian, B.; Ye, C.; Li, D.; Zhou, J.; Bao, H. *Org. Lett.* **2017,** *19,* 6120–6123. doi:10.1021/acs.orglett.7b02982
31. Cai, C.-Y.; Zheng, Y.-T.; Li, J.-F.; Xu, H.-C. *J. Am. Chem. Soc.* **2022,** *144,* 11980–11985. doi:10.1021/jacs.2c05126
32. Le Vaillant, F.; Waser, J. *Chem. Sci.* **2019,** *10,* 8909–8923. doi:10.1039/c9sc03033f

33. Le Du, E.; Waser, J. *Chem. Commun.* **2023,** *59,* 1589–1604. doi:10.1039/d2cc06168f
34. Ge, D.; Wang, X.; Chu, X.-Q. *Org. Chem. Front.* **2021,** *8,* 5145–5164. doi:10.1039/d1qo00798j
35. Zhou, Q.-Q.; Guo, W.; Ding, W.; Wu, X.; Chen, X.; Lu, L.-Q.; Xiao, W.-J. *Angew. Chem., Int. Ed.* **2015,** *54,* 11196–11199. doi:10.1002/anie.201504559
36. Jana, K.; Bhunia, A.; Studer, A. *Chem* **2020,** *6,* 512–522. doi:10.1016/j.chempr.2019.12.022
37. Capaldo, L.; Ravelli, D. *Org. Lett.* **2021,** *23,* 2243–2247. doi:10.1021/acs.orglett.1c00381
38. Zuo, Z.; Studer, A. *Org. Lett.* **2022,** *24,* 949–954. doi:10.1021/acs.orglett.1c04319
39. Wiles, R. J.; Molander, G. A. *Isr. J. Chem.* **2020,** *60,* 281–293. doi:10.1002/ijch.201900166
40. Sharma, S.; Singh, J.; Sharma, A. *Adv. Synth. Catal.* **2021,** *363,* 3146–3169. doi:10.1002/adsc.202100205
41. Xiong, P.; Long, H.; Song, J.; Wang, Y.; Li, J.-F.; Xu, H.-C. *J. Am. Chem. Soc.* **2018,** *140,* 16387–16391. doi:10.1021/jacs.8b08592
42. Cabrera-Afonso, M. J.; Sookezian, A.; Badir, S. O.; El Khatib, M.; Molander, G. A. *Chem. Sci.* **2021,** *12,* 9189–9195. doi:10.1039/d1sc02547c
43. Sheng, W.; Huang, X.; Cai, J.; Zheng, Y.; Wen, Y.; Song, C.; Li, J. *Org. Lett.* **2023,** *25,* 6178–6183. doi:10.1021/acs.orglett.3c02309
44. Sookezian, A.; Molander, G. A. *Org. Lett.* **2023,** *25,* 1014–1019. doi:10.1021/acs.orglett.3c00182
45. Borrel, J.; Waser, J. *Chem. Sci.* **2023,** *14,* 9452–9460. doi:10.1039/d3sc03309k
See for more details on the reaction scope; mechanistic studies.
46. Smyrnov, V.; Muriel, B.; Waser, J. *Org. Lett.* **2021,** *23,* 5435–5439. doi:10.1021/acs.orglett.1c01775
47. Amos, S. G. E.; Cavalli, D.; Le Vaillant, F.; Waser, J. *Angew. Chem., Int. Ed.* **2021,** *60,* 23827–23834. doi:10.1002/anie.202110257
48. Alektiar, S. N.; Wickens, Z. K. *J. Am. Chem. Soc.* **2021,** *143,* 13022–13028. doi:10.1021/jacs.1c07562
49. Williams, O. P.; Chmiel, A. F.; Mikhael, M.; Bates, D. M.; Yeung, C. S.; Wickens, Z. K. *Angew. Chem., Int. Ed.* **2023,** *62,* e202300178. doi:10.1002/anie.202300178
50. Shinomoto, Y.; Yoshimura, A.; Shimizu, H.; Yamazaki, M.; Zhdankin, V. V.; Saito, A. *Org. Lett.* **2015,** *17,* 5212–5215. doi:10.1021/acs.orglett.5b02543
51. Reichle, A.; Koch, M.; Sterzel, H.; Großkopf, L.-J.; Floss, J.; Rehbein, J.; Reiser, O. *Angew. Chem., Int. Ed.* **2023,** *62,* e202219086. doi:10.1002/anie.202219086
52. Day, C. S.; Fawcett, A.; Chatterjee, R.; Hartwig, J. F. *J. Am. Chem. Soc.* **2021,** *143,* 16184–16196. doi:10.1021/jacs.1c07330
53. Wu, Y.; Kim, D.; Teets, T. S. *Synlett* **2022,** *33,* 1154–1179. doi:10.1055/a-1390-9065
54. Garreau, M.; Le Vaillant, F.; Waser, J. *Angew. Chem., Int. Ed.* **2019,** *58,* 8182–8186. doi:10.1002/anie.201901922
55. Yu, Y.; Yuan, Y.; Ye, K.-Y. *Chem. Commun.* **2023,** *59,* 422–425. doi:10.1039/d2cc06246a
56. Motiwala, H. F.; Armaly, A. M.; Cacioppo, J. G.; Coombs, T. C.; Koehn, K. R. K.; Norwood, V. M., IV; Aubé, J. *Chem. Rev.* **2022,** *122,* 12544–12747. doi:10.1021/acs.chemrev.1c00749
57. Mitchell, T. A.; Bode, J. W. *J. Am. Chem. Soc.* **2009,** *131,* 18057–18059. doi:10.1021/ja906514s
58. Argintaru, O. A.; Ryu, D.; Aron, I.; Molander, G. A. *Angew. Chem., Int. Ed.* **2013,** *52,* 13656–13660. doi:10.1002/anie.201308036
59. Roscales, S.; Ortega, V.; Csákÿ, A. G. *J. Org. Chem.* **2013,** *78,* 12825–12830. doi:10.1021/jo402262m
60. Šterman, A.; Sosič, I.; Časar, Z. *Chem. Sci.* **2022,** *13,* 2946–2953. doi:10.1039/d1sc07065g
61. Wayner, D. D. M.; McPhee, D. J.; Griller, D. *J. Am. Chem. Soc.* **1988,** *110,* 132–137. doi:10.1021/ja00209a021
62. The content of this publication was adapted from: Borrel, J. Novel alkynylation methods through the combination of hypervalent iodine reagents and alkynyl-trifluoroborate salts. Ph.D. Thesis n° 10492, EPFL, Switzerland, 2024.

License and Terms

BEILSTEIN JOURNAL OF ORGANIC CHEMISTRY

Ortho-ester-substituted diaryliodonium salts enabled regioselective arylocyclization of naphthols toward 3,4-benzocoumarins

Ke Jiang[1], Cheng Pan[1], Limin Wang[1], Hao-Yang Wang[*2] and Jianwei Han[*1]

Letter

Open Access

Address:
[1]Key Laboratory for Advanced Materials and Feringa Nobel Prize Scientist Joint Research Center, Department of Fine Chemistry and Institute of Fine Chemicals, School of Chemistry and Molecular Engineering, East China University of Science and Technology, 130 Meilong Road, Shanghai 200237, P. R. China and [2]National Center for Organic Mass Spectrometry in Shanghai, Shanghai Institute of Organic Chemistry, The Chinese Academy of Sciences, 345 Lingling Road, Shanghai 200032, China

Email:
Hao-Yang Wang[*] - haoyangwang@sioc.ac.cn; Jianwei Han[*] - jianweihan@ecust.edu.cn

* Corresponding author

Keywords:
annulation; arylocyclization; 3,4-benzocoumarin; diaryliodonium salts; naphthol

Beilstein J. Org. Chem. **2024,** *20,* 841–851.
https://doi.org/10.3762/bjoc.20.76

Received: 25 November 2023
Accepted: 11 April 2024
Published: 18 April 2024

This article is part of the thematic issue "Hypervalent halogen chemistry".

Guest Editor: T. Gulder

Abstract

Cyclic annulation involving diaryliodonium salts is an efficient tool for the construction of two or more chemical bonds in a one-pot process. *Ortho*-functionalized diaryliodonium salts have showcased distinct reactivity in the exploration of benzocyclization or arylocyclization. With this strategy of *ortho*-ester-substituted diaryliodonium salts, herein, we utilized a copper catalyst to activate the C–I bond of diaryliodonium salts in the generation of aryl radicals, thus resulting in an annulation reaction with naphthols and substituted phenols. This approach yielded a diverse array of 3,4-benzocoumarin derivatives bearing various substituents.

Introduction

Diaryliodonium salts as electrophilic reagents have attracted significant attention in the field of organic synthesis owing to their efficiency and selectivity [1-7]. Particularly, they have been employed in benzocyclization and arylocyclization reactions, enabling intramolecular cyclization by forming aromatic or heterocyclic rings as a part of cyclic structures [8]. In these reactions, the dual activation of a C–I bond and vicinal C–H bonds/functional groups features a distinct advantage, facilitating the formation of two or more chemical bonds in a step-economic manner [9-13]. In a prior study, we reported a palladium-catalyzed efficient activation of both C–I bond and the adjacent C–H bond of diaryliodonium salts in the formation of 4,5-benzocoumarin derivatives, expanding the benzocoumarin family (Scheme 1b) [14]. Recently, *ortho*-functionalized

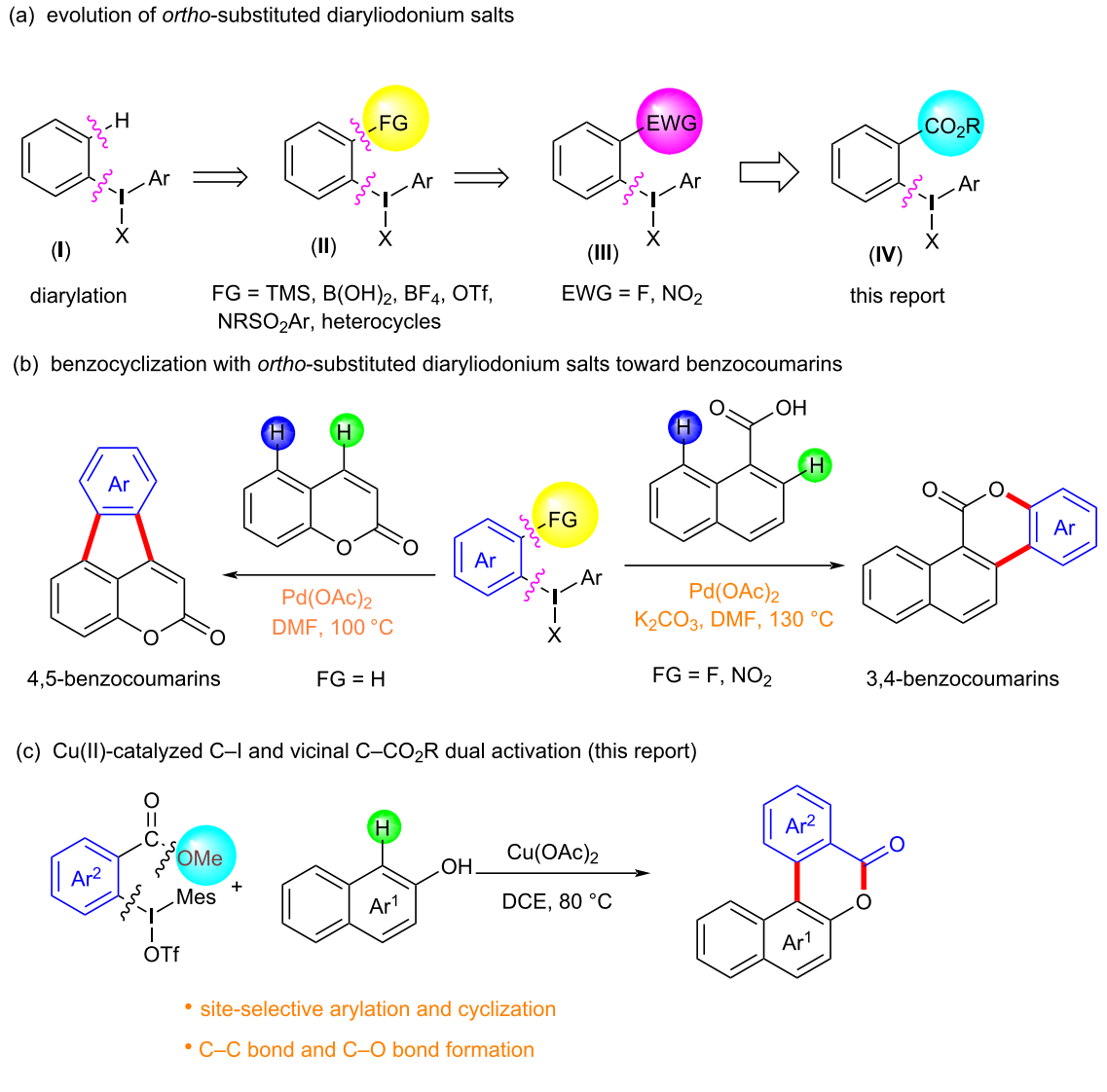

Scheme 1: Arylation reactions of aromatic compounds and reaction patterns of *ortho*-functionalized diaryliodonium salts.

diaryliodonium salts, due to their coordinating and electrophilic effects, have exhibited unique reactivity and chemoselectivity [15]. As such, a wide range of functional groups including the trimethylsilyl group, boronic acid, trifluoroborate moiety, trifluoromethanesulfonate, aryl sulfonamides, and heterocycles, have been incorporated into the *ortho*-position of diaryliodonium structures [16-21]. *Ortho*-trimethylsilyl or boronic acid-substituted diaryliodonium salts can serve as aryne precursors. *Ortho*-trifluoroborate-substituted diaryliodonium salts furnished iodonium zwitterions as bifunctional reagents [22-25]. Additionally, *ortho*-trifluoromethanesulfonate, *N*-sulfonyl, or tosylmethylene-substituted diaryliodonium salts can undergo intramolecular aryl migrations [26-28]. More recently, we explored the reactivity of *ortho*-functionalized diaryliodonium salts containing electron-withdrawing groups (EWGs) such as fluorine and nitro groups [29,30]. These *ortho*-substituted diaryliodonium salts undergo selective benzocyclizations and arylocyclizations with aromatic acids, leading to 3,4-benzocoumarin skeletons in the presence of palladium catalysts (Scheme 1b). Furthermore, Olofsson and colleagues described an unprecedented reaction pathway using *ortho*-fluoro-substituted diaryliodonium salts bearing strong electron-withdrawing groups, leading to novel diarylations of N-, O-, and S-nucleophiles [31-33]. Building on our great interest in *ortho*-functionalized diaryliodonium salts and their dual activation capabilities, we sought to incorporate carboxylic ester groups into the structures of *ortho*-substituted diaryliodonium salts to explore their properties and reactivity. Our previous investigations demonstrated the ability of diaryliodonium salts for selective mono-arylation of 2-naphthols [34]. In this context, we embark

on a strategy to modify the neighbouring position of the diaryliodonium salt with an ester group, presenting a novel copper-catalysed regioselective arylocyclization of naphthols and substituted phenols. This method represents an efficient approach to access 3,4-benzocoumarin derivatives (Scheme 1c).

Results and Discussion

To start the study, we used 2-naphthol (**1a**) and 1.1 equivalents of *ortho*-methyl formate-substituted diaryliodonium salt **2a** as template substrates. The reaction was performed in the presence of 10 mol % $Cu(OTf)_2$ and 1.0 equivalent of K_2CO_3 in DCE at a temperature of 80 °C. To our delight, the reaction afforded 3,4-benzocoumarin **3aa** in a 27% yield (Table 1, entry 1). The structure of **3aa** was confirmed through NMR spectroscopy and mass spectra analysis. Subsequently, we started to screen various bases such as Na_2CO_3, Cs_2CO_3, KOH, NaO*t*-Bu, LiHMDS, and DMAP (Table 1, entries 2–7). Fortunately, it was found that the reaction yield was increased to 50% in the absence of any base (Table 1, entry 8). Further investigations for assessing the influence of various solvents including dimethyl sulfoxide (DMSO), *N*,*N*-dimethylformamide (DMF), toluene, acetic acid (AcOH) and water (Table 1, entries 9–13) were carried out. However, polar solvents such as AcOH and H_2O were proved to be unsuitable for this reaction. For catalysts, we found that $Cu(OAc)_2$ gave the best results (Table 1, entries 15–18). Finally, the reaction temperature and time were optimized, **3aa** was produced in 61% yield at a temperature of 80 °C after 3 hours (Table 1, entry 15).

With the optimized reaction conditions in hand, we started to explore the substrate scope of the cyclization to construct a variety of 3,4-benzocoumarin derivatives. Our investigations commenced with 2-naphthol (**1**), and the results are presented in Table 2. Various substituted naphthols with a broad range of substituents on the naphthalene unit were well tolerated in the reaction, affording the corresponding products **3aa**–**aq** in gener-

Table 1: Optimization of reaction conditions.[a]

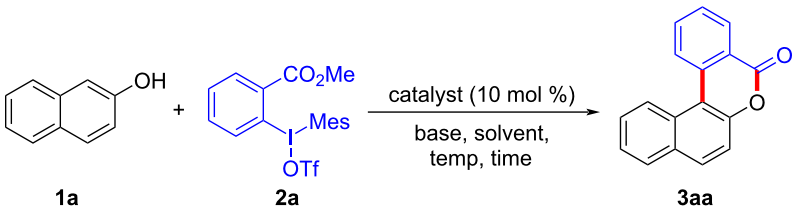

1a **2a** **3aa**

Entry	Solvent	Base	Catalyst	**3aa** (%)[b]
1	DCE	K_2CO_3	$Cu(OTf)_2$	27
2	DCE	Na_2CO_3	$Cu(OTf)_2$	25
3	DCE	Cs_2CO_3	$Cu(OTf)_2$	16
4	DCE	KOH	$Cu(OTf)_2$	24
5	DCE	DMAP	$Cu(OTf)_2$	26
6	DCE	NaO*t*-Bu	$Cu(OTf)_2$	35
7	DCE	LiHMDS	$Cu(OTf)_2$	30
8	DCE	–	$Cu(OTf)_2$	50
9	DMSO	–	$Cu(OTf)_2$	45[c] (40)[d]
10	DMF	–	$Cu(OTf)_2$	23
11	toluene	–	$Cu(OTf)_2$	10
12	AcOH	–	$Cu(OTf)_2$	0
13	H_2O	–	$Cu(OTf)_2$	0
14[e]	DCE	–	$Cu(OTf)_2$	48
15	DCE	–	$Cu(OAc)_2$	61
16	DCE	–	$Pd(OAc)_2$	22
17	DCE	–	$PdCl_2$	40
18	DCE	–	AgOAc	20

[a]Reaction conditions: **1a** (0.3 mmol, 1 equiv), **2a** (0.33 mmol, 1.1 equiv), base (0.3 mmol; 1 equiv), catalyst (10 mol %), solvent (2 mL), 80 °C, 3 hours. [b]Isolated yields were obtained after purification by column chromatography. [c]The reaction temperature was 110 °C. [d]The reaction temperature was 130 °C. [e]The reaction was quenched after 12 hours.

ally moderate to good yields of 22–83% (Table 2, entries 1–17). These substituents included halogen (Br), methyl, phenyl, aldehyde, ester, and methoxy groups, all of which were compatible with the reaction conditions. Notably, compounds **3ab**, **3ah**, **3aj**, **3am** and **3ap** bearing bromine are very useful modules for the synthesis of functional materials via cross-coupling reactions. Next, we extended our investigation to 1-naphthol in this reaction, and found that the arylation of 1-naphthol was achieved selectively at the C-2 position. The cascade cyclization resulted in the corresponding products **3an** and **3ao** in yields of 49% and 40%, respectively (Table 2, entries 14 and 15). When 5,6,7,8-tetrahydro-2-naphthol was subjected to the reaction, we obtained products **3ar** and **3as** as a mixture (40% and 10% yield, respectively, Table 2, entry 18). However, when naphthol bearing a strong electron-withdrawing group (such as a nitro group) in the *para* position was reacted, the corresponding product could not be obtained, but instead the O-arylated product **3at** was obtained (Table 2, entry 19). Apart from naphthol, we also tested substituted phenols under the standard conditions. The corresponding products of **3au** and **3av** were produced in 34% and 39% yields, respectively, in which methoxy and *tert*-butyl groups were located in the *para* position to the hydroxy group (Table 2, entries 20 and 21). In the case of **3al**, the mono-arylation of naphthol generated **3al'** in 20% isolated yield, which is the reason for the low yield of **3al**.

We subsequently turned our attention to explore the effect of structural diversity of the *ortho*-ester-substituted diaryliodonium salts. Firstly, a family of substituted diaryliodonium salts

Table 2: Scope of naphthols and phenols for the synthesis of 3,4-benzocoumarins.[a,b].

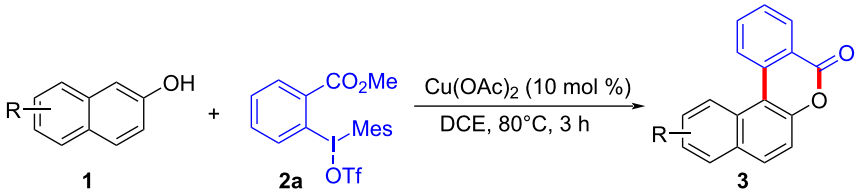

1 2a 3

Entry	1	Product	Yield (%)[b]
1	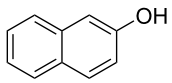	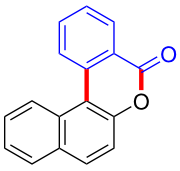 **3aa**	61
2	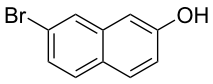	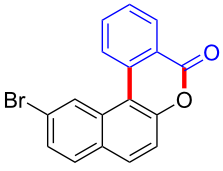 **3ab**	63
3	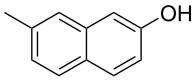	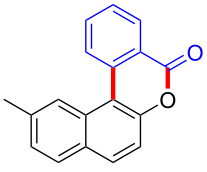 **3ac**	80
4	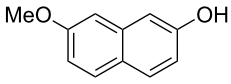	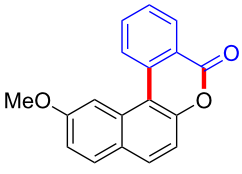 **3ad**	77

Table 2: Scope of naphthols and phenols for the synthesis of 3,4-benzocoumarins.[a,b]. (continued)

5	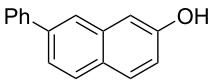	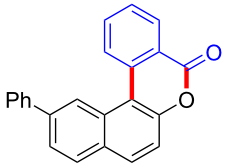 **3ae**		26
6	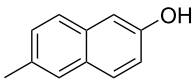	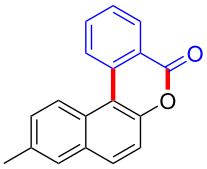 **3af**		31
7	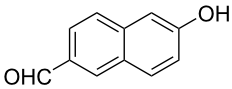	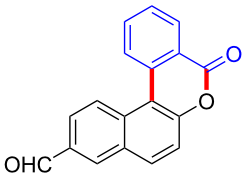 **3ag**		28
8	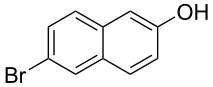	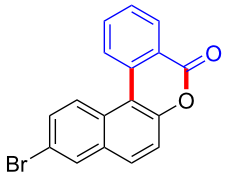 **3ah**		54
9	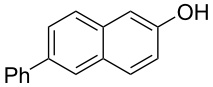	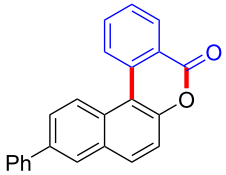 **3ai**		25
10	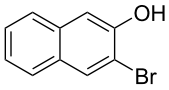	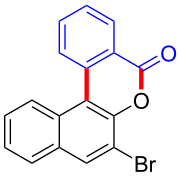 **3aj**		22
11	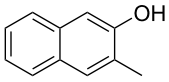	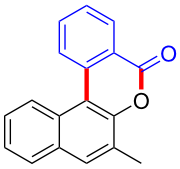 **3ak**		49
12	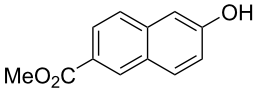	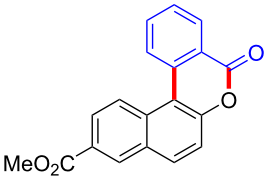 **3al**	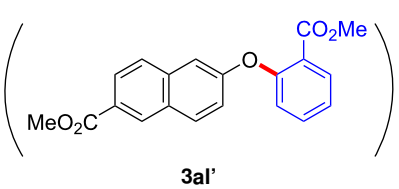 **3al'**	48 (20)

Table 2: Scope of naphthols and phenols for the synthesis of 3,4-benzocoumarins.[a,b]. (continued)

13	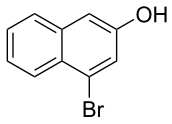	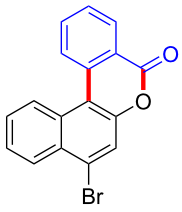 **3am**		3
14	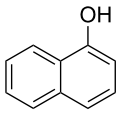	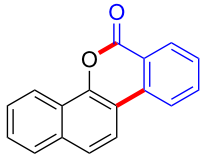 **3an**		49
15	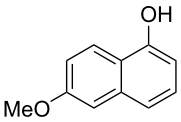	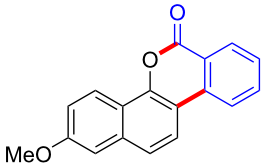 **3ao**		40
16	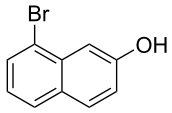	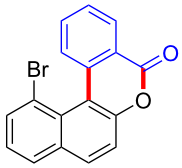 **3ap**		25
17	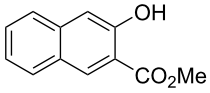	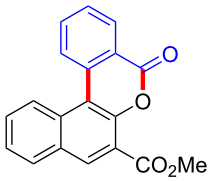 **3aq**		43
18	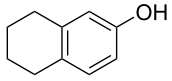	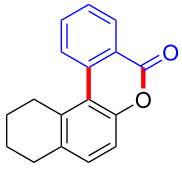 **3ar**	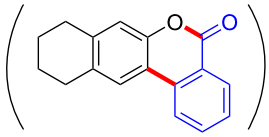 **3as**	45 (10)
19	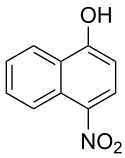	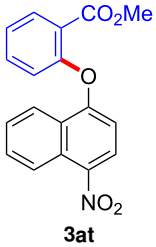 **3at**		51

Table 2: Scope of naphthols and phenols for the synthesis of 3,4-benzocoumarins.[a,b]. (continued)

20	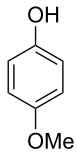	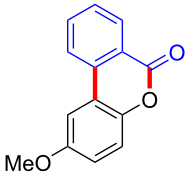 **3au**	34
21	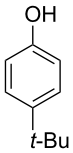	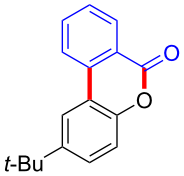 **3av**	39

[a]Reaction conditions: **1** (0.3 mmol, 1 equiv), **2a** (0.33 mmol, 1.1 equiv), $Cu(OAc)_2$ (10 mol %), DCE (2 mL), 80 °C, 3 hours. [b]Isolated yields were obtained after purification with column chromatography. Mes = 2,4,6-trimethylphenyl, OTf = trifluoromethansulfonate.

were synthesized in a one-pot procedure. These *ortho*-substituted diaryliodonium salts were isolated as stable solids, whose structures were fully characterized by NMR spectroscopy. As shown in Table 3, we utilized 2-naphthol and 1-naphthol as template substrates to react with various unsymmetrical 2-ester-substituted diaryliodonium salts. Remarkably, iodonium salts **2**

Table 3: Scope of *ortho*-ester-substituted diaryliodonium salts.[a]

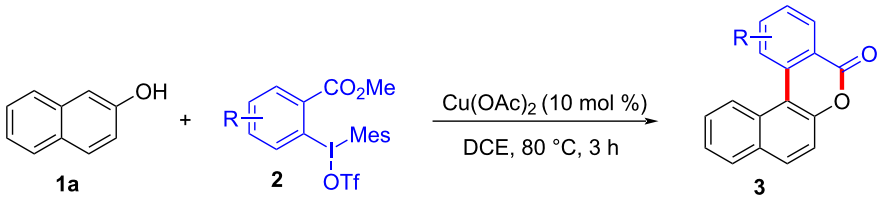

1a **2** **3**

Entry	**2**	Product	Yield (%)[b]
1	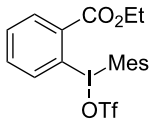 **2b**	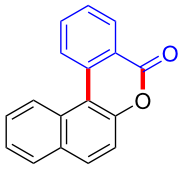 **3aa**	55
2	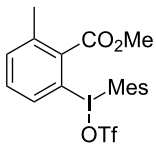 **2c**	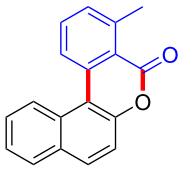 **3ca**	32
3	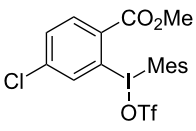 **2d**	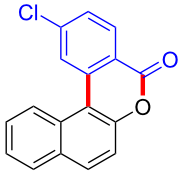 **3da**	50

Table 3: Scope of *ortho*-ester-substituted diaryliodonium salts.[a] (continued)

4	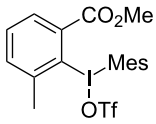 **2e**	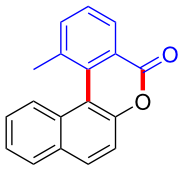 **3ea**	46
5	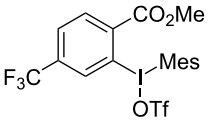 **2f**	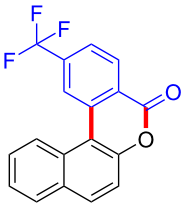 **3fa**	49
6	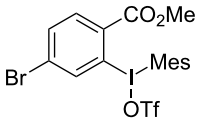 **2g**	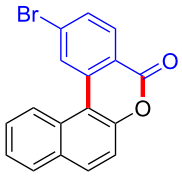 **3ga**	55
7	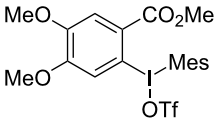 **2h**	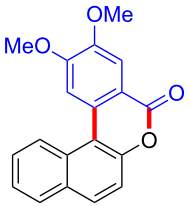 **3ha**	43
8	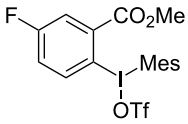 **2i**	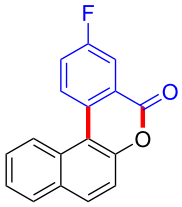 **3ia**	21
9	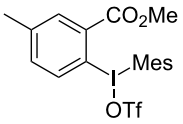 **2j**	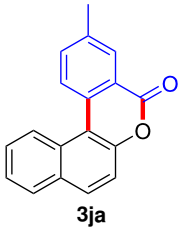 **3ja**	59
10[c]	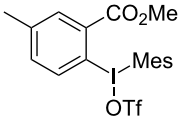 **2j**	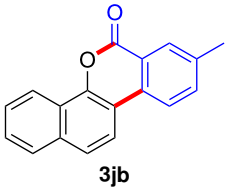 **3jb**	28

Table 3: Scope of *ortho*-ester-substituted diaryliodonium salts.[a] (continued)

11	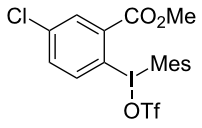 **2k**	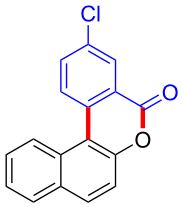 **3ka**	37
12[c]	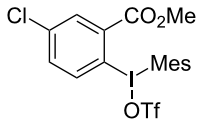 **2k**	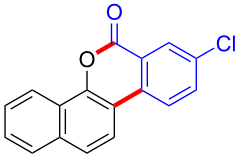 **3kb**	45
13	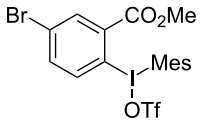 **2l**	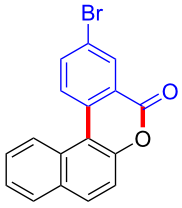 **3la**	35
14	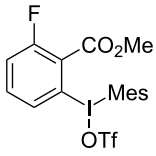 **2m**	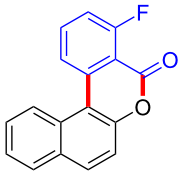 **3ma**	50

[a]Reaction conditions: **1** (0.3 mmol, 1 equiv), **2** (0.33 mmol, 1.1 equiv), $Cu(OAc)_2$ (10 mol %), DCE (2 mL), 80 °C, 3 hours. [b]Isolated yields were obtained after purification with column chromatography. [c]1-Naphthol was used instead of 2-naphthol. Mes = 2,4,6-trimethylphenyl, OTf = trifluoromethansulfonate.

proved to be versatile in this reaction, regardless of the electronic nature and position of the substituents. The desired 3,4-benzocoumarin products **3ba**–**ma** were obtained in yields of 21–59%. Notably, substituents such as halogens (F, Cl, and Br), methyl, methoxy, and trifluoromethyl groups at the *ortho*-, *meta*-, or *para*-positions to the ester group were all well-tolerated (Table 3).

To gain further insights into the reaction mechanism, we conducted control experiments. Given the utility of diaryliodonium salts in radical chemistry, we introduced 2 equivalents of 2,2,6,6-tetramethylpiperidine-1-oxyl (TEMPO) or 2 equivalents of butylated hydroxytoluene (BHT) into the template reaction. Remarkably, we observed that the desired product was not formed, suggesting a radical pathway. Subsequently, we investigated the bond-formation sequence in the benzocyclization reaction. A possible intermediate of **3al'** was prepared and tested in the reaction under the standard conditions, however, product **3aa** was not obtained.

Based on the literature known results and the experimental evidences [35,36], we proposed a plausible reaction mechanism (Scheme 2b). The reaction started with the formation of radical intermediate **A** from diaryliodonium salt **2a**. Naphthol **1a** forms intermediate **B** with **A** after participation with the Cu(II) catalyst. Intermediate **B** generates **C** by radical substitution. A final intramolecular transesterification yields the benzocoumarin product **3aa**.

Conclusion

In summary, we have employed *ortho*-ester-substituted diaryliodonium salts in a cascade cyclization, the cyclization features a copper-catalyzed activation strategy involving the cleavage of the C–I bond and esterification. The resulting cascade of selective arylation/intramolecular cyclization facilitated the synthesis of 3,4-benzocoumarin derivatives. The protocol enables the efficient formation of two chemical bonds in one pot, representing a valuable tool for the synthesis of polycyclic benzocoumarins. Our ongoing research endeavours

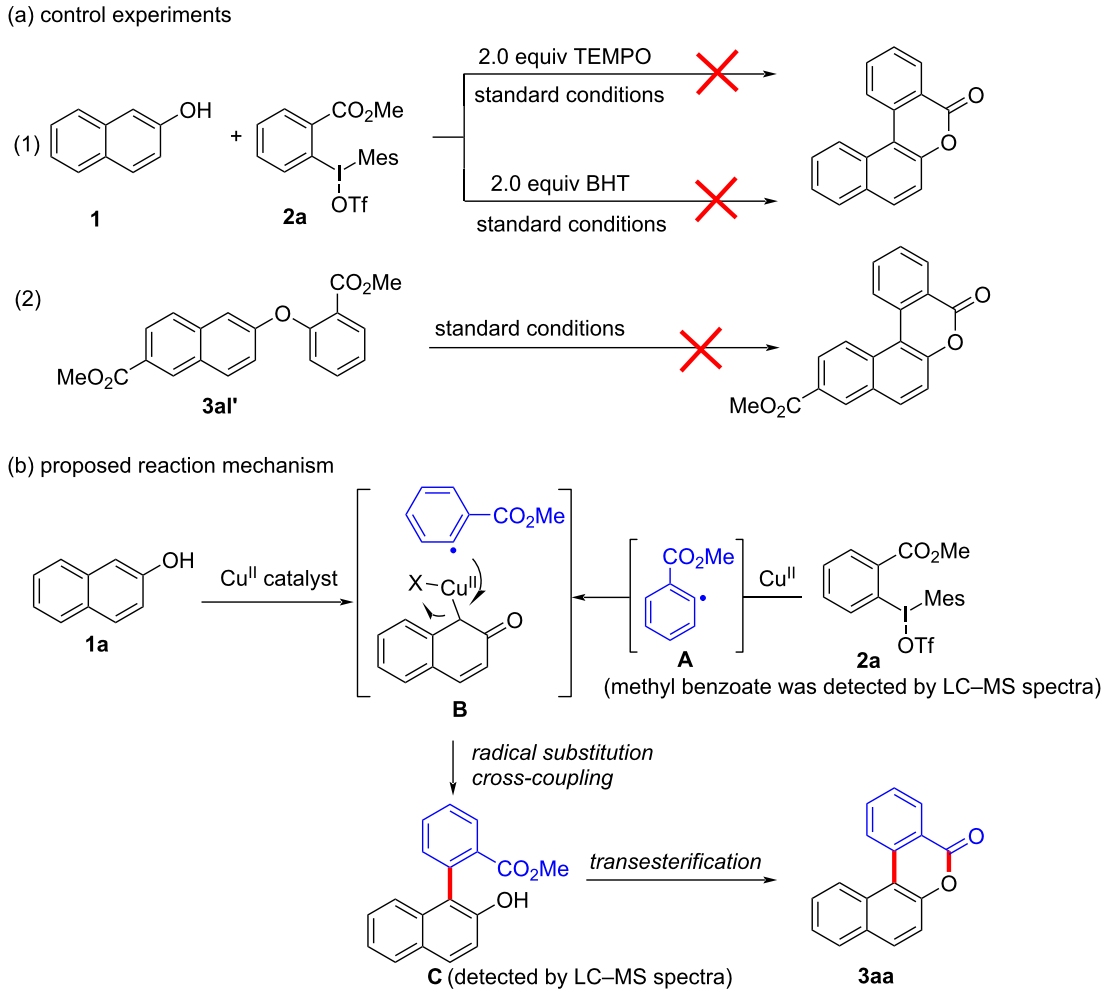

Scheme 2: Mechanism study. Standard conditions: **1** (0.3 mmol, 1 equiv), **2** (0.33 mmol, 1.1 equiv), $Cu(OAc)_2$ (10 mol %), DCE (2 mL), 80 °C, 3 hours. TEMPO = 2,2,6,6-tetramethylpiperidine-1-oxyl; BHT = butylated hydroxytoluene.

are dedicated to explore the detailed reaction mechanism with the ultimate aim of broadening the scope and applicability of this approach.

Supporting Information

Supporting Information File 1

Experimental procedures, LC–MS spectra and characterization data of all products, copies of ^{1}H, ^{13}C, ^{19}F NMR spectra of all compounds.
[https://www.beilstein-journals.org/bjoc/content/supplementary/1860-5397-20-76-S1.pdf]

Acknowledgements

The authors thank the Research Center of Analysis and Test of the East China University of Science and Technology for the help on the characterization and Professor Zhen-Jiang Xu from SIOC, CAS for helpful discussion and instrumental analysis.

Funding

The work was supported by the Industry-University-Research Collaborative Innovation Fund for Chinese Universities-DeZhou Project (2021DZ030) and the Natural Science Foundation of Shanghai (20ZR1413500); Shanghai Municipal Science and Technology Major Project (grant no. 2018SHZDZX03) and Program of Introducing Talents of Discipline to Universities (B16017).

ORCID® iDs

Jianwei Han - https://orcid.org/0000-0002-8354-5684

Data Availability Statement

The data that supports the findings of this study is available from the corresponding author upon reasonable request.

Preprint

A non-peer-reviewed version of this article has been previously published as a preprint: https://doi.org/10.3762/bxiv.2023.54.v1

References

1. Silva, J. L. F.; Olofsson, B. *Nat. Prod. Rep.* **2011,** *28,* 1722–1754. doi:10.1039/c1np00028d
2. Yoshimura, A.; Zhdankin, V. V. *Chem. Rev.* **2016,** *116,* 3328–3435. doi:10.1021/acs.chemrev.5b00547
3. Aradi, K.; Tóth, B.; Tolnai, G.; Novák, Z. *Synlett* **2016,** *27,* 1456–1485. doi:10.1055/s-0035-1561369
4. Cao, C.; Sheng, J.; Chen, C. *Synthesis* **2017,** *49,* 5081–5092. doi:10.1055/s-0036-1589515
5. Wang, Y.; An, G.; Wang, L.; Han, J. *Curr. Org. Chem.* **2020,** *24,* 2070–2105. doi:10.2174/1385272824999200507124328
6. Yang, X.-G.; Hu, Z.-N.; Jia, M.-C.; Du, F.-H.; Zhang, C. *Synlett* **2021,** *32,* 1289–1296. doi:10.1055/a-1492-4943
7. Peng, X.; Rahim, A.; Peng, W.; Jiang, F.; Gu, Z.; Wen, S. *Chem. Rev.* **2023,** *123,* 1364–1416. doi:10.1021/acs.chemrev.2c00591
8. Pan, C.; Wang, L.; Han, J. *Chem. Rec.* **2023,** *23,* e202300138. doi:10.1002/tcr.202300138
9. Wu, Y.; Peng, X.; Luo, B.; Wu, F.; Liu, B.; Song, F.; Huang, P.; Wen, S. *Org. Biomol. Chem.* **2014,** *12,* 9777–9780. doi:10.1039/c4ob02170c
10. Mehra, M. K.; Sharma, S.; Rangan, K.; Kumar, D. *Eur. J. Org. Chem.* **2020,** 2409–2413. doi:10.1002/ejoc.202000013
11. An, G.; Wang, L.; Han, J. *Org. Lett.* **2021,** *23,* 8688–8693. doi:10.1021/acs.orglett.1c03016
12. Xue, C.; Wang, L.; Han, J. *J. Org. Chem.* **2020,** *85,* 15406–15414. doi:10.1021/acs.joc.0c02192
13. Kitamura, T.; Yamane, M. *J. Chem. Soc., Chem. Commun.* **1995,** 983–984. doi:10.1039/c39950000983
14. Wu, X.; Yang, Y.; Han, J.; Wang, L. *Org. Lett.* **2015,** *17,* 5654–5657. doi:10.1021/acs.orglett.5b02938
15. Kikushima, K.; Elboray, E. E.; Jiménez-Halla, J. O. C.; Solorio-Alvarado, C. R.; Dohi, T. *Org. Biomol. Chem.* **2022,** *20,* 3231–3248. doi:10.1039/d1ob02501e
16. Kitamura, T.; Gondo, K.; Oyamada, J. *J. Am. Chem. Soc.* **2017,** *139,* 8416–8419. doi:10.1021/jacs.7b04483
17. Yoshimura, A.; Fuchs, J. M.; Middleton, K. R.; Maskaev, A. V.; Rohde, G. T.; Saito, A.; Postnikov, P. S.; Yusubov, M. S.; Nemykin, V. N.; Zhdankin, V. V. *Chem. – Eur. J.* **2017,** *23,* 16738–16742. doi:10.1002/chem.201704393
18. Robidas, R.; Guérin, V.; Provençal, L.; Echeverria, M.; Legault, C. Y. *Org. Lett.* **2017,** *19,* 6420–6423. doi:10.1021/acs.orglett.7b03307
19. Wu, Y.; Izquierdo, S.; Vidossich, P.; Lledós, A.; Shafir, A. *Angew. Chem., Int. Ed.* **2016,** *55,* 7152–7156. doi:10.1002/anie.201602569
20. Boelke, A.; Vlasenko, Y. A.; Yusubov, M. S.; Nachtsheim, B. J.; Postnikov, P. S. *Beilstein J. Org. Chem.* **2019,** *15,* 2311–2318. doi:10.3762/bjoc.15.223
21. Vlasenko, Y. A.; Kuczmera, T. J.; Antonkin, N. S.; Valiev, R. R.; Postnikov, P. S.; Nachtsheim, B. J. *Adv. Synth. Catal.* **2023,** *365,* 535–543. doi:10.1002/adsc.202201001
22. Chen, H.; Wang, L.; Han, J. *Chem. Commun.* **2020,** *56,* 5697–5700. doi:10.1039/d0cc01766c
23. Han, J.; Chen, H.; An, G.; Sun, X.; Li, X.; Liu, Y.; Zhao, S.; Wang, L. *J. Chem. Educ.* **2021,** *98,* 3992–3998. doi:10.1021/acs.jchemed.1c00546
24. Wang, Y.; Zhang, Y.; Wang, L.; Han, J. *Asian J. Org. Chem.* **2022,** *11,* e202100669. doi:10.1002/ajoc.202100669
25. Liu, X.; Wang, L.; Wang, H.-Y.; Han, J. *J. Org. Chem.* **2023,** *88,* 13089–13101. doi:10.1021/acs.joc.3c01293
26. Chen, H.; Han, J.; Wang, L. *Angew. Chem., Int. Ed.* **2018,** *57,* 12313–12317. doi:10.1002/anie.201806405
27. Chen, H.; Wang, L.; Han, J. *Org. Lett.* **2020,** *22,* 3581–3585. doi:10.1021/acs.orglett.0c01024
28. Wang, Y.; Pan, W.; Zhang, Y.; Wang, L.; Han, J. *Angew. Chem., Int. Ed.* **2023,** *62,* e202304897. doi:10.1002/anie.202304897
29. Pan, C.; Wang, L.; Han, J. *Org. Lett.* **2020,** *22,* 4776–4780. doi:10.1021/acs.orglett.0c01577
30. Liu, X.; Wang, L.; Han, J. *Org. Biomol. Chem.* **2022,** *20,* 8628–8632. doi:10.1039/d2ob01783k
31. Linde, E.; Bulfield, D.; Kervefors, G.; Purkait, N.; Olofsson, B. *Chem* **2022,** *8,* 850–865. doi:10.1016/j.chempr.2022.01.009
32. Mondal, S.; Di Tommaso, E. M.; Olofsson, B. *Angew. Chem., Int. Ed.* **2023,** *62,* e202216296. doi:10.1002/anie.202216296
33. Linde, E.; Olofsson, B. *Angew. Chem., Int. Ed.* **2023,** *62,* e202310921. doi:10.1002/anie.202310921
34. Qian, X.; Han, J.; Wang, L. *Tetrahedron Lett.* **2016,** *57,* 607–610. doi:10.1016/j.tetlet.2015.12.100
35. Phipps, R. J.; McMurray, L.; Ritter, S.; Duong, H. A.; Gaunt, M. J. *J. Am. Chem. Soc.* **2012,** *134,* 10773–10776. doi:10.1021/ja3039807
36. Wang, W.; Zhou, J.; Wang, C.; Zhang, C.; Zhang, X.-Q.; Wang, Y. *Commun. Chem.* **2022,** *5,* 145. doi:10.1038/s42004-022-00768-3

License and Terms

BEILSTEIN JOURNAL OF ORGANIC CHEMISTRY

Three-component *N*-alkenylation of azoles with alkynes and iodine(III) electrophile: synthesis of multisubstituted *N*-vinylazoles

Jun Kikuchi*, Roi Nakajima and Naohiko Yoshikai*

Full Research Paper

Open Access

Address:
Graduate School of Pharmaceutical Sciences, Tohoku University, 6-3 Aoba, Aramaki, Aoba-ku, Sendai 980-8578, Japan

Email:
Jun Kikuchi* - jun.kikuchi.e8@tohoku.ac.jp; Naohiko Yoshikai* - naohiko.yoshikai.c5@tohoku.ac.jp

* Corresponding author

Keywords:
alkynes; azoles; cross-coupling; hypervalent iodine

Beilstein J. Org. Chem. **2024,** *20,* 891–897.
https://doi.org/10.3762/bjoc.20.79

Received: 21 December 2023
Accepted: 11 April 2024
Published: 22 April 2024

This article is part of the thematic issue "Hypervalent halogen chemistry".

Guest Editor: J. Wencel-Delord

Abstract

A stereoselective *N*-alkenylation of azoles with alkynes and iodine(III) electrophile is reported. The reaction between various azoles and internal alkynes is mediated by benziodoxole triflate as the electrophile in a *trans*-fashion, affording azole-bearing vinylbenziodoxoles in moderate to good yields. The tolerable azole nuclei include pyrazole, indazole, 1,2,3-triazole, benzotriazole, and tetrazole. The iodanyl group in the product can be leveraged as a versatile synthetic handle, allowing for the preparation of hitherto inaccessible types of densely functionalized *N*-vinylazoles.

Introduction

N-Functionalized azoles are prevalent in bioactive natural products and pharmaceutical agents, including antifungal drugs [1-3], and hence their selective preparation has attracted considerable attention from the synthetic community. Compared to methods for the de novo construction of azole heterocycles, direct functionalization of the azole N–H bond offers the unique merit of enabling rapid access to structurally diverse *N*-functionalized azoles because one versatile method would potentially apply to various azole nuclei. In this context, the *N*-alkenylation of azoles represents an attractive transformation due to the occurrence of the *N*-vinylazole motif in bioactive compounds and the synthetic utility of its olefinic C=C bond. The most extensively explored approach to this transformation is the transition metal-catalyzed C–N coupling between azoles and vinylating agents, including vinyl halides [4], boronates [5], sulfonium salts [6-8], and iodonium salts [9], which usually occurs with the retention of the stereochemistry of the vinylating agents (Scheme 1a). Nonetheless, this approach is not necessarily suited for the stereoselective preparation of densely substituted *N*-vinylazoles because preparing the requisite multisubstituted vinylating agents, preferably with well-defined stereochemistry, is a nontrivial task.

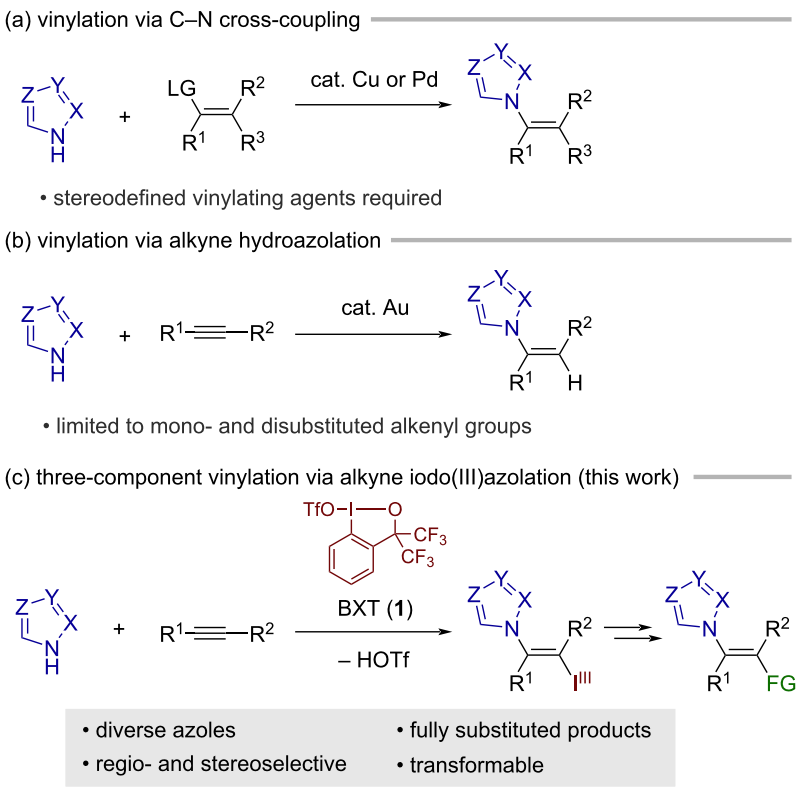

Scheme 1: Synthesis of *N*-vinylazoles.

The addition of azoles to alkynes represents an alternative approach to *N*-vinylazoles. For example, Nolan and co-workers recently reported a gold-catalyzed addition of azoles to alkynes (hydroazolation; Scheme 1b) [10]. The gold catalysis encompassed various azoles such as pyrazole, indazole, and (benzo)triazole, exhibiting high *Z*-selectivity. In addition, Cao et al. reported a gold-catalyzed addition of 5-substituted tetrazoles to terminal alkynes [11]. Analogous hydroazolation reactions of alkynes have also been achieved under other metal-catalyzed conditions [12,13] or base-mediated conditions [14], with varying scopes of azoles and alkynes. Despite such advances, the hydroazolation approach is intrinsically limited to the preparation of mono- or disubstituted vinylazoles. Herein, we report on a three-component *N*-vinylation reaction of azoles with alkynes and iodine(III) electrophile, benziodoxole triflate (BXT, **1**; Scheme 1c). Displaying exclusive *trans*-selectivity, the reaction tolerates a broad range of azoles, including pyrazole, 1,2,3-triazole, tetrazole, indazole, and benzotriazole, with internal alkynes as coupling partners. The resulting products represent a new class of functionalized vinylbenziodoxoles (VBXs) [15-21], which have recently emerged as unique vinylating agents [22-25]. Thus, the follow-up transformation of the iodanyl group in the present products allows for the preparation of hitherto inaccessible types of densely functionalized vinylazoles with tetrasubstituted olefinic moiety.

Results and Discussion

Our group has demonstrated benziodoxole triflate (BXT) [26] and related compounds as a versatile iodine(III) electrophile for the inter- and intramolecular difunctionalization of alkynes with various heteroatom and carbon nucleophiles [27-34]. Specifically, intermolecular *trans*-iodo(III)functionalization of alkynes has been achieved using oxygen nucleophiles such as alcohols [28,32], ethers [33], carboxylic acids [31], phosphate esters [31], and sulfonic acids [31]. On the other hand, nitrogen-based nucleophiles amenable to this reaction manifold have thus far been limited to nitriles in the context of Ritter-type iodo(III)amidation [29]. In light of the significance of vinylated azoles, our attention was attracted to the feasibility of iodo(III)azolation using various azoles (a single example of iodo(III)azolation using pyrazole was reported in [28]).

Table 1 summarizes the results of the optimization of the reaction conditions for the vinylation of pyrazole (**2a**) with 1-phenyl-1-propyne (**3a**) and BXT (**1**). Upon examination of various reaction parameters, the desired three-component *N*-alkenyla-

Table 1: Optimization of reaction conditions.[a]

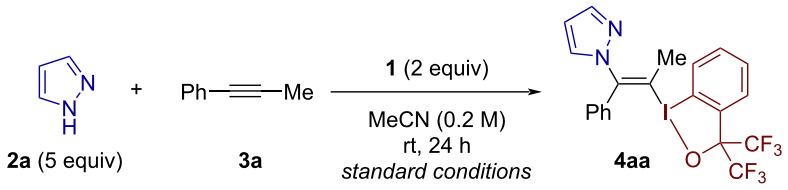

Entry	Deviation from standard conditions	Yield (%)[b]
1	none	77[c]
2	*c* = 0.1 M	50
3	*c* = 0.4 M	70
4	HFIP as the solvent (0.2 M)	16
5	Et_2O as the solvent (0.2 M)	22
6	3 equiv of **2a**	66
7	2 equiv of **2a**	55
8	2 equiv of **2a**, 2 equiv of K_2CO_3	trace

[a]The reaction was performed on a 0.1 mmol scale; [b]Determined by ^{1}H NMR using 1,1,2,2-tetrachloroethane as an internal standard; [c]Isolated yield.

tion was found to proceed smoothly by reacting **3a** with excess amounts of **1** (2 equiv) and **2a** (5 equiv) in MeCN (0.2 M) at room temperature, affording the *trans*-difunctionalized product **4aa** as a single regio- and stereoisomer in 77% yield (Table 1, entry 1). Decreasing or increasing the concentration did not improve the yield of **4aa** (Table 1, entries 2 and 3). The reaction became rather sluggish in different solvents such as HFIP and Et_2O (Table 1, entries 4 and 5). By reducing the equivalents of **2a** to 3 equiv and 2 equiv, the yield of **4aa** dropped to 66% and 55%, respectively (Table 1, entries 6 and 7). The addition of a base such as K_2CO_3 completely shut down the desired reaction (Table 1, entry 8). It is worth noting that the replacement of **1** with *N*-iodosuccinimide, a common iodine(I) electrophile, failed to promote an analogous iodoazolation reaction, highlighting the unique utility of the iodine(III) electrophile in the present alkyne difunctionalization.

With the standard conditions (Table 1, entry 1) in hand, we explored the scope of the three-component *N*-vinylation (Scheme 2). First, various azoles were subjected to the vinylation reaction using alkyne **3a** and BXT (**1**). 4-Bromo and 4-methylpyrazoles afforded the desired products **4ba** and **4ca** in 92% and 38% yields, respectively. 3-Phenylpyrazole underwent competitive alkenylation at the N1 and N2 positions, affording the N2-alkenylated product **4da** and its N1-regioisomer in 84% overall yield in a ratio of 7:3. Indazole and its 4-bromo and 6-methoxycarbonyl analogues afforded the expected N1-alkenylated products **4ea**–**4ga** in 43–68% yields. 1,2,3-Triazole and benzotriazole both smoothly participated in the reaction to give their respective products **4ha** and **4ia** in 60% and 81% yields, respectively. Tetrazole and 5-methyltetrazole both proved to be excellent substrates. Regardless of the presence or absence of the 5-substituent, they underwent preferential alkenylation at the N1 position over the N2 position with the identical regioselectivity of 7:3 (see **4ja** and **4ka**). Among other five-membered aromatic azacycles, imidazole completely failed to undergo the present *N*-alkenylation, whereas the reaction of 1,2,4-triazole was too sluggish to allow for the isolation and unambiguous characterization of the expected product.

Next, the reaction of pyrazole (**2a**) was explored using different alkynes. A series of (hetero)aryl(alkyl)alkynes were successfully engaged as reaction partners to give the products **4ab**–**4af** in moderate yields, displaying tolerance to *o*-tolyl (**4ad**), 2-thienyl (**4ae**), and methoxymethyl (**4af**) groups. A dialkylalkyne such as 5-decyne smoothly underwent the difunctionalization reaction to afford the product **4ag** in 62% yield. While sluggish, trimethylsilylacetylene was selectively azolated at the terminal position (see **4ah**), which could be rationalized by the better stabilization of a partial positive charge at this position by the β-silyl substituent. Finally, an oxazolidinone-substituted ynamide also proved to undergo iodo(III)azolation in a regio- and stereoselective fashion to give the product **4ai** in a moderate yield. Note that terminal alkynes such as phenylacetylene also took part in the reaction, albeit in a much-diminished yield (7% by ^{1}H NMR; data not shown). Observing no byproducts originating from phenylacetylene, we speculate that the lack of reactivity stems from the relatively low electron density of the ter-

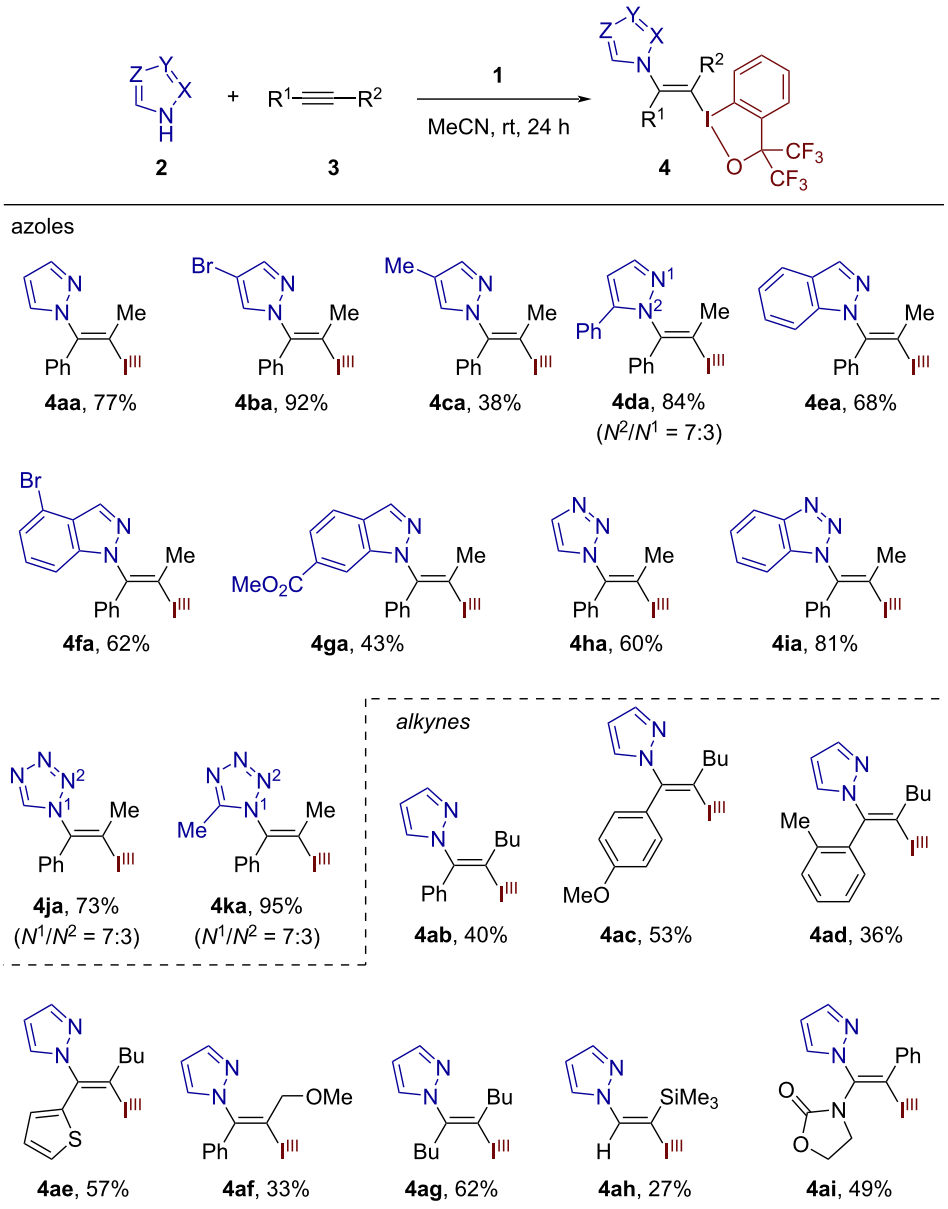

Scheme 2: Scope of three-component *N*-alkenylation of azoles.

minal alkyne, which likely leads to direct coordination of pyrazole to the iodine(III) reagent.

To probe the relative reactivity of different azoles, competition experiments were performed. The reaction of excess (5 equiv each) pyrazole (**2a**) and 1,2,3-triazole (**2h**) with the alkyne **3a** and **1** afforded a mixture of the corresponding products **4aa** and **4ha** in a ratio of 60:40 (Scheme 3a). Performed in the same manner, the competition between **2a** and tetrazole (**2j**) resulted in **4aa** as the major adduct, accompanied by the tetrazole adducts **4ja** and **4ja'** (the ratio **4aa**/**4ja**/**4ja'** = 71:21:8; Scheme 3b). Superficially, these results appear correlated with the acidity of the corresponding azoles (pK_a value: pyrazole, 19.8; 1,2,3-triazole, 13.9; tetrazole, 8.2), with the lowest-acidic pyrazole being the most competitive. However, we rather surmise that the Lewis basicity of the proton-free nitrogen atom of the azole would have more direct relevance to the results of the competition experiments, where the least Lewis basic tetrazole was the least competitive. Along with this conjecture, the present reaction is proposed to involve reversible complexation between the alkyne and the cationic iodine(III) electrophile and subsequent *trans*-addition of the azole nucleophile, the latter

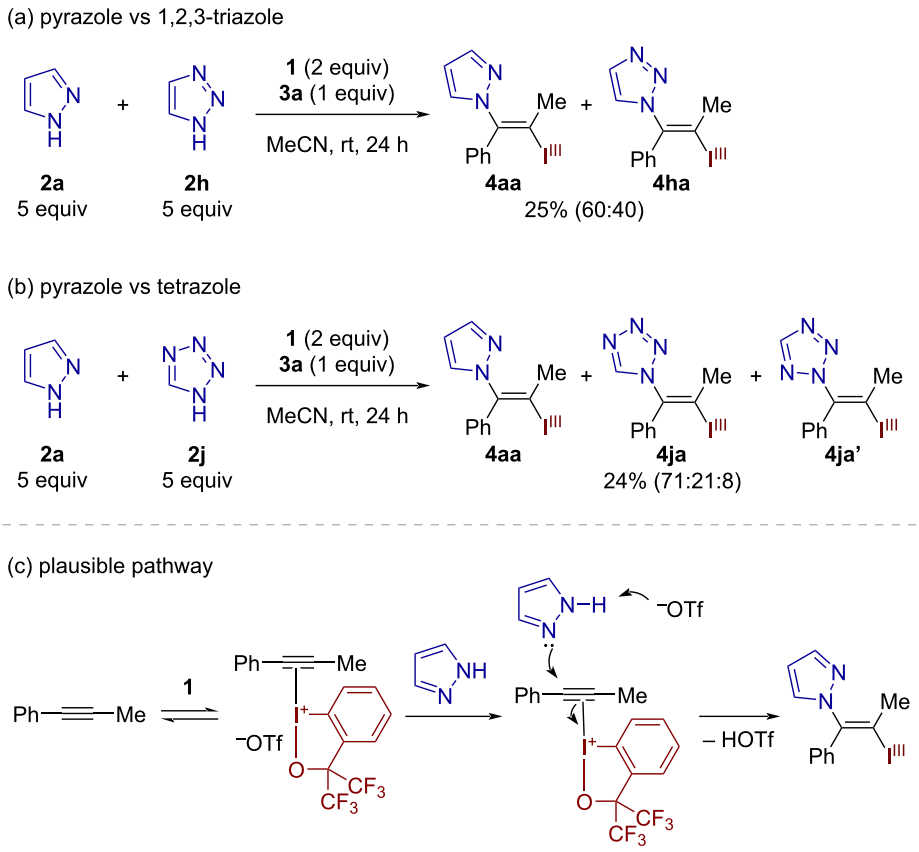

Scheme 3: Competition experiments and plausible reaction pathway.

step being coupled with concomitant deprotonation of the N–H bond by the triflate anion (Scheme 3c). It is important to note that the azole nucleophile preferentially adds to the carbon atom that can better stabilize a positive charge, as demonstrated by the regioselectivities observed with unsymmetrical alkynes. The failure of imidazole to participate in the iodo(III)azolation may be attributed to its much greater Lewis basicity compared to other azoles, likely killing the reactivity of the iodine(III) electrophile by direct coordination.

The present reaction could be performed on a preparative scale. Thus, 1 mmol-scale synthesis of the vinylazoles **4aa** and **4ba** could be successfully performed in 68% and 74% yields, respectively (Scheme 4a). Furthermore, the iodanyl group on these products serves as a versatile handle for downstream transformations, thus allowing for the stereoselective preparation of various trisubstituted *N*-vinylazoles (Scheme 4b). Pd-catalyzed C–C couplings such as Suzuki–Miyaura and Sonogashira couplings on **4aa** or **4ba** afforded the desired products **5** and **6** in 47% and 74% yields, respectively. In the former case, the C–Br bond on the pyrazole moiety remained intact, highlighting the superior leaving group ability of the BX group. Cu-catalyzed Ullmann coupling between **4ba** and 4-methoxybenzenethiol furnished the N,S-substituted olefin **7** in 59% yield. The treatment of **4aa** with stoichiometric CuI and L-proline effected the iodine(III)-to-iodine(I) conversion to give the vinyl iodide **8** in 76% yield. Compound **8** was used for the Ullmann coupling with imidazole, producing the vicinal *N*-heterocycle-substituted olefin **9** as a mixture of stereoisomers in 65% yield. Finally, **4aa** proved to be a viable nucleophilic VBX for the carboiodanation of 3-methoxybenzyne [35], furnishing the new *ortho*-alkenylated arylbenziodoxole **10** with exclusive C–C bond formation at the distal aryne carbon [36].

Conclusion

In summary, we have reported a three-component *N*-vinylation reaction of azoles with alkynes and iodine(III) electrophile. The present reaction represents a rare example of the installation of stereodefined trisubstituted alkenyl groups into the azole core, encompassing various azole nucleophiles including pyrazole, indazole, 1,2,3-triazole, benzotriazole, and tetrazole. The follow-up transformation of the iodanyl group provides a means to prepare hitherto inaccessible types of alkenylated azoles. Further exploration of the three-component alkenylation of

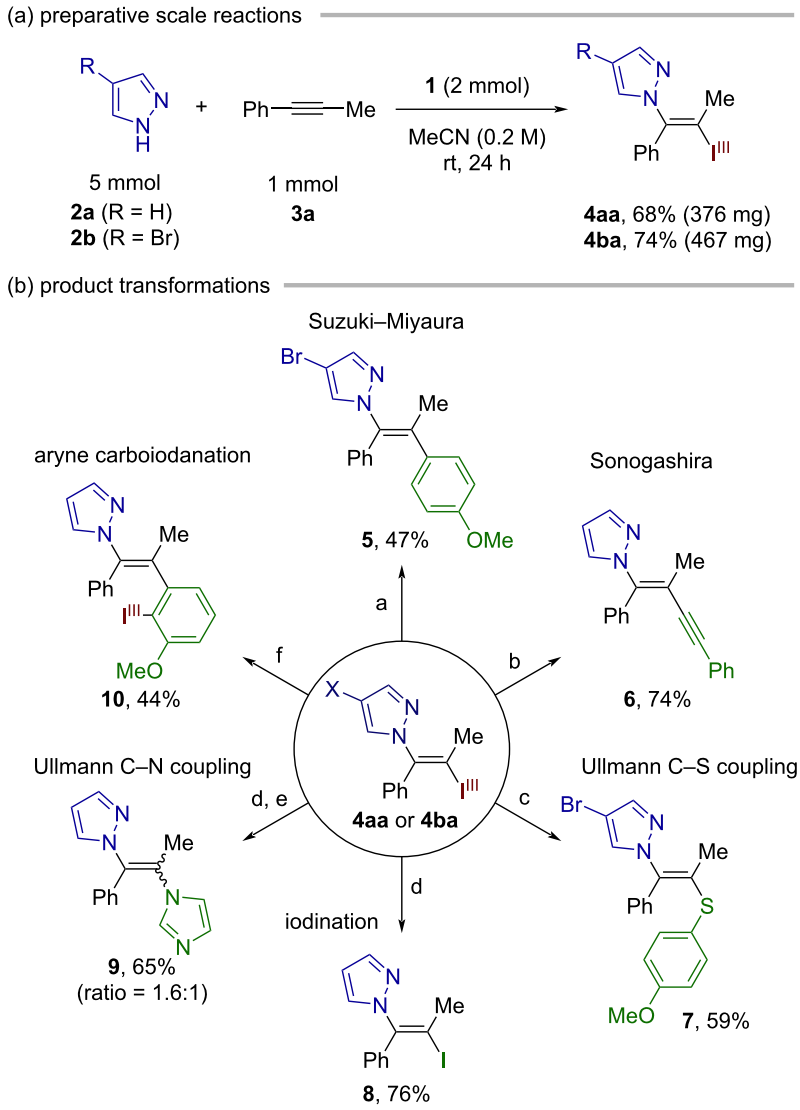

Scheme 4: Preparative-scale reaction and product transformations. Reaction conditions: (a) $Pd(PPh_3)_4$, 4-$MeOC_6H_4B(OH)_2$, Cs_2CO_3, DMF/H_2O, 60 °C, 18 h. (b) $Pd(OAc)_2$, PPh_3, CuI, phenylacetylene, Et_3N, 50 °C, 5 h. (c) CuI, neocuproine, 4-$MeOC_6H_4SH$, NaO*t*-Bu, toluene, 110 °C, 13 h. (d) CuI, L-proline, DMF, 80 °C, 14 h. (e) CuI, imidazole, Cs_2CO_3, DMF, 120 °C, 15 h. (f) 3-Methoxy-2-(trimethylsilyl)phenyl triflate, CsF, MeCN, rt, 18 h.

nitrogen and other heteroatom nucleophiles is currently underway.

Supporting Information

Supporting Information File 1

Experimental procedures and characterization data of new compounds.
[https://www.beilstein-journals.org/bjoc/content/supplementary/1860-5397-20-79-S1.pdf]

Acknowledgements

We thank the Central Glass Co., Ltd. for the generous donation of 1,1,1,3,3,3-hexafluoro-2-phenylpropan-2-ol (HFAB).

Funding

This work was supported by JSPS KAKENHI (Grant No. 20K23375 (N.Y.) and 19K15552 (J.K.)), The Uehara Memorial Foundation (N.Y.), Research Support Project for Life Science and Drug Discovery (Basis for Supporting Innovative Drug Discovery and Life Science Research (BINDS)) from AMED (Grant No. JP23ama121040 (N.Y.)).

ORCID® iDs

Jun Kikuchi - https://orcid.org/0000-0001-9892-8832
Naohiko Yoshikai - https://orcid.org/0000-0002-8997-3268

Data Availability Statement

All data that supports the findings of this study is available in the published article and/or the supporting information to this article.

References

1. Rezaei, Z.; Khabnadideh, S.; Pakshir, K.; Hossaini, Z.; Amiri, F.; Assadpour, E. *Eur. J. Med. Chem.* **2009,** *44,* 3064–3067. doi:10.1016/j.ejmech.2008.07.012
2. Vitaku, E.; Smith, D. T.; Njardarson, J. T. *J. Med. Chem.* **2014,** *57,* 10257–10274. doi:10.1021/jm501100b
3. Azevedo, M.-M.; Faria-Ramos, I.; Cruz, L. C.; Pina-Vaz, C.; Gonçalves Rodrigues, A. *J. Agric. Food Chem.* **2015,** *63,* 7463–7468. doi:10.1021/acs.jafc.5b02728
4. Liao, Q.; Wang, Y.; Zhang, L.; Xi, C. *J. Org. Chem.* **2009,** *74,* 6371–6373. doi:10.1021/jo901105r
5. Motornov, V.; Latyshev, G. V.; Kotovshchikov, Y. N.; Lukashev, N. V.; Beletskaya, I. P. *Adv. Synth. Catal.* **2019,** *361,* 3306–3311. doi:10.1002/adsc.201900225
6. Zhou, M.; Tan, X.; Hu, Y.; Shen, H. C.; Qian, X. *J. Org. Chem.* **2018,** *83,* 8627–8635. doi:10.1021/acs.joc.8b00682
7. Juliá, F.; Yan, J.; Paulus, F.; Ritter, T. *J. Am. Chem. Soc.* **2021,** *143,* 12992–12998. doi:10.1021/jacs.1c06632
8. Chen, S.-J.; Li, J.-H.; He, Z.-Q.; Chen, G.-S.; Zhuang, Y.-Y.; Chen, C.-P.; Liu, Y.-L. *J. Org. Chem.* **2022,** *87,* 15703–15712. doi:10.1021/acs.joc.2c02323
9. Csenki, J. T.; Mészáros, Á.; Gonda, Z.; Novák, Z. *Chem. – Eur. J.* **2021,** *27,* 15638–15643. doi:10.1002/chem.202102840
10. Michon, C.; Gilbert, J.; Trivelli, X.; Nahra, F.; Cazin, C. S. J.; Agbossou-Niedercorn, F.; Nolan, S. P. *Org. Biomol. Chem.* **2019,** *17,* 3805–3811. doi:10.1039/c9ob00587k
11. Cao, Z.; Zhao, C.; Zhu, J.; Yan, S.; Tian, L.; Sun, X.; Meng, X. *ChemistrySelect* **2019,** *4,* 11785–11789. doi:10.1002/slct.201902532
12. Tsuchimoto, T.; Aoki, K.; Wagatsuma, T.; Suzuki, Y. *Eur. J. Org. Chem.* **2008,** 4035–4040. doi:10.1002/ejoc.200800353
13. Das, U. K.; Mandal, S.; Anoop, A.; Bhattacharjee, M. *J. Org. Chem.* **2014,** *79,* 9979–9991. doi:10.1021/jo502151z
14. Garg, V.; Kumar, P.; Verma, A. K. *J. Org. Chem.* **2017,** *82,* 10247–10262. doi:10.1021/acs.joc.7b01746
15. Declas, N.; Pisella, G.; Waser, J. *Helv. Chim. Acta* **2020,** *103,* e2000191. doi:10.1002/hlca.202000191
16. Mironova, I. A.; Noskov, D. M.; Yoshimura, A.; Yusubov, M. S.; Zhdankin, V. V. *Molecules* **2023,** *28,* 2136. doi:10.3390/molecules28052136
17. Stridfeldt, E.; Seemann, A.; Bouma, M. J.; Dey, C.; Ertan, A.; Olofsson, B. *Chem. – Eur. J.* **2016,** *22,* 16066–16070. doi:10.1002/chem.201603955
18. Wu, J.; Deng, X.; Hirao, H.; Yoshikai, N. *J. Am. Chem. Soc.* **2016,** *138,* 9105–9108. doi:10.1021/jacs.6b06247
19. Wu, J.; Xu, K.; Hirao, H.; Yoshikai, N. *Chem. – Eur. J.* **2017,** *23,* 1521–1525. doi:10.1002/chem.201605772
20. Caramenti, P.; Declas, N.; Tessier, R.; Wodrich, M. D.; Waser, J. *Chem. Sci.* **2019,** *10,* 3223–3230. doi:10.1039/c8sc05573d
21. Shimbo, D.; Shibata, A.; Yudasaka, M.; Maruyama, T.; Tada, N.; Uno, B.; Itoh, A. *Org. Lett.* **2019,** *21,* 9769–9773. doi:10.1021/acs.orglett.9b03990
22. Pisella, G.; Gagnebin, A.; Waser, J. *Org. Lett.* **2020,** *22,* 3884–3889. doi:10.1021/acs.orglett.0c01150
23. Di Tommaso, E. M.; Norrby, P.-O.; Olofsson, B. *Angew. Chem., Int. Ed.* **2022,** *61,* e202206347. doi:10.1002/anie.202206347
24. Milzarek, T. M.; Waser, J. *Angew. Chem., Int. Ed.* **2023,** *62,* e202306128. doi:10.1002/anie.202306128
25. Bhaskar Pal, K.; Di Tommaso, E. M.; Inge, A. K.; Olofsson, B. *Angew. Chem., Int. Ed.* **2023,** *62,* e202301368. doi:10.1002/anie.202301368
26. Zhdankin, V. V.; Kuehl, C. J.; Krasutsky, A. P.; Bolz, J. T.; Simonsen, A. J. *J. Org. Chem.* **1996,** *61,* 6547–6551. doi:10.1021/jo960927a
27. Wu, B.; Wu, J.; Yoshikai, N. *Chem. – Asian J.* **2017,** *12,* 3123–3127. doi:10.1002/asia.201701530
28. Ding, W.; Chai, J.; Wang, C.; Wu, J.; Yoshikai, N. *J. Am. Chem. Soc.* **2020,** *142,* 8619–8624. doi:10.1021/jacs.0c04140
29. Chai, J.; Ding, W.; Wang, C.; Ito, S.; Wu, J.; Yoshikai, N. *Chem. Sci.* **2021,** *12,* 15128–15133. doi:10.1039/d1sc05240c
30. Laskar, R. A.; Ding, W.; Yoshikai, N. *Org. Lett.* **2021,** *23,* 1113–1117. doi:10.1021/acs.orglett.1c00039
31. Wang, C.-S.; Tan, P. S. L.; Ding, W.; Ito, S.; Yoshikai, N. *Org. Lett.* **2022,** *24,* 430–434. doi:10.1021/acs.orglett.1c04123
32. Kikuchi, J.; Maesaki, K.; Sasaki, S.; Wang, W.; Ito, S.; Yoshikai, N. *Org. Lett.* **2022,** *24,* 6914–6918. doi:10.1021/acs.orglett.2c02570
33. Chai, J.; Ding, W.; Wu, J.; Yoshikai, N. *Chem. – Asian J.* **2020,** *15,* 2166–2169. doi:10.1002/asia.202000653
34. Kikuchi, J.; Nagata, T.; Ito, S.; Yoshikai, N. *Org. Chem. Front.* **2024**. doi:10.1039/d4qo00489b
35. Arakawa, C.; Kanemoto, K.; Nakai, K.; Wang, C.; Morohashi, S.; Kwon, E.; Ito, S.; Yoshikai, N. *J. Am. Chem. Soc.* **2024,** *146,* 3910–3919. doi:10.1021/jacs.3c11524
36. Medina, J. M.; Mackey, J. L.; Garg, N. K.; Houk, K. N. *J. Am. Chem. Soc.* **2014,** *136,* 15798–15805. doi:10.1021/ja5099935

License and Terms

BEILSTEIN JOURNAL OF ORGANIC CHEMISTRY

Auxiliary strategy for the general and practical synthesis of diaryliodonium(III) salts with diverse organocarboxylate counterions

Naoki Miyamoto[1], Daichi Koseki[1], Kohei Sumida[1], Elghareeb E. Elboray[1,2], Naoko Takenaga[3], Ravi Kumar[*4] and Toshifumi Dohi[*1]

Letter

Open Access

Address:
[1]College of Pharmaceutical Sciences, Ritsumeikan University, 1-1-1, Nojihigashi, Kusatsu Shiga, 525-8577, Japan, [2]Department of Chemistry, Faculty of Science, South Valley University, Qena 83523, Egypt, [3]Faculty of Pharmacy, Meijo University, 150 Yagotoyama, Tempaku-ku, Nagoya 468-8503, Japan and [4]Department of Chemistry, J. C. Bose University of Science & Technology, YMCA Faridabad, NH-2, Sector-6, Mathura Road, Faridabad, Haryana, 121006, India

Email:
Ravi Kumar[*] - ravi.dhamija@rediffmail.com; Toshifumi Dohi[*] - td1203@ph.ritsumei.ac.jp

* Corresponding author

Keywords:
auxiliary ligand; diaryliodonium(III) salts; hybridization; hypervalent iodine; organocarboxylates

Beilstein J. Org. Chem. **2024,** *20,* 1020–1028.
https://doi.org/10.3762/bjoc.20.90

Received: 10 February 2024
Accepted: 22 April 2024
Published: 03 May 2024

This article is part of the thematic issue "Hypervalent halogen chemistry".

Guest Editor: J. Wencel-Delord

Abstract

Diaryliodonium(III) salts are versatile reagents that exhibit a range of reactions, both in the presence and absence of metal catalysts. In this study, we developed efficient synthetic methods for the preparation of aryl(TMP)iodonium(III) carboxylates, by reaction of (diacetoxyiodo)arenes or iodosoarenes with 1,3,5-trimethoxybenzene in the presence of a diverse range of organocarboxylic acids. These reactions were conducted under mild conditions using the trimethoxyphenyl (TMP) group as an auxiliary, without the need for additives, excess reagents, or counterion exchange in further steps. These protocols are compatible with a wide range of substituents on (hetero)aryl iodine(III) compounds, including electron-rich, electron-poor, sterically congested, and acid-labile groups, as well as a broad range of aliphatic and aromatic carboxylic acids for the synthesis of diverse aryl(TMP)iodonium(III) carboxylates in high yields. This method allows for the hybridization of complex bioactive and fluorescent-labeled carboxylic acids with diaryliodonium(III) salts.

Introduction

Hypervalent iodine compounds are an attractive class of reagents due to their stability, accessibility, and diverse chemical reactivity [1]. Diaryliodonium(III) salts, in particular, have been widely recognized as efficient arylating reagents for a range of carbon, nitrogen, oxygen, sulfur, and other nucleophiles, and can be employed in the presence or absence of tran-

sition metal catalysts under thermal or photochemical conditions [2-5]. Furthermore, these compounds have practical applications in the synthesis of radiochemicals utilized in positron emission tomography (PET) imaging [6], as well as serving as photoacid generators for photoinitiated radical polymerizations [7,8]. Consequently, there exists a growing interest in the development of more convenient synthetic routes for these compounds, facilitating the creation of structurally novel diaryliodonium(III) salts.

The counterions of diaryliodonium(III) salts play a crucial role in modifying their physical properties, and stability and controlling the reactivity of arylation processes, as demonstrated in various studies [9,10]. For instance, the Gaunt group reported that the use of a fluoride counterion in diaryliodonium(III) salt can trigger phenol *O*-arylation by activating the phenolic O–H group with a fluoride anion [11]. Additionally, Muñiz et al. found that the acetate counterion was more effective than chloride, hexafluorophosphate, and trifluoromethane sulfonate for the borylation of diaryliodonium(III) salts [12]. Recently, our group has developed a new method for phenol *O*-arylation using aryl(2,4,6-trimethoxyphenyl)iodonium(III) acetates [13]. In this process, the acetate ligand acted as a base to activate the phenol group and positioned it in proximity to accomplish the smooth S_NAr reaction.

The synthesis of diaryliodonium(III) salts with various counterions, such as triflate (TfO^-) [14], tetrafluoroborate (BF_4^-) [15], tosylate (TsO^-) [16], and others [17], has been extensively studied, as they play a key factor in the participation of iodonium salts in diverse arylation reactions. Recently, efficient syntheses of diaryliodonium(III) trifluoroacetates have been reported [18,19] (Scheme 1). The importance of the trimethoxyphenyl (TMP) group as an auxiliary (dummy) ligand on the iodonium salt has prompted researchers to synthesize aryl(TMP)iodonium(III) trifluoroacetates via oxidation of iodoarene with *m*-chloroperbenzoic acid (*m*CPBA) in the presence of trifluoroacetic acid, followed by coupling with 1,3,5-trimethoxybenzene [18] (Scheme 1A). This process demonstrated tolerance for a wide range of electron-rich and electron-deficient (hetero)aryl iodine(III) compounds. Wirth and colleagues reported the flow synthesis of diaryliodonium(III) trifluoroacetates using a cartridge filled with powdered oxone® for in situ generation of bis(trifluoroacetoxyiodo)arenes and their reaction with electron-rich arene or arylboronic acid [19] (Scheme 1B).

Carboxylic acids, such as acetic acid and benzoic acid, characterized by substantial difference in pK_a values when compared to trifluoroacetic acid, TfOH, HBF_4, and *p*-TsOH, present a wider substrate scope, including acid-sensitive groups, in the preparation of diaryliodonium(III) salts. While the counterion exchange of diaryliodonium(III) chloride with silver acetate was reported [20], this method required heating conditions and the use of an equimolar amount of the metal salt (Scheme 2A). Despite the expected advantage, direct synthesis of these diaryliodon-ium(III) carboxylates are scarce, and these compounds were synthesized by reacting (diacetoxyiodo)benzene and *N*-functionalized pyrrole in 2,2,2-trifluoroethanol (TFE, Scheme 2B) [21].

Our group previously reported the synthesis of diaryliodonium(III) salts by combining hypervalent iodine(III) reagents with electron-rich arenes in fluoroalcohol solvents, such as TFE or 1,1,1,3,3,3-hexafluoro-2-propanol [21,22]. These solvents stabilize the cationic intermediates in the synthesis of diaryliodonium(III) salts from Koser's reagents or (diacetoxyiodo)arenes. While iodonium salts with TfO^-, TsO^-, and

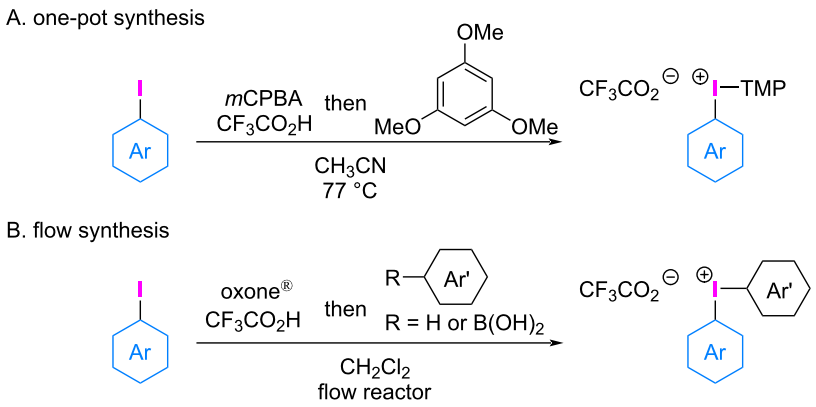

Scheme 1: Synthetic approaches of diaryliodonium(III) trifluoroacetates.

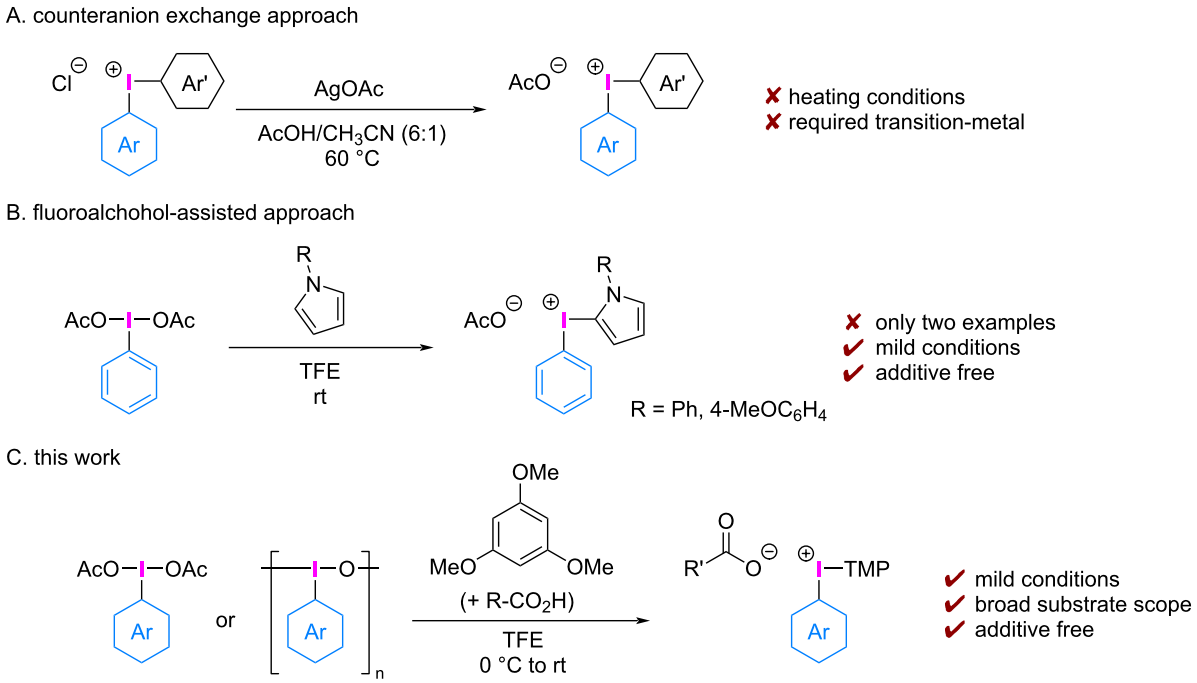

Scheme 2: Synthesis of diaryliodonium(III) carboxylates.

other counterions are common, the related diaryliodonium carboxylates are more attractive from a cost and safety standpoint. In this work, we present a more practical, direct approach for the synthesis of aryl(TMP)iodonium(III) carboxylates, utilizing readily accessible iodosoarenes or (diacetoxyiodo)arenes as starting materials in a fluoroalcohol solvent (Scheme 2C). This protocol allows for the synthesis of electron-rich, electron-poor, heterocyclic, and sterically hindered aryl(TMP)iodonium(III) carboxylates by combining the broad substrate scope of (hetero)aryl iodine(III) and carboxylic acids under mild conditions.

Results and Discussion

In the synthesis of diaryliodonium(III) salts and their application in arylation reactions, it is highly desirable to design diaryliodonium(III) salts including a commercially available and inexpensive auxiliary group to achieve efficient preparation of the salts and a high degree of chemoselectivity for transferring the required aryl group. Electron-rich aryl ligands derived from anisole, mesitylene, and particularly 1,3,5-trimethoxybenzene are highly recommended for chemoselective arylation processes. Aryl(TMP)iodonium(III) salts have been successfully used as transition metal-free arylating reagents for various nucleophiles such as nitrogen- [23-26], oxygen- [13,27-29], sulfur- [30], and carbon- [31] nucleophiles due to their excellent reactivity and aryl group selectivity over aryl(anisyl)iodonium(III) salts [32] and aryl(mesityl)iodonium(III) salts [33].

Based on our previously reported conditions for the synthesis of diaryliodonium(III) salts [21], we designed a more practical synthetic protocol for the extended numbers of diaryliodonium(III) carboxylates. Various electron-rich arenes were screened as auxiliary aryl groups in the reaction with $PhI(OAc)_2$ (**1a**) (Scheme 3). However, common partners such as toluene (**2a**), mesitylene (**2b**), and anisole (**2c**) failed to react with $PhI(OAc)_2$ (**1a**). Therefore, 1,3-dimethoxybenzene (**2d**) was used as a more electron-rich aryl group in the reaction with $PhI(OAc)_2$ (**1a**), resulting in the formation of the desired phenyl(2,4-dimethoxyphenyl)iodonium(III) acetate (**3ad**) in 69% yield. Notably, utilizing 1,3,5-trimethoxybenzene (**2e**) as an auxiliary aryl group under identical conditions yielded the corresponding phenyl(TMP)iodonium(III) acetate (**3ae**) in 96% yield.

Utilizing TMP as an auxiliary aryl group, we investigated the substrate scope of (diacetoxyiodo)arenes **1** for the synthesis of aryl(TMP)iodonium(III) acetates **4** (Scheme 4). The starting materials, (diacetoxyiodo)arenes **1**, can be prepared through the oxidation of iodoarenes with $NaBO_3{\cdot}4H_2O$ [34], AcOOH [35], *m*CPBA [36], and $NaClO{\cdot}5H_2O$ [37] in the presence of acetic acid. The reaction of (diacetoxyiodo)arenes bearing electron-donating (methyl (**1b**), methoxy (**1c**), and phenyl (**1d**)) and electron-withdrawing (methyl ester (**1e**), nitro (**1f**), and fluoro (**1g**)) groups proceeded efficiently to produce the corresponding aryl(TMP)iodonium(III) acetates **4b**–**g** in high yields. A sterically hindered *ortho*-disubstituted aryl group was also well-

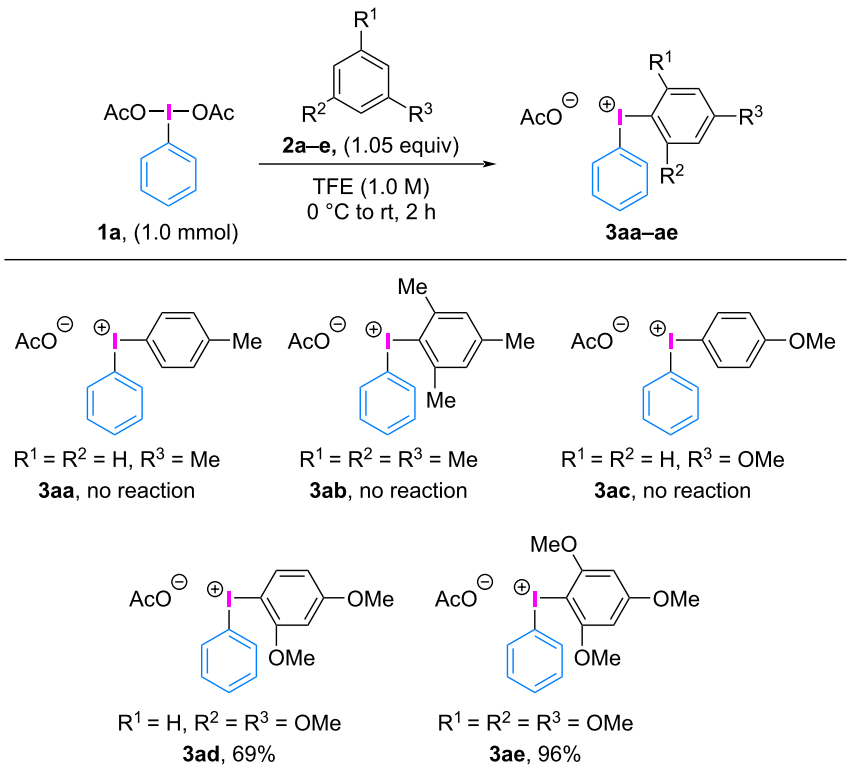

Scheme 3: Scope of dummy ligands.

tolerated, and the related *ortho*-disubstituted aryl(TMP)iodonium(III) acetate (**4h**) was obtained in 83% yield. Notably, this strategy allowed the synthesis of (diacetoxyiodo)arenes bearing acid-sensitive Boc protecting groups (**1i**) and heteroaromatic moieties such as pyridyl (**1j**) and thienyl (**1k**) groups. The reaction of bis(diacetoxyiodo)arene (**1l**) with 1,3,5-trimethoxybenzene (2.1 equiv) under the same conditions afforded the ditrigger iodonium salt **4l** in 88% yield, demonstrating the versatility of the process for the synthesis of multivalent precursors. Furthermore, phenyliodine(III) bis(trifluoroacetate) was used as a starting material under the optimized reaction conditions and the corresponding phenyl(TMP)iodonium(III) trifluoroacetate (**4m**) was obtained in 91% yield. These aryl(TMP)iodonium(III) acetates were recently utilized by our group for the arylation of phenols [13] and *N*-alkoxyamides [26,29], exhibiting excellent reactivity and aryl group selectivity.

In subsequent experiments, we sought to develop an alternative approach by reacting iodosobenzene (**5a**) with a range of aromatic and aliphatic carboxylic acids **6a–i** to form phenyl(TMP)iodonium(III) carboxylates **3ae**, **7aa–ai** (Scheme 5A). The reaction between benzoic acids (**6a**, **6b**) and heteroaromatic carboxylic acids (**6c**, **6d**) proceeded smoothly under the set conditions to form the corresponding phenyl(TMP)iodonium(III) carboxylates **7aa–ad** in high yield. Additionally, a range of aliphatic carboxylic acids such as acetic acid (**6e**), pivalic acid (**6f**), cyclohexanecarboxylic acid (**6g**), and aliphatic carboxylic acid with acidic α-proton (**6h**) was also tolerated under these conditions to produce the corresponding phenyl(TMP)iodonium(III) carboxylates (**3ae, 7af–ah**) in 63–81% yield without any signs of side reactions. The adenosine receptor antagonist acefylline (**6i**) was also used as a carboxylic acid to give the corresponding phenyl(TMP)iodonium(III) carboxylate **7ai** in 86% yield, opening up new avenues for structural modifications of drug candidates to improve their properties and consequently, bioactivities [38-40]. The umbelliferone-3-carboxylic acid derivative **6j** was also employed to produce the phenyl(TMP)iodonium(III) carboxylate **7aj** carrying a fluorescent-labeling group in 93% yield.

Iodosoarenes **5b–f** can be easily obtained by treating (dichloroiodo)arenes [41] or (diacetoxyiodo)arenes [42] with sodium hydroxide, by oxidation of iodoarenes with $NaClO{\cdot}5H_2O$ [43], or by electrolysis [44]. The reaction scope of iodosoarenes **5b–f** was explored with benzoic acid (**6a**) and 1,3,5-trimethoxybenzene (Scheme 5B). Iodosoarenes with electron-rich (**5b**, **5c**, **5f**), electron-deficient (**5d**), bromo (**5e**), and sterically hindered substituents (**5f**) were applicable to give the corresponding aryl(TMP)iodonium(III) benzoates **7ba–fa** in

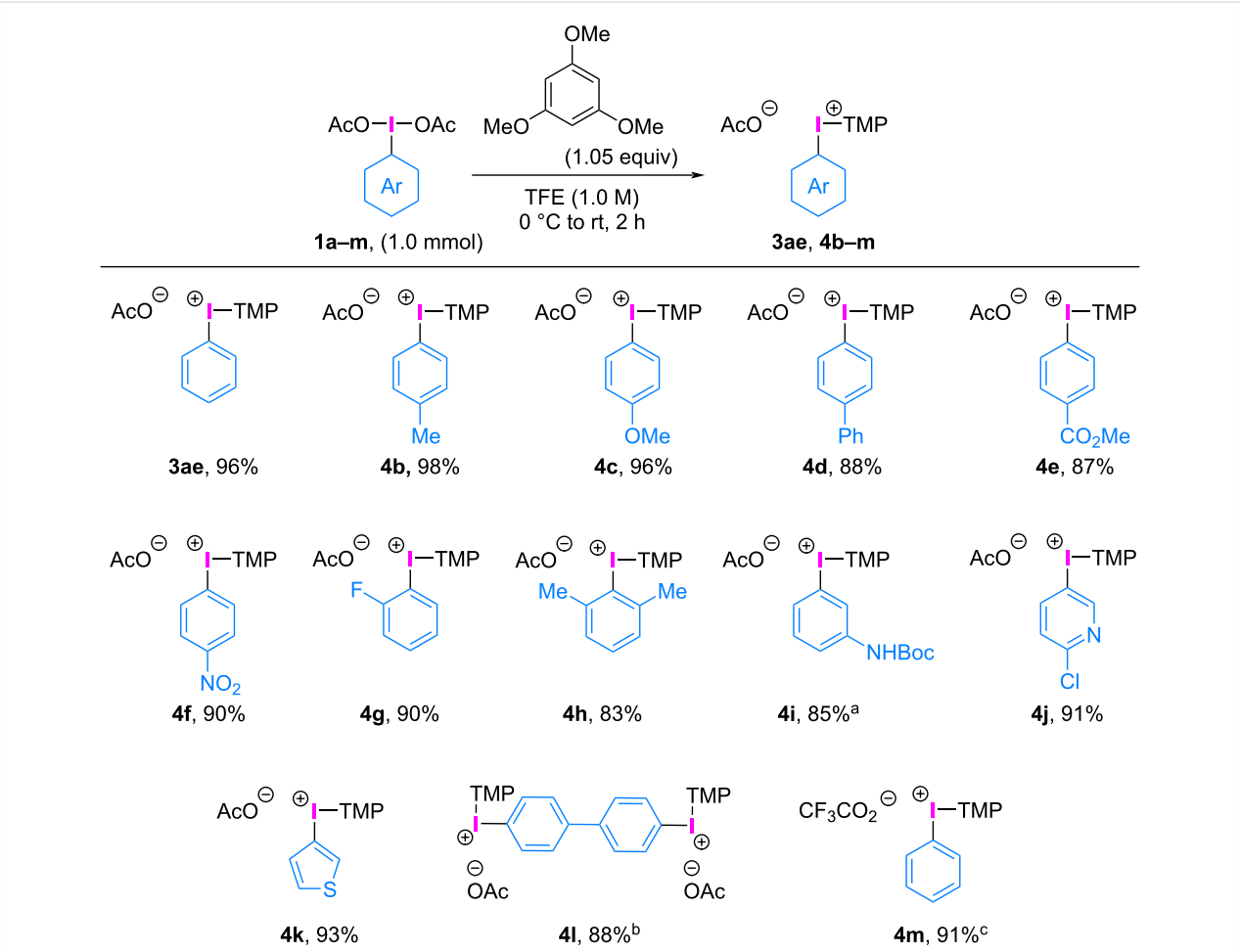

Scheme 4: Substrate scope of aryl(TMP)iodonium(III) acetates. a) 0.50 mmol scale of **1i**. b) 1,3,5-Trimethoxybenzene (2.1 equiv) was used. c) Bis(trifluoroacetoxyiodo)benzene was used instead of **1a**.

63–93% yield. It is worth noting that the products yielded by these protocols were easily separated as white amorphous solids by concentration and trituration of the obtained residue with diethyl ether. The color of the products indicates that the reactions proceeded without any signs of decomposition, consequently yielding the desired products in high yields. However, the common synthetic methods of diaryliodonium(III) triflates involving a strong oxidizing agent with a strong acid and an electron-rich arene often resulted in black/discolored products, indicating decomposition, poor yields, and lower productivity in arylation processes [45].

These aryl(TMP)iodonium(III) carboxylates are stable at room temperature and are available as amorphous solids that dissolve in specific solvents, such as chloroform, methanol, and dimethyl sulfoxide. The iodonium salt **7aa** does not decompose even at 70 °C, and further increase in temperature facilitates the ligand coupling between the phenyl group and the carboxylate counterion. When heated at 140 °C for 2.5 h under solvent-free conditions, iodonium salt **7aa** underwent carboxylate *O*-phenylation with complete phenyl group transfer, resulting in the formation of phenyl benzoate in 70% yield (Scheme 6A).

Furthermore, iodonium salt **7aj** with an umbelliferone-3-carboxylate counterion displayed extremely weak blue fluorescence emission under 365 nm UV light compared to free carboxylic acid **6j**. This unique property was utilized for tracing the counterion exchange process of the diaryliodonium(III) salt by irradiating with 365 nm UV light. The counterion exchange in umbelliferone carboxylate salt **7aj** with trifluoroacetic acid was rapid, and after 30 s, the completion of the reaction was confirmed by the emergence of strong blue fluorescence emission due to the liberation of the fluorescent-labeling carboxylic acid **6j** (see Supporting Information File 1, Figure S1). Thus, this post-fluorescence iodonium salt can be used for visual indication of the ligand exchange process, elucidating the arylation mechanism of diaryliodonium(III) salts for their further applications in organic chemistry and other scientific fields. The poten-

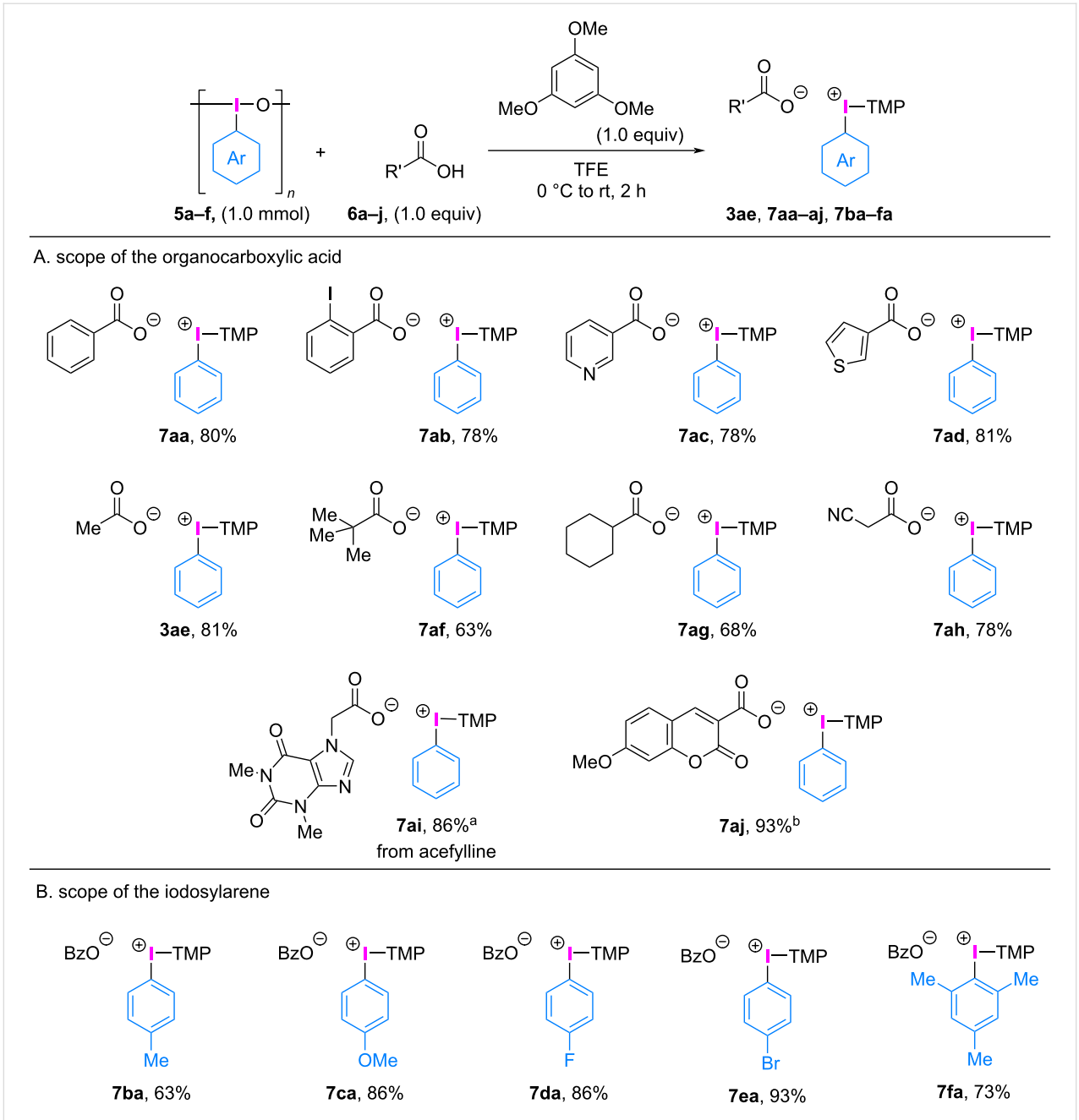

Scheme 5: Substrate scope of the carboxylic acids and iodosylarenes. a) The reaction was conducted for 4 h. b) 2.0 mL TFE was used.

tial of diaryliodonium(III) carboxylates obtained in this study (i.e., Scheme 6B,C) and the related amino acid derivatives [46-49] as new arylating reagents will be further explored by conducting reactions with various nucleophiles involving the counterion exchange process.

Conclusion

The absence of a widely applicable method for the synthesis of diaryliodonium(III) carboxylates has prompted our research group to devise a practical strategy for the synthesis of aryl(TMP)iodonium(III) carboxylates with minimal reagents without a counterion exchange step. By employing TMP as an auxiliary aryl group, we have successfully achieved the reaction between the hypervalent iodine compounds ($ArI(OAc)_2$ or ArIO) and 1,3,5-trimethoxybenzene in the presence of organocarboxylic acid under mild conditions. This process was completed in comparatively shorter time at room temperature, yielding high yields of the corresponding aryl(TMP)iodonium(III) carboxylates. Our method is compatible with a wide range of electronically and sterically

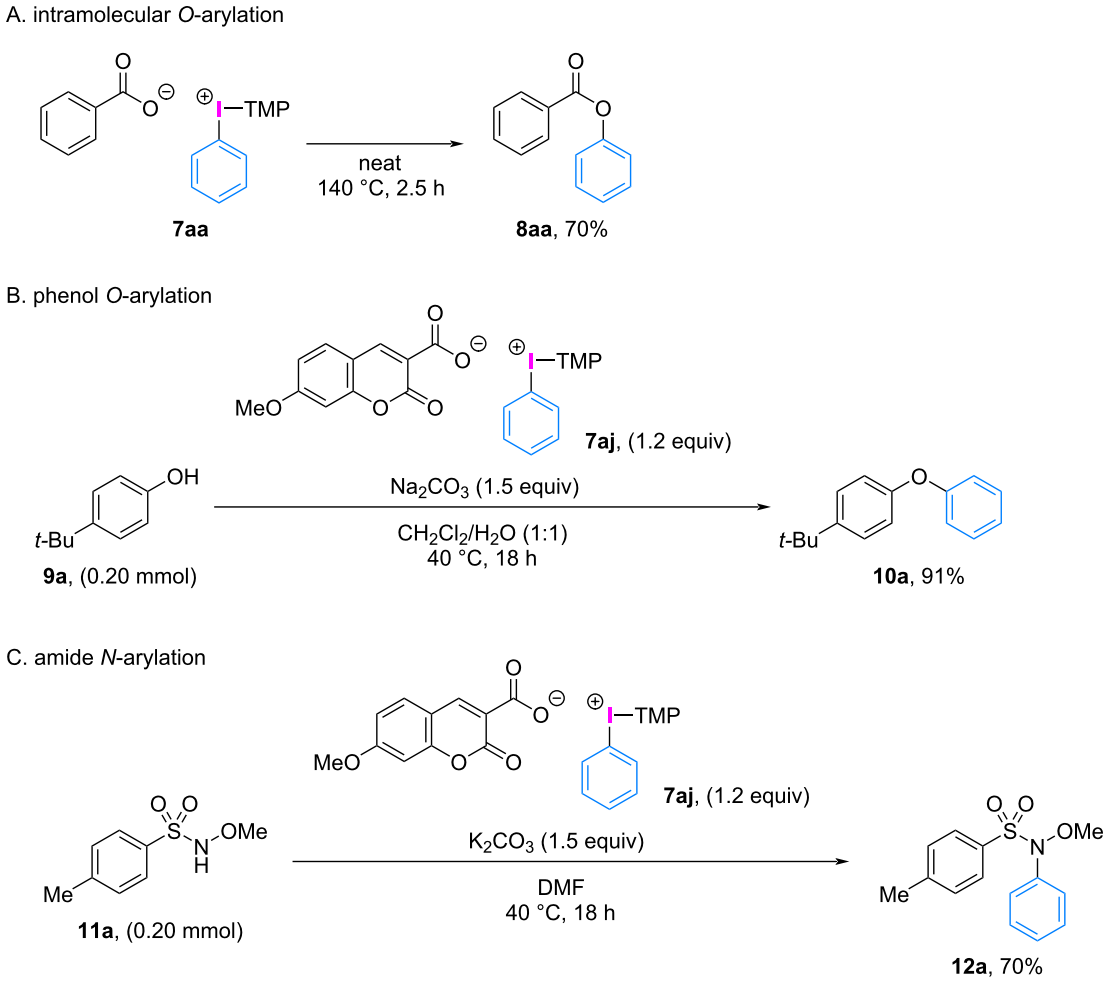

Scheme 6: Representative applications of aryl(TMP)iodonium(III) carboxylates.

diverse (hetero)aryl iodine(III) compounds, as well as aliphatic and aromatic carboxylic acids with a diverse series of functional groups. As a result, this process can be applied for the unique hybridization of biologically active and fluorescently-labeled carboxylic acids with diaryliodonium(III) salts. We anticipate that this study will encourage the incorporation of diaryliodonium(III) carboxylates in various new applications.

Supporting Information

Supporting Information File 1

Further experimental details and copies of ^{1}H, ^{13}C, and ^{19}F NMR spectra.
[https://www.beilstein-journals.org/bjoc/content/supplementary/1860-5397-20-90-S1.pdf]

Acknowledgements

T.D. thanks for the generous gift of fluoroalcohols from Central Glass Co., Ltd.

Funding

N.T. and T.D. acknowledge support from JSPS KAKENHI Grant Number 20K06980 (N.T.) and 19K05466 (T.D.), JST CREST grant number JPMJCR20R1 (T.D.), and the Ritsumeikan Global Innovation Research Organization (R-GIRO) project. R.K. is thankful to the J C Bose University of Science and Technology, YMCA, Faridabad (Seed Grant R&D/SG/2020-21/166) and Department of Science and Technology (DST), India for the PURSE grant (SR/PURSE/2022/126).

Author Contributions

Naoki Miyamoto: investigation; writing – original draft. Daichi Koseki: investigation. Kohei Sumida: investigation. Elghareeb

E. Elboray: investigation; writing – review & editing. Naoko Takenaga: investigation. Ravi Kumar: conceptualization; writing – review & editing. Toshifumi Dohi: conceptualization; methodology; supervision; writing – review & editing.

ORCID® iDs

Elghareeb E. Elboray - https://orcid.org/0000-0003-2261-0355
Naoko Takenaga - https://orcid.org/0000-0003-3776-9406
Ravi Kumar - https://orcid.org/0000-0002-5666-4506
Toshifumi Dohi - https://orcid.org/0000-0002-2812-9581

Data Availability Statement

All data that supports the findings of this study is available in the published article and/or the supporting information to this article.

References

1. Stang, P. J.; Zhdankin, V. V. *Chem. Rev.* **1996,** *96,* 1123–1178. doi:10.1021/cr940424+
2. Merritt, E. A.; Olofsson, B. *Angew. Chem., Int. Ed.* **2009,** *48,* 9052–9070. doi:10.1002/anie.200904689
3. Kikushima, K.; Elboray, E. E.; Jiménez-Halla, J. O. C.; Solorio-Alvarado, C. R.; Dohi, T. *Org. Biomol. Chem.* **2022,** *20,* 3231–3248. doi:10.1039/d1ob02501e
4. Senapati, S.; Parida, S. K.; Karandikar, S. S.; Murarka, S. *Org. Lett.* **2023,** *25,* 7900–7905. doi:10.1021/acs.orglett.3c03146
5. Meher, P.; Panda, S. P.; Mahapatra, S. K.; Thombare, K. R.; Roy, L.; Murarka, S. *Org. Lett.* **2023,** *25,* 8290–8295. doi:10.1021/acs.orglett.3c03365
6. Rong, J.; Haider, A.; Jeppesen, T. E.; Josephson, L.; Liang, S. H. *Nat. Commun.* **2023,** *14,* 3257. doi:10.1038/s41467-023-36377-4
7. Crivello, J. V.; Lam, J. H. W. *Macromolecules* **1977,** *10,* 1307–1315. doi:10.1021/ma60060a028
8. Honma, H.; Yasue, R.; Ichikawa, K. Aromatic heterocyclic compound acid generator, photoresist compositions, resist patterns formed thereby. Jap. Patent JP2023-69345, Nov 2, 2023.
9. Seidl, T. L.; Sundalam, S. K.; McCullough, B.; Stuart, D. R. *J. Org. Chem.* **2016,** *81,* 1998–2009. doi:10.1021/acs.joc.5b02833
10. Seidl, T. L.; Stuart, D. R. *J. Org. Chem.* **2017,** *82,* 11765–11771. doi:10.1021/acs.joc.7b01599
11. Chan, L.; McNally, A.; Toh, Q. Y.; Mendoza, A.; Gaunt, M. J. *Chem. Sci.* **2015,** *6,* 1277–1281. doi:10.1039/c4sc02856b
12. Miralles, N.; Romero, R. M.; Fernández, E.; Muñiz, K. *Chem. Commun.* **2015,** *51,* 14068–14071. doi:10.1039/c5cc04944j
13. Kikushima, K.; Miyamoto, N.; Watanabe, K.; Koseki, D.; Kita, Y.; Dohi, T. *Org. Lett.* **2022,** *24,* 1924–1928. doi:10.1021/acs.orglett.2c00294
14. Bielawski, M.; Zhu, M.; Olofsson, B. *Adv. Synth. Catal.* **2007,** *349,* 2610–2618. doi:10.1002/adsc.200700373
15. Bielawski, M.; Aili, D.; Olofsson, B. *J. Org. Chem.* **2008,** *73,* 4602–4607. doi:10.1021/jo8004974
16. Zhu, M.; Jalalian, N.; Olofsson, B. *Synlett* **2008,** 592–596. doi:10.1055/s-2008-1032050
17. Beringer, F. M.; Drexler, M.; Gindler, E. M.; Lumpkin, C. C. *J. Am. Chem. Soc.* **1953,** *75,* 2705–2708. doi:10.1021/ja01107a046
18. Carreras, V.; Sandtorv, A. H.; Stuart, D. R. *J. Org. Chem.* **2017,** *82,* 1279–1284. doi:10.1021/acs.joc.6b02811
19. Soldatova, N. S.; Postnikov, P. S.; Yusubov, M. S.; Wirth, T. *Eur. J. Org. Chem.* **2019,** 2081–2088. doi:10.1002/ejoc.201900220
20. Beringer, F. M.; Galton, S. A.; Huang, S. J. *J. Am. Chem. Soc.* **1962,** *84,* 2819–2823. doi:10.1021/ja00873a035
21. Dohi, T.; Yamaoka, N.; Kita, Y. *Tetrahedron* **2010,** *66,* 5775–5785. doi:10.1016/j.tet.2010.04.116
22. Dohi, T.; Hayashi, T.; Ueda, S.; Shoji, T.; Komiyama, K.; Takeuchi, H.; Kita, Y. *Tetrahedron* **2019,** *75,* 3617–3627. doi:10.1016/j.tet.2019.05.033
23. Sandtorv, A. H.; Stuart, D. R. *Angew. Chem., Int. Ed.* **2016,** *55,* 15812–15815. doi:10.1002/anie.201610086
24. Basu, S.; Sandtorv, A. H.; Stuart, D. R. *Beilstein J. Org. Chem.* **2018,** *14,* 1034–1038. doi:10.3762/bjoc.14.90
25. Roshandel, S.; Lunn, M. J.; Rasul, G.; Muthiah Ravinson, D. S.; Suri, S. C.; Prakash, G. K. S. *Org. Lett.* **2019,** *21,* 6255–6258. doi:10.1021/acs.orglett.9b02140
26. Kikushima, K.; Morita, A.; Elboray, E. E.; Bae, T.; Miyamoto, N.; Kita, Y.; Dohi, T. *Synthesis* **2022,** *54,* 5192–5202. doi:10.1055/a-1922-8846
27. Dohi, T.; Koseki, D.; Sumida, K.; Okada, K.; Mizuno, S.; Kato, A.; Morimoto, K.; Kita, Y. *Adv. Synth. Catal.* **2017,** *359,* 3503–3508. doi:10.1002/adsc.201700843
28. Gallagher, R. T.; Basu, S.; Stuart, D. R. *Adv. Synth. Catal.* **2020,** *362,* 320–325. doi:10.1002/adsc.201901187
29. Elboray, E. E.; Bae, T.; Kikushima, K.; Kita, Y.; Dohi, T. *Adv. Synth. Catal.* **2023,** *365,* 2703–2710. doi:10.1002/adsc.202300406
30. Saikia, R. A.; Hazarika, N.; Biswakarma, N.; Chandra Deka, R.; Thakur, A. J. *Org. Biomol. Chem.* **2022,** *20,* 3890–3896. doi:10.1039/d2ob00406b
31. Kikushima, K.; Yamada, K.; Umekawa, N.; Yoshio, N.; Kita, Y.; Dohi, T. *Green Chem.* **2023,** *25,* 1790–1796. doi:10.1039/d2gc04445e
32. Jalalian, N.; Petersen, T. B.; Olofsson, B. *Chem. – Eur. J.* **2012,** *18,* 14140–14149. doi:10.1002/chem.201201645
33. Qian, X.; Han, J.; Wang, L. *Adv. Synth. Catal.* **2016,** *358,* 940–946. doi:10.1002/adsc.201501013
34. McKillop, A.; Kemp, D. *Tetrahedron* **1989,** *45,* 3299–3306. doi:10.1016/s0040-4020(01)81008-5
35. Dohi, T.; Yamaoka, N.; Itani, I.; Kita, Y. *Aust. J. Chem.* **2011,** *64,* 529–535. doi:10.1071/ch11057
36. Iinuma, M.; Moriyama, K.; Togo, H. *Synlett* **2012,** *23,* 2663–2666. doi:10.1055/s-0032-1317345
37. Watanabe, A.; Miyamoto, K.; Okada, T.; Asawa, T.; Uchiyama, M. *J. Org. Chem.* **2018,** *83,* 14262–14268. doi:10.1021/acs.joc.8b02541
38. Nassar, A. F. Role of Structural Modifications of Drug Candidates to Enhance Metabolic Stability. In *Drug Metabolism Handbook: Concepts and Applications in Cancer Research,* 2nd ed.; Nassar, A. F.; Hollenberg, P. F.; Scatina, J.; Manna, S. K.; Zeng, S., Eds.; John Wiley & Sons: Hoboken, NJ, USA, 2023; pp 303–322. doi:10.1002/9781119851042.ch9
39. Nassar, A. F. Drug Design Strategies: Role of Structural Modifications of Drug Candidates to Improve PK Parameters of New Drugs. In *Drug Metabolism Handbook: Concepts and Applications in Cancer Research,* 2nd ed.; Nassar, A. F.; Hollenberg, P. F.; Scatina, J.; Manna, S. K.; Zeng, S., Eds.; John Wiley & Sons: Hoboken, NJ, USA, 2023; pp 323–343. doi:10.1002/9781119851042.ch10

40. Nassar, A. F. Chemical Structural Alert and Reactive Metabolite Concept as Applied in Medicinal Chemistry to Minimize the Toxicity of Drug Candidates. In *Drug Metabolism Handbook: Concepts and Applications in Cancer Research,* 2nd ed.; Nassar, A. F.; Hollenberg, P. F.; Scatina, J.; Manna, S. K.; Zeng, S., Eds.; John Wiley & Sons: Hoboken, NJ, USA, 2023; pp 345–372. doi:10.1002/9781119851042.ch11
41. Lucas, H. J.; Kennedy, E. R.; Formo, M. W. *Org. Synth.* **1942,** *22,* 70. doi:10.15227/orgsyn.022.0070
42. Saltzman, H.; Sharefkin, J. G. *Org. Synth.* **1963,** *43,* 60. doi:10.15227/orgsyn.043.0060
43. Miyamoto, K.; Watanabe, Y.; Takagi, T.; Okada, T.; Toyama, T.; Imamura, S.; Uchiyama, M. *ARKIVOC* **2021,** No. vii, 1–11. doi:10.24820/ark.5550190.p011.493
44. Zu, B.; Ke, J.; Guo, Y.; He, C. *Chin. J. Chem.* **2021,** *39,* 627–632. doi:10.1002/cjoc.202000501
45. Linde, E.; Mondal, S.; Olofsson, B. *Adv. Synth. Catal.* **2023,** *365,* 2751–2756. doi:10.1002/adsc.202300354
See for a solution to this problematic issue.
46. Koposov, A. Y.; Boyarskikh, V. V.; Zhdankin, V. V. *Org. Lett.* **2004,** *6,* 3613–3615. doi:10.1021/ol0484714
47. Li, H.; Gori, D.; Kouklovsky, C.; Vincent, G. *Tetrahedron: Asymmetry* **2010,** *21,* 1507–1510. doi:10.1016/j.tetasy.2010.05.016
48. Islam, M.; Tirukoti, N. D.; Nandi, S.; Hotha, S. *J. Org. Chem.* **2014,** *79,* 4470–4476. doi:10.1021/jo500465m
49. Kishore Vandavasi, J.; Hu, W.-P.; Chandru Senadi, G.; Chen, H.-T.; Chen, H.-Y.; Hsieh, K.-C.; Wang, J.-J. *Adv. Synth. Catal.* **2015,** *357,* 2788–2794. doi:10.1002/adsc.201500177

License and Terms

BEILSTEIN JOURNAL OF ORGANIC CHEMISTRY

Oxidative hydrolysis of aliphatic bromoalkenes: scope study and reactivity insights

Amol P. Jadhav and Claude Y. Legault*

Letter

Open Access

Address:
Department of Chemistry, Centre in Green Chemistry and Catalysis, Université de Sherbrooke, Québec J1K 2R1, Canada

Email:
Claude Y. Legault* - claude.legault@usherbrooke.ca

* Corresponding author

Keywords:
bromoalkenes; bromoketones; hypervalent iodine; oxidative hydrolysis; Ritter-type

Beilstein J. Org. Chem. **2024,** *20,* 1286–1291.
https://doi.org/10.3762/bjoc.20.111

Received: 21 March 2024
Accepted: 22 May 2024
Published: 03 June 2024

This article is part of the thematic issue "Hypervalent halogen chemistry".

Guest Editor: T. Gulder

Abstract

We have developed an operationally simple method for the synthesis of dialkyl α-bromoketones from bromoalkenes by utilizing a hypervalent iodine-catalyzed oxidative hydrolysis reaction. This catalytic process provides both symmetrical and unsymmetrical dialkyl bromoketones with moderate yields across a broad range of bromoalkene substrates. Our studies also reveal the formation of Ritter-type side products by an alternative reaction pathway.

Introduction

Organic synthesis heavily relies on oxidative transformations to facilitate chemical reactions. One popular method for achieving these transformations is using redox-active metals, inspired by Nature's metalloproteins. However, using toxic and expensive metals is not always practical, making alternative oxidative methodologies more appealing. Enter hypervalent iodine reagents – a leading metal-free choice for oxidation reactions. These robust and low-toxicity reagents have gained popularity due to their commercial availability [1-5] and versatility for phenolic dearomatizations, oxidative annulations, fragmentations, and oxidative rearrangements [6-11]. In particular, iodine(III) reagents have been proven effective for a wide range of oxidative transformations, cementing their position as a go-to option for organic chemists.

Based on our continued interest in iodine(III)-mediated chemistry, we have explored numerous strategies in oxidative transformations such as direct α-tosyloxylation of ketones [12-14], and the oxidation of enol esters [15,16], to access α-functionalized ketones. We recently developed the oxidative contraction of 3,4-dihydropyranones to access polysubstituted γ-butyrolactones [17]. In 2015 we demonstrated that [hydroxy(tosyloxy)iodo]benzene (HTIB) could be used to convert chloro- and bromoalkenes into their corresponding α-halo ketone products

in usually very high yields (Scheme 1a) [18,19]. However, the haloalkenes used in this previous study as α-substituted ketone precursors were limited to either styryl analogs or stilbene type haloalkenes, with the only exception of 1-bromocycloheptene as fully aliphatic substituted substrate which resulted in a low yield of the desired product. Also, this method involved using a stoichiometric amount of HTIB for the transformation.

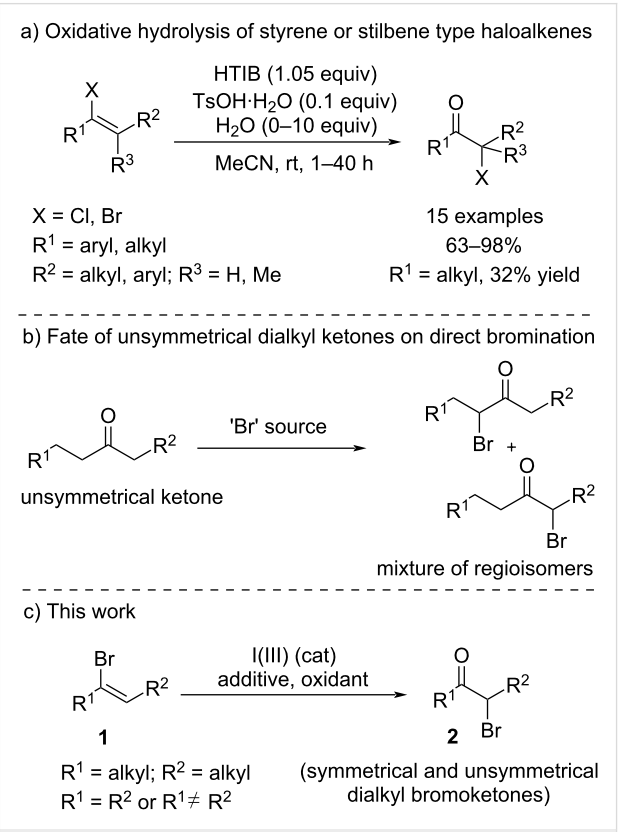

Scheme 1: (a) Oxidative hydrolysis of styrene or stilbene type haloalkenes. (b) Fate of unsymmetrical dialkyl ketones on direct bromination. (c) This work.

α-Haloketones are 1,2-difunctionalized synthons which are very versatile and essential building blocks for their role in the synthesis of heterocyclic compounds [20-22]. Particularly dialkyl bromoketones have been utilized in natural product synthesis [23-25], also as a precursor to reactive oxyallyl cation intermediates [26-28], and for their photochemical reactions [29]. However, the direct halogenation of unsymmetrical ketones for the synthesis of dialkyl bromoketones would result in a mixture of regioisomers given the presence of enolizable protons on each side of the ketone (Scheme 1b). Recently Toy et al. have disclosed the selective synthesis of unsymmetrical α-haloketones by reductive halogenation of an α,β-unsaturated ketones using external halide source [30]. We envisioned that dialkyl bromoalkenes **1** could be used as enol analogs with an improvement in reaction conditions in the presence of I(III) reagents to directly get both symmetrical and unsymmetrical dialkyl bromoketones **2** (Scheme 1c). Recent methods have been reported to access bromoalkenes such as **1** from easily accessible substrates, making the approach even more appealing [31,32].

Results and Discussion

Given its low volatility, we initiated our studies by testing the reactivity of (*E*/*Z*)-1,8-diphenyl-4-bromooct-4-ene (**1a**) with HTIB (1.1 equiv) and cat. $TsOH·H_2O$ (0.2 equiv) in acetonitrile. These reaction conditions afforded the desired product **2a** in moderate yield (51%), along with 21% mixture of regioisomers **3a** and **3a'** obtained from Ritter-type reaction of **1a** with CH_3CN in the presence of HTIB (Table 1, entry 1).

We explored the influence of different variables to counteract the formation of **3a** and **3a'**. We first envisioned that the use of the more hindered, mesityl-derived Koser's reagent, could drastically influence the formation of the side-products. Unfortunately, its use resulted in a drop of the yield for the desired α-bromoketone (Table 1, entry 2). In situ generation of Koser-like reagent by addition of excess $TsOH·H_2O$ (2.0 equiv) to either PIDA or *p*-OMe-PIDA did not further improve the yield for α-bromoketone (Table 1, entries 3 and 4). We envisioned that altering the iodonium intermediate counterion by replacing TsOH with either MsOH or $HNTf_2$ as an acid additive (2.0 equiv) could influence the formation of **3a**/**3a'**. The use of these acids in the presence of PIDA did not show any significantly altering reaction outcome (Table 1, entries 5 and 6). We then replaced acetonitrile with dichloromethane to completely prevent the formation of **3a**/**3a'**. Unfortunately, while it eliminated the side products, it further limited the yield for α-bromoketone, whereas no reactivity was seen when EtOAc and DMA were used as solvents (Table 1, entries 7–9). The use of HFIP led to complete conversion of **1a**, but no observation of the desired product **2a** (Table 1, entry 10).

We then explored catalytic conditions for the generation of the iodine(III) reagent. Remarkably, when catalytic PhI (0.2 equiv) was employed for in situ generation of Koser's reagent by using *m*-CPBA (1.2 equiv) as an oxidant, almost similar results were obtained (Table 2, entry 1) with those obtained by stoichiometric use of HTIB. Attempt to perform the reaction using a catalytic amount of 2-iodobenzoic acid (0.2) under similar oxidizing conditions resulted in slightly diminished yield for the desired *α*-bromoketone (Table 2, entry 2). Notably, the direct use of HTIB as the catalyst, with a catalytic amount of $TsOH·H_2O$ (0.2 equiv each), in the presence of *m*-CPBA (1.2 equiv) proved to be the most superior conditions (59% NMR yield, Table 2, entry 3). To rule out the possibility of direct involvement of *m*-CPBA in the oxidative hydrolysis reaction, **1a** was reacted in the absence of any hypervalent iodine

Table 1: Conditions screening (without oxidant)[a].

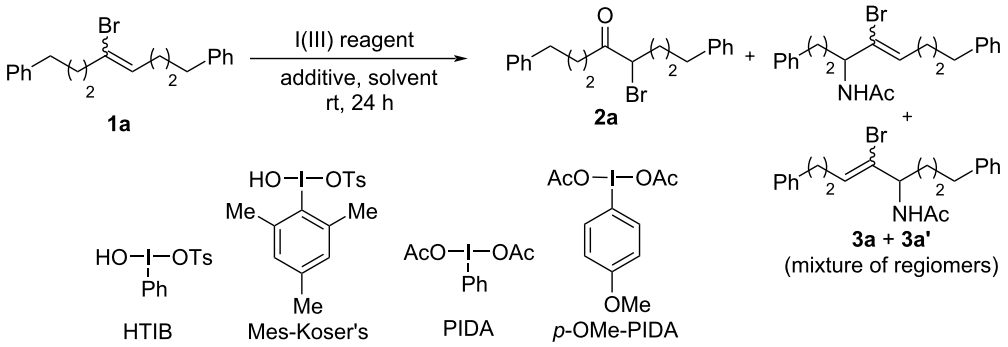

Entry	Solvent	HVI source (equiv)	Additive (equiv)	**2a** [%][b]	**3a** + **3a'** [%][b,c]
1	CH_3CN	HTIB (1.1)	$TsOH·H_2O$ (0.2)	51	21
2	CH_3CN	Mes-Koser's (1.1)	$TsOH·H_2O$ (0.2)	36	18
3	CH_3CN	PIDA (1.1)	$TsOH·H_2O$ (2.0)	42	28
4	CH_3CN	*p*-OMe-PIDA (1.1)	$TsOH·H_2O$ (2.0)	50	18
5[d]	CH_3CN	PIDA (1.1)	MsOH (2.0)	46	28
6[d]	CH_3CN	PIDA (1.1)	$HNTf_2$ (2.0)	35	trace
7	CH_2Cl_2	HTIB (1.1)	$TsOH·H_2O$ (0.2)	25	na
8	EtOAc	HTIB (1.1)	$TsOH·H_2O$ (0.2)	NR	na
9	DMA	HTIB (1.1)	$TsOH·H_2O$ (0.2)	NR	na
10	HFIP	HTIB (1.1)	$TsOH·H_2O$ (1.1)	0	na

[a]Unless otherwise stated 0.1 mmol of **1a** was used with 0.1 M conc. of solvent. [b]NMR yield determined by ^1H NMR of the crude reaction mixture using an internal standard. [c]Combined yield of regioisomers. [d]5.0 equiv H_2O were added to the reaction.

Table 2: Conditions screening (with oxidant)[a].

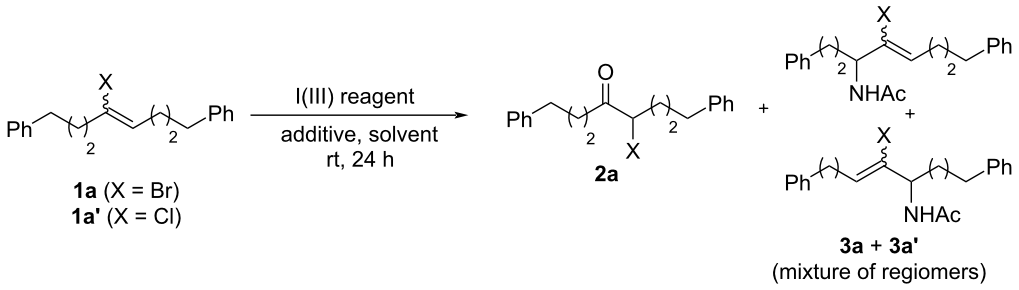

Entry	Solvent	Catalyst (equiv)	Additive (equiv)	Oxidant (equiv)	**2a** [%][b]	**3a** + **3a'** [%][b,c]
1	CH_3CN	PhI (0.2)	$TsOH·H_2O$ (0.2)	*m*-CPBA (1.2)	51	23
2	CH_3CN	2-I-$PhCO_2H$ (0.2)	$TsOH·H_2O$ (0.2)	*m*-CPBA (1.2)	41	22
3	CH_3CN	HTIB (0.2)	$TsOH·H_2O$ (0.2)	*m*-CPBA (1.2)	59	24
4	CH_3CN	none	none	*m*-CPBA (1.2)	5	20
5	CH_3CN	none	$TsOH·H_2O$ (1.1)	*m*-CPBA (1.2)	13	15
6[d]	CH_3CN	HTIB (0.2)	$TsOH·H_2O$ (0.2)	*m*-CPBA (1.2)	na	na

[a]Unless otherwise stated 0.1 mmol of **1a** was used with 0.1 M conc. of solvent. [b]NMR yield determined by ^1H NMR of the crude reaction mixture using an internal standard. [c]Combined yield of regioisomers. [d]X = Cl and the reaction was carried out both with or without addition of 5.0 equiv of H_2O.

source, which resulted in a significant decrease in the yield of **2a** (Table 2, entries 4 and 5). Importantly, when analogous chloroalkene (*E*/*Z*)-1,8-diphenyl-4-chlorooct-4-ene (**1a'**) was tested as a substrate under optimal conditions (without H_2O or with 5 equiv H_2O), no reactivity was seen at all, presumably due to the stronger inductive effect of the chlorine (Table 2, entry 6).

It was unfortunately not possible to prevent formation of side products **3a**/**3a'** using modifications of the reaction conditions. We thus next turned our attention to exploring the scope of the developed protocols, focusing both on symmetrical as well as unsymmetrical dialkyl bromoalkenes, in order to determine if the nature of the substrate could influence the reaction outcome. As shown in Scheme 2, the (*E*/*Z*) symmetrical dialkyl bromoalkenes reacted well with catalytic HTIB, irrespective of the chain length, affording the corresponding α-bromoketones (**2a**,**b**) in 49–54% isolated yields by oxidative transposition of the bromine atom in the reaction process. We then extended this scope by synthesizing unsymmetrical dialkyl bromoalkenes (**1c**–**g**) bearing side chains of varied length and steric character. The incorporation of *n*-pentyl or isobutyl groups at the distal side of bromoalkene was readily tolerated and yielded the products (**2c**,**d**) with consistent yields. Demonstrating additional generalizability, substrates bearing sterically demanding cyclohexyl or isopropyl groups as the near side chain of bromoalkene afforded the corresponding α-bromoketones (**2e**,**f**) with unaffected reactivity or yields. Notably, 15–20% Ritter-type side products were obtained with all these substrates as a mixture of regioisomers. Surprisingly, even substrate **2g** did not provide a higher yield of the desired α-bromoketone product, despite the absence of hydrogens on the allylic position (see Scheme 3 for explanations).

Our mechanistic understanding of the oxidative hydrolysis of styrene haloalkene analogs [19] lets us hypothesize an external bromide attack as the main reaction pathway for this catalytic oxidative transposition of dialkyl bromoalkenes (Scheme 3). No α-tosyloxy ketone products were observed in the crude reaction mixtures, either with catalytic or stoichiometric use of $TsOH{\cdot}H_2O$, even when the reactions were incomplete. These observations ruled out the possibility of double S_N2 attack by tosylate followed by bromide.

$TsOH{\cdot}H_2O$ accelerates the formation of the phenyl tosyloxy iodonium intermediate **A** from catalytic HTIB. Dialkyl bromoalkene **1** then associates with **A** followed by attack of tosyloxy or water, delivering iodonium intermediate **B**. Being a better leaving group, the bromide anion is then expelled, which becomes a counterion for the iodonium intermediate **C**. Liberation of PhI serves as the driving force for subsequent S_N2 attack by the bromide anion to give the dialkyl α-bromoketone **2**. *m*-CPBA then regenerates the hypervalent iodine (HTIB) catalyst by oxidizing PhI in the presence of $TsOH{\cdot}H_2O$. The forma-

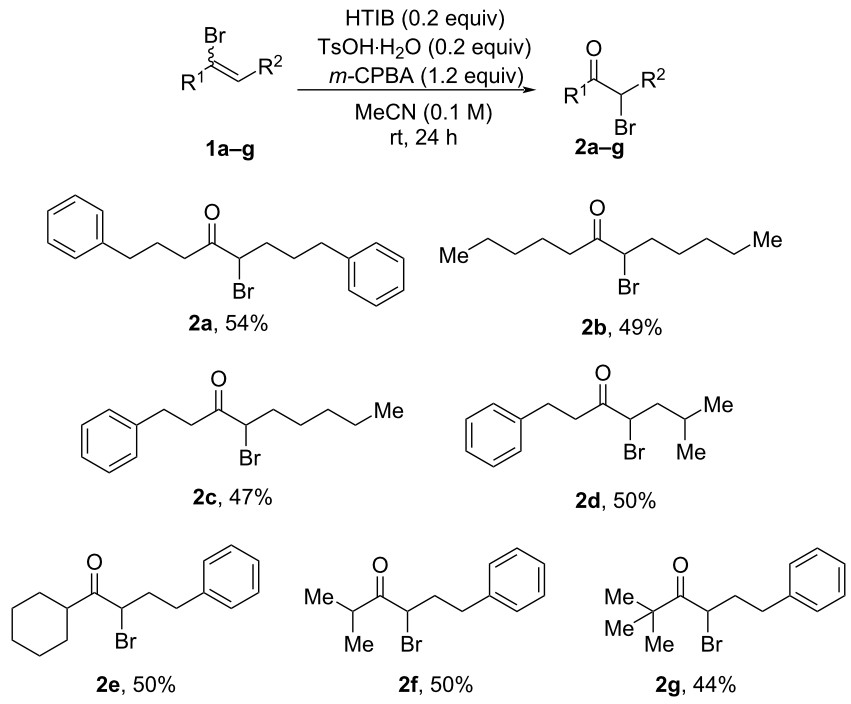

Scheme 2: Substrate scope. Unless otherwise stated 0.2 mmol of **1** was used and the isolated yields are given.

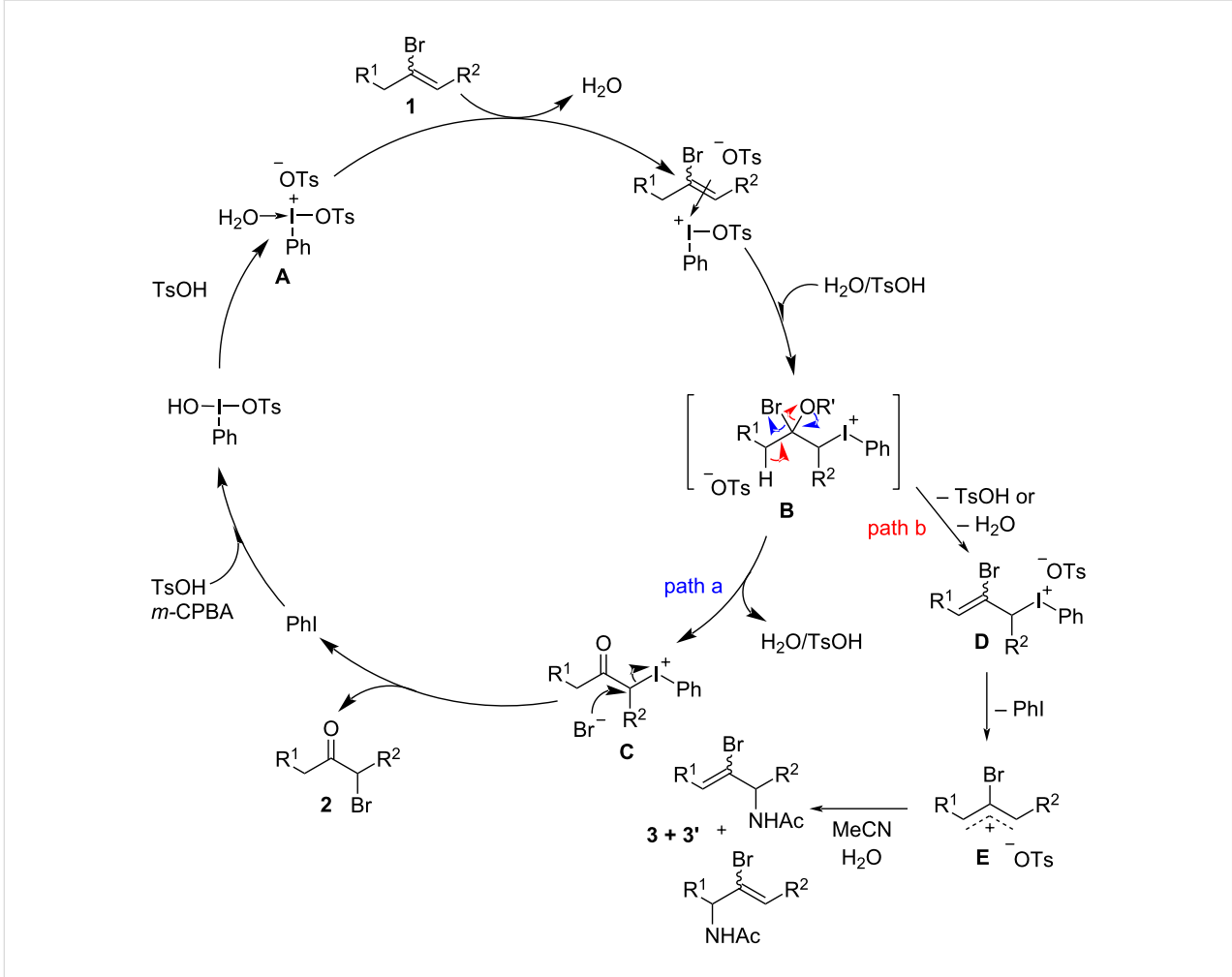

Scheme 3: Proposed catalytic cycle.

tion of the Ritter-type side products is proposed through path b (Scheme 3). The elimination of α-proton on the side chain of dialkyl bromoalkenes results in iodonium intermediate **D**, which on the expulsion of PhI gives a mixture of the allylic carbocation **E**, which ultimately gets trapped by MeCN in the presence of H_2O, giving the regioisomeric mixture of Ritter-type amidation side products **3**.

Conclusion

In summary we have developed a hypervalent iodine-catalyzed synthetic method for the oxidative hydrolysis of diverse dialkyl bromoalkenes. The current approach can tolerate both symmetrical as well as unsymmetrical dialkyl bromoalkenes as substrates delivering dialkyl α-bromoketones which are highly sought-after synthons in heterocycle synthesis and medicinal chemistry, thus overcoming the limitations of previous methods. The reaction accommodates sterically hindered bromoalkenes as substrates, leading to the corresponding α-bromoketone derivatives. While we could not further minimize the formation of Ritter-type side products (≈4:1 ratio of α-bromoketone vs Ritter-type side products), noticing these side products from common phenyl tosyloxy iodonium intermediate suggest that hypervalent iodine reagents could be utilized in the future for the α-acetamidation of dialkyl bromoalkenes. The present work provides an operationally simple catalytic method to access a diverse range of α-bromoketones, which are versatile building blocks for synthesizing various important hetero aromatics.

Supporting Information

Supporting Information File 1

Experimental procedures for reactions, and relevant spectra of all new compounds.
[https://www.beilstein-journals.org/bjoc/content/supplementary/1860-5397-20-111-S1.pdf]

Funding

This work was supported by the National Science and Engineering Research Council (NSERC) of Canada, the Canada Foundation for Innovation (CFI), the FRQNT Centre in Green Chemistry and Catalysis (CGCC), and the Université de Sherbrooke.

ORCID® iDs

Amol P. Jadhav - https://orcid.org/0000-0003-3962-6169
Claude Y. Legault - https://orcid.org/0000-0002-0730-0263

Data Availability Statement

All data that supports the findings of this study is available in the published article and/or the supporting information to this article.

References

1. Yoshimura, A.; Zhdankin, V. V. *Chem. Rev.* **2016,** *116,* 3328–3435. doi:10.1021/acs.chemrev.5b00547
2. Brown, M.; Farid, U.; Wirth, T. *Synlett* **2013,** *24,* 424–431. doi:10.1055/s-0032-1318103
3. Wirth, T. *Angew. Chem., Int. Ed.* **2005,** *44,* 3656–3665. doi:10.1002/anie.200500115
4. Zhdankin, V. V.; Stang, P. J. *Chem. Rev.* **2002,** *102,* 2523–2584. doi:10.1021/cr010003+
5. Varvoglis, A. *Hypervalent Iodine in Organic Synthesis;* Academic Press: San Diego, CA, USA, 1997.
6. Puthanveedu, M.; Antonchick, A. P. Aromatic C–H Functionalization. *Iodine Catalysis in Organic Synthesis;* Wiley-VCH: Weinheim, Germany, 2022; pp 151–184. doi:10.1002/9783527829569.ch6
7. Shetgaonkar, S. E.; Krishnan, M.; Singh, F. V. *Mini-Rev. Org. Chem.* **2021,** *18,* 138–158. doi:10.2174/1570193x17999200727204349
8. Zhang, B.; Li, X.; Guo, B.; Du, Y. *Chem. Commun.* **2020,** *56,* 14119–14136. doi:10.1039/d0cc05354f
9. Wu, W.-T.; Zhang, L.; You, S.-L. *Chem. Soc. Rev.* **2016,** *45,* 1570–1580. doi:10.1039/c5cs00356c
10. Roche, S. P.; Porco, J. A., Jr. *Angew. Chem., Int. Ed.* **2011,** *50,* 4068–4093. doi:10.1002/anie.201006017
11. Pouységu, L.; Deffieux, D.; Quideau, S. *Tetrahedron* **2010,** *66,* 2235–2261. doi:10.1016/j.tet.2009.12.046
12. Thérien, M.-È.; Guilbault, A.-A.; Legault, C. Y. *Tetrahedron: Asymmetry* **2013,** *24,* 1193–1197. doi:10.1016/j.tetasy.2013.08.002
13. Guilbault, A.-A.; Legault, C. Y. *ACS Catal.* **2012,** *2,* 219–222. doi:10.1021/cs200612s
14. Guilbault, A.-A.; Basdevant, B.; Wanie, V.; Legault, C. Y. *J. Org. Chem.* **2012,** *77,* 11283–11295. doi:10.1021/jo302393u
15. Jobin-Des Lauriers, A.; Legault, C. Y. *Asian J. Org. Chem.* **2016,** *5,* 1078–1099. doi:10.1002/ajoc.201600246
16. Basdevant, B.; Legault, C. Y. *J. Org. Chem.* **2015,** *80,* 6897–6902. doi:10.1021/acs.joc.5b00948
17. Dagenais, R.; Lussier, T.; Legault, C. Y. *Org. Lett.* **2019,** *21,* 5290–5294. doi:10.1021/acs.orglett.9b01893
18. Dagenais, R.; Jobin-Des Lauriers, A.; Legault, C. *Synthesis* **2017,** *49,* 2928–2932. doi:10.1055/s-0036-1588439
19. Jobin-Des Lauriers, A.; Legault, C. Y. *Org. Lett.* **2016,** *18,* 108–111. doi:10.1021/acs.orglett.5b03345
20. Ali, S. H.; Sayed, A. R. *Synth. Commun.* **2021,** *51,* 670–700. doi:10.1080/00397911.2020.1854787
21. Fülöpová, V.; Soural, M. *Synthesis* **2016,** *48,* 3684–3695. doi:10.1055/s-0035-1562519
22. Erian, A. W.; Sherif, S. M.; Gaber, H. M. *Molecules* **2003,** *8,* 793–865. doi:10.3390/81100793
23. Grenet, E.; Géant, P.-Y.; Salom-Roig, X. J. *Org. Lett.* **2021,** *23,* 8539–8542. doi:10.1021/acs.orglett.1c03237
24. Zhang, X.; Cai, X.; Huang, B.; Guo, L.; Gao, Z.; Jia, Y. *Angew. Chem., Int. Ed.* **2019,** *58,* 13380–13384. doi:10.1002/anie.201907523
25. Song, Y.-Y.; Kinami, K.; Kato, A.; Jia, Y.-M.; Li, Y.-X.; Fleet, G. W. J.; Yu, C.-Y. *Org. Biomol. Chem.* **2016,** *14,* 5157–5174. doi:10.1039/c6ob00720a
26. Pirovano, V.; Brambilla, E.; Moretti, A.; Rizzato, S.; Abbiati, G.; Nava, D.; Rossi, E. *J. Org. Chem.* **2020,** *85,* 3265–3276. doi:10.1021/acs.joc.9b03117
27. Li, H.; Wu, J. *Synthesis* **2014,** *47,* 22–33. doi:10.1055/s-0034-1378918
28. Tang, Q.; Chen, X.; Tiwari, B.; Chi, Y. R. *Org. Lett.* **2012,** *14,* 1922–1925. doi:10.1021/ol300591z
29. García-Santos, W. H.; Mateus-Ruiz, J. B.; Cordero-Vargas, A. *Org. Lett.* **2019,** *21,* 4092–4096. doi:10.1021/acs.orglett.9b01275
30. Lao, Z.; Zhang, H.; Toy, P. H. *Org. Lett.* **2019,** *21,* 8149–8152. doi:10.1021/acs.orglett.9b02324
31. Coombs, J. R.; Zhang, L.; Morken, J. P. *Org. Lett.* **2015,** *17,* 1708–1711. doi:10.1021/acs.orglett.5b00480
32. Yu, P.; Bismuto, A.; Morandi, B. *Angew. Chem., Int. Ed.* **2020,** *59,* 2904–2910. doi:10.1002/anie.201912803

BEILSTEIN JOURNAL OF ORGANIC CHEMISTRY

Hypervalent iodine-catalyzed amide and alkene coupling enabled by lithium salt activation

Akanksha Chhikara, Fan Wu, Navdeep Kaur, Prabagar Baskaran, Alex M. Nguyen, Zhichang Yin, Anthony H. Pham and Wei Li*

Letter

Open Access

Address:
Department of Chemistry and Biochemistry, School of Green Chemistry and Engineering, The University of Toledo, 2801 West Bancroft Street, Toledo, Ohio 43606, United States

Email:
Wei Li* - Wei.Li@Utoledo.edu*

* Corresponding author

Keywords:
amide coupling; hypervalent iodine catalysis; lithium salt activation; olefin oxyamination; oxazoline

Beilstein J. Org. Chem. **2024,** *20,* 1405–1411.
https://doi.org/10.3762/bjoc.20.122

Received: 21 March 2024
Accepted: 29 May 2024
Published: 24 June 2024

This article is part of the thematic issue "Hypervalent halogen chemistry".

Guest Editor: T. Gulder

Abstract

Hypervalent iodine catalysis has been widely utilized in olefin functionalization reactions. Intermolecularly, the regioselective addition of two distinct nucleophiles across the olefin is a challenging process in hypervalent iodine catalysis. We introduce here a unique strategy using simple lithium salts for hypervalent iodine catalyst activation. The activated hypervalent iodine catalyst allows the intermolecular coupling of soft nucleophiles such as amides onto electronically activated olefins with high regioselectivity.

Introduction

Hypervalent iodine(III) reagents, also known as λ^3–iodanes, have been well established and used in organic synthesis for the past decades [1-5]. The pioneering works of Fuchigami and Fugita, Ochiai, Kita, and later the development of chiral hypervalent iodines by Wirth, Kita, Ishihara, Muñiz, and many others, have firmly established these reagents as useful catalysts for a wide variety of chemical transformations [6-17]. A number of features, including low toxicity, high stability, ease of handling, and versatile reactivity, etc. render these catalysts highly attractive for adoption in organic synthesis. In particular, the field of olefin difunctionalization, known for its rapid assembly of molecular complexity, has been a fertile ground for innovation for hypervalent iodine catalysis, which often involves the catalytic use of an iodoarene with stoichiometric oxidants such as MCPBA, Selectfluor, etc. [18-20]. Earlier and recent hypervalent iodine-catalyzed olefin halofunctionalizations by several groups have predicated on the use of intramolecular olefin substrates tethered with a nucleophile to avoid the lack of regiochemical additions (Scheme 1a) [21-28]. Intermolecular hypervalent iodine-catalyzed olefin difunctionalizations

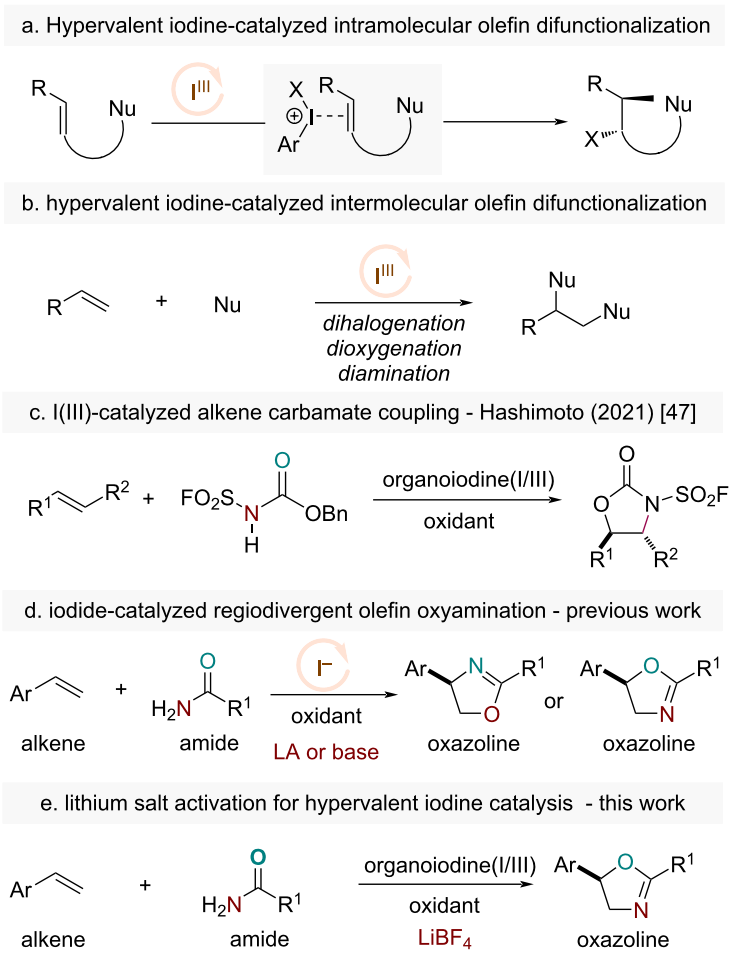

Scheme 1: Hypervalent iodine-catalyzed olefin difunctionalizations background.

have been realized for olefin dihalogenation, dioxygenation and diamination reactions, where often the same type of nucleophiles were incorporated (Scheme 1b) [29-40]. Intermolecular hypervalent iodine catalysis with the regioselective additions of two distinct nucleophilic functionalities across an olefin, however, remains challenging with limited solutions [41-46]. Notably, an interesting work by Hashimoto has recently enabled the intermolecular addition of *N*-(fluorosulfonyl)-protected carbamates as oxyamination reagents across a variety of olefin structures [47]. This work engages the hypervalent iodine catalyst in an anionic ligand exchange with the substrate, which then partitions into an ion pair suitable for olefin activation, followed by the addition of the bifunctional anionic carbamate (Scheme 1c).

Our hypothesis here aims to directly access the reactivity of the cationic hypervalent iodine catalyst through an initial activation first, which we reason will then enable soft nucleophiles such as unadorned amides to readily participate in the ensuing olefin addition. In this regard, we wondered if the hypervalent iodine with difluoro ligands could undergo salt metathesis with lithium salts such as $LiBF_4$ or $LiPF_6$ to afford the more reactive cationic hypervalent iodine catalyst. The cationic hypervalent iodine catalyst could then activate the olefin to allow the addition of bifunctional nucleophiles such as an amide to achieve an overall olefin oxyamination process. We have previously reported a series of iodide-catalyzed processes, in which the electrophilicity of the halogen source could be modulated to render different classes of nucleophiles for additions onto olefins in various olefin difunctionalization reactions [48-52]. In particular, we demonstrated that addition of either a Lewis acid or a base could activate amides to couple with alkenes regioselectively to furnish their respective oxazoline regioisomer (Scheme 1d). Herein, we report that lithium salts such as $LiBF_4$ or $LiPF_6$, which are often used in lithium-ion batteries, can be used to activate hypervalent iodine catalysts to enable olefin oxyamination reactions with simple bifunctional amide nucleophiles (Scheme 1e).

Results and Discussion

Our studies here focused on the development of hypervalent iodine-catalyzed amide and alkene coupling reaction [53-55]. In this case, we started with styrene (**1**) and benzamide (**2**) as the standard substrates. Using iodotoluene **A** as the hypervalent iodine catalyst precursor, Selectfluor as the oxidant, and $LiBF_4$ as the lithium salt for hypervalent iodine activation, we were gratified to observe the formation of the desired oxazoline **3** in 59% yield as the major regioisomer in nitromethane ($MeNO_2$) solvent (Table 1, entry 1). To further improve the reaction efficiency, we screened several additional parameters including solvents and concentration. In these cases, we found that while both acetonitrile and $MeNO_2$ (0.25 M) were suitable solvents, other solvents in general afforded no product formation (Table 1, entries 2–6). Lower catalyst loading and longer reaction time did not improve the overall reaction efficiency (Table 1, entries 6–8). Furthermore, we evaluated several salt additives containing different counterions, and found that $LiBF_4$ was the optimal additive (Table 1, entries 7, 9, and 10). The optimal conditions were shown in entry 7 in Table 1, resulting in the formation of the desired oxazoline product **3** in 61% isolated yield. Control reactions in the absence of either the precatalyst or oxidant afforded no product formation (Table 1, entries 11 and 12). The control reaction in the absence of the lithium salt only afforded 8% of the oxazoline product **3** (Table 1, entry 13). These reactions validated the critical roles of each individual component to achieve an efficient reaction.

To understand this coupling reaction better, we have also performed time studies to elucidate the effects of several key features in this reaction. First, we studied the iodoarene catalyst precursor and the lithium salt in terms of their effects on the overall reaction rate. In this case, we observed that the overall reaction proceeded faster with the more electron-rich iodoarene catalysts than electron-poor ones. Qualitatively, the electron-rich iodoarene catalysts are likely to be worse at activating the olefins than the electron-deficient hypervalent iodine catalysts. Therefore, the faster rate with the electron-rich catalyst precursor is because the electron-rich iodoarene catalyst precursors are more easily oxidized to the hypervalent iodine catalyst with difluoro ligands. Interestingly, the use of different lithium salts also impacted the overall reaction rate, with the reaction using the less coordinating $LiAsF_6$ salt proceeding faster than $LiPF_6$ and $LiBF_4$. This time study suggested that the hypervalent iodine precatalyst with the less coordinating counterion is more reactive to activate the olefin. We also conducted kinetic studies on how the olefin and amide structures impacted the overall reaction rate. The more electron-rich olefins generally proceeded faster than the electron-poor ones, suggesting that a significant positive charge was likely built up on the olefin prior

Table 1: Amide and alkene reaction optimization studies.

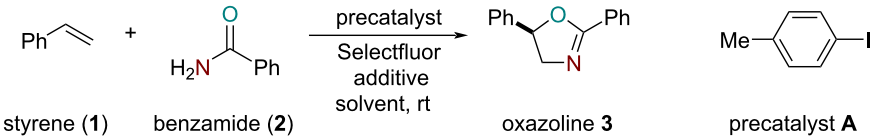

styrene (**1**) benzamide (**2**) oxazoline **3** precatalyst **A**

entry[a]	precatalyst (mol %)	solvent (M)	additive (mol %)	yield (%)[c]	rr
1	**A** (20)	$MeNO_2$ (0.5)	$LiBF_4$ (100)	59	>95:5
2	**A** (20)	MeCN (0.5)	$LiBF_4$ (100)	41	94:6
3	**A** (20)	MeOH (0.5)	$LiBF_4$ (100)	0	–
4	**A** (20)	DMF (0.5)	$LiBF_4$ (100)	0	–
5	**A** (20)	$MeNO_2$ (0.3)	$LiBF_4$ (100)	62	>95:5
6[b]	**A** (20)	$MeNO_2$ (0.25)	$LiBF_4$ (100)	64	>95:5
7	**A** (20)	$MeNO_2$ (0.25)	$LiBF_4$ (100)	65 (61)	>95:5
8	**A** (15)	$MeNO_2$ (0.5)	$LiBF_4$ (100)	55	>95:5
9	**A** (20)	$MeNO_2$ (0.5)	$LiPF_6$ (100)	56	>95:5
10	**A** (20)	$MeNO_2$ (0.5)	$AgBF_4$ (100)	12	>95:5
11	–	$MeNO_2$ (0.5)	$LiBF_4$ (100)	0	–
12[d]	**A** (20)	$MeNO_2$ (0.5)	$LiBF_4$ (100)	0	–
13	**A** (20)	$MeNO_2$ (0.5)	–	8	>95:5

[a]Optimized conditions: styrene (**1**, 0.25 mmol), iodotoluene **A** (20 mol %), $LiBF_4$ (100 mol %), Selectfluor (150 mol %), benzamide (**2**, 400 mol %), $MeNO_2$ (0.25 M), rt, 16 h. Yields were determined by crude ^1H NMR using 1,3-benzodioxole as the internal standard. [b]Reaction time is 24 hours. [c]The yield in parenthesis is isolated yield. [d]No Selectfluor added.

to the nucleophilic addition. On the other hand, the electronic nature of the para-substituted benzamides had little impact on the overall reaction rate as both electron-rich and electron-deficient benzamides proceeded with similar kinetic profiles. All the kinetic plots are shown in Figure 1.

With the optimized conditions and kinetic information in hand, we turned our attention to the amide substrate scope. In this case, both electron-rich and -deficient benzamides proceeded to the desired products in reasonable yields and high regioselectivities (Figure 2, products **4**–**7**). Concurring with our kinetic data, the electronic nature of the amide bears little impact on the overall reaction rate and in this case, on the final yields as well. Similarly, ortho- and meta-substituted benzamides with halogen functionalities could also generate the desired oxazoline products with reasonable yields (Figure 2, products **8**–**10**). Heteroaromatic amides could also furnish the oxazolines **11** and **12** with good efficiency. Naphthaleneamide also generated the desired product **13**, albeit with slightly lower efficiency. Interestingly, *o*- and *m*-methyl-substituted benzamides provided a significant yield boost to provide the oxazoline structures **14** and **15**. Finally, sterically encumbered tertiary amides participated in the reaction to afford the respective regioisomeric product **16**.

Encouraged by these results, we then turned our attention to explore the extent of alkene substrate scope using 3,4-dimethylbenzamide, which afforded the oxazoline product **17** in 70% yield (Figure 3). Based on this optimal amide structure, we examined various electronically activated olefins under the optimal reaction conditions. A number of styrenyl derivatives with para-substituted halogens, ester, and phthalimide proceeded smoothly with good yields and excellent regioselectivities to access the oxazoline products as single regioisomers (Figure 3, products **18**–**22**). The *o*-bromo-substituted styrene also afforded the corresponding product **23**. Furthermore, 1,1-di-substituted α-methylstyrene and α-phenylstyrene produced the respective oxazoline products with high regioselectivity and reasonable yields using iodoanisole as the catalyst precursor (Figure 3, products **24** and **25**).

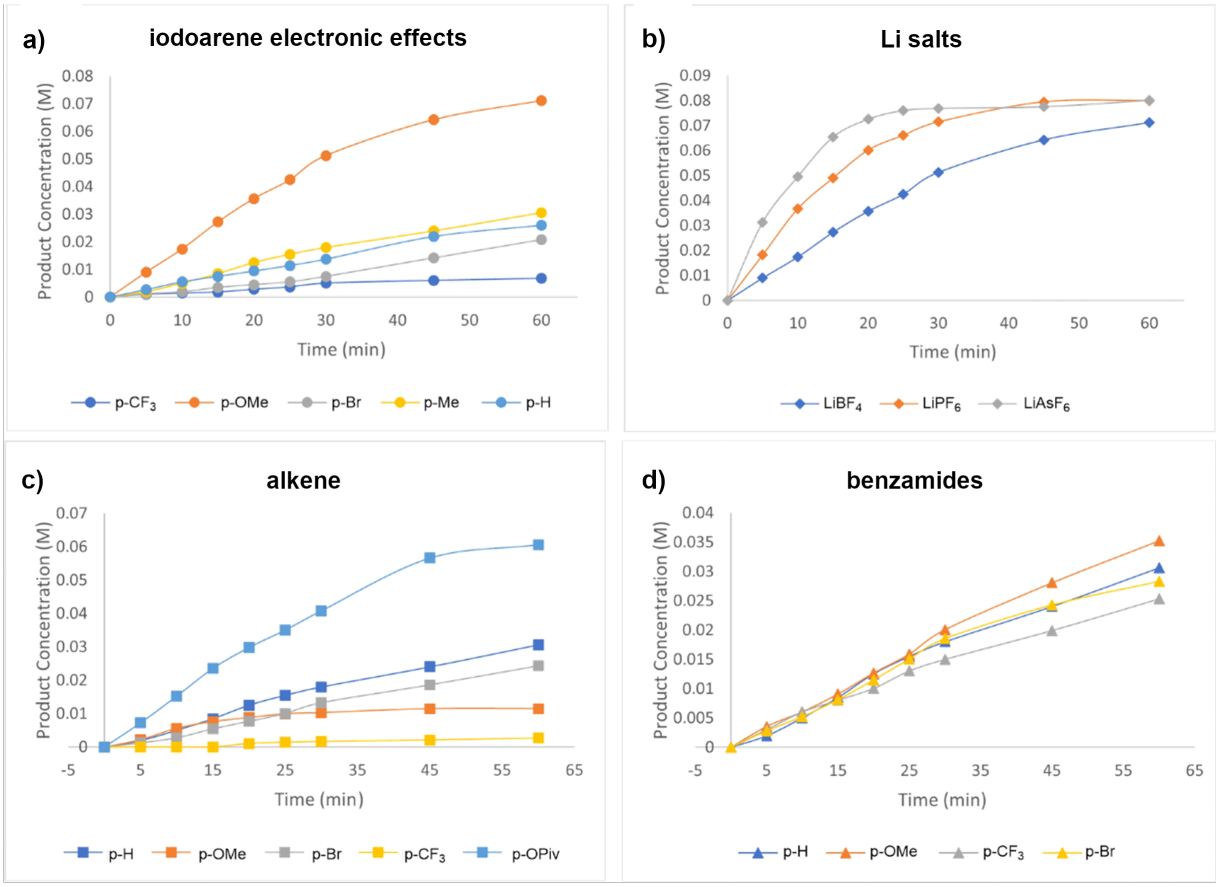

Figure 1: Time studies of the amide and alkene coupling. a) Iodoarene time studies: styrene (**1**), para-substituted iodoarenes, $LiBF_4$, and benzamide (**2**). b) Li salt time studies: styrene (**1**), iodoanisole, Li salts, and benzamide (**2**). c) Alkene time studies: para-substituted styrenes, iodotoluene **A**, $LiBF_4$, and benzamide (**2**). d) Benzamide time studies: styrene (**1**), iodotoluene **A**, $LiBF_4$, and para-substituted benzamides.

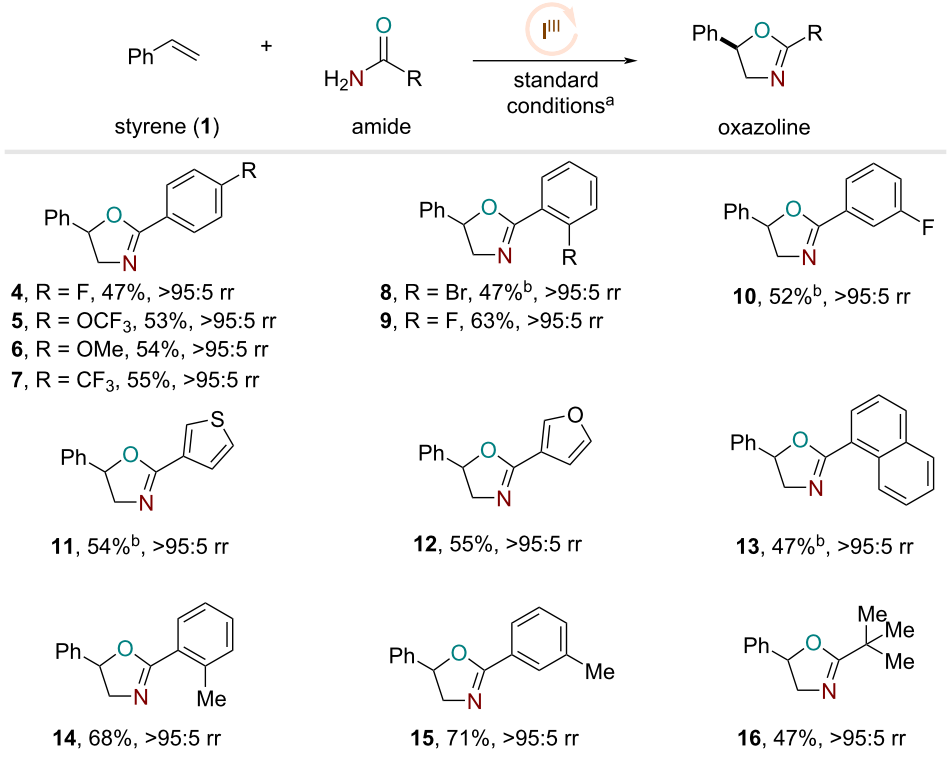

Figure 2: Amide substrate scope studies. a) Standard conditions: styrene (0.25 mmol), iodotoluene (20 mol %), $LiBF_4$ (100 mol %), Selectfluor (150 mol %), amide (400 mol %), $MeNO_2$ (0.25 M), rt, 16 h. b) Iodoanisole (20 mol %).

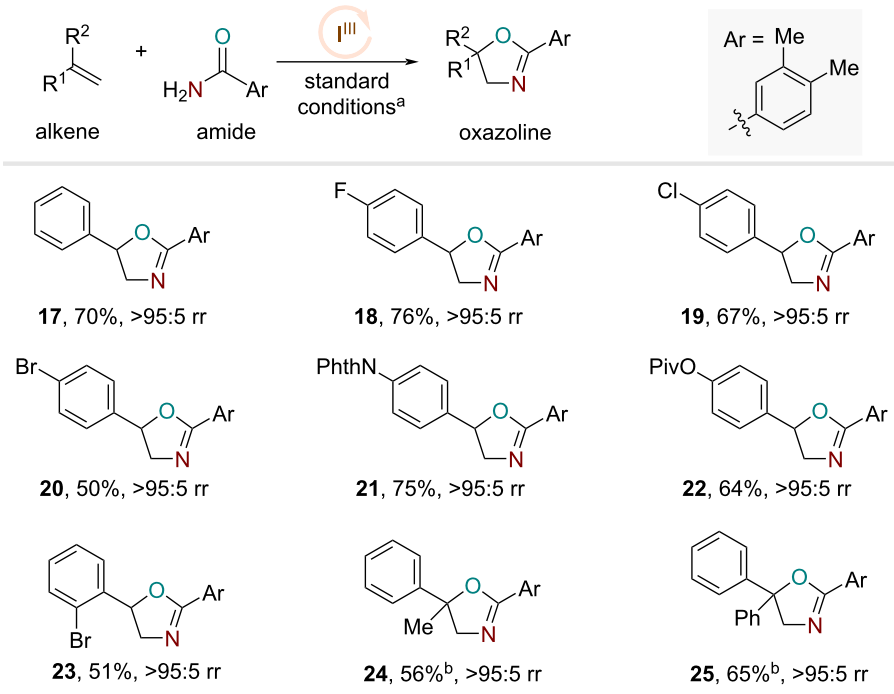

Figure 3: Alkene substrate scope studies. a) Standard conditions: alkene (0.25 mmol), iodotoluene (20 mol %), $LiBF_4$ (100 mol %), Selectfluor (150 mol %), 3,4-dimethylbenzamide (400 mol %), $MeNO_2$ (0.25 M), rt, 16 h. b) Iodoanisole (20 mol %), MeCN (0.25 M).

The proposed catalytic cycle (Figure 4) begins with iodotoluene **A** which is oxidized by Selectfluor salt into the difluorinated iodotoluene **B**. Then, $LiBF_4$ can perform a salt metathesis with **B** to produce LiF along with the active hypervalent iodoarene catalyst **C**. The activated hypervalent iodine catalyst **C** can coordinate to the alkene to form complex **D.** The nucleophilic oxygen of the amide will attack in the internal position and subsequent cyclization will furnish the desired oxazoline.

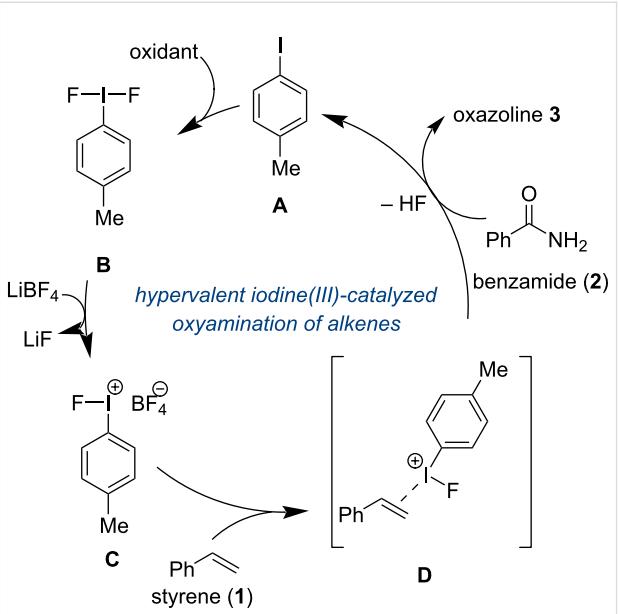

Figure 4: Proposed catalytic cycle for the hypervalent iodine-catalyzed amide and alkene coupling.

Conclusion

We have developed a hypervalent iodine-catalyzed amide and alkene coupling reaction. This reaction protocol furnished useful oxazoline products and introduced the use of lithium salts to activate hypervalent iodine catalysts. This strategy rendered the participation of simple and unadorned amides as bifunctional nucleophiles to achieve olefin oxyamination reactions. Time studies of these reactions further unveiled interesting mechanistic features that will be useful for our future catalysis development and asymmetric reaction designs.

Supporting Information

Supporting Information File 1

Spectral characterization of the products and kinetic studies.
[https://www.beilstein-journals.org/bjoc/content/supplementary/1860-5397-20-122-S1.pdf]

Acknowledgements

We thank Dr. Yong W. Kim (University of Toledo) for NMR assistance. Mr. Babatunde Obadawo (University of Toledo) is acknowledged for collecting the high-resolution mass spectrometry data. We acknowledge Dr. Navdeep Kaur's Ph. D. for her contributions in her Ph. D. thesis titled "Selective Conversion of Chemical Feedstock to O- and N-Containing Heterocycles".

Funding

We thank the National Institute of General Medical Sciences of the National Institutes of Health under Award Number R15GM139156 for supporting this work. We thank the University of Toledo for an internal seed grant from the Summer Research Awards and Fellowship Programs for supporting our initial work.

ORCID® iDs

Navdeep Kaur - https://orcid.org/0009-0009-5200-5106
Wei Li - https://orcid.org/0000-0001-8524-217X

Data Availability Statement

The data that supports the findings of this study is available from the corresponding author upon reasonable request.

References

1. Zhdankin, V. V.; Stang, P. J. *Chem. Rev.* **2002,** *102,* 2523–2584. doi:10.1021/cr010003+
2. Zhdankin, V. V.; Stang, P. J. *Chem. Rev.* **2008,** *108,* 5299–5358. doi:10.1021/cr800332c
3. Wirth, T. *Top. Curr. Chem.* **2003,** *224,* 1–4.
4. Merritt, E. A.; Olofsson, B. *Angew. Chem., Int. Ed.* **2009,** *48,* 9052–9070. doi:10.1002/anie.200904689
5. Yoshimura, A.; Zhdankin, V. V. *Chem. Rev.* **2016,** *116,* 3328–3435. doi:10.1021/acs.chemrev.5b00547
6. Ochiai, M.; Miyamoto, K. *Eur. J. Org. Chem.* **2008,** 4229–4239. doi:10.1002/ejoc.200800416
7. Dohi, T.; Kita, Y. *Chem. Commun.* **2009,** 2073–2085. doi:10.1039/b821747e
8. Fuchigami, T.; Fujita, T. *J. Org. Chem.* **1994,** *59,* 7190–7192. doi:10.1021/jo00103a003
9. Ochiai, M.; Takeuchi, Y.; Katayama, T.; Sueda, T.; Miyamoto, K. *J. Am. Chem. Soc.* **2005,** *127,* 12244–12245. doi:10.1021/ja0542800
10. Dohi, T.; Maruyama, A.; Yoshimura, M.; Morimoto, K.; Tohma, H.; Kita, Y. *Angew. Chem., Int. Ed.* **2005,** *44,* 6193–6196. doi:10.1002/anie.200501688
11. Hirt, U. H.; Spingler, B.; Wirth, T. *J. Org. Chem.* **1998,** *63,* 7674–7679. doi:10.1021/jo980475x
12. Dohi, T.; Maruyama, A.; Takenaga, N.; Senami, K.; Minamitsuji, Y.; Fujioka, H.; Caemmerer, S. B.; Kita, Y. *Angew. Chem., Int. Ed.* **2008,** *47,* 3787–3790. doi:10.1002/anie.200800464
13. Farid, U.; Wirth, T. *Angew. Chem., Int. Ed.* **2012,** *51,* 3462–3465. doi:10.1002/anie.201107703
14. Uyanik, M.; Yasui, T.; Ishihara, K. *Angew. Chem., Int. Ed.* **2010,** *49,* 2175–2177. doi:10.1002/anie.200907352

15. Guilbault, A.-A.; Basdevant, B.; Wanie, V.; Legault, C. Y. *J. Org. Chem.* **2012,** *77,* 11283–11295. doi:10.1021/jo302393u
16. Quindeau, S.; Lyvinec, G.; Marguerit, M.; Bathany, K.; Ozanne-Beaudenon, A.; Buffeteau, T.; Cavagnat, D.; Chénedé, A. *Angew. Chem., Int. Ed.* **2009,** *48,* 4605–4609. doi:10.1002/anie.200901039
17. Ishihara, K.; Muñiz, K. *Iodine Catalysis in Organic Synthesis;* Wiley-VCH: Weinheim, Germany, 2022. doi:10.1002/9783527829569
18. Li, X.; Chen, P.; Liu, G. *Beilstein J. Org. Chem.* **2018,** *14,* 1813–1825. doi:10.3762/bjoc.14.154
19. Romero, R. M.; Wöste, T. H.; Muñiz, K. *Chem. – Asian J.* **2014,** *9,* 972–983. doi:10.1002/asia.201301637
20. Lee, J. H.; Choi, S.; Hong, K. B. *Molecules* **2019,** *24,* 2634. doi:10.3390/molecules24142634
21. Ngatimin, M.; Frey, R.; Levens, A.; Nakano, Y.; Kowalczyk, M.; Konstas, K.; Hutt, O. E.; Lupton, D. W. *Org. Lett.* **2013,** *15,* 5858–5861. doi:10.1021/ol4029308
22. Braddock, D. C.; Cansell, G.; Hermitage, S. A. *Chem. Commun.* **2006,** 2483–2485. doi:10.1039/b604130b
23. Fabry, D. C.; Stodulski, M.; Hoerner, S.; Gulder, T. *Chem. – Eur. J.* **2012,** *18,* 10834–10838. doi:10.1002/chem.201201232
24. Kong, W.; Feige, P.; de Haro, T.; Nevado, C. *Angew. Chem., Int. Ed.* **2013,** *52,* 2469–2473. doi:10.1002/anie.201208471
25. Suzuki, S.; Kamo, T.; Fukushi, K.; Hiramatsu, T.; Tokunaga, E.; Dohi, T.; Kita, Y.; Shibata, N. *Chem. Sci.* **2014,** *5,* 2754–2760. doi:10.1039/c3sc53107d
26. Alhalib, A.; Kamouka, S.; Moran, W. J. *Org. Lett.* **2015,** *17,* 1453–1456. doi:10.1021/acs.orglett.5b00333
27. Mennie, K. M.; Banik, S. M.; Reichert, E. C.; Jacobsen, E. N. *J. Am. Chem. Soc.* **2018,** *140,* 4797–4802. doi:10.1021/jacs.8b02143
28. Woerly, E. M.; Banik, S. M.; Jacobsen, E. N. *J. Am. Chem. Soc.* **2016,** *138,* 13858–13861. doi:10.1021/jacs.6b09499
29. Stodulski, M.; Goetzinger, A.; Kohlhepp, S. V.; Gulder, T. *Chem. Commun.* **2014,** *50,* 3435–3438. doi:10.1039/c3cc49850f
30. Zhao, Z.; Jameel, I.; Murphy, G. K. *Synthesis* **2019,** *51,* 2648–2659. doi:10.1055/s-0037-1611562
31. Molnár, I. G.; Gilmour, R. *J. Am. Chem. Soc.* **2016,** *138,* 5004–5007. doi:10.1021/jacs.6b01183
32. Banik, S. M.; Medley, J. W.; Jacobsen, E. N. *J. Am. Chem. Soc.* **2016,** *138,* 5000–5003. doi:10.1021/jacs.6b02391
33. Yan, J.; Wang, H.; Yang, Z.; He, Y. *Synlett* **2009,** 2669–2672. doi:10.1055/s-0029-1217977
34. Zhong, W.; Liu, S.; Yang, J.; Meng, X.; Li, Z. *Org. Lett.* **2012,** *14,* 3336–3339. doi:10.1021/ol301311e
35. Haubenreisser, S.; Wöste, T. H.; Martínez, C.; Ishihara, K.; Muñiz, K. *Angew. Chem., Int. Ed.* **2016,** *55,* 413–417. doi:10.1002/anie.201507180
36. Gelis, C.; Dumoulin, A.; Bekkaye, M.; Neuville, L.; Masson, G. *Org. Lett.* **2017,** *19,* 278–281. doi:10.1021/acs.orglett.6b03631
37. Kong, A.; Blakey, S. B. *Synthesis* **2012,** *44,* 1190–1198. doi:10.1055/s-0031-1290591
38. Mizar, P.; Laverny, A.; El-Sherbini, M.; Farid, U.; Brown, M.; Malmedy, F.; Wirth, T. *Chem. – Eur. J.* **2014,** *20,* 9910–9913. doi:10.1002/chem.201403891
39. Röben, C.; Souto, J. A.; González, Y.; Lishchynskyi, A.; Muñiz, K. *Angew. Chem., Int. Ed.* **2011,** *50,* 9478–9482. doi:10.1002/anie.201103077
40. Muñiz, K.; Barreiro, L.; Romero, R. M.; Martínez, C. *J. Am. Chem. Soc.* **2017,** *139,* 4354–4357. doi:10.1021/jacs.7b01443
41. Qurban, J.; Elsherbini, M.; Wirth, T. *J. Org. Chem.* **2017,** *82,* 11872–11876. doi:10.1021/acs.joc.7b01571
42. Ulmer, A.; Stodulski, M.; Kohlhepp, S. V.; Patzelt, C.; Pöthig, A.; Bettray, W.; Gulder, T. *Chem. – Eur. J.* **2015,** *21,* 1444–1448. doi:10.1002/chem.201405888
43. Li, M.; Yu, F.; Qi, X.; Chen, P.; Liu, G. *Angew. Chem., Int. Ed.* **2016,** *55,* 13843–13848. doi:10.1002/anie.201607248
44. Qi, X.; Yu, F.; Chen, P.; Liu, G. *Angew. Chem., Int. Ed.* **2017,** *56,* 12692–12696. doi:10.1002/anie.201706401
45. Yoshimura, A.; Middleton, K. R.; Todora, A. D.; Kastern, B. J.; Koski, S. R.; Maskaev, A. V.; Zhdankin, V. V. *Org. Lett.* **2013,** *15,* 4010–4013. doi:10.1021/ol401815n
46. Xiang, C.; Li, T.; Yan, J. *Synth. Commun.* **2014,** *44,* 682–688. doi:10.1080/00397911.2013.834364
47. Wata, C.; Hashimoto, T. *J. Am. Chem. Soc.* **2021,** *143,* 1745–1751. doi:10.1021/jacs.0c11440
48. Gembreska, N. R.; Vogel, A. K.; Ziegelmeyer, E. C.; Cheng, E.; Wu, F.; Roberts, L. P.; Vesoulis, M. M.; Li, W. *Synlett* **2020,** *32,* 539–544. doi:10.1055/a-1277-8669
49. Wu, F.; Stewart, S.; Ariyarathna, J. P.; Li, W. *ACS Catal.* **2018,** *8,* 1921–1925. doi:10.1021/acscatal.7b04060
50. Wu, F.; Ariyarathna, J. P.; Alom, N.-E.; Kaur, N.; Li, W. *Org. Lett.* **2020,** *22,* 884–890. doi:10.1021/acs.orglett.9b04432
51. Wu, F.; Alom, N.-E.; Ariyarathna, J. P.; Naß, J.; Li, W. *Angew. Chem., Int. Ed.* **2019,** *58,* 11676–11680. doi:10.1002/anie.201904662
52. Wu, F.; Kaur, N.; Alom, N.-E.; Li, W. *JACS Au* **2021,** *1,* 734–741. doi:10.1021/jacsau.1c00103
53. Gratia, S. S.; Vigneau, E. S.; Eltayeb, S.; Patel, K.; Meyerhoefer, T. J.; Kershaw, S.; Huang, V.; De Castro, M. *Tetrahedron Lett.* **2014,** *55,* 448–452. doi:10.1016/j.tetlet.2013.11.054
54. Minakata, S.; Morino, Y.; Ide, T.; Oderaotoshi, Y.; Komatsu, M. *Chem. Commun.* **2007,** 3279–3281. doi:10.1039/b706572h
55. Mumford, E. M.; Hemric, B. N.; Denmark, S. E. *J. Am. Chem. Soc.* **2021,** *143,* 13408–13417. doi:10.1021/jacs.1c06750

License and Terms

BEILSTEIN JOURNAL OF ORGANIC CHEMISTRY

A comparison of structure, bonding and non-covalent interactions of aryl halide and diarylhalonium halogen-bond donors

Nicole Javaly, Theresa M. McCormick and David R. Stuart*

Full Research Paper

Open Access

Address:
Department of Chemistry, Portland State University, 1719 SW 10th Ave, Portland OR 97201, United States

Email:
David R. Stuart* - dstuart@pdx.edu

* Corresponding author

Keywords:
aryl halide; diarylhalonium; halogen; halogen bond; non-covalent interaction

Beilstein J. Org. Chem. **2024,** *20,* 1428–1435.
https://doi.org/10.3762/bjoc.20.125

Received: 26 March 2024
Accepted: 18 June 2024
Published: 27 June 2024

This article is part of the thematic issue "Hypervalent halogen chemistry".

Guest Editor: T. Gulder

Abstract

Halogen bonding permeates many areas of chemistry. A wide range of halogen-bond donors including neutral, cationic, monovalent, and hypervalent have been developed and studied. In this work we used density functional theory (DFT), natural bond orbital (NBO) theory, and quantum theory of atoms in molecules (QTAIM) to analyze aryl halogen-bond donors that are neutral, cationic, monovalent and hypervalent and in each series we include the halogens Cl, Br, I, and At. Within this diverse set of halogen-bond donors, we have found trends that relate halogen bond length with the van der Waals radii of the halogen and the non-covalent or partial covalency of the halogen bond. We have also developed a model to calculate ΔG of halogen-bond formation by the linear combination of the % p-orbital character on the halogen and energy of the σ-hole on the halogen-bond donor.

Introduction

Halogen bonding has emerged as an important attractive interaction in a wide range of applications that include crystal engineering, drug discovery and light-emitting materials [1-4]. Although, halogen bonding was first "observed" over 200 years ago [5,6] and the structural characteristics were elucidated in the latter half of the nineteenth century [7], the term "halogen bond" entered the chemical literature in the latter half of twentieth century [8]. Detailed studies of halogen bonding that followed in the late 1990s and early 2000s primarily focused on inorganic molecular and interhalogens, and inorganic and organic halides that are monovalent (Scheme 1a) [1-4]. Hypervalent halogen compounds, specifically diaryliodonium salts, have also been known to form Lewis acid–base adducts [9,10] and a relative scale to quantify this property has recently been reported [11,12]. Consequently, there has been a recent surge in the use of diarylhalonium salts in halogen-bonding catalysis [13-19].

Crabtree has outlined the similarity in molecular orbitals (MO) formed in halogen bonds and hypervalent bonds (and hydrogen

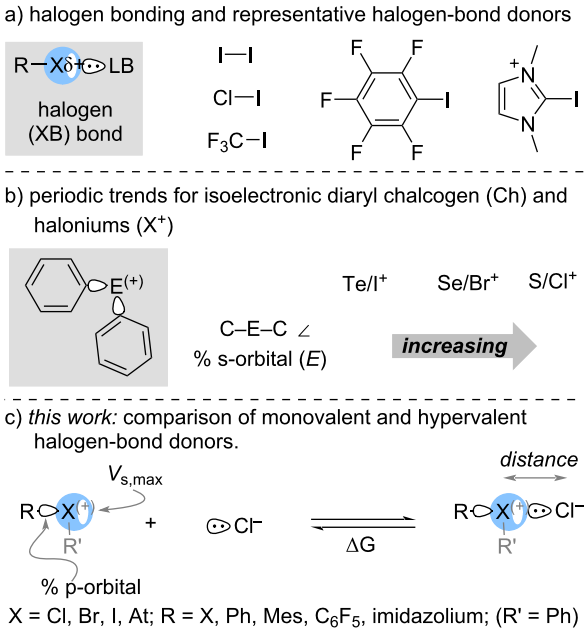

Scheme 1: Overview of halogen bonding.

bonds) [20]. Recently, we [21], and Legault and Huber [22], independently investigated the connection between electronic structure (bonding) and molecular structure (geometry) in diarylhalonium salts. We found a periodic trend with respect to the percentage of s- and p-orbital character used by the central atom to bond to the aryl substituents for a series of isoelectronic diaryl chalcogen and diarylhalonium compounds (Scheme 1b) [21]. The amount of s-character in the orbital used by the central atom (both chalcogen and halogen) to bond with the aryl groups decreases moving down the respective group (16 and 17) [21]. We also found with a limited set of six compounds that the association constant (K_a) for the halogen-bond interaction of diarylhalonium salts with pyridine decreased with increasing s-character used by the central halogen atom in the bond opposite the halogen bond; this is effectively the s-character in the σ*-orbital [21].

Conceptually, halogen-bond donors are commonly described by the electropositive σ-hole region, which is quantitatively described by $V_{s,max}$ on the halogen, though other factors have also been considered (Scheme 1a) [1-4,23-25]. Huber and co-workers have posed the question: "Is There a Single Ideal Parameter for Halogen-Bonding Based Lewis Acidity?", and concluded that, for a set of monovalent iodine-based halogen-bond donors, a linear combination of σ-hole and σ* energy provides a superior predictive ability than σ-hole alone [26]. In this work we compare a set of both monovalent and nominally hypervalent halogen-bond donors in which the central halogen atom is Cl, Br, I, and At. We have used density functional theory (DFT) to uncover periodic trends in the orbitals used by the central halogen atom in forming covalent and non-covalent interactions and how this impacts the interatomic distance and energy of halogen-bond interactions (Scheme 1c).

Results and Discussion

This study evolved from a parallel exploration of reactions involving unsymmetrical phenyl(mesityl)halonium salts, i.e., Ph(Mes)X$^+$. DFT analysis revealed similar structural trends to our previous work [21] when we expanded the halogens to include astatine (At). Due to its radioactivity and short half-life it would be very challenging to synthesize astatine analogs of diarylhalonium salts and almost no experimental data exists on halogen bonding with astatine for comparison with DFT-generated data. However, the inclusion of molecules containing At in this study provides an opportunity to expand the theoretical framework describing the structure, bonding, and reactivity of diarylhalonium compounds [27]. Although some relativistic effects of astatine may not be sufficiently incorporated in calculations [28], others have shown in theoretical and limited experimental studies that astatine does engage in halogen-bonding interactions [29,30]. In this work, a series of halogen-bond donor molecules and their halogen bond complexes with chloride anion were optimized at the M062x/6-311+G(d) level of theory [31] with def2-tzvpp used for iodine and astatine, and with SMD solvation in tetrahydrofuran (THF) incorporating Huber, Truhlar, and Cramer's correction for bromine and iodine [32] using Gaussian 09 [33]. Our prior work on the orbital analysis of diarylhalonium salts [21], showed good agreement between crystal structure data and energy-minimized structures at the B3LYP/cc-pvtz level with def2-qzvpp for iodine and tellurium and in the gas phase. In our present work using M06-2x/6-311+G(d) with def2-txvpp for iodine and astatine, we observed excellent agreement in the correlation between orbitals used on the halonium center and the C–X–C bond angle, i.e., molecular geometry, from our prior work (Scheme 2).

Given the similarities drawn between hypervalent and halogen bonding [20], we considered the association of the diarylhalonium cations **1**–**8** with chloride anion as well as the association of the monovalent subunits **25**–**36** with chloride anion (Scheme 3). We also considered the association of cationic monovalent halogen-bond donors **37**–**40** with chloride as the imidazolium iodide is a well-established core of halogen-bonding catalysts [34,35] (Scheme 3). In general, we observed that more exergonic association of the halogen-bond donors with chloride were associated with closer X---Cl contacts (Scheme 3). The monovalent halogen-bond donors of phenyl, mesityl, and pentafluorophenyl derivatives **25**–**35** had endergonic association with chloride (Scheme 3). Pentafluorophenyl astitide (**36**) was the only neutral monovalent halogen-bond

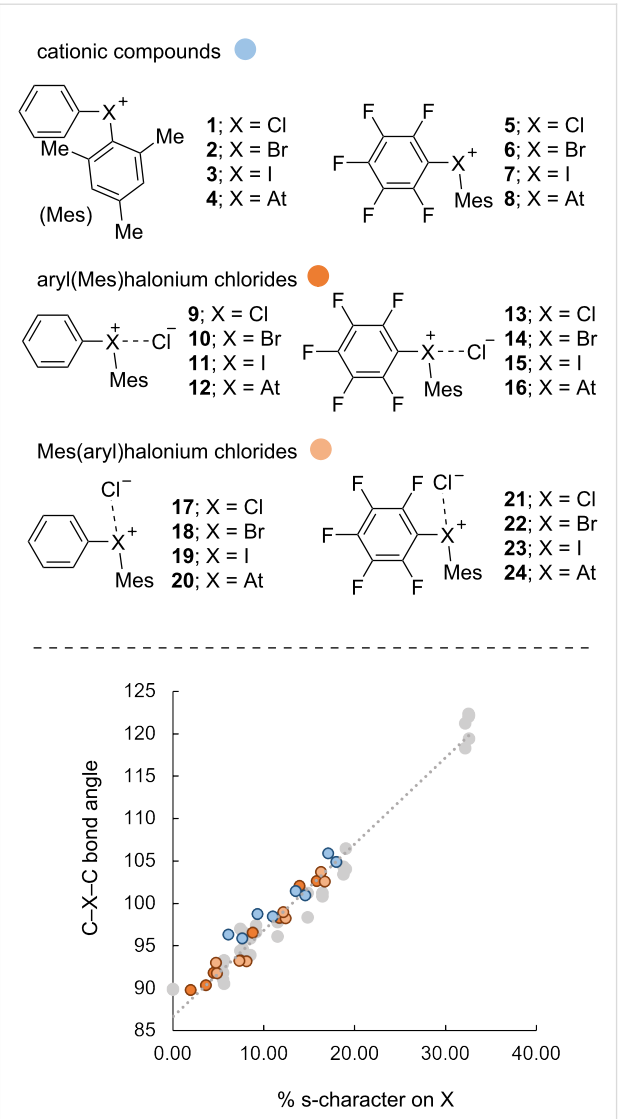

Scheme 2: Correlation of orbital character on halogen with C–X–C bond angle for compounds **1**–**24**; data from prior work is represented by grey dots [21].

donor with an exergonic association with chloride (ΔG = −5.0 kcal/mol). The X---Cl distance calculated for the halogen-bonding complexes **41** and **45** of phenyl chloride (**25**) and mesityl chloride (**29**) with chloride anion were 3.85 and 3.71 Å, respectively. These values are larger than the sum of the van der Waals radii (3.5 Å) for two chlorine atoms [36] and therefore unlikely to represent a substantial halogen-bonding interaction. The hypervalent halogen-bond donors **1**–**8** had substantially more exergonic association with chloride than their monovalent subunits. For instance, the association of chloride with pentafluorophenyl bromide (**34**) was ΔG = 1.6 kcal/mol, whereas the association of chloride with pentafluorophenyl(mesityl)bromonium (**6**) was ΔG = −13.2 kcal/mol. The overall charge on the halogen-bond donor also has an impact on the energy of association. The association of chloride with the diarylhalonium cations **1**–**8** had ΔG values that ranged from −5.9 to −23.1 kcal/mol (see Supporting Information File 1 for exact values). Likewise, the association of chloride with imidazolium halides **37**–**40** ranged from −3.7 to −14.3 kcal/mol, which overlaps with the range observed for the diarylhalonium cations.

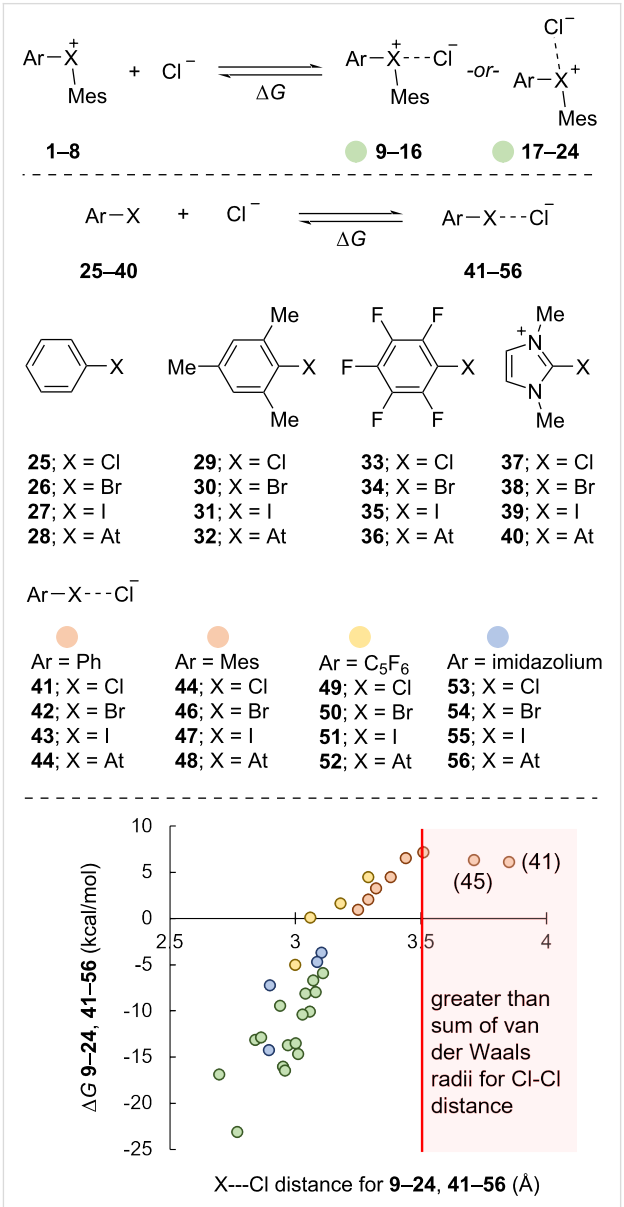

Scheme 3: Correlation of ΔG for XB bond formation and X---Cl distance for compounds **9**–**24** (green dots), **41**–**48** (orange dots), **49**–**52** (yellow dots), and **53**–**56** (blue dots).

We delved deeper into the periodic trends related to the X---Cl distance for halogen-bond complexes **9**–**24**, **42**–**44**, and **46**–**56**; representative examples are shown in Scheme 4. As a reference we considered the trend in X–Cl covalent bond distance with

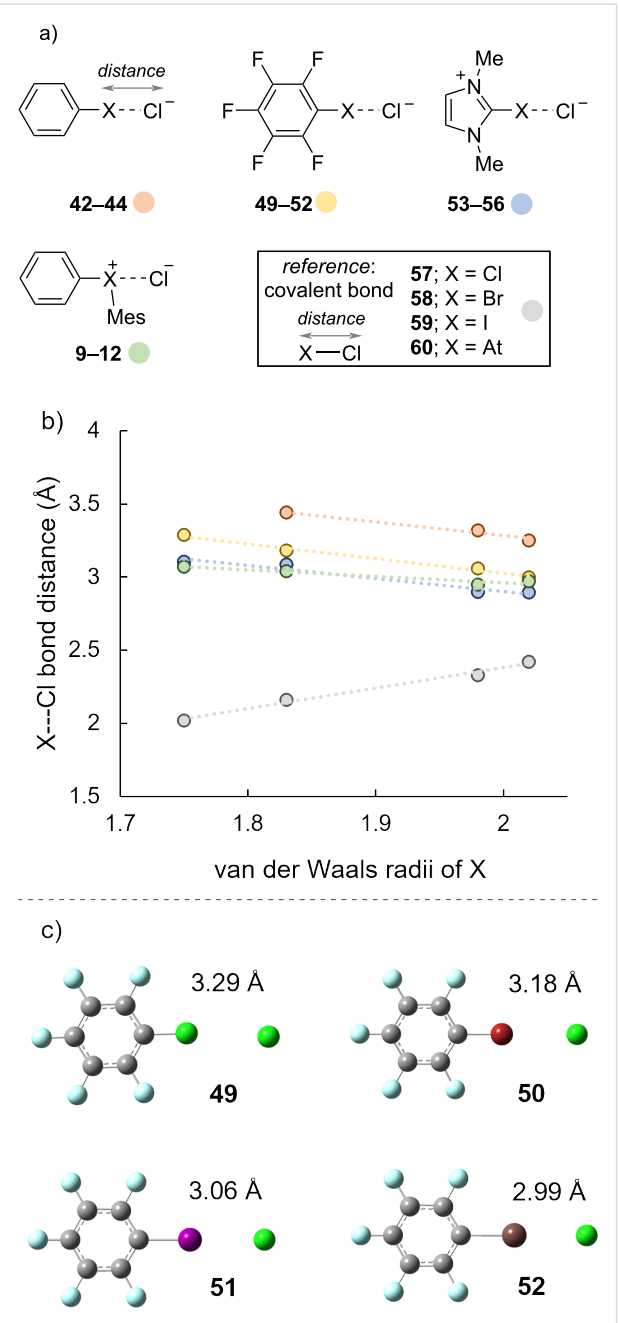

Scheme 4: Correlation of X---Cl distance with van der Waals radii of X.

respect to the van der Waals radii of X [36], and we observed a linear trend with a positive slope (Scheme 4b, grey dots). That is the length of the X–Cl (**57**–**60**) covalent bond increases with increasing van der Waals radii of X. Notably, this trend is also replicated for ionic bonds of the halides with sodium; longer ionic bond lengths are observed for larger halides [37]. On the other hand, halogen-bond complexes that we studied here revealed an opposite trend (Scheme 4b, orange, yellow, blue, and green dots). The halogen-bond length decreased with increasing van der Waals radii of X and the trend was more pronounced for monovalent halogen-bond donors. This is exemplified by halogen-bond complexes of the pentafluorophenyl halide series with chloride anion (Scheme 4c, **49**–**52**). A similar trend for decreasing bond length with increasing van der Waals radii has also been observed for some [38], though not all [39], series of chalcogen bonds. Generally, shorter bonds are stronger and longer bonds are weaker, and the trend we observe here for halogen bonding aligns with that rule of thumb (Scheme 3). The conceptual frameworks underpinning covalent and ionic bonds are orbital overlap and electrostatic attraction, respectively. Therefore, if larger van der Waals radii are associated with longer, weaker bonds where both these phenomena (orbital overlap and electrostatics) are operative (covalent and ionic bonds), our observations suggest a unique feature of halogen bonding that relates to bond length. Pauli repulsion and dispersion are additional factors that have been included in defining halogen bonds [25]. Smaller halogens that are less able to disperse lone-pairs may have greater destabilizing repulsive forces associated with them that ultimately lengthen the halogen bond relative to those of larger halogens [22,40].

Further analysis of the XB complexes revealed additional distinctions in the nature of the halogen bonds (Scheme 5). We used Bader's quantum theory of atoms in molecules (QTAIM) [41] and assessed ρ(r), ∇2(r), and associated values. However, to minimize complexity we elected to focus on the distance between the bond critical points (BCP) and the atomic centers (available in Supporting Information File 1, Table S8) and the electronic energy at the BCPs, *E*(r) (Scheme 5). On the bond-

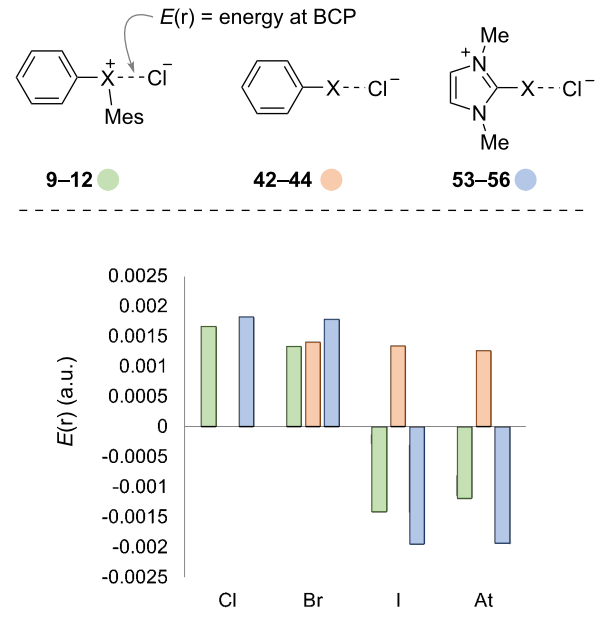

Scheme 5: Comparison of *E*(r) for XB complexes **9**–**12**, **42**–**44**, and **53**–**56**.

ing continuum positive values of E(r) are generally associated non-covalent bonds and negative values of E(r) indicate increasing covalency [42]. We observed a switch from positive E(r) values for the lighter hypervalent phenyl(mesityl)haloniums **9** and **10** (X = Cl and Br) to negative E(r) values for the heavier haloniums **11** and **12** (X = I and At, Scheme 5, green bars). Uchiyama previously suggested that the diarylchloronium **9** has a "breakdown of the hypervalent bond" [43], and our data suggest that the interaction (halogen or hypervalent bond) between chloride anion and diarylchloronium cation **9** is non-covalent and likely dominated by electrostatic attraction. A similar switch from non-covalent halogen bond for the lighter (X = Cl and Br) to partially covalent halogen bond for the heavier (X = I and At) was also observed for the cationic imidazolium series of XB donors **53**–**56** (Scheme 5, blue bars). The neutral monovalent XB donors **26**–**28** formed halogen-bonding complexes **42**–**44** with non-covalent interactions in all cases, even those with heavier halogen iodine and astatine (Scheme 5, orange bars).

We turned our attention from periodic trends in XB length to periodic trends in XB strength. The σ-bond oriented 180° relative to the halogen bond plays a central role in tuning the halogen bond properties [1-4]. Indeed, it impacts the size of the σ-hole ($V_{s,max}$), and the energy of the σ* orbital has been shown be a key component of a predictive model for halogen-bond strength [26]. However, a confounding, though rarely discussed, factor for halogen-bond strength is the composition (s/p-character) of the orbital on the halogen atom that is engaged in the σ-bond (Scheme 6a). We have previously shown that larger association constants (K_{eq}) were measured for hypervalent halogen-bond donors with greater calculated p-character on the halogen participating in the σ-bond opposite the hypervalent (or halogen) bond; both K_{eq} and p-character on X increased in the order Cl < Br < I [21]. We conducted a similar analysis here in which we plotted the percent p-orbital contribution on the XB donor against ΔG determined by DFT (Scheme 6b). Although, we found that this feature is a poor global predictor of ΔG, clear periodic trends are observed when related groups of XB donors are considered (Scheme 6b). When the halogen-bond donors are clustered into hypervalent **1**–**8** (Scheme 6b, green dots), monovalent aryl **26**–**28** and **30**–**32** (Scheme 6b, orange dots), perfluorophenyl **33**–**36** (Scheme 6b, yellow dots), and imidazolium **37**–**40** (Scheme 6b, blue dots) linear correlations with similar slopes are observed for p-orbital character and ΔG (Scheme 6b). Analysis in this way also provides an opportunity for comparison between these groups for the same halogen, that is a comparison between monovalent and hypervalent halogen-bond donors, and neutral and cationic halogen-bond donors. First, when the halogen is held constant it can be seen that the different classes of halogen-bond donors (monovalent vs hypervalent) use similar orbital composition to form the σ-bond with the aryl group (Scheme 6b). The percentage of p-character in the σ-orbital for halogen-bond donors with X = Cl is ≈80-82%, X = Br is ≈84–86%, X = I is ≈88–91%, and X = At is ≈92–94%. Interestingly, monovalent halogen-bond donors use slightly more p-orbital character to bond with the aryl group than their hypervalent counterparts. For example, in phenyl iodide (**27**) the iodine atom uses 88.97% p-character to bond with the phe-

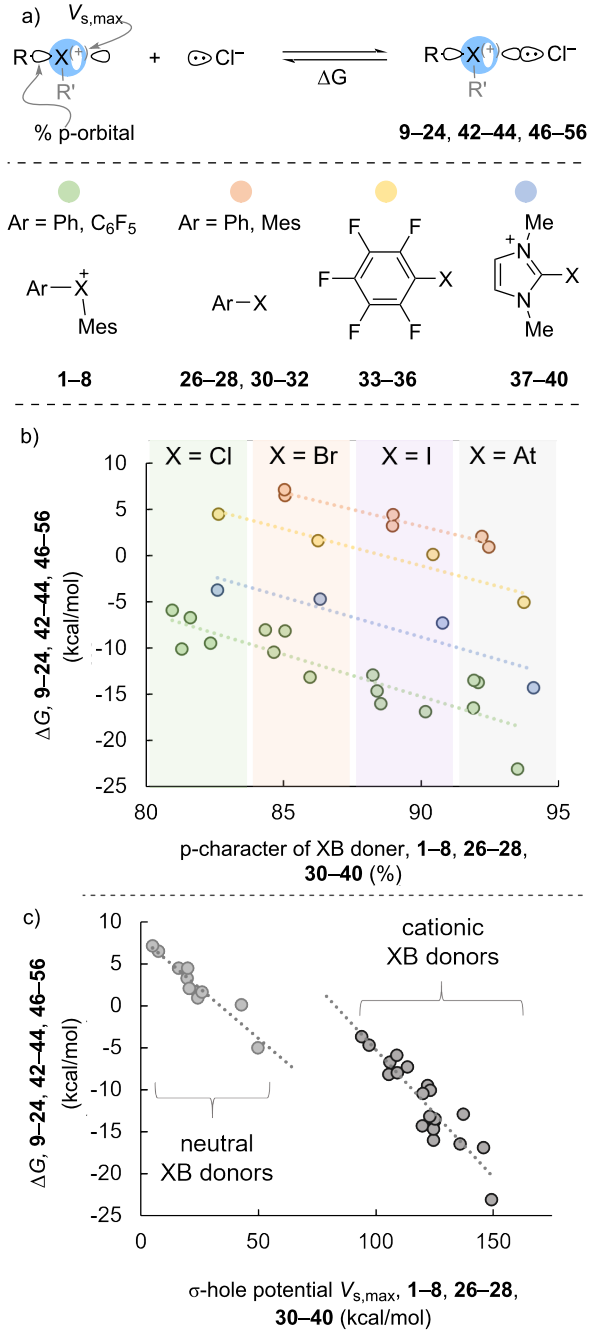

Scheme 6: Correlation of p-character and $V_{s,max}$ on X of XB donor with ΔG of XB bond.

nyl group, whereas in phenyl(mesityl)iodonium cation (**3**) the iodine atom uses 88.54% p-character to bond with the phenyl group. Phenyl iodide (**27**) has three lone-pairs, whereas the phenyl(mesityl)iodonium cation (**3**) has two lone-pairs (though it does have another aryl group), and therefore this observation is consistent with Bent's rule in which lone-pairs are stabilized by being in orbitals with more s-character [44]. An additional observation regarding the p-character directed at the aryl group by the halogen center relates to the charge on the halogen-bond donor. The halogen of the cationic imidazolium halogen-bond donors **37**–**40** has the largest amount of p-orbital character in bonding with the aryl group, this was followed by the perfluorophenyl monovalent halogen bond donors **33**–**36**, then monovalent aryl halogen-bond donors **26**–**28** and **30**–**32**, and finally hypervalent halogen-bond donors **1**–**8**. This observation is also consistent with Bent's rule in which greater p-character is directed toward more electronegative ligands [44].

We also consider a correlation between $V_{s,max}$ of the halogen-bond donor and ΔG of the halogen bond (Scheme 6c) [45]. Although a modest linear correlation ($R^2 = 0.90$) was observed over all data points, in which XB donors with larger $V_{s,max}$ values also had more exergonic associations, we actually observed two almost parallel clusters of data (Scheme 6c). In this case, neutral XB donors **26**–**28**, and **30**–**36** had $V_{s,max}$ values ≈5–50 kcal/mol and a slope of −0.24 (Scheme 6c, light grey dots), whereas cationic XB donors **1**–**8** and **37**–**40** had $V_{s,max}$ values ≈100–150 kcal/mol and a slope of −0.30 (Scheme 6c, dark grey dots). So, the distinction in our data set regarding $V_{s,max}$ is not between monovalent and hypervalent halogen-bond donors, but rather between neutral and cationic halogen-bond donors. Three additional points regarding these data sets warrant comment. First, within the neutral XB donors it is perhaps not surprising that perfluoroaryl XB donors **32**–**36** had substantially larger $V_{s,max}$ values than their non-fluorinated counter parts. Second, two data points are especially representative of the discontinuity in these data sets, the pentafluorophenyl astitide XB donor **36** has a $V_{s,max}$ = 49.8 kcal/mol and ΔG = −5.0 kcal/mol, on the other hand cationic imidazolium chloride XB donor **37** has a $V_{s,max}$ = 94.0 kcal/mol (almost two fold that of **36**) yet has a ΔG = −3.7 kcal/mol (less than that of **36**). Third, within the cationic XB donors the hypervalent haloniums **1**–**8** in which the positive charge is primarily located on the halogen had larger $V_{s,max}$ values than the imidazolium halides **37**–**40** in which the positive charge is primarily delocalized on the imidazolium ring.

We have developed a model for ΔG of the halogen bonds investigated in this work by merging the two concepts of p-orbital character and $V_{s,max}$ of the XB donor (Scheme 7). Although we considered other characteristics of XB donors, including NPA charges and Hirshfeld charges (available in Supporting Information File 1, Table S5), the linear combination of p-character (%) and σ-hole ($V_{s,max}$) provided the highest correlation based on linear regression analysis of ΔG_{DFT} vs ΔG_{calc}, wherein ΔG_{calc} is obtained from Equation 1 [46].

$$\Delta G_{calc} = -1.95\ (\%\ \text{p orbital}) - 7.56\ (V_{s,max}) - 6.78 \quad (1)$$

Our model was developed with normalized parameters of % p-orbital character and $V_{s,max}$ and therefore a comparison of the parameter coefficients reveals that $V_{s,max}$ is a more dominant term than % p-orbital character in predicting ΔG (Equation 1 and Scheme 7). However, the % p-character term is non-negligible and demonstrates that this highly intuitive parameter contributes to the prediction of ΔG for halogen bonding. It is important to point out that this model is limited to the halogen-bond donors studied here and their interaction with chloride anion, although it is likely that prediction of ΔG with Equation 1 for structurally similar halogen-bond donors would be successful provided the parameters (% p-character and $V_{s,max}$) are known. However, ΔG cannot be predicted for halogen-bond acceptors other than chloride and a more general predictive model should include parameters to describe the Lewis basic halogen-bond acceptor.

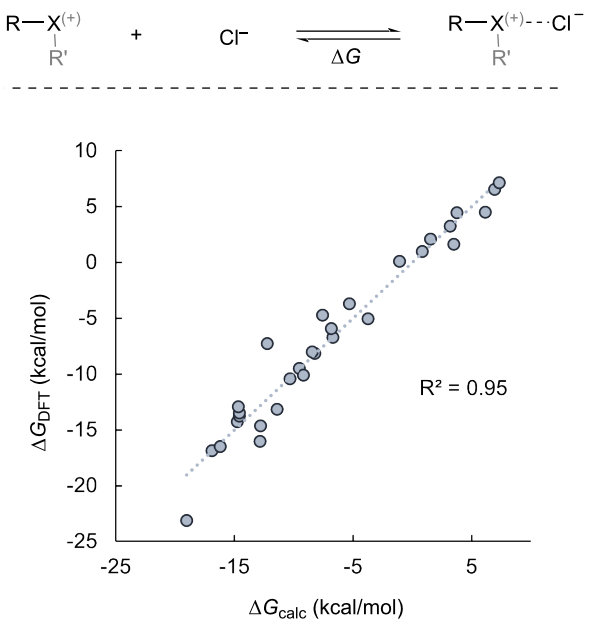

Scheme 7: Model for ΔG based on Equation 1.

Conclusion

In this work, we have compared the characteristics of monovalent, hypervalent, neutral, and cationic XB donors and their XB

complexes with chloride anion by DFT. The structural characteristics of the diaryliodonium cations (XB donors) and diaryliodonium chloride salts (XB complexes) are consistent with our previous model that correlates s/p-orbital composition and C–X–C bond angle. The XB complexes that we studied generally follow the heuristic that stronger bonds are associated with shorter bonds. We found, however, that unlike covalent and ionic bonds, the halogen bonds studied decrease in length with increasing van der Waals radii of the halogen, and we suggest that this is possibly due to greater dispersive and lesser repulsive forces for larger halogens. This finding may prove useful in catalyst design where close spatial proximity of the substrate to other important structural information (i.e., chirality) has an impact on selectivity. Our analysis of selected XB complexes by QTAIM revealed that for cationic XB donors of the lighter halogens (X = Cl and Br) have non-covalent halogen bonds and those of the heavier halogens (X = I and At) have partially covalent halogen bonds. Clustered analysis of the XB donor parameters % p-orbital character and σ-hole potential ($V_{s,max}$) showed linear correlations with ΔG_{DFT} of the halogen bond. The linear combination of the normalized parameters (% p-orbital character and $V_{s,max}$) provides a model to calculate ΔG of the halogen bond.

Supporting Information

Supporting Information File 1

Computational data.
[https://www.beilstein-journals.org/bjoc/content/supplementary/1860-5397-20-125-S1.pdf]

Supporting Information File 2

Coordinates of optimized structures.
[https://www.beilstein-journals.org/bjoc/content/supplementary/1860-5397-20-125-S2.xyz]

Funding

This work was funded by the National Science Foundation (CHE 2154500). The NSF provided funding for the high-performance computing cluster at PSU (DMS 1624776).

Author Contributions

Nicole Javaly: data curation; formal analysis; methodology; visualization; writing – original draft; writing – review & editing. Theresa M. McCormick: conceptualization; formal analysis; funding acquisition; supervision; writing – review & editing. David R. Stuart: conceptualization; formal analysis; funding acquisition; methodology; supervision; visualization; writing – original draft; writing – review & editing.

ORCID® iDs

David R. Stuart - https://orcid.org/0000-0003-3519-9067

Data Availability Statement

All data that supports the findings of this study is available in the published article and/or the supporting information to this article.

References

1. Cavallo, G.; Metrangolo, P.; Milani, R.; Pilati, T.; Priimagi, A.; Resnati, G.; Terraneo, G. *Chem. Rev.* **2016,** *116,* 2478–2601. doi:10.1021/acs.chemrev.5b00484
2. Beale, T. M.; Chudzinski, M. G.; Sarwar, M. G.; Taylor, M. S. *Chem. Soc. Rev.* **2013,** *42,* 1667–1680. doi:10.1039/c2cs35213c
3. Gilday, L. C.; Robinson, S. W.; Barendt, T. A.; Langton, M. J.; Mullaney, B. R.; Beer, P. D. *Chem. Rev.* **2015,** *115,* 7118–7195. doi:10.1021/cr500674c
4. Kolář, M. H.; Hobza, P. *Chem. Rev.* **2016,** *116,* 5155–5187. doi:10.1021/acs.chemrev.5b00560
5. Colin, M. M.; Gaultier de Claubry, H. *Ann. Chim. (Cachan, Fr.)* **1814,** *90,* 87–100.
6. Colin, M. M. *Ann. Chim. (Cachan, Fr.)* **1814,** *91,* 252–272.
7. Guthrie, F. *J. Chem. Soc.* **1863,** *16,* 239–244. doi:10.1039/js8631600239
8. Zingaro, R. A.; Hedges, R. M. *J. Phys. Chem.* **1961,** *65,* 1132–1138. doi:10.1021/j100825a010
9. Ochiai, M.; Suefuji, T.; Miyamoto, K.; Tada, N.; Goto, S.; Shiro, M.; Sakamoto, S.; Yamaguchi, K. *J. Am. Chem. Soc.* **2003,** *125,* 769–773. doi:10.1021/ja0211205
10. Ochiai, M.; Suefuji, T.; Shiro, M.; Yamaguchi, K. *Heterocycles* **2006,** *67,* 391. doi:10.3987/com-05-s(t)8
11. Labattut, A.; Tremblay, P.-L.; Moutounet, O.; Legault, C. Y. *J. Org. Chem.* **2017,** *82,* 11891–11896. doi:10.1021/acs.joc.7b01616
12. Mayer, R. J.; Ofial, A. R.; Mayr, H.; Legault, C. Y. *J. Am. Chem. Soc.* **2020,** *142,* 5221–5233. doi:10.1021/jacs.9b12998
13. Zhang, Y.; Han, J.; Liu, Z.-J. *RSC Adv.* **2015,** *5,* 25485–25488. doi:10.1039/c5ra00209e
14. Heinen, F.; Engelage, E.; Dreger, A.; Weiss, R.; Huber, S. M. *Angew. Chem., Int. Ed.* **2018,** *57,* 3830–3833. doi:10.1002/anie.201713012
15. Heinen, F.; Engelage, E.; Cramer, C. J.; Huber, S. M. *J. Am. Chem. Soc.* **2020,** *142,* 8633–8640. doi:10.1021/jacs.9b13309
16. Heinen, F.; Reinhard, D. L.; Engelage, E.; Huber, S. M. *Angew. Chem., Int. Ed.* **2021,** *60,* 5069–5073. doi:10.1002/anie.202013172
17. Nishida, Y.; Suzuki, T.; Takagi, Y.; Amma, E.; Tajima, R.; Kuwano, S.; Arai, T. *ChemPlusChem* **2021,** *86,* 741–744. doi:10.1002/cplu.202100089
18. Yoshida, Y.; Ishikawa, S.; Mino, T.; Sakamoto, M. *Chem. Commun.* **2021,** *57,* 2519–2522. doi:10.1039/d0cc07733j
19. Yunusova, S. N.; Novikov, A. S.; Soldatova, N. S.; Vovk, M. A.; Bolotin, D. S. *RSC Adv.* **2021,** *11,* 4574–4583. doi:10.1039/d0ra09640g
20. Crabtree, R. H. *Chem. Soc. Rev.* **2017,** *46,* 1720–1729. doi:10.1039/c6cs00688d
21. Karandikar, S. S.; Bhattacharjee, A.; Metze, B. E.; Javaly, N.; Valente, E. J.; McCormick, T. M.; Stuart, D. R. *Chem. Sci.* **2022,** *13,* 6532–6540. doi:10.1039/d2sc02332f
22. Robidas, R.; Reinhard, D. L.; Huber, S. M.; Legault, C. Y. *ChemPhysChem* **2023,** *24,* e202200634. doi:10.1002/cphc.202200634

23. Řezáč, J.; de la Lande, A. *Phys. Chem. Chem. Phys.* **2017,** *19,* 791–803. doi:10.1039/c6cp07475h
24. Riley, K. E.; Hobza, P. *Phys. Chem. Chem. Phys.* **2013,** *15,* 17742. doi:10.1039/c3cp52768a
25. Thirman, J.; Engelage, E.; Huber, S. M.; Head-Gordon, M. *Phys. Chem. Chem. Phys.* **2018,** *20,* 905–915. doi:10.1039/c7cp06959f
26. Engelage, E.; Reinhard, D.; Huber, S. M. *Chem. – Eur. J.* **2020,** *26,* 3843–3861. doi:10.1002/chem.201905273
27. Rossi, E.; De Santis, M.; Sorbelli, D.; Storchi, L.; Belpassi, L.; Belanzoni, P. *Phys. Chem. Chem. Phys.* **2020,** *22,* 1897–1910. doi:10.1039/c9cp06293a
28. Gamboni, G.; Belpassi, L.; Belanzoni, P. *ChemPhysChem* **2024,** e202400310. doi:10.1002/cphc.202400310
29. Devore, D. P.; Ellington, T. L.; Shuford, K. L. *J. Phys. Chem. A* **2024,** *128,* 1477–1490. doi:10.1021/acs.jpca.3c06894
30. Guo, N.; Maurice, R.; Teze, D.; Graton, J.; Champion, J.; Montavon, G.; Galland, N. *Nat. Chem.* **2018,** *10,* 428–434. doi:10.1038/s41557-018-0011-1
31. Wang, Y.; Verma, P.; Jin, X.; Truhlar, D. G.; He, X. *Proc. Natl. Acad. Sci. U. S. A.* **2018,** *115,* 10257–10262. doi:10.1073/pnas.1810421115
32. Engelage, E.; Schulz, N.; Heinen, F.; Huber, S. M.; Truhlar, D. G.; Cramer, C. J. *Chem. – Eur. J.* **2018,** *24,* 15983–15987. doi:10.1002/chem.201803652
33. *Gaussian 09,* Revision D.01; Gaussian, Inc.: Wallingford, CT, 2013.
34. Gliese, J.-P.; Jungbauer, S. H.; Huber, S. M. *Chem. Commun.* **2017,** *53,* 12052–12055. doi:10.1039/c7cc07175b
35. Sutar, R. L.; Erochok, N.; Huber, S. M. *Org. Biomol. Chem.* **2021,** *19,* 770–774. doi:10.1039/d0ob02503h
36. Mantina, M.; Chamberlin, A. C.; Valero, R.; Cramer, C. J.; Truhlar, D. G. *J. Phys. Chem. A* **2009,** *113,* 5806–5812. doi:10.1021/jp8111556
37. CCCBDB bond length model; NIST Computational Chemistry Comparison and Benchmark Database; NIST Standard Reference Database Number 101, Release 22; May 2022; Russell, D. Johnson, III. https://cccbdb.nist.gov/bondlengthmodel2x.asp?method=51&basis=20 (accessed March 19, 2024).
38. Oliveira, V.; Cremer, D.; Kraka, E. *J. Phys. Chem. A* **2017,** *121,* 6845–6862. doi:10.1021/acs.jpca.7b06479
39. de Azevedo Santos, L.; van der Lubbe, S. C. C.; Hamlin, T. A.; Ramalho, T. C.; Matthias Bickelhaupt, F. *ChemistryOpen* **2021,** *10,* 391–401. doi:10.1002/open.202000323
40. Ramasami, P.; Murray, J. S. *J. Mol. Model.* **2024,** *30,* 81. doi:10.1007/s00894-024-05869-5
41. Bader, R. F. W. *Chem. Rev.* **1991,** *91,* 893–928. doi:10.1021/cr00005a013
42. Miller, D. K.; Chernyshov, I. Y.; Torubaev, Y. V.; Rosokha, S. V. *Phys. Chem. Chem. Phys.* **2022,** *24,* 8251–8259. doi:10.1039/d1cp05441d
43. Nakajima, M.; Miyamoto, K.; Hirano, K.; Uchiyama, M. *J. Am. Chem. Soc.* **2019,** *141,* 6499–6503. doi:10.1021/jacs.9b02436
44. Bent, H. A. *Chem. Rev.* **1961,** *61,* 275–311. doi:10.1021/cr60211a005
45. Donald, K. J.; Pham, N.; Ravichandran, P. *J. Phys. Chem. A* **2023,** *127,* 10147–10158. doi:10.1021/acs.jpca.3c05797
46. Santiago, C. B.; Guo, J.-Y.; Sigman, M. S. *Chem. Sci.* **2018,** *9,* 2398–2412. doi:10.1039/c7sc04679k

License and Terms

BEILSTEIN JOURNAL OF ORGANIC CHEMISTRY

Predicting bond dissociation energies of cyclic hypervalent halogen reagents using DFT calculations and graph attention network model

Yingbo Shao[‡1], Zhiyuan Ren[‡1], Zhihui Han[1], Li Chen[*1], Yao Li[*2] and Xiao-Song Xue[*2,3]

Letter

Open Access

Address:
[1]State Key Laboratory of Elemento-Organic Chemistry, College of Chemistry, Nankai University, Tianjin 300071, P. R. China, [2]Key Laboratory of Fluorine and Nitrogen Chemistry and Advanced Materials, Shanghai Institute of Organic Chemistry, University of Chinese Academy of Sciences, Shanghai 200032, P. R. China, and [3]School of Chemistry and Material Sciences, Hangzhou Institute for Advanced Study, University of Chinese Academy of Sciences, Hangzhou 310024, P. R. China

Email:
Li Chen[*] - chenliyss@nankai.edu.cn; Yao Li[*] - liyao@sioc.ac.cn; Xiao-Song Xue[*] - xuexs@sioc.ac.cn

* Corresponding author ‡ Equal contributors

Keywords:
BDE; cyclic hypervalent halogen reagents; DFT calculation; graph attention network; machine learning

Beilstein J. Org. Chem. **2024,** *20,* 1444–1452.
https://doi.org/10.3762/bjoc.20.127

Received: 15 March 2024
Accepted: 17 June 2024
Published: 28 June 2024

This article is part of the thematic issue "Hypervalent halogen chemistry".

Guest Editor: J. Wencel-Delord

Abstract

Although hypervalent iodine(III) reagents have become staples in organic chemistry, the exploration of their isoelectronic counterparts, namely hypervalent bromine(III) and chlorine(III) reagents, has been relatively limited, partly due to challenges in synthesizing and stabilizing these compounds. In this study, we conduct a thorough examination of both homolytic and heterolytic bond dissociation energies (BDEs) critical for assessing the chemical stability and functional group transfer capability of cyclic hypervalent halogen compounds using density functional theory (DFT) analysis. A moderate linear correlation was observed between the homolytic BDEs across different halogen centers, while a strong linear correlation was noted among the heterolytic BDEs across these centers. Furthermore, we developed a predictive model for both homolytic and heterolytic BDEs of cyclic hypervalent halogen compounds using machine learning algorithms. The results of this study could aid in estimating the chemical stability and functional group transfer capabilities of hypervalent bromine(III) and chlorine(III) reagents, thereby facilitating their development.

Introduction

Hypervalent iodine reagents are increasingly gaining attention in the fields of organic synthesis and catalysis due to their environmental benefits, accessibility, and cost-efficiency [1-11]. Over the last three decades, a series of cyclic hypervalent iodine(III) reagents has been developed [12-17] (Figure 1), including the well-known Zhdankin reagents [13] and Togni

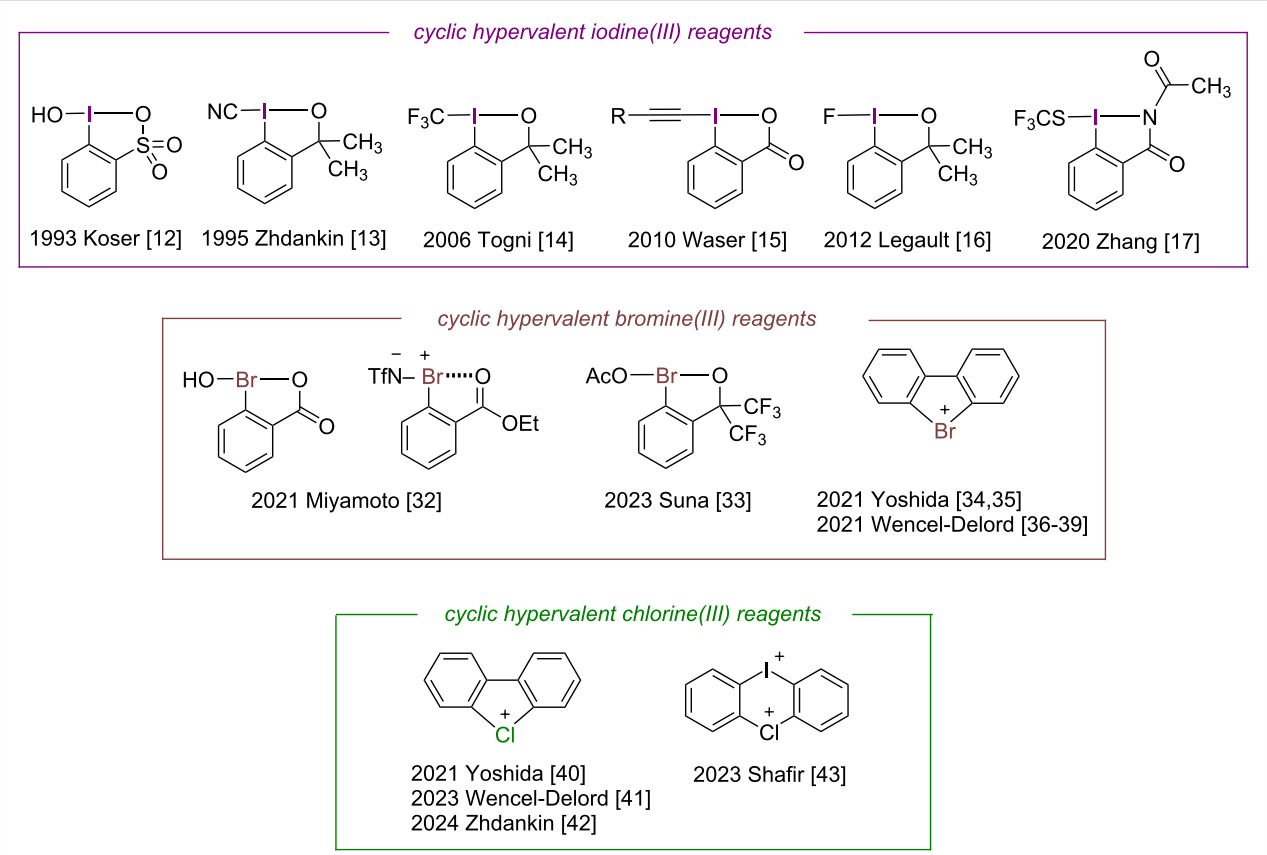

Figure 1: Examples of cyclic hypervalent halogen reagents.

reagents [14]. These reagents are popularly used as electrophilic group transfer reagents [18,19] in a variety of reactions, such as C–H functionalization [20-22], unsaturated alkane addition [23,24], and cyclization [25,26].

Despite the rapid development of hypervalent iodine(III) reagents, the exploration of isoelectronic hypervalent bromine(III) and chlorine(III) reagents has been comparatively limited despite their demonstrated potential for unique applications [27-30]. For example, hypervalent bromine(III) reagents enable C–H amination and alkene aziridination reactions without the need for additional Lewis acid activation [31-33]. However, challenges in the synthesis and stabilization of cyclic hypervalent bromine and chlorine reagents have impeded their development relative to their iodine(III) analogs [27-30]. Cyclic hypervalent bromine(III) reagents were pioneered by Miyamoto [32] and have since been developed to a certain extent [33]. Biphenyl hypervalent bromine(III) reagents [34-39] have been synthesized by Yoshida and Wencel-Delord (Figure 1). Cyclic hypervalent chlorine(III) reagents with similar skeletal structures have not been reported yet, and only biphenyl hypervalent chlorine(III) reagents [40-42] and cyclic diaryliodonium salts [43] have been synthesized.

Previous investigations [44-47] have highlighted the critical role of bond dissociation energy (BDE) in understanding the group transfer capabilities and chemical stability of hypervalent iodine(III) reagents. In this context, detailed knowledge of the BDE of hypervalent bromine(III) and chlorine(III) reagents is especially crucial for designing novel reagents. Yet, the BDE values of hypervalent bromine(III) and chlorine(III) reagents remain largely elusive, hampering the design and synthesis of novel reagents.

In recent years, machine learning has emerged as a promising and cost-effective alternative to traditional DFT calculations for predicting key properties of organic molecules such as BDE, nucleophilicity, and electrophilicity [48-60]. Recently, applications of the Elastic Net model with Avalon fingerprints [55] and the deployment of artificial neural network (ANN) models [57] with the Mordred cheminformatics package have demonstrated considerable success in predicting the BDEs of hypervalent iodine(III) reagents. However, previous studies have been limited to the prediction of hypervalent iodine(III) reagents. Driven by their proven effectiveness and our ongoing interest in hypervalent halogen chemistry [61-72], we are motivated to develop a machine learning model for a broader array of cyclic

hypervalent halogen reagents, thereby integrating different halogen centers and making it easier to predict the group transfer capacity and chemical stability of different cyclic hypervalent halogen reagents.

Results and Discussion

We selected five different skeletons and twenty common transfer groups for combination (Figure 2) and calculated their BDEs. Referring to the previous computational studies of hypervalent iodine [61-76] and the computational database of organic species by Paton and co-workers [77], geometry optimizations and single point energy calculations for homolytic BDEs are both performed using M06-2X/def2-TZVPP [78-80] in the gas phase at 298.15 K by Gaussian 16 [81]. Frequency calculations confirmed that optimized structures are minima (no imaginary frequency). The accuracy of computational BDEs of halides using M06-2X/def2-TZVPP is also evaluated and compared to experimental BDEs, demonstrating the reliability of the method (see Supporting Information File 1).

The computational homolytic BDEs are presented in Table 1. From the perspective of halogen centers, hypervalent iodine(III) reagents exhibit the highest homolytic BDEs, followed by hypervalent bromine(III) reagents, while hypervalent chlorine(III) reagents have the lowest. Generally, the homolytic BDEs of cyclic hypervalent iodine(III) reagents are above 30.0 kcal/mol, consistent with their good chemical stability. The homolytic BDEs of some cyclic hypervalent bromine(III) and most cyclic hypervalent chlorine(III) reagents are below 20 kcal/mol, implying these reagents should be too reactive to be isolated. From the perspective of transfer groups, the homolytic BDEs of groups with strong trans effects [82-84] such as -F, -CCH, -CN, -OCF_3, -OTf, -OTs are elevated, while those of -N_3, -NH_2, -SCF_3, etc. are smaller. These results are consistent with our previous studies on the group transfer ability of hypervalent iodine(III) reagents [44]. According to the calculation results, skeleton 5 may be a better candidate for synthesizing cyclic hypervalent bromine(III) and chlorine(III) reagents. The groups with strong trans effects, such as -F, -CCH, -CN, -OTf, can help stabilize cyclic hypervalent bromine(III) and chlorine(III) reagents.

In addition, we also calculated the heterolytic BDEs of cyclic hypervalent halogen reagents [46,47] to comprehensively examine the strength of chemical bonds (Table 2). Geometry optimizations and single point energy calculations for heterolytic BDEs are performed using M06-2X/def2-TZVPP in the SMD (acetonitrile) Implicit solvent model at 298.15 K. Due to the instability of some transfer group cations, such as $^{+}OCH_3$, $^{+}OCF_3$, $^{+}OCOCF_3$, $^{+}OCOPh$, ^{+}OTf and $^{+}SCF_3$, it is difficult for us to investigate their heterolytic BDEs. From Table 2, it can be seen that, except for CF_3 and $CHCH_2$, all other transfer groups exhibit high heterolytic BDEs with hypervalent halogen centers.

To elucidate the relationships between halogen centers and their corresponding homolytic BDEs, the homolytic BDEs of cyclic hypervalent halogen reagents were plotted against those of reagents with different halogen centers, giving moderate linear relationships (Figure 3a). For heterolytic BDEs, we found a strong linear relationship between different halogen centers, as illustrated in Figure 3b. This indicates that based on any kind of cyclic hypervalent halogen reagents, we can obtain a rough estimation of the BDEs for others with different halogen centers.

With these homolytic and heterolytic BDEs in hand, we next attempted to develop a predictive model for BDEs of hypervalent halogen compounds using machine learning algorithms. Graph attention network (GAT) [85] embeds local chemical environment information into the graph network by taking atomic information as node inputs, thus achieving higher predictive capabilities [86]. Building upon the computational studies, we constructed two compound datasets separately, consisting of 296 homolytic BDE data points and 209 heterolytic BDE data points. Taking homolytic BDE datasets as an example (Figure 4a), the distribution of this dataset is illustrated with key bond energy values normalized using min–max scaling. This approach ensures both data consistency and improves training efficiency.

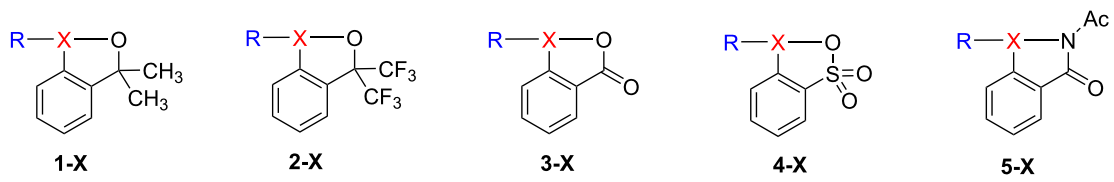

Figure 2: Common cyclic hypervalent halogen skeletons and transfer groups.

Table 1: Computational homolytic BDEs (kcal/mol) of cyclic hypervalent halogen reagents.

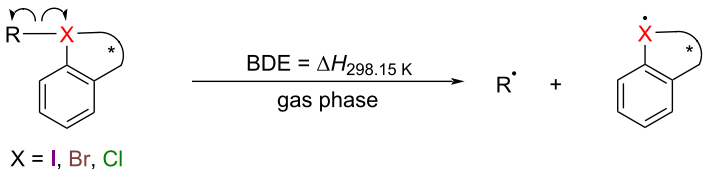

X = I, Br, Cl

		1-X			2-X			3-X			4-X			5-X		
R		X = I	X = Br	X = Cl	X = I	X = Br	X = Cl	X = I	X = Br	X = Cl	X = I	X = Br	X = Cl	X = I	X = Br	X = Cl
a	F	78.6	50.5	30.5	81.9	56.6	35.5	80.8	54.3	33.3	80.6	61.4	29.4	84.0	62.0	42.9
b	Cl	55.3	29.4	10.1	58.1	35.6	14.0	57.4	33.1	12.1	57.1	40.9	10.7	60.1	40.3	21.3
c	Br	44.7	19.8	0.2	47.3	24.9	4.3	46.7	23.0	2.4	46.5	31.2	2.0	49.3	30.2	11.4
d	CH_3	33.2	13.4	−0.3	42.4	28.7	16.5	42.8	29.6	20.0	49.1	49.3	40.0	39.9	28.9	22.2
e	CF_3	33.5	13.5	−0.8	39.0	24.5	11.8	38.5	23.6	12.5	41.2	39.0	25.1	37.2	24.5	12.6
f	$CHCH_2$	40.4	21.4	8.7	49.6	36.5	25.8	49.6	36.8	28.1	56.0	58.2	47.1	46.8	36.1	27.0
g	CCH	66.1	42.0	24.5	73.1	53.9	38.2	72.6	53.0	39.2	76.3	68.5	48.5	71.1	53.8	39.0
h	CN	68.8	43.6	24.2	72.6	51.6	33.4	71.6	49.7	32.7	72.8	61.6	37.9	71.9	53.0	34.8
i	N_3	32.1	7.6	−11.2	35.8	14.6	−4.5	34.8	12.3	−6.3	36.3	23.3	−4.8	36.5	17.9	0.1
j	NH_2	37.7	12.6	−4.3	45.5	25.1	9.6	45.0	24.1	8.3	49.4	40.2	16.7	44.5	27.5	11.7
k	NHAc	47.6	22.0	2.6	53.4	31.6	13.0	52.7	30.0	12.2	55.8	43.4	18.8	53.0	33.7	15.7
l	OH	53.0	26.4	6.5	58.7	35.7	15.9	57.7	33.5	14.1	60.1	44.9	16.3	58.7	38.3	19.5
m	OCH_3	40.7	15.3	−3.5	46.2	24.6	6.1	45.2	22.4	4.3	47.9	34.5	7.7	46.2	26.9	9.1
n	OCF_3	62.9	37.0	18.4	64.4	40.5	19.8	63.5	38.1	17.4	62.7	45.0	13.3	67.0	46.6	28.6
o	$OCOCH_3$	54.6	27.4	7.5	58.1	33.7	12.3	57.5	31.1	9.9	57.6	39.3	8.6	59.1	37.1	17.4
p	$OCOCF_3$	62.3	36.1	17.4	63.5	39.0	18.0	62.7	36.7	15.8	61.2	43.4	11.3	65.9	45.1	27.0
q	OCOPh	55.8	28.5	8.7	58.9	33.8	12.4	58.4	31.8	10.4	58.4	40.5	9.0	60.1	38.0	19.1
r	OTf	66.3	41.9	25.8	65.1	41.3	21.3	64.3	39.0	18.7	62.0	43.6	11.1	69.8	50.8	35.4
s	OTs	61.8	36.5	18.4	62.4	38.4	18.3	62.3	36.2	15.5	61.0	43.0	12.9	65.8	45.8	28.9
t	SCF_3	40.1	16.1	−3.1	44.6	23.3	4.0	43.2	21.6	3.0	44.9	33.7	14.0	44.2	26.2	7.9

Table 2: Computational heterolytic BDEs (kcal/mol) of cyclic hypervalent halogen reagents.

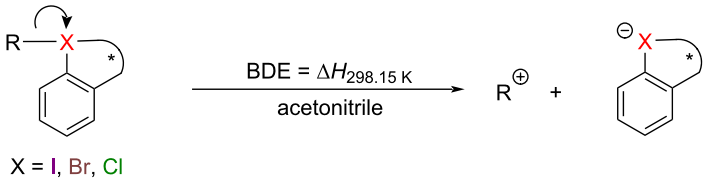

X = I, Br, Cl

		1-X			2-X			3-X			4-X			5-X		
R		X = I	X = Br	X = Cl	X = I	X = Br	X = Cl	X = I	X = Br	X = Cl	X = I	X = Br	X = Cl	X = I	X = Br	X = Cl
a	F	375.2	346.9	327.5	354.4	322.1	301.1	345.0	309.7	290.0	324.1	286.4	263.3	353.0	321.5	303.1
b	Cl	239.5	214.1	195.2	217.7	188.5	166.9	208.4	176.3	156.5	187.6	154.8	134.6	216.4	188.0	170.2
c	Br	212.7	188.4	169.0	190.8	163.3	142.0	181.6	151.3	131.9	160.7	130.9	111.9	189.5	162.2	143.8
d	CH_3	83.8	66.1	55.6	74.0	57.4	47.9	67.9	51.4	47.8	58.6	44.5	43.0	66.2	48.7	43.4
e	CF_3	77.5	56.5	42.1	61.7	40.4	29.3	53.7	30.9	24.2	37.8	19.8	18.9	55.2	32.0	20.9

Table 2: Computational heterolytic BDEs (kcal/mol) of cyclic hypervalent halogen reagents. (continued)

f	$CHCH_2$	71.2	54.2	43.9	60.3	44.9	37.7	54.2	38.4	34.9	44.0	28.8	29.3	53.0	35.9	30.7
g	CCH	231.7	207.2	189.8	216.5	192.5	178.7	208.7	183.3	174.1	194.4	171.4	163.5	210.1	183.8	171.0
h	CN	254.7	227.8	207.7	235.6	206.1	189.3	226.6	194.4	181.2	207.8	177.1	166.7	231.0	200.5	181.2
i	N_3	159.6	134.1	115.4	139.5	111.3	92.2	130.4	99.5	83.4	111.6	81.9	68.2	136.6	107.7	89.5
j	NH_2	145.5	121.4	103.8	133.0	108.4	94.0	124.9	99.2	89.9	111.7	87.7	79.7	125.5	99.9	86.9
k	NHAc	113.6	87.8	68.3	97.6	71.5	55.2	89.3	61.4	49.0	73.5	47.9	37.6	92.2	64.2	47.2
l	OH	244.1	217.6	197.1	227.3	199.1	179.6	218.4	187.7	170.9	200.9	170.3	154.0	222.9	193.6	174.0
m	OCH_3	–	–	–	–	–	–	–	–	–	–	–	–	–	–	–
n	OCF_3	–	–	–	–	–	–	–	–	–	–	–	–	–	–	–
o	$OCOCH_3$	149.1	122.7	102.9	128.7	100.4	78.1	119.6	87.4	67.7	99.4	67.8	47.0	127.0	97.5	77.2
p	$OCOCF_3$	–	–	–	–	–	–	–	–	–	–	–	–	–	–	–
q	OCOPh	–	–	–	–	–	–	–	–	–	–	–	–	–	–	–
r	OTf	–	–	–	–	–	–	–	–	–	–	–	–	–	–	–
s	OTs	104.8	79.7	62.4	80.2	50.0	29.1	70.9	37.0	18.5	47.8	13.2	-7.6	/	52.5	37.9
t	SCF_3	–	–	–	–	–	–	–	–	–	–	–	–	–	–	–

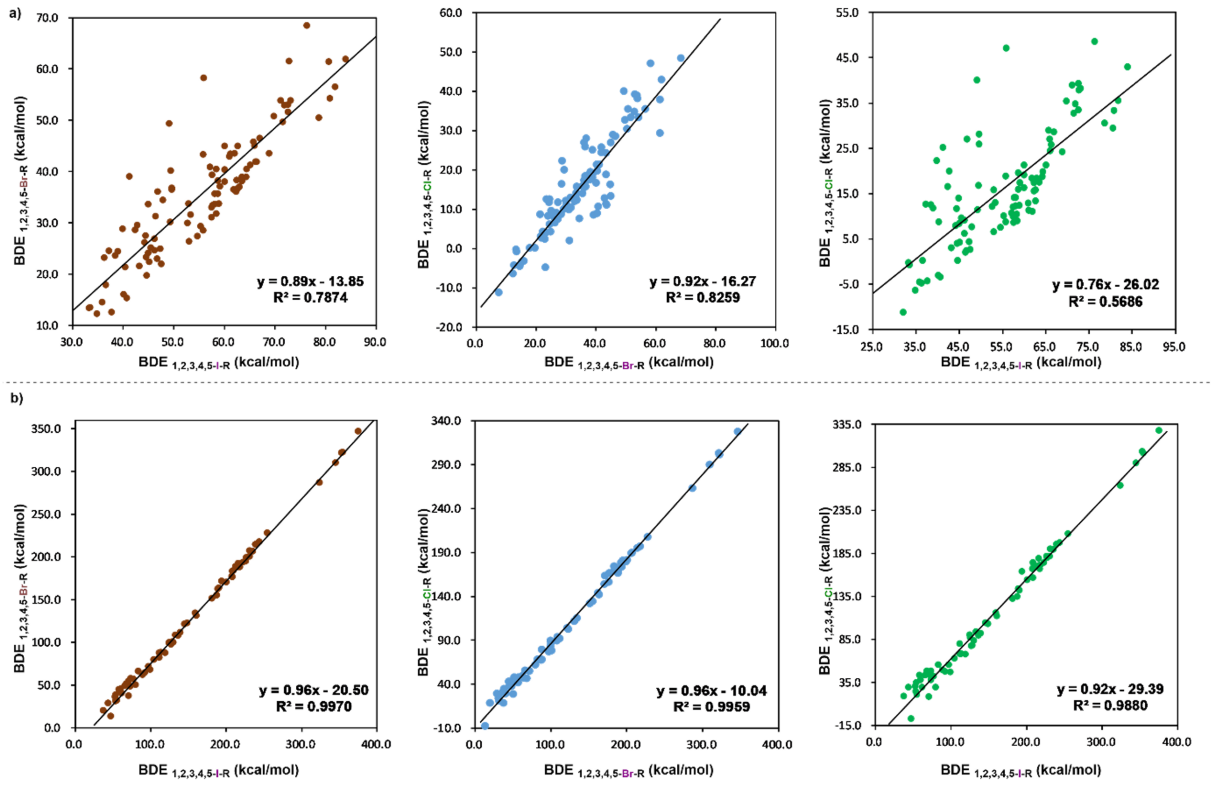

Figure 3: a) Linear dependence between the homolytic BDEs of cyclic hypervalent halogen reagents; b) linear dependence between the heterolytic BDEs of cyclic hypervalent halogen reagents.

We used the GAT model as the core framework, incorporating ten selected atomic descriptors as local information within the graph structure. Effective molecular transformations into molecular graphs (Figure 4b) were achieved using the RDKit and Deep Graph Library [87]. The dataset was randomly divided into training and testing sets in a 9:1 ratio. Notably, our analysis of descriptor testing revealed that individual inputs, such as neighboring atomic information, atomic charge, and atomic species, did not yield satisfactory results. However, combining all three inputs resulted in highly effective predictions (Figure 4c, see Supporting Information File 1 for detail). The R^2, MAE, and RMSE metrics exhibited outstanding perfor-

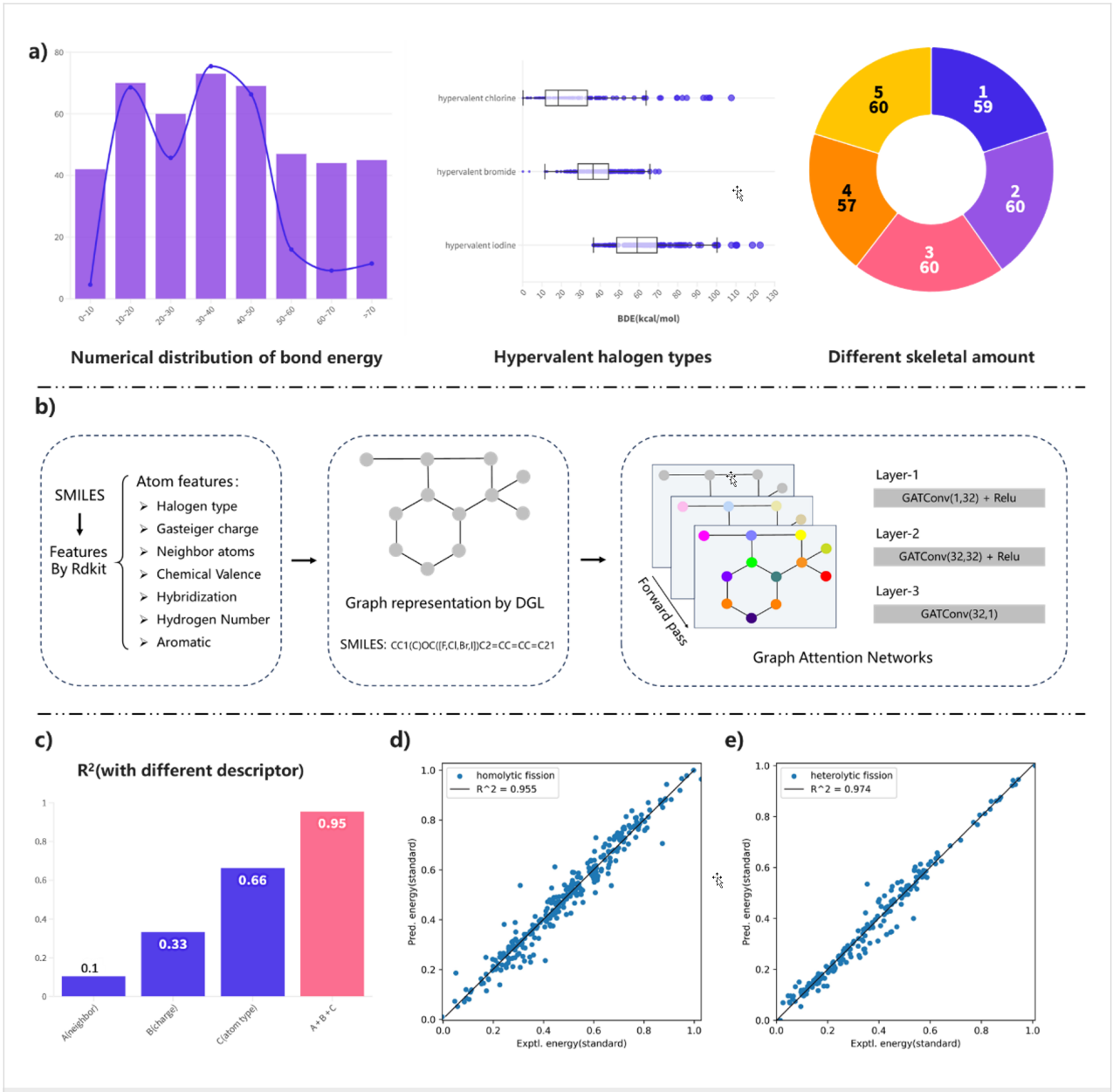

Figure 4: a) Composition and distribution of homolytic BDE dataset; b) graph attention network (GAT) model architecture and workflow; c) comparison of prediction performance on the training set using different descriptors (see more details in Supporting Information File 1); d) prediction performance for homolytic BDEs on the test set; e) prediction performance for heterolytic BDEs on the test set.

mance. The final predictive results yielded excellent performance with an R^2 value of 0.955 for homolytic BDEs (Figure 4d) and an R^2 value of 0.974 for heterolytic BDEs (Figure 4e). Furthermore, we achieved superior predictive results by not distinguishing between halogen categories in the dataset. This approach is reliable and efficient in assisting chemists in estimating the bond energy ranges of novel cyclic hypervalent halogen reagents.

We conducted additional tests with cyclic hypervalent halogen reagents beyond the training set, employing linear dependence equations and the GAT model for predictions (Table 3). The comparison of the two methods reveals that the GAT model is more reliable, as indicated by the lower root mean square error (RMSE). Moreover, the linear dependence method requires the BDEs of known cyclic hypervalent iodine(III) reagents to deduce the BDEs of the cyclic hypervalent bromine(III) and chlorine(III) reagents. In contrast, the GAT model is more straightforward, relying solely on structural information. Therefore, the GAT model is a superior method to predict the BDEs of cyclic hypervalent halogen reagents.

Table 3: Predictional BDEs of cyclic hypervalent halogen reagents.

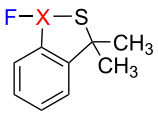

6-X-F

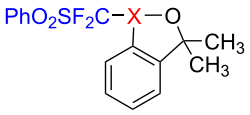

1-X-CF_2SO_2Ph

homolytic BDEs								heterolytic BDEs							
methods	**6-X-F**			**1-X-CF_2SO_2Ph**			RMSE	methods	**6-X-F**			**1-X-CF_2SO_2Ph**			RMSE
	X = I	X = Br	X = Cl	X = I	X = Br	X = Cl			X = I	X = Br	X = Cl	X = I	X = Br	X = Cl	
DFT[a]	68.3	44.1	26.2	32.6	10	−6.2	–	DFT[b]	367.4	342.7	328.8	79.9	57.6	41.7	–
LE[c]	–	47	26.1	–	15.2	−1.2	3.9	LE[d]	–	332.2	308.6	–	56.2	44.1	11.4
ML[e]	72.7	45.2	27.2	38.1	13.3	−4.5	3.3	ML[e]	375.8	336.8	329.1	86.3	56.6	48.9	5.7

[a]DFT calculations: M06-2X/def2-TZVPP in gas phase; [b]DFT calculations: M06-2X/def2-TZVPP in SMD (acetonitrile); [c]linear dependence equations: these predicted BDEs for hypervalent bromine and hypervalent chlorine are obtained by inserting the calculated hypervalent iodine BDEs into the linear dependence equations: y = 0.89x−13.85 and y = 0.76x−26.02; [d]linear dependence equations: y = 0.96x−20.50 and y = 0.92x−29.39; [e]machine learning.

Conclusion

We have undertaken an extensive computational investigation into the BDEs of cyclic hypervalent halogen reagents. Leveraging this dataset, we have developed a predictive model for both homolytic and heterolytic BDEs of hypervalent halogen compounds employing a graph attention network. We anticipate that the findings from our research will aid the design and development of new hypervalent bromine(III) and chlorine(III) reagents, an area that remains largely underexplored.

Supporting Information

Supporting Information File 1

Machine learning details and calculation data.
[https://www.beilstein-journals.org/bjoc/content/supplementary/1860-5397-20-127-S1.pdf]

Acknowledgements

Thanks to Prof. Dr. Jun Zhang (Shenzhen Bay Laboratory) and Ms. Qiufen Chen (Shenzhen Bay Laboratory & Southern University of Science and Technology) for their help in machine learning as well as Prof. Dr. Xin Li (Nankai University) and Haihe Laboratory of Sustainable Chemical Transformations for computational resources.

Funding

This work was supported by the Ministry of Science and Technology of China (2021YFF0701700), the National Natural Science Foundation of China (Nos. 22122104, 22193012, and 21933004), the CAS Project for Young Scientists in Basic Research (grant no. YSBR-052 and YSBR-095), and the Strategic Priority Research Program of the Chinese Academy of Sciences (grant no. XDB0590000).

ORCID® iDs

Yao Li - https://orcid.org/0000-0003-1370-6662
Xiao-Song Xue - https://orcid.org/0000-0003-4541-8702

Data Availability Statement

The data that supports the findings of this study is available from the corresponding author upon reasonable request.

References

1. Stang, P. J.; Zhdankin, V. V. *Chem. Rev.* **1996,** *96,* 1123–1178. doi:10.1021/cr940424+
2. Zhdankin, V. V.; Stang, P. J. *Chem. Rev.* **2002,** *102,* 2523–2584. doi:10.1021/cr010003+
3. Wirth, T. *Angew. Chem., Int. Ed.* **2005,** *44,* 3656–3665. doi:10.1002/anie.200500115
4. Zhdankin, V. V.; Stang, P. J. *Chem. Rev.* **2008,** *108,* 5299–5358. doi:10.1021/cr800332c
5. Dohi, T.; Kita, Y. *Chem. Commun.* **2009,** 2073–2085. doi:10.1039/b821747e
6. Yoshimura, A.; Zhdankin, V. V. *Chem. Rev.* **2016,** *116,* 3328–3435. doi:10.1021/acs.chemrev.5b00547
7. Li, X.; Chen, P.; Liu, G. *Beilstein J. Org. Chem.* **2018,** *14,* 1813–1825. doi:10.3762/bjoc.14.154
8. Parra, A. *Chem. Rev.* **2019,** *119,* 12033–12088. doi:10.1021/acs.chemrev.9b00338

9. Flores, A.; Cots, E.; Bergès, J.; Muñiz, K. *Adv. Synth. Catal.* **2019,** *361,* 2–25. doi:10.1002/adsc.201800521
10. Zhdankin, V. V. *ARKIVOC* **2020,** No. iv, 1–11. doi:10.24820/ark.5550190.p011.145
11. Singh, F. V.; Shetgaonkar, S. E.; Krishnan, M.; Wirth, T. *Chem. Soc. Rev.* **2022,** *51,* 8102–8139. doi:10.1039/d2cs00206j
12. Koser, G. F.; Sun, G.; Porter, C. W.; Youngs, W. J. *J. Org. Chem.* **1993,** *58,* 7310–7312. doi:10.1021/jo00077a071
13. Zhdankin, V. V.; Kuehl, C. J.; Krasutsky, A. P.; Bolz, J. T.; Mismash, B.; Woodward, J. K.; Simonsen, A. J. *Tetrahedron Lett.* **1995,** *36,* 7975–7978. doi:10.1016/0040-4039(95)01720-3
14. Eisenberger, P.; Gischig, S.; Togni, A. *Chem. – Eur. J.* **2006,** *12,* 2579–2586. doi:10.1002/chem.200501052
15. Fernández González, D.; Brand, J. P.; Waser, J. *Chem. – Eur. J.* **2010,** *16,* 9457–9461. doi:10.1002/chem.201001539
16. Legault, C. Y.; Prévost, J. *Acta Crystallogr., Sect. E: Struct. Rep. Online* **2012,** *68,* o1238. doi:10.1107/s1600536812012822
17. Ren, J.; Du, F.-H.; Jia, M.-C.; Hu, Z.-N.; Chen, Z.; Zhang, C. *Angew. Chem., Int. Ed.* **2021,** *60,* 24171–24178. doi:10.1002/anie.202108589
18. Li, Y.; Hari, D. P.; Vita, M. V.; Waser, J. *Angew. Chem., Int. Ed.* **2016,** *55,* 4436–4454. doi:10.1002/anie.201509073
19. Yoshimura, A.; Saito, A.; Zhdankin, V. V. *Adv. Synth. Catal.* **2023,** *365,* 2653–2675. doi:10.1002/adsc.202300275
20. Wang, Y.; Hu, X.; Morales-Rivera, C. A.; Li, G.-X.; Huang, X.; He, G.; Liu, P.; Chen, G. *J. Am. Chem. Soc.* **2018,** *140,* 9678–9684. doi:10.1021/jacs.8b05753
21. Zhang, Y.; Lu, J.; Lan, T.; Cheng, S.; Liu, W.; Chen, C. *Eur. J. Org. Chem.* **2021,** 436–442. doi:10.1002/ejoc.202001373
22. Poeira, D. L.; Negrão, A. C. R.; Faustino, H.; Coelho, J. A. S.; Gomes, C. S. B.; Gois, P. M. P.; Marques, M. M. B. *Org. Lett.* **2022,** *24,* 776–781. doi:10.1021/acs.orglett.1c04312
23. Ilchenko, N. O.; Tasch, B. O. A.; Szabó, K. J. *Angew. Chem., Int. Ed.* **2014,** *53,* 12897–12901. doi:10.1002/anie.201408812
24. Zheng, L.; Wang, Z.; Li, C.; Wu, Y.; Liu, Z.; Ning, Y. *Chem. Commun.* **2021,** *57,* 9874–9877. doi:10.1039/d1cc04268h
25. Yuan, W.; Szabó, K. J. *Angew. Chem., Int. Ed.* **2015,** *54,* 8533–8537. doi:10.1002/anie.201503373
26. Ulmer, A.; Brunner, C.; Arnold, A. M.; Pöthig, A.; Gulder, T. *Chem. – Eur. J.* **2016,** *22,* 3660–3664. doi:10.1002/chem.201504749
27. Farooq, U.; Shah, A.-u.-H. A.; Wirth, T. *Angew. Chem., Int. Ed.* **2009,** *48,* 1018–1020. doi:10.1002/anie.200805027
28. Ochiai, M. *Synlett* **2009,** 159–173. doi:10.1055/s-0028-1087355
29. Miyamoto, K.; Uchiyama, M. *Chem. Lett.* **2021,** *50,* 832–838. doi:10.1246/cl.200849
30. Winterson, B.; Patra, T.; Wirth, T. *Synthesis* **2022,** *54,* 1261–1271. doi:10.1055/a-1675-8404
31. Ochiai, M.; Miyamoto, K.; Kaneaki, T.; Hayashi, S.; Nakanishi, W. *Science* **2011,** *332,* 448–451. doi:10.1126/science.1201686
32. Miyamoto, K.; Saito, M.; Tsuji, S.; Takagi, T.; Shiro, M.; Uchiyama, M.; Ochiai, M. *J. Am. Chem. Soc.* **2021,** *143,* 9327–9331. doi:10.1021/jacs.1c04536
33. Sokolovs, I.; Suna, E. *Org. Lett.* **2023,** *25,* 2047–2052. doi:10.1021/acs.orglett.3c00405
34. Yoshida, Y.; Ishikawa, S.; Mino, T.; Sakamoto, M. *Chem. Commun.* **2021,** *57,* 2519–2522. doi:10.1039/d0cc07733j
35. Yoshida, Y.; Ao, T.; Mino, T.; Sakamoto, M. *Molecules* **2023,** *28,* 384. doi:10.3390/molecules28010384
36. Lanzi, M.; Dherbassy, Q.; Wencel-Delord, J. *Angew. Chem., Int. Ed.* **2021,** *60,* 14852–14857. doi:10.1002/anie.202103625
37. Lanzi, M.; Ali Abdine, R. A.; De Abreu, M.; Wencel-Delord, J. *Org. Lett.* **2021,** *23,* 9047–9052. doi:10.1021/acs.orglett.1c03278
38. Lanzi, M.; Wencel-Delord, J. *Chem. Sci.* **2024,** *15,* 1557–1569. doi:10.1039/d3sc05382b
39. De Abreu, M.; Rogge, T.; Lanzi, M.; Saiegh, T. J.; Houk, K. N.; Wencel-Delord, J. *Angew. Chem., Int. Ed.* **2024,** *63,* e202319960. doi:10.1002/anie.202319960
40. Yoshida, Y.; Mino, T.; Sakamoto, M. *ACS Catal.* **2021,** *11,* 13028–13033. doi:10.1021/acscatal.1c04070
41. Lanzi, M.; Rogge, T.; Truong, T. S.; Houk, K. N.; Wencel-Delord, J. *J. Am. Chem. Soc.* **2023,** *145,* 345–358. doi:10.1021/jacs.2c10090
42. Huss, C. D.; Yoshimura, A.; Rohde, G. T.; Mironova, I. A.; Postnikov, P. S.; Yusubov, M. S.; Saito, A.; Zhdankin, V. V. *ACS Omega* **2024,** *9,* 2664–2673. doi:10.1021/acsomega.3c07512
43. Chen, W. W.; Artigues, M.; Font-Bardia, M.; Cuenca, A. B.; Shafir, A. *J. Am. Chem. Soc.* **2023,** *145,* 13796–13804. doi:10.1021/jacs.3c02406
44. Yang, J.-D.; Li, M.; Xue, X.-S. *Chin. J. Chem.* **2019,** *37,* 359–363. doi:10.1002/cjoc.201800549
45. Internet Bond-energy Databank (pK_a and BDE)-*i*BonD: http://ibond.chem.tsinghua.edu.cn or http://ibond.nankai.edu.cn.
46. Lohithakshamenon, R.; Prasanthkumar, K. P.; Femina, C.; Sajith, P. K. *J. Phys. Chem. A* **2024,** *128,* 727–737. doi:10.1021/acs.jpca.3c06378
47. Jiang, H.; Sun, T.-Y.; Chen, Y.; Zhang, X.; Wu, Y.-D.; Xie, Y.; Schaefer, H. F., III. *Chem. Commun.* **2019,** *55,* 5667–5670. doi:10.1039/c9cc01320b
48. Schütt, K. T.; Arbabzadah, F.; Chmiela, S.; Müller, K. R.; Tkatchenko, A. *Nat. Commun.* **2017,** *8,* 13890. doi:10.1038/ncomms13890
49. Schütt, K. T.; Sauceda, H. E.; Kindermans, P.-J.; Tkatchenko, A.; Müller, K.-R. *J. Chem. Phys.* **2018,** *148,* 241722. doi:10.1063/1.5019779
50. Yang, Q.; Li, Y.; Yang, J.-D.; Liu, Y.; Zhang, L.; Luo, S.; Cheng, J.-P. *Angew. Chem., Int. Ed.* **2020,** *59,* 19282–19291. doi:10.1002/anie.202008528
51. St. John, P. C.; Guan, Y.; Kim, Y.; Kim, S.; Paton, R. S. *Nat. Commun.* **2020,** *11,* 2328. doi:10.1038/s41467-020-16201-z
52. Jeong, W.; Stoneburner, S. J.; King, D.; Li, R.; Walker, A.; Lindh, R.; Gagliardi, L. *J. Chem. Theory Comput.* **2020,** *16,* 2389–2399. doi:10.1021/acs.jctc.9b01297
53. Wen, M.; Blau, S. M.; Spotte-Smith, E. W. C.; Dwaraknath, S.; Persson, K. A. *Chem. Sci.* **2021,** *12,* 1858–1868. doi:10.1039/d0sc05251e
54. Yu, H.; Wang, Y.; Wang, X.; Zhang, J.; Ye, S.; Huang, Y.; Luo, Y.; Sharman, E.; Chen, S.; Jiang, J. *J. Phys. Chem. A* **2020,** *124,* 3844–3850. doi:10.1021/acs.jpca.0c01280
55. Nakajima, M.; Nemoto, T. *Sci. Rep.* **2021,** *11,* 20207. doi:10.1038/s41598-021-99369-8
56. S. V., S. S.; Kim, Y.; Kim, S.; St. John, P. C.; Paton, R. S. *Digital Discovery* **2023,** *2,* 1900–1910. doi:10.1039/d3dd00169e
57. Liu, Y.; Yang, Q.; Cheng, J.; Zhang, L.; Luo, S.; Cheng, J.-P. *ChemPhysChem* **2023,** *24,* e202300162. doi:10.1002/cphc.202300162
58. Saini, V.; Kataria, R.; Rajput, S. *Artif. Intell. Chem.* **2024,** *2,* 100032. doi:10.1016/j.aichem.2023.100032
59. Li, Y.; Huang, W.-S.; Zhang, L.; Su, D.; Xu, H.; Xue, X.-S. *Artif. Intell. Chem.* **2024,** *2,* 100043. doi:10.1016/j.aichem.2024.100043

60. Gelžinytė, E.; Öeren, M.; Segall, M. D.; Csányi, G. *J. Chem. Theory Comput.* **2024,** *20,* 164–177. doi:10.1021/acs.jctc.3c00710
61. Yan, T.; Zhou, B.; Xue, X.-S.; Cheng, J.-P. *J. Org. Chem.* **2016,** *81,* 9006–9011. doi:10.1021/acs.joc.6b01642
62. Zhou, B.; Yan, T.; Xue, X.-S.; Cheng, J.-P. *Org. Lett.* **2016,** *18,* 6128–6131. doi:10.1021/acs.orglett.6b03134
63. Zhou, B.; Xue, X.-s.; Cheng, J.-p. *Tetrahedron Lett.* **2017,** *58,* 1287–1291. doi:10.1016/j.tetlet.2017.02.040
64. Zhou, B.; Haj, M. K.; Jacobsen, E. N.; Houk, K. N.; Xue, X.-S. *J. Am. Chem. Soc.* **2018,** *140,* 15206–15218. doi:10.1021/jacs.8b05935
65. Zheng, H.; Sang, Y.; Houk, K. N.; Xue, X.-S.; Cheng, J.-P. *J. Am. Chem. Soc.* **2019,** *141,* 16046–16056. doi:10.1021/jacs.9b08243
66. Zheng, H.; Xue, X.-S. *Curr. Org. Chem.* **2020,** *24,* 2106–2117. doi:10.2174/1385272824999200620223218
67. Zhang, D.; Shao, Y.; Zheng, H.; Zhou, B.; Xue, X.-S. *Acta Chim. Sin. (Chin. Ed.)* **2021,** *79,* 1394–1400. doi:10.6023/a21080358
68. Chen, Y.; Gu, Y.; Meng, H.; Shao, Q.; Xu, Z.; Bao, W.; Gu, Y.; Xue, X.-S.; Zhao, Y. *Angew. Chem., Int. Ed.* **2022,** *61,* e202201240. doi:10.1002/anie.202201240
69. Zheng, H.; Cai, L.; Pan, M.; Uyanik, M.; Ishihara, K.; Xue, X.-S. *J. Am. Chem. Soc.* **2023,** *145,* 7301–7312. doi:10.1021/jacs.2c13295
70. Ge, Y.; Shao, Y.; Wu, S.; Liu, P.; Li, J.; Qin, H.; Zhang, Y.; Xue, X.-s.; Chen, Y. *ACS Catal.* **2023,** *13,* 3749–3756. doi:10.1021/acscatal.3c00230
71. Shao, Y.; Ren, Z.; Zheng, C.; Xue, X.-S. *Adv. Synth. Catal.* **2023,** *365,* 2737–2743. doi:10.1002/adsc.202300375
72. Gao, B.; Cai, L.; Zhang, Y.; Huang, H.; Li, Y.; Xue, X.-S. *CCS Chem.* **2024,** in press. doi:10.31635/ccschem.024.202303774
73. Jiang, H.; Sun, T.-Y.; Wang, X.; Xie, Y.; Zhang, X.; Wu, Y.-D.; Schaefer, H. F., III. *Org. Lett.* **2017,** *19,* 6502–6505. doi:10.1021/acs.orglett.7b03167
74. Hyun, S.-M.; Yuan, M.; Maity, A.; Gutierrez, O.; Powers, D. C. *Chem* **2019,** *5,* 2388–2404. doi:10.1016/j.chempr.2019.06.006
75. Matsumoto, K.; Nakajima, M.; Nemoto, T. *J. Phys. Org. Chem.* **2019,** *32,* e3961. doi:10.1002/poc.3961
76. Sun, T.-Y.; Chen, K.; Zhou, H.; You, T.; Yin, P.; Wang, X. *J. Comput. Chem.* **2021,** *42,* 470–474. doi:10.1002/jcc.26469
77. St. John, P. C.; Guan, Y.; Kim, Y.; Etz, B. D.; Kim, S.; Paton, R. S. *Sci. Data* **2020,** *7,* 244. doi:10.1038/s41597-020-00588-x
78. Zhao, Y.; Truhlar, D. G. *Acc. Chem. Res.* **2008,** *41,* 157–167. doi:10.1021/ar700111a
79. Weigend, F.; Ahlrichs, R. *Phys. Chem. Chem. Phys.* **2005,** *7,* 3297–3305. doi:10.1039/b508541a
80. Zhao, Y.; Truhlar, D. G. *Chem. Phys. Lett.* **2011,** *502,* 1–13. doi:10.1016/j.cplett.2010.11.060
81. *Gaussian 16,* Revision A.03; Gaussian, Inc.: Wallingford, CT, 2016.
82. Ochiai, M.; Sueda, T.; Miyamoto, K.; Kiprof, P.; Zhdankin, V. V. *Angew. Chem., Int. Ed.* **2006,** *45,* 8203–8206. doi:10.1002/anie.200603055
83. Sajith, P. K.; Suresh, C. H. *Inorg. Chem.* **2012,** *51,* 967–977. doi:10.1021/ic202047g
84. Sajith, P. K.; Suresh, C. H. *Inorg. Chem.* **2013,** *52,* 6046–6054. doi:10.1021/ic400399v
85. Veličković, P.; Cucurull, G.; Casanova, A.; Romero, A.; Liò, P.; Bengio, Y. *arXiv* **2017,** 1710.10903. doi:10.48550/arxiv.1710.10903
86. Chen, Q.; Zhang, Y.; Gao, P.; Zhang, J. *Artif. Intell. Chem.* **2023,** *1,* 100010. doi:10.1016/j.aichem.2023.100010
87. Wang, M.; Zheng, D.; Ye, Z.; Gan, Q.; Li, M.; Song, X.; Zhou, J.; Ma, C.; Yu, L.; Gai, Y.; Xiao, T.; He, T.; Karypis, G.; Li, J.; Zhang, Z. *arXiv* **2019,** 1909.01315. doi:10.48550/arxiv.1909.01315

License and Terms

BEILSTEIN JOURNAL OF ORGANIC CHEMISTRY

Synthesis of 4-functionalized pyrazoles via oxidative thio- or selenocyanation mediated by $PhICl_2$ and NH_4SCN/KSeCN

Jialiang Wu[1], Haofeng Shi[1], Xuemin Li[1], Jiaxin He[1], Chen Zhang[2], Fengxia Sun[*2] and Yunfei Du[*1]

Letter

Open Access

Address:
[1]Tianjin Key Laboratory for Modern Drug Delivery & High-Efficiency, School of Pharmaceutical Science and Technology, Tianjin University, Tianjin 300072, China and [2]Hebei Research Center of Pharmaceutical and Chemical Engineering, Hebei University of Science and Technology, Shijiazhuang 050018, China

Email:
Fengxia Sun[*] - fxsun001@163.com; Yunfei Du[*] - duyunfeier@tju.edu.cn

* Corresponding author

Keywords:
$PhICl_2$; pyrazoles; selenocyanation; thiocyanation; thiocyanogen chloride

Beilstein J. Org. Chem. **2024,** *20,* 1453–1461.
https://doi.org/10.3762/bjoc.20.128

Received: 17 March 2024
Accepted: 12 June 2024
Published: 28 June 2024

This article is part of the thematic issue "Hypervalent halogen chemistry".

Guest Editor: T. Gulder

Abstract

A series of 4-thio/seleno-cyanated pyrazoles was conveniently synthesized from 4-unsubstituted pyrazoles using NH_4SCN/KSeCN as thio/selenocyanogen sources and $PhICl_2$ as the hypervalent iodine oxidant. This metal-free approach was postulated to involve the in situ generation of reactive thio/selenocyanogen chloride (Cl–SCN/SeCN) from the reaction of $PhICl_2$ and NH_4SCN/KSeCN, followed by an electrophilic thio/selenocyanation of the pyrazole skeleton.

Introduction

Pyrazoles and their derivatives are an important class of five-membered heterocyclic compounds [1-5] that have drawn increasing attention from organic chemists, due to their potential biological and pharmaceutical properties including anti-inflammatory [6], antiviral [7], antibacterial [8], antifungal [9], cytotoxic [10], antioxidant [11], and analgesic [12] activities. For instance, celecoxib (**I**, Figure 1) (for treating rheumatoid arthritis and osteoarthritis), tepoxalin (**II**, Figure 1) (a veterinary painkiller used to relieve pain from muscle and bone diseases), dimetilan (**III**, Figure 1) (demonstrating excellent insecticidal effects) [13-15] all possess a pyrazole framework in their respective chemical structure. Considering the pharmaceutical significance of pyrazole compounds, there has been growing interest in the development of efficient strategies for accessing functionalized pyrazole derivatives.

Thio/selenocyano groups are widely existing in the core structural motifs of various natural products and pharmaceutical agents [16-20]. Many S/SeCN-containing bioactive small molecules have been proved to possess wide-ranging biological ac-

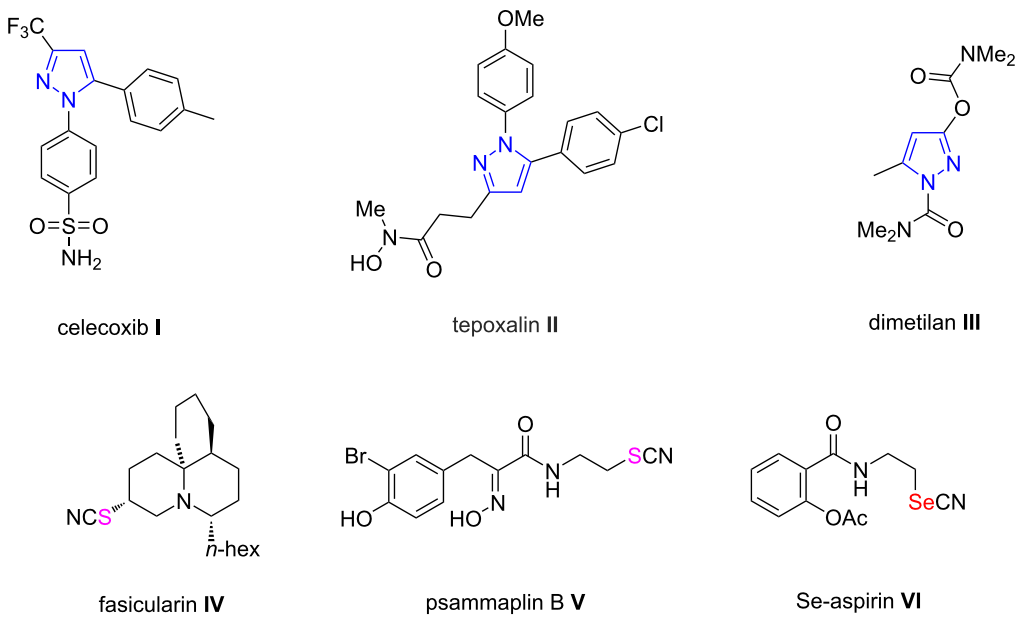

Figure 1: Representative pyrazoles with pharmacological activities and S/Se-containing pharmaceutical molecules.

tivities. Specifically, representative examples include fasicularin (**IV**, Figure 1), which possesses cytotoxic properties [21] and psammaplin B (**V**, Figure 1), which shows antimicrobial and mild tyrosine kinase inhibition activities [22]. In addition, Se-aspirin (**VI**, Figure 1) has been used as an effective anti-inflammatory pharmaceutical [23]. On the other hand, organic thiocyanates usually serve as useful synthetic intermediates that can be conveniently converted to sulfur-containing derivatives including sulfides [24], disulfides [25], thiocarbamates [26], and trifluoromethyl thioethers [27]. Likewise, selenocyanates can be used as versatile precursors for the synthesis of a variety of selenium-containing compounds [28-32].

As the S/SeCN-containing organic compounds play an important role in organic and medicinal chemistry, organic chemists have devoted a great deal of efforts to developing efficient thio/selenocyanation approaches [33-41]. Specifically, a plethora of synthetic strategies have been reported for the thiocyanation of heteroaromatic compounds including arenes, indoles, carbazoles, pyrroles, and imidazopyridines [42-45]. However, the electrophilic thiocyanation of biologically important pyrazoles has been less explored [46-48]. Among them, the majority of the reported methods proceed through a radical pathway, with the SCN radical generated by the reaction of the thiocyanate source with a corresponding oxidant (Scheme 1a–c) [49]. For example, Xu reported that a series of 4-thiocyanated 5-hydroxy-1*H*-pyrazoles was synthesized by a $K_2S_2O_8$-promoted direct thiocyanation of pyrazolin-5-ones at room temperature, using NH_4SCN as thiocyanogen source (Scheme 1a) [20]. Similarly, utilizing NH_4SCN and $K_2S_2O_8$, Yotphan and colleagues realized a direct thiocyanation of *N*-substituted pyrazolones under metal-free conditions [49]. Besides, Choudhury and co-workers developed an additive and metal-free methodology for the C–H thiocyanation of aminopyrazoles, using H_2O_2 as a benign oxidizing agent (Scheme 1b) [41]. Pan presented a method for the C–H thiocyanation of pyrazoles by using a sustainable catalyst of graphite-phase carbon nitride (g-C_3N_4) under visible light irradiation (Scheme 1c) [2]. Furthermore, Yao harnessed an electrochemical approach to form the electrophilic SCN^+ intermediate, which reacted with pyrazoles to give the corresponding thiocyanated pyrazoles (Scheme 1d) [50]. However, to our knowledge, there are only few reports on the electrophilic selenocyanation of heterocycles [51-53] including the biologically important pyrazoles. In this regard, it should be highly desirable to develop an efficient method for a smooth selenocyanation of pyrazole compounds.

Results and Discussion

In our previous work we reported that a regioselective C-5 thiocyanation of the 2-pyridone skeleton could be realized via a $PhICl_2$-mediated electrophilic thiocyanation approach [54]. Inspired by this previous work, we were interested at investigating whether a direct C-4 selenocyanation as well as a thiocyanation of the pyrazole skeleton could be realized using the same protocol. At the outset of the study, 3,5-dimethyl-1-phenyl-1*H*-pyrazole (**1a**, 1 equiv) was chosen as the model substrate to

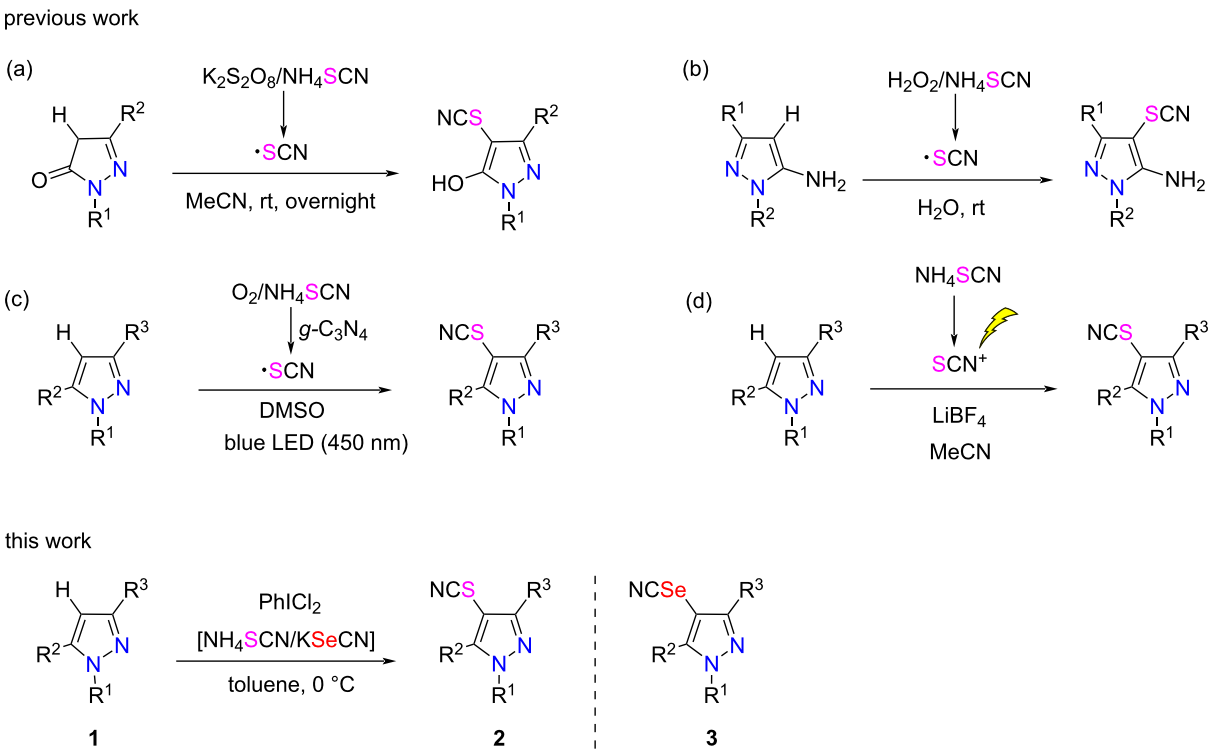

Scheme 1: Approaches for thio/selenocyanation of the pyrazole skeleton.

react with NH_4SCN (1 equiv) and $PhICl_2$ (1 equiv) in THF at 0 °C under N_2 atmosphere. To our delight, the desired thiocyanated product **2a** was obtained in 68% yield (Table 1, entry 1). Encouraged by this result, we proceeded to investigate the other parameters that would possibly affect the efficiency of the reaction. First, upon a comparison of different reaction temperatures, we found that the reaction operated at 0 °C gave the best result (Table 1, entries 1–3). Then, other SCN-containing inorganic salts including KSCN, AgSCN, and CuSCN were screened, and the results showed that none of them gave better results than NH_4SCN (Table 1, entries 4–6). Next, other oxidants including phenyliodine(III) diacetate (PIDA), phenyliodine(III) bis(trifluoroacetate) (PIFA), iodosobenzene (PhIO), and NCS were applied, and the results indicated that $PhICl_2$ was the most effective oxidant (Table 1, entries 7–10). Later on, when the dosage of $PhICl_2$ and NH_4SCN was increased to 2.0 equivalents, the yield of product **2a** significantly increased to 82% (Table 1, entry 11). However, when the loading of $PhICl_2$ and NH_4SCN were further increased to 3.0 equivalents, the reaction did not afford a better outcome (Table 1, entry 12). Furthermore, solvent screening showed that toluene was the most appropriate solvent, while the reaction led to a much lower yield when DMF, MeOH, MeCN, or DCM were used as solvents (Table 1, entries 13–17). On the basis of the above experimental results, the optimized conditions for the thiocyanation of the model substrate were concluded to be: 2.0 equivalents of $PhICl_2$ and NH_4SCN in toluene at 0 °C, under N_2 atmosphere (Table 1, entry 17).

With the optimized reaction conditions in hand, the substrate scope of this thiocyanation approach was next investigated (Scheme 2). The results showed that the newly established $PhICl_2/NH_4SCN$ protocol was suitable for a wide range of substrates. Specifically, when *N*-aryl substrates containing electron-donating groups (-Me, -OMe) were subjected to the standard reaction conditions, the corresponding products **2b–e** were obtained in good yields (80–91%). It was found that there was no significant influence on the outcome of the reactions of various *N*-aryl-substituted pyrazoles with a methyl group at the *ortho*-, *meta*- or *para*- positions of the phenyl group. Next, *N*-arylated substrates bearing electron-withdrawing groups (-F, -Cl, -Br, -I, $-CF_3$, $-NO_2$) were tested, and the desired products **2f–k** were conveniently obtained in moderate to good yields. Notably, the reaction of the substrate bearing a $-CF_3$ group afforded the corresponding product **2j** in 93% yield. However, the substrate possessing a $-NO_2$ substituent gave an inferior yield of the product **2k**. Then, we proceeded to investigate the effects of different substituents R^2 and R^3. When the methyl substituent (R^2) was replaced with an aryl group, the corresponding thiocyanated products **2l–o** could be obtained in acceptable to mod-

Table 1: Optimization of oxidative thiocyanation of pyrazole.[a]

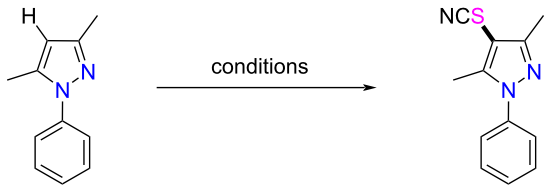

1a **2a**

Entry	Oxidant (equiv)	[SCN] (equiv)	Solvent	*T* (°C)	Yield (%)[b]
1	$PhICl_2$ (1.0)	NH_4SCN (1.0)	THF	0	68
2	$PhICl_2$ (1.0)	NH_4SCN (1.0)	THF	25	43
3	$PhICl_2$ (1.0)	NH_4SCN (1.0)	THF	40	40
4	$PhICl_2$ (1.0)	KSCN (1.0)	THF	0	10
5	$PhICl_2$ (1.0)	AgSCN (1.0)	THF	0	15
6	$PhICl_2$ (1.0)	CuSCN (1.0)	THF	0	12
7	PIDA (1.0)	NH_4SCN (1.0)	THF	0	NR[c]
8	PIFA (1.0)	NH_4SCN (1.0)	THF	0	NR
9	PhIO (1.0)	NH_4SCN (1.0)	THF	0	NR
10	NCS (1.0)	NH_4SCN (1.0)	THF	0	ND[d]
11	$PhICl_2$ (2.0)	NH_4SCN (2.0)	THF	0	82
12	$PhICl_2$ (3.0)	NH_4SCN (3.0)	THF	0	80
13	$PhICl_2$ (2.0)	NH_4SCN (2.0)	DMF	0	NR
14	$PhICl_2$ (2.0)	NH_4SCN (2.0)	MeOH	0	10
15	$PhICl_2$ (2.0)	NH_4SCN (2.0)	MeCN	0	58
16	$PhICl_2$ (2.0)	NH_4SCN (2.0)	DCM	0	55
17	**$PhICl_2$ (2.0)**	**NH_4SCN (2.0)**	**toluene**	**0**	**91**

[a]Reaction conditions: under N_2 atmosphere, a mixture of oxidant and [SCN] in solvent (2 mL) was stirred at 0 °C for 0.5 h, then **1a** (0.20 mmol) was added, and stirring continued at 0 °C for 8 h. [b]Yield of the isolated product. [c]NR = no reaction. [d]ND = no desired product.

erate yields. On the other hand, the method was equally applicable to the substrate bearing two aryl substituents (R^2 and R^3), albeit the reaction afforded product **2n** in a much lower yield, possibly caused by steric congestion. In addition, when the aryl substituent of R^1 was replaced with a *tert*-butyl group, this method also worked well to give product **2o** in moderate yield. Notably, when the C3 and C5-unsubstituted substrate **1p** was subjected to the standard conditions, the 4-thiocyanated product **2p** was obtained regioselectively in 87% yield. Strikingly, the thiocyanation of the pharmaceutically active compound edaravone could also be realized under the optimized conditions, affording the corresponding product **2q** in good yield.

Furthermore, we turned our attention to the applicability of this protocol for the selenocyanation of the pyrazole skeleton (Scheme 3). Gratifyingly, the method was equally applicable to selenocyanation of pyrazoles bearing various substituents, with the corresponding selenocyanated products **3a**–**o** achieved in acceptable to good yields. Similarly, the selenocyanation of C3- and C5-unsubstituted substrate **1p** regioselectively furnished the 4-selenocyanated pyrazole **3p** in good yield.

The utility of this approach was further demonstrated by a scale-up experiment. When 10.0 mmol of compound **1a** were treated with 20.0 mmol of NH_4SCN/KSeCN and $PhICl_2$ under the standard reaction conditions, the desired products **2a** and **3a** were obtained in 88% and 80% yield, respectively (Scheme 4).

The obtained 4-thio/selenocyanated pyrazoles could be further derivatized by known approaches. Specifically, products **2a** and **3a** could react with $TMSCF_3$ in the presence of Cs_2CO_3 [55] to give the corresponding SCF_3- and $SeCF_3$-containing compounds **2r** and **3q** in moderate yields. Moreover, products **2a** and **3a** could be conveniently transformed into thiomethyl and selenomethyl-substituted pyrazole derivatives **2s** and **3r** by treatment with CH_3MgBr in THF [56] (Scheme 4).

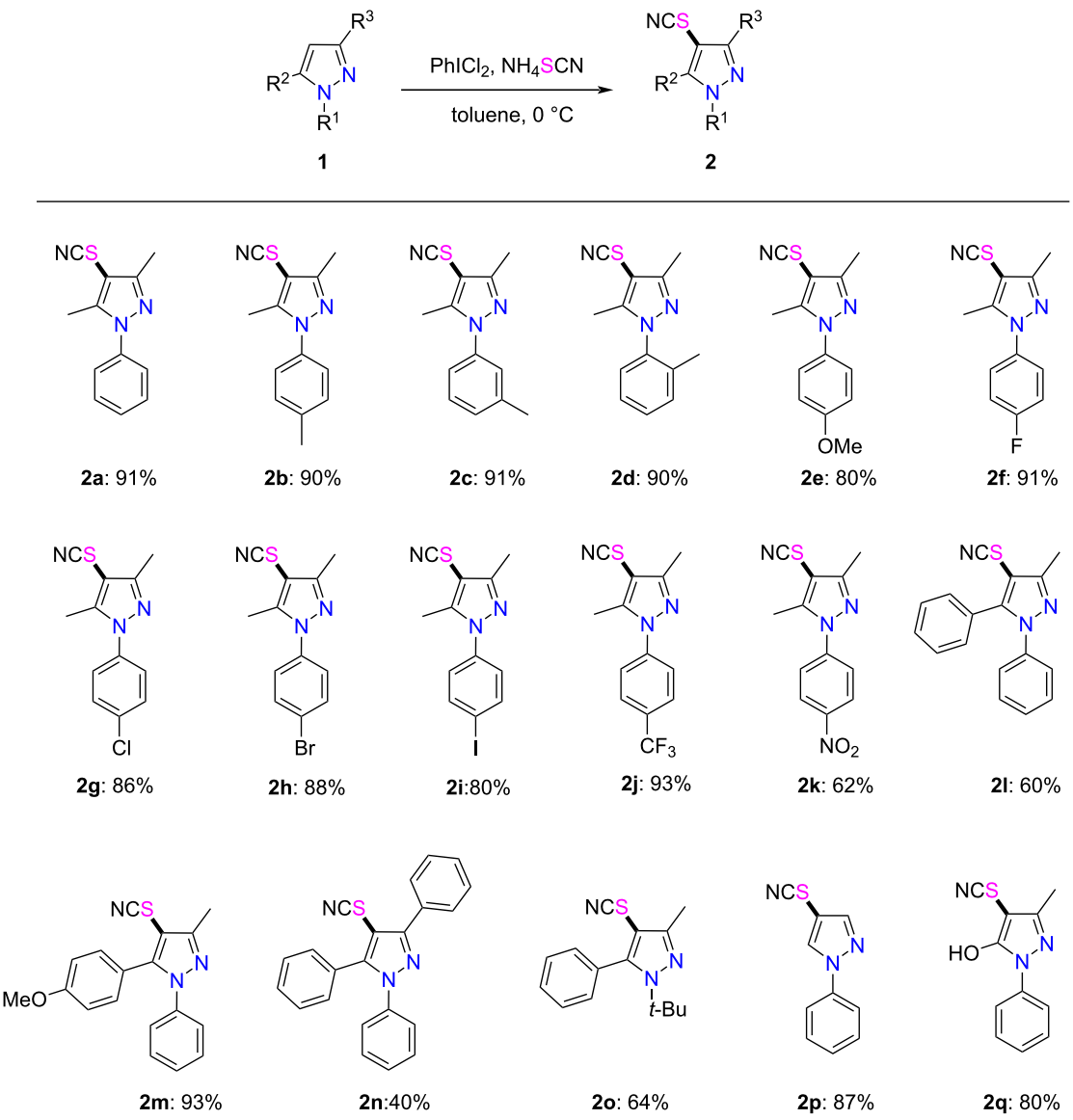

Scheme 2: $PhICl_2$/NH_4SCN-mediated thiocyanation of pyrazoles. Reaction conditions: under N_2 atmosphere, a mixture of $PhICl_2$ (2.00 mmol) and NH_4SCN (2.00 mmol) in toluene (5 mL) was stirred at 0 °C for 0.5 h, then **1a** (1.00 mmol) was added and stirring continued at 0 °C for 8 h. Isolated yields are given.

Based on the previous reports [54,57-59], a possible mechanism of this selenocyanation reaction was proposed (Scheme 5). First, the reaction of $PhICl_2$ with KSeCN produces selenocyanogen chloride (Cl–SeCN), which further reacts with selenocyanate to give $(SeCN)_2$ [60]. Then, one selenium atom of $(SeCN)_2$ nucleophilically attacks the iodine center in $PhICl_2$ to generate intermediate **A**, which was further transformed into intermediate **B** by release of one molecule of iodobenzene. Next, the nucleophilic attack of chloride anion to the bivalent selenium center of intermediate **B** resulted in the formation of two molecules of Cl–SeCN. Subsequently, Cl–SeCN undergoes an electrophilic addition reaction with pyrazole **1** to give intermediate **C**, which, after deprotonative rearomatization affords the 4-selenocyanated pyrazole **3**.

Conclusion

In conclusion, we have accomplished the synthesis of a series of C-4 thio/selenocyanated pyrazoles via a hypervalent iodine-mediated electrophilic thio/selenocyanation approach under mild reaction conditions. Furthermore, the obtained S/SeCN-containing pyrazoles can be converted to S/$SeCF_3$- and S/SeMe-containing pyrazole derivatives. Further investigations

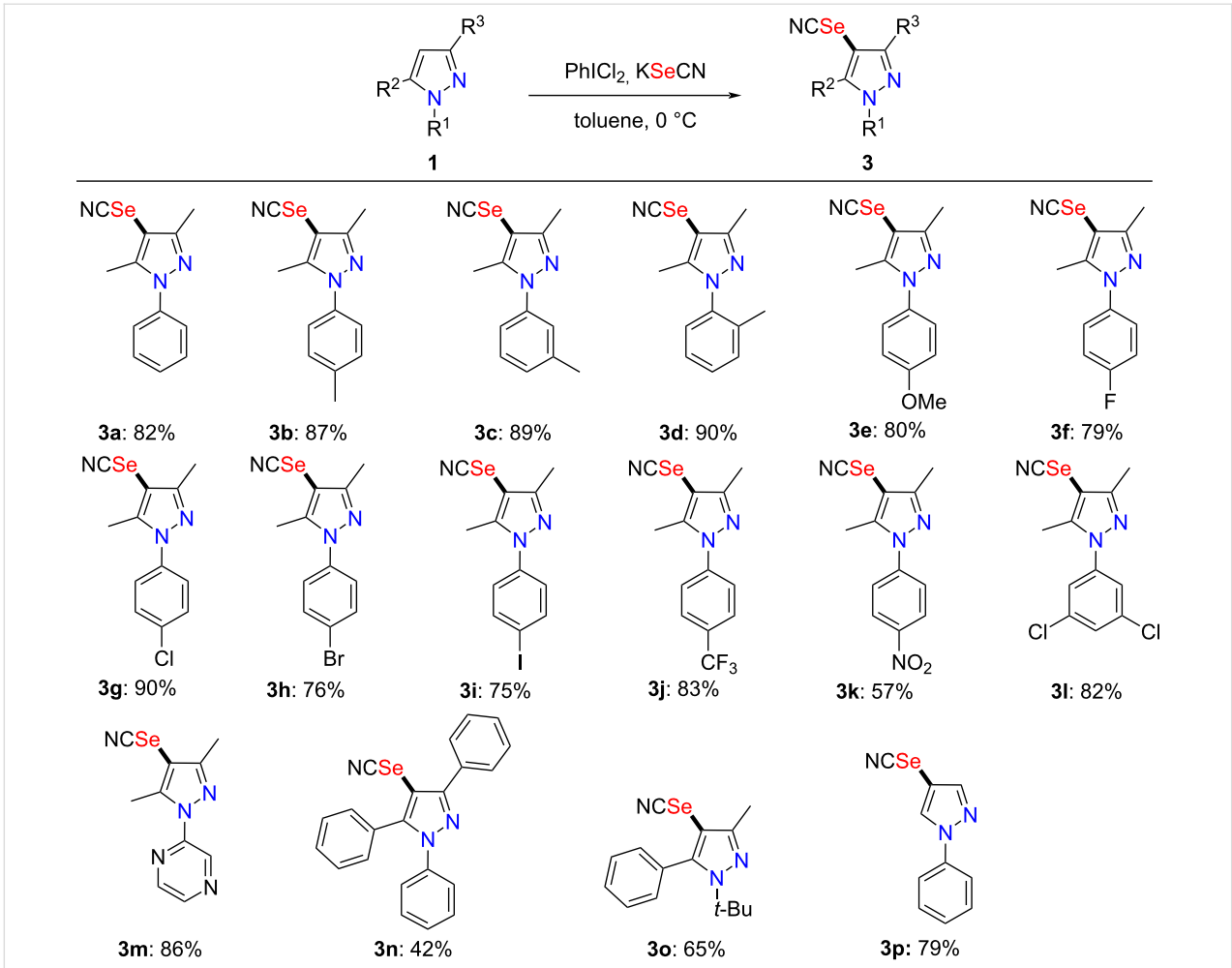

Scheme 3: $PhICl_2$/KSeCN-mediated selenocyanation of pyrazoles. Reaction conditions: under N_2 atmosphere, a mixture of $PhICl_2$ (2.00 mmol) and KSeCN (2.00 mmol) in toluene (5 mL) was stirred at 0 °C for 0.5 h, then **1a** (1.00 mmol) was added and stirring continued at 0 °C for 8 h. Isolated yields are given.

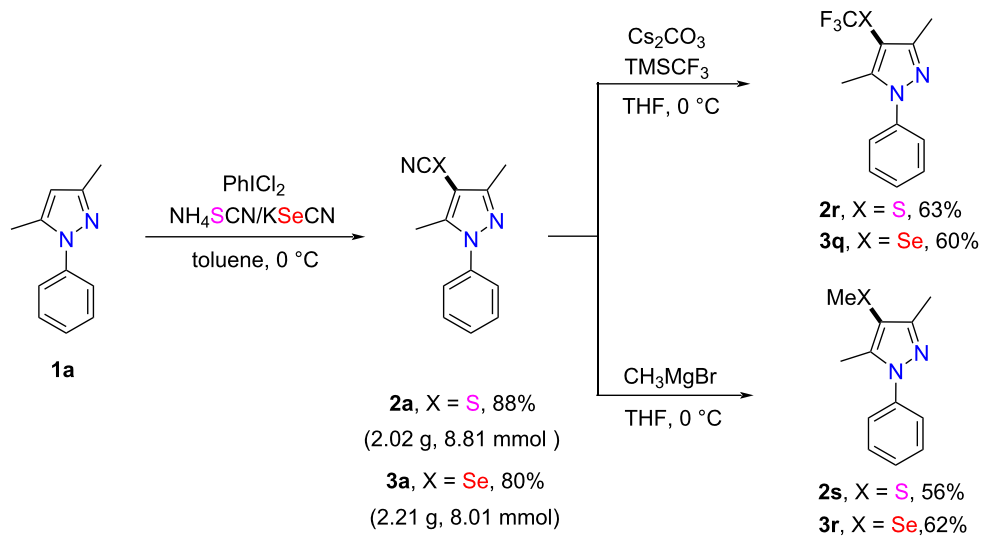

Scheme 4: Gram-scale synthesis of compounds **2a** and **3a** and their derivatization.

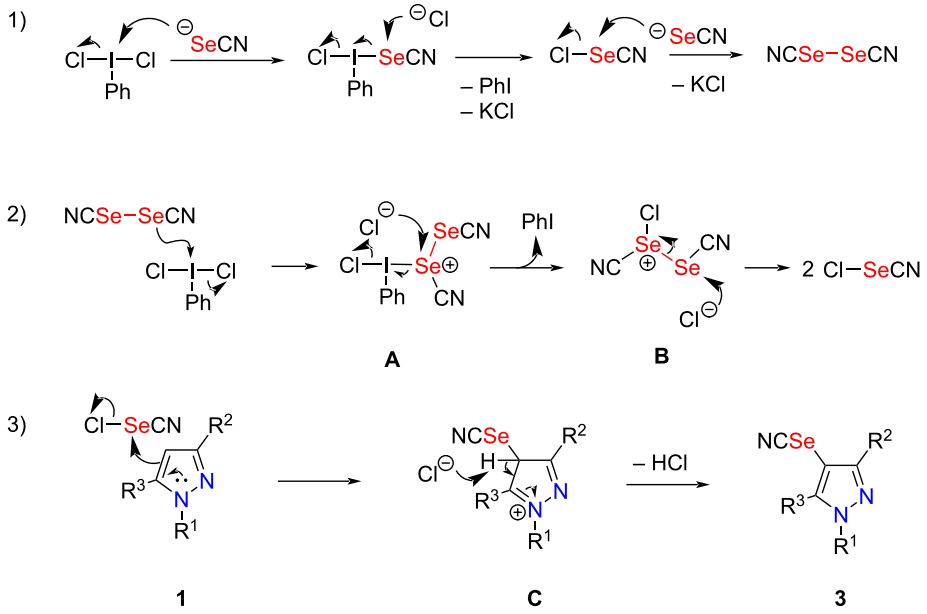

Scheme 5: Plausible reaction mechanism.

of the synthetic utility of this approach are currently ongoing in our lab.

Supporting Information

Supporting Information File 1

Synthetic details and compound characterization data.
[https://www.beilstein-journals.org/bjoc/content/supplementary/1860-5397-20-128-S1.pdf]

Funding

We acknowledge the National Key Research and Development Program of China (2019YFA0905100), the National Natural Science Foundation of China (No. 22071175) and Tianjin Graduate Research and Innovation Project (No.2021YJSB196) and for financial supports.

Author Contributions

Jialiang Wu: formal analysis; investigation; project administration; writing – original draft. Haofeng Shi: data curation; formal analysis. Xuemin Li: formal analysis; resources. Jiaxin He: data curation; resources. Chen Zhang: formal analysis; resources. Fengxia Sun: conceptualization; funding acquisition; methodology; supervision. Yunfei Du: conceptualization; funding acquisition; methodology; project administration; supervision; validation; visualization; writing – review & editing.

ORCID® iDs

Yunfei Du - https://orcid.org/0000-0002-0213-2854

Data Availability Statement

All data that supports the findings of this study is available in the published article and/or the supporting information to this article.

Preprint

A non-peer-reviewed version of this article has been previously published as a preprint: https://doi.org/10.3762/bxiv.2024.14.v1

References

1. Sangani, C. B.; Mungra, D. C.; Patel, M. P.; Patel, R. G. *Chin. Chem. Lett.* **2012,** *23,* 57–60. doi:10.1016/j.cclet.2011.09.012
2. Pan, J.; Liu, C.; Wang, J.; Dai, Y.; Wang, S.; Guo, C. *Tetrahedron Lett.* **2021,** *77,* 153253. doi:10.1016/j.tetlet.2021.153253
3. Mamaghani, M.; Hossein Nia, R.; Shirini, F.; Tabatabaeian, K.; Rassa, M. *Med. Chem. Res.* **2015,** *24,* 1916–1926. doi:10.1007/s00044-014-1271-y
4. El-Sabbagh, O. I.; Baraka, M. M.; Ibrahim, S. M.; Pannecouque, C.; Andrei, G.; Snoeck, R.; Balzarini, J.; Rashad, A. A. *Eur. J. Med. Chem.* **2009,** *44,* 3746–3753. doi:10.1016/j.ejmech.2009.03.038
5. Li, G.; Cheng, Y.; Han, C.; Song, C.; Huang, N.; Du, Y. *RSC Med. Chem.* **2022,** *13,* 1300–1321. doi:10.1039/d2md00206j
6. Gawad, N. M. A.-E.; Georgey, H. H.; Ibrahim, N. A.; Amin, N. H.; Abdelsalam, R. M. *Arch. Pharmacal Res.* **2012,** *35,* 807–821. doi:10.1007/s12272-012-0507-y
7. Ouyang, G.; Cai, X.-J.; Chen, Z.; Song, B.-A.; Bhadury, P. S.; Yang, S.; Jin, L.-H.; Xue, W.; Hu, D.-Y.; Zeng, S. *J. Agric. Food Chem.* **2008,** *56,* 10160–10167. doi:10.1021/jf802489e

8. Lupsor, S.; Aonofriesei, F.; Iovu, M. *Med. Chem. Res.* **2012,** *21,* 3035–3042. doi:10.1007/s00044-011-9839-2
9. Mert, S.; Kasımoğulları, R.; İça, T.; Çolak, F.; Altun, A.; Ok, S. *Eur. J. Med. Chem.* **2014,** *78,* 86–96. doi:10.1016/j.ejmech.2014.03.033
10. Hassan, G. S.; Kadry, H. H.; Abou-Seri, S. M.; Ali, M. M.; Mahmoud, A. E. E.-D. *Bioorg. Med. Chem.* **2011,** *19,* 6808–6817. doi:10.1016/j.bmc.2011.09.036
11. Rangaswamy, J.; Vijay Kumar, H.; Harini, S. T.; Naik, N. *Bioorg. Med. Chem. Lett.* **2012,** *22,* 4773–4777. doi:10.1016/j.bmcl.2012.05.061
12. Palaska, E.; Aytemir, M.; Uzbay, İ. T.; Erol, D. *Eur. J. Med. Chem.* **2001,** *36,* 539–543. doi:10.1016/s0223-5234(01)01243-0
13. Eftekhari-Sis, B.; Zirak, M.; Akbari, A. *Chem. Rev.* **2013,** *113,* 2958–3043. doi:10.1021/cr300176g
14. Ansari, A.; Ali, A.; Asif, M.; Shamsuzzaman, S. *New J. Chem.* **2017,** *41,* 16–41. doi:10.1039/c6nj03181a
15. Kang, E.; Kim, H. T.; Joo, J. M. *Org. Biomol. Chem.* **2020,** *18,* 6192–6210. doi:10.1039/d0ob01265c
16. Yasman; Edrada, R. A.; Wray, V.; Proksch, P. *J. Nat. Prod.* **2003,** *66,* 1512–1514. doi:10.1021/np030237j
17. Brown, S. P.; Smith, A. B., III. *J. Am. Chem. Soc.* **2015,** *137,* 4034–4037. doi:10.1021/ja512880g
18. Lawson, A. P.; Long, M. J. C.; Coffey, R. T.; Qian, Y.; Weerapana, E.; El Oualid, F.; Hedstrom, L. *Cancer Res.* **2015,** *75,* 5130–5142. doi:10.1158/0008-5472.can-15-1544
19. Yang, H.; Duan, X.-H.; Zhao, J.-F.; Guo, L.-N. *Org. Lett.* **2015,** *17,* 1998–2001. doi:10.1021/acs.orglett.5b00754
20. Mao, X.; Ni, J.; Xu, B.; Ding, C. *Org. Chem. Front.* **2020,** *7,* 350–354. doi:10.1039/c9qo01174a
21. Dutta, S.; Abe, H.; Aoyagi, S.; Kibayashi, C.; Gates, K. S. *J. Am. Chem. Soc.* **2005,** *127,* 15004–15005. doi:10.1021/ja053735i
22. Jiménez, C.; Crews, P. *Tetrahedron* **1991,** *47,* 2097–2102. doi:10.1016/s0040-4020(01)96120-4
23. Plano, D.; Karelia, D. N.; Pandey, M. K.; Spallholz, J. E.; Amin, S.; Sharma, A. K. *J. Med. Chem.* **2016,** *59,* 1946–1959. doi:10.1021/acs.jmedchem.5b01503
24. Nguyen, T.; Rubinstein, M.; Wakselman, C. *J. Org. Chem.* **1981,** *46,* 1938–1940. doi:10.1021/jo00322a047
25. Prabhu, K. R.; Ramesha, A. R.; Chandrasekaran, S. *J. Org. Chem.* **1995,** *60,* 7142–7143. doi:10.1021/jo00127a017
26. Riemschneider, R.; Wojahn, F.; Orlick, G. *J. Am. Chem. Soc.* **1951,** *73,* 5905–5907. doi:10.1021/ja01156a552
27. Goossen, L.; Matheis, C.; Wang, M.; Krause, T. *Synlett* **2015,** *26,* 1628–1632. doi:10.1055/s-0034-1378702
28. Higuchi, H.; Otsubo, T.; Ogura, F.; Yamaguchi, H.; Sakata, Y.; Misumi, S. *Bull. Chem. Soc. Jpn.* **1982,** *55,* 182–187. doi:10.1246/bcsj.55.182
29. Mullen, G. P.; Luthra, N. P.; Dunlap, R. B.; Odom, J. D. *J. Org. Chem.* **1985,** *50,* 811–816. doi:10.1021/jo00206a017
30. Krief, A.; Dumont, W.; Delmotte, C. *Angew. Chem., Int. Ed.* **2000,** *39,* 1669–1672. doi:10.1002/(sici)1521-3773(20000502)39:9<1669::aid-anie1669>3.0.co;2-6
31. Yu, F.; Li, C.; Wang, C.; Zhang, H.; Cao, Z.-Y. *Org. Lett.* **2021,** *23,* 7156–7160. doi:10.1021/acs.orglett.1c02564
32. Tao, S.; Jiang, L.; Du, Y. *Asian J. Org. Chem.* **2022,** *11,* e202200595. doi:10.1002/ajoc.202200595
33. Barbero, M.; Degani, I.; Diulgheroff, N.; Dughera, S.; Fochi, R. *Synthesis* **2001,** 585–590. doi:10.1055/s-2001-12362
34. Sun, N.; Che, L.; Mo, W.; Hu, B.; Shen, Z.; Hu, X. *Org. Biomol. Chem.* **2015,** *13,* 691–696. doi:10.1039/c4ob02208d
35. Fujiki, K.; Yoshida, E. *Synth. Commun.* **1999,** *29,* 3289–3294. doi:10.1080/00397919908085956
36. Takagi, K.; Takachi, H.; Sasaki, K. *J. Org. Chem.* **1995,** *60,* 6552–6556. doi:10.1021/jo00125a047
37. Teng, F.; Yu, J.-T.; Yang, H.; Jiang, Y.; Cheng, J. *Chem. Commun.* **2014,** *50,* 12139–12141. doi:10.1039/c4cc04578e
38. Yang, X.; She, Y.; Chong, Y.; Zhai, H.; Zhu, H.; Chen, B.; Huang, G.; Yan, R. *Adv. Synth. Catal.* **2016,** *358,* 3130–3134. doi:10.1002/adsc.201600304
39. Zhang, X.-Z.; Ge, D.-L.; Chen, S.-Y.; Yu, X.-Q. *RSC Adv.* **2016,** *6,* 66320–66323. doi:10.1039/c6ra13303g
40. Jiang, G.; Zhu, C.; Li, J.; Wu, W.; Jiang, H. *Adv. Synth. Catal.* **2017,** *359,* 1208–1212. doi:10.1002/adsc.201601142
41. Ali, D.; Panday, A. K.; Choudhury, L. H. *J. Org. Chem.* **2020,** *85,* 13610–13620. doi:10.1021/acs.joc.0c01738
42. Khalili, D. *New J. Chem.* **2016,** *40,* 2547–2553. doi:10.1039/c5nj02314a
43. Fotouhi, L.; Nikoofar, K. *Tetrahedron Lett.* **2013,** *54,* 2903–2905. doi:10.1016/j.tetlet.2013.02.106
44. Yadav, J. S.; Reddy, B. V. S.; Shubashree, S.; Sadashiv, K. *Tetrahedron Lett.* **2004,** *45,* 2951–2954. doi:10.1016/j.tetlet.2004.02.073
45. Yadav, J. S.; Reddy, B. V. S.; Krishna, A. D.; Reddy, C. S.; Narsaiah, A. V. *Synthesis* **2005,** 961–964. doi:10.1055/s-2005-861852
46. Thiruvikraman, S. V.; Seshadri, S. *Bull. Chem. Soc. Jpn.* **1985,** *58,* 785–786. doi:10.1246/bcsj.58.785
47. Kokorekin, V. A.; Sigacheva, V. L.; Petrosyan, V. A. *Tetrahedron Lett.* **2014,** *55,* 4306–4309. doi:10.1016/j.tetlet.2014.06.028
48. Finar, I. L.; Godfrey, K. E. *J. Chem. Soc.* **1954,** 2293–2298. doi:10.1039/jr9540002293
49. Kittikool, T.; Yotphan, S. *Eur. J. Org. Chem.* **2020,** 961–970. doi:10.1002/ejoc.201901770
50. Zhang, Y.; Xu, S.; Zhu, Y.; Xu, Q.; Gao, H.; Liang, Z.; Yao, X. *Eur. J. Org. Chem.* **2023,** *26,* e202201278. doi:10.1002/ejoc.202201278
51. Dey, A.; Hajra, A. *Adv. Synth. Catal.* **2019,** *361,* 842–849. doi:10.1002/adsc.201801232
52. Chen, X.-Y.; Kuang, X.; Wu, Y.; Zhou, J.; Wang, P. *Chin. J. Chem.* **2023,** *41,* 1979–1986. doi:10.1002/cjoc.202300188
53. Zhang, X.; Wang, C.; Jiang, H.; Sun, L. *RSC Adv.* **2018,** *8,* 22042–22045. doi:10.1039/c8ra04407d
54. Tao, S.; Xiao, J.; Li, Y.; Sun, F.; Du, Y. *Chin. J. Chem.* **2021,** *39,* 2536–2546. doi:10.1002/cjoc.202100278
55. Jouvin, K.; Matheis, C.; Goossen, L. J. *Chem. – Eur. J.* **2015,** *21,* 14324–14327. doi:10.1002/chem.201502914
56. Adams, R.; Bramlet, H. B.; Tendick, F. H. *J. Am. Chem. Soc.* **1920,** *42,* 2369–2374. doi:10.1021/ja01456a033
57. Ito, Y.; Touyama, A.; Uku, M.; Egami, H.; Hamashima, Y. *Chem. Pharm. Bull.* **2019,** *67,* 1015–1018. doi:10.1248/cpb.c19-00352
58. Tao, S.; Huo, A.; Gao, Y.; Zhang, X.; Yang, J.; Du, Y. *Front. Chem. (Lausanne, Switz.)* **2022,** *10,* 859995. doi:10.3389/fchem.2022.859995
59. Tao, S.; Xu, L.; Yang, K.; Zhang, J.; Du, Y. *Org. Lett.* **2022,** *24,* 4187–4191. doi:10.1021/acs.orglett.2c01468
60. For our previous clarification on identifying the formation of $(SeCN)_2$ and Cl–SeCN intermediates, see references [54,58,59].

BEILSTEIN JOURNAL OF ORGANIC CHEMISTRY

Tetrabutylammonium iodide-catalyzed oxidative α-azidation of β-ketocarbonyl compounds using sodium azide

Christopher Mairhofer‡, David Naderer‡ and Mario Waser*

Full Research Paper

Open Access

Address:
Institute of Organic Chemistry, Johannes Kepler University Linz, Altenbergerstrasse 69, 4040 Linz, Austria

Email:
Mario Waser* - mario.waser@jku.at

* Corresponding author ‡ Equal contributors

Keywords:
azidation; nitration; organocatalysis; oxidation; quaternary ammonium iodides

Beilstein J. Org. Chem. **2024,** *20,* 1510–1517.
https://doi.org/10.3762/bjoc.20.135

Received: 28 March 2024
Accepted: 28 June 2024
Published: 05 July 2024

This article is part of the thematic issue "Hypervalent halogen chemistry".

Guest Editor: T. Gulder

Abstract

We herein report the oxidative α-azidation of carbonyl compounds by using NaN_3 in the presence of dibenzoyl peroxide catalyzed by tetrabutylammonium iodide (TBAI). By utilizing these readily available bulk chemicals a variety of cyclic β-ketocarbonyl derivatives can be efficiently α-azidated under operationally simple conditions. Control experiments support a mechanistic scenario involving in situ formation of an ammonium hypoiodite species which first facilitates the α-iodination of the pronucleophile, followed by a phase-transfer-catalyzed nucleophilic substitution by the azide. Furthermore, we also show that an analogous α-nitration by using $NaNO_2$ under otherwise identical conditions is possible as well.

Introduction

Organic compounds containing an azide functionality are highly valuable synthesis targets that offer considerable potential for various applications and further manipulations [1-14]. For example, such molecules can be utilized to access free amines [3,13] and undergo Staudinger-type ligations [14]. Furthermore, they can be very efficiently employed for triazole-forming 1,3-dipolar cycloadditions with alkynes ("click-chemistry") [9-12]. As a consequence, the synthesis of organic azides is an important task and it comes as no surprise that a variety of conceptually complementary strategies to install azide groups in organic molecules have been reported [1-8]. α-Azido carbonyl derivatives are especially interesting targets which can be accessed by different approaches [6-8]. Maybe the most classical way to access organic azides is based on the utilization of pre-functionalized starting materials where a suited leaving group undergoes substitution using nucleophilic azide sources such as NaN_3 or $TMSN_3$ [6,7,15]. In addition, the recent years have seen remarkable progress in utilizing electrophilic azide-transfer reagents, i.e., hypervalent iodine-based compounds, for (asymmetric) α-azidations [16-23]. Besides these valuable ap-

proaches, which either require appropriate pre-functionalization of the starting materials (nucleophilic approach), or rely on more advanced N_3-transfer agents (electrophilic approach), over the course of the last years also α-azidations of enolate-type precursors using nucleophilic azide sources under oxidative conditions have been introduced very successfully [24-31]. Such oxidative coupling strategies of two inherently nucleophilic species allow for the direct utilization of simple starting materials in an efficient manner and especially the use of quaternary ammonium iodides as redox active catalysts has emerged as a powerful catalysis concept for such transformations [32-36]. These oxidative approaches, which usually proceed via the in situ formation of catalytically-competent ammonium hypoiodite species, can normally be carried out under operationally simple conditions, thus allowing for the use of easily accessible starting materials. Our group has a longstanding research interest in α-heterofunctionalization reactions under oxidative conditions [37-39] and we [30], as well as others [28,29,31], have recently also explored the use of simple quaternary ammonium iodides for oxidative α-azidations of carbonyl compounds (Scheme 1A). Hereby different strategies using different quaternary ammonium iodide derivatives and different azide sources were investigated and especially Uyanik's and Ishihara's recent approach using NaN_3 in combination with the carefully designed achiral catalyst **C1** represents a remarkable advancement in this field (Scheme 1B [31]). In contrast to previous oxidative quaternary ammonium iodide catalysis reports [28-30], this method does not require the use of $TMSN_3$, thus presenting an efficient oxidative α-azidation protocol utilizing NaN_3, which arguably represents the most easily available and cheapest nucleophilic N_3 source (for other remarkable approaches using alternative catalysts and oxidants see references [24-26]). In addition to the racemic approach, they also showed that this reaction can be rendered enantioselective by using advanced Maruoka-type quaternary ammonium iodides [40]. Interestingly, designer catalyst **C1** was found being catalytically superior compared to Bu_4NI (TBAI) when using H_2O_2 as the oxidant. Furthermore, it turned out that addition of PBN (phenyl *N*-*t*ert-butylnitrone) has a beneficial effect on the reaction and that carefully buffered conditions are best-suited. We have recently established the use of dibenzoyl peroxide (DBPO) as a very powerful oxidant for oxidative heterofunctionalization reactions using simple nucleophilic inorganic salts as heteroatom transfer reagents [39,41]. This was successfully demonstrated for the non-catalyzed α-S(e)CN-functionalization of different pronucleophiles [39] as well as the benzylic azidation of alkylphenol derivatives with NaN_3 using TBAI as a catalyst [41]. Considering the fact that TBAI clearly represents one of the most easily available quaternary ammonium iodides and keeping in mind our successfully demonstrated matching combination of this catalyst with NaN_3 and DBPO for our benzylic azidations [41], we were thus wondering if the use of these simple bulk chemicals also allows for the oxidative α-azidation of different carbonyl-based pronucleophiles. As outlined in this contribution, this reagent/catalyst system allows indeed for high yielding direct α-azidations of different (cyclic) β-ketocarbonyl derivatives (Scheme 1C), thus resulting in an operationally simple protocol to access α-azidated carbonyl derivatives. In addition, we have also carried out some test reactions using $NaNO_2$ instead of NaN_3 under otherwise identical conditions and obtained a first proof-of-concept for the analogous, to the best of our knowledge so far unprecedented, quaternary ammonium hypoiodite-mediated α-nitration reaction.

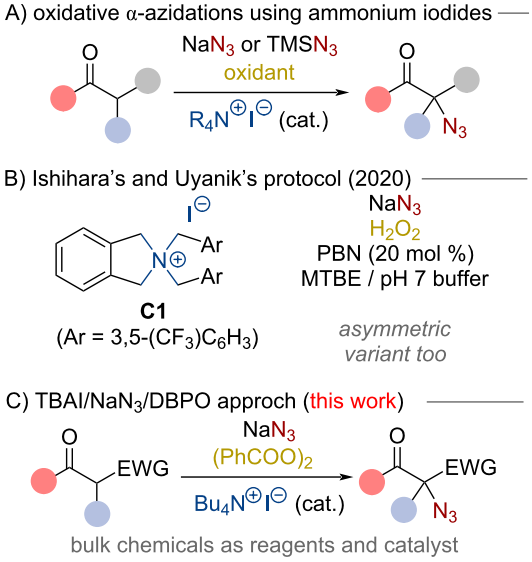

Scheme 1: General illustration of the oxidative α-azidation of carbonyl derivatives using quaternary ammonium iodides (A), Ishihara's protocol using NaN_3 (B), and the herein reported combination of Bu_4NI (TBAI), NaN_3 and DBPO ($(PhCOO)_2$) (C).

Results and Discussion

We started our investigations by optimizing the α-azidation of the *tert*-butyl-containing β-ketoester **1a** (Table 1 gives an overview of the most significant results obtained hereby). First experiments testing different oxidants in combination with Bu_4NI (30 mol %) in 1,2-dichloroethane (DCE), a solvent that we found to be well-suited for oxidative α-heterofunctionalizations before [39], showed that DBPO clearly outperforms all the other oxidants tested under these conditions (Table 1, entries 1–5). While H_2O_2 gave **2a** in low yield only (Table 1, entry 1), the use of mCPBA (Table 1, entry 3) and *t*-BuOOH (Table 1, entry 4) mainly resulted in the formation of the α-OH-ketoester **4**. On the other hand, oxone performed significantly better (Table 1, entry 2) but was also found to be inferior as compared to DBPO, which allowed for the more or less quantitative "spot-to-spot" formation of **2a** without any noteworthy side-product

Table 1: Optimization of the α-azidation of β-ketoester **1a**[a].

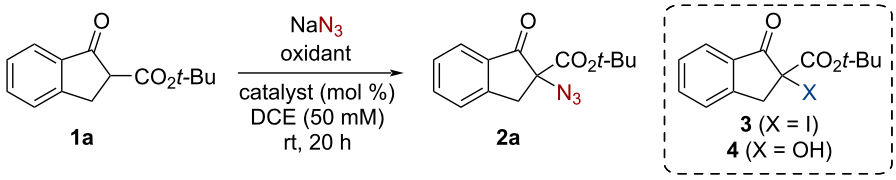

Entry	Cat. (mol %)	Equiv NaN_3	Oxidant (equiv)	**2a** (%)[b]	**3** (%)[c]	**4** (%)[c]
1	Bu_4NI (30)	2.2	H_2O_2 (2)	20	0	traces
2	Bu_4NI (30)	2.2	oxone (2)	85	5	0
3	Bu_4NI (30)	2.2	mCPBA (2)	20	0	50
4	Bu_4NI (30)	2.2	*t*-BuOOH (2)	30	traces	60
5	Bu_4NI (30)	2.2	DBPO (2)	>95	0	0
6	–	2.2	DBPO (2)	0	0	10
7	Bu_4NBr (30)	2.2	DBPO (2)	>95	0	0
8	Bu_4NCl (30)	2.2	DBPO (2)	15[d]	0	0
9	Bu_4NHSO_4 (30)	2.2	DBPO (2)	0[d]	0	0
10	KI (50)	2.2	DBPO (2)	60	30	0
11	Bu_4NI (30)	2.2	DBPO (1.2)	>95	0	0
12	Bu_4NI (30)	2.2	DBPO (0.5)	45	0	0
13	Bu_4NI (30)	1.2	DBPO (1.2)	>95	0	0
14	Bu_4NI (20)	1.2	DBPO (1.2)	95 (94)[e]	0	0
15	Bu_4NI (10)	1.2	DBPO (1.2)	85	0	0

[a]Unless otherwise stated, all reactions were carried out by stirring **1a** (0.1 mmol), the indicated amount of NaN_3, the catalyst, and the oxidant in 1,2-dichloroethane (DCE, 50 mM based on **1a**) at rt for 20 h. [b]NMR yield using 1,3,5-trimethoxybenzene as an internal standard (given in 5% intervals). [c]Determined by ^1H NMR of the crude product (given in 5% intervals). [d]Complete conversion of **1a** but giving a rather complex reaction mixture. [e]Isolated yield on 1 mmol scale.

formation (Table 1, entry 5). Screening different catalyst/DBPO combinations next (Table 1, entries 5–10), showed that the reaction requires a quaternary ammonium halide containing an easily oxidizable counter anion, i.e., iodide or bromide (Table 1, entries 5 and 7). No product formation was observed in the absence of any catalyst (Table 1, entry 6) or in the presence of Bu_4NHSO_4 (Table 1, entry 9) and the use of Bu_4NCl (Table 1, entry 8) was not satisfying either. On the other hand, the beneficial effect of the quaternary ammonium functionality was clearly underscored by employing KI instead of Bu_4NI (compare Table 1, entries 10 and 5). While Bu_4NI allowed for the clean and selective formation of **1a**, we observed significant amounts of the α-I-ketoester **3** when using KI instead. Having established the combination of DBPO and Bu_4NI as the best-suited catalyst/oxidant combination for the α-azidation of **1a** using NaN_3, we finally optimized stoichiometry and catalyst loading (Table 1, entries 11–15). Hereby we found the use of 1.2 equiv of NaN_3 with 1.2 equiv of DBPO and 20 mol % Bu_4NI as the best-suited and most economic reagent/catalyst combination, which allowed for the synthesis of **2a** in high isolated yield on 1 mmol scale as well (Table 1, entry 14). Tests using other solvents under these optimized conditions were also carried out (details not given in Table 1, which showed that CH_2Cl_2 (95% NMR yield), toluene (95% NMR yield), acetonitrile (90% NMR yield), and THF (85% NMR yield) are also very well-tolerated.

Having identified high-yielding conditions for the synthesis of **2a**, we next carried out a series of control experiments in order to address the role of the catalyst's counter anion and the oxidant (Table 2). Running the reaction of **1a** and NaN_3 in the presence of stoichiometric amounts of Bu_4NI_3, I_2, Bu_4NIO_3, or Bu_4NIO_4 did not lead to any noteworthy levels of product formation (Table 2, entries 1–4). In sharp contrast, the use of $Bu_4NOH + I_2$, which is known to give Bu_4NIO in situ [41-44], results in the formation of **2a** in a yield comparable to the above-described catalytic system. Accordingly, and in strong analogy to previous reports [31,41-43], the herein reported protocol most likely proceeds via in situ formation of a catalytically competent quaternary ammonium hypoiodite species which then facilities the coupling of the two inherently nucleophilic reaction partners. To get further mechanistic insights we also carried out our standard reaction (Table 1, entry 14) in the presence of well-established radical traps like TEMPO, di-*tert*-

butylhydroxytoluene (BHT), or 1,1-diphenylethene (DPE). In neither case any influence on the yield was observed, thus ruling out a mechanism involving radical species.

Table 2: Control experiments using different hypervalent iodine species[a].

Entry	Oxidant (1 equiv)	**2a** (%)[b]
1	Bu_4NI_3	0
2	I_2	15
3	Bu_4NIO_3	0
4	Bu_4NIO_4	0
5	I_2/Bu_4NOH[c]	95

[a]Carried out by reacting **1a** (0.1 mmol) and NaN_3 (2.2 equiv) in the presence of 1 equiv of the indicated oxidant in DCE at rt for 20 h. [b]NMR yield using 1,3,5-trimethoxybenzene as an internal standard (given in 5% intervals). [c]Resulting in the formation of Bu_4NIO [41-44].

Based on these mechanistic details obtained so far, we were also wondering if we could get any hints concerning possible reaction intermediates. Ishihara's group recently showed that their α-azidation protocol proceeds via in situ α-iodination first, followed by nucleophilic displacement by the azide [31]. Not surprisingly, when we analyzed reactions shortly after the addition of all reagents we detected notable amounts of the α-iodinated β-ketoester **3** which then converted to the final product **2a** over time. Furthermore, we also synthesized compound **3** independently (by reacting **1a** with TBAI and additional KI in the presence of DBPO) and then resubmitted this compound to our ammonium salt-catalyzed azidation reaction conditions, observing full conversion to **2a** as well. Considering all these details we thus propose a mechanistic scenario as outlined in Scheme 2. The catalyst gets oxidized to Bu_4NIO first, which then facilitates the α-iodination of **1a** (hereby either the formed benzoate or the hypoiodite itself may serve as a base). Intermediate **3** then undergoes a phase-transfer-catalyzed nucleophilic substitution with NaN_3 thus delivering the final product **2a**.

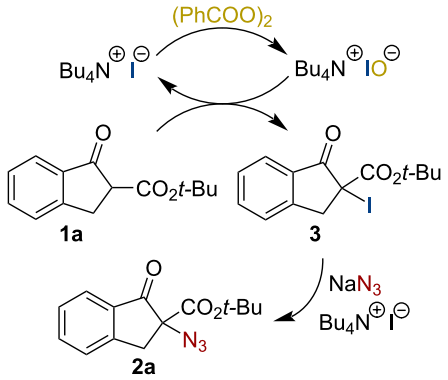

Scheme 2: Proposed mechanistic scenario.

With optimized conditions and a plausible mechanistic understanding at hand, we next investigated the application scope and limitations of this methodology. As outlined in Scheme 3, a series of differently substituted α-azido-β-ketoesters **2** as well as analogous α-azido-β-ketoketones **5** and the α-azido-β-ketoamide **6** could be accessed straightforwardly. Furthermore, this procedure was also successfully extended to γ-butyrolactone-based products **7**. Unfortunately, this methodology came to its limits when using tetralone-based β-ketoesters like compound **8**, which resulted in a complex product mixture, or the acylic β-ketoester **9**, which did not show any conversion under

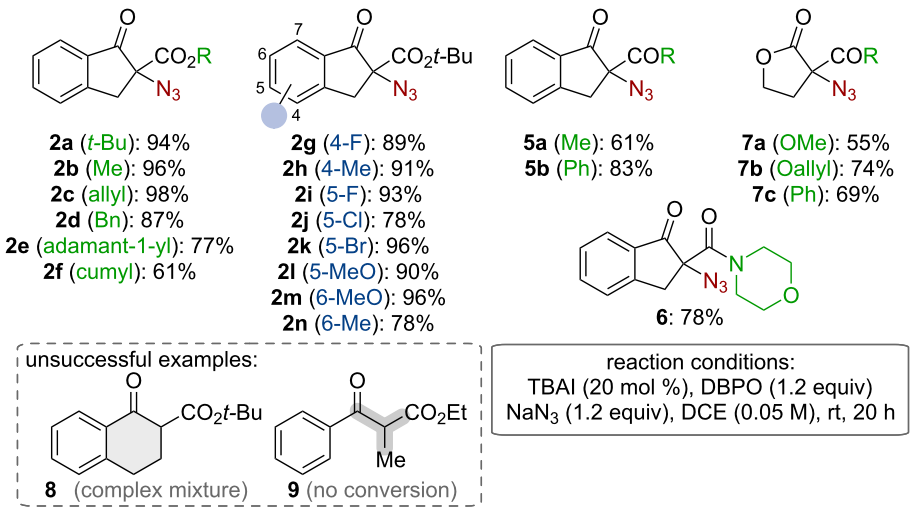

Scheme 3: Application scope.

these conditions. The later limitation shows a clear difference between our methodology and Uyanik's and Ishihara's protocol [31], underscoring the higher reactivity of their designer catalyst (Scheme 1B).

Having established the TBAI/DBPO-mediated α-azidation using NaN_3, we also briefly tested whether this concept can be extended to an analogous α-nitration approach. Different strategies for α-nitrations of carbonyl compounds have been reported [45-50], but the use of $NaNO_2$ under simple oxidative conditions has so far received relatively little attention [51]. Gratifyingly, employing $NaNO_2$ (2.2 equiv) under our established oxidative α-azidation conditions we found it possible to access the α-NO_2-β-ketoesters **10a–c** as well (Scheme 4), which in our opinion represents an interesting proof-of-concept for an ammonium hypoiodite-mediated α-nitration. In this case we observed intermediate formation of the α-iodinated β-ketoester **3** as well (vide supra), which suggests an analogous mechanistic scenario as for the azidation (compare with Scheme 3). However, it should also be stated that the α-nitro products **10** were found to be not too stable, undergoing some unspecific decomposition and also some decarboxylation during column chromatography or upon prolonged reaction times. Also, tests with analogous β-ketoketones and β-ketoamides (compare with azidation products **5** and **6**, Scheme 3) did not give any products but resulted in the formation of a variety of unidentified side-products, thus illustrating that this α-nitration methodology seems to be less general than the α-azidation, which can most likely be attributed to the sensitivity of the products (containing a carbon with three electron-withdrawing groups).

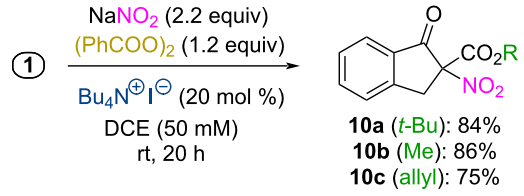

Scheme 4: Proof-of-concept for the analogous oxidative α-nitration.

Conclusion

α-Azidation reactions of carbonyl derivatives are powerful approaches to access valuable organic azides. In this contribution we report the direct α-azidation of cyclic β-ketocarbonyl compounds using NaN_3. This coupling of two inherently nucleophilic species is possible by carrying out the reaction under oxidative conditions using dibenzoyl peroxide in the presence of a catalytic amount of tetrabutylammonium iodide (TBAI). Control experiments support a mechanistic scenario proceeding via in situ formation of a catalytically competent quaternary ammonium hypoiodite first. This higher oxidation state species then facilitates the α-iodination of the pronucleophile, followed by a phase-transfer-catalyzed nucleophilic substitution by the azide. Furthermore, we also obtained a first proof-of-concept for the conceptually analogous α-nitration by using $NaNO_2$ under otherwise identical conditions.

Experimental

General details

^1H, ^{13}C and ^{19}F NMR spectra were recorded on a Bruker Avance III 300 MHz spectrometer with a broad band observe probe and a sample changer for 16 samples, on a Bruker Avance DRX 500 MHz spectrometer, and on a Bruker Avance III 700 MHz spectrometer with an Ascend magnet and TCI cryoprobe, which are all property of the Austro Czech NMR Research Center "RERI uasb". All NMR spectra were referenced on the solvent residual peak ($CDCl_3$: δ = 7.26 ppm for ^1H NMR, δ = 77.16 ppm for ^{13}C NMR, ^{19}F NMR unreferenced). IR spectra were recorded on a Bruker Alpha II FTIR spectrometer with diamond ATR-module using the OPUS software package. HRMS spectra were recorded on an Agilent QTOF 6520 spectrometer with an ESI source. Melting points are recorded using a Büchi M-560 apparatus and are reported uncorrected. TLC was performed on Macherey-Nagel precoated TLC plates (silica gel, 60 F254, 0.20 mm, ALUGRAM® Xtra SIL). Preparative column chromatography was carried out using Davisil LC 60 Å 70-200 MICRON silica gel. All chemicals were purchased from commercial suppliers and used without further purification unless otherwise stated.

General α-azidation procedure

Sodium azide (7.8 mg, 120 µmol, 1.2 equiv) and TBAI (7.4 mg, 20 µmol, 20 mol %) were suspended in a stirred solution of the respective starting material (100 µmol, 1.00 equiv) in 1.0 mL of DCE at rt. Then, a solution of anhydrous dibenzoyl peroxide (29.1 mg, 120 µmol, 1.2 equiv) in 1.0 mL of DCE was added to the suspension and the mixture was stirred for 20 h. The reaction solution was then diluted with 8 mL dichloromethane and extracted with 5 mL of sat. aq $NaHCO_3$. The aqueous phase was then extracted twice with 10 mL of DCM. The organic layer and the extracts were then filtered consecutively through a pad of anhydr. sodium sulfate and deactivated silica gel. The solvents were removed in vacuo. In most cases the products were already obtained in sufficiently high purity (>95%) after this work up. If necessary, further purification by silica gel column chromatography can be carried out.

Safety considerations: It is known that the combination of inorganic azides and halogenated compounds can lead to the formation of explosive diazido compounds and thus we have also demonstrated that the azidation chemistry is possible in other solvents as well (vide supra). However, to the best of our know-

ledge this is mainly an issue with dichloromethane [52,53], whereas the reaction between NaN_3 and dichloroethane usually requires higher temperatures and represents a slow process [54] and we did not detect any diazidoethane by ^{1}H NMR in any of our crude products [55].

Analytical details for the parent compound 2a: Obtained in 94% yield (25.7 mg, 94.0 µmol). cf.: 1.0 mmol scale, 94% yield (256.9 mg, 940.0 µmol; purified by column chromatography on silica gel (eluent: heptanes/EtOAc = 19:1)). Yellowish-white solid; Analytical data match those reported in literature [30]. ^{1}H NMR (300 MHz, $CDCl_3$, 298 K, δ/ppm) 7.82 (d, J = 7.7 Hz, 1H), 7.66 (t, J = 7.5 Hz, 1H), 7.48–7.39 (m, 2H), 3.64 (d, J = 17.2 Hz, 1H), 2.99 (d, J = 17.2 Hz, 1H), 1.45 (s, 9H); ^{13}C NMR (75 MHz, $CDCl_3$, 298 K, δ/ppm) 198.1, 167.4, 152.3, 136.4, 133.3, 128.4, 126.5, 125.6, 84.6, 70.6, 38.6, 28.0; IR (neat, FT-ATR, 298 K, $\tilde{\nu}$/cm^{-1}): 2984, 2928, 2853, 2110, 1747, 1736, 1718, 1604, 1589, 1548, 1466, 1431, 1397, 1372, 1353, 1326, 1271, 1259, 1215, 1145, 1091, 1054, 1027, 961, 913, 871, 844, 834, 818, 804, 756, 729, 711, 688, 661, 623, 598, 561, 533, 459, 416; HRMS (ESI$^+$-QqTOF, m/z): $[M + NH_4]^+$ calcd for $C_{14}H_{19}N_4O_3$, 291.1452; found, 291.1452 (major); TLC (silica gel K60, 200 µm, F254, heptanes/EtOAc = 7:3, 298 K, R_f 0.64; mp: 65.0–67.5 °C.

General α-nitration procedure

Sodium nitrite (15.2 mg, 220 µmol, 2.2 equiv) and TBAI (7.4 mg, 20 µmol, 20 mol %) were suspended in a stirred solution of the respective starting material (100 µmol, 1.00 equiv) in 1.0 mL of DCE at rt. Then, a solution of anhydrous dibenzoyl peroxide (29.1 mg, 120 µmol, 1.2 equiv) in 1.0 mL of DCE was added to the suspension and the mixture was stirred for 20 h. The reaction solution was then diluted with 8 mL dichloromethane and extracted with 5 mL of sat. aq $NaHCO_3$. The aqueous phase was then extracted twice with 10 mL of DCM. The organic layer and the extracts were then filtered consecutively through a pad of anhydr. sodium sulfate and deactivated silica gel. The solvents were removed in vacuo. In most cases the products were already obtained in sufficient purity (>95%) after this work up. If necessary, further purification can be achieved by fast silica gel column chromatography (the products tend to decompose on silica gel).

Analytical details for the parent compound 10a: Obtained in 84% yield (23.3 mg, 94.0 µmol). white solid; ^{1}H NMR (700 MHz, $CDCl_3$, 298 K, δ/ppm) 7.86 (d, J = 7.7 Hz, 1H), 7.71 (t, J = 7.5 Hz, 1H), 7.53 (d, J = 7.7 Hz, 1H), 7.48 (t, J = 7.5 Hz, 1H), 4.11 (d, J = 17.9 Hz, 1H), 3.99 (d, J = 17.9 Hz, 1H), 1.49 (s, 9H); ^{13}C NMR (126 MHz, $CDCl_3$, 298 K, δ/ppm) 188.4, 162.0, 150.1, 137.0, 132.9, 129.1, 126.5, 126.2, 96.7, 86.1, 37.5, 27.8; IR (neat, FT-ATR, 298 K, $\tilde{\nu}$/cm^{-1}): 2984, 2930, 2878, 2854, 1748, 1719, 1656, 1604, 1589, 1548, 1465, 1431, 1396, 1371, 1353, 1325, 1272, 1260, 1215, 1145, 1091, 1056, 1026, 961, 912, 871, 844, 834, 818, 803, 755, 730, 711, 688, 661, 625, 598, 561, 533, 459, 414; HRMS (ESI$^+$-QqTOF, m/z): $[M + H]^+$ calcd for $C_{14}H_{16}NO_5$, 278.1023; found, 278.1024; TLC (silica gel K60, 200 µm, F254, heptanes/EtOAc = 7:3, 298 K, R_f 0.47; mp: 75.9–78.4 °C.

Supporting Information

Supporting Information File 1

Full experimental and analytical details and copies of NMR spectra.
[https://www.beilstein-journals.org/bjoc/content/supplementary/1860-5397-20-135-S1.pdf]

Acknowledgements

We are grateful to Prof. Dr. Himmelsbach (Institute of Analytical Chemistry, JKU Linz) for support with HRMS analysis and Anna-Malin Draxler (Institute of Org. Chemistry, JKU Linz) for experimental support.

Funding

The used NMR spectrometers were acquired in collaboration with the University of South Bohemia (CZ) with financial support from the European Union through the EFRE INTERREG IV ETC-AT-CZ program (project M00146, "RERI-uasb").

ORCID® iDs

David Naderer - https://orcid.org/0009-0001-1378-4495
Mario Waser - https://orcid.org/0000-0002-8421-8642

Data Availability Statement

All data that supports the findings of this study is available in the published article and/or the supporting information to this article.

Preprint

A non-peer-reviewed version of this article has been previously published as a preprint: https://doi.org/10.3762/bxiv.2024.20.v1

References

1. Bräse, S.; Banert, K., Eds. *Organic Azides: Syntheses and Applications;* John Wiley & Sons: New York, NY, USA, 2009. doi:10.1002/9780470682517
2. Bräse, S.; Gil, C.; Knepper, K.; Zimmermann, V. *Angew. Chem., Int. Ed.* **2005,** *44,* 5188–5240. doi:10.1002/anie.200400657
3. Scriven, E. F. V.; Turnbull, K. *Chem. Rev.* **1988,** *88,* 297–368. doi:10.1021/cr00084a001

4. Huang, D.; Yan, G. *Adv. Synth. Catal.* **2017,** *359,* 1600–1619. doi:10.1002/adsc.201700103
5. Goswami, M.; de Bruin, B. *Eur. J. Org. Chem.* **2017,** 1152–1176. doi:10.1002/ejoc.201601390
6. Patonay, T.; Konya, K.; Juhasz-Toth, E. *Chem. Soc. Rev.* **2011,** *40,* 2797–2847. doi:10.1039/c0cs00101e
7. Faiz, S.; Zahoor, A. F.; Rasool, N.; Yousaf, M.; Mansha, A.; Zia-Ul-Haq, M.; Jaafar, H. Z. E. *Molecules* **2015,** *20,* 14699–14745. doi:10.3390/molecules200814699
8. Ding, P.-G.; Hu, X.-S.; Zhou, F.; Zhou, J. *Org. Chem. Front.* **2018,** *5,* 1542–1559. doi:10.1039/c8qo00138c
9. Bock, V. D.; Hiemstra, H.; van Maarseveen, J. H. *Eur. J. Org. Chem.* **2006,** 51–68. doi:10.1002/ejoc.200500483
10. Sletten, E. M.; Bertozzi, C. R. *Angew. Chem., Int. Ed.* **2009,** *48,* 6974–6998. doi:10.1002/anie.200900942
11. Liang, L.; Astruc, D. *Coord. Chem. Rev.* **2011,** *255,* 2933–2945. doi:10.1016/j.ccr.2011.06.028
12. Singh, M. S.; Chowdhury, S.; Koley, S. *Tetrahedron* **2016,** *72,* 5257–5283. doi:10.1016/j.tet.2016.07.044
13. Gololobov, Y. G.; Kasukhin, L. F. *Tetrahedron* **1992,** *48,* 1353–1406. doi:10.1016/s0040-4020(01)92229-x
14. Köhn, M.; Breinbauer, R. *Angew. Chem., Int. Ed.* **2004,** *43,* 3106–3116. doi:10.1002/anie.200401744
15. Phan, T. B.; Mayr, H. *J. Phys. Org. Chem.* **2006,** *19,* 706–713. doi:10.1002/poc.1063
16. Zhdankin, V. V. *Hypervalent Iodine Chemistry, Preparation, Structure, and Synthetic Applications of Polyvalent Iodine Compounds;* Wiley-VCH: Weinheim, Germany, 2013. doi:10.1002/9781118341155
17. Simonet-Davin, R.; Waser, J. *Synthesis* **2023,** *55,* 1652–1661. doi:10.1055/a-1966-4974
18. Mironova, I. A.; Kirsch, S. F.; Zhdankin, V. V.; Yoshimura, A.; Yusubov, M. S. *Eur. J. Org. Chem.* **2022,** e202200754. doi:10.1002/ejoc.202200754
19. Zhdankin, V. V.; Krasutsky, A. P.; Kuehl, C. J.; Simonsen, A. J.; Woodward, J. K.; Mismash, B.; Bolz, J. T. *J. Am. Chem. Soc.* **1996,** *118,* 5192–5197. doi:10.1021/ja954119x
20. Vita, M. V.; Waser, J. *Org. Lett.* **2013,** *15,* 3246–3249. doi:10.1021/ol401229v
21. Deng, Q.-H.; Bleith, T.; Wadepohl, H.; Gade, L. H. *J. Am. Chem. Soc.* **2013,** *135,* 5356–5359. doi:10.1021/ja402082p
22. He, C.; Wu, Z.; Zhou, Y.; Cao, W.; Feng, X. *Org. Chem. Front.* **2022,** *9,* 703–708. doi:10.1039/d1qo01634b
23. Yanagisawa, A.; Takagi, K.; Horiguchi, M.; Dezaki, K.; Marui, T.; Saito, E.; Ebihara, T.; Russell, G. M.; Watanabe, T.; Midorikawa, K. *Asian J. Org. Chem.* **2023,** *12,* e202300213. doi:10.1002/ajoc.202300213
24. Harschneck, T.; Hummel, S.; Kirsch, S. F.; Klahn, P. *Chem. – Eur. J.* **2012,** *18,* 1187–1193. doi:10.1002/chem.201102680
25. Klahn, P.; Erhardt, H.; Kotthaus, A.; Kirsch, S. F. *Angew. Chem., Int. Ed.* **2014,** *53,* 7913–7917. doi:10.1002/anie.201402433
26. Erhardt, H.; Häring, A. P.; Kotthaus, A.; Roggel, M.; Tong, M. L.; Biallas, P.; Jübermann, M.; Mohr, F.; Kirsch, S. F. *J. Org. Chem.* **2015,** *80,* 12460–12469. doi:10.1021/acs.joc.5b02328
27. Galligan, M. J.; Akula, R.; Ibrahim, H. *Org. Lett.* **2014,** *16,* 600–603. doi:10.1021/ol403504z
28. Dhineshkumar, J.; Prabhu, K. R. *Eur. J. Org. Chem.* **2016,** 447–452. doi:10.1002/ejoc.201501374
29. Yasui, K.; Kojima, K.; Kato, T.; Odagi, M.; Kato, M.; Nagasawa, K. *Tetrahedron* **2016,** *72,* 5350–5354. doi:10.1016/j.tet.2016.07.015
30. Tiffner, M.; Stockhammer, L.; Schörgenhumer, J.; Röser, K.; Waser, M. *Molecules* **2018,** *23,* 1142. doi:10.3390/molecules23051142
31. Uyanik, M.; Sahara, N.; Tsukahara, M.; Hattori, Y.; Ishihara, K. *Angew. Chem., Int. Ed.* **2020,** *59,* 17110–17117. doi:10.1002/anie.202007552
32. Uyanik, M.; Ishihara, K. *ChemCatChem* **2012,** *4,* 177–185. doi:10.1002/cctc.201100352
33. Wu, X.-F.; Gong, J.-L.; Qi, X. *Org. Biomol. Chem.* **2014,** *12,* 5807–5817. doi:10.1039/c4ob00276h
34. Claraz, A.; Masson, G. *Org. Biomol. Chem.* **2018,** *16,* 5386–5402. doi:10.1039/c8ob01378k
35. Uyanik, M. Catalytic Oxidative α-Functionalization of Carbonyls. In *Iodine Catalysis in Organic Synthesis;* Ishihara, K.; Muniz, K., Eds.; Wiley-VCH: Weinheim, Germany, 2022; pp 275–298. doi:10.1002/9783527829569.ch10
36. Odagi, M.; Nagasawa, K. *ChemCatChem* **2023,** *15,* e202300820. doi:10.1002/cctc.202300820
37. Mairhofer, C.; Novacek, J.; Waser, M. *Org. Lett.* **2020,** *22,* 6138–6142. doi:10.1021/acs.orglett.0c02198
38. Röser, K.; Scheucher, A.; Mairhofer, C.; Bechmann, M.; Waser, M. *Org. Biomol. Chem.* **2022,** *20,* 3273–3276. doi:10.1039/d2ob00463a
39. Mairhofer, C.; Röser, K.; Aryafard, M.; Himmelsbach, M.; Waser, M. *Eur. J. Org. Chem.* **2023,** *26,* e202300969. doi:10.1002/ejoc.202300969
40. Lee, H.-J.; Maruoka, K. *Chem. Rec.* **2023,** *23,* e202200286. doi:10.1002/tcr.202200286
41. Mairhofer, C.; Waser, M. *Adv. Synth. Catal.* **2023,** *365,* 2757–2762. doi:10.1002/adsc.202300405
42. Uyanik, M.; Okamoto, H.; Yasui, T.; Ishihara, K. *Science* **2010,** *328,* 1376–1379. doi:10.1126/science.1188217
43. Uyanik, M.; Hayashi, H.; Ishihara, K. *Science* **2014,** *345,* 291–294. doi:10.1126/science.1254976
44. Yamada, S.; Morizono, D.; Yamamoto, K. *Tetrahedron Lett.* **1992,** *33,* 4329–4332. doi:10.1016/s0040-4039(00)74252-3
45. Feuer, H.; Vincent, E. F., Jr. *J. Org. Chem.* **1964,** *29,* 939–940. doi:10.1021/jo01027a501
46. Feuer, H.; Monter, R. P. *J. Org. Chem.* **1969,** *34,* 991–995. doi:10.1021/jo01256a048
47. Sifniades, S. *J. Org. Chem.* **1975,** *40,* 3562–3566. doi:10.1021/jo00912a020
48. Fischer, R. H.; Weitz, H. M. *Synthesis* **1980,** 261–282. doi:10.1055/s-1980-28990
49. Zhang, Z.-Q.; Chen, T.; Zhang, F.-M. *Org. Lett.* **2017,** *19,* 1124–1127. doi:10.1021/acs.orglett.7b00040
50. Wei, W.-T.; Zhu, W.-M.; Ying, W.-W.; Wang, Y.-N.; Bao, W.-H.; Gao, L.-H.; Luo, Y.-J.; Liang, H. *Adv. Synth. Catal.* **2017,** *359,* 3551–3554. doi:10.1002/adsc.201700870
51. Dighe, S. U.; Mukhopadhyay, S.; Priyanka, K.; Batra, S. *Org. Lett.* **2016,** *18,* 4190–4193. doi:10.1021/acs.orglett.6b01807
52. Conrow, R. E.; Dean, W. D. *Org. Process Res. Dev.* **2008,** *12,* 1285–1286. doi:10.1021/op8000977
53. Treitler, D. S.; Leung, S. *J. Org. Chem.* **2022,** *87,* 11293–11295. doi:10.1021/acs.joc.2c01402
54. Kantheti, S.; Narayan, R.; Raju, K. V. S. N. *J. Coat. Technol. Res.* **2013,** *10,* 609–619. doi:10.1007/s11998-013-9494-2
55. Betzler, F. M.; Klapötke, T. M.; Sproll, S. M. *Eur. J. Org. Chem.* **2013,** 509–514. doi:10.1002/ejoc.201201201

BEILSTEIN JOURNAL OF ORGANIC CHEMISTRY

Divergent role of PIDA and PIFA in the AlX_3 (X = Cl, Br) halogenation of 2-naphthol: a mechanistic study

Kevin A. Juárez-Ornelas[1], Manuel Solís-Hernández[2], Pedro Navarro-Santos[*2], J. Oscar C. Jiménez-Halla[*1] and César R. Solorio-Alvarado[*1]

Full Research Paper

Open Access

Address:
[1]Departamento de Química, División de Ciencias Naturales y Exactas, Universidad de Guanajuato, Campus Gto, Noria Alta S/N 36050, Guanajuato, México and [2]CONAHCYT - Instituto de Investigaciones Químico Biológicas, Universidad Michoacana de San Nicolás de Hidalgo, Avenida Francisco J. Múgica S/N 58030, Morelia, Michoacán, México

Email:
Pedro Navarro-Santos[*] - pnavarrosa@conacyt.mx;
J. Oscar C. Jiménez-Halla[*] - jjimenez@ugto.mx;
César R. Solorio-Alvarado[*] - csolorio@ugto.mx

* Corresponding author

Keywords:
aromatic bromination; aromatic chlorination; density functional theory (DFT); hypervalent iodine; iodine(III)

Beilstein J. Org. Chem. **2024,** *20,* 1580–1589.
https://doi.org/10.3762/bjoc.20.141

Received: 20 March 2024
Accepted: 27 June 2024
Published: 15 July 2024

This article is part of the thematic issue "Hypervalent halogen chemistry" and is dedicated to the memory of our friend Kevin Juarez who unfortunately passed away.

Guest Editor: J. Wencel-Delord

Abstract

The reaction mechanism for the chlorination and bromination of 2-naphthol with PIDA or PIFA and AlX_3 (X = Cl, Br), previously reported by our group, was elucidated via quantum chemical calculations using density functional theory. The chlorination mechanism using PIFA and $AlCl_3$ demonstrated a better experimental and theoretical yield compared to using PIDA. Additionally, the lowest-energy chlorinating species was characterized by an equilibrium of Cl–I(Ph)–OTFA–$AlCl_3$ and [Cl–I(Ph)][OTFA–$AlCl_3$], rather than $PhICl_2$ being the active species. On the other hand, bromination using PIDA and $AlBr_3$ was more efficient, wherein the intermediate Br–I(Ph)–OAc–$AlBr_3$ was formed as active brominating species. Similarly, $PhIBr_2$ was higher in energy than our proposed species. The reaction mechanisms are described in detail in this work and were found to be in excellent agreement with the experimental yield. These initial results confirmed that our proposed mechanism was energetically favored and therefore more plausible compared to halogenation via $PhIX_2$.

Introduction

Hypervalent iodine(III) reagents have gained attention as strong oxidants with a low toxicity [1-8] and due to the ability to mimic reactivity [9] usually associated with transition metals [10,11]. Iodine(III) compounds have been used for the formation of different bond types, such as C–C [12,13], C–O [14,15], C–N [16], C–S [17], C–CN [18], C–F [19-21], C–I [22,23], C–NO_2 [24,25] and, in the context of this work, C–X (X = Cl, Br) [26-31]. So far, different protocols for the halogenation of arenes using iodine(III) reagents have been described, mainly using (diacetoxyiodo)benzene (PIDA)/TMSCl, PIDA/TMSBr

[32], and [bis(trifluoroacetoxy)iodo]benzene (PIFA)/TMSBr [33]. We have recently developed a new protocol for the oxidative chlorination and bromination of naphthols using the PIFA/$AlCl_3$ [26] and PIDA/$AlBr_3$ [28,29] systems. These unprecedented protocols combined iodine(III) reagents and aluminum salts to achieve chlorination and bromination of electron-rich arenes under mild and experimentally straightforward conditions (Scheme 1).

The synthesis of aryl halides is of great academic and industrial importance. Recently, our research group has developed a new procedure for the *ortho*-selective chlorination of phenols under mild conditions in a short reaction time [26]. The chlorinating species was generated in situ simply by mixing PIFA with a Lewis acid, in this case $AlCl_3$. The importance of this protocol arises from the oxidation of an $AlCl_3$-based chlorine atom, which is an available and cheap reagent. Then it is used as an electrophile source in the chlorination process with an umpolung reactivity. In contrast to the suggested traceroute where the chlorine or bromine atom is attached to the hypervalent iodine center of the plausible reagent $PhIX_2$ (X = Cl, Br), our new protocol opens up a broad path for the reaction through different halogenating species. For a deeper understanding of these reactions, we explored different pathways of the reaction mechanisms for the *ortho*-halogenation using 2-naphthol as a model substrate (Scheme 2). In such a way, we found a reaction pathway that was energetically favored.

Based on our successful procedure for chlorination, we also developed an efficient protocol for the electrophilic bromination of arenes, mainly phenols [28,29]. Accordingly, the bromination reaction was initially explored by mixing PIFA and $AlBr_3$, which gave an acceptable yield (84%). However, other iodine(III) reagents were tested as oxidants during the optimization process. Thus, when mixing PIDA with aluminum bromide, the reaction occurred with an unexpectedly higher yield

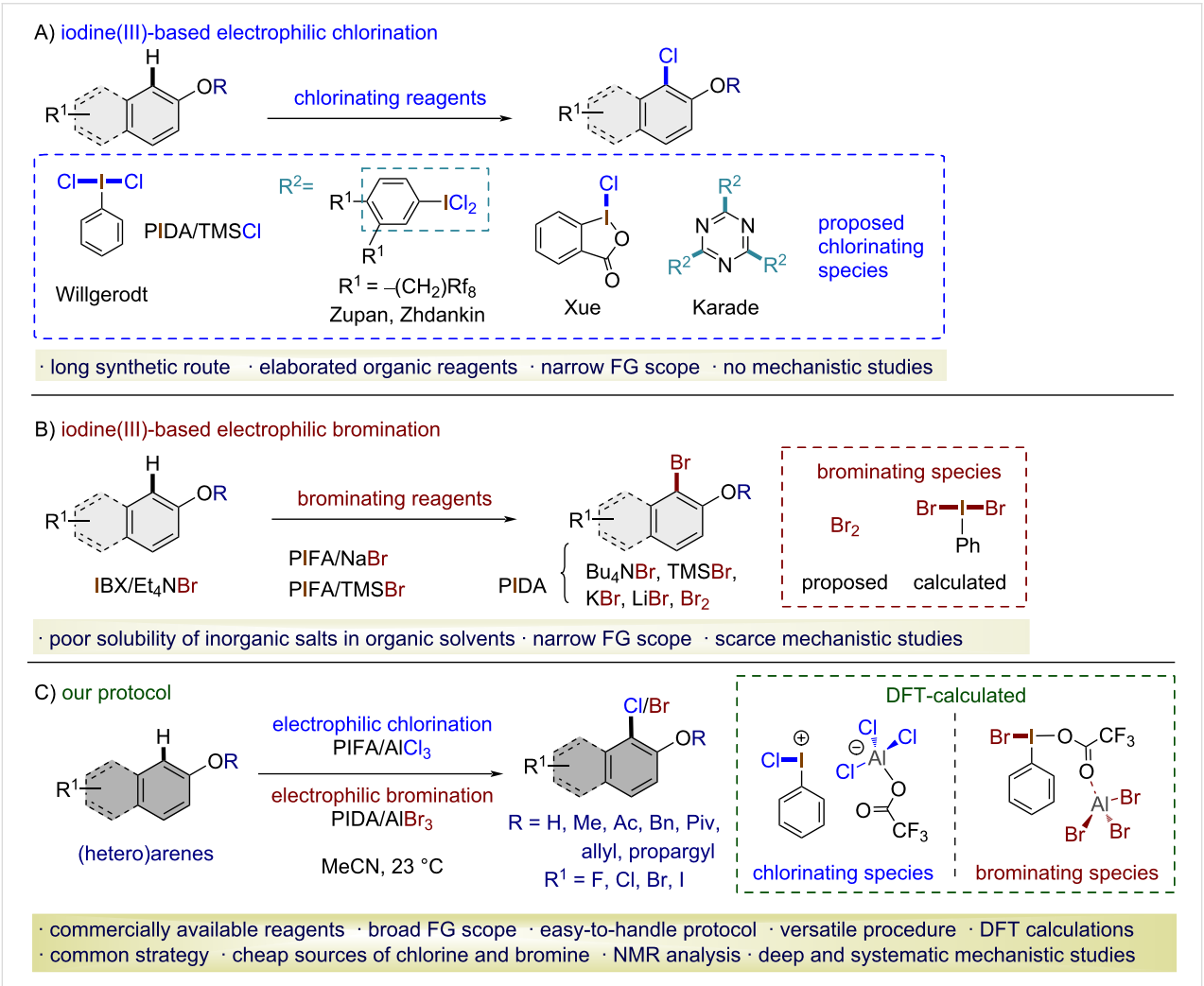

Scheme 1: Representative protocols for the oxidative aromatic chlorination and bromination with iodine(III) reagents.

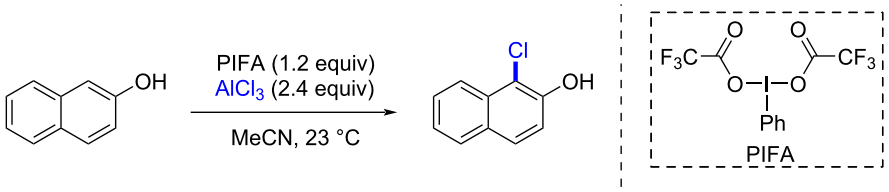

Scheme 2: Chlorination of 2-naphthol using the PIFA/$AlCl_3$, 1:2 system.

(93%) than with PIFA. Therefore, the bromination reaction proceeded in the presence of PIDA/$AlBr_3$ as a brominating system using MeCN as solvent (Scheme 3).

In light of the relevance of this newly discovered reactivity and the scarce mechanistic and theoretical studies available [33], we computationally explored all of the different plausible pathways to elucidate the most feasible route that allowed the reported halogenation under these new reaction conditions. In this work, we systematically investigated the influence of PIDA and PIFA in the chlorination and bromination reactions. Interestingly, we found an excellent agreement between the theoretical predictions and the experimental results.

Results and Discussion

Computational details

The equilibrium geometry of reagents and products, the stationary points, and transition-state structures were optimized by density functional theory (DFT) calculations employing the software Gaussian 16 [34]. Although the B3LYP functional could be suitable for these calculations, e.g., for tracing reaction pathways, nitrations, halogenations, or FC acylations in solution, we found the ω-B97XD functional [35] appropriate for this study because it considered dispersion interactions through a range separation (22% for short range and 100% Hartree–Fock for long range), which properly describes thermochemistry and noncovalent interactions. When searching for the critical points along the potential surface energy of the possible chlorination and bromination pathways studied in this work, Br and I atoms were treated with the revised version of the LANL2DZ basis set and effective core potential, referred to as LANL08(d), providing d-type polarization functions. Meanwhile, the 6-31G(d) basis set was used for the other atoms (i.e., H, C, O, F, Al, etc.).

Geometry optimizations were carried out without any symmetry constraints, and the stationary points were characterized by analytical frequency calculations, i.e., energy minima (reactants, intermediates, and products) must exhibit only positive harmonic frequencies, whereas each energy maximum (transition state) exhibited only one negative frequency. From these last calculations, zero-point energy, thermal, and entropy corrections were obtained, which were added to the electronic energy to express the calculated values as Gibbs free energy at 298 K and 1 atm.

All our calculations were performed in the gas phase. Then, the solvent effects were included according to the polarizable continuum model via the solvent model density (SMD) option considering Truhlar's model [36-40] and MeCN as the solvent. Single-point calculations were improved using a mixed basis set of triple-ζ quality with a polarization function, 6-311G(d,p) for all atoms except for Br and I, which were treated with the LANL08d relativistic pseudopotential [41-43], i.e., the composite level of theory used is the following: (SMD: MeCN) ω-B97XD/(6-311G(d,p),LANL08d)//ω-B97XD/6-31G(d), LANL08d.

Chlorination mechanism

The reaction mechanism for the chlorination of 2-naphthol using one equivalent of PIFA and two equivalents of aluminum chloride is outlined in Scheme 4.

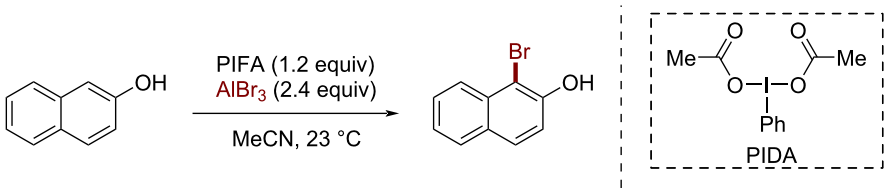

Scheme 3: Bromination of 2-naphthol using the PIDA/$AlBr_3$, 1:2 system.

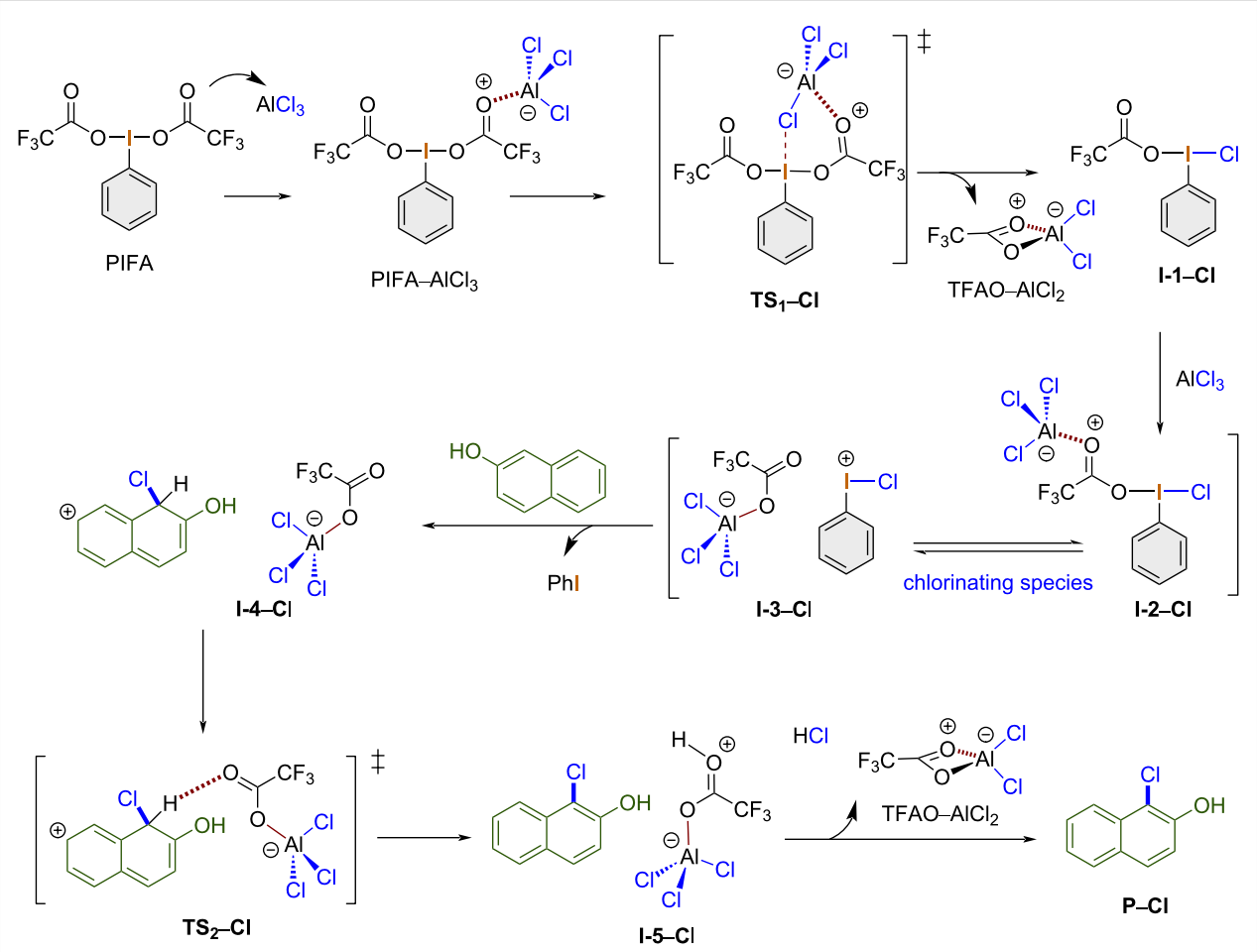

Scheme 4: Reaction mechanism for the chlorination of 2-naphthol using the PIFA/$AlCl_3$, 1:2 system.

The chlorination mechanism starts when PIFA coordinates the first equivalent of aluminum chloride to give the corresponding adduct PIFA–$AlCl_3$. Next, a chlorine atom is transferred to the iodine(III) center to yield **I-1–Cl** via **TS_1–Cl** with the release of the complex TFAO–$AlCl_2$. Then, the second equivalent of aluminum chloride coordinates the TFAO ligand, giving rise to the chlorinating species **I-2–Cl** in equilibrium with **I-3–Cl**. At this point, 2-naphthol reacts, leading to the formation of the ion pair **I-4–Cl** via chlorine atom transfer, which then yields the adduct **I-5–Cl** trough transition state **TS_2–Cl**. Then, the release of the second equivalent of the TFAO–$AlCl_2$ complex yields the final product 1-chloro-2-naphthol (**P–Cl**).

The calculated mechanism for the chlorination reaction starts with coordination of a PIFA oxygen atom to aluminum chloride. This generates a highly exergonic PIFA–$AlCl_3$ adduct. In Figure 1, the Gibbs free energy of this adduct is set as 0 kcal/mol for more clarity. Herein, one chlorine atom is transferred from aluminum to the hypervalent iodine(III) center through six-membered-ring transition state **TS_1–Cl** ($\Delta G^{\ddagger}$ = 9.7 kcal/mol, selected bond lengths 2.76, 1.22, 1.27, 1.78, 2.60, and 2.86 Å for I–O, O–C, C–O, O–Al, Al–Cl, and Cl–I, respectively). Then, the tetracoordinate TFAO–$AlCl_2$ salt is released, giving rise to intermediate **I-1–Cl** (ΔG = −25.2 kcal/mol), which contains the key Cl–I(III) bond, in a formal TFAO/Cl ligand exchange. The Cl–I bond length is 2.46 Å, with the halogen atom sharing the hypervalent iodine bond in the equatorial position. Next, the second equivalent of aluminum chloride coordinates to the TFAO ligand, forming active chlorinating species **I-2–Cl** (ΔG = −18.3 kcal/mol). This energetically favored step is in equilibrium with the ion pair **I-3–Cl** (ΔG = −0.5 kcal/mol). It is worth mentioning that the slight difference in energy between both states indicates the importance of the spontaneous interconversion of both species, which is observed only in the presence of two equivalents of the Lewis acid.

After the addition of 2-naphthol, the chlorine atom is introduced barrier-free into the phenolic ring, producing the nonaromatic intermediate **I-4–Cl** (ΔG = −23.1 kcal/mol). Next, aroma-

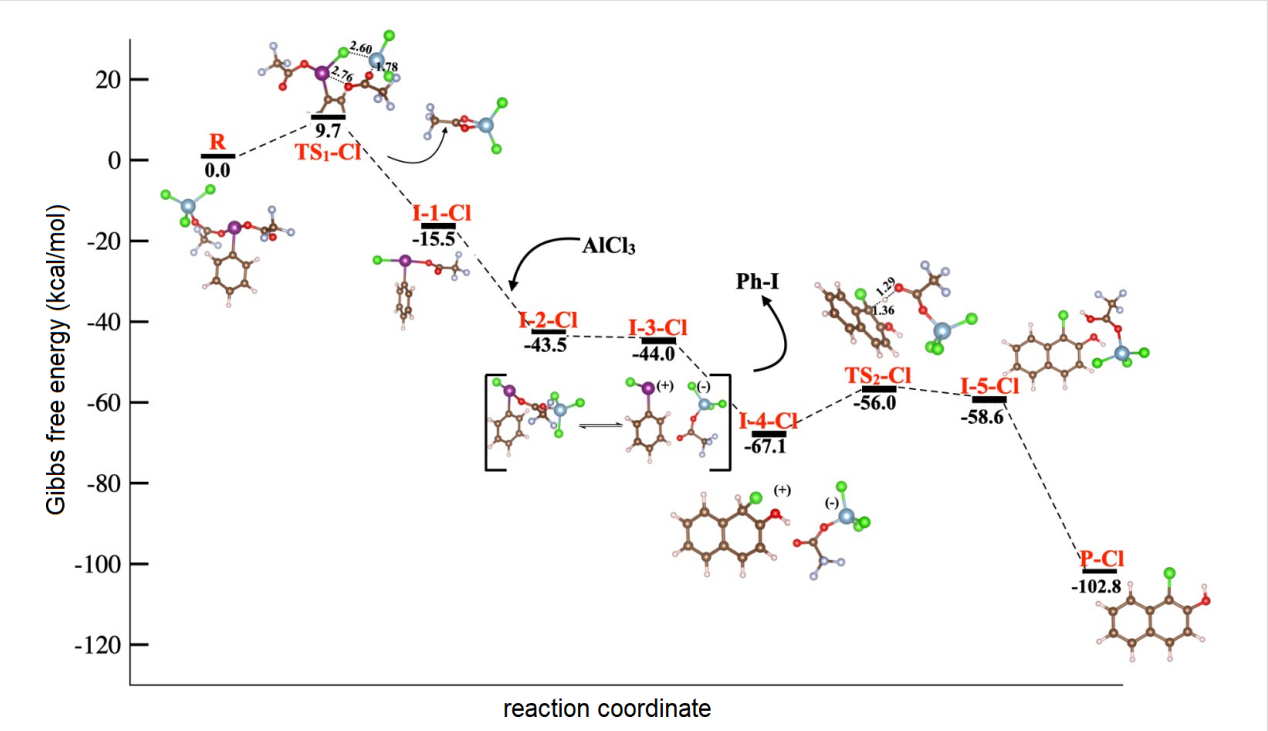

Figure 1: Energy profile for the chlorination of 2-naphthol in the presence of PIFA and $AlCl_3$.

tization assisted by TFAO–$AlCl_2$ via **TS_2–Cl** ($\Delta G^{\ddagger}$ = 11.1 kcal/mol) and hydrogen transfer from the nonaromatic intermediate to TFAO–$AlCl_2$ are observed. In **TS_2–Cl**, the energy barrier must be overcome to give rise to the 1-chloro-2-naphthol adduct with TFA–OH–$AlCl_2$, **I-5–Cl** (ΔG = −2.6 kcal/mol), which spontaneously yields the final 1-chloro-2-naphthol (**P–Cl**) with concomitant release of TFAO–$AlCl_2$ in a highly exothermic process (ΔG = −44.2 kcal/mol, Figure 1).

Other relevant routes for this chlorination process, which involve a different stoichiometry or the formation of $PhICl_2$ as chlorinating species, were also investigated and ruled out. Thus, for the chlorination of 2-naphthol with the PIFA/$AlCl_3$, 1:1 system, we found that in general, once the intermediate **I-1–Cl** is formed, the following coordination of 2-naphthol with the TFAO ligand via **TS_2** is energetically less favored ($\Delta G^{\ddagger}$ = 16.2 kcal/mol, see Supporting Information File 1 for details of the explored chlorination and bromination mechanisms). Additionally, for this mechanism, we identified that the formation of **TS_4** has the highest energy barrier ($\Delta G^{\ddagger}$ = 20.2 kcal/mol), becoming a less probable route. This result also confirms the relevance of using two equivalents of aluminum chloride.

The aromatic chlorination with iodine(III) reagents broadly employs $PhICl_2$ [7]. Thus, we explored two alternatives for the chlorination of 2-naphthol to identify or rule out this potential reaction pathway. The first explored mechanism involves PIFA/$AlCl_3$ and the second PIDA/$AlCl_3$ (see Figures S2 and S3, respectively, Supporting Information File 1). In both cases, the route involves the formation of $PhICl_2$ as the chlorinating reagent by considering two equivalents of $AlCl_3$ (PIFA/$AlCl_3$ or PIDA/$AlCl_3$, 1:2). Overall, we characterized four transition states along the reaction coordinates for both pathways. Although the PIFA-assisted mechanism follows a similar route to that described in Figure 1 until the formation of the active chlorinating species, in this case, the formation of **TS_2** requires 18.1 kcal/mol, which is an energetically more demanding process than the equilibration between **I-2–Cl** and ion pair **I-3–Cl**, proposed as active chlorinating species in Figure 1 and requiring less than 1 kcal/mol. It is worth mentioning that once $PhICl_2$ is formed, the energy barrier to **TS_3** is 21.5 kcal/mol. These energy differences suggest that the traceroute $PhICl_2$ is less viable for the chlorination of 2-naphthol.

On the other hand, in the presence of PIDA (Figure S3, Supporting Information File 1), when the reaction occurs through the chlorinating species $PhICl_2$, we found that **TS_1**, **TS_2**, and **TS_4** require 17.7, 13.8, and 16.5 kcal/mol, respectively. Considering the high transition-state energy barrier in the proposed mechanism shown in Figure 1 for **TS_2–Cl** (11.1 kcal/mol), this route is less probable. Additionally, we observed that chlorination of naphthol (the formation of **I-6**) could be the determining step since we found a coupling between the ring of the chlorinating species and naphthol during **TS_4**, i.e., it could disfavor

the PIDA-assisted chlorination traceroute via $PhICl_2$. Thus, using PIFA and two equivalents of $AlCl_3$ resulted in the highest yield, which is in agreement with our experiments.

As a consequence of the previous analysis, the chlorination process is energetically favored in the presence of PIFA/$AlCl_3$, 1:2 through the formation of PhICl–TFAO–$AlCl_3$ in equilibrium with [PhICl][TFAO–$AlCl_3$] as chlorinating species.

Bromination mechanism

The reaction mechanism for the bromination of 2-naphthol using one equivalent of PIDA and two equivalents of aluminum bromide is shown in Scheme 5.

PIDA coordinates the first equivalent of aluminum bromide to form the adduct PIDA–$AlBr_3$, which spontaneously dissociates, giving ion pair **I-1–Br**. Next, via **TS_1–Br**, complex AcO–$AlBr_2$

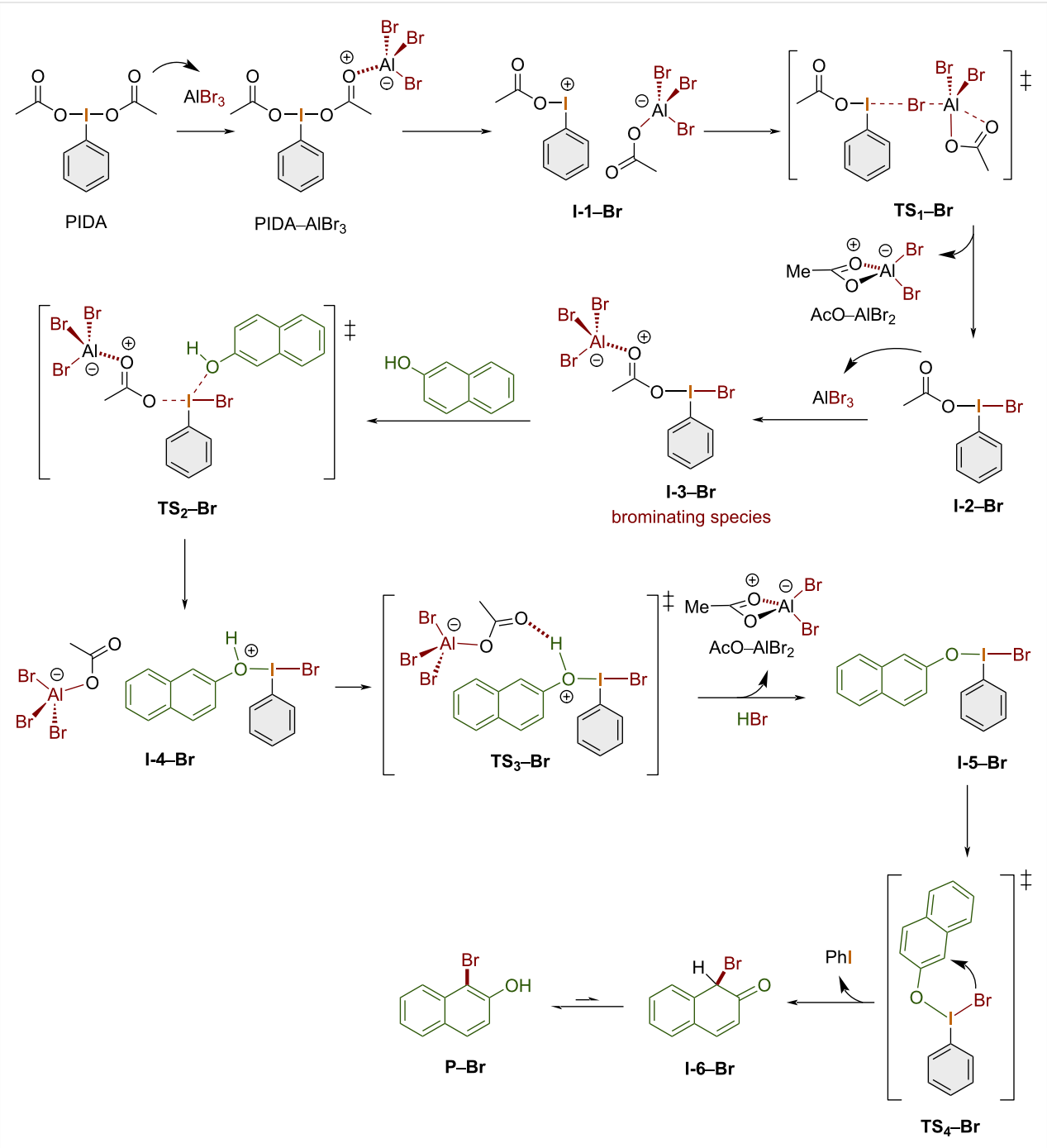

Scheme 5: Calculated reaction mechanism for the bromination of 2-naphthol using the PIDA/$AlBr_3$, 1:2 system.

is released with subsequent formation of intermediate **I-2–Br**. Then, the second equivalent of aluminum bromide coordinates to an acetate ligand, forming adduct **I-3–Br**, which is the brominating species. At this point, 2-naphthol reacts and forms **I-4–Br** via **TS$_2$–Br**. Afterwards, the second equivalent of the AcO–AlBr$_2$ complex and HBr are released with concomitant formation of **I-5–Br** trough **TS$_2$–Br**. Then, **I-5–Br** spontaneously isomerizes to give **I-6–Br** via the transition state **TS$_4$–Br**. Finally, **I-6–Br** tautomerizes, yielding the experimentally observed 1-bromo-2-naphthol (**P–Br**).

Based on our calculations, the bromination reaction proceeds through a stepwise mechanism. Thus, the reaction starts with the coordination of aluminum bromide to an acetate ligand in PIDA to form the PIDA–AlBr$_3$ adduct in a highly exergonic process. Similar to the previous section, the Gibbs free energy at this point was set as 0 kcal/mol for reference. At this stage, the PIDA–AlBr$_3$ adduct undergoes ionization, giving rise to the corresponding ion pair **I-1–Br** (ΔG = −31.3 kcal/mol) in a highly exergonic and energetically favorable process. Next, an intramolecular S_N2 reaction of the formed aluminum anion transfers a bromine atom to the electrophilic iodine(III) center through **TS$_1$–Br**, which has a feasible energy barrier of 8.3 kcal/mol. The I–Br and Br–Al bond lengths are 3.15 and 2.78 Å, respectively, and the I–Br–Al angle is 93.1°, which is close to the common T-shape of such hypervalent iodine(III) species. This step releases the tetracoordinate AcO–AlBr$_2$ salt and gives rise to the intermediate **I-2–Br** (ΔG = −9 kcal/mol), which contains the key Br–I(III) bond with a length of 2.65 Å. Herein, we could identify an energetically favored AcO/Br ligand exchange that releases 35.2 kcal/mol. At this point, the second equivalent of aluminum bromide is coordinated by an acetate ligand to produce the active brominating species Br–I(Ph)–OAc–AlBr$_3$ (**I-3–Br**). Then, 2-naphthol adds to the iodine(III) species to release the activated Br$_3$Al–OAc ligand through transition state **TS$_2$–Br** ($\Delta G^{\ddagger}$ = 11.7 kcal/mol), which leads to the protonated intermediate **I-4–Br**. The next step is a deprotonation assisted by the released Br$_3$Al–OAc species. This allows the formation of the AcO–AlBr$_2$ salt via **TS$_3$–Br** and the *trans* intermediate **I-5–Br**, which contains a Br–I(Ph)–O–naphthyl bond of 2.14 Å length. The last step is the bromination of **I-5–Br** by isomerization to the *cis* transition state **TS$_4$–Br** ($\Delta G^{\ddagger}$ = 16.1 kcal/mol), which yields the brominated nonaromatic intermediate **I-6–Br** in a highly exothermic step (ΔG = −52.3 kcal/mol). Finally, **I-6–Br** undergoes spontaneous aromatization, converting it into the experimentally observed 1-bromo-2-naphthol (**P–Br**), which is more stable than **I-6–Br** by 2.6 kcal/mol (Figure 2).

We also explored the plausible mechanisms for the bromination of 2-naphthol mediated by PIFA in a 1:2 ratio (Figure S4, Supporting Information File 1). In this proposal, we observed that the energy barriers to reach **TS$_1$** (10.6 kcal/mol) and **TS$_2$** (16.7 kcal/mol) are higher than those calculated for the mechanism shown in Figure 2, namely 8.3 kcal/mol for **TS$_1$–Br** and 16.1 kcal/mol for **TS$_4$–Br**.

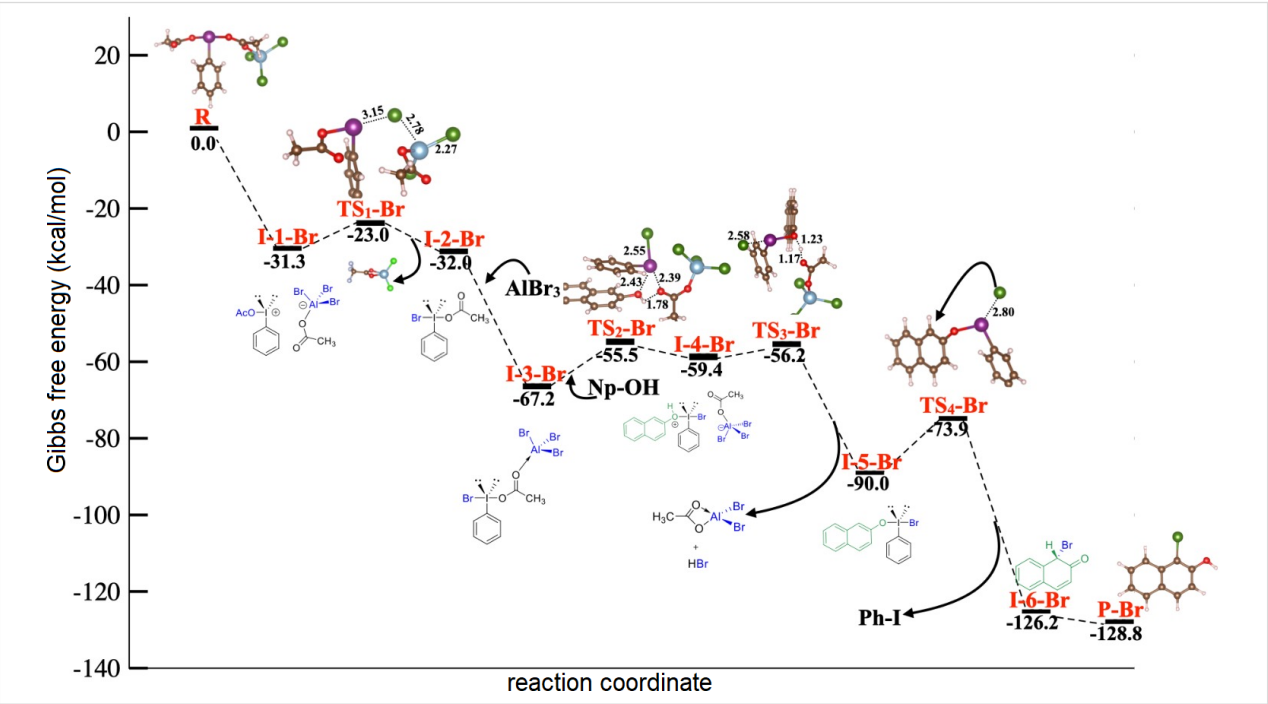

Figure 2: Calculated mechanism for the bromination of 2-naphthol in the presence of PIDA and AlBr$_3$.

Other possible mechanisms involve the formation of $PhIBr_2$. For these scenarios, the reaction pathway with PIDA and PIFA, respectively, involves two equivalents of $AlBr_3$ (Figures S5 and S6, Supporting Information File 1). Calculations indicated that each of these pathways proceeds along four transition states. Moreover, we found that the coordination of $AlBr_3$ to **I-2** to form $\mathbf{TS_2}$ has the highest energy barrier (determining step, $\Delta G^{\ddagger}$ for $\mathbf{TS_2}$ 53.3 kcal/mol) in the presence of PIDA. Meanwhile, formation of $\mathbf{TS_3}$ ($\Delta G^{\ddagger}$ = 21.3 kcal/mol) is the limiting step of the mechanism in the presence of PIFA.

Then, in the presence of the PIFA/$AlBr_3$ system, bromination of 2-naphthol is the energetically most favored pathway. Although all these reactions occur through four transition states, significant energy differences exist concerning the PIDA/$AlBr_3$ system. For example, the activation barrier of $\mathbf{TS_2}$ was 41.6 kcal/mol higher in energy than that in the mechanism in Figure 2. A similar energy profile was obtained for the bromination of 2-naphthol in the presence of PIFA (and 2 equivalents of $AlBr_3$) compared to Figure 2. The energy difference from **I-1** to $\mathbf{TS_1}$ (2.3 kcal/mol for the reaction in the presence of PIFA) could be the reason why the experimental yield is higher in the presence of PIDA and two equivalents $AlBr_3$ rather than PIFA and two equivalents $AlBr_3$ when considering the different hypervalent iodine reagents for this reaction.

To find the correlations between experiments and theoretical calculations, chlorination and bromination of 2-naphthol using PIFA/$AlCl_3$ and PIDA/$AlBr_3$ were carried out. Consequently, we found an excellent correlation between the yield and the energy barrier (Table 1).

Table 1: Experimental yield by using different hypervalent iodine(III) reagents.

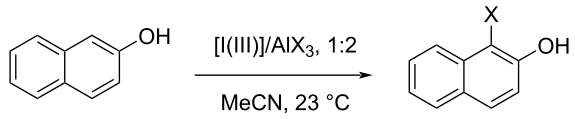

reaction	PIFA	PIDA	AlX_3
chlorination	63%	48%	$AlCl_3$
bromination	84%	93%	$AlBr_3$

Conclusion

We elucidated the energetically most viable pathway for the chlorination and bromination of 2-naphthol using the novel systems PIFA/$AlCl_3$ and PIDA/$AlBr_3$ in a 2:1 ratio in both cases. We found that the energetically most favored reaction proceeds through the chlorinating species **I-2–Cl** and **I-3–Cl** (rather than $PhICl_2$), which are in an equilibrium. The bromination is more efficient with PIDA/$AlBr_3$ through the formation of the intermediate **I-3–Br** as active brominating species. Similarly, involvement of $PhIBr_2$ is energetically less favored compared to our proposed pathway. One key step is the coordination of a second equivalent of AlX_3 to TFAO or AcO in PIFA or PIDA to promote the formation of the active halogenating species **I-2** and **I-3** for chlorination and bromination, respectively. Although bromination reactions in the presence of PIDA and PIFA give an excellent experimental yield, slight energy differences in the pathways explained why PIFA/$AlCl_3$ for chlorination and PIDA/$AlBr_3$ for bromination are better choices for these reactions.

Supporting Information

Supporting Information File 1

Optimized Cartesian coordinates of all structures and alternative mechanisms.
[https://www.beilstein-journals.org/bjoc/content/supplementary/1860-5397-20-141-S1.pdf]

Acknowledgements

We acknowledge the facilities of the DCNyE, the Chemistry Department, and the Supercomputing Center facilities of the National Laboratory UG-CONACyT (LACAPFEM) of the University of Guanajuato. We also thank Fernando Murillo for the kind discussion.

Funding

K. A. J.-O. thanks CONAHCyT for financial support (Ph.D. fellowship).

Author Contributions

Kevin A. Juárez-Ornelas: data curation; formal analysis; methodology; software; visualization. Manuel Solís-Hernández: formal analysis; investigation; methodology. Pedro Navarro-Santos: conceptualization; data curation; formal analysis; investigation; methodology; project administration; writing – review & editing. J. Oscar C. Jiménez-Halla: data curation; formal analysis; methodology; software. César R. Solorio-Alvarado: conceptualization; funding acquisition; investigation; methodology; software; supervision; visualization; writing – review & editing.

ORCID® iDs

Manuel Solís-Hernández - https://orcid.org/0000-0002-1678-0107
César R. Solorio-Alvarado - https://orcid.org/0000-0001-6082-988X

Data Availability Statement

Additional research data is not shared.

Preprint

A non-peer-reviewed version of this article has been previously published as a preprint: https://doi.org/10.3762/bxiv.2024.16.v1

References

1. Yoshimura, A.; Zhdankin, V. V. *Chem. Rev.* **2016,** *116,* 3328–3435. doi:10.1021/acs.chemrev.5b00547
2. Zhdankin, V. V. *ARKIVOC* **2009,** No. i, 1–62.
3. Zhdankin, V. V. *Hypervalent Iodine Chemistry: Preparation, Structure and Synthetic Applications of Polyvalent Iodine Compounds;* Wiley-VCH: Weinheim, Germany, 2014. doi:10.1002/9781118341155
4. Chávez-Rivera, R.; Navarro-Santos, P.; Chacón-García, L.; Ortiz-Alvarado, R.; Solorio Alvarado, C. R. *ChemistrySelect* **2023,** *8,* e202303425. doi:10.1002/slct.202303425
5. Segura-Quezada, L. A.; Torres-Carbajal, K. R.; Juárez-Ornelas, K. A.; Navarro-Santos, P.; Granados-López, A. J.; González-Garcia, G.; Ortiz-Alvarado, R.; de León-Solis, C.; Solorio-Alvarado, C. R. *Curr. Org. Chem.* **2022,** *26,* 1954–1968. doi:10.2174/1385272826666220621142211
6. Kikushima, K.; Elboray, E. E.; Jiménez-Halla, J. O. C.; Solorio-Alvarado, C. R.; Dohi, T. *Org. Biomol. Chem.* **2022,** *20,* 3231–3248. doi:10.1039/d1ob02501e
7. Segura-Quezada, L. A.; Torres-Carbajal, K. R.; Juárez-Ornelas, K. A.; Alonso-Castro, A. J.; Ortiz-Alvarado, R.; Dohi, T.; Solorio-Alvarado, C. R. *Org. Biomol. Chem.* **2022,** *20,* 5009–5034. doi:10.1039/d2ob00741j
8. Segura-Quezada, L. A.; Torres-Carbajal, K. R.; Satkar, Y.; Juárez Ornelas, K. A.; Mali, N.; Patil, D. B.; Gámez-Montaño, R.; Zapata-Morales, J. R.; Lagunas-Rivera, S.; Ortíz-Alvarado, R.; Solorio-Alvarado, C. R. *Mini-Rev. Org. Chem.* **2021,** *18,* 159–172. doi:10.2174/1570193x17999200504095803
9. Wang, B.; Graskemper, J. W.; Qin, L.; DiMagno, S. G. *Angew. Chem., Int. Ed.* **2010,** *49,* 4079–4083. doi:10.1002/anie.201000695
10. Segura-Quezada, L. A.; Torres-Carbajal, K. R.; Mali, N.; Patil, D. B.; Luna-Chagolla, M.; Ortiz-Alvarado, R.; Tapia-Juárez, M.; Fraire-Soto, I.; Araujo-Huitrado, J. G.; Granados-López, A. J.; Gutiérrez-Hernández, R.; Reyes-Estrada, C. A.; López-Hernández, Y.; López, J. A.; Chacón-García, L.; Solorio-Alvarado, C. R. *ACS Omega* **2022,** *7,* 6944–6955. doi:10.1021/acsomega.1c06637
11. Nahide, P. D.; Jiménez-Halla, J. O. C.; Wrobel, K.; Solorio-Alvarado, C. R.; Ortiz Alvarado, R.; Yahuaca-Juárez, B. *Org. Biomol. Chem.* **2018,** *16,* 7330–7335. doi:10.1039/c8ob02056f
12. Kita, Y.; Dohi, T.; Morimoto, K. *J. Synth. Org. Chem., Jpn.* **2011,** *69,* 1241–1250. doi:10.5059/yukigoseikyokaishi.69.1241
13. Satkar, Y.; Wrobel, K.; Trujillo-González, D. E.; Ortiz-Alvarado, R.; Jiménez-Halla, J. O. C.; Solorio-Alvarado, C. R. *Front. Chem. (Lausanne, Switz.)* **2020,** *8,* 10.3389/fchem.2020.563470. doi:10.3389/fchem.2020.563470
14. Dohi, T.; Maruyama, A.; Yoshimura, M.; Morimoto, K.; Tohma, H.; Kita, Y. *Angew. Chem., Int. Ed.* **2005,** *44,* 6193–6196. doi:10.1002/anie.200501688
15. Yahuaca-Juárez, B.; González, G.; Ramírez-Morales, M. A.; Alba-Betancourt, C.; Deveze-Álvarez, M. A.; Mendoza-Macías, C. L.; Ortiz-Alvarado, R.; Juárez-Ornelas, K. A.; Solorio-Alvarado, C. R.; Maruoka, K. *Synth. Commun.* **2020,** *50,* 539–548. doi:10.1080/00397911.2019.1707225
16. Dohi, T.; Maruyama, A.; Minamitsuji, Y.; Takenaga, N.; Kita, Y. *Chem. Commun.* **2007,** 1224–1226. doi:10.1039/b616510a
17. Kumar, R. K.; Manna, S.; Mahesh, D.; Sar, D.; Punniyamurthy, T. *Asian J. Org. Chem.* **2013,** *2,* 843–847. doi:10.1002/ajoc.201300151
18. Dohi, T.; Morimoto, K.; Takenaga, N.; Goto, A.; Maruyama, A.; Kiyono, Y.; Tohma, H.; Kita, Y. *J. Org. Chem.* **2007,** *72,* 109–116. doi:10.1021/jo061820i
19. Karam, O.; Jacquesy, J.-C.; Jouannetaud, M.-P. *Tetrahedron Lett.* **1994,** *35,* 2541–2544. doi:10.1016/s0040-4039(00)77165-6
20. Zhao, Z.; To, A. J.; Murphy, G. K. *Chem. Commun.* **2019,** *55,* 14821–14824. doi:10.1039/c9cc08310c
21. Chai, H.; Zhen, X.; Wang, X.; Qi, L.; Qin, Y.; Xue, J.; Xu, Z.; Zhang, H.; Zhu, W. *ACS Omega* **2022,** *7,* 19988–19996. doi:10.1021/acsomega.2c01791
22. Mali, N.; Ibarra-Gutiérrez, J. G.; Lugo Fuentes, L. I.; Ortíz-Alvarado, R.; Chacón-García, L.; Navarro-Santos, P.; Jiménez-Halla, J. O. C.; Solorio-Alvarado, C. R. *Eur. J. Org. Chem.* **2022,** 10.1002/ejoc.202201067. doi:10.1002/ejoc.202201067
23. Satkar, Y.; Yera-Ledesma, L. F.; Mali, N.; Patil, D.; Navarro-Santos, P.; Segura-Quezada, L. A.; Ramírez-Morales, P. I.; Solorio-Alvarado, C. R. *J. Org. Chem.* **2019,** *84,* 4149–4164. doi:10.1021/acs.joc.9b00161
24. Patil, D. B.; Gámez-Montaño, R.; Ordoñez, M.; Solis-Santos, M.; Jiménez-Halla, J. O. C.; Solorio-Alvarado, C. R. *Eur. J. Org. Chem.* **2022,** e202201295. doi:10.1002/ejoc.202201295
25. Juárez-Ornelas, K. A.; Jiménez-Halla, J. O. C.; Kato, T.; Solorio-Alvarado, C. R.; Maruoka, K. *Org. Lett.* **2019,** *21,* 1315–1319. doi:10.1021/acs.orglett.8b04141
26. Nahide, P. D.; Ramadoss, V.; Juárez-Ornelas, K. A.; Satkar, Y.; Ortiz-Alvarado, R.; Cervera-Villanueva, J. M. J.; Alonso-Castro, Á. J.; Zapata-Morales, J. R.; Ramírez-Morales, M. A.; Ruiz-Padilla, A. J.; Deveze-Álvarez, M. A.; Solorio-Alvarado, C. R. *Eur. J. Org. Chem.* **2018,** 485–493. doi:10.1002/ejoc.201701399
27. Cheng, D. P.; Chen, Z. C.; Zheng, Q. G. *J. Chem. Res., Synop.* **2002,** 624–625. doi:10.3184/030823402103171032
28. Satkar, Y.; Ramadoss, V.; Nahide, P. D.; García-Medina, E.; Juárez-Ornelas, K. A.; Alonso-Castro, A. J.; Chávez-Rivera, R.; Jiménez-Halla, J. O. C.; Solorio-Alvarado, C. R. *RSC Adv.* **2018,** *8,* 17806–17812. doi:10.1039/c8ra02982b
29. Segura-Quezada, A.; Satkar, Y.; Patil, D.; Mali, N.; Wrobel, K.; González, G.; Zárraga, R.; Ortiz-Alvarado, R.; Solorio-Alvarado, C. R. *Tetrahedron Lett.* **2019,** *60,* 1551–1555. doi:10.1016/j.tetlet.2019.05.019
30. Qin, Y.; Qi, L.; Zhen, X.; Wang, X.; Chai, H.; Ma, X.; Jiang, X.; Cai, X.; Zhu, W. *J. Org. Chem.* **2023,** *88,* 4359–4371. doi:10.1021/acs.joc.2c02967
31. Juárez-Ornelas, K. A.; Báez, J. E.; Solorio-Alvarado, C. R.; Jiménez-Halla, J. O. C. Starting Computational Study of the Chlorination Mechanism Reaction of 2-Naphthol with PIDA and $AlCl_3$ via $PhICl_2$ Formation as a Chlorinating Reagent. In *Proceedings of the 24th International Electronic Conference on Synthetic Organic Chemistry,* Nov 15–Dec 15, 2020; MDPI: Basel, Switzerland, 2020. doi:10.3390/ecsoc-24-08358
32. Evans, P. A.; Brandt, T. A. *Tetrahedron Lett.* **1996,** *37,* 6443–6446. doi:10.1016/0040-4039(96)01427-x

33. Granados, A.; Shafir, A.; Arrieta, A.; Cossío, F. P.; Vallribera, A. *J. Org. Chem.* **2020,** *85,* 2142–2150. doi:10.1021/acs.joc.9b02784
34. *Gaussian 16,* Revision C.01; Gaussian, Inc.: Wallingford, CT, 2009.
35. Chai, J.-D.; Head-Gordon, M. *Phys. Chem. Chem. Phys.* **2008,** *10,* 6615–6620. doi:10.1039/b810189b
36. Marenich, A. V.; Cramer, C. J.; Truhlar, D. G. *J. Phys. Chem. B* **2009,** *113,* 6378–6396. doi:10.1021/jp810292n
37. Barone, V.; Cossi, M. *J. Phys. Chem. A* **1998,** *102,* 1995–2001. doi:10.1021/jp9716997
38. Cossi, M.; Barone, V.; Mennucci, B.; Tomasi, J. *Chem. Phys. Lett.* **1998,** *286,* 253–260. doi:10.1016/s0009-2614(98)00106-7
39. Barone, V.; Cossi, M.; Tomasi, J. *J. Comput. Chem.* **1998,** *19,* 404. doi:10.1002/(sici)1096-987x(199803)19:4<404::aid-jcc3>3.3.co;2-l
40. Tomasi, J.; Mennucci, B.; Cammi, R. *Chem. Rev.* **2005,** *105,* 2999–3094. doi:10.1021/cr9904009
41. Wadt, W. R.; Hay, P. J. *J. Chem. Phys.* **1985,** *82,* 284–298. doi:10.1063/1.448800
42. Hay, P. J.; Wadt, W. R. *J. Chem. Phys.* **1985,** *82,* 299–310. doi:10.1063/1.448975
43. Roy, L. E.; Hay, P. J.; Martin, R. L. *J. Chem. Theory Comput.* **2008,** *4,* 1029–1031. doi:10.1021/ct8000409

License and Terms

BEILSTEIN JOURNAL OF ORGANIC CHEMISTRY

Oxidation of benzylic alcohols to carbonyls using *N*-heterocyclic stabilized λ^3-iodanes

Thomas J. Kuczmera[1], Pim Puylaert[2] and Boris J. Nachtsheim[*1]

Full Research Paper

Open Access

Address:
[1]Institute for Organic and Analytical Chemistry, University of Bremen, Bremen, Germany and [2]Institute for Inorganic Chemistry and Crystallography, University of Bremen, Bremen, Germany

Email:
Boris J. Nachtsheim[*] - nachtsheim@uni-bremen.de

* Corresponding author

Keywords:
alcohol oxidation; hypervalent iodine; *N*-heterocycles

Beilstein J. Org. Chem. **2024,** *20,* 1677–1683.
https://doi.org/10.3762/bjoc.20.149

Received: 26 February 2024
Accepted: 12 July 2024
Published: 19 July 2024

This article is part of the thematic issue "Hypervalent halogen chemistry".

Guest Editor: J. Wencel-Delord

Abstract

We present *N*-heterocycle-stabilized iodanes (NHIs) as suitable reagents for the mild oxidation of activated alcohols. Two different protocols, both involving activation by chloride additives, were used to synthesize benzylic ketones and aldehydes without overoxidation in up to 97% yield. Based on MS experiments an activated hydroxy(chloro)iodane is proposed as the reactive intermediate.

Introduction

The oxidation of alcohols to aldehydes and ketones is an essential transformation in organic chemistry [1,2]. Generating aldehydes is particularly challenging as they are easily overoxidized to carboxylic acids. Over the past decades a variety of methods have been developed, utilizing toxic heavy metals such as pyridinium dichromate (PDC) [3-5] or manganese dioxide (Figure 1) [6,7]. Molecular oxygen [8] and peroxides [9,10] can also be used as inexpensive terminal oxidants in combination with transition-metal catalysts. Metal-free methods employ chlorodimethylsulfonium compounds as the reactive species and have gained great popularity under the name Swern oxidation or the Corey–Kim oxidation [11]. Hypervalent iodine compounds have also been studied and are well established in several oxidative transformations including the synthesis of complex molecules and drugs [12,13]. The most prominent examples are the pentavalent derivatives 2-iodoxybenzoic acid (IBX) and Dess–Martin periodinane (DMP) [14,15]. Although mild and selective oxidants, these highly oxidized λ^5-iodanes have drawbacks, in particular low solubility and moisture sensitivity [11]. Hypervalent iodine compounds in a lower oxidation state (λ^3-iodanes), such as iodosobenzene $(PhIO)_n$ or phenyliodine(III) diacetate (PIDA) have been reported in alcohol oxidations but they often result in overoxidation to the corresponding carboxylic acids [16]. Additives such as bromide salts or Al_2O_3 can eliminate this problem and allow selective oxidation to some extent [17-20].

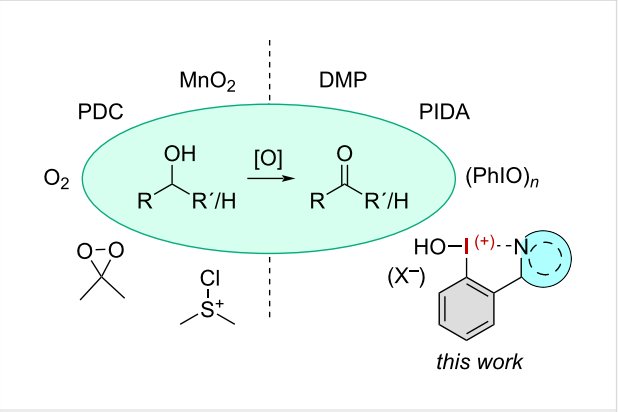

Figure 1: Overview of common non-iodine-based (left) and iodine-based (right) oxidizing reagents for the generation of carbonyls from the corresponding alcohols.

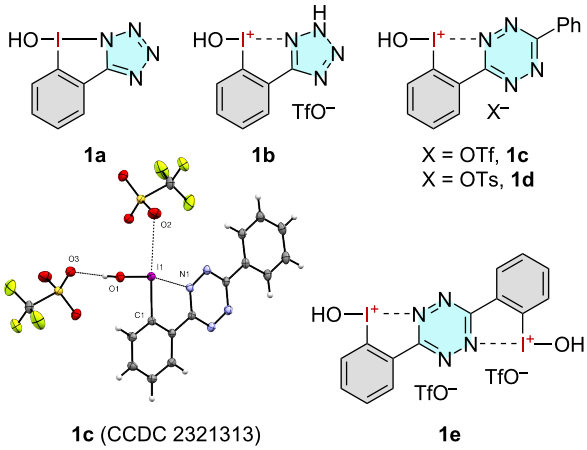

Figure 2: NHIs investigated for the oxidation of benzylic alcohols and the crystal structure (ORTEP drawing) of **1c** (CCDC 2321313), showing the coordination of the triflate to two positions of the iodane. Thermal ellipsoids are displayed with 50% probability. Selected bond lengths and angles: I1–N1: 2.44(4) Å; I1–O1: 1.94(9) Å; I1–O2: 3.04(1) Å; C1–I1–N1: 73.5(8)°; O1–I1–N1: 166.6(5)°; N1–I1–C1–O1: 177.8(3)°.

During the past years, *N*-heterocycle-stabilized iodanes (NHIs) were demonstrated as suitable tools for various applications among them group transfer reactions [21] and as building blocks [22-24]. The synthetic potential of NHIs has been previously studied in model transformations such as thioanisole oxygenation, oxidative lactonization, or diacetoxylation of alkenes [25-28]. In this work, we want to apply NHIs in a mild oxidation of primary and secondary benzylic alcohols to aldehydes and ketones as an alternative to λ^5-iodanes.

Results and Discussion

Initially, we investigated a variety of pyrazole-, triazole-, and oxazole-substituted hydroxy-NHIs previously developed by our group [25]. However, none of them proved to be effective in a model oxidation reaction of *n*-octanol (**2**). Since previous investigations have repeatedly shown that the number of heteroatoms in the *N*-heterocycle correlates with the NHIs activity, a series of tetrazole- and tetrazine-substituted NHIs **1a**–**e** was synthesized (Figure 2) [29,30]. A crystal structure was additionally obtained for tetrazine **1c**. Bond lengths and angles were similar to those of known five-membered NHIs [25], including a strong intramolecular interaction between the nitrogen of the tetrazine and the hypervalent iodine atom (I1–N1: 2.44(4) Å; the sum of VdW radii: 3.61 Å [31]).

Beginning with the electron-deficient and thereby highly reactive NHIs **1a** and **1c**, we explored the potential for a ligand-exchange process on the iodane via ^{1}H NMR spectroscopy by combining equimolar quantities of NHI and *n*-octanol (**2**). When the tetrazole-substituted hydroxy(aryl)iodane **1a** was added, no significant shifts in the NMR spectral signals were detected, probably due to the poor solubility of the iodane. Conversely, with the addition of the red tetrazine salt **1c**, a significant downfield shift was observed for the *alpha*-carbon protons from 3.51 ppm to 4.55 ppm, as illustrated in Figure 3a.

This indicates a ligand exchange of the hydroxy group resulting in a loss of electron density and the formation of the alkoxy-NHI **2'**. The chemical shift is consistent with previously measured alkoxyiodanes [32].

The experiments were repeated using activated *p*-tolylmethanol (**3a**), again showing no reaction with iodane **1a**. Utilizing the tetrazine **1c**, *p*-methylbenzaldehyde (**4a**) was observed as a new species at 9.94 ppm (Figure 3b). The reaction reached 31% conversion after 72 h, however, *p*-methylbenzoic acid (**4a'**) was formed in 35% as well, showing an undesired overreaction. In this experiment no formation of an alkoxyiodane was observed, indicating that the formation of this ligand-exchanged intermediate is slower than the dehydrogenation. As a consequence, we attempted to accelerate the ligand exchange through the addition of a Lewis acid and the performance of the NHIs was compared with common iodine(III) reagents by ^{1}H NMR spectroscopy (Figure 4). After 60 h the measurements revealed a higher yield of aldehyde **4a** using **1a** (68%) compared to **1c** (30%) under the influence of $AlCl_3$. As a comparison, the use of PIDA (**5b**) and IBA (**5c**) with the additive resulted in a significantly lower oxidation of the alcohol. Only small amounts of benzoic acid **4a'** were observed in all reactions with additional $AlCl_3$, suggesting that the additive inhibits the previously observed overoxidation.

Surprisingly $AlCl_3$ activated the cyclic tetrazole iodane **1a** but had almost no influence on the reactivity of the tetrazine salt **1c**. Based on these results, the reaction conditions were further optimized using NHI **1a** with the benzyl alcohols **3a** (electron-rich)

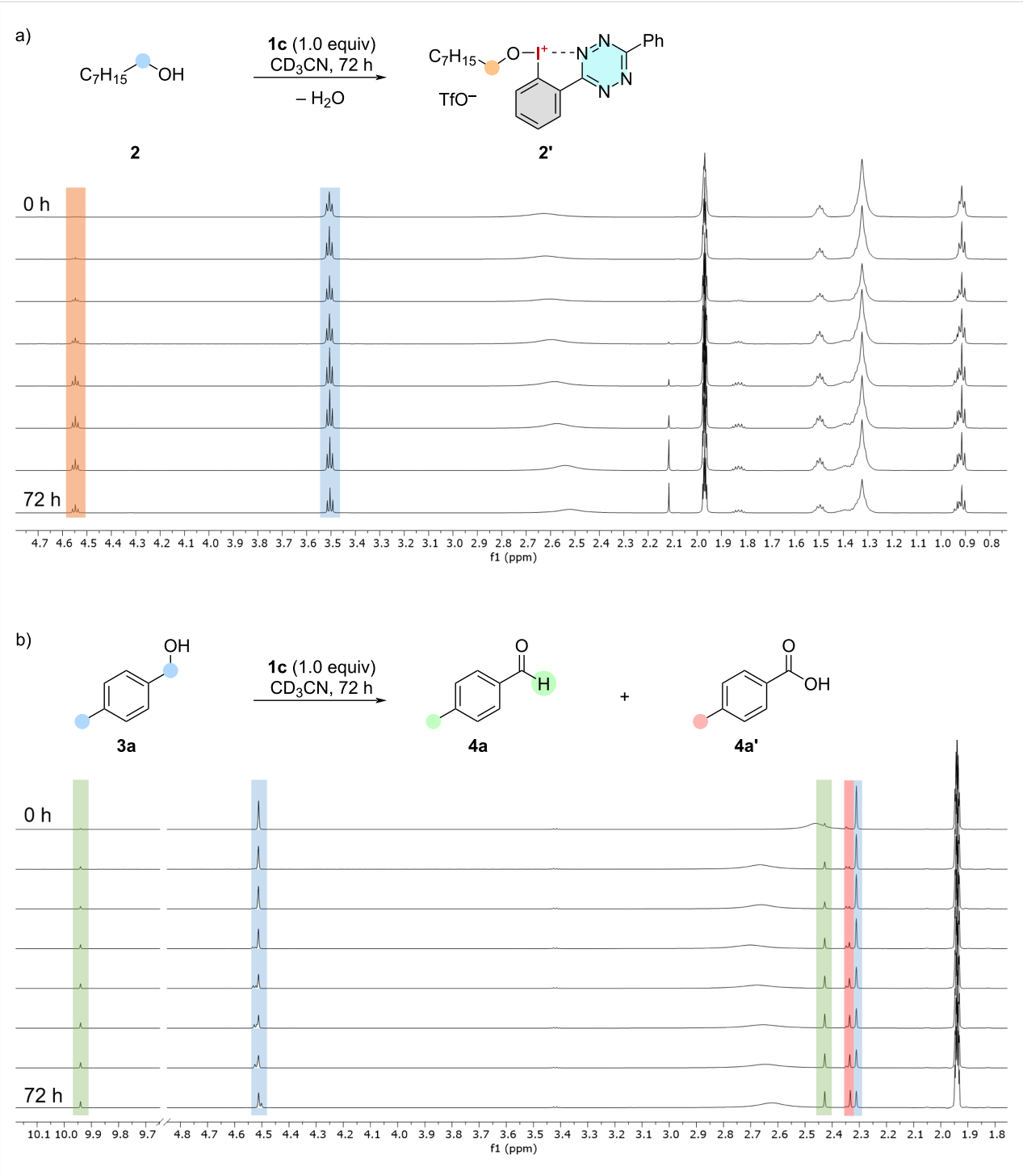

Figure 3: ^{1}H NMR spectra of the time-dependent formation of a) an alkoxy-NHI which is causing a significant downfield shift of the protons in *alpha*-position (orange) compared to the free alcohol **2** (blue) and b) oxidation of *p*-tolylmethanol (**3a**, blue) to the aldehyde **4a** (green) and carboxylic acid **4a'** (red). Reaction conditions: An equimolar mixture of NHI **1c** (10.0 µmol) and alcohol (**2** or **3a**, 10.0 µmol) were dissolved in CD_3CN (600 µL) and ^{1}H NMR spectra were recorded.

and **3b** (electron-poor) as the model substrates. First, the reaction temperature was increased, finding 60 °C to be the optimal value in EtOAc (Table 1, entry 1). At this temperature, the reaction time was significantly reduced to 2.5 h. A variety of other additives were tested next, revealing TsOH or NaOTs inhibiting the reaction (Table 1, entries 2 and 3). The addition of tetrabutylammonium halides showed the chloride salt being superior, giving comparable or even better yields than $AlCl_3$ (Table 1,

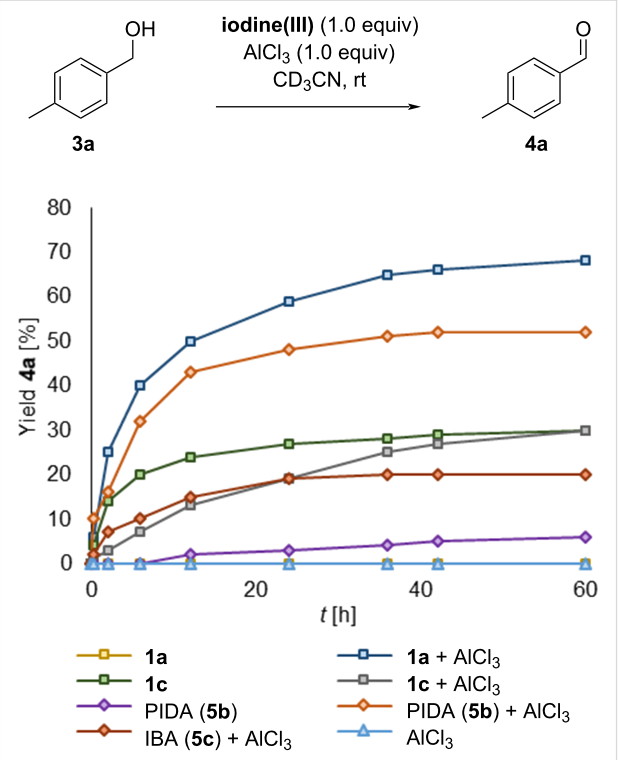

Figure 4: Oxidation of **3a** to **4a** using different iodine(III) reagents with $AlCl_3$ as an additive. Conditions: The turnover of an equimolar mixture of **3a**, iodine(III), and $AlCl_3$ (10.0 µmol, respectively) in CD_3CN (500 µL) was monitored via ^1H NMR spectroscopy.

entries 4–7). Investigation of other chloride sources resulted in a reduced yield in the case of ammonium chloride and an improved yield of 82% of **4a** when concentrated aqueous HCl was added (Table 1, entries 8 and 9). Other solvents did not further increase the yield (see the full table in Supporting Information File 1).

However, when electron-deficient *p*-chlorobenzyl alcohol (**3b**) was used the highest yield of **4b** (69%) was achieved with TBACl as the chloride source in MeCN (Table 1, entry 10). These optimizations lead to the conclusion that $AlCl_3$, as proposed in the initial experiments is not a Lewis acid activator but just a chloride source. Further optimization studies improved the yield to 78% of **4b** using a concentration of 0.20 M of the alcohol and 1.4 equiv of **1a** (see Supporting Information File 1). Finally, all NHIs were tested under the optimized conditions, revealing the tetrazole-substituted iodane **1a** to be the best oxidant for this reaction (Table 2).

The two suitable methods (A: HCl in EtOAc; B: TBACl in MeCN) were then applied to a variety of activated alcohols. The best option is shown in Figure 5. Model substrate **4a** could be isolated in a high yield of 84% with reisolation of the 5-(2-iodophenyl)-1*H*-tetrazole (**6**) in 90% yield. Other *para*-halogenated benzaldehydes **4b–f** were isolated in good yields of up to 88%. *ortho*-Substitution led to a lower yield of the iodinated product **4g** (43%) compared to the *para*-iodinated analogues **4d** (75%). The *ortho*-phenyl-substituted aldehyde **4h** was isolated in 85% yield, while the *ortho*-methoxy substrate did not convert to **4i**.

Table 1: Varying the additive and solvent in the oxidation of electron-rich and electron-deficient benzylic alcohols with **1a**.[a]

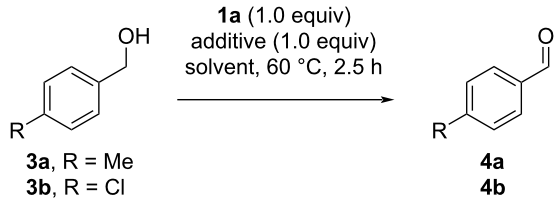

Entry	Additive	Solvent	Yield [%]	
			4a	**4b**
1	$AlCl_3$	EtOAc	65	39
2	$TsOH·H_2O$	EtOAc	1	1
3	NaOTs	EtOAc	1	1
4	TBAF	EtOAc	9	19
5	TBACl	EtOAc	67	62
6	TBABr	EtOAc	58	47
7	TBAI	EtOAc	40	36
8	NH_4Cl	EtOAc	37	26
9	HCl	EtOAc	82	44
10	TBACl	MeCN	64	69
11[b]	TBACl	MeCN	74	78
12[b]	HCl	EtOAc	90	53

[a]Reaction conditions: **1a** (100 µmol), **3a**/**3b** (100 µmol), and the additive (100 µmol) were stirred in the given solvent (1 mL) at 60 °C for 2.5 h and quenched with Me_2S (200 µmol). [b]Optimum reaction conditions were used: **1a** (100 µmol), **3a**/**3b** (100 µmol), and the additive (100 µmol) were stirred in the given solvent (0.5 mL) at 60 °C for 2.5 h and quenched with Me_2S (200 µmol). The yield was determined via ^1H NMR using tetraethylsilane as an internal standard.

Table 2: Testing different NHIs under the optimum conditions for oxidation of electron-deficient substrate **3b**.[a]

Iodane	Yield of **4b** [%]
1a	78
1b	71
1c	46
1d	29
1e	41

[a]Reaction conditions: NHI (**1a–d**: 140 µmol, **1e**: 70.0 µmol), *p*-chlorobenzyl alcohol (**3b**, 100 µmol) and TBACl (100 µmol) in MeCN (500 µL) were stirred at 60 °C for 2.5 h and quenched with Me_2S (200 µmol). The yield was determined via ^1H NMR with tetraethylsilane as an internal standard.

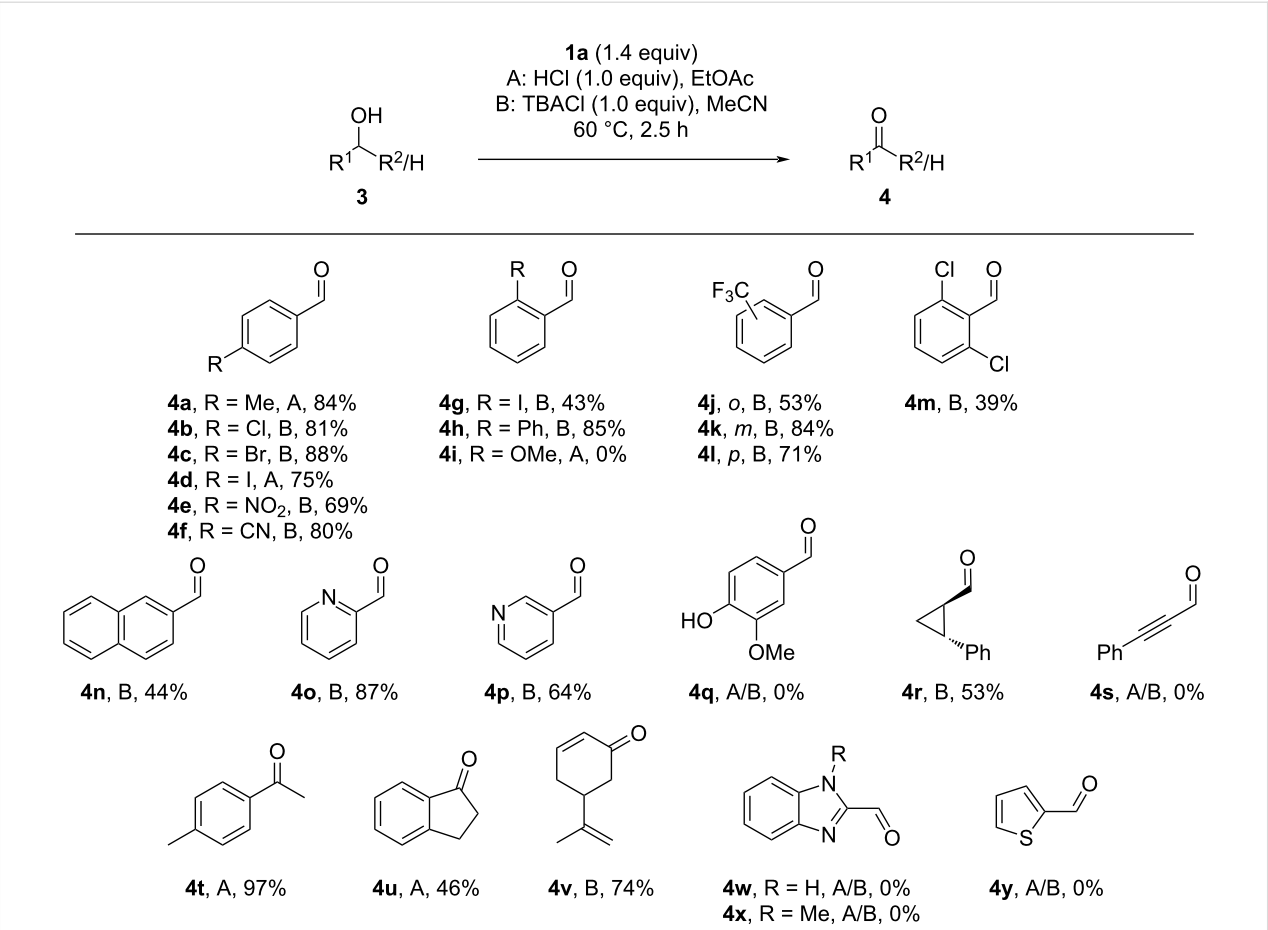

Figure 5: Substrate scope of aldehydes and ketones synthesized from the corresponding alcohols. Isolated yields. Reaction conditions: **1a** (700 µmol), alcohol (500 µmol), and method A HCl (37%, 500 µmol) in EtOAc (2.5 mL) or method B TBACl (500 µmol) in MeCN (2.5 mL), respectively, were stirred at 60 °C for 2.5 h and quenched with Me_2S (1.40 mmol).

The *ortho*-, *meta*- and *para*-permutation of a CF_3 group showed lower reactivity for the *ortho*-substituted **4j** (53%), while the *meta*- and *para*-derivatives **4k** and **4l** gave higher yields of 84% and 71%, respectively. The steric inhibition of a doubly substituted phenyl ring was observed in a diminished formation of 2,6-dichlorobenzaldehyde (**4m**) in 39% yield. Naphthalen-2-ylmethanol gave aldehyde **4n** in 44% yield. Pyridines **4o** and **4p** were also compatible and gave good yields of 87% and 64%, respectively. Unfortunately, the synthesis of vanillin (**4q**) was unsuccessful due to undesirable oxidation reactions of the electron-rich arene. The cyclopropane derivative **4r** was generated from the cyclopropylmethanol in 53% yield. The acetylene derivative **4s** could not be isolated due to undesired oxidations of the triple bond. The behavior of secondary benzylic alcohols was tested next, giving 4-methylacetophenone (**4t**) in an excellent yield of 97% and 1-indanone (**4u**) in 46%. It is worth noting that for some derivatives oxidized by method A, an acylation of the alcohol was detected as a side reaction via mass spectrometry. Vinyl alcohols were also studied, giving carvone (**4v**) in 74% yield without oxidation of the double bonds. Finally, other heterocyclic benzylic alcohols were investigated, which led to undesired chlorinations in the case of benzimidazoles **3w** and **3x** and decomposition for thiophenylmethanol **3y**.

Regarding the reaction mechanism, two plausible pathways can be discussed based on literature examples (Scheme 1, path a [17] and path b [33]). In either path, initial ligand exchange to the hydroxy(chloro)iodane **I-OH** is proposed. For getting an indication of a chloride-activated iodane of this type, a mixture of NHI **1a** and HCl in EtOAc was stirred for 1 h at 60 °C and an ESI(−) mass spectrum was recorded afterward, showing an ion **I-OMe** with *m/z* 337.0 [**1a** – OH + MeO + Cl]$^-$ (Scheme 1c). It is known that methanol, which is used as a solvent in the mass spectrometer, can be exchanged with the hydroxy group of the NHI [21]. No such ion was measured in the mixture before heating. This ion therefore indicates an I–Cl bond in the activated iodane. Starting from **I-OH**, in a potential path a) formation of hypochlorous acid is suggested, which consequently

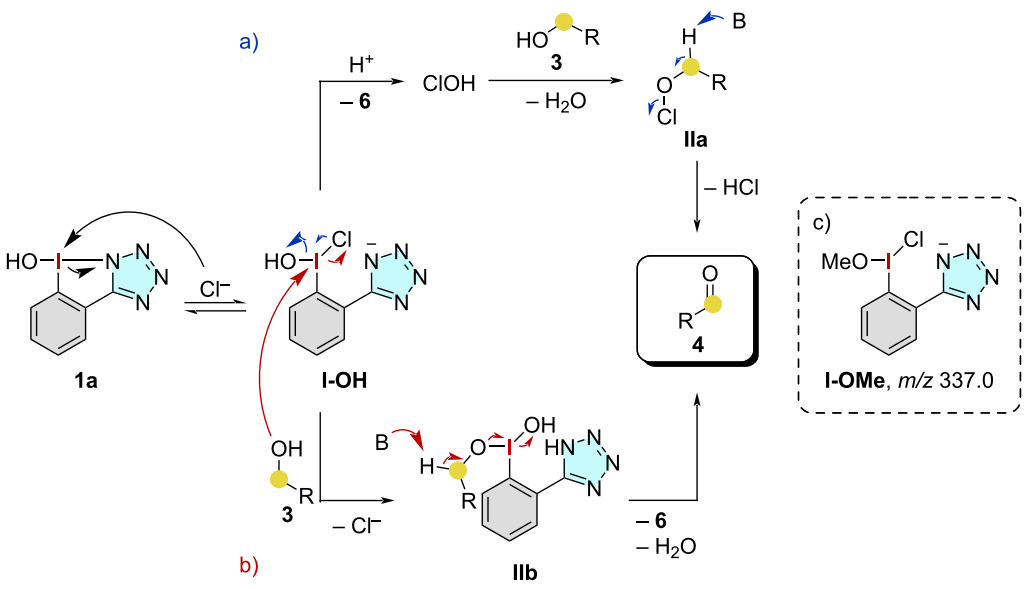

Scheme 1: Possible reaction mechanisms via the formation of a) a Cl(I) species and b) the formation of an alkoxyiodane **IIb**. Both are initialized by the activated iodane **I-OH**, which was observed as c) **I-OMe** species in the ESI(–) MS.

oxidizes the alcohol through the alkyl hypochlorite **IIa**. The second mechanism (path b) requires a direct ligand exchange of **I-OH** with the alcohol and subsequent β-elimination of the alkoxy(hydroxy)iodane **IIb** to form the desired aldehyde **4**.

Conclusion

In conclusion, this study has successfully introduced *N*-heterocycle-stabilized iodanes (NHIs) as effective λ^3-iodane oxidants for the selective synthesis of ketones and aldehydes, avoiding overoxidation to carboxylic acids. The developed protocols proved particularly effective for benzylic alcohols, yielding good to excellent results. The beneficial role of chloride salt additives was investigated, potentially leading to the formation of a hydroxy(chloro)iodane intermediate. This intermediate either liberates hypochlorous acid as the terminal oxidant or undergoes a direct ligand exchange with the alcohol, followed by oxidative elimination to form the aldehyde. Thus, these reagents offer a viable alternative to traditional aryl-λ^5-iodane-based oxidants, although further studies are necessary to fully understand their reaction mechanisms.

Experimental

General procedure for oxidation of benzylic alcohols

1a (700 µmol, 201 mg, 1.40 equiv), benzylic alcohol (**3**, 500 µmol, 1.00 equiv) and method A: aqueous HCl (37%, 500 µmol, 41.6 µL, 1.00 equiv) in EtOAc (2.5 mL) or method B: TBACl (500 µmol, 137 mg, 1.00 equiv) in MeCN (2.5 mL), respectively, were stirred at 60 °C for 2.5 h, quenched with Me_2S (2.00 equiv) and the reaction mixture was purified via flash column chromatography on silica.

Supporting Information

Supporting Information File 1

Experimental part and copies of spectra.
[https://www.beilstein-journals.org/bjoc/content/supplementary/1860-5397-20-149-S1.pdf]

Author Contributions

Thomas J. Kuczmera: investigation; writing – original draft. Pim Puylaert: investigation. Boris J. Nachtsheim: conceptualization; funding acquisition; project administration; resources; supervision; writing – review & editing.

ORCID® iDs

Thomas J. Kuczmera - https://orcid.org/0000-0002-6834-5828
Pim Puylaert - https://orcid.org/0000-0003-3397-2677
Boris J. Nachtsheim - https://orcid.org/0000-0002-3759-2770

Data Availability Statement

All data that supports the findings of this study is available in the published article and/or the supporting information to this article

Preprint

A non-peer-reviewed version of this article has been previously published as a preprint: https://doi.org/10.26434/chemrxiv-2024-t3b6h

References

1. Arterburn, J. B. *Tetrahedron* **2001,** *57,* 9765–9788. doi:10.1016/s0040-4020(01)01009-2
2. Caron, S.; Dugger, R. W.; Ruggeri, S. G.; Ragan, J. A.; Ripin, D. H. B. *Chem. Rev.* **2006,** *106,* 2943–2989. doi:10.1021/cr040679f
3. Guziec, F. S., Jr.; Luzzio, F. A. *J. Org. Chem.* **1982,** *47,* 1787–1789. doi:10.1021/jo00348a045
4. Collins, J. C.; Hess, W. W.; Frank, F. J. *Tetrahedron Lett.* **1968,** *9,* 3363–3366. doi:10.1016/s0040-4039(00)89494-0
5. Corey, E. J.; Suggs, J. W. *Tetrahedron Lett.* **1975,** *16,* 2647–2650. doi:10.1016/s0040-4039(00)75204-x
6. Lou, J.-D.; Xu, Z.-N. *Tetrahedron Lett.* **2002,** *43,* 6149–6150. doi:10.1016/s0040-4039(02)01345-x
7. Highet, R. J.; Wildman, W. C. *J. Am. Chem. Soc.* **1955,** *77,* 4399–4401. doi:10.1021/ja01621a062
8. Sigman, M. S.; Jensen, D. R. *Acc. Chem. Res.* **2006,** *39,* 221–229. doi:10.1021/ar040243m
9. Trost, B. M.; Masuyama, Y. *Tetrahedron Lett.* **1984,** *25,* 173–176. doi:10.1016/s0040-4039(00)99832-0
10. Bovicelli, P.; Truppa, D.; Sanetti, A.; Bernini, R.; Lupattelli, P. *Tetrahedron* **1998,** *54,* 14301–14314. doi:10.1016/s0040-4020(98)00885-0
11. Tidwell, T. T. *Synthesis* **1990,** 857–870. doi:10.1055/s-1990-27036
12. Tohma, H.; Kita, Y. *Adv. Synth. Catal.* **2004,** *346,* 111–124. doi:10.1002/adsc.200303203
13. Varala, R.; Seema, V.; Dubasi, N. *Organics* **2023,** *4,* 1–40. doi:10.3390/org4010001
14. Yoshimura, A.; Zhdankin, V. V. *Chem. Rev.* **2016,** *116,* 3328–3435. doi:10.1021/acs.chemrev.5b00547
15. Dess, D. B.; Martin, J. C. *J. Org. Chem.* **1983,** *48,* 4155–4156. doi:10.1021/jo00170a070
16. Tohma, H.; Takizawa, S.; Maegawa, T.; Kita, Y. *Angew. Chem.* **2000,** *112,* 1362–1364. doi:10.1002/(sici)1521-3757(20000403)112:7<1362::aid-ange1362>3.0.co;2-g
17. Salvo, A.; Campisciano, V.; Beejapur, H.; Giacalone, F.; Gruttadauria, M. *Synlett* **2015,** *26,* 1179–1184. doi:10.1055/s-0034-1380196
18. Takenaga, N.; Goto, A.; Yoshimura, M.; Fujioka, H.; Dohi, T.; Kita, Y. *Tetrahedron Lett.* **2009,** *50,* 3227–3229. doi:10.1016/j.tetlet.2009.02.020
19. Varma, R. S.; Dahiya, R.; Saini, R. K. *Tetrahedron Lett.* **1997,** *38,* 7029–7032. doi:10.1016/s0040-4039(97)01660-2
20. Deng, Y.; Lu, S.-C.; Yue, L.-L.; Gong, Y.-L.; Guan, X.-D. *Synth. Commun.* **2022,** *52,* 2198–2204. doi:10.1080/00397911.2022.2134799
21. Kuczmera, T. J.; Boelke, A.; Nachtsheim, B. J. *Eur. J. Org. Chem.* **2022,** e202200276. doi:10.1002/ejoc.202200276
22. Kuczmera, T. J.; Dietz, A.; Boelke, A.; Nachtsheim, B. J. *Beilstein J. Org. Chem.* **2023,** *19,* 317–324. doi:10.3762/bjoc.19.27
23. Vlasenko, Y. A.; Postnikov, P. S.; Trusova, M. E.; Shafir, A.; Zhdankin, V. V.; Yoshimura, A.; Yusubov, M. S. *J. Org. Chem.* **2018,** *83,* 12056–12070. doi:10.1021/acs.joc.8b01995
24. Tolstaya, T. P.; Egorova, L. D.; Lisichkina, I. N. *Chem. Heterocycl. Compd.* **1985,** *21,* 392–396. doi:10.1007/bf00504396
25. Boelke, A.; Lork, E.; Nachtsheim, B. J. *Chem. – Eur. J.* **2018,** *24,* 18653–18657. doi:10.1002/chem.201804957
26. Boelke, A.; Sadat, S.; Lork, E.; Nachtsheim, B. J. *Chem. Commun.* **2021,** *57,* 7434–7437. doi:10.1039/d1cc03097c
27. Abazid, A. H.; Clamor, N.; Nachtsheim, B. J. *ACS Catal.* **2020,** *10,* 8042–8048. doi:10.1021/acscatal.0c02321
28. Aertker, K.; Rama, R. J.; Opalach, J.; Muñiz, K. *Adv. Synth. Catal.* **2017,** *359,* 1290–1294. doi:10.1002/adsc.201601178
29. Kumar, R.; Sayala, K. D.; Camdzic, L.; Siegler, M.; Vaish, A.; Tsarevsky, N. *ChemRxiv* **2021**. doi:10.26434/chemrxiv-2021-gsp7q-v2
30. Vaish, A.; Sayala, K. D.; Tsarevsky, N. V. *Tetrahedron Lett.* **2019,** *60,* 150995. doi:10.1016/j.tetlet.2019.150995
31. Bondi, A. *J. Phys. Chem.* **1964,** *68,* 441–451. doi:10.1021/j100785a001
32. Sakakibara, Y.; Murakami, K.; Itami, K. *Org. Lett.* **2022,** *24,* 602–607. doi:10.1021/acs.orglett.1c04030
33. Tohma, H.; Maegawa, T.; Takizawa, S.; Kita, Y. *Adv. Synth. Catal.* **2002,** *344,* 328–337. doi:10.1002/1615-4169(200206)344:3/4<328::aid-adsc328>3.0.co;2-s

License and Terms

BEILSTEIN JOURNAL OF ORGANIC CHEMISTRY

Oxidative fluorination with Selectfluor: A convenient procedure for preparing hypervalent iodine(V) fluorides

Samuel M. G. Dearman[1], Xiang Li[2], Yang Li[2], Kuldip Singh[1] and Alison M. Stuart[*1]

Full Research Paper

Open Access

Address:
[1]School of Chemistry, University of Leicester, Leicester, LE1 7RH, UK and [2]School of Chemical Engineering, Dalian University of Technology, No. 2 Linggong Road, Dalian, 116024, P. R. China

Email:
Alison M. Stuart[*] - Alison.Stuart@le.ac.uk

* Corresponding author

Keywords:
fluorination; fluorobenziodoxoles; halogen bonding; hypervalent iodine; Selectfluor

Beilstein J. Org. Chem. **2024,** *20,* 1785–1793.
https://doi.org/10.3762/bjoc.20.157

Received: 30 April 2024
Accepted: 03 July 2024
Published: 29 July 2024

This article is part of the thematic issue "Hypervalent halogen chemistry".

Guest Editor: T. Gulder

Abstract

The ability to investigate hypervalent iodine(V) fluorides has been limited primarily by their difficult preparation traditionally using harsh fluorinating reagents such as trifluoromethyl hypofluorite and bromine trifluoride. Here, we report a mild and efficient route using Selectfluor to deliver hypervalent iodine(V) fluorides in good isolated yields (72–90%). Stability studies revealed that bicyclic difluoro(aryl)-λ^5-iodane **6** was much more stable in acetonitrile-d_3 than in chloroform-d_1, presumably due to acetonitrile coordinating to the iodine(V) centre and stabilising it via halogen bonding.

Introduction

An important strategy in the drug discovery process is the incorporation of fluorine into biologically active molecules because fluorine can improve bioactivity and pharmacokinetic properties [1]. Consequently, 22% of all small-molecule drugs contain at least one fluorine atom [2]. Hypervalent iodine(III) fluorides, such as difluoroiodotoluene **1** and fluoroiodane **2**, have been key to the development of numerous, new synthetic procedures for C–F bond formation over the last decade. Since difluoroiodotoluene **1** has low chemical stability and is highly hygroscopic, it is often prepared in situ and Gilmour [3-8] has reported a range of fluorination protocols utilising hypervalent iodine(I/III) catalysis (Scheme 1A). Lennox has also demonstrated that **1** can be generated cleanly by electrochemical oxidation [9,10]. In an alternative approach, we reported the first application of using fluoroiodane **2** as a fluorinating reagent in 2013 [11]. The chelate sidearm makes **2** an air-stable, easy-to-handle solid with excellent fluorinating ability and it often exhibits different reactivity to that observed with fluoroaza reagents such as Selectfluor (Scheme 1B) [12-20].

In contrast to the chemistry of hypervalent iodine(III) reagents, very little is known about hypervalent iodine(V) fluorides. One

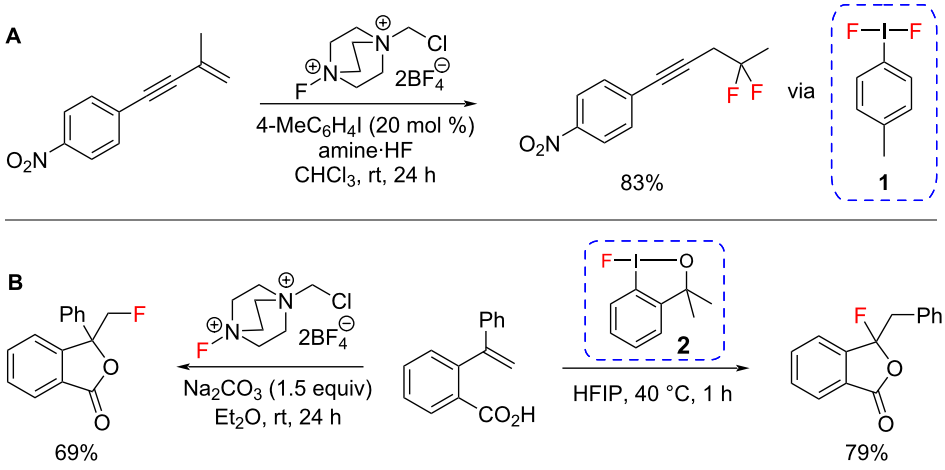

Scheme 1: Examples of fluorination using hypervalent iodine(III) reagents **1** and **2**.

problem that has blocked research into these compounds has been the lack of synthetic procedures to access them easily because they normally require harsh fluorinating reagents. The synthesis of hypervalent iodine(V) fluoride **3** was reported by Amey and Martin in 1979 using the highly toxic gas, trifluoromethyl hypofluorite (Scheme 2A), and they later prepared bicyclic hypervalent iodine(V) fluoride **4** using bromine trifluoride (Scheme 2B) [21,22]. They also showed that hypervalent iodine(V) fluoride **3** fluorinated phenylmagnesium bromide in Freon-113 to form fluorobenzene in 90% yield (Scheme 2A) and so, it is very surprising that this reagent has not been investigated further. Since then, Gruber [23] reacted a perfluorinated iodine(III) compound with XeF_2 and postulated the formation of a (perfluoroalkyl)iodine(V) difluoride intermediate which underwent a reductive elimination to afford perfluorinated products (Scheme 2C). In 2019 Togni reported a safer route to a range of acyclic iodine(V) fluorides such as **5** (Scheme 2D) using large excesses of trichloroisocyanuric acid (TCCA) and potassium fluoride [24]. The iodine(V) fluorides were formed in good spectroscopic yields (79–94%), but only one product, tetrafluoro(4-fluorophenyl)-λ^5-iodane **5**, was isolated from the reaction mixture by performing multiple extractions into hexane under a nitrogen atmosphere in a glovebox. A similar synthetic approach to acyclic iodine(V) fluorides was developed more recently by Ismalaj and co-workers by reacting iodoarenes with 6 equivalents of KF and ex situ-generated chlorine gas within a two-chamber reactor setup, but again the iodine(V) fluorides were not isolated [25].

We became interested in developing a convenient procedure to access these intriguing reagents and to investigate their ability to fluorinate aryl Grignard reagents. In this paper, we report a straightforward route to hypervalent iodine(V) fluorides by reacting iodine(III) precursors with commercially available Selectfluor. The method avoids large excesses of reagents and pure iodine(V) fluorides are isolated after a simple work-up.

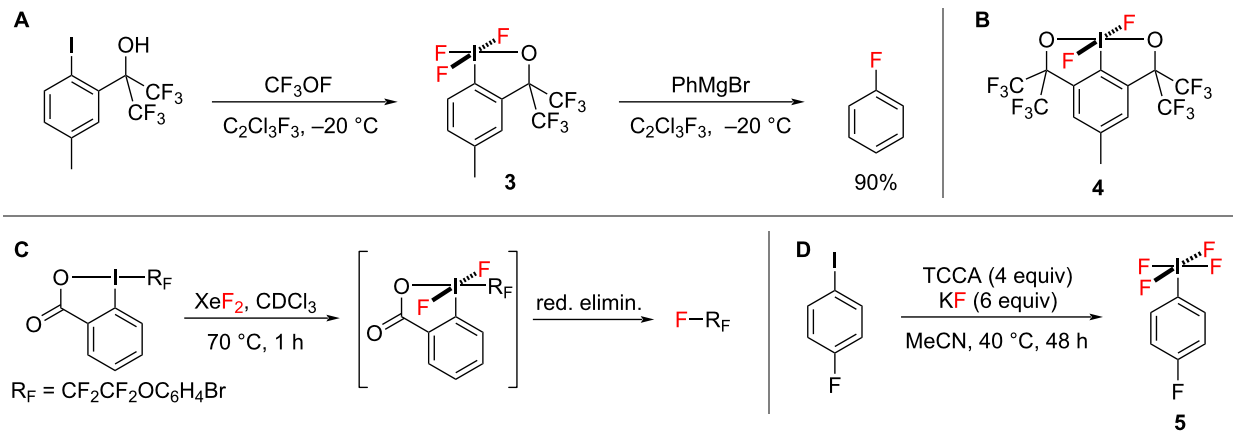

Scheme 2: Preparations and reactions of hypervalent iodine(V) fluorides.

Results and Discussion

Preparation of bicyclic difluoro(aryl)-λ^5-iodanes

Two different types of bicyclic difluoro(aryl)-λ^5-iodanes were designed originally because of the stabilisation afforded from two five-membered rings (Figure 1). We started our investigation with bicyclic difluoro(aryl)-λ^5-iodane **6**, building on the hypervalent iodine core skeleton used in fluoroiodane **2**, with an additional 5-membered ring to stabilise the iodine(V) centre. Both sidearms were also changed to amides because the NR group is a point of diversity which could be used to modulate the sterics and electronics of these novel hypervalent iodine(V) compounds.

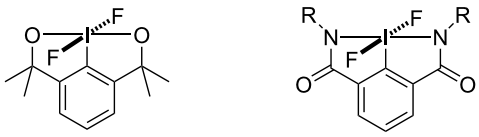

6 **7a** R = CH_2Ph **7b** R = $CH(CH_3)_2$

Figure 1: Bicyclic difluoro(aryl)-λ^5-iodanes.

Initially, we applied Togni's oxidative fluorination protocol to iodine(I) precursor **8** (Table 1). Reacting **8** with 4 equivalents of trichloroisocyanuric acid (TCCA) and 6 equivalents of potassium fluoride in dry acetonitrile at 40 °C for 48 hours formed difluoroiodane **6** in a 90% spectroscopic yield (Table 1, entry 1). An iodosyl decomposition product **9** was also formed during the work-up procedure in air. When the reaction time was shortened to 24 hours, a complex reaction mixture was obtained (Table 1, entry 2). Reducing the amount of TCCA to 3 equivalents (Table 1, entry 3) delivered difluoroiodane **6** in the same 90% yield. Finally, we performed the reaction and work-up under inert conditions and an excellent 99% yield of difluoroiodane **6** was achieved. The main issue with this procedure, however, was that we could not extract the pure difluoroiodane **6** into hexane and separate it from the large excesses of TCCA. Selectfluor was therefore explored as an oxidative fluorinating reagent (Table 1, entry 5). When **8** was reacted with 4 equivalents of freeze-dried Selectfluor in dry acetonitrile at 40 °C for 48 hours, difluoroiodane **6** was formed in 85% spectroscopic yield. However, the iodosyl decomposition product **9** was also produced in 15% spectroscopic yield, despite working the reaction up under inert conditions.

Consequently, we decided to investigate the oxidative fluorination of iodine(III) substrate **10** with Selectfluor (Table 2). We were delighted that difluoroiodane **6** was formed in 93% spectroscopic yield and the iodosyl byproduct **9** was formed in a much lower 7% spectroscopic yield, when **10** was reacted with a large excess of Selectfluor (5.1 equivalents) in dry acetonitrile at 40 °C for 48 hours (Table 2, entry 1). More importantly, difluoroiodane **6** was isolated successfully in an excellent 91% yield by a simple extraction into dry dichloromethane providing an efficient separation from the excess Selectfluor and its byproduct. Reducing the amount of Selectfluor to 2.5 equivalents and the reaction time to 24 hours (Table 2, entry 2) resulted in a similar high yield of difluoroiodane **6**. The reaction also proceeded well at either room temperature for 24 hours (Table 2, entry 3) or at 40 °C for 6 hours (Table 2, entry 4). Finally, reducing the amount of Selectfluor to 1.5 equivalents

Table 1: Oxidative fluorination of iodine(I) substrate **8**.

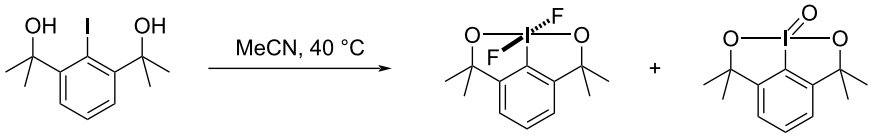

8 **6** **9**

Entry	Reaction conditions	Time (h)	Yield[a]	
			6 (%)	**9** (%)
1	TCCA (4 equiv), KF (6 equiv)	48	90	10
2	TCCA (4 equiv), KF (6 equiv)	24	complex mixture	
3	TCCA (3 equiv), KF (6 equiv)	48	90	10
4	TCCA (3 equiv), KF (6 equiv), work-up under N_2	48	99	1
5	Selectfluor (4 equiv), work-up under N_2	48	85 (56)	15

[a]Yield calculated by ^{1}H NMR spectroscopy, isolated yield shown in parenthesis.

Table 2: Oxidative fluorination with Selectfluor[a].

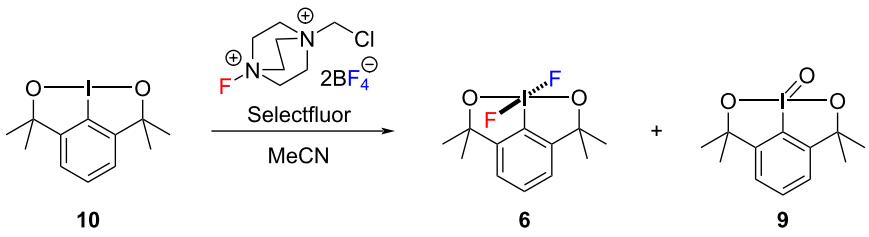

10 **6** **9**

Entry	Selectfluor (equiv)	Temp. (°C)	Time (h)	Conversion (%)	Yield[b]	
					6 (%)	**9** (%)
1	5.1	40	48	100	93 (91)	7
2	2.5	40	24	100	98 (80)	2
3	2.5	25	24	97	98 (58)	2
4	2.5	40	6	99	95 (55)	5
5	1.5	40	24	99	96 (90)	4

[a]All reactions performed in dry acetonitrile with freeze-dried Selectfluor under nitrogen and work-ups performed in dry solvents under nitrogen; [b]Yield calculated by ^{1}H NMR spectroscopy, isolated yield shown in parenthesis.

led to an excellent 90% isolated yield and the conclusion that Selectfluor delivered one electrophilic fluorine (from the N–F) and one nucleophilic fluoride (from the tetrafluoroborate, BF_4^-) to form difluoroiodane **6**.

The formation of difluoroiodane **6** was identified by a singlet at −23.0 ppm in the ^{19}F NMR spectrum. As expected, the aromatic signals in the ^{1}H NMR spectrum shifted downfield from a doublet at 7.21 ppm and a triplet at 7.56 ppm for iodine(III) substrate **10** to 7.71 ppm and 7.96 ppm, respectively, for iodine(V) product **6**. Similarly, the ^{13}C NMR spectrum showed a major downfield shift for the aromatic carbon attached to iodine from a chemical shift of 105.3 ppm in iodine(III) substrate **10** to 132.4 ppm for difluoroiodane(V) product **6**.

Since Selectfluor was shown to be the best reagent for preparing bicyclic iodine(V) difluoride **6**, this route was first investigated for the oxidative fluorinations of hypervalent iodine(III) amides **11a** and **11b** (Scheme 3). Unfortunately, these reactions did not work and difluoro(aryl)-λ^5-iodanes **7a** and **7b** were not produced. Togni's protocol using TCCA (4 equivalents) and KF (6 equivalents) was then applied to both bicyclic iodine(III) amides **11a** and **11b**, but these reactions also failed to form either difluoroiodane **7a** or **7b**.

Following the successful preparation and isolation of difluoroiodane **6**, we investigated its ability to fluorinate PhMgBr as reported with iodine(V) fluoride **3** by Amey and Martin [21]. Difluoroiodane **6** was first reacted with phenylmagnesium chloride in dry toluene at 0 °C, but fluorobenzene was not formed

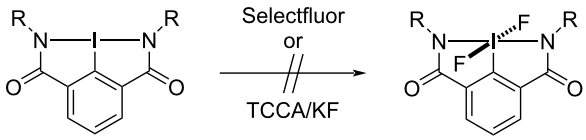

11a R = CH_2Ph
11b R = $CH(CH_3)_2$

7a R = CH_2Ph
7b R = $CH(CH_3)_2$

Scheme 3: Attempted oxidative fluorination of hypervalent iodine(III) amides.

under these reaction conditions. The reaction was then repeated using phenylmagnesium bromide, but disappointingly, no fluorination was observed. The disparity in reactivity between difluoroiodane **6** and trifluoroiodane **3** towards aryl Grignard reagents could be attributed to the different relationships between the fluorine ligands on the iodine(V) centre. In difluoroiodane **6** the fluorine ligands are restricted to a *trans*-configuration because of the bicyclic carbon skeleton. Trifluoroiodane **3**, on the other hand, has both *trans*- and *cis*-configurations of the fluorine ligands which could play a key role in the reductive elimination step in the fluorination of phenylmagnesium bromide. Trifluoroiodane **3** also contains two trifluoromethyl groups in the sidearm which could alter the electronic effects significantly. We therefore decided to prepare a small series of monocyclic trifluoro(aryl)-λ^5-iodanes, where the sidearm substituents were changed stepwise from methyl to trifluoromethyl groups, so that we also formed an analogue of Amey and Martin's monocyclic trifluoroiodane **3**.

Preparation of monocyclic trifluoro(aryl)-λ^5-iodanes

Our investigation into the synthesis of monocyclic trifluoro(aryl)-λ^5-iodanes began with the preparation of the key iodine(III) precursors for our oxidative fluorination protocol. Fluoroiodane **2** was already available in our laboratory [11] and the three-step synthesis of methyl(trifluoromethyl)fluoroiodane **15** is shown in Scheme 4. The first step was a diazotisation of 2'-aminoacetophenone **12** to form 2'-iodoacetophenone **13**, which was then reacted with Ruppert's reagent (CF_3SiMe_3) to afford iodoalcohol **14** in 93% yield. In the final step iodoalcohol **14** underwent an oxidative fluorination with Selectfluor at room temperature to deliver methyl(trifluoromethyl)fluoroiodane **15** in a good 68% yield after recrystallisation from toluene.

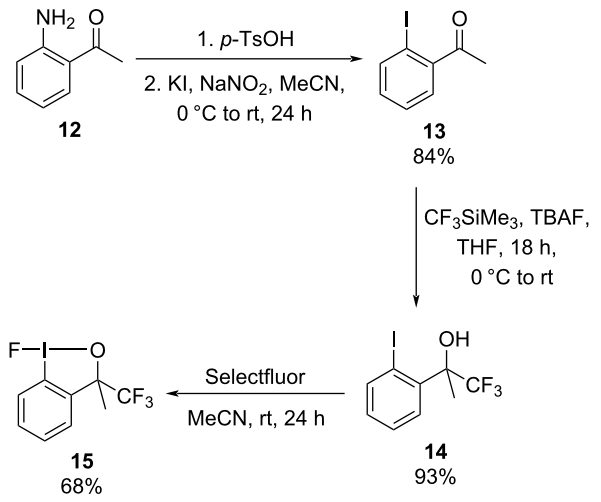

Scheme 4: Synthesis of methyl(trifluoromethyl)fluoroiodane **15**.

Although bis(trifluoromethyl)fluoroiodane **19** has been reported before [26-28], we developed a new synthetic route which is shown in Scheme 5. In the first step trifluoromethylketone **17** was prepared by a nucleophilic acyl substitution of methyl 2-iodobenzoate **16** with Ruppert's reagent. Ketone **17** was then reacted with an excess of Ruppert's reagent and TBAF in order to form bis(trifluoromethyl)iodoalcohol **18**, which was treated with Selectfluor in the final step to deliver bis(trifluoromethyl)fluoroiodane **19** in 72% yield.

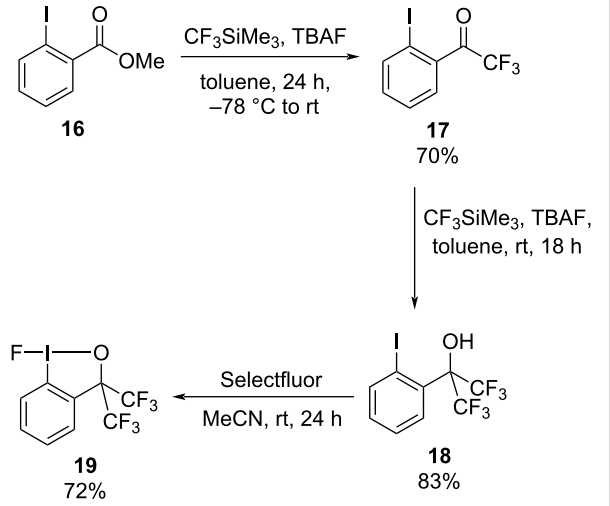

Scheme 5: Synthesis of bis(trifluoromethyl)fluoroiodane **19**.

A small series of trifluoro(aryl)-λ^5-iodanes were successfully prepared and isolated in good yields (Table 3). Dimethyltrifluoroiodane **20** was readily formed under mild reaction conditions using 2.5 equivalents of Selectfluor at 40 °C for 24 hours. However, the introduction of trifluoromethyl groups to the

Table 3: Oxidative fluorination of monocyclic fluoroiodanes.

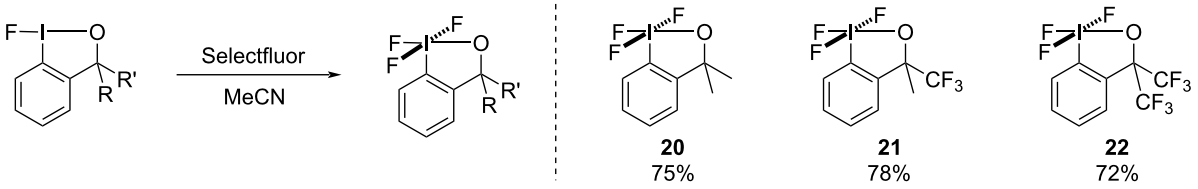

Entry	R/R'	Product	Selectfluor (equiv)	Temp. (°C)	Time (h)	Yield[a] (%)
1	CH_3/CH_3	**20**	2.5	40	24	75
2	CH_3/CF_3	**21**	3.0	60	48	78
3	CF_3/CF_3	**22**	3.0	80	72	72

[a]Isolated yield.

sidearm of the iodine(III) fluoroiodanes led to harsher oxidative fluorination conditions being required because the increased electron-withdrawing effect made the fluoroiodane precursors more resistant to oxidation. Consequently, higher temperatures, longer reaction times and more equivalents of Selectfluor were required to prepare trifluoroiodanes **21** and **22**. Trifluoro(aryl)-λ^5-iodane **22** was also prepared directly from its iodine(I) precursor **18** in 73% isolated yield in a one-pot procedure using 5.5 equivalents of Selectfluor (see Supporting Information File 1).

Unfortunately, we were never able to replicate Amey and Martin's fluorination of phenylmagnesium bromide using bis(trifluoromethyl)trifluoroiodane **22** (Scheme 6). The major products were phenyliodane **23**, presumably a result of ligand exchange and reduction, and iodoalcohol **18**. Different solvents, temperatures and activators were investigated and the results are shown in Table S3 in Supporting Information File 1. Fluorobenzene was only ever observed in trace amounts (1–3 % spectroscopic yield) when $BF_3{\cdot}OEt_2$ was added to the reaction mixture.

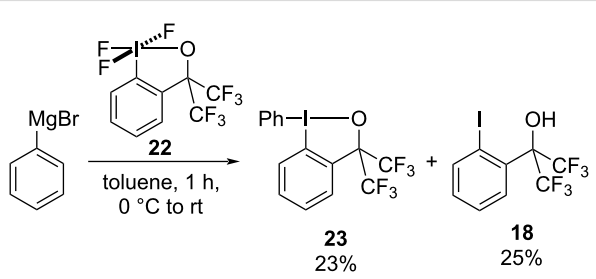

Scheme 6: Reaction of phenylmagnesium bromide with bis(trifluoromethyl)trifluoroiodane **22**.

X-ray crystallography and DFT calculations

The solid-state structure of difluoroiodane **6** is shown in Figure 2 and displays the expected square pyramidal geometry around the iodine atom, with only minor distortion (τ_5 = 0.191). Since there were two unique molecules in the unit cell, Table 4 compares the average bond lengths and average bond angles of difluoroiodane **6** with trifluoroiodane **20**, which was reported by Togni [24], and fluoroiodane **2** [11]. The I–F bond lengths in difluoroiodane **6** (range from 1.959(4) to 1.990(4) Å) are very similar to those in trifluoroiodane **20** (range from 1.956(4) to 1.984(4) Å), but are shorter than that in fluoroiodane **2** (2.048(3) to 2.058(3) Å) suggesting that fluorine is bound more strongly to the iodine(V) centre than in iodine(III) compounds. There is a similar contraction in the I–O bond lengths when comparing iodine(V) compounds, difluoroiodane **6** (range from

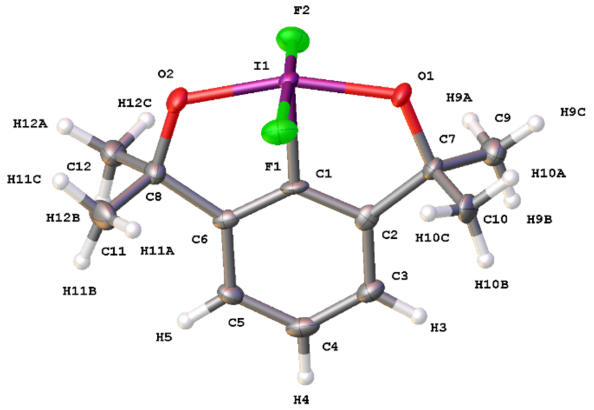

Figure 2: Molecular structure of difluoroiodane **6** showing 50% displacement ellipsoids.

Table 4: Selected average bond lengths (Å) and average bond angles (°) with estimated standard deviations (e.s.d.s.) in parenthesis for difluoroiodane **6**, trifluoroiodane **20** and fluoroiodane **2**.

Average bond lengths (Å) and bond angles (°)	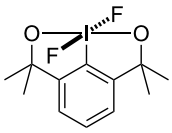 **6**	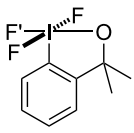 **20**	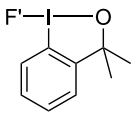 **2**
C–I	2.031(6)	2.072(7)	2.089(5)
I–F	1.975(4)	1.963(4)	–
I–F'	–	1.979(4)	2.053(3)
I–O	1.986(4)	1.924(5)	2.029(3)
F'/O–I–O	161.4(2)	167.9(2)	166.7(2)
F–I–F	172.9(2)	168.5(2)	–
C–I–F	86.7(2)	85.8(3)	–
C–I–F'	–	85.8(3)	86.8(2)
C–I–O	80.7(2)	82.5(2)	80.4(2)

1.977(4) to 1.993(4) Å) and trifluoroiodane **20** (1.924(5) Å), with their respective iodine(III) precursors, **10** (2.096(2) Å) [29] and fluoroiodane **2** (2.029(3) Å). The F–I–F bond angle for difluoroiodane **6** (172.2(2)° to 173.6(2)°) deviates from 180°, but not to the same extent as seen with the aryl-IF_4 compounds (169.9(1) to 170.4(1)°) or with trifluoroiodane **20** (167.9(2)° to 169.0(2)°) [24]. On the other hand, the O–I–O bond angle for difluoroiodane **6** (161.4(2)°) is much smaller than the F'–I–O bond angles in both trifluoroiodane **20** (167.2(2)° to 168.6(2)°) and fluoroiodane **2** (166.7(2)°), presumably due to the strain caused by the two five-membered rings. Similar to trifluoroiodane **20**, there are two short intermolecular I···F contacts of 2.942(4) Å and 2.999(4) Å in the packing diagram of difluoroiodane **6** (see Figure S1 in Supporting Information File 1).

DFT calculations were carried out to gain further insight into the structures of iodine(V) fluorides **21** and **22** whose X-ray structures could not be obtained, and hypothetical iodine(V) amides **7a** and **7b** which could not be made. Comparisons were made with iodine(V) compounds **6** and **20**, as well as with iodine(III) compounds **2** and **19**. Geometry optimisations were performed on all the compounds using Gaussian 16 at wB97xD/cc-pvdz, with a cc-pvdz-PP basis set used for the iodine atom. The calculated bond lengths and bond angles are reported in Table 5 and are in good agreement with the solid state structures. As expected, the calculated atomic charge on iodine was much higher for the iodine(V) fluorides (1.689–1.766) than in the iodine(III) fluorides (0.957–1.009) resulting in shorter I–F and I–O bond lengths. Interestingly, there is a slightly lower charge on iodine in bicyclic iodane **6** (1.689) compared to monocyclic trifluoroiodanes **20**–**22** (1.738–1.766) and the ipso carbon atom is slightly less electronegative (−0.355 vs −0.414) resulting in a less polar, but slightly shorter C–I bond in difluoroiodane **6** (2.031(6) Å) compared to trifluoroiodane **20** (2.072(7) Å). As you go across the series of monocyclic trifluoroiodanes **20** to **22**, the I–O bond length increases slightly due to the electron-withdrawing effect of the trifluoromethyl groups in the sidearms and consequently, the synergistic effect of the 3-centre-4-electron bond causes the I–F' bond length to decrease slightly. The only major difference between the bicyclic and monocyclic iodine(V) fluorides is the much smaller O–I–O bond angle (161.4(2) °) in difluoroiodane **6** compared to the F'–I–O bond angle (167.9(2) ° in **20**) in the monocyclic iodanes **20**–**22**. In fact, DFT calculations predicted that hypothetical difluoroiodanes **7a** and **7b** containing the amide sidearms would have an even more acute N–I–N bond angle (156.6–156.9 °). Furthermore, the internal chelate NCC bond angle in **7a/b** (111.7°) was calculated to be bigger than the corresponding OCC angle (108.3(5)° to 109.2(5)°) in **6** due to the sp^2-hybridised carbon in **7a/b** and an sp^3-hybridised carbon in **6**. This NCC bond angle (111.7°) would certainly increase the angle strain in **7a/b** and this, combined with the acute N–I–N bond angle (156.6–156.9°) caused by these two five-membered rings, could be the reason that we could not prepare these compounds.

Stability studies of hypervalent iodine(V) fluorides in solution

The stability of hypervalent iodine(V) fluorides **6**, **20**, **21** and **22** was studied in dry acetonitrile-d_3 by ^{1}H and ^{19}F NMR spectroscopy over 7 days under an argon atmosphere. All four hypervalent iodine(V) fluorides were stable for the 7-day period. When the same experiment was repeated in air, iodine(V) fluorides **6**, **21** and **22** decomposed to 55–65% remaining after 7 days presumably due to the moisture in the air, whereas trifluoroiodane **20** was less stable with only 37% remaining. Difluoro-

Table 5: Comparing properties of hypervalent iodine(V) fluorides with hypervalent iodine(III) fluorides **2** and **19**[a].

	d(C–I) (Å)	d(I–F) (Å)	d(I–F') (Å)	d(I-O/N) (Å)	q_C	q_I	q_F	$q_{F'}$	$q_{O/N}$	$\theta_{F–I–F}$ (°)	$\theta_{O\text{-}I\text{-}O/F'}$/ $\theta_{N\text{-}I\text{-}N}$ (°)
6	2.04	2.00[b]	–	2.03	−0.355	1.689	−0.460	–	−0.561	173.6	161.1
7a	2.06	2.00	–	2.12	−0.312	1.668	−0.426	–	−0.609	175.9	156.6
7b	2.05	1.99[b]	–	2.12	−0.314	1.667	−0.444	–	−0.591	176.7	156.9
20	2.09	1.98[b]	1.99	1.99	−0.419	1.738	−0.453	−0.449	−0.556	171.8	168.8
21	2.09	1.98[c]	1.98	2.01	−0.415	1.753	−0.445[d]	−0.439	−0.550	171.7	168.6
22	2.10	1.97[b]	1.97	2.03	−0.407	1.766	−0.438	−0.428	−0.540	171.4	168.5
2	2.10	–	2.04	2.07	−0.403	0.957	–	−0.490	−0.574	–	167.9
19	2.10	–	2.02	2.09	−0.387	1.009	–	−0.469	−0.552	–	167.8

[a]Calculations performed at wB97xD/cc-pvdz, with a cc-pvdz-PP basis set used for the iodine atom. C refers to ipso carbon atom, F and F' refers to fluorine atom bound to iodine. [b]Structure is nearly symmetric about F–I–F (mirror plane). [c]Average between 1.99 and 1.97. [d]Average between −0.441 and −0.449.

iodane **6** was also stable in dry chloroform-d_1 under argon over 7 days, but it decomposed completely to iodosyl **9** after just 48 hours in dry chloroform-d_1 in air (red line in Figure 3). The difference in the stability of difluoroiodane **6** in $CDCl_3$ and CD_3CN was attributed to the ability of acetonitrile to coordinate to the iodine(V) centre. Stabilisation via halogen bonding is well-established in hypervalent iodine(III) compounds and Dutton showed that pyridine formed a weak complex with dichloroiodobenzene via halogen bonding [30-32]. We therefore added dry pyridine (2.4 equivalents) to difluoroiodane **6** in $CDCl_3$ to help stabilise the iodine(V) centre and the rate of decomposition was reduced significantly (green line in Figure 3).

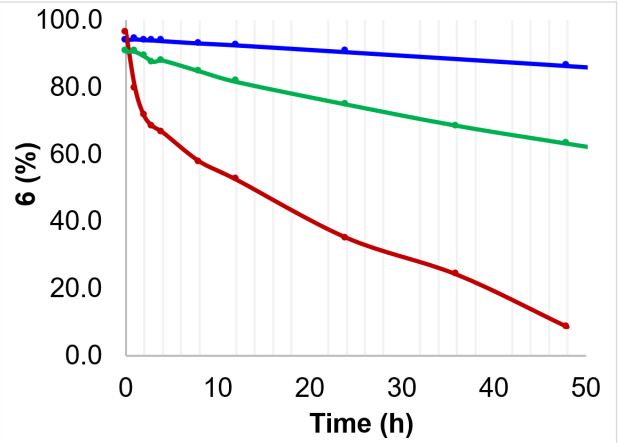

Figure 3: Stability of difluoroiodane **6** in air in dry CD_3CN (blue line), dry $CDCl_3$ with 2.4 equivalents of dry pyridine (green line), and dry $CDCl_3$ (red line).

The hydrolysis of the four hypervalent iodine(V) fluorides was also investigated in acetonitrile-d_3 by adding 5 equivalents of water. All four compounds decomposed to their corresponding iodosyl compounds and the order of stability is shown in Figure 4. Difluoroiodane **6**, containing two 5-membered rings, was the most stable iodine(V) fluoride whereas monocyclic trifluoroiodane **20** was the least stable and decomposed completely within the first minute. As expected, the stability of the monocyclic trifluoroiodanes **21** and **22** was increased by the stepwise incorporation of the trifluoromethyl groups into the sidearm, but trifluoroiodane **22** was less stable than bicyclic difluoro(aryl)-λ^5-iodane **6**.

Conclusion

In summary, we have developed a new strategy using Selectfluor for the convenient preparation and isolation of hypervalent iodine(V) fluorides in good yields (72–90%). Unfortunately, none of the iodine(V) fluorides reacted with phenylmagnesium bromide to form fluorobenzene and we were never able to repeat Amey and Martin's fluorination of phenylmagnesium bromide. A solid-state structure of **6** and DFT calculations on **6** and **20**–**22** gave insights into the geometries of the iodine(V) fluorides compared to the iodine(III) precursors. DFT results also suggested a possible reason for not being able to make iodine(V) amides **7a** and **7b**. An investigation into the hydrolysis of the four hypervalent iodine(V) fluorides revealed that bicyclic difluoro(aryl)-λ^5-iodane **6** was more stable than monocyclic trifluoro(aryl)-λ^5-iodanes **20**–**22** due to the incorporation of the second 5-membered ring in the 3-centre-4-electron bond.

Experimental

Dioxoiodane **10** (0.58 g, 1.8 mmol), Selectfluor (0.97 g, 2.7 mmol) and dry acetonitrile (10 mL) were charged to a dry Schlenk flask under a nitrogen atmosphere. The flask was sealed and heated to 40 °C for 24 hours. After cooling the reaction mixture to room temperature, the solvent was removed in vacuo to afford a crude orange solid. The orange solid was extracted with dry dichloromethane (3 × 5 mL) under a nitrogen atmosphere and the dichloromethane was removed in vacuo to afford difluoroiodane **6** as a pale orange solid (0.58 g, 90%).

Supporting Information

Crystallographic data (excluding structure factors) for the structures reported in this paper have been deposited with the Cambridge Crystallographic Data Centre and allocated the deposition numbers CCDC: 2351949 and 2351950.

Supporting Information File 1

Experimental procedures, characterisation data, DFT calculations and ^1H, ^{13}C and ^{19}F NMR spectra and crystallographic data.
[https://www.beilstein-journals.org/bjoc/content/supplementary/1860-5397-20-157-S1.pdf]

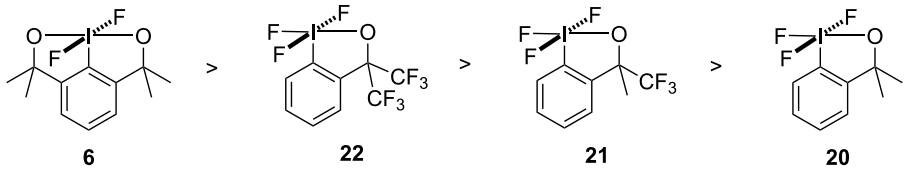

Figure 4: Order of hydrolytic stability for the four hypervalent iodine(V) fluorides.

Funding

SMGD and AMS thank the School of Chemistry, University of Leicester, for their generous support. AMS also thanks the EPSRC for research grant EP/W02151X/1.

ORCID® iDs

Samuel M. G. Dearman - https://orcid.org/0009-0003-5421-1647
Yang Li - https://orcid.org/0000-0002-5719-9044
Alison M. Stuart - https://orcid.org/0000-0001-5984-4919

Data Availability Statement

All data that supports the findings of this study is available in the published article and/or the supporting information to this article.

References

1. Inoue, M.; Sumii, Y.; Shibata, N. *ACS Omega* **2020,** *5,* 10633–10640. doi:10.1021/acsomega.0c00830
2. Han, J.; Remete, A. M.; Dobson, L. S.; Kiss, L.; Izawa, K.; Moriwaki, H.; Soloshonok, V. A.; O'Hagan, D. *J. Fluorine Chem.* **2020,** *239,* 109639. doi:10.1016/j.jfluchem.2020.109639
3. Wang, Z.-X.; Livingstone, K.; Hümpel, C.; Daniliuc, C. G.; Mück-Lichtenfeld, C.; Gilmour, R. *Nat. Chem.* **2023,** *15,* 1515–1522. doi:10.1038/s41557-023-01344-5
4. Häfliger, J.; Ruyet, L.; Stübke, N.; Daniliuc, C. G.; Gilmour, R. *Nat. Commun.* **2023,** *14,* 3207. doi:10.1038/s41467-023-38957-w
5. Yu, Y.-J.; Schäfer, M.; Daniliuc, C. G.; Gilmour, R. *Angew. Chem., Int. Ed.* **2023,** *62,* e202214906. doi:10.1002/anie.202214906
6. Neufeld, J.; Daniliuc, C. G.; Gilmour, R. *Helv. Chim. Acta* **2023,** *106,* e202200183. doi:10.1002/hlca.202200183
7. Meyer, S.; Göbel, L.; Livingstone, K.; Roblick, C.; Daniliuc, C. G.; Gilmour, R. *Tetrahedron* **2022,** *126,* 132925. doi:10.1016/j.tet.2022.132925
8. Neufeld, J.; Stünkel, T.; Mück-Lichtenfeld, C.; Daniliuc, C. G.; Gilmour, R. *Angew. Chem., Int. Ed.* **2021,** *60,* 13647–13651. doi:10.1002/anie.202102222
9. Doobary, S.; Sedikides, A. T.; Caldora, H. P.; Poole, D. L.; Lennox, A. J. J. *Angew. Chem., Int. Ed.* **2019,** *58,* 1155–1160. doi:10.1002/anie.201912119
10. Doobary, S.; Poole, D. L.; Lennox, A. J. J. *J. Org. Chem.* **2021,** *86,* 16095–16103. doi:10.1021/acs.joc.1c01946
11. Geary, G. C.; Hope, E. G.; Singh, K.; Stuart, A. M. *Chem. Commun.* **2013,** *49,* 9263–9265. doi:10.1039/c3cc44792h
12. Geary, G. C.; Hope, E. G.; Stuart, A. M. *Angew. Chem., Int. Ed.* **2015,** *54,* 14911–14914. doi:10.1002/anie.201507790
13. Minhas, H. K.; Riley, W.; Stuart, A. M.; Urbonaite, M. *Org. Biomol. Chem.* **2018,** *16,* 7170–7173. doi:10.1039/c8ob02236d
14. Abudken, A. M. H.; Hope, E. G.; Singh, K.; Stuart, A. M. *Org. Biomol. Chem.* **2020,** *18,* 6140–6146. doi:10.1039/d0ob01401j
15. Riley, W.; Jones, A. C.; Singh, K.; Browne, D. L.; Stuart, A. M. *Chem. Commun.* **2021,** *57,* 7406–7409. doi:10.1039/d1cc02587b
16. Ilchenko, N. O.; Tasch, B. O. A.; Szabó, K. J. *Angew. Chem., Int. Ed.* **2014,** *53,* 12897–12901. doi:10.1002/anie.201408812
17. Yuan, W.; Eriksson, L.; Szabó, K. J. *Angew. Chem., Int. Ed.* **2016,** *55,* 8410–8415. doi:10.1002/anie.201602137
18. Ilchenko, N. O.; Cortés, M. A.; Szabó, K. J. *ACS Catal.* **2016,** *6,* 447–450. doi:10.1021/acscatal.5b02022
19. Ulmer, A.; Brunner, C.; Arnold, A. M.; Pöthig, A.; Gulder, T. *Chem. – Eur. J.* **2016,** *22,* 3660–3664. doi:10.1002/chem.201504749
20. Zhao, P.; Wang, W.; Gulder, T. *Org. Lett.* **2023,** *25,* 6560–6565. doi:10.1021/acs.orglett.3c02384
21. Amey, R. L.; Martin, J. C. *J. Am. Chem. Soc.* **1979,** *101,* 5294–5299. doi:10.1021/ja00512a030
22. Nguyen, T. T.; Amey, R. L.; Martin, J. C. *J. Org. Chem.* **1982,** *47,* 1024–1027. doi:10.1021/jo00345a026
23. Gruber, S.; Ametamey, S. M.; Schibli, R. *Chem. Commun.* **2018,** *54,* 8999–9002. doi:10.1039/c8cc04558e
24. Häfliger, J.; Pitts, C. R.; Bornemann, D.; Käser, R.; Santschi, N.; Charpentier, J.; Otth, E.; Trapp, N.; Verel, R.; Lüthi, H. P.; Togni, A. *Chem. Sci.* **2019,** *10,* 7251–7259. doi:10.1039/c9sc02162k
25. Ullah, K.; Kordnezhadian, R.; Demaerel, J.; De Borggraeve, W. M.; Ismalaj, E. *J. Fluorine Chem.* **2024,** *275,* 110276. doi:10.1016/j.jfluchem.2024.110276
26. Chai, J.; Ding, W.; Wu, J.; Yoshikai, N. *Chem. – Asian J.* **2020,** *15,* 2166–2169. doi:10.1002/asia.202000653
27. Cvengroš, J.; Stolz, D.; Togni, A. *Synthesis* **2009,** 2818–2824. doi:10.1055/s-0029-1217406
28. Milzarek, T. M.; Ramirez, N. P.; Liu, X.-Y.; Waser, J. *Chem. Commun.* **2023,** *59,* 12637–12640. doi:10.1039/d3cc04525k
29. Gao, W.-C.; Zhang, C. *Tetrahedron Lett.* **2014,** *55,* 2687–2690. doi:10.1016/j.tetlet.2014.03.034
30. Pinto de Magalhães, H.; Togni, A.; Lüthi, H. P. *J. Org. Chem.* **2017,** *82,* 11799–11805. doi:10.1021/acs.joc.7b01716
31. Matoušek, V.; Václavík, J.; Hájek, P.; Charpentier, J.; Blastik, Z. E.; Pietrasiak, E.; Budinská, A.; Togni, A.; Beier, P. *Chem. – Eur. J.* **2016,** *22,* 417–424. doi:10.1002/chem.201503531
32. Poynder, T. B.; Chamorro Orué, A. I.; Tania; Sharp-Bucknall, L.; Flynn, M. T.; Wilson, D. J. D.; Athukorala Arachchige, K. S.; Clegg, J. K.; Dutton, J. L. *Chem. Commun.* **2021,** *57,* 4970–4973. doi:10.1039/d1cc01567b

BEILSTEIN JOURNAL OF ORGANIC CHEMISTRY

Solvent-dependent chemoselective synthesis of different isoquinolinones mediated by the hypervalent iodine(III) reagent PISA

Ze-Nan Hu‡, Yan-Hui Wang‡, Jia-Bing Wu, Ze Chen, Dou Hong and Chi Zhang*

Full Research Paper

Open Access

Address:
State Key Laboratory of Elemento-Organic Chemistry, The Research Institute of Elemento-Organic Chemistry, College of Chemistry, Nankai University, 94 Weijin Road, Tianjin 300071, P. R. China

Email:
Chi Zhang* - zhangchi@nankai.edu.cn

* Corresponding author ‡ Equal contributors

Keywords:
annulation; C–H amination; hypervalent iodine reagent; iodine(III); isoquinolinone; solvent-dependence

Beilstein J. Org. Chem. **2024,** *20,* 1914–1921.
https://doi.org/10.3762/bjoc.20.167

Received: 23 April 2024
Accepted: 22 July 2024
Published: 07 August 2024

This article is part of the thematic issue "Hypervalent halogen chemistry".

Guest Editor: J. Wencel-Delord

Abstract

Isoquinolinone is an important heterocyclic framework in natural products and biologically active molecules, and the efficient synthesis of this structural motif has received much attention in recent years. Herein, we report a (phenyliodonio)sulfamate (PISA)-mediated, solvent-dependent synthesis of different isoquinolinone derivatives. The method provides highly chemoselective access to 3- or 4-substituted isoquinolinone derivatives by reacting *o*-alkenylbenzamide derivatives with PISA in either acetonitrile or wet hexafluoro-2-isopropanol.

Introduction

Isoquinolinone is an important heterocyclic structure found in many natural products and biologically active compounds, including pharmaceuticals [1]. For instance, lycoricidine, found in the medicinal plant *Lycoris radiata*, may inhibit the MCPyV LT protein activity and thus block cancer formation [2]. Alangiumkaloids A, an isoquinolinone alkaloid isolated from *Alangium salviiforlium*, was reported to exhibit cytotoxic activity against cancer cells [3]. In 2018, duvelisib, a dual inhibitor of phosphoinositide-3 kinases, was firstly approved by the FDA for the treatment of adult patients with relapsed or refractory chronic lymphocytic leukaemia or small lymphocytic lymphoma [4]. Palonosetron is a key component of Akynzeo®, used for the prevention of acute and delayed nausea and vomiting of cancer patients who are receiving chemotherapy [5]. As an active compound, PF-06821497 showed potent tumor growth inhibition in mouse xenograft models [6]. CRA-680 was efficacious in both a house dust mouse model of allergic lung inflammation and a guinea pig allergen challenge model of lung inflammation [7]. In addition, isoquinolinone compounds not only prevent and control plant diseases but also have some

herbicidal activity. Compound **I** showed good inhibitory activity against *Sclerotinia sclerotiorum* on detached oilseed rape leaves [8], and compound **II** has excellent herbicidal activity against dicot weeds, such as *Zinnia elegans* Jacq. and *Abutilon theophrasti* Medicus (Figure 1) [9]. Therefore, in recent years, isoquinolinone derivatives have attracted considerable attention, and successful synthetic methods involving the isoquinolinone framework have been reported.

A number of appealing methods for the synthesis of isoquinolinone scaffolds using transition metal reagents, including cobalt [10], copper [11], rhodium [12-14], palladium [15-17], silver [18], and gold [19] catalysts, have been reported. However, compared to the widespread use of metal catalysts, the synthesis of isoquinolinone scaffolds mediated by environmentally friendly nonmetallic reagents as an attractive alternative is less developed. In 2014, Antonchick and Manna firstly reported the synthesis of a series of 3,4-diaryl-substituted isoquinolinone derivatives through oxidative annulation between alkynes and benzamide derivatives using iodobenzene as a catalyst and peracetic acid as a terminal oxidant [20]. Recently, Kočovský et al. disclosed a method employing 2-methylbenzamide and benzonitrile to yield 3-aryl-substituted isoquinolinone derivatives in the presence of *n*-butyllithium [21]. On the other hand, the intramolecular oxidative cyclization is also a viable option for the preparation of isoquinolinone derivatives. In 2020, two reports have been published on the conversion of alkyne-tethered *N*-alkoxybenzamides to isoquinolinones by intramolecular oxidative annulation, either electrochemically or using the hypervalent iodine reagent phenyliodine(III) diacetate (PIDA) [22,23]. And more recently, Du and our group have developed a method for the chemoselective cycloisomerization of *o*-alkenylbenzamides to 3-arylisoquinolinones, using PhIO as oxidant in combination with a catalytic amount of trimethylsilyl trifluoromethanesulfonate [24]. Although considerable progress has been made in the synthesis of isoquinolinone derivatives, there is still the need to develop chemoselective strategies based on easily adjustable factors, such as solvent selection to obtain 3- or 4-substituted isoquinolinone derivatives.

In 2018, our group has reported the zwitterionic water-soluble hypervalent iodine reagent (phenyliodonio)sulfamate (PISA). In water, PISA is strongly acidic, and the pH value can reach 2.05 in a saturated aqueous solution. With PISA, various indoles have been synthesized via C–H amination of 2-alkenylanilines involving an aryl migration–intramolecular cyclization cascade with excellent chemoselectivity in aqueous CH_3CN [25]. Herein, as part of our continuing studies of heterocyclic scaffold synthesis mediated by hypervalent iodine reagents, we present the solvent-dependent chemoselective synthesis of a series of isoquinolinones mediated by PISA using 2-alkenylbenzamide derivatives as substrates (Scheme 1).

Results and Discussion

We began by exploring the reaction of *N*-methoxy-2-(prop-1-en-2-yl)benzamide (**1a**) with PISA (1.5 equiv) in anhydrous acetonitrile at room temperature under argon atmosphere. 4-Methylisoquinolinone **2a** was the sole product in the reaction, with a yield of 86% in 20 minutes (Table 1, entry 1). Encouraged by this result, we added additives to the reaction with the aim of further increasing the chemical yield of **2a**. When 1.5 equivalents of water were added to the reaction, the yield of **2a** dropped to 79% (Table 1, entry 2). The reduced yield of **2a** indicated that this reaction could benefit from a dry solvent.

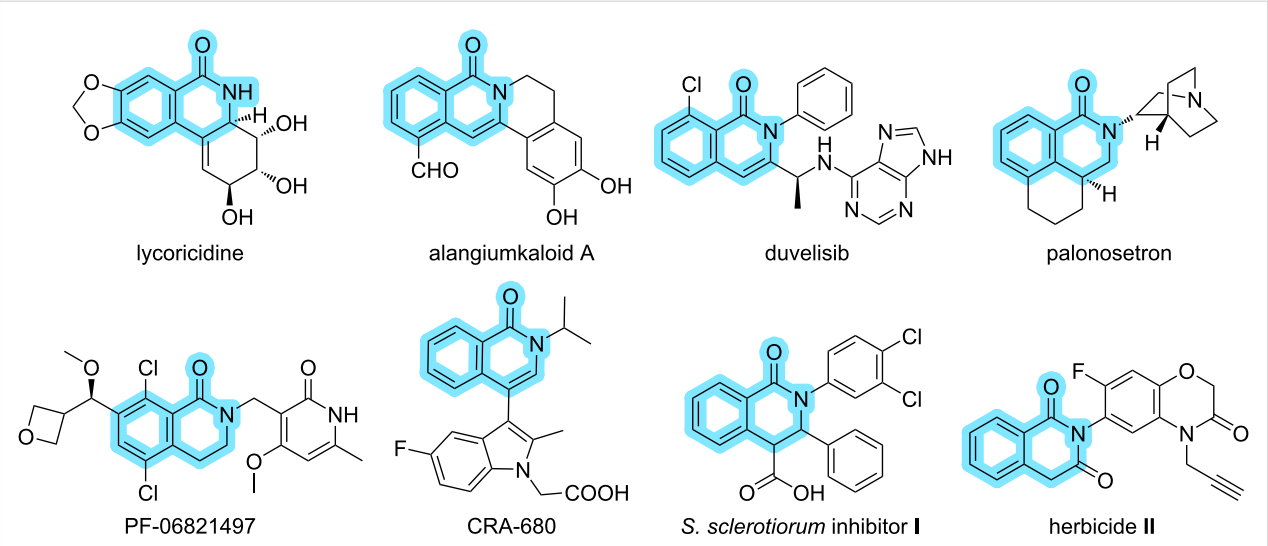

Figure 1: Selected natural products, pharmaceuticals, and biologically active compounds having an isoquinolinone scaffold.

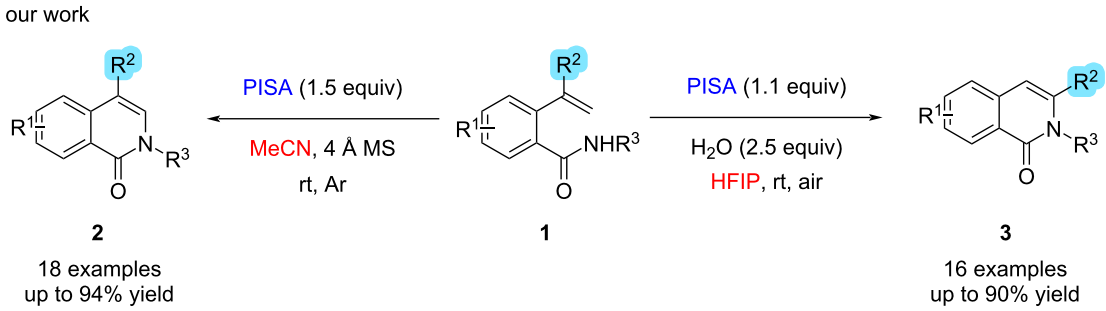

Scheme 1: Chemoselective and PISA-mediated, solvent-controlled synthesis of different isoquinolinone derivatives **2** and **3**.

Therefore, 4 Å molecular sieves or anhydrous sodium sulfate were added to the reaction mixture. When 4 Å molecular sieves were added, the yield of **2a** slightly increased to 88%, which was superior to using Na_2SO_4 (Table 1, entries 3 and 4). Next, different commercially available iodanes were employed as oxidants, such as PIDA, phenyliodine(III) bis(trifluoroacetate) (PIFA), *N*-tosyliminobenzyliodinane (PhINTs), iodosylbenzene (PhIO), and Koser's reagent (HTIB) (Table 1, entries 5–9). Of the reagents tested, PISA gave the best result. Furthermore, screening of different solvents showed that acetonitrile was superior for this reaction (Table S1, Supporting Information File 1). Based on the screening results, the optimized reaction conditions for the conversion of **1a** to the 4-subsitituted isoquinolinone **2a** were as follows: 1.5 equivalents of PISA and 4 Å MS in anhydrous CH_3CN (0.1 M of **2a**) under argon atmosphere at room temperature for 20 min.

With the optimal reaction conditions in hand, we explored the scope of the method by testing various 2-alkenylbenzamide derivatives **1** (Scheme 2). When R^1 was ethyl, isopropyl, cyclopropyl, phenyl, or hydrogen, respectively, the intramolecular amination smoothly gave the corresponding 4-substituted isoquinolinone products **2b**,**c**,**d**–**f** in 51–94% yield. Notably, when **1c** was used as the substrate, the cycloisomerization product **2c'** was observed in 31% yield besides **2c** in 51% yield. Additional experiments were then carried out using *N*-methoxy-2-(prop-1-en-2-yl)benzamide with different substituents R^2. Both electron-donating (methyl, alkoxy, dimethylamino) and electron-withdrawing substituents (fluoro, chloro, trifluoromethyl) were well tolerated on the phenyl ring and gave the desired products **2g**–**n** in 68–95% yield. Furthermore, a substrate containing a naphthalene moiety was also compatible with the reaction conditions, giving the corresponding ring-fused product **2o** in 40% yield. It is worth noting that when the *N*-substituent was phenyl, benzyloxy, or phenylamino, the reaction still proceeded well, and the corresponding products **2p**,**q**,**r** were obtained in 69%, 41%, and 40% yield, respectively.

Table 1: Optimization of the reaction conditions for the synthesis of 4-substituted isoquinolinone **2a**[a].

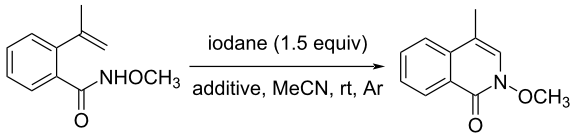

1a (0.2 mmol) **2a**

entry	iodane	additive	yield of **2a**, %[b]
1	PISA	—	86
2	PISA	H_2O (1.5 equiv)	79
3	**PISA**	**4 Å MS**	**88**
4	PISA	Na_2SO_4	81
5	PIDA	4 Å MS	52
6	PIFA	4 Å MS	77
7	PhINTs	4 Å MS	61
8	PhIO	4 Å MS	0
9	HTIB	4 Å MS	52

[a]Reactions were carried out using **1a** (0.2 mmol), hypervalent iodine reagent (1.5 equiv), and 4 Å MS (7.6 mg) in MeCN (2.0 mL) at room temperature under argon atmosphere. [b]Isolated yield.

Interestingly, when screening solvents for the synthesis of 4-methylisoquinolinones, we were surprised to discover that when hexafluoro-2-propanol (HFIP) was used as the solvent, 3-methylisoquinolinone **3a**, an isomer of **2a**, was formed in 51% yield. Apparently, the change of solvent resulted in a different chemoselectivity of the reaction. With this in mind, we investigated the reaction conditions (see Supporting Information File 1 for details) and obtained the optimal conditions for the synthesis of 3-methylisoquinolinone as follows: reacting 1.1 equivalents of PISA in HFIP (0.1 M of **1a**) containing 2.5 equivalents of H_2O at room temperature for 20 minutes (Scheme 3).

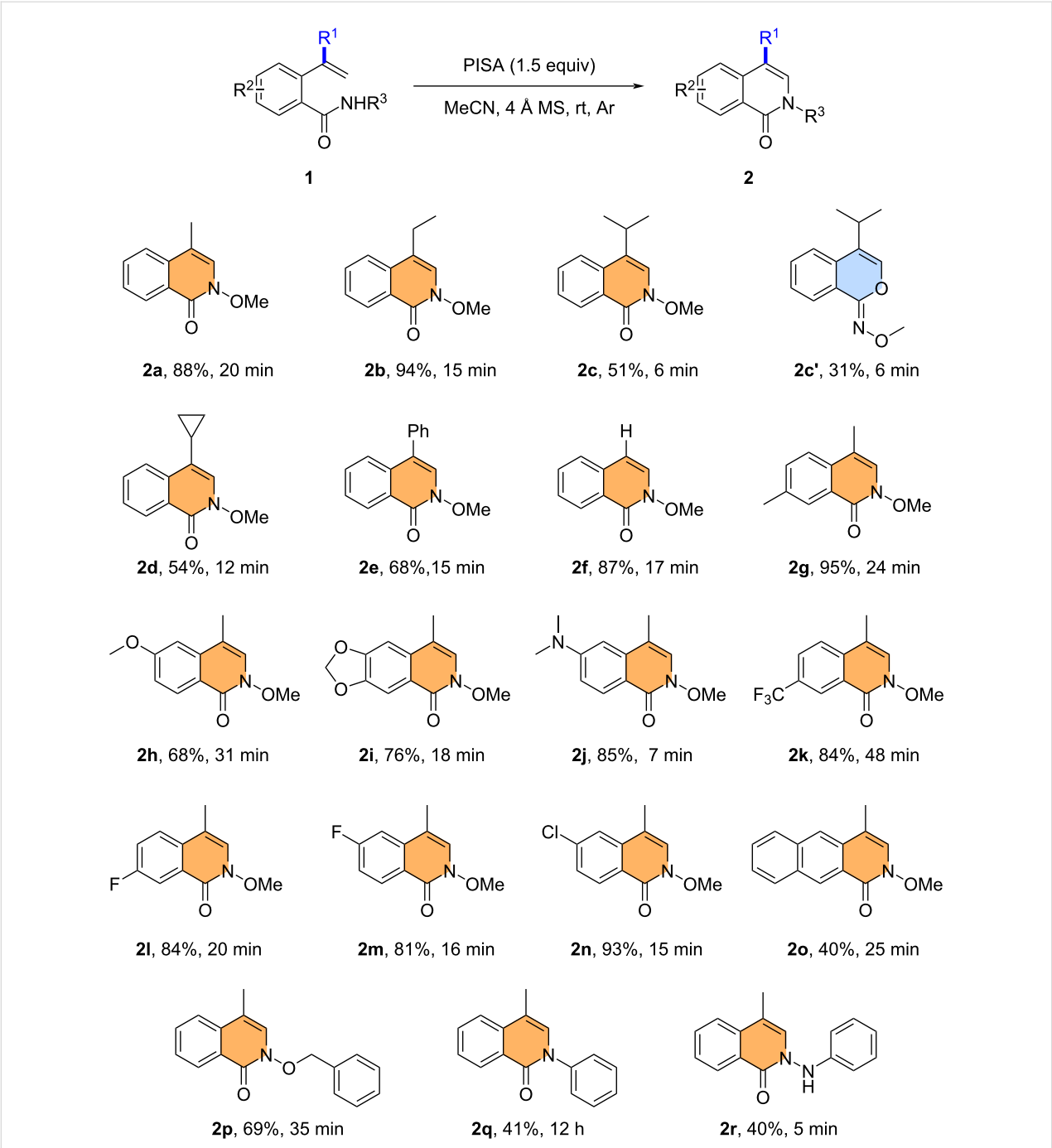

Scheme 2: Substrate scope for the synthesis of 4-substituted isoquinolinones **2**. Reaction conditions: **1** (0.3 mmol), PISA (1.5 equiv), and 4 Å MS (10 mg) in MeCN (3.0 mL).

The general applicability of PISA in wet HFIP solvent was studied. When R^1 was ethyl, isopropyl, cyclopropyl, or hydrogen, respectively, the substrates could be successfully converted to the products **3b**–**d** and **2f** in 52–87% yield with this method. In addition, a good or high yield of 3-methylisoquinolinones **3e**–**k**, with different substituents on the phenyl ring, was also obtained. It is worth noting that when an electron-withdrawing group (trifluoromethyl, fluoro, chloro) was located on the phenyl ring, various amounts of 4-substituted isoquinolinone derivatives **2k**,**m**,**n** were observed along with the formation of **3h**,**j**,**k**, respectively. Furthermore, a substrate containing a naphthalene unit was also compatible with the reaction conditions, leading to **3l**. In particular, the presence of diverse nitrogen protecting groups, such as benzyloxy, phenyl, and

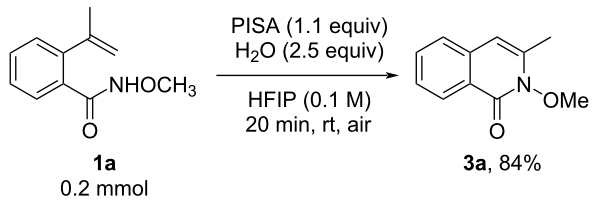

Scheme 3: Optimal reaction conditions for the synthesis of 3-substituted isoquinolinone **3a**.

alkyl, did not affect the smooth reaction, affording **3m–o** in a moderate yield of 32–64% (Scheme 4). Just by changing the solvent of the reaction, we were able to obtain the isomeric 3- or 4-substituted isoquinolinone derivatives with excellent chemoselectivity. These interesting findings led us to investigate the reaction mechanism.

To gain insight into the mechanism and chemoselectivity of the reactions above, we performed a control experiment. With acetonitrile as the solvent, a radical clock experiment was carried out with **1d** under the optimal reaction conditions, resulting in the formation of **2d** in 54% yield, and no cyclopropyl ring opening products were observed. This result suggested that no radical intermediates were generated during the reaction (Scheme 5).

According to the aforementioned control experiment and literature precedents, we proposed a mechanism for the formation of 4-substituted isoquinolinone derivatives, including **2a**. The reaction begins by tautomerization of **1a**, and PISA undergoes an electrophilic reaction with **1a'** to form the iodane intermediate **A**. The iodane **A** then undergoes a proton shift to provide intermediate **B**. Intermediate **B** collapses via reductive elimina-

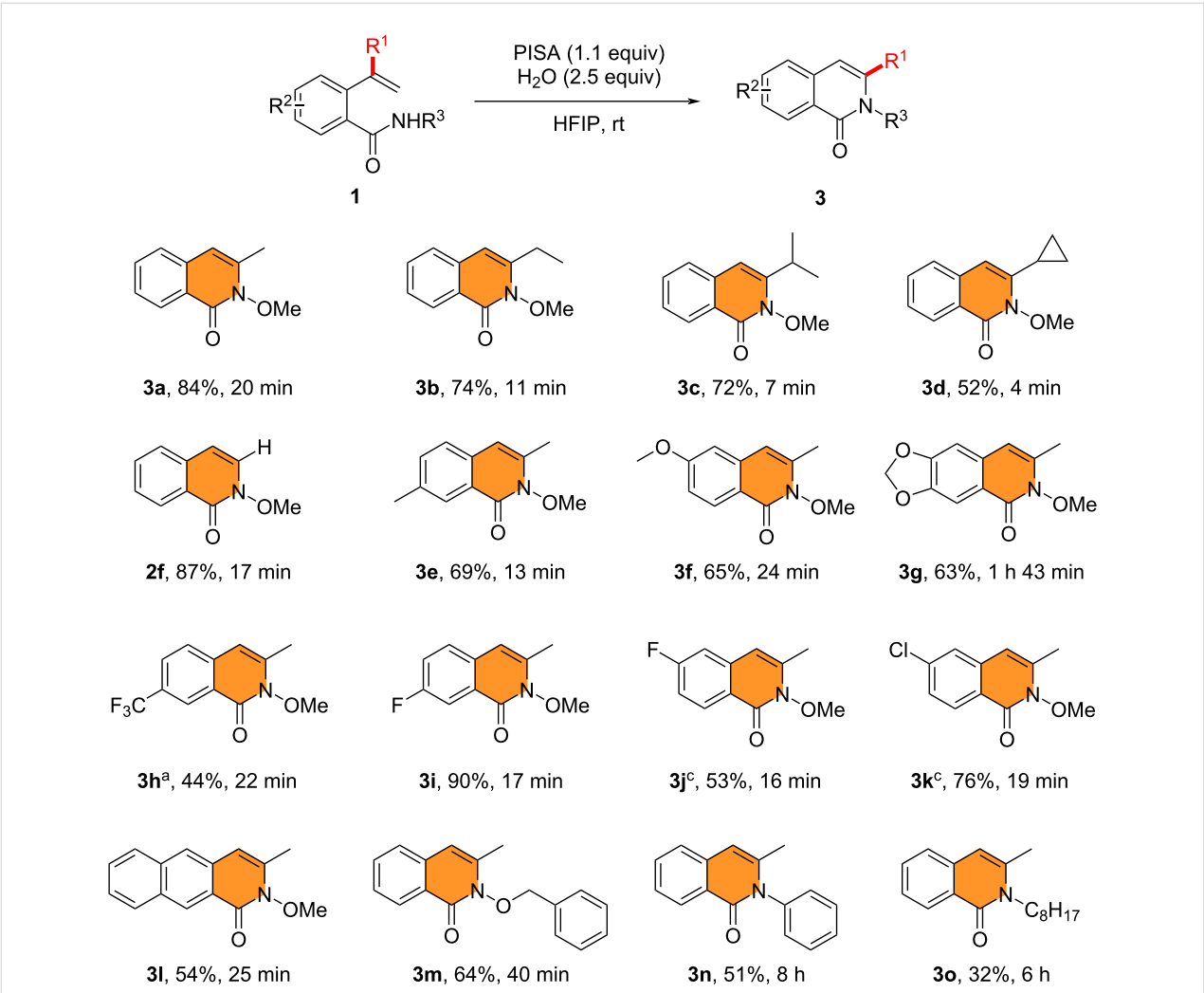

Scheme 4: Substrate scope for the synthesis of 3-substituted isoquinolinones **3**. Reaction conditions: **1** (0.3 mmol), PISA (1.1 equiv), and H_2O (2.5 equiv) in HFIP (3.0 mL) at room temperature. Isolated yield is stated. [a]The yield of **2k** was 56%. [b]The yield of **2m** was 24%. [c]The yield of **2n** was 11%.

Scheme 5: Control experiment to test for radical intermediates.

tion to give nitrenium ion **C**, along with the release of iodobenzene and sulfamate. Finally, nucleophilic attack of the olefin moiety of **C** on the electrophilic nitrogen atom, followed by the deprotonation with sulfamate, gives the 4-substituted isoquinolinone derivative **2a** (Scheme 6).

Looking into the formation of **2c'** from **1c** (Scheme 2), two other resonance structures for the initially formed intermediate **1CC**, namely **1CC'** and **1CC''**, are shown in Scheme 7. The oxygen atom in the amide motif of the substrate **1c** may act as an electrophilic center, forming a C–O bond with the alkenyl group to give the isochromen-1-one oxime product **2c'**.

When wet HFIP was used as the solvent, the reaction followed a different pathway. HFIP, a strong hydrogen bonding donor [26-28], interacts with the amide moiety of the substrate, and thus preventing the possible interaction between the amide moiety and PISA, as opposed to CH_3CN. The olefin moiety of the complex then interacts with the exposed central iodine(III) atom in PISA [25], forming the intermediate **D**. Similar cyclic iodonium intermediates were also postulated for the synthesis of

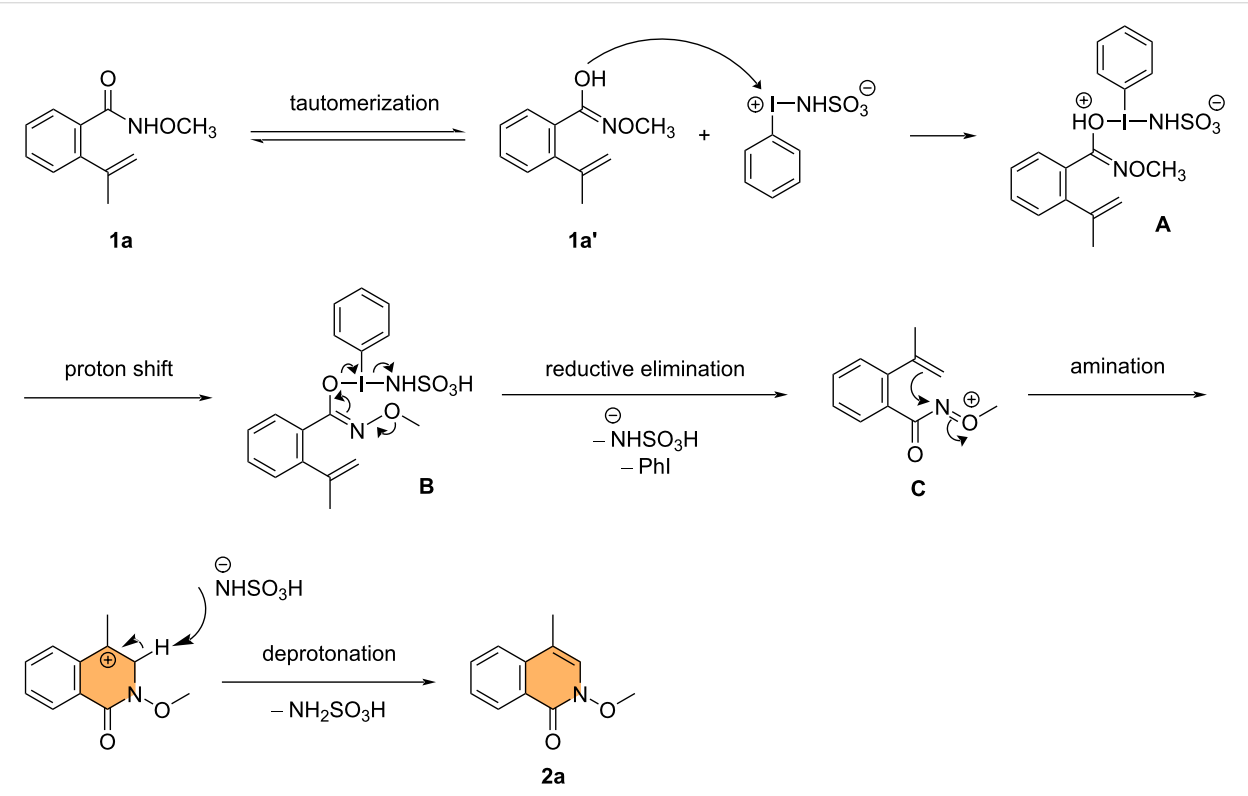

Scheme 6: Proposed mechanism for the reaction between **1a** and PISA in anhydrous acetonitrile.

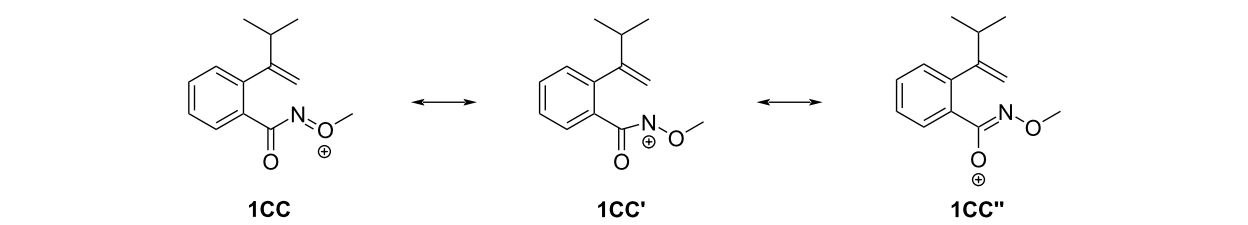

Scheme 7: Two other resonance structures of the intermediate **1CC**.

benzofuran derivatives from styrene derivatives by iodane reagents [29,30]. Subsequently, intermediate **D** is attacked by H_2O at the benzylic carbon atom to afford intermediate **E**. Intramolecular proton shift occurs, generating the intermediate **F**, which undergoes phenyl migration and reductive elimination, along with the release of iodobenzene and sulfamic acid. Cyclization of protonated **G** takes place to afford the intermediate **H**. Finally, release of water and β-proton elimination produces the rearranged product **3a** (Scheme 8).

Conclusion

In summary, we reported the efficient synthesis of isoquinolinone derivatives using a PISA-mediated methodology that chemoselectively yielded 3- or 4-substituted isoquinolinone derivatives by simply adjusting the solvent. When acetonitrile was used, the 4-substituted isoquinolinone derivatives were the reaction products, whereas hexafluoro-2-propanol led to 3-substituted isoquinolinones. The solvent-dependent chemoselective synthesis of isoquinolinone derivatives is interesting and unprecedented. Further research on synthetic utility of PISA, a unique zwitterionic hypervalent iodine(III) reagent, is underway in our laboratory.

Supporting Information

Supporting Information File 1

Experimental details, optimization studies, compound characterization data, and spectra.
[https://www.beilstein-journals.org/bjoc/content/supplementary/1860-5397-20-167-S1.pdf]

Funding

This work was financially supported by the National Natural Science Foundation of China (numbers 22071116 and 21772096).

Author Contributions

Ze-Nan Hu: investigation; writing – original draft. Yan-Hui Wang: investigation; writing – original draft. Jia-Bing Wu: investigation. Ze Chen: investigation. Dou Hong: investigation. Chi Zhang: conceptualization; funding acquisition; project administration; resources; supervision; visualization; writing – original draft.

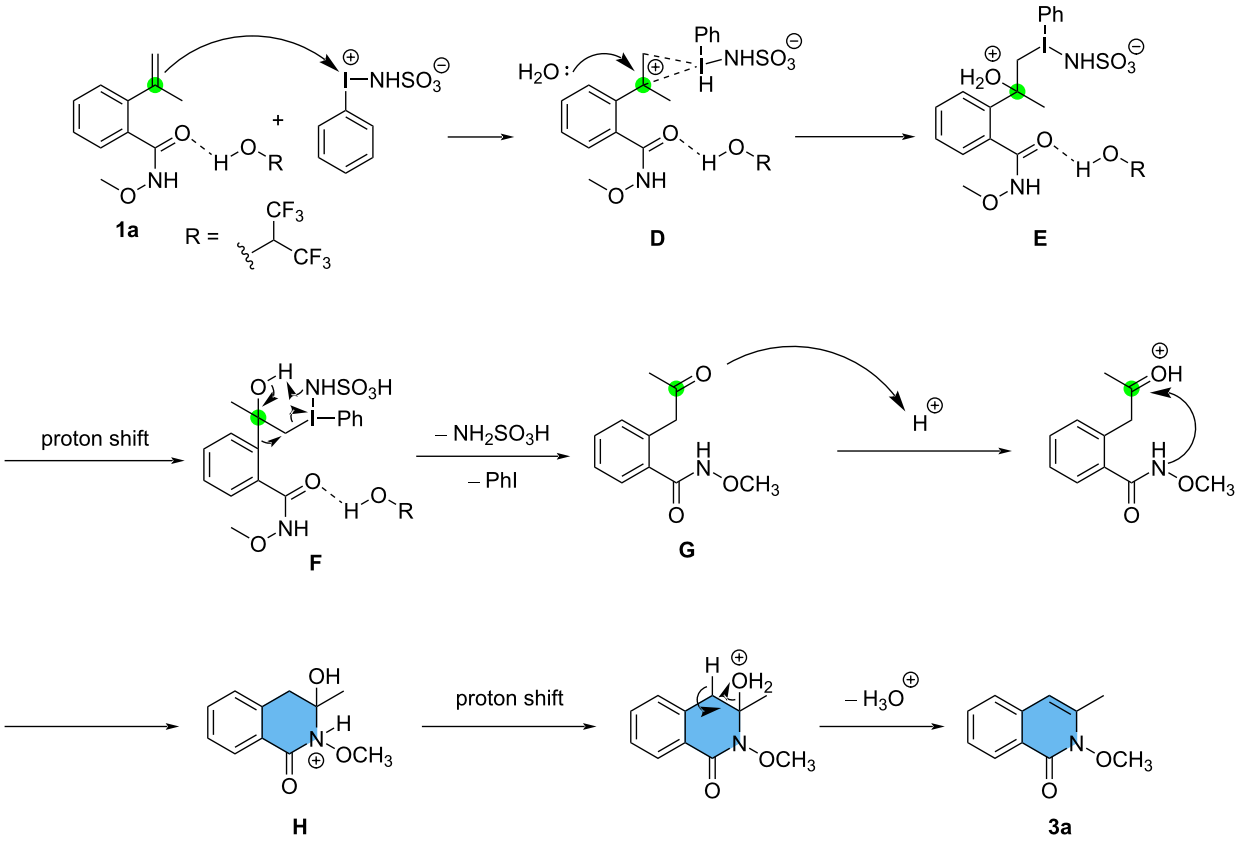

Scheme 8: Proposed mechanism for the reaction between **1a** and PISA in wet HFIP.

ORCID® iDs

Dou Hong - https://orcid.org/0000-0002-1431-5068
Chi Zhang - https://orcid.org/0000-0001-9050-076X

Data Availability Statement

All data that supports the findings of this study is available in the published article and/or the supporting information to this article.

References

1. Rao, L. B.; Sreenivasulu, C.; Kishore, D. R.; Satyanarayana, G. *Tetrahedron* **2022,** *127,* 133093. doi:10.1016/j.tet.2022.133093
2. Asseri, A. H.; Alam, M. J.; Alzahrani, F.; Khames, A.; Pathan, M. T.; Abourehab, M. A. S.; Hosawi, S.; Ahmed, R.; Sultana, S. A.; Alam, N. F.; Alam, N.-U.; Alam, R.; Samad, A.; Pokhrel, S.; Kim, J. K.; Ahammad, F.; Kim, B.; Tan, S. C. *Pharmaceuticals* **2022,** *15,* 501. doi:10.3390/ph15050501
3. Nishiyama, T.; Hironaka, M.; Taketomi, M.; Taguchi, E.; Kotouge, R.; Shigemori, Y.; Hatae, N.; Ishikura, M.; Choshi, T. *Eur. J. Org. Chem.* **2018,** 673–678. doi:10.1002/ejoc.201701557
4. Blair, H. A. *Drugs* **2018,** *78,* 1847–1853. doi:10.1007/s40265-018-1013-4
5. Gao, A.; Guan, S.; Sun, Y.; Wang, L.; Meng, F.; Liu, X.; Gu, L.; Li, G.; Zhong, D.; Zhang, L. *BMC Cancer* **2023,** *23,* 609. doi:10.1186/s12885-023-11070-3
6. Kung, P.-P.; Bingham, P.; Brooun, A.; Collins, M.; Deng, Y.-L.; Dinh, D.; Fan, C.; Gajiwala, K. S.; Grantner, R.; Gukasyan, H. J.; Hu, W.; Huang, B.; Kania, R.; Kephart, S. E.; Krivacic, C.; Kumpf, R. A.; Khamphavong, P.; Kraus, M.; Liu, W.; Maegley, K. A.; Nguyen, L.; Ren, S.; Richter, D.; Rollins, R. A.; Sach, N.; Sharma, S.; Sherrill, J.; Spangler, J.; Stewart, A. E.; Sutton, S.; Uryu, S.; Verhelle, D.; Wang, H.; Wang, S.; Wythes, M.; Xin, S.; Yamazaki, S.; Zhu, H.; Zhu, J.; Zehnder, L.; Edwards, M. *J. Med. Chem.* **2018,** *61,* 650–665. doi:10.1021/acs.jmedchem.7b01375
7. Kaila, N.; Follows, B.; Leung, L.; Thomason, J.; Huang, A.; Moretto, A.; Janz, K.; Lowe, M.; Mansour, T. S.; Hubeau, C.; Page, K.; Morgan, P.; Fish, S.; Xu, X.; Williams, C.; Saiah, E. *J. Med. Chem.* **2014,** *57,* 1299–1322. doi:10.1021/jm401509e
8. Li, M.; Yuan, C.; Fang, Y.; Zhang, Z.; Wang, D. *Chin. J. Pestic. Sci.* **2023,** *25,* 62–72. doi:10.16801/j.issn.1008-7303.2022.0102
9. Li, B.; Wu, H.; Cui, D.; Yu, H.; Xu, J.; Yang, H. Isoquinolinone compounds and their applications. Chin. Patent CN1687061, Oct 26, 2005.
10. Li, X.; Huang, T.; Song, Y.; Qi, Y.; Li, L.; Li, Y.; Xiao, Q.; Zhang, Y. *Org. Lett.* **2020,** *22,* 5925–5930. doi:10.1021/acs.orglett.0c02016
11. Zhao, S.; Gong, X.; Gan, Z.; Yan, Q.; Liu, X.; Yang, D. *Chin. J. Org. Chem.* **2021,** *41,* 258–266. doi:10.6023/cjoc202008045
12. Bian, M.; Mawjuda, H.; Gao, H.; Xu, H.; Zhou, Z.; Yi, W. *Org. Lett.* **2020,** *22,* 9677–9682. doi:10.1021/acs.orglett.0c03734
13. Mochida, S.; Umeda, N.; Hirano, K.; Satoh, T.; Miura, M. *Chem. Lett.* **2010,** *39,* 744–746. doi:10.1246/cl.2010.744
14. Huang, J.-R.; Bolm, C. *Angew. Chem., Int. Ed.* **2017,** *56,* 15921–15925. doi:10.1002/anie.201710776
15. Zhong, R.; Xu, Y.; Sun, M.; Wang, Y. *J. Org. Chem.* **2021,** *86,* 5255–5264. doi:10.1021/acs.joc.1c00150
16. Zhong, H.; Yang, D.; Wang, S.; Huang, J. *Chem. Commun.* **2012,** *48,* 3236–3238. doi:10.1039/c2cc17859a
17. Zheng, Z.; Alper, H. *Org. Lett.* **2008,** *10,* 4903–4906. doi:10.1021/ol801991m
18. Dell'Acqua, M.; Castano, B.; Cecchini, C.; Pedrazzini, T.; Pirovano, V.; Rossi, E.; Caselli, A.; Abbiati, G. *J. Org. Chem.* **2014,** *79,* 3494–3505. doi:10.1021/jo5002559
19. Wang, A.; Xie, X.; Zhang, C.; Liu, Y. *Chem. Commun.* **2020,** *56,* 15581–15584. doi:10.1039/d0cc06875f
20. Manna, S.; Antonchick, A. P. *Angew. Chem., Int. Ed.* **2014,** *53,* 7324–7327. doi:10.1002/anie.201404222
21. Matouš, P.; Májek, M.; Kysilka, O.; Kuneš, J.; Maříková, J.; Růžička, A.; Pour, M.; Kočovský, P. *J. Org. Chem.* **2021,** *86,* 8078–8088. doi:10.1021/acs.joc.1c00561
22. Zhang, L.-B.; Geng, R.-S.; Wang, Z.-C.; Ren, G.-Y.; Wen, L.-R.; Li, M. *Green Chem.* **2020,** *22,* 16–21. doi:10.1039/c9gc03290h
23. Wen, L.-R.; Ren, G.-Y.; Geng, R.-S.; Zhang, L.-B.; Li, M. *Org. Biomol. Chem.* **2020,** *18,* 225–229. doi:10.1039/c9ob02430a
24. He, J.; Du, F.-H.; Zhang, C.; Du, Y. *Commun. Chem.* **2023,** *6,* 126. doi:10.1038/s42004-023-00930-5
25. Xia, H.-D.; Zhang, Y.-D.; Wang, Y.-H.; Zhang, C. *Org. Lett.* **2018,** *20,* 4052–4056. doi:10.1021/acs.orglett.8b01615
26. An, X.-D.; Xiao, J. *Chem. Rec.* **2020,** *20,* 142–161. doi:10.1002/tcr.201900020
27. Tian, F.-X.; Qu, J. *J. Org. Chem.* **2022,** *87,* 1814–1829. doi:10.1021/acs.joc.1c02361
28. Cheng, Y.-X.; Yang, X.-G.; Du, F.-H.; Zhang, C. *Green Chem.* **2024,** *26,* 5914–5920. doi:10.1039/d4gc00622d
29. Mangaonkar, S. R.; Shetgaonkar, S. E.; Vernekar, A. A.; Singh, F. V. *ChemistrySelect* **2020,** *5,* 10754–10758. doi:10.1002/slct.202002860
30. Singh, F. V.; Mangaonkar, S. R. *Synthesis* **2018,** *50,* 4940–4948. doi:10.1055/s-0037-1610650

License and Terms

BEILSTEIN JOURNAL OF ORGANIC CHEMISTRY

Hydrogen-bond activation enables aziridination of unactivated olefins with simple iminoiodinanes

Phong Thai, Lauv Patel, Diyasha Manna and David C. Powers*

Full Research Paper

Open Access

Address:
Department of Chemistry, Texas A&M University, College Station TX, 77843, USA

Email:
David C. Powers* - powers@chem.tamu.edu

* Corresponding author

Keywords:
aziridination; electrochemistry; H-bond activation; hypervalent iodine; nitrene transfer

Beilstein J. Org. Chem. **2024,** *20,* 2305–2312.
https://doi.org/10.3762/bjoc.20.197

Received: 23 May 2024
Accepted: 05 September 2024
Published: 11 September 2024

This article is part of the thematic issue "Hypervalent halogen chemistry".

Guest Editor: T. Gulder

Abstract

Iminoiodinanes comprise a class of hypervalent iodine reagents that is often encountered in nitrogen-group transfer (NGT) catalysis. In general, transition metal catalysts are required to effect efficient NGT to unactivated olefins because iminoiodinanes are insufficiently electrophilic to engage in direct aziridination chemistry. Here, we demonstrate that 1,1,1,3,3,3-hexafluoroisopropanol (HFIP) activates *N*-arylsulfonamide-derived iminoiodinanes for the metal-free aziridination of unactivated olefins. ^{1}H NMR and cyclic voltammetry (CV) studies indicate that hydrogen-bonding between HFIP and the iminoiodinane generates an oxidant capable of direct NGT to unactivated olefins. Stereochemical scrambling during aziridination of 1,2-disubstituted olefins is observed and interpreted as evidence that aziridination proceeds via a carbocation intermediate that subsequently cyclizes. These results demonstrate a simple method for activating iminoiodinane reagents, provide analysis of the extent of activation achieved by H-bonding, and indicate the potential for chemical non-innocence of fluorinated alcohol solvents in NGT catalysis.

Introduction

Hypervalent iodine reagents find widespread application in selective oxidation chemistry due to the combination of synthetically tunable iodine-centered electrophilicity and the diversity of substrate functionalization mechanisms that can be accessed [1,2]. Large families of iodine(III)- and iodine(V)-based reagents have been developed – including iodobenzene diacetate ($PhI(OAc)_2$, PIDA), Koser's reagent (PhI(OH)OTs), Zhdankin's reagent ($C_6H_4(o\text{-}COO)IN_3$, ABX), and Dess–Martin periodinane (DMP) – and find application in an array of synthetically important transformations including olefin difunctionalization, carbonyl desaturation, alcohol oxidation, and C–H functionalization [3,4]. Iminoiodinanes (ArI=NR) are a subclass of hypervalent iodine reagents that function as nitrene equivalents in synthesis [5,6]. The direct reaction of iminoiodinanes with olefins, which could be envisioned to give rise to aziridines directly, is typically not observed and thus

families of transition metal catalysts or photochemical procedures have been developed to enable this transformation [7-9].

The reactivity of hypervalent iodine reagents can be enhanced via Lewis acid catalysis [10]. For example, PIDA becomes a stronger oxidant upon coordination of $BF_3{\cdot}OEt_2$, enabling chemistry that was not available in the absence of Lewis acid activation (Scheme 1a) [11,12]. A variety of Lewis acid activators have been reported [13-22] in an array of group-transfer reactions, including trifluoromethylation, cyanation, and fluorination. Brønsted acid activation has also been described in some group-transfer schemes [23-25], and in particular, fluorinated alcohol solvents, such as 1,1,1,3,3,3-hexafluoroisopropanol (HFIP), have been reported to enhance hypervalent iodine reactivity by providing a H-bonding solvent cluster that enhances the electrophilicity of the iodine center [26,27]. Despite the prevalence of acid-activation in promoting carbon [28], oxygen [29,30], sulfur [31], chlorine [32], and fluorine [33] transfer reactions of hypervalent iodine compounds, these strategies have not been applied to activation of iminoiodinanes for nitrene transfer chemistry.

We recently developed a metal-free aziridination of unactivated olefins via the intermediacy of an *N*-pyridinium iminoiodinane (Scheme 1b) [34]. We rationalized the enhanced reactivity towards olefin aziridination as a result of charge-enhanced iodine-centered electrophilicity arising from the cationic *N*-pyridinium substituent. Based on those observations, we reasoned that similarly enhanced reactivity might be accessed by Lewis acid or H-bond activated iminoiodinanes. Here, we describe the HFIP-promoted aziridination of unactivated olefins with *N*-sulfonyl iminoiodinane reagents, which are among the most frequently encountered iminoiodinanes in NGT catalysis (Scheme 1c). This simple procedure afforded the formal transfer of various nitrogen groups, including those derived from complex amines, and is complementary to other metal-free aziridinations of unactivated olefins [35-39].

Results and Discussion

Treatment of cyclohexene (**1a**) with a stoichiometric amount of simple iminoiodinane such as PhINTs (**2a**) in CH_2Cl_2 resulted in <10% conversion to the corresponding *N*-sulfonylaziridine **3a**, which is consistent with the previously reported need for transition metal catalysts to promote nitrene transfer catalysis (Table 1, entry 1) [40,41]. In contrast, combination of PhINTs (2.0 equiv) with **1a** in HFIP afforded **3a** in 67% NMR yield (Table 1, entry 2). Lowering the loading of iminoiodinane **2a** to 1.5 or 1.0 equivalents decreased the reaction yield to 28% and 22%, respectively (Table 1, entries 3 and 4). Increasing the reaction temperature negatively affected the efficiency of azirid-

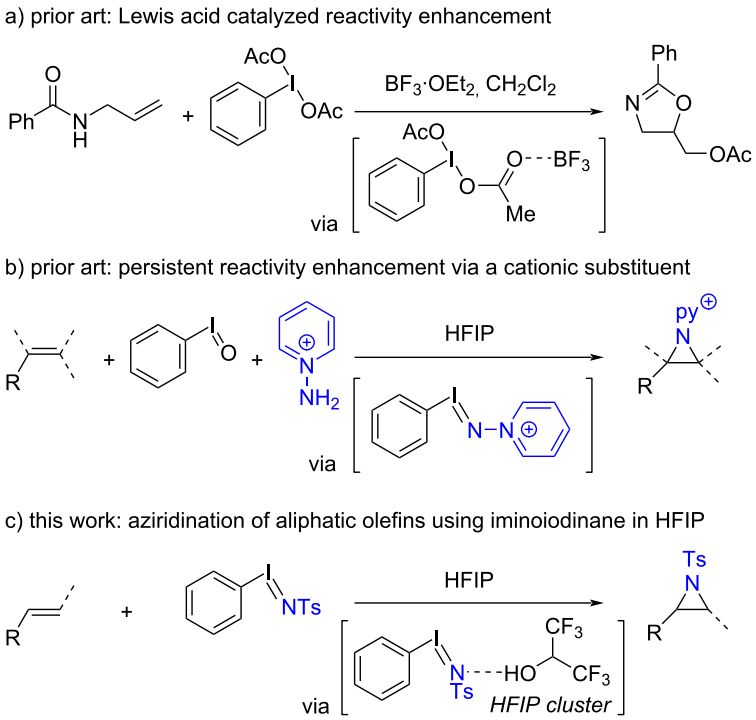

Scheme 1: a) Lewis acid activation of hypervalent iodine reagents can enhance the reactivity of these reagents. b) Charge-tagged iminoiodinanes display enhanced reactivity in aziridination reactions with unactivated olefins (ref. [34]). c) Here, we demonstrate that H-bonding between fluorinated alcohol solvents and iminoiodinanes can enable direct metal-free aziridination of unactivated olefins with simple iminoiodinanes.

Table 1: Optimization of HFIP-promoted aziridination of cyclohexene (**1a**). Conditions: 0.20 mmol **1a**, 0.40 mmol PhINTs **2a**, 1.0 mL HFIP, N_2 atmosphere, 20 °C, 16 h. Yield was determined via ^{1}H NMR using triethyl 1,3,5-benzenetricarboxylate as internal standard.

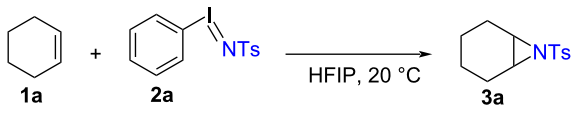

1a + 2a → 3a

Entry	Deviation from standard conditions	Yield (%)
1	CH_2Cl_2	<10%
2	none	67
3	1.5 equiv PhINTs	28
4	1.0 equiv PhINTs	22
5	30 °C	50
6	50 °C	43
7	TFE	16
8	10 equiv HFIP in CH_2Cl_2	38
9	5 equiv $BF_3{\cdot}Et_2O$, TfOH, or $Zn(OTf)_2$ in CH_2Cl_2,	0
10	1 equiv **4** and 1 equiv **5** instead of **2a**	19
11	1 equiv **4** and 2 equiv **5** instead of **2a**	27
12	no ambient light	64

ination: Reactions performed at 30 or 50 °C afforded **3a** in 50% and 43% yield, respectively (Table 1, entries 5 and 6). Replacing HFIP with 2,2,2-trifluoroethanol (TFE), which is also a commonly encountered fluorinated alcohol solvent, resulted in a 16% yield of **3a** (Table 1, entry 7). Performing aziridination with 10 equivalents of HFIP in CH_2Cl_2 resulted in a 38% yield (Table 1, entry 8). The aziridine product **3a** was not observed when other Lewis or Brønsted acids, such as $BF_3{\cdot}Et_2O$, TfOH, or $Zn(OTf)_2$, were employed in CH_2Cl_2 (Table 1, entry 9). Attempts to generate **2a** in situ using 1 equivalent of $TsNH_2$ (**4**) in combination with 1 or 2 equivalents of PhIO (**5**) resulted in aziridination yields of 19% and 27%, respectively (Table 1, entries 10 and 11). Finally, exclusion of ambient light had no impact of the aziridination of **1a** with PhINTs (Table 1, entry 12) [42,43].

With metal-free aziridination conditions in hand, we explored the scope and limitations of the HFIP-promoted aziridination of unactivated olefins (Scheme 2). For cyclic substrates, aziridination of cyclopentene, cyclohexene, and cycloheptene afforded the corresponding aziridines in modest to high isolated yields: **3b** (80%), **3a** (46%), and **3c** (36%), respectively. Acyclic olefin 1-hexene underwent aziridination to **3d** in 79% yield (reaction performed at 50 °C); aziridination of vinylcyclohexane proceeded in 67% yield of **3e**. Allylbenzene engaged in aziridination to deliver **3f** in 53% yield, while homoallylbenzene and pent-4-en-1-ylbenzene underwent aziridination in yields of 54% (**3g**) and 26% (**3h**), respectively. The procedure was compatible with various commonly encountered functional groups, such as chloride (**3i**), bromide (**3j**), and benzoyl (**3k**). Noticeably, an unprotected alcohol is tolerated in our procedure, with product **3l** delivered at 50% NMR yield; **3l** is sensitive to column chromatography, and thus aziridine-opening to a cyclic ether was observed (31% isolated yield) during purification. Aziridination of *cis*- or *trans*-4-octene afforded aziridine **3m** as a 1.3:1.0 *trans*/*cis* mixture in 72% and 64% yield, respectively. While many styrene derivatives polymerize in HFIP [44], 1,2-disubstituted styrene derivatives were sufficiently stable to engage in the developed aziridination reaction, with *cis*- or *trans*-β-methylstyrene **1n** furnishing aziridine **3n** as diastereomeric mixtures with comparable yields of 38% (1.0:2.0 *trans*/*cis*, from *cis*-**1n**) and 35% (1.7:1.0 *trans*/*cis*, from *trans*-**1n**). Olefins containing *N*-heteroaromatics such as phthalimide and pyridine underwent aziridination to give **3o** (32% yield) and **3p** (26% yield). Similarly, 1,4-cyclohexadiene was compatible in this procedure, giving product **3q** in 21% yield (see Supporting Information File 1, Figure S1 for other challenging substrates). Finally, ibuprofen-derived olefin **1r** underwent aziridination to afford **3r** in 31% yield. Overall, these results highlight the efficacy of a simple activation protocol and the generality of H-bond activation of iminoiodinanes for direct aziridination, albeit with modest efficiency for some substrates.

The impact of the iminoiodinane structure on the efficiency of HFIP-promoted direct aziridination was next investigated (Scheme 3). For this purpose, cyclopentene was selected as it underwent efficient aziridination with PhINTs. A family of iminoiodinanes **2** was synthesized from PIDA and the corresponding sulfonamide derivative. Reaction of phenylsulfonamide-derived iminoiodinane with cyclopentene afforded *N*-phenylsulfonylaziridine **6b** in 45% yield, while *N*-(*p*-trifluoromethylsulfonyl)aziridine **6c** was furnished in 47% yield. Similarly, 2,6-difluorosulfonyl-substituted iminoiodinane **2d** afforded aziridine **6d** in 52% yield. The aziridination procedure was tolerant of heterocyclic substituents on the iminoiodinane, *N*-(5-methylpyridin-2-ylsulfonyl)aziridine **6e** could be obtained in 46% yield. The *N*-Tces group (Tces = trichloroethylsulfamate) could also be transferred to afford **6f** in 39% yield. Finally, the iminoiodinane derived from celecoxib (**2i**) could be used to transfer this drug moiety to furnish aziridine **6i** in 46% yield. In general, the efficiency of aziridination correlates with the stability of the relevant iminoiodinane reagent, with higher yields attributed to more electron-rich sulfonamide substitution such as **2a**. Relatively electron-deficient iminoiodinanes are less efficient but are also more prone to decomposition (see Supporting Information File 1, Figure S2 for challenging iminoiodinanes). In situ preparation of the iminoiodinane intermediates is possible, and for those reagents that undergo facile decomposi-

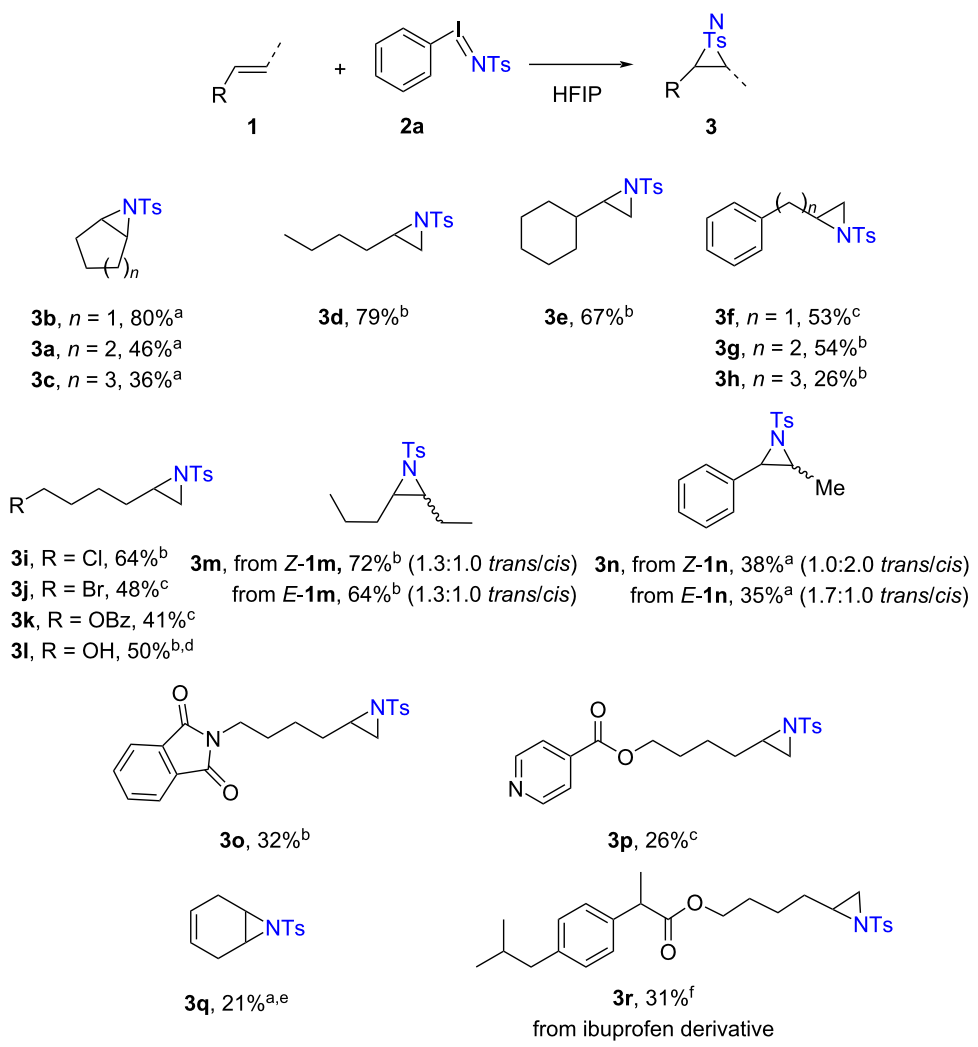

Scheme 2: Scope and limitations of HFIP-promoted direct aziridination with iminoiodinane reagents. Conditions: 0.20 mmol **1**, 0.40 mmol **2a**, 1.0 mL HFIP, N_2 atmosphere. a) 20 °C for 16 h, b) 50 °C for 16 h, c) 50 °C for 48 h, d) NMR yield, e) 1.2 equiv PhINTs was used, and f) 4.0 equiv of PhINTs at 20 °C for 48 h.

tion, aziridination is more efficient using these conditions (yields for in situ-generated iminoiodinanes are in parentheses in Scheme 3, with *N*-*o*-methyl (**6g**) and *N*-*p*-methoxysulfonyl (**6h**) aziridines obtained each in 22% yield; the drug topiramate could also be transferred to furnish aziridine **6j** in 11% yield).

We carried out a series of experiments to clarify the origin of the observed reactivity enhancement of *N*-arylsulfonyliminoiodinanes in the presence of HFIP (Scheme 4). First, ^{1}H NMR was employed to examine the interaction between HFIP and iminoiodinane **2c** in CD_3CN (compound **2c** was chosen over **2a** due to its increased solubility in nonprotic solvents). In a sample of **2c** with 4 equivalents of HFIP, a broad signal for O–H proton of HFIP was observed at 5.52 ppm with a FWHM = 56.6 Hz (Scheme 4a). This resonance was broader and more downfield than that of free HFIP in CD_3CN (5.41 ppm with FWHM = 5.0 Hz), suggesting a hydrogen bonding interaction between HFIP and **2c**, and similar observations were also reported for the hydrogen bonding between HFIP and PIDA [30,33]. During this experiment, a small amount of hydrolysis product 4-(trifluoromethyl)benzenesulfonamide was also observed (1.2 mM, signals at 8.0, 7.9, and 5.86 ppm), but this compound did not greatly contribute to the broadening of O–H proton signal of HFIP as a separate 4.0 mM sample of the sulfonamide resulted in O–H proton signal of HFIP being at 5.64 ppm with FWHM = 11.3 Hz. Second, to evaluate the impact of HFIP on the redox chemistry of PhINTs, we collected cyclic voltammograms (CVs) of iminoiodinane **2c** in MeCN in the presence of varying HFIP increments (Scheme 4b). The CV of 25 µL HFIP in MeCN showed no electrochemical events between −2.0–0 V. The CV of **2c** in the absence of HFIP showed a reductive current (i_p = −0.80 mA) at peak potential (E_{pr}) of

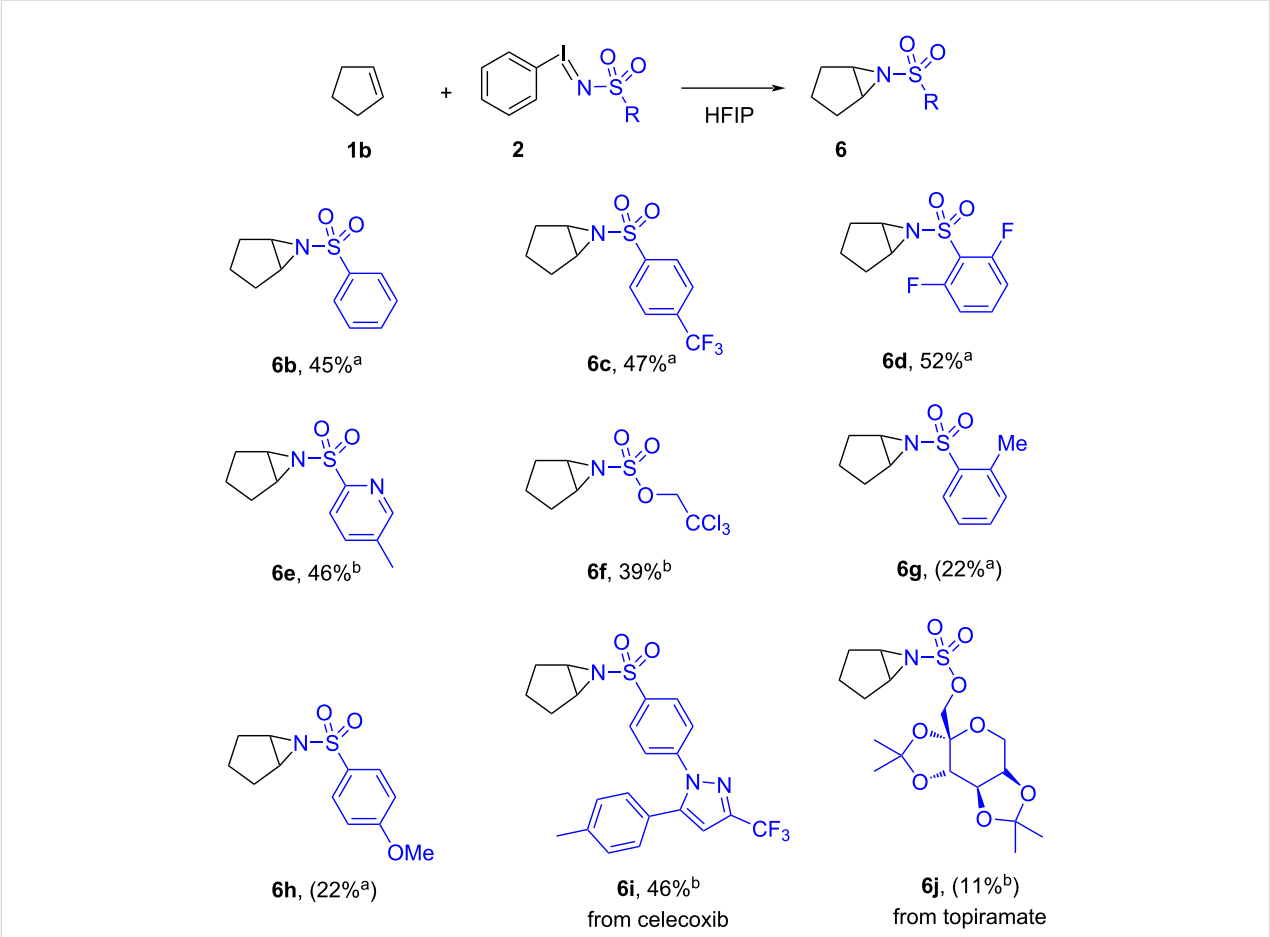

Scheme 3: Scope of nitrogen group transfer in the aziridination of aliphatic olefins. Conditions using synthesized iminoiodinane: 0.20 mmol cyclopentene (**1b**), 0.40 mmol iminoiodinane **2**, 1.0 mL HFIP, N_2 atmosphere. Conditions using in situ-generated iminoiodinane: 0.20 mmol cyclopentene (**1b**), 0.20 mmol sulfonamide, 0.40 mmol iodosylbenzene (PhIO), 1.0 mL HFIP, N_2 atmosphere. a) 20 °C for 16 h, b) 40 °C for 16 h.

–1.72 V vs Fc^+/Fc. Upon addition of 5.0 µL of HFIP (1.2 equiv with respect to **2c**), the current increased to −1.22 mA, signaling the binding of HFIP to **2c** enhanced the electron transfer kinetics between the hypervalent iodine reagent and the electrode [45]. Further additions of HFIP further increased the current response and shifted the peak potential, with 10 µL and 15 µL of HFIP showing responses with E_{pr} at −1.55 V and −1.52 V, respectively. The titration showed a saturation point at 25 µL of HFIP (6.0 equiv with respect to **2c**), at which the CV of **2c** showed an E_{pr} = –1.47 V and –1.52 mA current. Overall, the addition of HFIP results in a 250 mV shift in the reduction of **2c**. The increased facility of reduction is consistent with H-bonding between HFIP and **2c**, which results in a more potent oxidant and gives rise to the observed HFIP-promoted olefin aziridination chemistry.

A number of observations are relevant to the mechanism by which unactivated olefin aziridination is accomplished by the HFIP-activated iminoiodinanes: First, the reaction of PhINTs with either *cis*- or *trans*-β-methylstyrene (**1n**) in HFIP afforded aziridine **3n** as a mixture of 2.0:1.0 *cis*/*trans* (from *cis*-**1n**) and 1.0:1.7 *cis*/*trans* (from *trans*-**1n**) (Scheme 4c). The formation of diastereomeric mixtures suggests that aziridination proceeds in a stepwise fashion. The dissimilarity of the diastereomeric ratios from *cis*- and *trans*- starting materials indicates that the potential intermediate is too short lived for complete ablation of the starting material stereochemistry. Second, the aziridination of cyclopentene by PhINTs in the presence of a radical trap *N*-*tert*-butyl-α-phenylnitrone (PBN) afforded the aziridine product **3b** in 60% NMR yield (Scheme 4d), suggesting a radical pathway was unlikely to be operative.

An ^{1}H NMR experiment was carried out to probe the speciation of **2a** in HFIP, and we observed that **2a** underwent reversible ligand exchange with alcohol solvent to afford $ArI(OR)_2$ and $TsNH_2$ (Supporting Information File 1, Figure S3); similar solvolysis of PhIO in HFIP has been reported [10]. Reaction between cyclohexene and PhIO (2 equiv) in HFIP delivered <10%

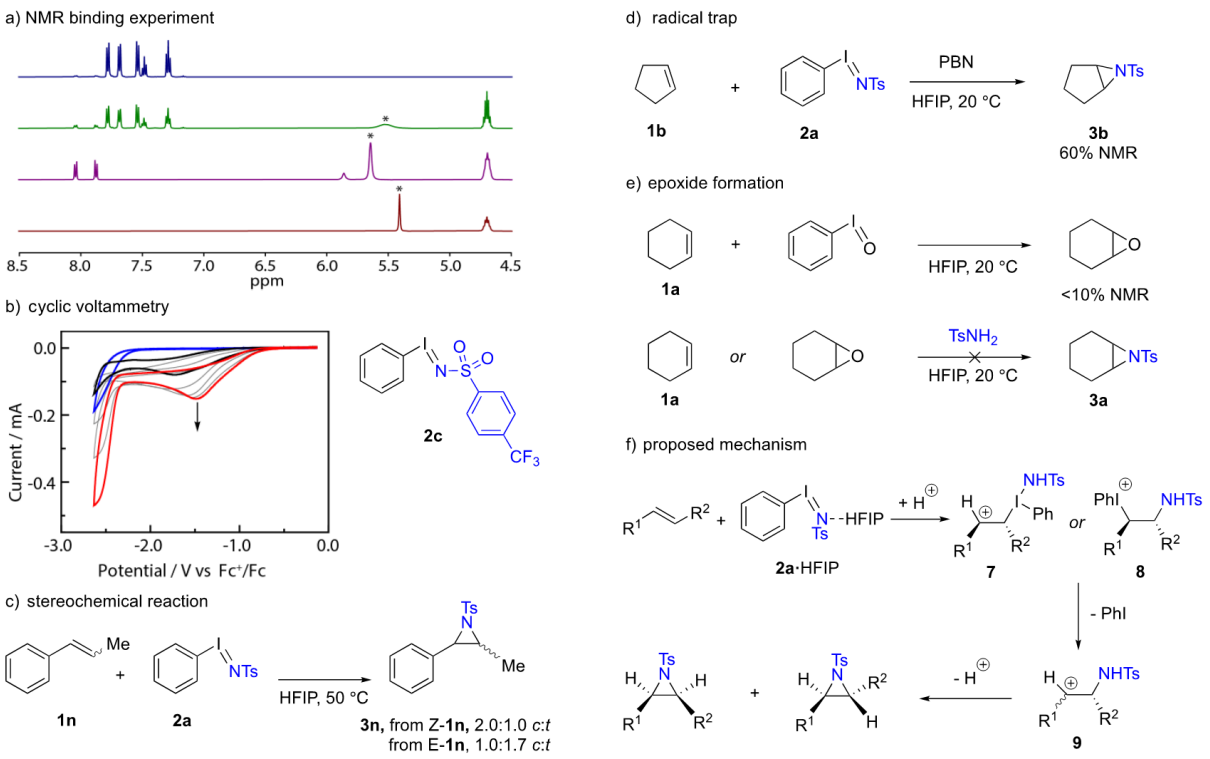

Scheme 4: a) The broadening of the hydroxide proton (denoted by asterisk *) of HFIP in the presence of iminoiodinane **2c** suggesting hydrogen bonding observed in ^{1}H NMR spectra (CD_3CN) of: 8.0 mM **2c** with no HFIP (blue line), 8.0 mM **2c** with 32 mM HFIP (green line), 4.0 mM of 4-(trifluoromethyl)benzenesulfonamide with 32 mM HFIP (purple line), only 32 mM HFIP (red line). b) Cyclic voltammogram of iminoiodinane **2c** (8.0 mM) with varying amounts of HFIP in 5.0 mL solution of MeCN (0.10 M $TBABF_4$) under N_2 atmosphere: **2c** with no HFIP (black line); **2c** with 5, 10, 15 µL HFIP (grey line); **2c** with 25 µL HFIP (red line); only 25 µL (blue line). c) Diastereomeric mixtures of aziridines are obtained from aziridination reactions of *cis*- or *trans*-β-methylstyrene, suggesting aziridine formation likely to operate via a step-wise pathway. d) Aziridination is not impacted by the presence of potential radical traps. e) PhIO, potentially generated by PhINTs hydrolysis, can give rise to epoxidation products. Epoxides are not on-path to the observed aziridines. f) Proposed reaction mechanism.

of cyclohexene oxide; meanwhile, both cyclohexene and cyclohexene oxide were shown to be unreactive towards sulfonamide (Scheme 4e), suggesting that epoxidation is not on path to the observed aziridines. For discussion of side-products and reaction mass balance, see Figure S4 (Supporting Information File 1). Based on these observations, we favor a mechanism in which H-bond activated iminoiodinane reacts directly with the olefin to generate a short-lived alkyl-bound iodinane **7** or iodonium species **8** (Scheme 4f). Ligand coupling from **7** or extrusion of iodobenzene from **8** would furnish a carbocation intermediate **9** which could undergo C–C bond rotation prior to ring closure to form the aziridine product. Such a process would account for the simultaneous stereochemical scrambling observed and the lack of radical trapping noted.

Conclusion

In conclusion, we describe the activation of simple iminoiodinane reagents by fluorinated alcohols, such as HFIP. While most iminoiodinane reagents do not engage aliphatic olefins in the absence of transition metal catalysts, the addition of HFIP enables direct aziridination to be observed. The enhanced reactivity is rationalized as resulting from H-bonding between HFIP and the nitrogen center of the iminoiodinane reagents. ^{1}H NMR data are consistent with such an association and electrochemical data collected in the presence of increasing HFIP concentrations are consistent with H-bonding affording an increasingly strong oxidant. These results demonstrate a simple method for activating iminoiodinane reagents and indicate the potential for chemical non-innocence of fluorinated alcohol solvents in NGT catalysis.

Supporting Information

Supporting Information File 1

Experimental procedures and characterization data, original spectra of new compounds, and optimization details.
[https://www.beilstein-journals.org/bjoc/content/supplementary/1860-5397-20-197-S1.pdf]

Funding

The authors acknowledge the Welch Foundation (A-1907) and the National Science Foundation (CAREER 1848135) for financial support.

Author Contributions

Phong Thai: conceptualization; investigation; validation; writing – original draft; writing – review & editing. Lauv Patel: investigation; validation; writing – review & editing. Diyasha Manna: investigation; validation; writing – review & editing. David C. Powers: conceptualization; funding acquisition; project administration; supervision; writing – review & editing.

ORCID® iDs

Phong Thai - https://orcid.org/0000-0001-6283-9344
Diyasha Manna - https://orcid.org/0009-0009-2647-0776
David C. Powers - https://orcid.org/0000-0003-3717-2001

Data Availability Statement

All data that supports the findings of this study is available in the published article and/or the supporting information to this article.

References

1. Wang, X.; Studer, A. *Acc. Chem. Res.* **2017,** *50,* 1712–1724. doi:10.1021/acs.accounts.7b00148
2. Yoshimura, A.; Zhdankin, V. V. *Chem. Rev.* **2016,** *116,* 3328–3435. doi:10.1021/acs.chemrev.5b00547
3. Akiba, K. *Chemistry of hypervalent compounds;* Wiley-VCH: Weinheim, Germany, 1998.
4. Zhdankin, V. V. *Hypervalent iodine chemistry: preparation, structure, and synthetic applications of polyvalent iodine compounds;* John Wiley & Sons: Chichester, UK, 2013. doi:10.1002/9781118341155
5. Dauban, P.; Dodd, R. H. *Synlett* **2003,** 1571–1586. doi:10.1055/s-2003-41010
6. Hui, C.; Antonchick, A. P. *Org. Chem. Front.* **2022,** *9,* 3897–3907. doi:10.1039/d2qo00739h
7. Ju, M.; Schomaker, J. M. *Nat. Rev. Chem.* **2021,** *5,* 580–594. doi:10.1038/s41570-021-00291-4
8. Degennaro, L.; Trinchera, P.; Luisi, R. *Chem. Rev.* **2014,** *114,* 7881–7929. doi:10.1021/cr400553c
9. Guo, Y.; Pei, C.; Koenigs, R. M. *Nat. Commun.* **2022,** *13,* 86. doi:10.1038/s41467-021-27687-6
10. Cardenal, A. D.; Maity, A.; Gao, W.-Y.; Ashirov, R.; Hyun, S.-M.; Powers, D. C. *Inorg. Chem.* **2019,** *58,* 10543–10553. doi:10.1021/acs.inorgchem.9b01191
11. Izquierdo, S.; Essafi, S.; del Rosal, I.; Vidossich, P.; Pleixats, R.; Vallribera, A.; Ujaque, G.; Lledós, A.; Shafir, A. *J. Am. Chem. Soc.* **2016,** *138,* 12747–12750. doi:10.1021/jacs.6b07999
12. Dasgupta, A.; Thiehoff, C.; Newman, P. D.; Wirth, T.; Melen, R. L. *Org. Biomol. Chem.* **2021,** *19,* 4852–4865. doi:10.1039/d1ob00740h
13. Koller, R.; Stanek, K.; Stolz, D.; Aardoom, R.; Niedermann, K.; Togni, A. *Angew. Chem., Int. Ed.* **2009,** *48,* 4332–4336. doi:10.1002/anie.200900974
14. Yuan, W.; Szabó, K. J. *Angew. Chem., Int. Ed.* **2015,** *54,* 8533–8537. doi:10.1002/anie.201503373
15. Deng, Q.-H.; Wadepohl, H.; Gade, L. H. *J. Am. Chem. Soc.* **2012,** *134,* 10769–10772. doi:10.1021/ja3039773
16. He, Y.-T.; Li, L.-H.; Yang, Y.-F.; Zhou, Z.-Z.; Hua, H.-L.; Liu, X.-Y.; Liang, Y.-M. *Org. Lett.* **2014,** *16,* 270–273. doi:10.1021/ol403263c
17. Zhou, B.; Yan, T.; Xue, X.-S.; Cheng, J.-P. *Org. Lett.* **2016,** *18,* 6128–6131. doi:10.1021/acs.orglett.6b03134
18. Ilchenko, N. O.; Tasch, B. O. A.; Szabó, K. J. *Angew. Chem.* **2014,** *126,* 13111–13115. doi:10.1002/ange.201408812
19. Nagata, T.; Matsubara, H.; Kiyokawa, K.; Minakata, S. *Org. Lett.* **2017,** *19,* 4672–4675. doi:10.1021/acs.orglett.7b02313
20. Zhao, Z.; Racicot, L.; Murphy, G. K. *Angew. Chem., Int. Ed.* **2017,** *56,* 11620–11623. doi:10.1002/anie.201706798
21. Narobe, R.; Murugesan, K.; Schmid, S.; König, B. *ACS Catal.* **2022,** *12,* 809–817. doi:10.1021/acscatal.1c05077
22. Matoušek, V.; Pietrasiak, E.; Sigrist, L.; Czarniecki, B.; Togni, A. *Eur. J. Org. Chem.* **2014,** 3087–3092. doi:10.1002/ejoc.201402225
23. Shu, S.; Li, Y.; Jiang, J.; Ke, Z.; Liu, Y. *J. Org. Chem.* **2019,** *84,* 458–462. doi:10.1021/acs.joc.8b02741
24. Thai, P.; Frey, B. L.; Figgins, M. T.; Thompson, R. R.; Carmieli, R.; Powers, D. C. *Chem. Commun.* **2023,** *59,* 4308–4311. doi:10.1039/d3cc00549f
25. Brantley, J. N.; Samant, A. V.; Toste, F. D. *ACS Cent. Sci.* **2016,** *2,* 341–350. doi:10.1021/acscentsci.6b00119
26. Colomer, I.; Chamberlain, A. E. R.; Haughey, M. B.; Donohoe, T. J. *Nat. Rev. Chem.* **2017,** *1,* 0088. doi:10.1038/s41570-017-0088
27. Motiwala, H. F.; Armaly, A. M.; Cacioppo, J. G.; Coombs, T. C.; Koehn, K. R. K.; Norwood, V. M., IV; Aubé, J. *Chem. Rev.* **2022,** *122,* 12544–12747. doi:10.1021/acs.chemrev.1c00749
28. Koller, R.; Huchet, Q.; Battaglia, P.; Welch, J. M.; Togni, A. *Chem. Commun.* **2009,** 5993–5995. doi:10.1039/b913962a
29. Choudhuri, K.; Maiti, S.; Mal, P. *Adv. Synth. Catal.* **2019,** *361,* 1092–1101. doi:10.1002/adsc.201801510
30. Colomer, I.; Batchelor-McAuley, C.; Odell, B.; Donohoe, T. J.; Compton, R. G. *J. Am. Chem. Soc.* **2016,** *138,* 8855–8861. doi:10.1021/jacs.6b04057
31. Yang, X.-G.; Zheng, K.; Zhang, C. *Org. Lett.* **2020,** *22,* 2026–2031. doi:10.1021/acs.orglett.0c00405
32. Sarie, J. C.; Neufeld, J.; Daniliuc, C. G.; Gilmour, R. *ACS Catal.* **2019,** *9,* 7232–7237. doi:10.1021/acscatal.9b02313
33. Minhas, H. K.; Riley, W.; Stuart, A. M.; Urbonaite, M. *Org. Biomol. Chem.* **2018,** *16,* 7170–7173. doi:10.1039/c8ob02236d
34. Tan, H.; Thai, P.; Sengupta, U.; Deavenport, I. R.; Kucifer, C. M.; Powers, D. C. *ChemRxiv* **2024**. doi:10.26434/chemrxiv-2024-s8gcj
35. Cheng, Q.-Q.; Zhou, Z.; Jiang, H.; Siitonen, J. H.; Ess, D. H.; Zhang, X.; Kürti, L. *Nat. Catal.* **2020,** *3,* 386–392. doi:10.1038/s41929-020-0430-4
36. Farndon, J. J.; Young, T. A.; Bower, J. F. *J. Am. Chem. Soc.* **2018,** *140,* 17846–17850. doi:10.1021/jacs.8b10485
37. Holst, D. E.; Wang, D. J.; Kim, M. J.; Guzei, I. A.; Wickens, Z. K. *Nature* **2021,** *596,* 74–79. doi:10.1038/s41586-021-03717-7
38. Huang, Y.; Zhu, S.-Y.; He, G.; Chen, G.; Wang, H. *J. Org. Chem.* **2024,** *89,* 6263–6273. doi:10.1021/acs.joc.4c00253
39. Jat, J. L.; Chandra, D.; Kumar, P.; Singh, V.; Tiwari, B. *Synthesis* **2022,** *54,* 4513–4520. doi:10.1055/a-1879-7974
40. Satheesh, V.; Alahakoon, I.; Shrestha, K. K.; Iheme, L. C.; Marszewski, M.; Young, M. C. *Eur. J. Org. Chem.* **2024,** e202301114. doi:10.1002/ejoc.202301114
41. He, L.; Chan, P. W. H.; Tsui, W.-M.; Yu, W.-Y.; Che, C.-M. *Org. Lett.* **2004,** *6,* 2405–2408. doi:10.1021/ol049232j

42. Li, F.; Zhu, W. F.; Empel, C.; Datsenko, O.; Kumar, A.; Xu, Y.; Ehrler, J. H. M.; Atodiresei, I.; Knapp, S.; Mykhailiuk, P. K.; Proschak, E.; Koenigs, R. M. *Science* **2024,** *383,* 498–503. doi:10.1126/science.adm8095
43. Jurberg, I. D.; Nome, R. A.; Crespi, S.; Atvars, T. D. Z.; König, B. *Adv. Synth. Catal.* **2022,** *364,* 4061–4068. doi:10.1002/adsc.202201095
44. Kuznetsov, D. M.; Tumanov, V. V.; Smit, W. A. *J. Polym. Res.* **2013,** *20,* 128. doi:10.1007/s10965-013-0128-2
45. Noel, M.; Vasu, K. *Cyclic Voltammetry and the Frontiers of Electrochemistry;* Oxford & IBH Publishing: New Dehli, India, 1990.

License and Terms

BEILSTEIN JOURNAL OF ORGANIC CHEMISTRY

Evaluating the halogen bonding strength of a iodoloisoxazolium(III) salt

Dominik L. Reinhard‡, Anna Schmidt‡, Marc Sons, Julian Wolf, Elric Engelage and Stefan M. Huber*

Letter

Open Access

Address:
Fakultät für Chemie und Biochemie, Ruhr-Universität Bochum, Universitätsstraße 150, 44801 Bochum, Germany

Email:
Stefan M. Huber* - stefan.m.huber@ruhr-uni-bochum.de

* Corresponding author ‡ Equal contributors

Keywords:
diaryliodonium; gold catalysis; halogen bonding; hypervalent iodine; non-covalent interactions

Beilstein J. Org. Chem. **2024,** *20,* 2401–2407.
https://doi.org/10.3762/bjoc.20.204

Received: 13 June 2024
Accepted: 02 September 2024
Published: 23 September 2024

This article is part of the thematic issue "Hypervalent halogen chemistry".

Guest Editor: T. Gulder

Abstract

Diaryliodonium(III) salts have been established as powerful halogen-bond donors in recent years. Herein, a new structural motif for this compound class was developed: iodoloisoxazolium salts, bearing a cyclic five-membered iodolium core fused with an isoxazole ring. A derivative of this class was synthesized and investigated in the solid state by X-ray crystallography. Finally, the potential as halogen-bonding activator was benchmarked in solution in the gold-catalyzed cyclization of a propargyl amide.

Introduction

The compound class of diaryliodonium (DAI) salts has been known since the end of the 19th century and their use as aryl-transfer reagents has been widely explored [1-3]. The application as Lewis acid catalysts, on the other hand, has only gained interest in the last ten years after a first report by Han and Liu in 2015 on their use as catalysts in a Mannich reaction [4]. In 2018, our group showed in a proof-of-principle study [5] that the Lewis acid catalysis by DAI salts is based on halogen bonding (XB), an interaction between a Lewis base (XB acceptor) and an electrophilic halogen atom in the Lewis acid (XB donor) [6-10]. In organocatalysis, previously only iodine(I)-based Lewis acids had been applied. However, after this study, the application of DAI salts as XB donors gained increasing interest and was investigated by several groups [11]. In the last years, important information about structure–activity relationships was also obtained: in a titration study by Mayer and Legault it was determined that cyclic five-membered DAI salts, so-called iodolium compounds, are significantly stronger Lewis acids than their less-stable acyclic counterparts [12]. By using the activation of alkyl halides as a benchmark, our group later reported that six-membered core structures are also weaker XB donors (iodininium $\mathbf{3}^{\mathbf{OTf}}$) than iodolium $\mathbf{1}^{\mathbf{OTf}}$ [13]. Further-

more, the importance of substituents in the core and on the outer rings was demonstrated (XB donors 2^{OTf} and 4^{OTf}). Nachtsheim reported the synthesis of *N*-heterocyclic substituted monocationic iodolium salts like derivatives 5^{Z} and 6^{Z} (Figure 1) [14,15]. Their benchmark studies showed significant activity differences amongst them and superior performance compared to prototypical iodolium 1^{Z}. Significant upgrades to DAI-based XB catalysts were made in the form of bidentate and dicationic XB donors [16,17] from our group as well as of dicationic *N*-heterocyclic-substituted monodentate catalysts by Nachtsheim [15]. While such compounds are necessary to activate neutral substrates in more challenging reactions, monodentate and monocationic congeners provide sufficient activation in halide abstractions, e.g. to activate gold chloride complexes [18,19]. Therefore, besides the development of new bidentate catalyst motifs, we were still interested in the optimization of these "simpler" derivatives. Thus, we designed a new catalyst motif [20] featuring an isoxazole ring, XB donor 7^{Z}, and compared it with our known iodonium species in the activation of Au(I)–Cl bonds.

Results and Discussion

As immediate precursor to the target structure 7^{Z}, the literature-known isoxazole **10** was synthesized via a Cu(I)-catalyzed cycloaddition between (2-iodophenyl)acetylene (**8**) and benzyl nitrile oxide, which is produced in situ from the imidoyl chloride **9** [21]. The one-pot oxidation and ring-closure reaction [22,23] to iodoloisoxazolium(III) salt 7^{OTf} and the salt metathesis with sodium tetrakis(3,5-bis(trifluoromethyl)phenyl)borate ($NaBArF_{24}$) were then realized with 85% and 72% yield, respectively (Scheme 1).

The triflate salt 7^{OTf} was transformed into the corresponding bromide salt by XB-activated solvolysis of α-methylbenzyl bro-

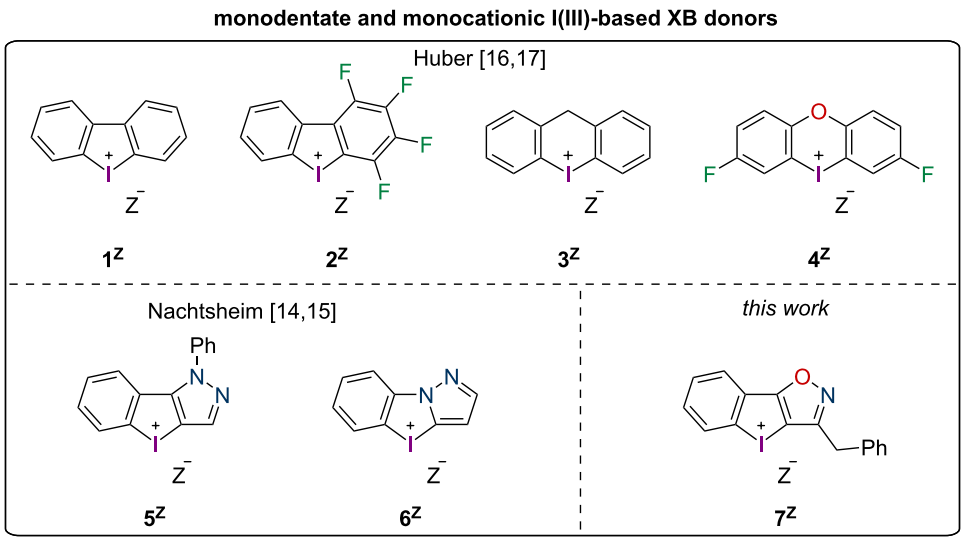

Figure 1: Set of literature-known monocationic cyclic diaryliodonium(III) salts that were applied as XB donors (Z = OTf, $BArF_{24}$).

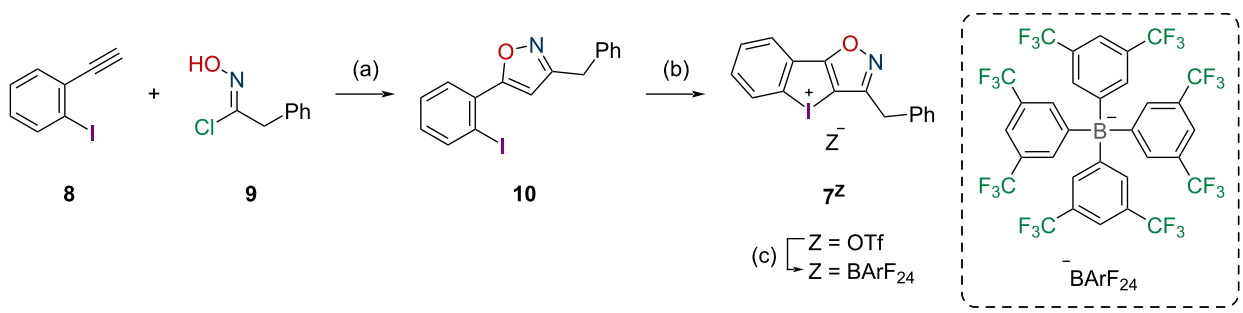

Scheme 1: Synthesis of the iodoloisoxazolium salts 7^{Z}: (a) 1.5 equiv **9**, 0.2 equiv CuI, 2.0 equiv K_2CO_3, (THF), 0.1 M, 135 h at rt, 43%, (b) 1.5 equiv mCPBA, 3.0 equiv TfOH (at 0 °C), (DCM), 0.1 M, 20 h at rt, 85%, (c) 1.0 equiv $NaBArF_{24}$, (acetone), 0.5 M, 2 h at 50 °C under microwave irradiation, 72%.

mide in wet acetonitrile [13]. The DAI salt $\mathbf{7}^{\mathbf{Br}}$ crystallized from this solution in the monoclinic space group $P2_1/n$ with a cell volume of 1447.91(3) Å^3 (a = 5.4707(1) Å, b = 10.9139(1) Å, c = 24.3668(3) Å, β = 95.601(1)°) and a density of 2.01865 g/cm^3. Two units of the cationic XB donor form a dimer, which is bridged via two bromide ions (Figure 2). As usual for DAI salts, two XB axes are found on the elongations of the C–I bonds. On the one *trans* to the isoxazolium unit, halogen bonding [I1···Br1 = 3.0610(5) Å, 80% of Σr, and C8–I1···Br1 = 171.67(9)°] and hydrogen bonding were found [H2···Br1 = 2.7991(4) Å, 95% of Σr, C2···Br1 = 3.545(4) Å, 100% of Σr and C2–H2···Br1 = 136.1(2)°]. On the other axis, no ortho proton is present, so only XB is observed [I1···Br1 = 3.2023(5) Å, 84% of Σr, and C1–I1···Br1 = 176.08(9)°]. The bond distances indicate that the hydrogen bond is noticeably weaker than the two XBs and thus constitutes merely an assisting interaction.

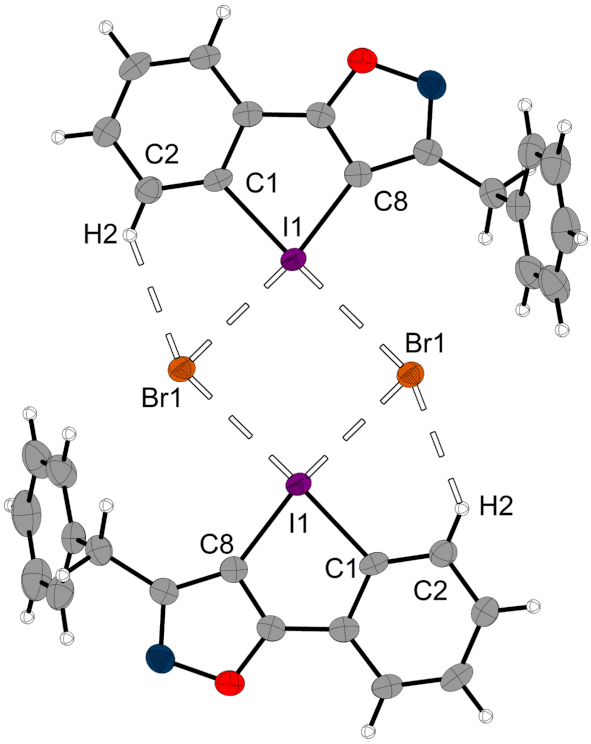

Figure 2: Halogen bonding dimer found in the crystal structure of $\mathbf{7}^{\mathbf{Br}}$. Ellipsoids are shown at 50% probability (carbon: grey, nitrogen: blue, oxygen: red, bromine: orange, iodine: purple) and hydrogen atoms are shown in standard ball-and-stick model (white). Halogen and hydrogen bonding is indicated dashed.

The XB interactions in this crystal structure were compared to the ones in the literature-known co-crystal of prototypic iodolium $\mathbf{1}^{\mathbf{BArF}}$ with bromide (CCDC: 1145291) [5]. For the latter, such a dimeric binding motif was also found, with I–Br bond lengths of 3.1936(9) Å [83% of Σr] and 3.2299(9) Å [84% of Σr]. It can be concluded that stronger halogen bonding can be found in the crystal structure of iodoloisoxazolium $\mathbf{7}^{\mathbf{Br}}$, which hints that also in solution stronger binding to Lewis bases and therefore higher activity as catalyst may be expected (compared to prototypic iodolium $\mathbf{1}^{\mathbf{Z}}$).

As a benchmark for the halogen-bonding strength in solution, the activation of $(PPh_3)AuCl$ was chosen. The activated gold(I) complex was applied as catalyst for the cyclization of propargylic amide **11**, a typical benchmark reaction in gold catalysis (Scheme 2) [24-27], which had previously already been activated by iodine(I) and iodine(III)-based XB donors [15,18].

To evaluate the activity of the new iodoloisoxazolium $\mathbf{7}^{\mathbf{BArF}}$, it was compared to the four monodentate iodine(III)-based XB donors $\mathbf{1}^{\mathbf{BArF}}$–$\mathbf{4}^{\mathbf{BArF}}$ (Scheme 2), which had been applied in a previous study by our group as triflate salts and which had shown strong differences in XB donor strength [13]. While the six-membered iodininium salt $\mathbf{3}^{\mathbf{OTf}}$ proved to be markedly

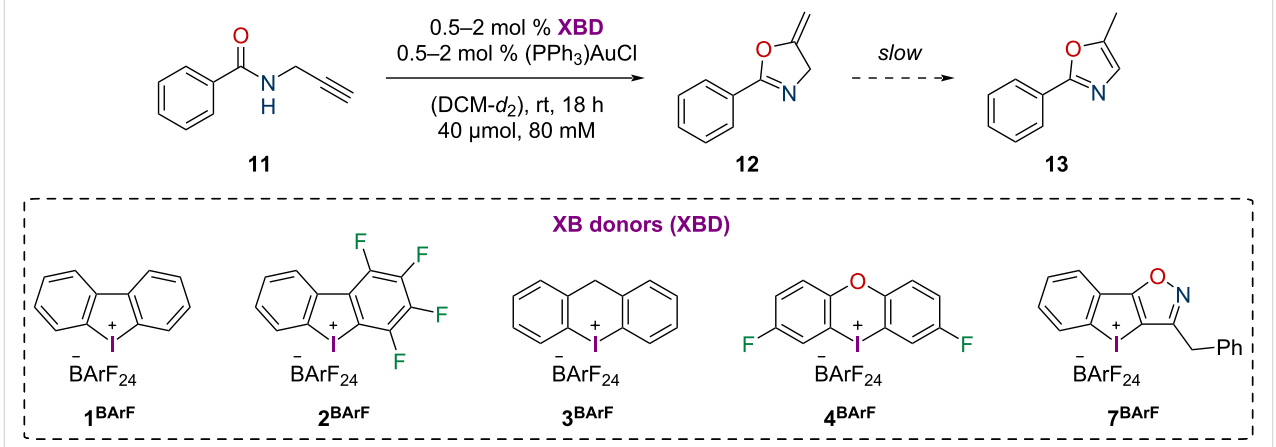

Scheme 2: Gold(I)-catalyzed cyclization of propargylic amide **11** as benchmark reaction for Au–Cl activation.

weaker than prototypic iodolium $\mathbf{1}^{\mathbf{OTf}}$, the oxygen-bridged iodoxinium $\mathbf{4}^{\mathbf{OTf}}$ exhibited improved performance and the polyfluorinated iodolium $\mathbf{2}^{\mathbf{OTf}}$ was by far the most active. A previous study on gold activation by halogen bonding showed significantly higher activity when the weakly coordinating counteranion tetrakis[3,5-bis(trifluoromethyl)phenyl]borate ($^{-}BArF_{24}$) was used instead of triflate [18]. Therefore, standard anion metathesis procedures were employed to prepare the salts $\mathbf{1}^{\mathbf{BArF}}$–$\mathbf{4}^{\mathbf{BArF}}$ (see Supporting Information File 1).

Similarly to our previous report on this gold activation, the gold complex $(PPh_3)AuCl$ was applied with a catalyst loading of 2 mol %, activated by an equal amount of the DAI salt. Due to solubility issues, the reaction had to be performed in methylene chloride instead of chloroform. The gold-catalyzed cyclization reaction (Scheme 2) was followed via ^{1}H NMR spectroscopy (Figure 3).

When applying the six-membered cyclic DAI salt $\mathbf{3}^{\mathbf{BArF}}$ as an activator, the lowest activity was observed, reaching ≈80% conversion after 18 h (≈5% after 2 h). It has to be noted that a sigmoidal curve was observed. This indicates that the activity of the catalyst system increases over time. A preactivation process between the XB donor, the gold complex, or the amide can be assumed. Such a sigmoidal curve for this reaction has also been observed in one of the previous studies on the XB activation of gold complexes [15]. The prototypic iodolium $\mathbf{1}^{\mathbf{BArF}}$ showed significantly better results reaching ≈85% conversion after already 4 h (≈55% after 2 h) and the oxygen-bridged iodoxinium $\mathbf{4}^{\mathbf{BArF}}$ performed slightly better (≈70% after 2 h). For these two catalysts, a very slight sigmoidal curve shape was also observed. The polyfluorinated XB donor $\mathbf{2}^{\mathbf{BArF}}$ performed the best, with ≈90% conversion after 2 h. The resulting order of catalytic activity of these halogen-bond donors is in line with the above-mentioned previous benchmark of these activators [13]. Finally, also the new iodoloisoxazolium salt $\mathbf{7}^{\mathbf{BArF}}$ was applied and a comparably high activity was observed (ca. 85% conversion after 2 h). This result marks this halogen-bond donor as the second-best activator out of this set of compounds. Furthermore, the three strongest XB donors $\mathbf{2}^{\mathbf{BArF}}$, $\mathbf{4}^{\mathbf{BArF}}$, and $\mathbf{7}^{\mathbf{BArF}}$ were also applied at a catalyst loading of 0.5 mol % (with an equimolar amount of $(PPh_3)AuCl$). Both, the tetrafluoroiodolium $\mathbf{2}^{\mathbf{BArF}}$ and the iodoloisoxazolium $\mathbf{7}^{\mathbf{BArF}}$ are still effective activators even at such low catalyst-system loadings. The tetrafluoroiodolium $\mathbf{2}^{\mathbf{BArF}}$ yields a conversion of almost 80% and the iodoloisoxazolium $\mathbf{7}^{\mathbf{BArF}}$ one of almost 70% after

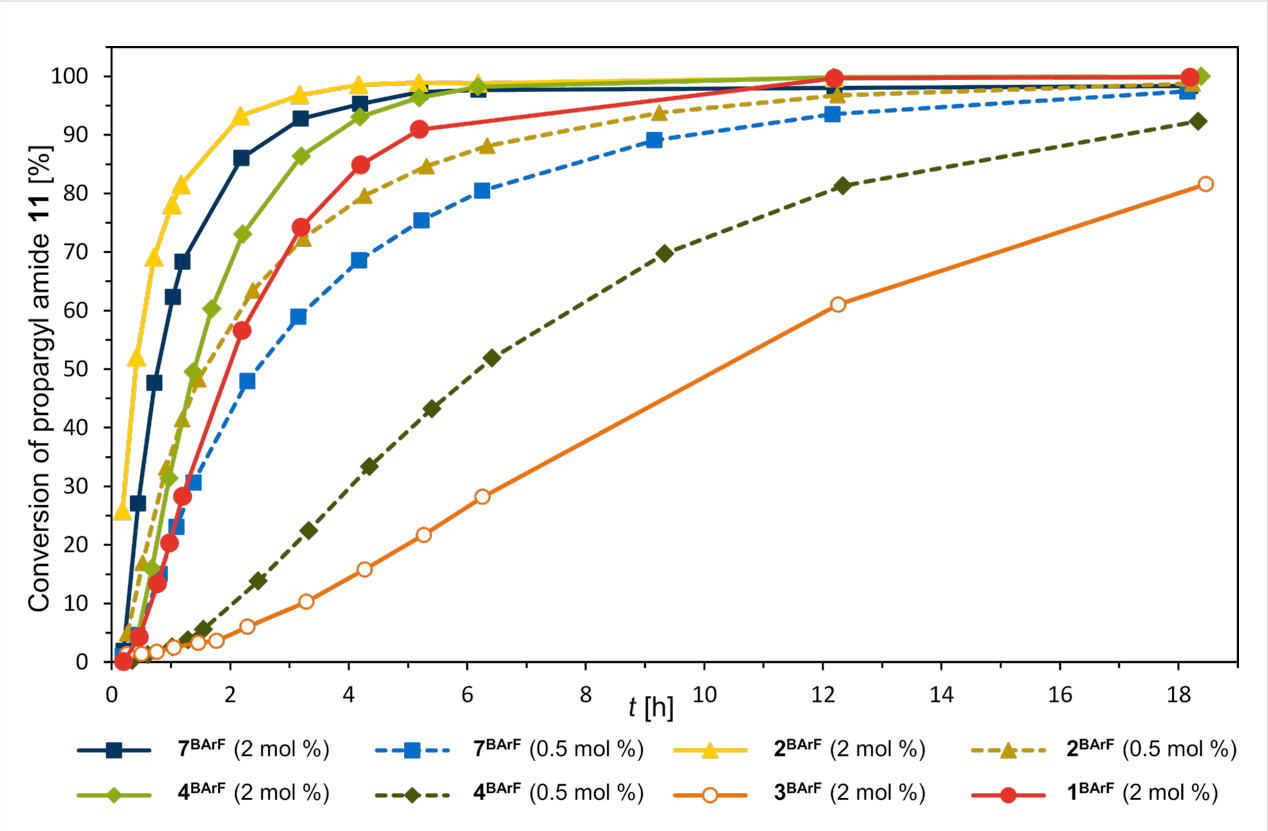

Figure 3: ^{1}H NMR kinetics of the gold-catalyzed cyclization shown in Scheme 2. An equimolar amount of the gold complex was applied, respectively. Every experiment was performed three times (see Supporting Information File 1).

4 h. In comparison, the iodoxinium salt $\mathbf{4}^{\mathbf{BArF}}$ also featured a sigmoidal curve shape and a significantly slower activation, which results in an amide consumption of only ca. 30% after 4 hours. To quantify the activity differences of these XB donors, the reaction kinetics were fitted according to a pseudo-first-order rate. Only selected periods (the first four data points within the first 1.5 hours of reaction) were considered, as such a coarse approximation cannot be applied after reaching the plateau due to equilibrium processes (see Supporting Information File 1 for further details). The determined TOF of tetrafluoroiodolium salt $\mathbf{2}^{\mathbf{BArF}}$ reaches a value of 80 h^{-1}, almost 1.7 times as high as the TOF of iodoloisoxazolium $\mathbf{7}^{\mathbf{BArF}}$ with 48 h^{-1}. Both TOFs are much higher (almost 5 and 3 times higher) than the one of iodoxinium $\mathbf{4}^{\mathbf{BArF}}$ with 17 h^{-1} (Table 1).

Table 1: Determined TOFs of the strongest activators $\mathbf{2}^{\mathbf{BArF}}$, $\mathbf{7}^{\mathbf{BArF}}$, and $\mathbf{4}^{\mathbf{BArF}}$ (and their calculated standard deviation). The TOFs were determined from the kinetics (see Supporting Information File 1 for further details).

XB donor	TOF [h^{-1}]
$\mathbf{2}^{\mathbf{BArF}}$	80 ± 7
$\mathbf{7}^{\mathbf{BArF}}$	48 ± 4
$\mathbf{4}^{\mathbf{BArF}}$	17 ± 1

Since the three compounds $\mathbf{2}^{\mathbf{BArF}}$–$\mathbf{4}^{\mathbf{BArF}}$ have not been tested in this reaction before, and iodoloisoxazolium salt $\mathbf{7}^{\mathbf{BArF}}$ has not been tested in any reaction at all, several control experiments were also performed, even though the benchmark reaction has already been established in halogen-bonding activation. In the presence of 2 mol % of either the unactivated gold complex $(PPh_3)AuCl$ or the XB donors $\mathbf{1}^{\mathbf{BArF}}$–$\mathbf{4}^{\mathbf{BArF}}$ + $\mathbf{7}^{\mathbf{BArF}}$, ^1H NMR showed no conversion within 18 h, indicating that the activated gold complex is the catalytically active species. Furthermore, stability measurements (^1H and ^{19}F NMR) of 1:1 mixtures of the gold complex and the XB donors were performed in order to investigate the stability of the cationic iodonium structures towards the gold complex [28]. For all catalyst systems, decomposition of the $^-BArF_{24}$ anion was observed via ^1H and ^{19}F NMR spectroscopy, which is known to happen in the presence of activated gold complexes [29]. The stability of the DAI cations was checked with ^1H NMR: the characteristic doublets belonging to the respective iodonium structures $\mathbf{1}^+$, $\mathbf{2}^+$, $\mathbf{3}^+$, and $\mathbf{7}^+$ were found to be constant (see Supporting Information File 1). The signals of the iodoxinium cation $\mathbf{4}^+$ were overlapping with signals of the anion. However, the stability of $\mathbf{4}^+$ (as well as of $\mathbf{2}^+$) could be confirmed by ^{19}F NMR measurements: no decomposition of the signals belonging to the core structure of the cations was observed. These results indicate that the DAI cations are still intact and do not decompose in the presence of the gold complex. In previous works, the mode of activation by several XB donors including DAI salts was investigated, suggesting that halide abstraction is the crucial step towards the formation of a catalytically active gold species [18,19]. Furthermore, iodonium species $\mathbf{1}^{\mathbf{BArF}}$–$\mathbf{4}^{\mathbf{BArF}}$ have been shown to be halide abstracting agents in the Ritter-type solvolysis of α-methylbenzyl bromide and via the crystal structures of $\mathbf{1}^{\mathbf{Cl}}$, $\mathbf{2}^{\mathbf{Cl}}$, and $\mathbf{3}^{\mathbf{Cl}}$ which resulted from crystallization of the respective cation with the abstracted chloride from the Ritter-type solvolysis of benzhydryl chloride [13]. The crystal structure of $\mathbf{5}^{\mathbf{Br}}$ was also obtained directly from the halide-abstraction reaction (see Supporting Information File 1). These three facts and the considerations mentioned before, strongly hint that the same kind of halide abstraction from the gold(I) species is occurring here with the presented XB donors $\mathbf{1}^{\mathbf{BArF}}$–$\mathbf{4}^{\mathbf{BArF}}$ and $\mathbf{7}^{\mathbf{BArF}}$.

Conclusion

In this study, we reported the synthesis of a new cyclic diaryliodonium motif: the iodoloisoxazolium unit bearing a five-membered iodolium core fused with an isoxazole ring. The derivatives $\mathbf{7}^{\mathbf{Z}}$ (Z = OTf, $BArF_{24}$) were synthesized and the crystal structure of the corresponding bromide salt was determined. Its analysis provided cases of strong halogen bonding, which was further investigated in solution via the activation of the gold–chlorine bond in the catalyst $(PPh_3)AuCl$. Here, the new diaryliodonium motif outcompeted other XB donors like the prototypical iodolium $\mathbf{1}^{\mathbf{BArF}}$ and showed a similar activity as the polyfluorinated XB donor $\mathbf{2}^{\mathbf{BArF}}$. The results illustrate the potential of the iodoloisoxazolium for halogen-bonding activation and catalysis. Studies on the synthesis and application of chiral and/or bidentate dicationic derivatives are currently underway in our laboratory.

Supporting Information

Supporting Information File 1

Synthesis, catalyses, and characterization data.
[https://www.beilstein-journals.org/bjoc/content/supplementary/1860-5397-20-204-S1.pdf]

Supporting Information File 2

Crystallographic information file of $\mathbf{7}^{\mathbf{Br}}$.
[https://www.beilstein-journals.org/bjoc/content/supplementary/1860-5397-20-204-S2.cif]

Supporting Information File 3

Crystallographic data.
[https://www.beilstein-journals.org/bjoc/content/supplementary/1860-5397-20-204-S3.xlsx]

Supporting Information File 4
Crystallographic data.
[https://www.beilstein-journals.org/bjoc/content/supplementary/1860-5397-20-204-S4.zip]

Funding

Funding by the *Fonds der Chemischen Industrie* (Kekulé scholarship for D.L.R. and Dozentenstipendium for S.M.H.) and by the *Deutsche Forschungsgemeinschaft* (DFG, German Research Foundation, Germany's Excellence Strategy, EXC 2033 – 390677874 – RESOLV) is gratefully acknowledged.

ORCID® iDs

Dominik L. Reinhard - https://orcid.org/0009-0005-2373-7317
Anna Schmidt - https://orcid.org/0009-0000-4708-0958
Elric Engelage - https://orcid.org/0000-0003-4640-6260
Stefan M. Huber - https://orcid.org/0000-0002-4125-159X

Data Availability Statement

The data that supports the findings of this study is available from the corresponding author upon reasonable request.

References

1. Zhdankin, V. V.; Stang, P. J. *Chem. Rev.* **2008,** *108,* 5299–5358. doi:10.1021/cr800332c
2. Olofsson, B. *Top. Curr. Chem.* **2015,** *373,* 135–166. doi:10.1007/128_2015_661
3. Merritt, E. A.; Olofsson, B. *Angew. Chem.* **2009,** *121,* 9214–9234. doi:10.1002/ange.200904689
   Angew. Chem. Int. Ed. **2009,** *48,* 9052–9070. doi:10.1002/anie.200904689
4. Zhang, Y.; Han, J.; Liu, Z.-J. *RSC Adv.* **2015,** *5,* 25485–25488. doi:10.1039/c5ra00209e
5. Heinen, F.; Engelage, E.; Dreger, A.; Weiss, R.; Huber, S. M. *Angew. Chem., Int. Ed.* **2018,** *57,* 3830–3833. doi:10.1002/anie.201713012
   Angew. Chem. 2018, 130, 3892-3896. doi:10.1002/ange.201713012
6. Erdélyi, M. *Chem. Soc. Rev.* **2012,** *41,* 3547. doi:10.1039/c2cs15292d
7. Cavallo, G.; Metrangolo, P.; Milani, R.; Pilati, T.; Priimagi, A.; Resnati, G.; Terraneo, G. *Chem. Rev.* **2016,** *116,* 2478–2601. doi:10.1021/acs.chemrev.5b00484
8. Brown, A.; Beer, P. D. *Chem. Commun.* **2016,** *52,* 8645–8658. doi:10.1039/c6cc03638d
9. Mukherjee, A.; Tothadi, S.; Desiraju, G. R. *Acc. Chem. Res.* **2014,** *47,* 2514–2524. doi:10.1021/ar5001555
10. Sutar, R. L.; Huber, S. M. *ACS Catal.* **2019,** *9,* 9622–9639. doi:10.1021/acscatal.9b02894
11. Robidas, R.; Reinhard, D. L.; Legault, C. Y.; Huber, S. M. *Chem. Rec.* **2021,** *21,* 1912–1927. doi:10.1002/tcr.202100119
12. Mayer, R. J.; Ofial, A. R.; Mayr, H.; Legault, C. Y. *J. Am. Chem. Soc.* **2020,** *142,* 5221–5233. doi:10.1021/jacs.9b12998
13. Reinhard, D. L.; Heinen, F.; Stoesser, J.; Engelage, E.; Huber, S. M. *Helv. Chim. Acta* **2021,** *104,* e2000221. doi:10.1002/hlca.202000221
14. Boelke, A.; Kuczmera, T. J.; Caspers, L. D.; Lork, E.; Nachtsheim, B. J. *Org. Lett.* **2020,** *22,* 7261–7266. doi:10.1021/acs.orglett.0c02593
15. Boelke, A.; Kuczmera, T. J.; Lork, E.; Nachtsheim, B. J. *Chem. – Eur. J.* **2021,** *27,* 13128–13134. doi:10.1002/chem.202101961
16. Heinen, F.; Reinhard, D. L.; Engelage, E.; Huber, S. M. *Angew. Chem., Int. Ed.* **2021,** *60,* 5069–5073. doi:10.1002/anie.202013172
    Angew. Chem. 2021, 133, 5127-5132.
17. Reinhard, D. L.; Kutzinski, D.; Hatta, M.; Engelage, E.; Huber, S. M. *Synlett* **2024,** *35,* 209–214. doi:10.1055/a-2198-3914
18. Wolf, J.; Huber, F.; Erochok, N.; Heinen, F.; Guérin, V.; Legault, C. Y.; Kirsch, S. F.; Huber, S. M. *Angew. Chem., Int. Ed.* **2020,** *59,* 16496–16500. doi:10.1002/anie.202005214
    Angew. Chem. 2020, 132, 16638-16643. doi:10.1002/ange.202005214
19. Jónsson, H. F.; Sethio, D.; Wolf, J.; Huber, S. M.; Fiksdahl, A.; Erdelyi, M. *ACS Catal.* **2022,** *12,* 7210–7220. doi:10.1021/acscatal.2c01864
20. Su, J.; Liu, Y.; Jing, Y.; Liu, Y.; Ke, Z. *Asian J. Org. Chem.* **2023,** *12,* e202300210. doi:10.1002/ajoc.202300210
    While this monocationic motif has to the best of our knowledge never been investigated, an *N*-methylated dicationic derivative has been part of a purely theoretical study.
21. Yuan, H.; Wang, M.; Xu, Z.; Gao, H. *Adv. Synth. Catal.* **2019,** *361,* 4386–4392. doi:10.1002/adsc.201900435
22. Bielawski, M.; Olofsson, B. *Chem. Commun.* **2007,** 2521–2523. doi:10.1039/b701864a
23. Bielawski, M.; Zhu, M.; Olofsson, B. *Adv. Synth. Catal.* **2007,** *349,* 2610–2618. doi:10.1002/adsc.200700373
24. Hashmi, A. S. K.; Weyrauch, J. P.; Frey, W.; Bats, J. W. *Org. Lett.* **2004,** *6,* 4391–4394. doi:10.1021/ol0480067
25. Wegener, M.; Huber, F.; Bolli, C.; Jenne, C.; Kirsch, S. F. *Chem. – Eur. J.* **2015,** *21,* 1328–1336. doi:10.1002/chem.201404487
26. Tšupova, S.; Rudolph, M.; Rominger, F.; Hashmi, A. S. K. *Adv. Synth. Catal.* **2016,** *358,* 3999–4005. doi:10.1002/adsc.201600615
27. Schießl, J.; Schulmeister, J.; Doppiu, A.; Wörner, E.; Rudolph, M.; Karch, R.; Hashmi, A. S. K. *Adv. Synth. Catal.* **2018,** *360,* 2493–2502. doi:10.1002/adsc.201800233
28. The measurements were performed with a concentration of 5 mM, which is higher in comparison to the concentration of the active complex during catalysis experiments: 1.6 mM with a catalyst loading of 2 mol % and 0.4 mM with a catalyst load of 0.5 mol %.
29. Weber, S. G.; Zahner, D.; Rominger, F.; Straub, B. F. *Chem. Commun.* **2012,** *48,* 11325. doi:10.1039/c2cc36171j

BEILSTEIN JOURNAL OF ORGANIC CHEMISTRY

Hypervalent iodine-mediated cyclization of bishomoallylamides to prolinols

Smaher E. Butt‡[1], Konrad Kepski‡[1], Jean-Marc Sotiropoulos*[2] and Wesley J. Moran*[3]

Full Research Paper

Open Access

Address:
[1]Department of Physical and Life Sciences, University of Huddersfield, Queensgate, Huddersfield HD1 3DH, United Kingdom, [2]Université de Pau et des Pays de l'Adour, IPREM (CNRS-UMR 5254), Technopole Hélioparc, 2 Avenue du Président Pierre Angot, 64053 Pau Cedex 09, France and [3]School of Pharmacy and Bioengineering, Keele University, Keele, Staffordshire ST5 5JX, United Kingdom

Email:
Jean-Marc Sotiropoulos* - jean-marc.sotiro@univ-pau.fr;
Wesley J. Moran* - w.j.moran@keele.ac.uk

* Corresponding author ‡ Equal contributors

Keywords:
cyclization; DFT; hypervalent iodine; mechanism; proline

Beilstein J. Org. Chem. **2024,** *20,* 2455–2460.
https://doi.org/10.3762/bjoc.20.209

Received: 14 May 2024
Accepted: 13 September 2024
Published: 30 September 2024

This article is part of the thematic issue "Hypervalent halogen chemistry".

Guest Editor: J. Wencel-Delord

Abstract

A change in mechanism was observed in the hypervalent iodine-mediated cyclization of *N*-alkenylamides when the carbon chain between the alkene and the amide increased from two to three atoms. In the latter case, cyclization at the amide nitrogen to form the pyrrolidine ring was favored over cyclization at the amide oxygen. A DFT study was undertaken to rationalize the change in mechanism of this cyclization process. In addition, reaction conditions were developed, and the scope of this cyclization studied.

Introduction

Proline is one of the 20 DNA-encoded proteinogenic amino acids that are essential to life [1,2]. In addition, the pyrrolidine core is present in many organocatalysts [3-5], natural products (e.g., the potent α-glucosidase inhibitor (−)-codonopsinol B) [6,7], and pharmaceutical drug molecules such as saxagliptin and ramipril (Figure 1) [8]. Accordingly, the development of methods to access substituted prolines and pyrrolidines is an important area of study as this ring system is prevalent in many useful molecules. Typical literature procedures include multi-step derivations of proline itself, e.g., the destruction of the stereocenter and then its reinstallation by an enantioselective conjugate addition [9]. Other methods include the enantioselective conjugate addition to α,β-unsaturated pyroglutamic acid derivatives followed by deoxygenation [10], and the enantioselective organocatalytic reaction between 2-acylaminomalonates and α,β-unsaturated aldehydes [11,12].

The development of new synthetic methods using hypervalent iodine reagents has become increasingly popular in recent years probably due to their useful reactivity, ease of handling, and low toxicity [13]. In particular, hypervalent iodine compounds have been shown to be effective reagents and catalysts for a

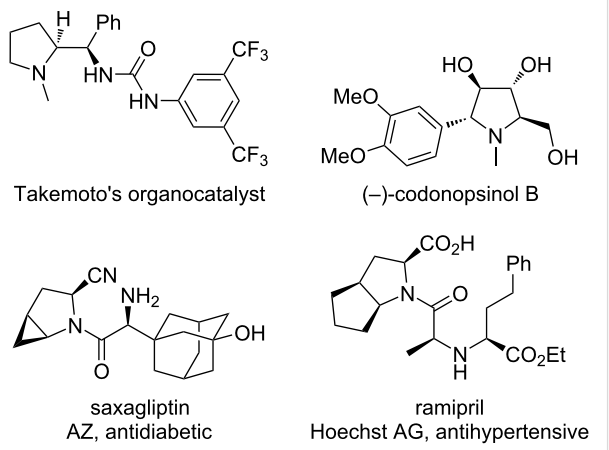

Figure 1: Functional molecules containing a substituted pyrrolidine core.

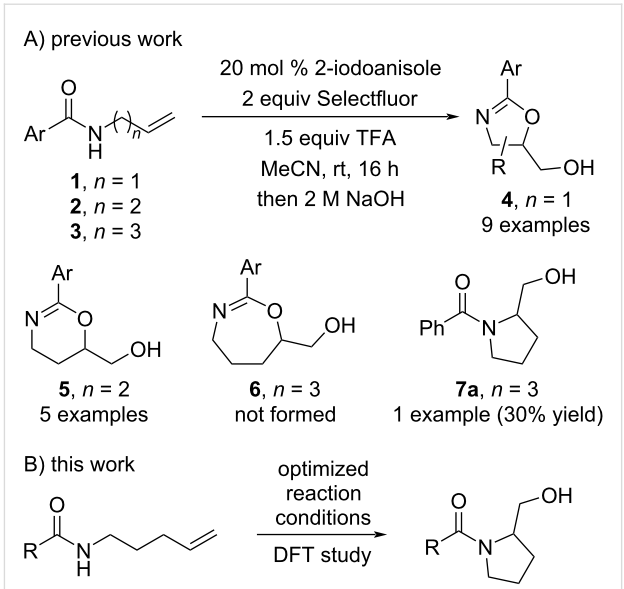

Scheme 1: A) Our previous report on *N*-alkenylamide cyclizations. B) An overview of the present work.

range of cyclization reactions [14]. In 2015, we reported the iodoarene-catalyzed cyclization of *N*-allylamides **1** and *N*-homoallylamides **2** to 2-oxazolines **4** and dihydrooxazines **5**, respectively (Scheme 1A) [15]. We also reported that an *N*-bishomoallylamide **3** (n = 3) was cyclized under the reaction conditions, but in just 30% yield. It turned out that the product of this reaction was the five-membered prolinol **7a** rather than the initially assigned isomeric seven-membered tetrahydrooxazepine **6** [16]. Subsequently, we set out to understand the *O*- versus *N*-chemoselectivity by DFT modelling, and to develop an effective synthetic protocol for the preparation of prolinols **7** in high yield (Scheme 1B). Notably, we are unaware of any reported method to achieve this specific transformation in the literature. Although, Tellitu and co-workers have reported a related preparation of indoline derivatives mediated by bis(trifluoroacetoxy)iodobenzene (PIFA) [17].

Results and Discussion

In 2019, we reported our DFT study on the cyclization of *N*-allylbenzamide (**1a**) to the 2-oxazoline **4a**, i.e., where n = 1 and Ar = Ph [18]. This work indicated that the alkene is activated by the iodine(III) species and that this triggers cyclization. Intrigued by the change in mechanism from *O*- to *N*-cyclization onto the alkene when n = 3, we modelled this reaction using DFT calculations (Scheme 2). Similarly, we concluded that the present reaction commences with activation of the olefin in **3a** by the hypervalent iodine species **8**, which is generated under the reaction conditions. The activation occurs via an associative pathway where one of the TFA ligands dissociates from **8** upon approaching the substrate and forms the intermediate **9**. The calculated $\Delta G^{\ddagger}$ value is quite high here, which could explain the low yield obtained after 16 hours. However, for the cyclization of *N*-allylbenzamide (**1a**), we found that the transition state was stabilized by 4.1 kcal·mol^{-1} by an extra molecule of trifluoroacetic acid. A similar stabilizing interaction was not identified in this case with **3a**, despite significant effort, but it cannot be ruled out. The cyclization of **9** was shown to be possible by attack of the amide at both the oxygen and the nitrogen, however, the $\Delta G^{\ddagger}$ value for the latter was lower by 2.5 kcal·mol^{-1}. This demonstrates a clear kinetic preference for formation of the five-membered ring over the seven-membered one [19]. Subsequent deprotonation of **11** leads to tertiary amide **12**.

Upon cyclization, the iodane moiety in **12** is eliminated by an intramolecular attack by the amide nitrogen to form the aziridinium **13**. Finally, ring-opening by S_N2 attack of trifluoroacetate leads to the final product **14** [20]. In this case, the kinetic pyrrolidine product is obtained due to the electron-withdrawing benzoyl group on the nitrogen atom preventing equilibration to the thermodynamic piperidine product [21]. Basic workup hydrolyzes the trifluoroacetoxy ester in **14** to alcohol **7a**. Consideration of the literature NMR data for the three possible isomeric products (i.e., pyrrolidine, piperidine, and tetrahydrooxazepine) as well as DEPT, HSQC, and HMBC data for **7a** support the assignment of the pyrrolidine structure.

The next stage of the project was to improve the yield of the reaction. We initiated our study by using our initially developed conditions using 20 mol % 2-iodoanisole and found that the reaction outcome led to variable yields of product in the range of 10–25%. Increasing the quantity of 2-iodoanisole to 150 mol % provided a reproducible 30% yield of **7a** (Table 1, entry 1). We then varied the iodoarene to see the impact on the reaction outcome. Using iodobenzene, 2-iodobiphenyl, and

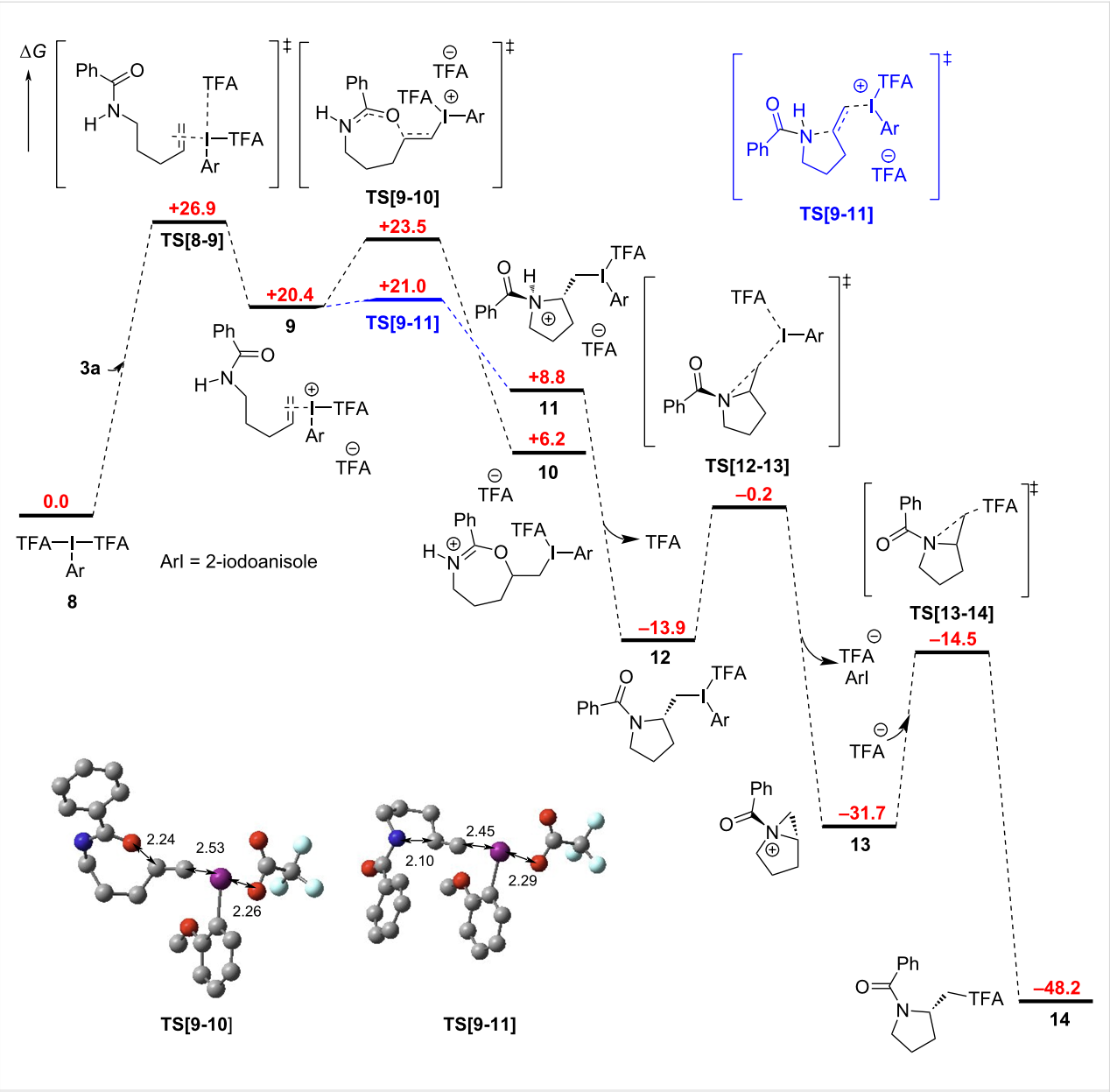

Scheme 2: Calculated mechanism for the cyclization of amide **3a** optimized at the B3LYP/ 6-31+G(d,p) level of theory with SDDall used for iodine. Solvent effects were considered using the CPCM model. All Δ*G* values are in kcal·mol^{-1}. Optimized structures are shown for the cyclization transition states (hydrogen atoms are omitted for clarity and bond lengths are given in Å).

3-iodotoluene provided slight improvements in yield (Table 1, entries 2–4). The more electron-rich 2-iodo-1,3-dimethoxybenzene led to a further increase in yield to 44% (Table 1, entry 5). 1,2-Diiodobenzene has been reported to be a superior precatalyst in intermolecular C–H aminations of arenes but only provided 40% yield in the present case [22]. 1-Iodonaphthalene led to an increase in yield to 49% (Table 1, entry 7). 1-Iodo-2,4-dimethoxybenzene afforded the highest yield of all with 59% of tertiary amide being isolated (Table 1, entry 8). Leaving the reaction to stir for an extended period led to a further increase in yield to 68% (Table 1, entry 9). Using the even more electron-rich 2-iodo-1,3,5-trimethoxybenzene only gave 45% yield (Table 1, entry 10). Our previous studies have shown that the oxidized form of 2-iodo-1,3,5-trimethoxybenzene is unstable in solution and decomposes destructively [18]. Iodoethane was also shown to be an effective reagent furnishing the product in up to 56% upon heating to 40 °C (Table 1, entries 11 and 12). It was envisaged that oxidation of iodoethane led to formation of oxidized forms of iodide by C–I-bond cleavage, therefore tetrabutylammonium iodide was utilized to see if the result could be replicated and it was (Table 1, entry 13). Finally, the reaction was shown to occur using PIFA (bistrifluoroacetoxyiodoben-

Table 1: Optimization of cyclization reaction.

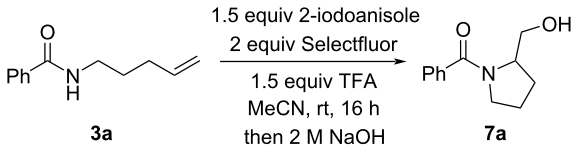

Entry	Deviation from conditions	Yield [%][a]
1	none	30
2	iodobenzene	37
3	2-iodobiphenyl	37
4	3-iodotoluene	39
5	2-iodo-1,3-dimethoxybenzene	44
6	1,2-diiodobenzene	40
7	1-iodonaphthalene	49
8	1-iodo-2,4-dimethoxybenzene	59
9	1-iodo-2,4-dimethoxybenzene, 48 h	68
10	2-iodo-1,3,5-trimethoxybenzene	45
11	iodoethane	38
12	iodoethane, 40 °C	56
13	Bu_4NI	40
14	PIFA, no selectfluor, no TFA	40

[a]The yields are for isolated compounds. TFA = trifluoroacetic acid. PIFA = bis(trifluoroacetoxy)iodobenzene.

zene), which is envisaged to be produced in the reaction mixture when using iodobenzene as reagent, and a similar yield was obtained (Table 1, entry 14 vs entry 2). The cyclization of amide **3a** did not occur in the absence of an iodine source. Other oxidants, solvents, and acids were screened but superior conditions were not discovered.

With the optimized conditions in hand, the scope of the cyclization was investigated (Scheme 3). We examined the cyclization of *para*-substituted benzamides and chloro- (**7b**), bromo- (**7c**), phenyl- (**7d**), and methoxy- (**7e**) derivatives were all isolated in moderate yields. The *ortho*-substituted derivatives **7f**, **7g**, and **7h** were also successfully prepared. Alkylamides were found to be ambiguous substrates as the acetamide **7i** and pivalamide **7j** were formed in trace quantities whereas the benzyl derivative **7k** was isolable. The enamide **7l** was not observed. Intriguingly, cyclopropyl and cyclohexyl derivatives **7m** and **7n**, respectively, were formed and isolated in moderate yields. Furyl derivative **7o** was isolated in 63% yield. Installing a geminal dimethyl group on the alkyl linker was anticipated to lead to an improvement in cyclization, however, very low conversion was observed and the product **7p** was isolated in 10% yield.

We then investigated the cyclization of *cis*-disubstituted alkene **3q** and were delighted to observe that only one diastereomer of

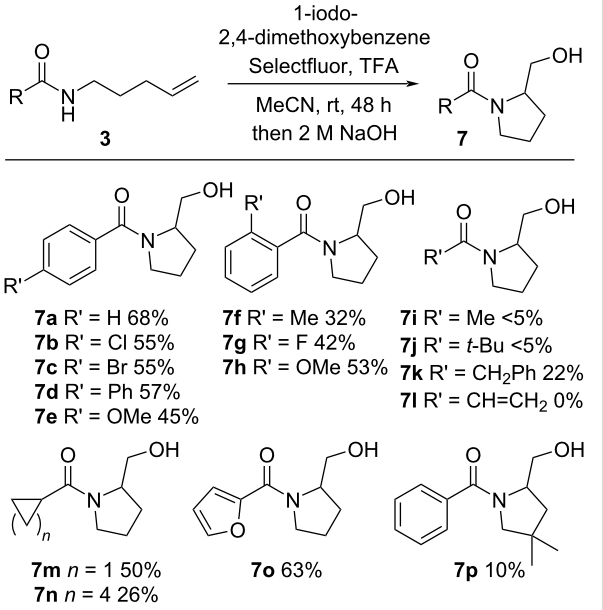

Scheme 3: Scope of cyclization reaction.

7q was formed (Scheme 4). This result is in accordance with the calculated mechanism. The more electron-rich trisubstituted alkene **3r** reacted directly with Selectfluor leading to a tertiary carbocation which was trapped by acetonitrile in a Ritter-type process to generate bisamide **15** [23]. As would be expected, one regioisomer and a 1:1 mixture of diastereomers was formed.

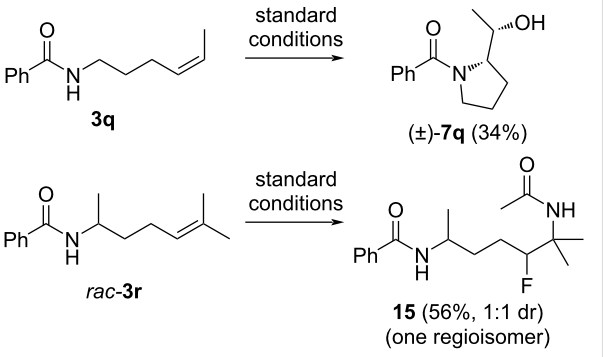

Scheme 4: Reactions of di- and trisubstituted alkene substrates.

Conclusion

We have demonstrated that a change in mechanism occurs in the cyclization of *N*-alkenylamides when increasing the chain length between the amide and the alkene. When there are one or two carbon atoms separating the functional groups, cyclization at the amide oxygen occurs to generate five- and six-membered

rings, respectively. However, when there is a three-carbon atom link, the corresponding seven-membered ring is not formed. Instead, cyclization at nitrogen occurs to generate a five-membered ring. We have performed DFT calculations to support the proposed change in mechanism and developed superior reaction conditions to effect this transformation. Finally, we have explored the substrate scope of this cyclization.

Supporting Information

Supporting Information File 1

Experimental procedures, compound characterization data, copies of NMR spectra, cartesian coordinates and energies of calculated structures.
[https://www.beilstein-journals.org/bjoc/content/supplementary/1860-5397-20-209-S1.pdf]

Acknowledgements

We thank Professor Mark Heron for his useful discussions and Dr Neil McLay for his NMR expertise. We also acknowledge Joshua Gauntlett for assistance with synthesis of some intermediates.

Funding

This study was supported by an EPSRC Doctoral Training Partnership (grant number EP/T51813X/1) held at the University of Huddersfield (K.K.), a University of Huddersfield funded Ph.D. studentship (S.B.), and by the Université de Pau et des Pays de l'Adour for access to their computer cluster.

ORCID® iDs

Jean-Marc Sotiropoulos - https://orcid.org/0000-0001-9513-3639
Wesley J. Moran - https://orcid.org/0000-0002-5768-3629

Data Availability Statement

The data that supports the findings of this study is available from the corresponding author upon reasonable request.

Preprint

A non-peer-reviewed version of this article has been previously published as a preprint: https://doi.org/10.3762/bxiv.2024.31.v1

References

1. Patriarca, E. J.; Cermola, F.; D'Aniello, C.; Fico, A.; Guardiola, O.; De Cesare, D.; Minchiotti, G. *Front. Cell Dev. Biol.* **2021,** *9,* 728576. doi:10.3389/fcell.2021.728576
2. Then, A.; Mácha, K.; Ibrahim, B.; Schuster, S. *Sci. Rep.* **2020,** *10,* 15321. doi:10.1038/s41598-020-72174-5
3. Vachan, B. S.; Karuppasamy, M.; Vinoth, P.; Vivek Kumar, S.; Perumal, S.; Sridharan, V.; Menéndez, J. C. *Adv. Synth. Catal.* **2020,** *362,* 87–110. doi:10.1002/adsc.201900558
4. Cobb, A. J. A.; Shaw, D. M.; Longbottom, D. A.; Gold, J. B.; Ley, S. V. *Org. Biomol. Chem.* **2005,** *3,* 84–96. doi:10.1039/b414742a
5. Okino, T.; Hoashi, Y.; Takemoto, Y. *J. Am. Chem. Soc.* **2003,** *125,* 12672–12673. doi:10.1021/ja036972z
6. Mauger, A. B. *J. Nat. Prod.* **1996,** *59,* 1205–1211. doi:10.1021/np9603479
7. Wakana, D.; Kawahara, N.; Goda, Y. *Chem. Pharm. Bull.* **2013,** *61,* 1315–1317. doi:10.1248/cpb.c13-00516
8. Lenci, E.; Trabocchi, A. *Symmetry* **2019,** *11,* 558. doi:10.3390/sym11040558
9. Huy, P.; Neudörfl, J.-M.; Schmalz, H.-G. *Org. Lett.* **2011,** *13,* 216–219. doi:10.1021/ol102613z
10. Perni, R. B.; Farmer, L. J.; Cottrell, K. M.; Court, J. J.; Courtney, L. F.; Deininger, D. D.; Gates, C. A.; Harbeson, S. L.; Kim, J. L.; Lin, C.; Lin, K.; Luong, Y.-P.; Maxwell, J. P.; Murcko, M. A.; Pitlik, J.; Rao, B. G.; Schairer, W. C.; Tung, R. D.; Van Drie, J. H.; Wilson, K.; Thomson, J. A. *Bioorg. Med. Chem. Lett.* **2004,** *14,* 1939–1942. doi:10.1016/j.bmcl.2004.01.078
11. Rios, R.; Ibrahem, I.; Vesely, J.; Sundén, H.; Córdova, A. *Tetrahedron Lett.* **2007,** *48,* 8695–8699. doi:10.1016/j.tetlet.2007.10.028
12. Chung, J. Y. L.; Wasicak, J. T.; Arnold, W. A.; May, C. S.; Nadzan, A. M.; Holladay, M. W. *J. Org. Chem.* **1990,** *55,* 270–275. doi:10.1021/jo00288a045
13. Yoshimura, A.; Zhdankin, V. V. *Chem. Rev.* **2016,** *116,* 3328–3435. doi:10.1021/acs.chemrev.5b00547
14. Sihag, M.; Soni, R.; Rani, N.; Kinger, M.; Kumar Aneja, D. *Org. Prep. Proced. Int.* **2023,** *55,* 1–62. doi:10.1080/00304948.2022.2113964
15. Alhalib, A.; Kamouka, S.; Moran, W. J. *Org. Lett.* **2015,** *17,* 1453–1456. doi:10.1021/acs.orglett.5b00333
16. Verbraeken, B.; Hullaert, J.; van Guyse, J.; Van Hecke, K.; Winne, J.; Hoogenboom, R. *J. Am. Chem. Soc.* **2018,** *140,* 17404–17408. doi:10.1021/jacs.8b10918
17. Correa, A.; Tellitu, I.; Domínguez, E.; SanMartin, R. *J. Org. Chem.* **2006,** *71,* 8316–8319. doi:10.1021/jo061486q
18. Butt, S. E.; Das, M.; Sotiropoulos, J.-M.; Moran, W. J. *J. Org. Chem.* **2019,** *84,* 15605–15613. doi:10.1021/acs.joc.9b02623
19. Casadei, M. A.; Galli, C.; Mandolini, L. *J. Am. Chem. Soc.* **1984,** *106,* 1051–1056. doi:10.1021/ja00316a039
20. O'Brien, P.; Towers, T. D. *J. Org. Chem.* **2002,** *67,* 304–307. doi:10.1021/jo010824e
21. Hayashi, K.; Kujime, E.; Katayama, H.; Sano, S.; Shiro, M.; Nagao, Y. *Chem. Pharm. Bull.* **2009,** *57,* 1142–1146. doi:10.1248/cpb.57.1142
22. Lucchetti, N.; Scalone, M.; Fantasia, S.; Muñiz, K. *Adv. Synth. Catal.* **2016,** *358,* 2093–2099. doi:10.1002/adsc.201600191
23. Stavber, S.; Pecan, T. S.; Papež, M.; Zupan, M. *Chem. Commun.* **1996,** 2247–2248. doi:10.1039/cc9960002247

BEILSTEIN JOURNAL OF ORGANIC CHEMISTRY

Recent advances in transition-metal-free arylation reactions involving hypervalent iodine salts

Ritu Mamgain, Kokila Sakthivel and Fateh V. Singh*

Review

Open Access

Address:
Department of Chemistry, SAS, Vellore Institute of Technology Chennai, Chennai-600 127, Tamil Nadu, India

Email:
Fateh V. Singh* - fatehveer.singh@vit.ac.in

* Corresponding author

Keywords:
arylation reaction; diaryliodonium salts; electrophilic arylation reagent; metal-free arylation; rearrangement reaction

Beilstein J. Org. Chem. **2024,** *20,* 2891–2920.
https://doi.org/10.3762/bjoc.20.243

Received: 11 June 2024
Accepted: 15 October 2024
Published: 13 November 2024

This article is part of the thematic issue "Hypervalent halogen chemistry".

Guest Editor: J. Wencel-Delord

Abstract

Diaryliodonium salts have become widely recognized as arylating agents in the last two decades. Both, symmetrical and unsymmetrical forms of these salts serve as effective electrophilic arylating reagents in various organic syntheses. The use of diaryliodoniums in C–C and carbon–heteroatom bond formations, particularly under metal-free conditions, has further enhanced the popularity of these reagents. In this review, we concentrate on various arylation reactions involving carbon and other heteroatoms, encompassing rearrangement reactions in the absence of any metal catalyst, and summarize advancements made in the last five years.

Introduction

The chemistry of hypervalent iodine compounds is well-established and they are prevalent as oxidants and electrophilic reagents in organic conversions [1-3]. They have gained significant attention due to their high reactivity and ability to carry out various useful transformations under mild, eco-friendly reaction conditions [4-11]. Various review articles [12-26] and books [27,28] have appeared on the chemistry of hypervalent iodine compounds. In the past two decades, diaryliodonium salts (DAIS), a versatile category of hypervalent iodine compounds, have seen significant progress in hypervalent iodine chemistry. Their efficiency and environmentally friendly characteristics have positioned DAIS as next-generation arylation reagents [29,30]. Other than aromatic electrophiles in aryl-transfer processes, DIAS are frequently employed as photoinitiators for cationic polymerizations [31-33], Lewis acids [34], oxidants [35,36] and in the field of macromolecular chemistry [37,38]. Additionally, biological activity is also exhibited by iodonium salts, often due to their capability to function as radical initiators.

The use of diaryliodonium salts as efficient electrophilic arylating reagents in a wide range of organic transformations is due to their unique features such as solid-state nature, excellent stability, and the presence of a robust leaving group [39-42].

They offer several advantages over traditional reagents, including low toxicity, high reactivity, and excellent selectivity [43] under simple reaction conditions. The distinctive reactivity of DIAS enables the smooth arylation of various carbon and heteroatom nucleophiles under gentle conditions, with or without the use of transition metals [44]. Thus, they address both the financial and environmental challenges associated with organic synthesis by acting as environmentally benign substitutes for costly organometallic catalysts and heavy-metal-based oxidants.

Diaryl iodide salts consist of two aryl groups attached to an iodine atom and an associated "anion". X-ray studies revealed that these iodine(III) compounds typically have a T-type structure **1** (Figure 1). In solution, they dissociate into Ar_2I^+ and X^- counterions **2**, with the degree of dissociation influenced by the solvent and the nature of X^- [45,46]. Anions like tetrafluoroborate, hexafluorophosphate, and trifluoromethanesulfate are commonly used in DAIS due to their good solubility and weak nucleophilicity. If the two aryl groups (Ar^1 and Ar^2) in DAIS are different, they are termed unsymmetric diaryliodonium salts **3**. The chemoselectivity of the product is primarily determined by the steric hindrance and electrophilicity of the aryl groups [17]. When the two aryl groups form a cyclic structure with a central iodine atom, they are referred to as cyclic diaryliodonium salts **4** (Figure 1). Cyclic DAISs are predominantly found in simple five to seven-membered cyclic compounds [47].

Arylation reactions using diaryliodonium salts can occur through four distinct mechanisms. First, the arylation can occur under metal-free conditions, involving the formation of a three-membered ring transition state through ligand coupling, leading to the formation of the Nu–Ar product and aryl iodide [21]. Second, the arylation can take place in the presence of a metal catalyst via oxidative addition, followed by reduction elimination [48,49]. Thirdly, it proceeds through a ligand-coupled arylation which involves a five-membered transition state to yield the respective arylation product [50,51]. Lastly, arylation can occur through single-electron transfer (SET), where a cation radical obtained from aromatic hydrocarbons with high electron density yields the desired arylated product [52]. In this review article, we will provide a comprehensive overview of arylation of carbon and heteroatom substrates via diaryliodonium salts in metal-free conditions. This review emphasizes the significance and potential of DIASs in contemporary organic chemistry.

Review

C-Arylation

Over the past decade, there has been a surge of interest in metal-catalyzed C-arylations utilizing diaryliodonium salts, marked by significant contributions, notably from research teams led by Sanford [53] and Gaunt [54]. The synthesis of carbon–carbon bonds through metal-free approaches serves as a valuable complement to transition-metal-catalyzed couplings. This is particularly significant as it circumvents the use of costly and hazardous metals and ligands which are commercially not available.

In order to obtain a variety of synthetically desirable tetra-substituted α-aryl-α-fluoroacetoacetamides **7**, Zaheer et al. disclosed a straightforward, metal-free technique for the α-arylation of α-fluoroacetoacetamides **5** utilising unsymmetric DIAS **6**. Various α-fluoroacetoacetamides **5** with electronically different aliphatic, aryl ring, and heterocyclic substitutions were discovered to be easily arylated using this method. The products were obtained within 30 minutes in the presence of Cs_2CO_3 as shown in Scheme 1. The substrate scope exhibits that on using electron-deficient diaryliodonium salts as an arylating agent, α-fluoroacetamides **8** were obtained in moderate to good yields through a spontaneous arylation/deacylation cascade. The deacylation reaction is considered due to the presence of fluorine and a newly installed electron-deficient aryl group on α-carbon which increases electrophilicity of the α-carbon center [55].

The proposed reaction mechanism (Scheme 2) begins with the formation of one of two potential iodine intermediates, labeled as **I** or **II**. These intermediates arise upon binding of the enolate molecule to iodine either through a carbon–iodine or an oxygen–iodine bond. Both intermediates, **I** and **II**, are in rapid equilibrium with each other and further undergo two different types of reactions: [1,2]-ligand coupling and [2,3]-rearrangement (Scheme 2). Either of these reactions leads to the formation of the desired arylated α-aryl-α-fluoroacetoacetamides **7**.

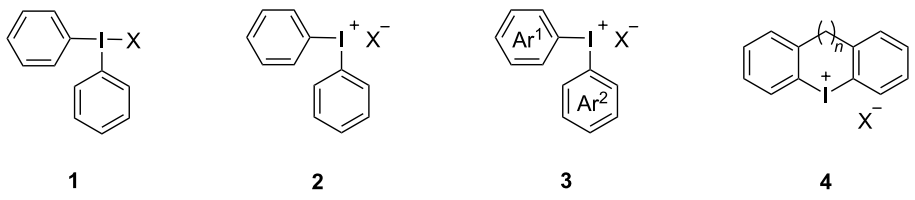

Figure 1: Various structures of iodonium salts.

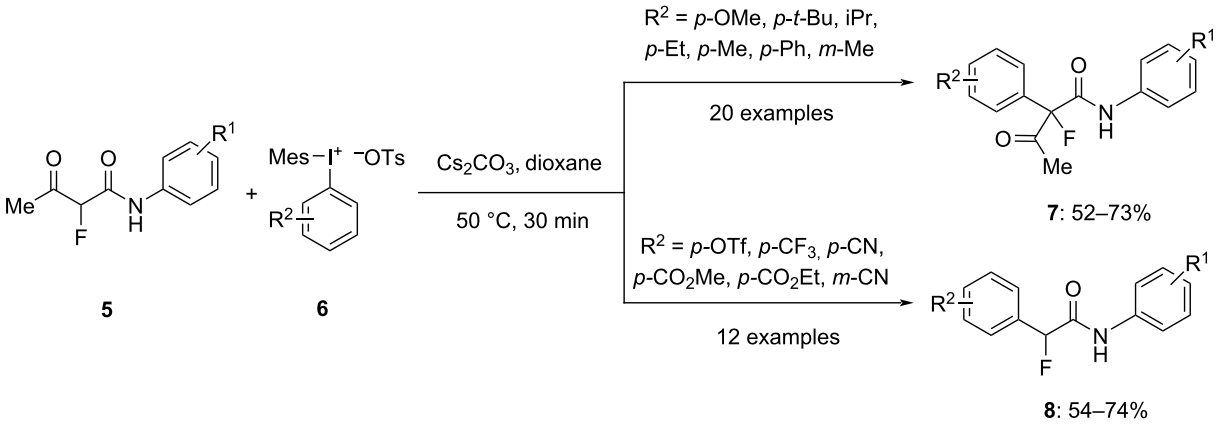

Scheme 1: Arylation of α-fluoroacetoacetamides **5** to α-aryl-α-fluoroacetoacetamides **7** and α-fluoroacetamides **8** using diaryliodonium salts **6**.

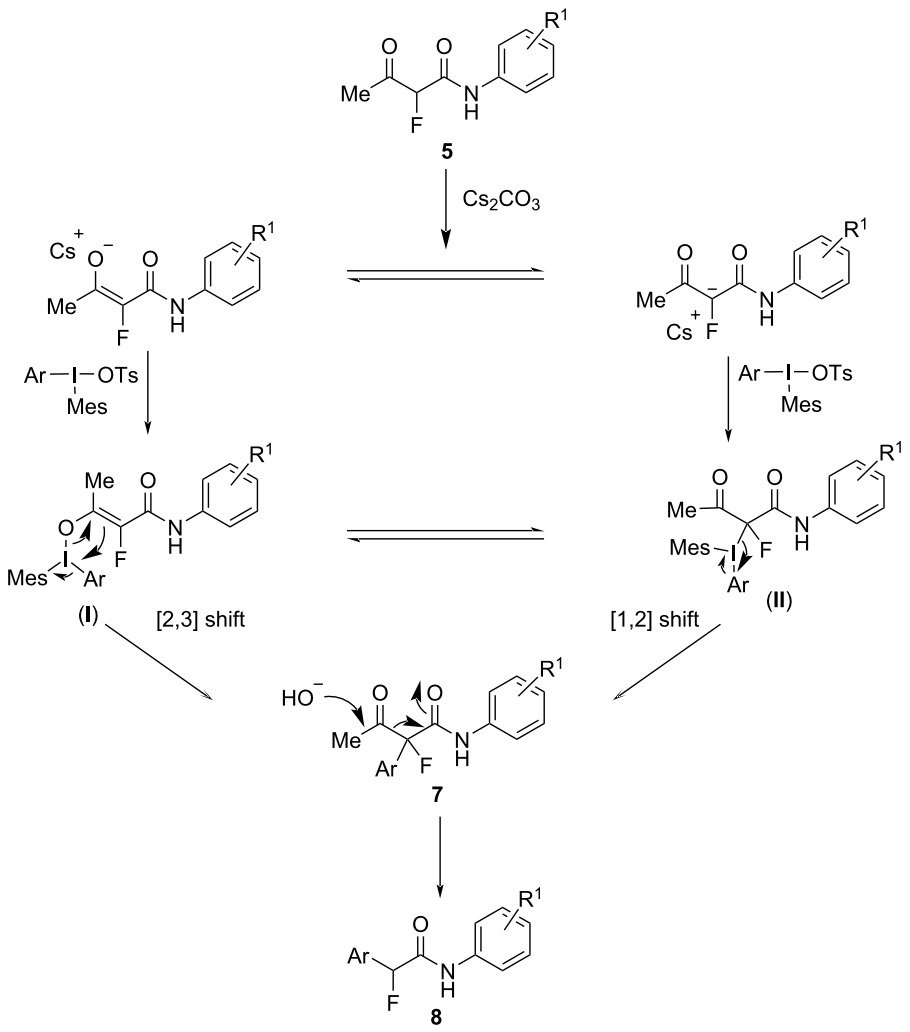

Scheme 2: Proposed mechanism for the arylation of α-fluoroacetoacetamides **5** to α-aryl-α-fluoroacetoacetamides **7** and α-fluoroacetamides **8**.

The tetrasubstituted fluorocarbon center becomes more electrophilic in the presence of an electron-deficient aryl (Ar) group. This increased electrophilicity facilitates a base-mediated deacylation reaction, resulting in arylfluoroacetamides **8** as final products.

Further, Zaheer and group developed an α-arylation of synthetically valuable α-fluoro-α-nitroacetamides (**9**, R = NO_2, Scheme 3) under gentle conditions to form a quaternary benzylic fluorocarbon center. The protocol was found to be effective for the α-arylation of α-cyano-α-fluoroacetamides (**9**, R = CN), too. Aryl(mesityl)iodonium salts **6** (which are unsymmetrical diaryliodonium salts) were used as hypervalent iodine salts in both reactions. To achieve the C(sp^3)-arylation of the α-nitro derivative of compounds **9** within 2 h to yield products **10**, K_2CO_3 as base and toluene as solvent were required (Scheme 3). On the other hand, for the α-arylation of the α-cyano derivative of compounds **9**, *t*-BuOK as base and THF as a solvent were useful to yield the products in a short reaction time (30 min). All the products with a wide range of electronically varied arenes were attained in good to excellent yields [56]. Additionally, the same reaction was further explored by using α-fluoro-α-nitrosulfonylmethanes as starting material under modified reaction conditions to yield the arylated α-fluoronitrosulfonylmethane [57]. Phenyl(mesityl)iodonium salt was employed to achieve the fluorinated products having a tetrasubstituted benzylic carbon center in good to excellent yields. The strategy was also used for the synthesis of α-arylated α-fluoro(arylsulfonyl)acetonitriles in good yield.

In a recent study, Dohi et al. achieved the arylation along with decarboxylation of α,α-difluoro-β-keto acid esters **11** with the help of aryl(TMP)iodonium tosylates **12** in toluene at 100 °C to yield α,α-difluoroketones **13** in excellent yield (Scheme 4). The reaction proceeds via ligand exchange between the fluorinated carboxylate and the tosylate anion of the hypervalent iodine salt, subsequently leading to decarboxylative C–C coupling. Notably, this method achieves the incorporation of two fluorine atoms in the benzyl position without resorting to hazardous fluorination reagents, transition-metal catalysts, or organometallic compounds. The utility of this reaction is underscored by the successful conversion of various α,α-difluoromethyl ketone groups into corresponding esters, amides, and difluoromethyl groups [58].

In 2021, Nilova and colleagues outlined an approach for the synthesis of highly hindered 1,2,3,4-tetrasubstituted benzenoid rings **15** using arynes generated from **6** on reacting with arynophiles **14** (Scheme 5) [59]. The reaction is unique due to its ability to functionalize position 3, despite its greater steric

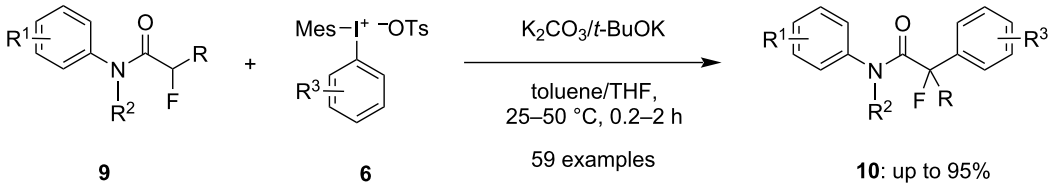

Scheme 3: α-Arylation of α-nitro- and α-cyano derivatives of α-fluoroacetamides **9** employing unsymmetrical DAISs **6**.

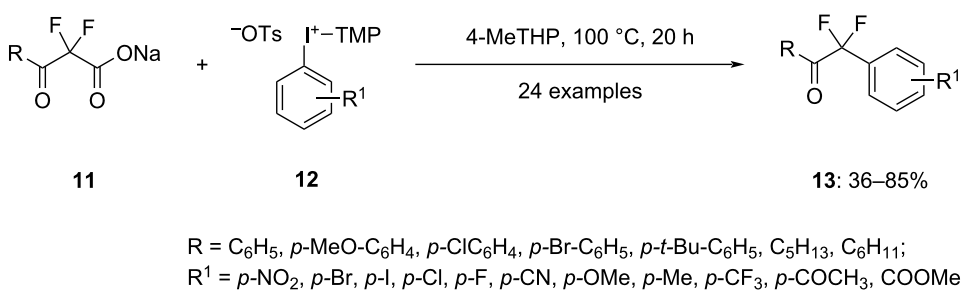

Scheme 4: Synthesis of α,α-difluoroketones **13** by reacting α,α-difluoro-β-keto acid esters **11** with aryl(TMP)iodonium tosylates **12**.

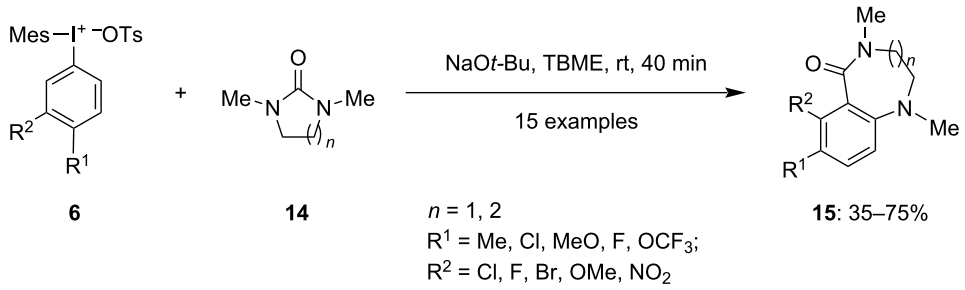

Scheme 5: Coupling reaction of arynes generated by iodonium salts **6** and arynophiles **14** for the synthesis of tetrasubstituted arenes **15**.

hindrance compared to position 5. The process involves deprotonation at the 3-position of the aryl(Mes)iodonium salts, followed by exit of a leaving group from position 4, and then regioselective vicinal functionalization of the generated aryne. The method's compatibility with halide-substituted aryl compounds enhances its versatility and practicality. Moreover, the completion of reaction within a mere 40 minutes at room temperature underscores its efficiency and effectiveness as a synthetic approach.

Furthermore, a transition-metal-free arylation of quinoxalines **17** and quinoxalinones **19** via aryl radicals was discussed by Li and co-workers in 2022. In this report the aryl radicals were generated by planetary ball milling of diaryliodonium salts **16** at a frequency of 35 Hz in the presence of the piezoelectric material $BaTiO_3$ (size < 4 μm). The results were obtained within 2 h when triethylamine was used as a base (Scheme 6) [60]. Both, symmetrically and unsymmetrically substituted diaryliodonium salts were employed for the reaction and it was revealed that in unsymmetrical diaryliodonium salts the transfer of the aryl group with the relatively lower electron density and less steric hindrance was favoured. A range of electron-rich and electron-deficient substituents positioned *para* to the aryl ring in the diaryliodonium salts were found to be well tolerated in the reaction. Quinoxalines substituted at various positions resulted in the corresponding arylation products **18** in moderate yields. Under similar reaction conditions various substituted quinoxalinones yielded products **20** in moderate to good yields. The $BaTiO_3$ used in the reaction could be easily recycled just by washing it with ethanol, retaining its catalytic activity for arylation up to three cycles without any compromise. Thus, this procedure could be considered economic as well as environment-friendly.

In 2019, Kalek and co-workers reported the regioselective C–H arylation of 2-naphthols **21** by using iodonium salts **16** as the source of the aryl group (Scheme 7) [61]. Through optimization, it was determined that the presence of Na_2CO_3 as base and cyclohexane as solvent facilitated the C–C cross-coupling reaction. The products were obtained in satisfactory yields using various diaryliodonium salts regardless of their differing counter-anions. A range of 2-naphthol substrates, including those bearing alkyl and aryl groups, halogens, trimethylsilyl, and protected hydroxy at positions 6 and 7, exhibited good

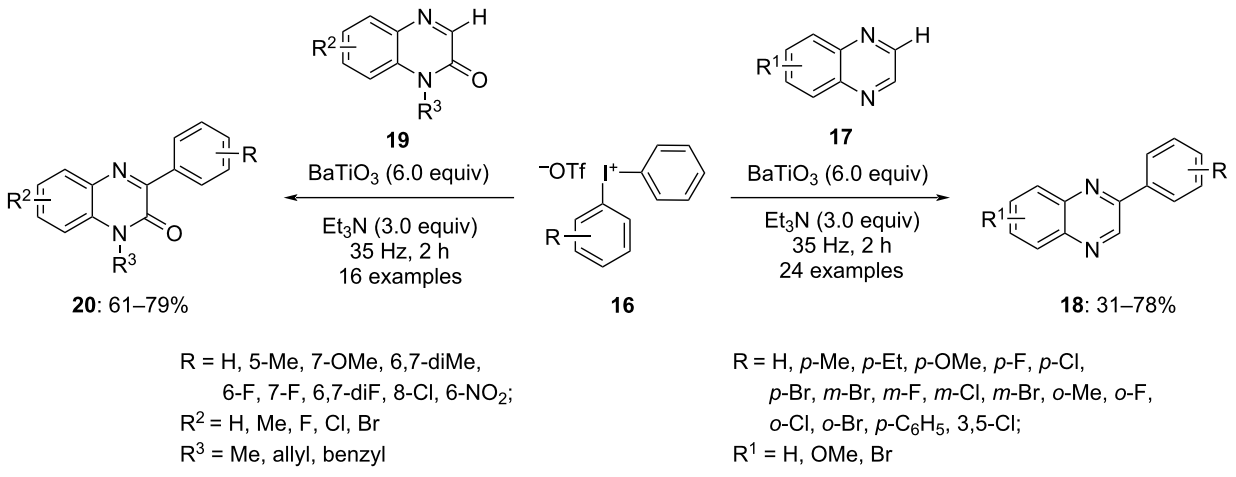

Scheme 6: Metal-free arylation of quinoxalines **17** and quinoxalinones **19** with DAISs **16**.

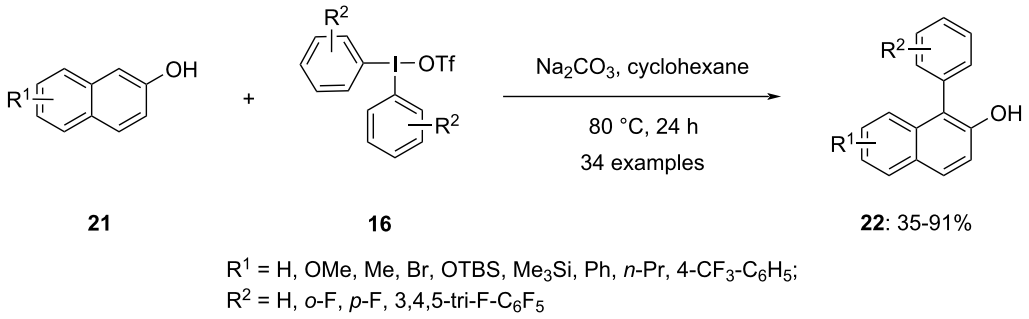

Scheme 7: Transition-metal-free, C–C cross-coupling of 2-naphthols **21** to 1-arylnapthalen-2-ols **22** employing diaryliodonium salts **16** as the aryl source.

tolerance. However, the reaction with 1-naphthol did not yield positive results. Notably, the efficiency of the cross-coupling reaction was observed to increase with the transfer of electron-poor aryl groups from the hypervalent iodine salt. Thus, electron-withdrawing substituents such as trifluoromethyl, *m*-chloro, and fluorine on the aryl group promoted efficient coupling.

Moreover, C–C bond formation was reported by Chen and colleagues in 2020 via the arylation of vinyl pinacol boronates **23** by using diaryliodonium salts **16** to yield *trans*-arylvinylboronates **24** in the absence of a metal catalyst [62]. The optimized reaction conditions involve the reaction of substituted diaryliodonium salts **16** with different substituted vinyl pinacol boronates **23** in dichloromethane as solvent at 100 °C in a sealed tube in the presence of a wet inorganic base (Scheme 8). Both K_2CO_3 and Li_2CO_3 were found to be compatible with the reaction, and it was observed that no product was obtained in the absence of a base. Additionally, the presence of 40 equivalents of water proved to be crucial for the reaction, as altering the amount of water significantly impacted the product yield, indicating the importance of water in the reaction mechanism. A diverse range of functionalized diaryliodonium salts, including di- and trisubstituted ones, were well tolerated in the reaction, providing products **24** with good stereoselectivity in moderate to good yields. Moreover, the reaction was successfully conducted with various substituted vinyl pinacol boronates and di(4-tolyl)iodonium triflate, resulting in moderate to good yields of the corresponding products. The vinyl boronates obtained from the aforementioned reaction were subsequently subjected to a Suzuki coupling with the remaining aryl iodides obtained from **16** in the presence of a palladium catalyst. This step facilitated the formation of functionalized olefins, showcasing an efficient utilization of aryliodonium salts in the process.

Later in the same year, Song and colleagues reported a protocol for the efficient synthesis of 2-aryl-substituted quinolines **27** and pyridine *N*-oxides **29** [63]. This reaction involved the selective arylation at the C2 position of quinoline *N*-oxides and pyridine *N*-oxides, utilizing hypervalent iodine salts as the arylation reagents. The reaction was facilitated by visible light in conjunction with a photocatalyst. The absence of either the photocatalyst or light resulted in only trace amounts of the product, underscoring their essential roles in product formation. Optimized conditions comprised the reaction of the quinoline *N*-oxides **25** (1 equiv) with diaryliodonium tetrafluoroborates **26** (2 equiv) as the arylating agent, 1,4-benzoquinone (BQ) as an additive (2 equiv), the photocatalyst eosin Y (10 mol %), and

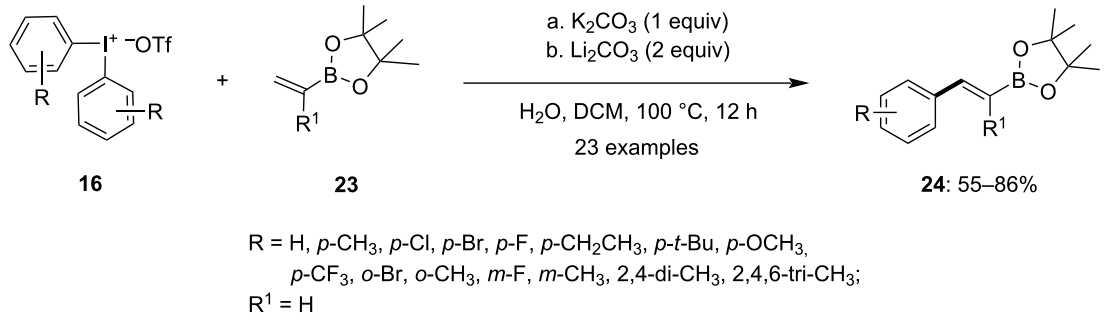

Scheme 8: Arylation of vinyl pinacol boronates **23** to *trans*-arylvinylboronates **24** in presence of hypervalent iodine salt **16**.

Cs_2CO_3 (1 equiv) as the base in methanol under a nitrogen atmosphere, with 5 W LEDs irradiation for 3 days (Scheme 9). Various substituted quinone *N*-oxides yielded the corresponding products in satisfactory to moderate yields. Notably, electron-withdrawing groups generated higher yields compared to electron-donating groups. The reaction exhibited high selectivity, with substitution at the C3 position not impeding the reaction. Different substituted diaryliodonium tetrafluoroborates were also investigated, yielding good product yields. The above protocol for the arylation of pyridine *N*-oxides **28**, resulted in corresponding products in moderate to good yields. The reaction conditions remained consistent, except $K_2S_2O_8$ was found to be a superior additive compared to BQ. The reaction exhibited good tolerance even towards strong electron-withdrawing groups.

A control experiment was conducted to investigate the reaction mechanism by adding 2 equivalents of TEMPO to the reaction mixture. The absence of the desired product indicated the involvement of a radical pathway in the process. The proposed reaction mechanism begins with the activation of eosin Y by visible light from 5 W blue LEDs, transitioning it to its excited state, eosin Y*. This excited state further undergoes oxidation via a single-electron-transfer (SET) reaction with Ar_2IBF_4 **26**, producing eosin Y^+ and a phenyl radical **30** (Scheme 10). The radical intermediate **30** selectively binds to the C2 position of either quinoline or pyridine *N*-oxide, forming intermediate **I**. Furthermore, intermediate **I** subsequently undergoes another SET reaction, resulting in intermediate **II** and the regeneration of the photocatalyst. Intermediate **II** undergoes deprotonation, facilitated by the presence of Cs_2CO_3 as base, to yield the final products **27** or **29**. Additives like BQ likely assist in the deprotonation of intermediate **II** to produce final products **27**, while $K_2S_2O_8$ aids in the oxidation of the photocatalyst in the case of pyridine *N*-oxide.

In another photoinduced reaction procedure, Murarka et al. reported the formation of aryl radicals from a tetrameric electron donor–acceptor (EDA) complex. The complex is formed of triphenylphosphine, sodium iodide and *N*,*N*,*N*,*N*-tetramethylethylenediamine (TMEDA) with diaryliodonium reagents (DAIRs) [64]. This activates DAIRs **16** to generate an aryl radical which is utilized in the C–H arylation of various heterocycles **31** to yield the corresponding heteroaryl–aryl compounds **32** in moderate to good yield. The use of blue LEDs (456 nm), nitrogen atmosphere, and HFIP/H_2O 4:1 solvent mixture improved the yield of the product by up to 90%. Various substituted azauracils were used to study the reaction and it was observed that different substituted N2/N4 azauracils were easily converted to the corresponding products in good to excellent yield. Furthermore, diverse DAIRs were subjected to the reaction which again provided the desired products **32** in moderate

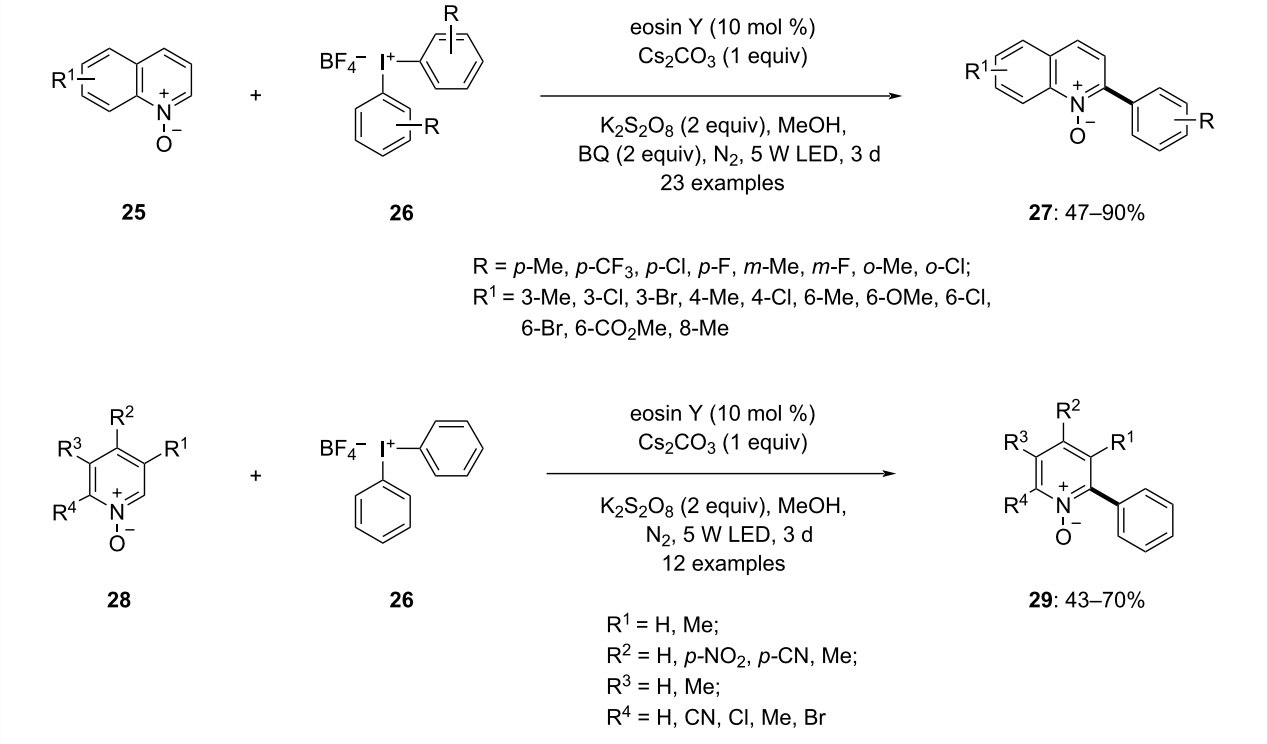

Scheme 9: Light-induced selective arylation at C2 of quinoline *N*-oxides **25** and pyridine *N*-oxides **28** in the presence of **26**.

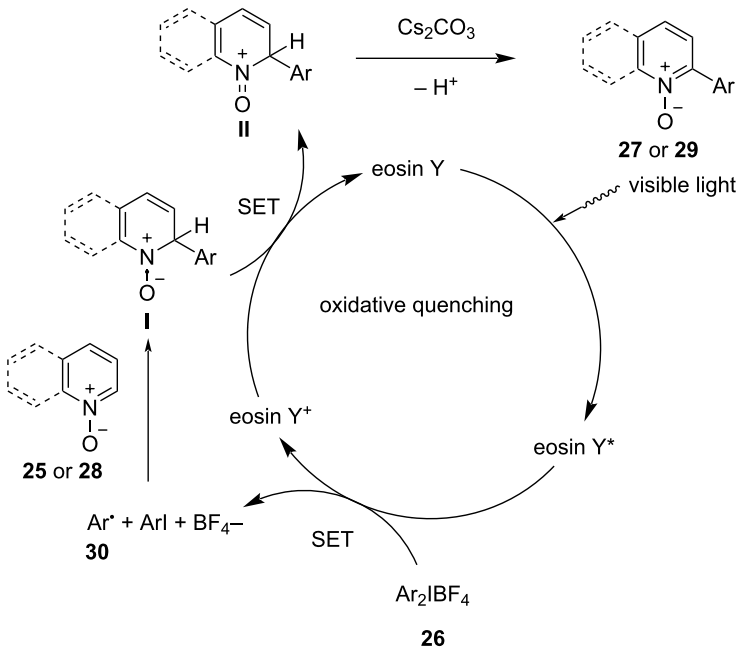

Scheme 10: Plaussible mechanism for the light-induced selective arylation of *N*-heterobiaryls.

to excellent yield (Scheme 11). The study suggests that the unsymmetrical DAIRs transfer the aryl ring which is less sterically hindered. The reaction conditions enabled to furnish results with various aromatic and nonaromatic heterocycles and *N*-heterocyles. The reaction was able to facilitate late-stage diversification of drug molecules such as nimesulide and gemfibrozil to corresponding products. The radical path was considered for the reaction mechanism as on adding TEMPO as radical scavenger the radical trapping adduct was detected by HRMS.

Simultaneously with the above work, Murarka and co-workers also reported an organophotoredox-catalyzed stereoselective allylic arylation method for Morita–Baylis–Hillman (MBH) acetates using a variety of diaryliodonium triflates [65]. The reaction was carried out with MBH acetate **33** and diphenyliodonium triflate **16** in the presence of different photocatalysts and bases. Methylene blue trihydrate (MB·3H_2O) was identified as a highly active photosensitizer and DIPEA was effective as a base (Scheme 12). The reaction yielded the *E*-isomers in a solvent mixture of methanol/water 5:1 under blue LED light (467 nm) irradiation in good yields. Various DAIRs substituted at different positions were found to be suitable for the reaction giving the respective products in moderate to good yield. Additionally, unsymmetrical DAIRs showed a preference for transferring an electron-poor and sterically less

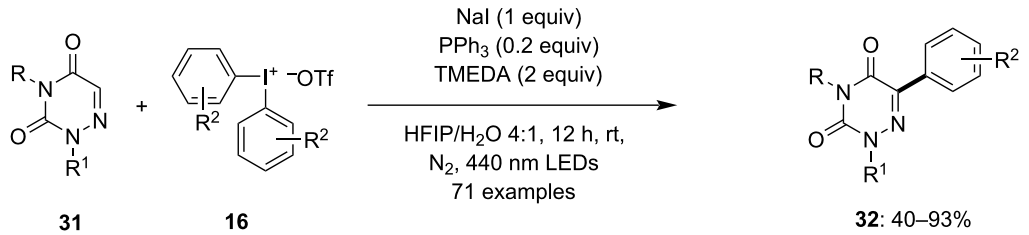

R = Me, Et, allyl, propargyl, CH_2COPh, CH_2COOEt;
R^1 = H, Bn, *p*-$BrC_6H_4CH_2$, $CH_2C_{10}H_7$, CH_2CHCH_2;
R^2 = 4-Me, 4-*t*-Bu, 4-OMe, 4-F, 4-Cl, 4-Br, 4-CF_3, 4-OCF_3, 4-CO_2Me, 3-Me, 3-Cl, 3-Br, 3-CN, 2-Me, 2-Cl

Scheme 11: Photoinduced arylation of heterocycles **31** with the help of diaryliodonium salts **16** activated through donor–acceptor complex formation.

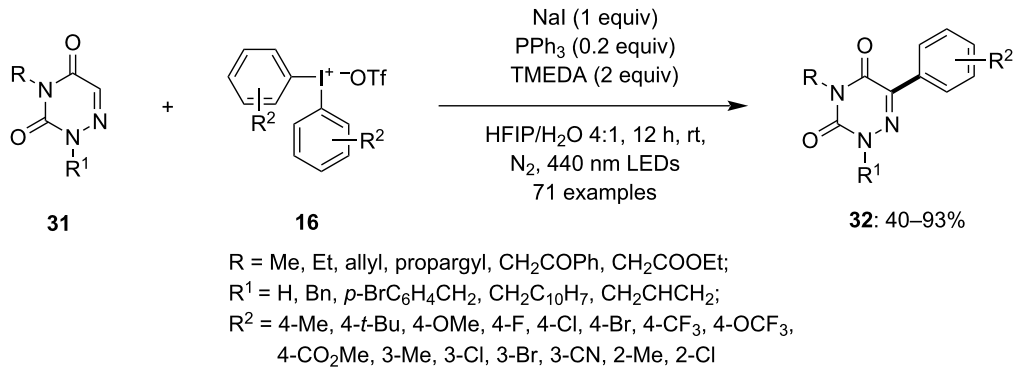

Scheme 12: Arylation of MBH acetates **33** with DIPEA and DAIRs **16**.

hindered aryl ring. The scope of MBH acetates was further explored, demonstrating compatibility with a wide range of substituted aromatic ethyl acrylates and various substituents on the aromatic ring. Additionally, a variety of substituted esters, ketones, and nitriles were found to be compatible with the reaction.

Additionally, the same approach was used for the aryl sulfonylation. Trisubstituted allylic sulfones **35** were synthesized by reacting MBH acetate **33** and diphenyliodonium triflates **16** using an optimal sulfur dioxide surrogate, 1,4-diazabicyclo[2.2.2]octane bis(sulfur dioxide) (DABSO, Scheme 13). The *Z*-isomer of the desired products was obtained by optimizing the reaction conditions. The involvement of radicals in both the arylation and aryl sulfonylation was confirmed as no product was found when carrying out the reaction in the presence of radical scavengers. Stern–Volmer studies indicated a significant fluorescence emission quenching of methylene blue by DIPEA, suggesting a reductive quenching of methylene blue during the reaction. Experiments involving variations in light exposure and quantum yield established the need for continuous irradiation and eliminated the possibility of a radical chain mechanism for the reaction.

Recently in 2023, Yadav and colleagues demonstrated that diaryliodonium salts are effective for arylating and cyclizing trifluoromethylated acrylamides **36** under environmentally friendly conditions [66]. When the reaction mixture of acrylamides **36** and diaryliodonium tetrafluoroborates **26** dissolved in water was irradiated with light of 390 nm wavelength, the desired oxindole products **37** were obtained in good yields (Scheme 14). The reaction was notably more successful with CF_3-acrylamide than with CH_3-acrylamide, likely because the former dissolves more readily in water. The reaction tolerated diverse substitutions at different positions on the aryl groups of acrylamides **36** and diaryliodonium salts **26**. Both electron-withdrawing and electron-donating substituents at the *para*-position of the *N*-arylacrylamide led to good yields. In cases of *meta*-substitution, a mixture of C6 and C4-substituted oxindole products were obtained, whereas *ortho*-substitution resulted in the desired oxindoles in moderate yields. Nitrogen substitution was also found to be tolerable in the reaction. Interestingly,

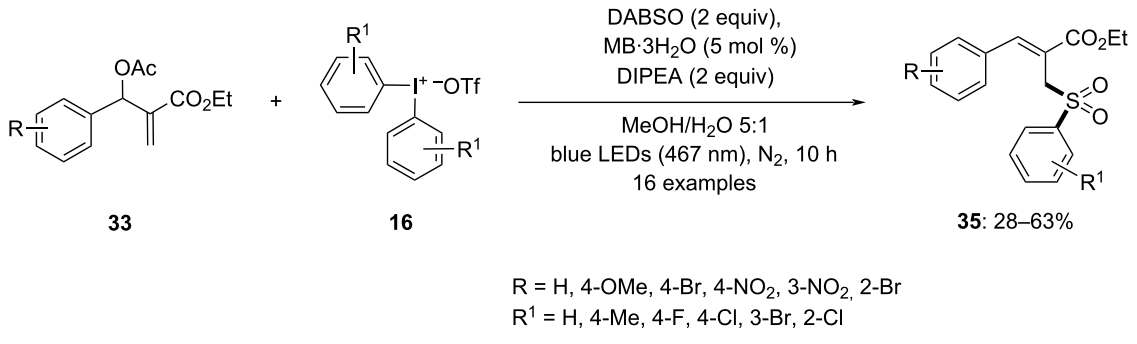

Scheme 13: Aryl sulfonylation of MBH acetates **33** with DABSO and diphenyliodonium triflates **16**.

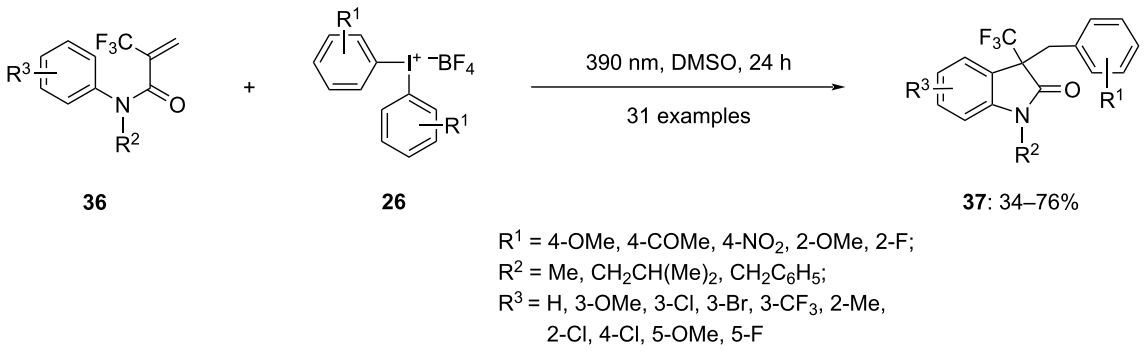

Scheme 14: Synthesis of oxindoles **37** from *N*-arylacrylamides **36** and diaryliodonium salts **26**.

substituting the *para*-position of the aryliodonium salts with an electron-donating group resulted in a moderate product yield, while electron-withdrawing groups led to decreased yields of the desired product.

N-Arylation

Nitrogen-containing heteroaromatic compounds serve as crucial scaffolds in pharmaceuticals. Therefore, the synthesis of *N*-substituted heteroaromatic derivatives under mild and environmentally friendly conditions is highly valued. The use of electrophilic diaryliodonium salts for nitrogen arylation has been investigated. Working on this Li and Jiang, created an effective ball-milling process for the *N*-arylation of amines **38** with the assistance of diaryliodonium salts **16** (Scheme 15) [67]. The arylation of an amino group or nitrogen heterocycle occurred effectively when the reaction is performed under solvent-free conditions or when a minimal quantity of water was used as a solvent in the presence of a base. The ball-milling method efficiently simplified the reaction process because, in contrast to typical solution methods, it may realize product formation without being affected by the solubility of the substrate and other additives. An efficient conversion was detected when the substrate contains electron-rich functionalities. In contrast, the yield dropped notably when the amines were substituted with electron-deficient functionalities. In addition, asymmetric diaryliodonium salts were examined, and the transfer of the aryl group with a less hindered portion is observed. The mechanism revealed the reaction undergoes the homolytic cleavage of the diaryliodonium salt to produce an iodoaryl radical cation, which further reacts with the amine to acquire the corresponding diaryl amines. Moreover, a similar reaction tried with a copper catalyst afforded nearly better results for the arylated products.

In 2022, Linde et al., demonstrated a conventional approach for achieving arylations of nitrogen- and oxygen nucleophiles via S_NAr reaction, using *o*-fluorinated diaryliodonium salts **40**, which enabled access to a greater range of compounds (Scheme 16) [68]. The novel iodine(III) intermediate was generated through nucleophilic substitution of a heteroatom nucleophile, which initiated the reaction. A subsequent aryl migration from the iodine to the heteroatom resulted in the formation of the arylated nucleophile. In addition to accepting a wide variety of protective and functional groups, the method creates products with an iodine substituent that is easily accessible for product derivatization. Moreover, it is a convenient methodology for both *N*-arylation and *O*-arylation. The arylation of amines **38** was achieved in acetonitrile as solvent, whereas the arylation of ammonia was achieved by using ethyl acetate as solvent along with potassium carbonate as a base. Likewise, water was arylated using cesium carbonate as a base.

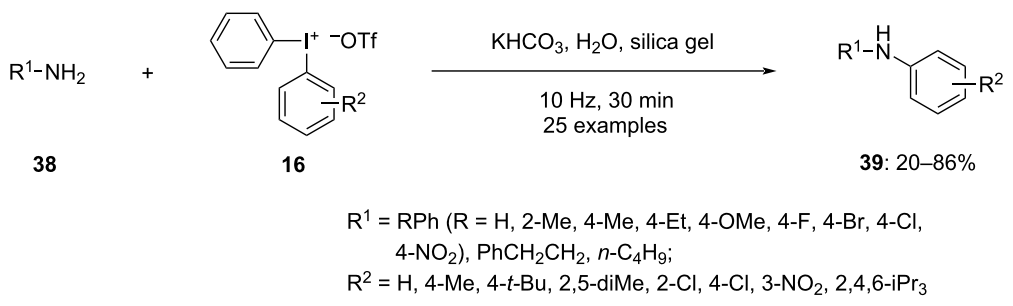

Scheme 15: Mechanically induced *N*-arylation of amines **38** using diaryliodonium salts **16**.

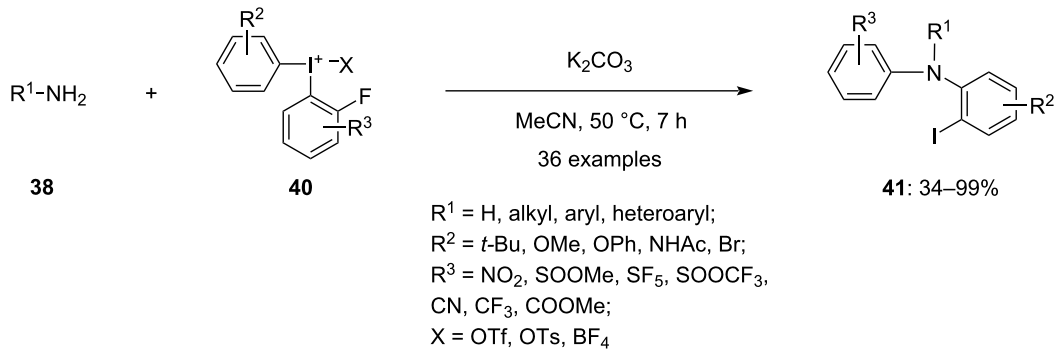

Scheme 16: *o*-Fluorinated diaryliodonium salts **40**-mediated diarylation of amines **38**.

The *N*-arylation reactions were performed under strict anhydrous conditions.

The reported mechanistic hypothesis (Scheme 17) suggests that the reaction initiates with an S_NAr at the *ortho*-carbon, forming a Meisenheimer complex **I** and a novel iodine(III) intermediate **II**. This type of reactivity is unprecedented, as past reactions between nucleophiles and diaryliodonium salts usually lead to a reduction of iodine(III) to iodine(I). Intermediate **II** then undergoes an intramolecular aryl migration, yielding the diarylated products **41**, analogous to the known iodoniumphenolate reactions that produce diaryl ethers.

The same research group meliorated the *N*-arylation of aliphatic cyclic amines with the same fluorinated diaryliodonium salts **40** (Scheme 18) [69], which however, does not produce the diarylated compounds. The intramolecular aryl migration from the iodine to the nitrogen leads to a quaternary ammonium ion intermediate **A**. Consequently, a nucleophilic ring opening of cyclic amine in **42** occurred via cleavage of the strong C–N bond. The ring opening incorporated nitrogen, oxygen, sulfur, carbon, and halogen-containing nucleophiles and their derivatives. The substrate scope was examined with numerous aryl groups on iodonium salts **40** and the progress of aryl migration happens fruitfully by considering electronic factors like steric hindrance. The ring opening proceeded smoothly when nucleophiles with higher nucleophilicity are used yielding up to 99% of the desired products **43**.

The *N*-arylation of amino acid esters **44** was established with the utility of substituted phenyl(anisyl)iodonium triflate salts **45** (Scheme 19) [70]. According to the screening studies, a mixture of enantiomers was obtained, with one enantiomer predominating (95 to >98% ee) under the optimized conditions. The phenyl with electron-deficient groups is well tolerated and produces outstanding yields. Moreover, the phenyl with a bulky substituent also participated with the high yield of corresponding product. Further, the reaction with iodonium salts with electron-donating substituents in the aryl ring required an extension of the reaction duration to 24 hours. Furthermore, the scope of substrates was investigated, with a focus on the benzyl ester generated rather than the corresponding methyl esters. The reaction was also performed with a 6-membered cyclic diaryliodonium salt, which proceeded successfully and produced the respective iodo-containing arylated product in 59% yield with 76% ee after 24 h. Using the same reaction conditions, the arylation of tyrosine methyl ester was also performed. The resulting compound was arylated at both *O*- and *N*-positions. The investigations were continued with the unsymmetric anisyl salts, and the results showed high chemoselectivity for *N*-arylation. Iodonium salts containing the anisyl auxiliary enhanced the arylation yields.

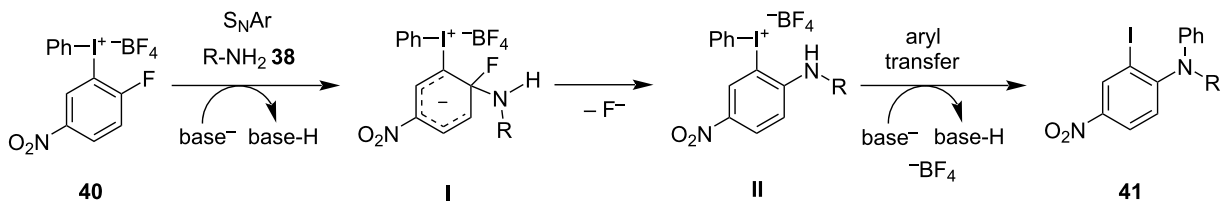

Scheme 17: Proposed mechanism for the diarylation of amines **38** using *o*-fluorinated diaryliodonium salts **40**.

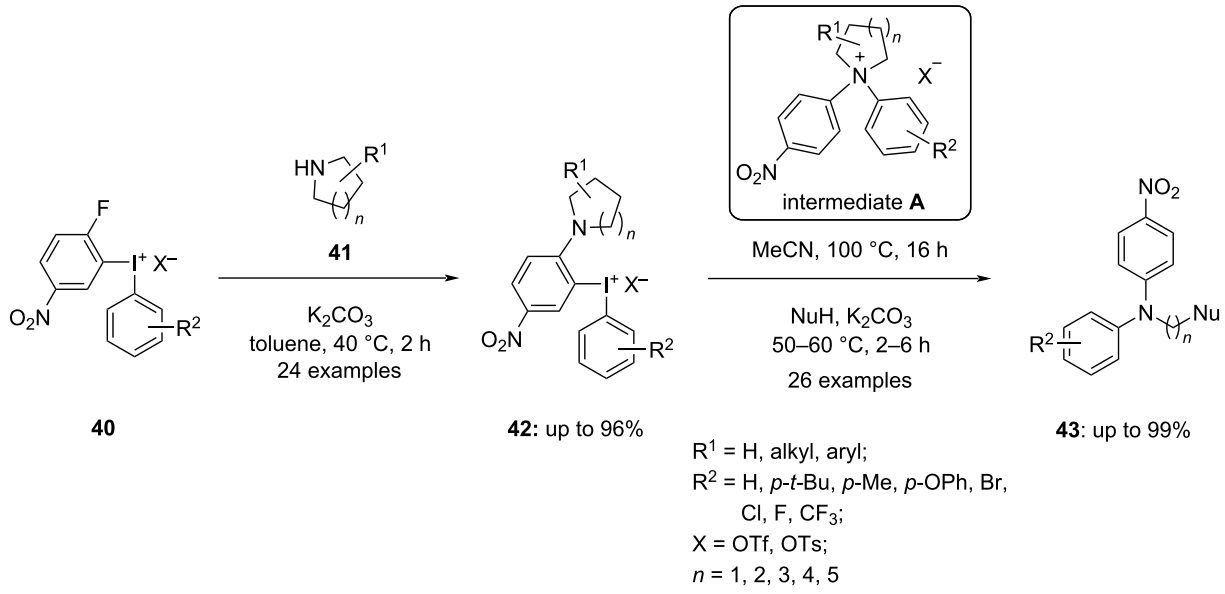

Scheme 18: Ring-opening difunctionalization of aliphatic cyclic amines **41**.

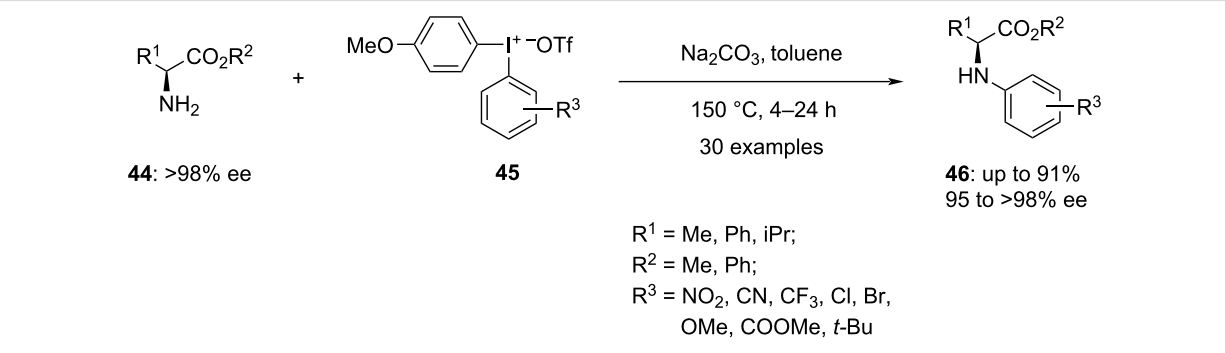

Scheme 19: *N*-Arylation of amino acid esters **44** using hypervalent iodonium salts **45**.

Hypervalent iodonium salts are also useful to achieve the *N*-arylation of azoles. Prakash and co-workers applied iodonium salts **48** in the presence of a base to obtain regioselectively the N2-arylated products of 1,2,3-triazoles via ligand exchange followed by reductive elimination in exceptional yields (Scheme 20) [71]. Although screening studies indicated the possibility of achieving the *N*-arylation at both, the N1- and N2-positions of the triazoles, N2-arylation was predominantly observed. It was incredible to achieve splendid regioselectivity without the usage of directing groups and any metal catalyst. Also, the electronic nature of a substituent at the C4 position of the starting triazole did not negatively impact the regioselectivity. Further, C4 and C5 disubstituted triazoles also produced the N2-arylated product. Remarkably, this is the only approach providing regioselective access to N2-arylated products along with high yields. The synthetic route could also be applied for the synthesis of N2-arylbenzotriazoles which are promising scaffolds for pharmaceuticals. Subsequently, the impact of the aryl group present in the diaryl iodonium salts on the reaction efficiency and selectivity was explored. A high selectivity was found for electron-withdrawing moieties, resulting in high yields of the N2-substituted products. Also, tetrazole **50** was arylated using the same hypervalent iodonium salts as a follow-up, but less than 14% of the targeted product were obtained. However, the yield of products **52** could be improved up to 66% by using iodonium salt **51** having the TMP group substituted with anisyl (Scheme 21) [72].

Switching the base in the arylation process can influence the chemoselectivity of the reaction as was reported by Onomura and group. They observed that the reaction of 2-pyridones **53** gave either the *N*- (**54**) or *O*-arylated product **55** as major component depending on the base used. Ultimately, the study progressed to optimized conditions leading selectively to either

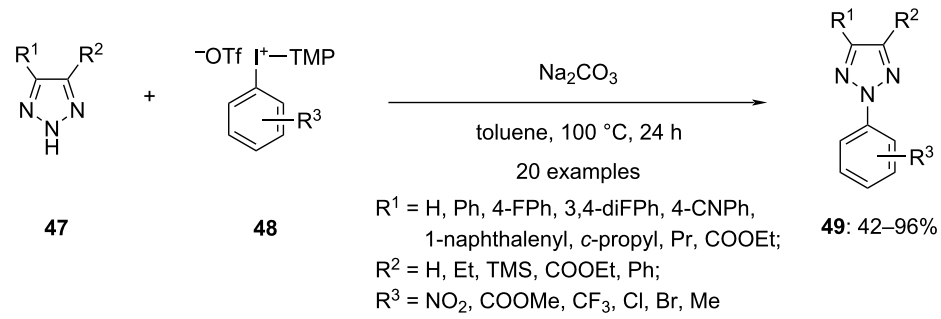

Scheme 20: Regioselective *N*-arylation of triazole derivatives **47** by hypervalent iodonium salts **48**.

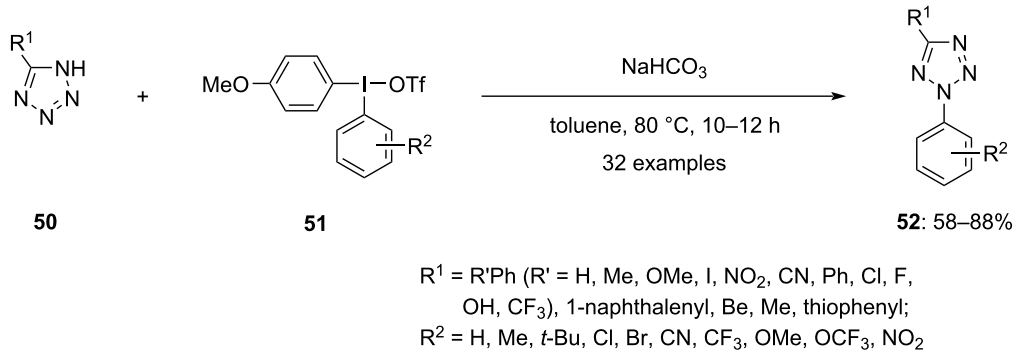

Scheme 21: Regioselective *N*-arylation of tetrazole derivatives **50** by hypervalent iodonium salt **51**.

product. Briefly, when diethylaniline was used as a base in fluorobenzene, the *N*-arylated compounds **54** were produced. On the other hand, the *O*-arylated compounds **55** emerged as major product when quinoline was used as the replacement base and chlorobenzene as the solvent in the reaction (Scheme 22). The effect of the substituent on the aryl group in the hypervalent iodonium salt, was investigated, and the ratio of aryl group migration was found to depend on steric and anti-*ortho* effects [73].

Oxygen-bridged cyclic diaryliodonium salts are novel arylating reagents recently developed by Linde et al. and were utilized to arylate carbon and heteroatoms. However, the reactivity of these cyclic salts was found to be limited, which prompted the authors to synthesize the corresponding acyclic iodonium salt **56** to increase the reactivity. It was subsequently employed in various arylation processes of several substrates. Remarkably, as much as 98% of the targeted *N*-arylated compound **57** was obtained by treating hypervalent iodine salt **56** with $NaNO_2$ in the presence of DBU as the base (Scheme 23). This salt was also studied for the arylation of sulfur, oxygen, and carbon giving good yields of corresponding products [74].

O-Arylation

Arylation of oxygen is a significant chemical reaction that results in the formation of diaryl ethers. Diaryl ethers are impor-

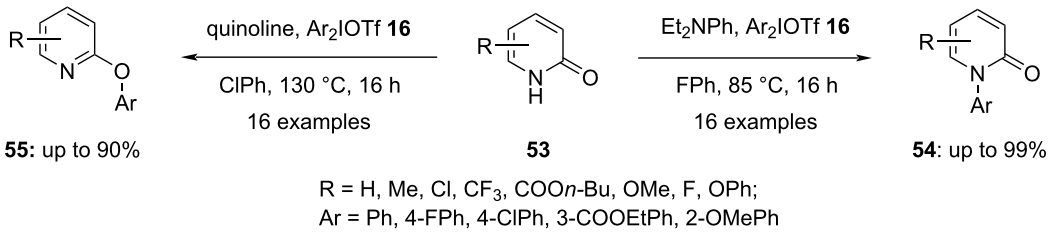

Scheme 22: Selective arylation at nitrogen and oxygen of pyridin-2-ones **53** by iodonium salts **16** depending on the base and solvent used.

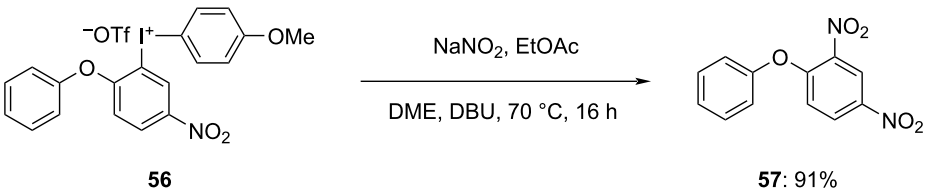

56 57: 91%

Scheme 23: *N*-Arylation using oxygen-bridged acyclic diaryliodonium salt **56**.

tant structural motifs in pharmaceuticals and agrochemicals due to their diverse biological activities. Since the 1950s, one of the most used methods for the synthesis of diaryl ethers involves the reaction of phenol with diaryliodonium salts. Recent advancements in this field have focused on the development of practically simple and scalable methods for the arylation of oxygen using diaryliodonium salts. By modifying the counter anions attached to the iodonium ion, the stability and reactivity of new symmetrical and unsymmetrical diaryliodonium salts could be improved which were subsequently used to synthesize new oxygen arylated products.

Solorio-Alvarado and co-workers introduced a one-pot double arylation of naphthols through the consecutive C–C/O–C bond formation in the presence of hypervalent iodine salts **16** as the aryl donor (Scheme 24) [75]. The reaction worked very well at room temperature under base-free conditions. In this one-pot synthesis of double arylation of naphthols **58**, a novel radical precursor, [1,1´-oxybis(2,2,6,6-tetramethylpiperidine)] (**59**), was employed. This precursor undergoes spontaneous homolytic fragmentation in solution, producing tetramethylpiperidinyl radical and the TEMPO radical. The tetramethylpiperidinyl radical interacts with 2-naphthol derivatives **58**, leading to the generation of an oxygen-centered radical through hydrogen atom transfer, which resonates with its respective carbon-centered radical. Subsequently, these O- and C-centered naphthyl radicals selectively react with hypervalent iodine salts **16** at their more electron-poor hypervalent bond, preferentially transferring the more electron-deficient aryl group to yield the double arylated products **60** in moderate to good yields.

A synthetic protocol for diaryl ethers via an in situ generation of a hypervalent iodine salt was introduced by Stuart and co-workers in 2020. To study the scope of the reaction first various substituted aryl(TMP)iodonium salts **12** were reacted with different substituted phenols **61** in the presence of K_2CO_3 at 55 °C to yield the corresponding products **62** in good to excellent yield (Scheme 25) [76]. It was observed that both electronic as well as steric effects on the aryl electrophile and phenol nucleophile were well tolerated. Further, this study was used for the one-pot synthesis of diaryl ethers **62**, starting with aryl iodides and phenols **61**. In this metal-free reaction, aryl(TMP)iodonium salts **12** were prepared in situ from aryl iodides via treatment with *m*-CPBA, TsOH, and TMB at 55 °C in acetonitrile, which subsequently react with the substituted phenols **61** to produce the *O*-arylated products **62**. Acetonitrile was identified as a suitable solvent for this reaction, resulting in moderate to good yields of the products. The three main steps in the reaction were oxidation of the aryl iodide, addition of the TMP auxiliary, and C–O coupling reaction.

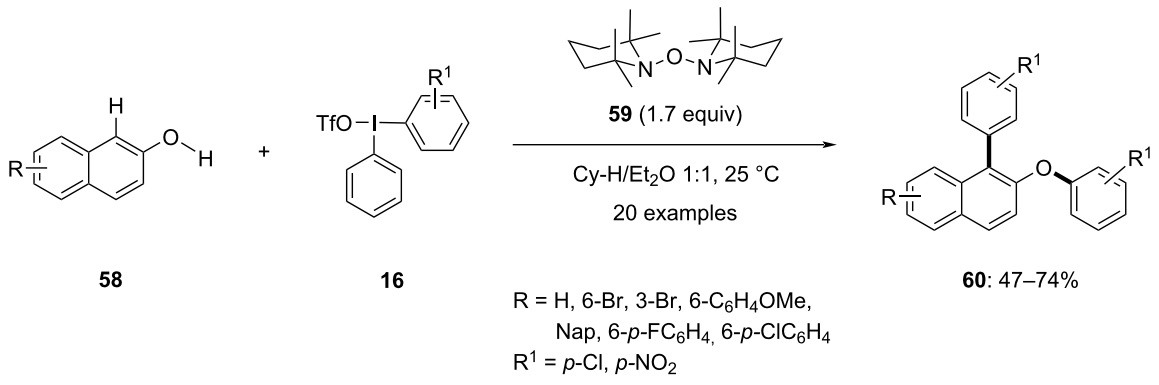

58 16 60: 47–74%

R = H, 6-Br, 3-Br, 6-C_6H_4OMe, Nap, 6-*p*-FC_6H_4, 6-*p*-ClC_6H_4
R^1 = *p*-Cl, *p*-NO_2

Scheme 24: The successive C(sp^2)–C(sp^2)/O–C(sp^2) bond formation of naphthols **58**.

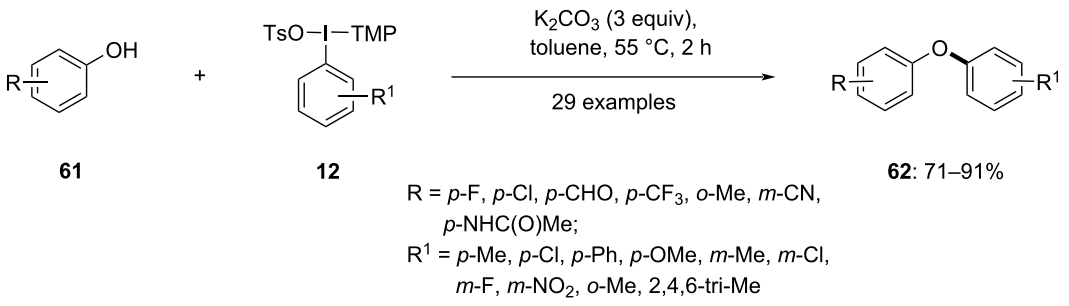

Scheme 25: Synthesis of diarylethers **62** via in situ generation of hypervalent iodine salts.

Olofsson et al. worked towards the synthesis of O3-arylated galactosides **64** by reacting benzyl-protected galactoside **63** with diphenyliodonium triflates **16** at room temperature in the presence of potassium *tert*-butoxide as the base (Scheme 26) [77]. This transition-metal-free approach simplifies the synthesis process. Electron-pushing and -pulling groups at the *para* and *meta*-position of the aryl group were compatible with the reaction leading to moderate to good yields of products. In contrast, products with substitutions at the *ortho* position were obtained only after heating the reaction mixture to 60 °C. These compounds were further assessed as inhibitors of galectin-9 and were found to exhibit selectivity and potency against galectin-9.

In 2021, Chen and colleagues developed a method to synthesize naproxen-containing diaryliodonium salts **67** using naproxen methyl ester **65** and ArI(OH)OTs **66**, activated by trimethylsilyl trifluoromethanesulfonate (TMSOTf). This synthesis was conducted in a mixture of 2,2,2-trifluoroethanol (TFE) and dichloromethane [78]. The synthesized naproxen-containing diaryliodonium salt **67** was further used to modify the aromatic ring of naproxen methyl ester **68** (Scheme 27). Various functionalization reactions which include arylation, iodination, alkynylation, thiophenolation, amination, and esterification, were carried out. Among these reactions, esterification was achieved in moderate yield under metal-free conditions by reacting the synthesized naproxen methyl ester (2-methoxyphenyl)iodonium trifluoromethanesulfonate with *p*-toluic acid in the presence of *t*-BuOH.

Moreover, later in 2022 Chen et al. modified the aromatic ring of gemfibrozil (**69**) and its methyl ester using gemfibrozil-derived diaryliodonium salts **72** synthesized by the aforementioned procedure [79]. On reacting gemfibrozil **69** in the presence of bis(4-methoxyphenyl)iodonium diacetate (**70**) or ArI(OH)OTs highly regioselective gemfibrozil methyl ester derived iodonium salts **71** were obtained in moderate to good yield. These salts were then used for various modifications like alkynylation, arylation, esterification, etherification, fluorination, and iodination of the gemfibrozil aromatic ring by reacting them with the corresponding nucleophiles. Notably, reactions with phenol, thiophenol and benzoic acid using salts **71** in the presence of *t*-BuOK led to the corresponding products **72** with 61%, 69%, and 77% yields, respectively (Scheme 28). These reactions occurred under mild conditions and without any need of transition-metal catalysts.

In 2023, Wu and colleagues successfully synthesized a range of *meta*-substituted biaryl ethers. The reaction involves phenols **61**

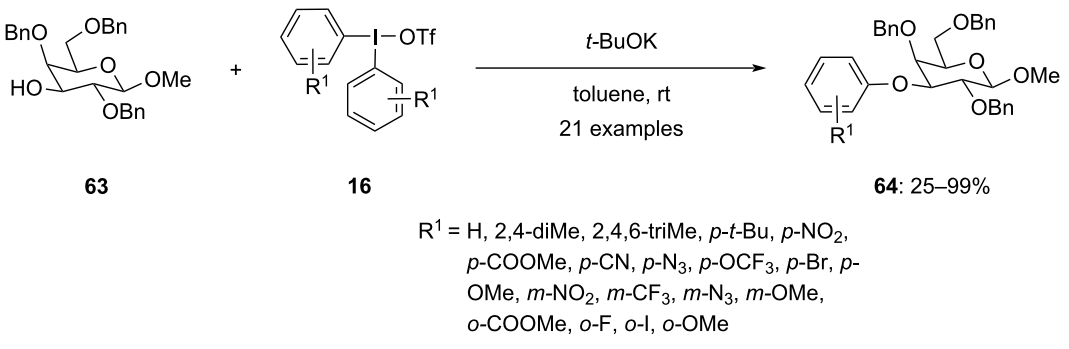

Scheme 26: *O*-Arylated galactosides **64** by reacting protected galactosides **63** with hypervalent iodine salts **16** in the presence of base.

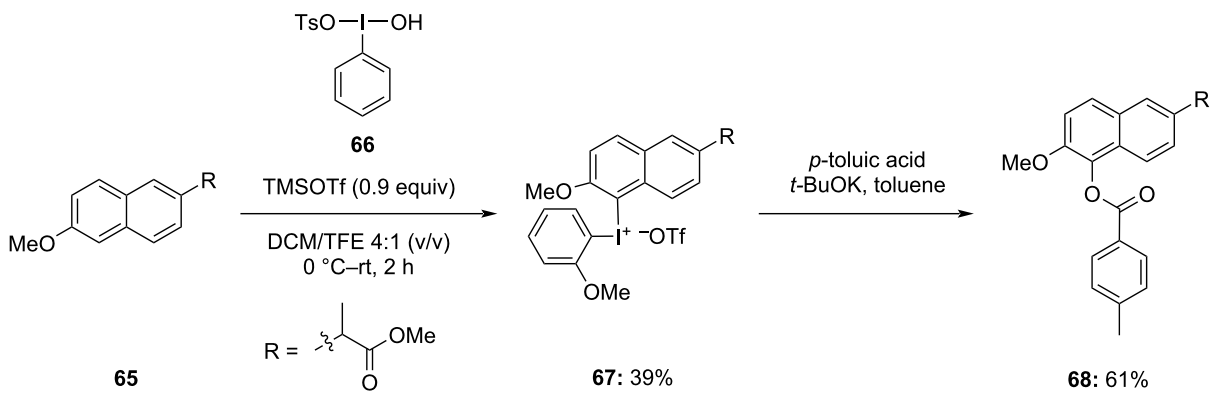

Scheme 27: Esterification of naproxen methyl ester **65** via formation and reaction of naproxen-containing diaryliodonium salt **67** with *p*-toluic acid.

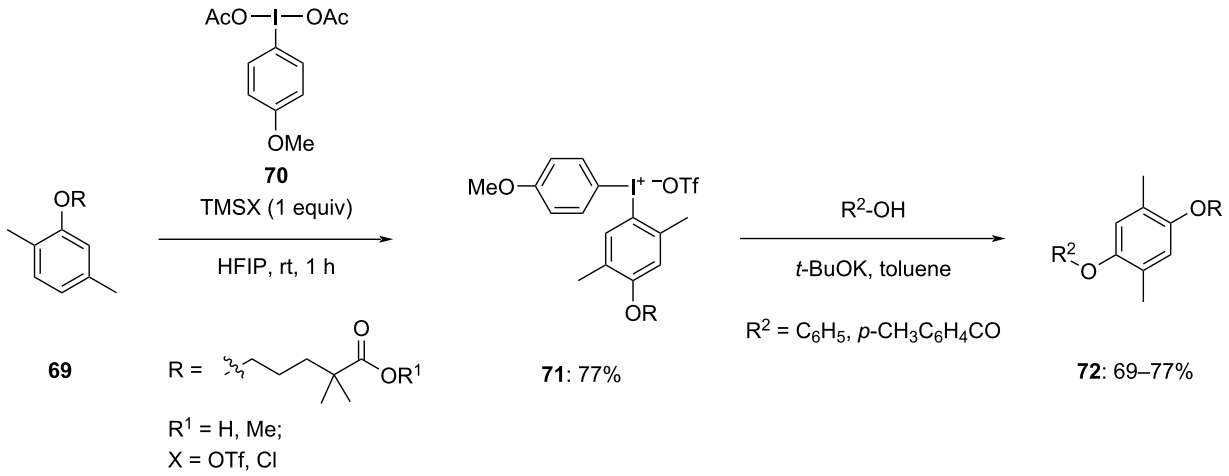

Scheme 28: Etherification and esterification products **72** through gemfibrozil methyl ester-derived diaryliodonium salts **71**.

and cyclic diaryliodonium salts **73**, dissolved in *tert*-butyl alcohol, in the presence of the base Cs_2CO_3 yielding iodine-containing *meta*-functionalized biaryl ethers **74** (Scheme 29) [80]. Notably, the reaction occurs under transition-metal-free conditions, making it environmentally friendly. The team explored the substrate scope by introducing various substitu-

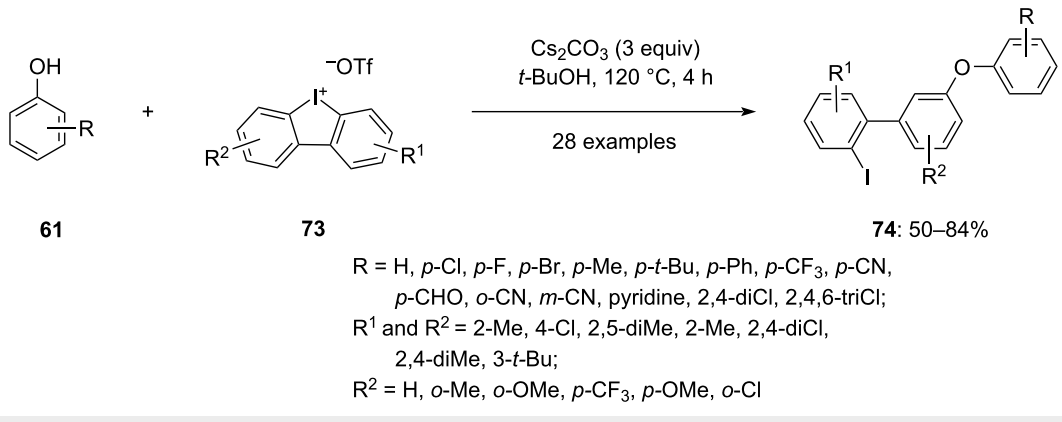

Scheme 29: Synthesis of iodine containing *meta*-substituted biaryl ethers **74** by reacting phenols **61** and cyclic diaryliodonium salts **73**.

tions on both phenols **61** and diaryliodonium salts **73**. Remarkably, the method exhibited high regioselectivity, with the substitution at the *meta* position being observed with up to 99% selectivity in comparison to the *ortho* position. Specifically, only electron-withdrawing groups like OMe or CF_3 when substituted at the *m*-position relative to the iodine center give the *ortho*-substituted products in good yield. Additionally, *ortho*-disubstituted diaryliodonium salts also led to the formation of *ortho*-substituted biaryl ethers in good yield with 99% selectivity and the reason given was the high torsional strain caused by the *ortho*-disubstitution on the diaryliodonium salts.

The reaction mechanism involves the deprotonation of the phenol **61** and diaryliodonium salts **73** via base under high temperature to get phenolate **I** and benzyne intermediate **II**, respectively. The phenolate nucleophile reacts with the benzyne intermediate to create a C–O bond, leading to the formation of the carbanion intermediate **III**. Lastly, this intermediate is protonated by bicarbonate to yield the final product **74** (Scheme 30).

Furthermore, Wang and his team introduced a novel method to synthesize *ortho*-iodo diaryl ethers **77** using intramolecular aryl migration in trifluoromethanesulfonate-substituted diaryliodonium salts **76** [81]. This reaction occurs under basic conditions at temperatures ranging from room temperature to 50 °C and is completed within 12 hours (Scheme 31). The process is atom-efficient as no aryl residue is wasted as a byproduct. Various functional groups on both aromatic rings were investigated, and based on the obtained yields of the products it was concluded that the reaction is compatible with electron-donating, electron-

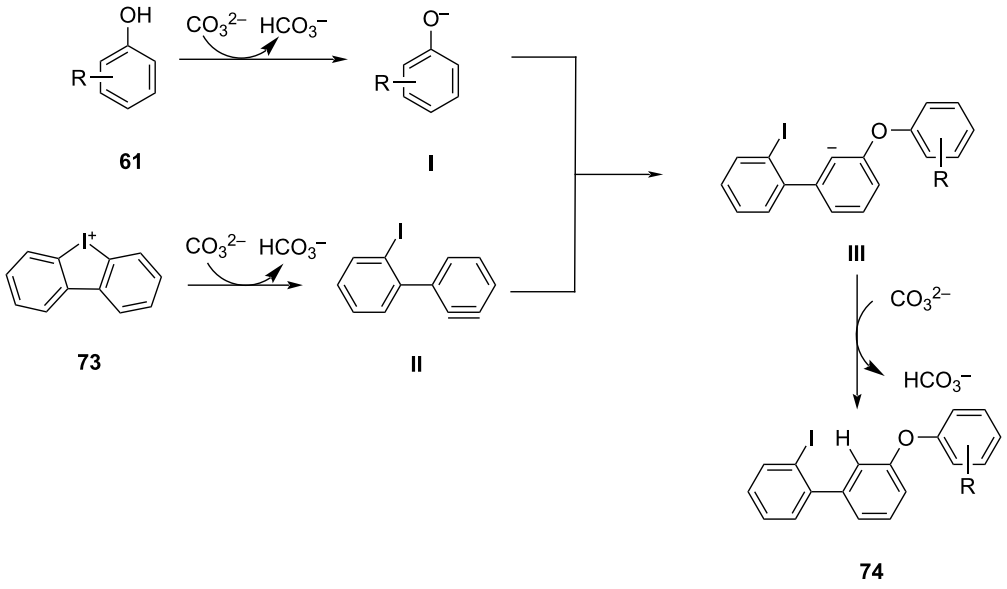

Scheme 30: Plausible mechanism for the synthesis of *meta*-functionalized biaryl ethers **74**.

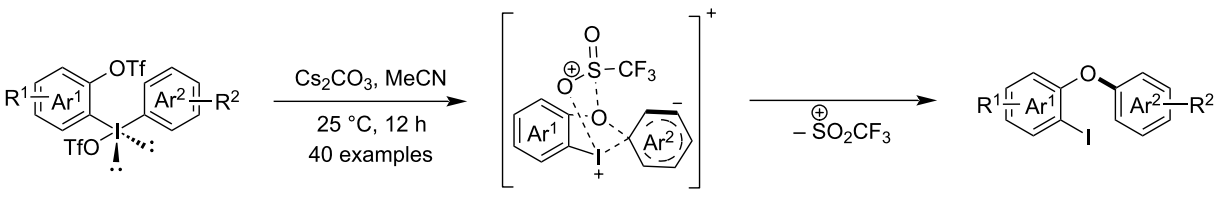

R^1 = *p*-Cl, *p*-F, *p*-Br, *p*-Me, *p*-COOMe, *m*-Me, *m*-*t*-Bu, *m*-Br, *m*-CF_3, *m*-NO_2, *m*-COOMe;
R^2 = H, *p*-Me, *p*-*t*-Bu, *p*-OMe, *p*-F, *p*-Cl, *p*-Br, *p*-CN, *p*-Ph, *p*-NO_2, *p*-COOMe, *m*-Me, *m*-Cl

Scheme 31: Intramolecular aryl migration of trifluoromethane sulfonate-substituted diaryliodonium salts **75**.

withdrawing, and electron-neutral substitutions. Mechanistic studies, including a cross-over reaction, indicated that the aryl migration is intramolecular. In the presence of a base, the triflate anion is extracted, forming a cationic trifluoromethanesulfonyl group as an intermediate. Thus, the products are believed to form via a sulfonyl-directed nucleophilic aromatic substitution pathway. Finally, the products are obtained through the dissociation of the SO_2CF_3 leaving group from the intermediate.

For the late-stage substitution of coumarins, Han and colleagues developed a method, using hypervalent iodine reagents. At 50 °C in the presence of a base, coumarin-based aryliodonium salts are produced. These salts undergo an intramolecular aryl rearrangement to form C(sp^2)–O bonds without the need of metal catalysts [82]. In 2023, this approach was expanded to synthesize complex functionalized aromatic ring diaryliodonium salts [83]. Various aromatic rings, including multisubstituted arenes, conjugated arenes, oxygen and nitrogen heterocycles **78** were utilized to prepare these salts using *ortho*-triflate-substituted iodobenzene acetate **79**. All synthesized diaryliodonium salts underwent successful aryl migrations, yielding the expected products **80** efficiently (Scheme 32). The advantages of this method include late-stage site-selective *O*-arylation, transition metal-free conditions, and the presence of a C–I bond in the product, allowing for further functionalization through various coupling reactions, making the reaction method highly attractive.

In 2022, Dohi and colleagues emphasized the high reactivity of TMP-iodonium acetates in the *O*-arylation of phenol derivatives [84]. The study revealed that the blend of the TMP ligand and the acetate anion in iodonium salts **82** synergistically increased electrophilic reactivity. The *ortho*-methoxy groups of TMP boost the basicity of the acetate anion by coordinating with the iodine(III) center, which facilitates the deprotonation of phenols. This method was well-suited for various functional groups, yielding diaryl ethers with significantly improved yields compared to other diaryliodonium salt reactions. Furthermore, the same research group extended the use of aryl(trimethoxyphenyl)iodonium salts for *O*-arylation of *N*-alkoxybenzamides **81** in absence of metal catalsyt at low temperatures [85]. The reaction resulted in the two products *O*-arylated **83** and *N*-arylated **84** amides (Scheme 33). By reacting various substituted diaryliodonium salts and the amide it was concluded that the chemoselectivity between *O*- and *N*-arylation could be controlled by adjusting the steric and/or electronic properties of the diaryliodonium salt and the amide. This approach was helpful in the formation of *O*-arylimidates previously unattainable using metal-catalyzed methods.

S-Arylation

The aryl sulfide moiety is widely present in biologically active compounds and natural products. Consequently, the synthesis of aryl sulfides has drawn increasing attention. Diaryliodonium salts have been reported to be utilized to arylate thiols in a number of publications in recent years [44,86,87]. In 2022, Sarkar et

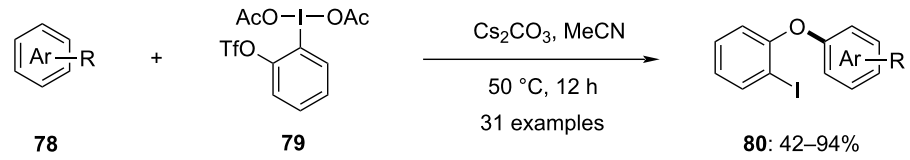

78 **79** **80**: 42–94%

Ar = coumarin, xanthone, 4-chromone, thiophene, C_6H_5;
R = *p*-C_6H_{11}, 3-Br, 4-OMe, *p*-CH_2CHCH_2, *p*-OC_6H_5,
p-OC_6H_4Br, *p*-$(CH_2)_3Br$, 2,4,6-Br, $OCH_2C_6H_5$

Scheme 32: Synthesis of diaryl ethers **80** via site-selective aryl migration.

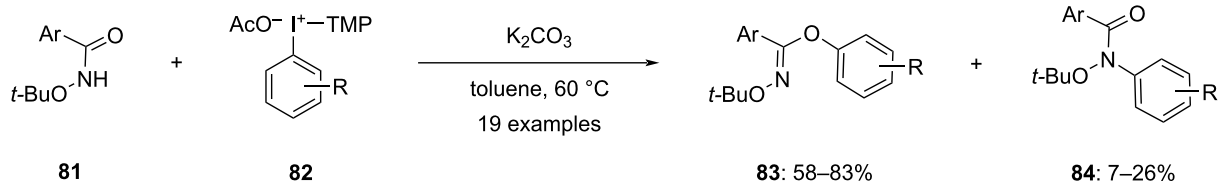

81 **82** **83**: 58–83% **84**: 7–26%

R = *p*-Me, 3,5-diMe, *o*-OMe, *p*-Ph, *m*-F, *p*-Br, *p*-NO_2, *p*-COOMe
Ar = Ph, *p*-$OMeC_6H_4$, *o*-$OMeC_6H_4$, Nap, pyridine, thiophene, $(CH)_2C_6H_5$

Scheme 33: Synthesis of *O*-arylated *N*-alkoxybenzamides **83** using aryl(trimethoxyphenyl)iodonium salts **82**.

al. demonstrated a synthesis of aryl sulfides **85** from thiols **84** using diaryliodonium salts **16** in basic conditions (Scheme 34). A multitude of thiols and diaryliodonium salts was examined in the reaction under optimized conditions, yielding exceptional yields [88].

To embrace the chemical process, DFT calculations were performed in the study. The results demonstrated that the diphenyliodonium triflate has a feasible energy barrier of 21.5 kcal/mol and can be readily converted into a stable iodonium thiolate species. This species can further undergo a C–S bond-forming reductive elimination, providing the sulfide product. As a result of C–S bond formation, the oxidation state of iodine is reduced from +III to +I, causing the loss of hypervalency. This process is extremely exergonic and provides the driving force for the reaction. Additionally, the alternative mechanism of a direct attack of the thiolate nucleophile on the aryl group of the iodonium salt was also investigated. A potential radical-mediated mechanism was evaluated.

Under mild conditions, a base-promoted arylation of general sulfinates **86** without the need for transition metals was introduced using diaryliodonium salts **16** as an aryl source (Scheme 35). Inspired by these encouraging outcomes, Wang and co-workers looked at the range of substrates that diaryliodonium salts could occupy. Numerous diaryl sulfoxides **87** were synthesized from the respective substrates **86** bearing electron-releasing, electron-neutral, and electron-attracting substituents at various positions of the aryl group. All the tested anions were well-tolerated. Moreover, the rate of productivity of the reaction was not significantly impacted by the steric barrier of the substituents on the sulfonate anions. Further, diaryliodonium salts with electron-releasing substituents at the *para* position of the phenyl groups were good reaction partners. Additionally, a few electron-withdrawing groups also proved to be better coupling partners. The tolerance of unsymmetrical diaryliodonium salts was further verified, resulting in the formation of two distinct products. Notably, the yield of the product with the aryl-containing bulky group was significantly higher compared to the smaller substituents. The arylation of sulfonate anions by transfer of the aryl group with an iPr substituent gave good results on using OTf as the counter anion instead of BF_4 [89].

With regard to the mechanism, the base-mediated deprotonation of substrates **86** produces the corresponding ester enolate. This enolate undergoes a retro-Michael reaction, generating sulfenate anion **A**. The sulfenate anion **A** then nucleophilically

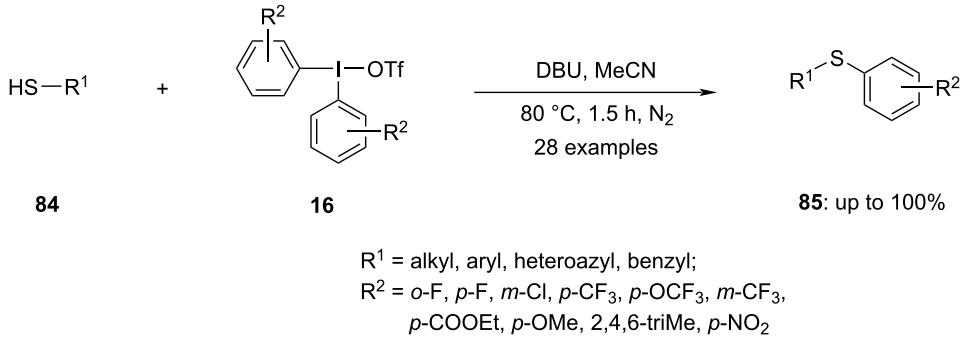

Scheme 34: Synthesis of aryl sulfides **85** from thiols **84** using diaryliodonium salts **16** in basic conditions.

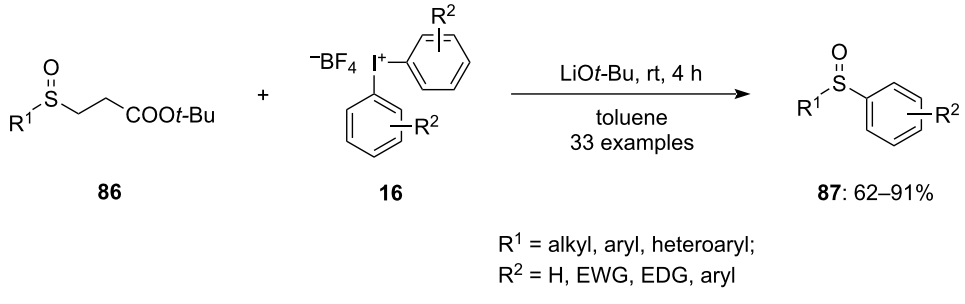

Scheme 35: Base-promoted synthesis of diarylsulfoxides **87** via arylation of general sulfinates **86**.

attacks the diaryliodonium salts **16**, forming hypervalent iodine intermediates **B**. Finally, reductive elimination of intermediate **C** yields the desired sulfoxides **87** (Scheme 36).

Recently, a detailed study by Thakur and group on the metal-free arylation of tetrazole-5-thiols **88**, exploring various substrate scopes under optimized conditions was conducted (Scheme 37) [90]. The findings indicated a broad functional group tolerance to steric hindrance and electronic factors within this protocol. Investigating the chemoselectivity of unsymmetrical diaryliodonium salts, the researchers noted their comparable electronic factors. Interestingly, the simple phenyl group was transferred easily rather than the phenyl with substituents, when an unsymmetrical diaryliodonium salt was employed. If both phenyls were substituted, then the phenyl ring bearing electron-withdrawing groups led to minor products, with other compounds becoming dominant. Further, replacing one aryl group of the diaryliodonium salt with thiophene favored the formation of phenylated products as the major outcome. Additionally, mercaptoazoles were found to be compatible with this protocol, expanding its applicability to include these compounds.

The functionalization of peptides and proteins plays a vital role in the development of therapeutics, particularly in antibody–drug conjugates (ADCs). Cysteine (Cys) holds a special place in this context due to the distinctive nucleophilicity of its thiol side chain. The cysteine thiol group offers a reactive handle for site-selective modifications, allowing for the attachment of various functional entities. In 2021, Byrne et al. published an impressive report detailing a novel protocol for the chemoselective late-stage variation of proteins and peptides at cysteine residues **91** and **94** in an aqueous buffer in the presence of suitably functionalized diaryliodonium salts **92** and **95** (Scheme 38) [91]. This method manifests the synthesis of stable thioether-linked synthetic conjugates **93** and **96** displaying its efficacy via the alteration of the affibody zEGFR and the histone protein H2A. The procedure involved synthesizing the diaryliodonium salt and appraising the proficiency of oxime ligation chemistry on the histone H2A protein. The protein was demonstrated as the T120C mutant via site-directed mutagenesis in *Escherichia coli* and decontaminated by HPLC. A notable reconciliation was changing the aqueous buffer from HEPES to phosphate owing to side-product generation during the arylation in HEPES. The reaction of H2A with the

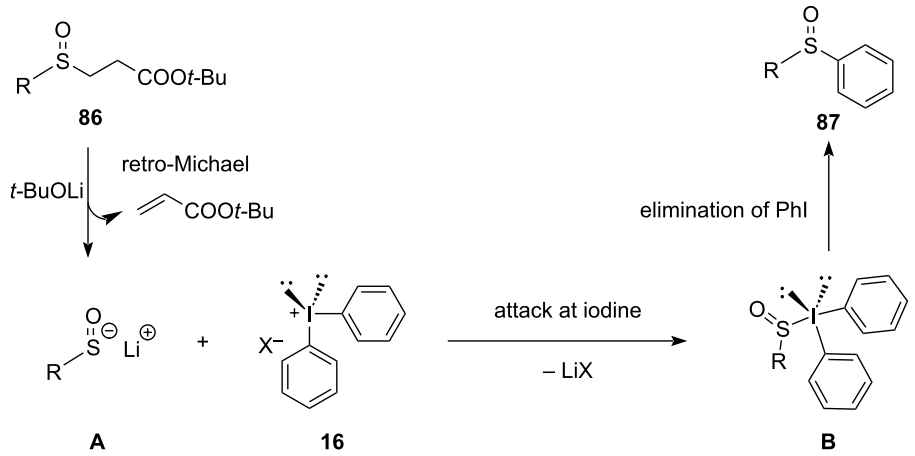

Scheme 36: Plausible mechanism for the arylation of sulfinates **86** via sulfenates **A** to give diaryl sulfoxides **87**.

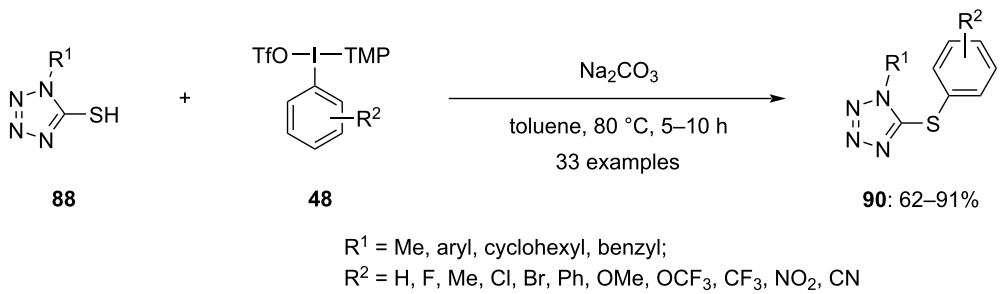

Scheme 37: *S*-Arylation reactions of aryl or heterocyclic thiols **88**.

diaryliodonium salt in phosphate buffer resulted in the expected arylated conjugate in an hour with a maximum of 98% conversion, yielding sulfur arylated product in 54% isolated yield after purification by HPLC.

Additionally, the functionalization of the ketone with a protein conjugate was effectively done with various hydroxylamines with the assistance of the nucleophilic catalyst 5-methoxyanthranilic acid. The resultant histone protein conjugates were functionalized with TAMRA, biotin and the cell-penetrating peptide 'penetratin' through oxime ligation, achieving high conversions (83–93%) in 1–20 hours. Purification by HPLC yielded the isolated oxime conjugates in excellent amounts. This methodology presents a promising approach for the late-stage variation of proteins and peptides, offering versatility and efficiency in aqueous environments.

In addition to thiols, sulfoxides and sulfilimines have received significant attention in chemical biology and synthetic chemistry due to their versatile properties. Traditional approaches to sulfilimine synthesis typically include the oxidative imination of sulfides, often relying on transition-metal catalysts, which can present limitations. However, a more efficient method for synthesizing sulfilimines emerged in 2023, involving the selective *S*-arylation of sulfenamides **97** with diaryliodonium salts **98** at ambient temperature in the presence of air (Scheme 39). These innovative approaches offer promising alternatives for sulfilimine synthesis, potentially overcoming some of the drawbacks associated with traditional methods. The choice of base used in the reaction can influence both the reaction duration and the yield. When the reaction was performed in acetonitrile in the presence of Cs_2CO_3 as a base at room temperature for 18 h, the yield was quite high (conditions A) [92]. Meanwhile, a similar yield was obtained in 2 h, when NaOH (conditions B) was used as a base (R^2 = acyl). Upon moving to other substrates (R^2 = aryl), the yield dropped significantly. By replacing the strong base with K_2CO_3, (conditions C) the product yield increased [93]. Similarly, the arylation of sulfonamides can also be achieved by using *t*-BuONa in toluene for an hour at room temperature in the presence of air (conditions D) [94].

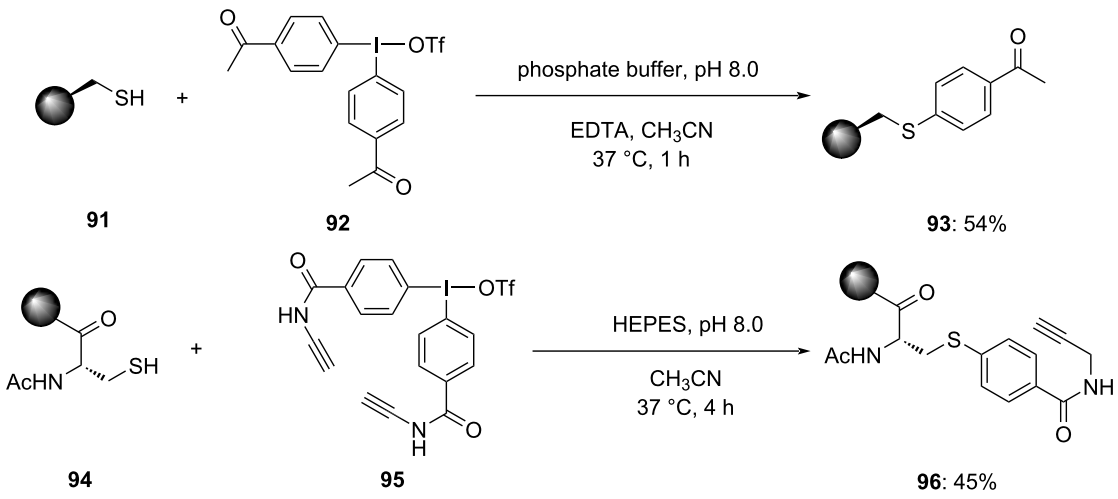

Scheme 38: Site-selective *S*-arylation reactions of cysteine thiol groups in **91** and **94** in the presence of diaryliodonium salts **92** and **95** as aryl source.

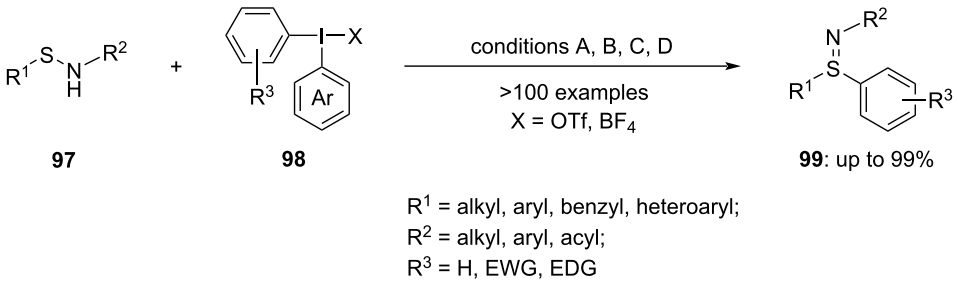

Scheme 39: The selective *S*-arylation of sulfenamides **97** using diphenyliodonium salts **98**.

The mechanism of the reaction involves formation of anionic intermediates **I** and **II** by the action of the base on *N*-sulfenamides **97**. Both, the divalent N-centered anion intermediate **I** and S-centered anionic intermediate **II** are the resonating structures which further react with the diaryliodonium salt to obtain intermediate **III** along with the elimination of triflate. Finally, intermediate **III** undergoes reductive elimination to produce the desired sulfilimine **99** (Scheme 40) [92].

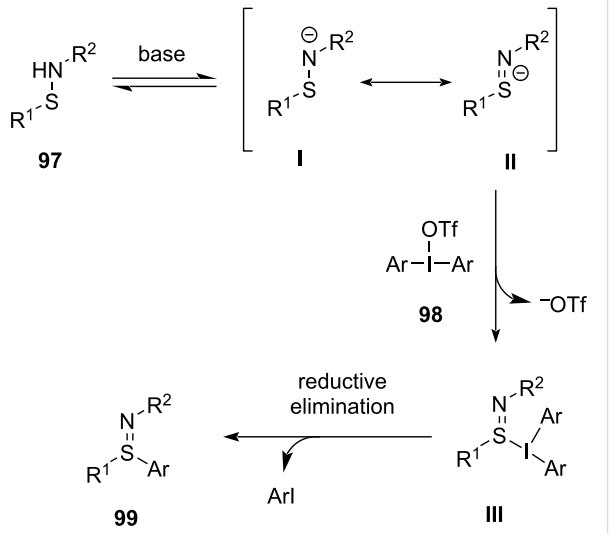

Scheme 40: Plausible mechanism for the synthesis of sulfilimines **99**.

Synthesizing *S*-aryl xanthates through transition-metal-catalyzed or S_NAr reactions presents challenges due to potential additional transformations occurring under the reaction conditions. However, employing diaryliodonium salts **101** for the *S*-arylation of potassium *O*-alkyl xanthates **100** offers a simpler approach [95]. This method operates under mild conditions, facilitating the creation of substituted *S*-aryl xanthates **102** (Scheme 41). Utilizing diaryliodonium salts for the arylation of xanthate anions provides a pathway for the reaction to proceed under gentle conditions. This prevents the subsequent transformation of the obtained *S*-aryl xanthates, thereby facilitating their isolation with satisfactory to excellent yields. During the assessment of the reaction's versatility, first variously substituted (4-anisyl)(aryl)iodonium salts were explored. The incorporation of the 4-anisyl group was expected to enhance selectivity for transferring unsubstituted phenyl groups. As anticipated, utilizing this component under optimized conditions led to highly selective reactions. This generated a diverse range of substituted *S*-aryl xanthates, with yields spanning from 65% to 91%. The promising biological properties of the *S*-aryl *O*-alkyl xanthates, makes them desirable targets for synthesis, and thus the exploration of the reaction's scope was broadened to encompass xanthate salts with diverse *O*-alkyl substituents.

Another potassium salt, potassium thiocyanate (**104**), was utilized as a sulfur source, with the sulfur serving as the anionic counterpart of diaryliodonium salts **105**. The subsequent arylation involved the arylating action of the counter cationic part of diaryliodonium salts **103** on the anionic thiocyanate component. These arylation studies primarily concentrated on iodonium salts represented by 8-membered cyclic heterotetramer **I** and 4-membered cyclic heterotetramer structures **II**, depicted in Figure 2. The research benefited from the strong regioselectivity of TMP-substituted iodonium cations in nucleophilic substitution reactions.

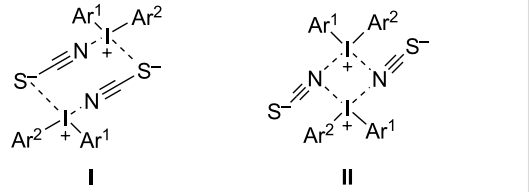

Figure 2: Structured of the 8-membered and 4-membered heterotetramer **I** and **II**.

The reactions were conducted at 100 °C, both in the solid-state and in DMSO-d_6 solution, for comparison. The conventional *S*-arylation reactions worked very well in DMSO-d_6 solution yielding the aryl-SCN products **106** (Scheme 42). However, a

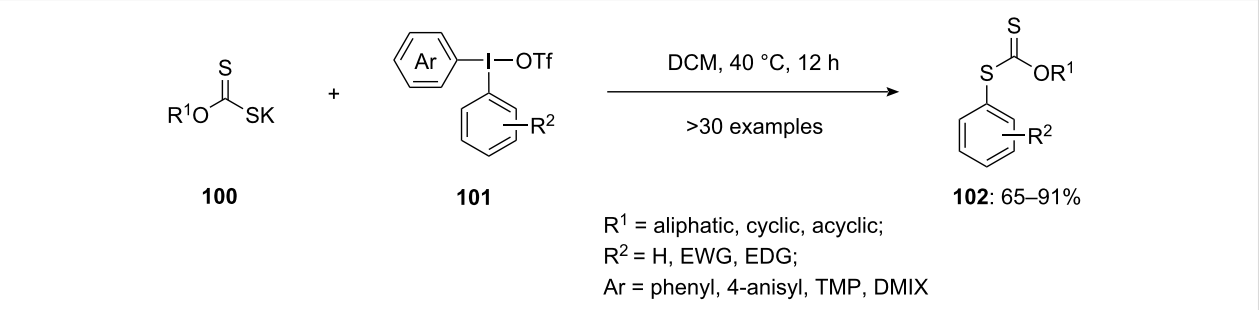

Scheme 41: Synthesis of *S*-arylxanthates **102** by reacting DAIS **101** with potassium alkyl xanthates **100**.

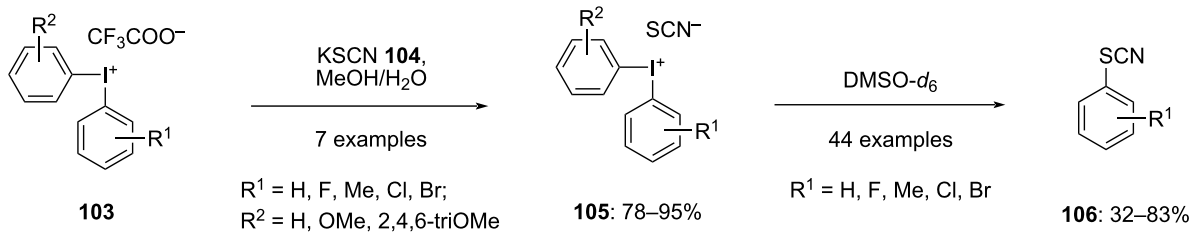

Scheme 42: *S*-Arylation by diaryliodonium cations **103** using KSCN (**104**) as a sulfur source.

significant difference was observed in the solid-state reactions, particularly with iodonium salts exhibiting 4-membered cyclic heterotetrameric structural motifs. Here, the major product was the *N*-arylation compounds ArNCS, contrasting with the predominantly *S*-arylation products obtained in DMSO-d_6 solution reactions [96].

Sarkar and Kalek showcased a novel technique involving the *S*-arylation of phosphorothioate diesters **107** through the utilization of diaryliodonium salts **108** (Scheme 43) [97]. This approach enables the facile synthesis of a diverse array of *S*-aryl phosphorothioates **109**, encompassing complex molecules, and various other organophosphorus compounds that are arylated at a chalcogen. Notably, the reaction retains the stereochemistry at the phosphorus atom, thereby providing a simple method for the synthesis of P-chiral products.

Computational studies employing DFT calculations were conducted to delve into the mechanism of the reaction. Specifically, the focus was on understanding the intricacies of the S–Ar bond formation and providing a rationale for the selectivity favoring *S*-arylation over *O*-arylation. Despite numerous attempts, a direct nucleophilic attack of a phosphorothioate on the phenyl ring of the diphenyliodonium salt by substituting an iodine-based leaving group in an S_N2 reaction mechanism, could not be located. The results showed the phosphorothioate gets attached in the inner coordination sphere of iodine giving intermediates with either P–S–I or P–O–I linkages (**109** and **110**, respectively). Both the intermediates **109** and **110** were energetically similar to each other, suggesting an equilibrium between these species. Homolytic cleavage of the S/O–I bond in **109**/**110** was found to be highly endergonic, excluding the radical pathway of the reaction. This was supported by a study including DPE and TEMPO. The intermediates obtained in the reaction could undergo aryl transfer by two different pathways, which included transition states with three- or five-membered rings (**111** and **112**, respectively) leading to *O*- and *S*-arylation products (Scheme 44). The energetically preferred S–Ar forming **112** (from intermediate **110**) and **111** (from intermediate **109**) explained the observed selective *S*-arylation. It was observed that the five-membered rings were favored transition states due to less strain on the ring. The inner sphere mechanism shared similarities with other aryl transfers using hypervalent iodine salts, with the unique presence of the transition state with a five-membered ring (**109** and **110**) attributed to the structural arrangement of the phosphorothioate diester. Computational studies also indicated stereospecific *S*-arylation of P-chiral phosphorothioates, consistent with the experimental observations of retention of configuration at the phosphorus atom throughout the mechanistic pathway.

Expanding the application of the developed arylation conditions, other P–S nucleophiles and related selenium compounds were investigated. Aryl transfer to the selenium atom of phos-

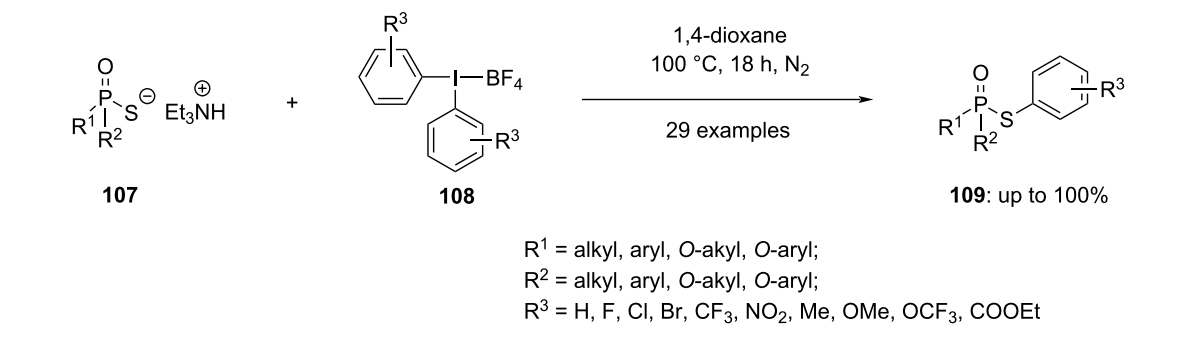

Scheme 43: *S*-Arylation of phosphorothioate diesters **107** through the utilization of diaryliodonium salts **108**.

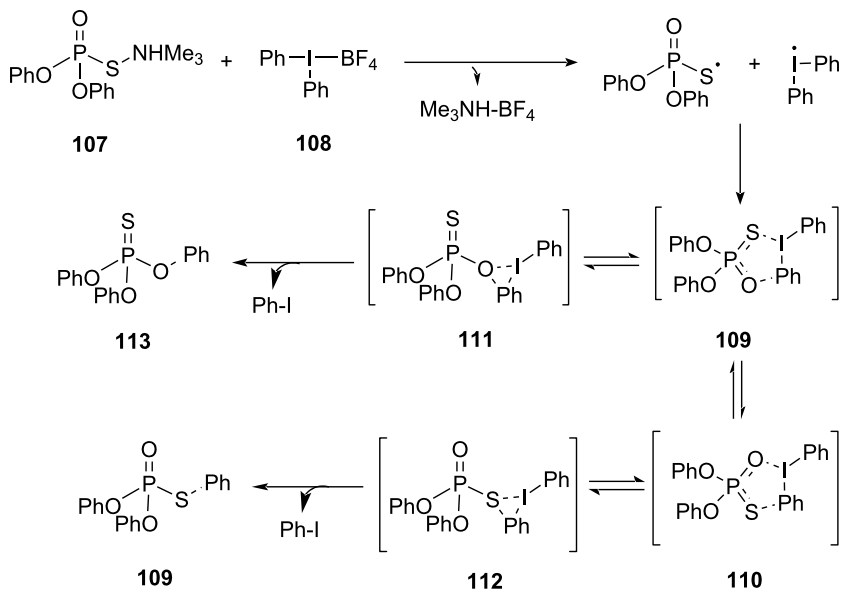

Scheme 44: Transfer of the aryl group from the hypervalent iodonium salt **108** to phosphorothioate diester **107**.

phoroselenoates **116** was achieved, though with reduced efficiency. To address this limitation, Radzhbov introduced a novel method for the metal-free diarylation of selenocyanate using trimethoxyphenyl-substituted iodonium salts **114**. This approach facilitated the synthesis of diarylselenides **118** containing electron-donating TMP groups in a two-step reaction without the need for isolating intermediate products (Scheme 45) [98].

To investigate how electron-rich groups influence the arylation, 1,3,5-trimethoxybenzene in the iodonium salts was replaced with 1,3-dimethoxybenzene. Arylation of $SeCN^-$ proceeded smoothly in all cases, producing selenocyanides with high selectivity. Surprisingly, when ArSeCN was reacted with 1-iodo-2,6-dimethoxybenzene, it exclusively formed symmetrical diselenides in excellent yields, rather than diarylselanes as expected.

P-Arylation

Bugaenko et al. established a light-promoted metal-free and catalyst-free arylation of tertiary phosphines **119** using diaryliodonium triflate salts **120**, yielding quaternary phosphonium salts **121** (Scheme 46). Using this novel protocol, a series of substituted aryl(mesityl)iodonium triflates **120** with varying electronic and steric effects were examined. The triflates bearing either electron-pushing or electron-pulling groups at different positions of the phenyl ring reacted efficiently with excellent selectivity of the aryl group transfer. Moreover, the reaction shows good compatibility across functional groups. Further, aryls with various electronic substituents are transferred for all aryl(mesityl)iodonium salts examined, when the mesityl group is considered to be a "auxiliary" group. Notably, when electron-rich aryls were transferred, the time duration of the reaction was elevated to obtain maximum yields. Since the reaction appears to exhibit electronic preferences

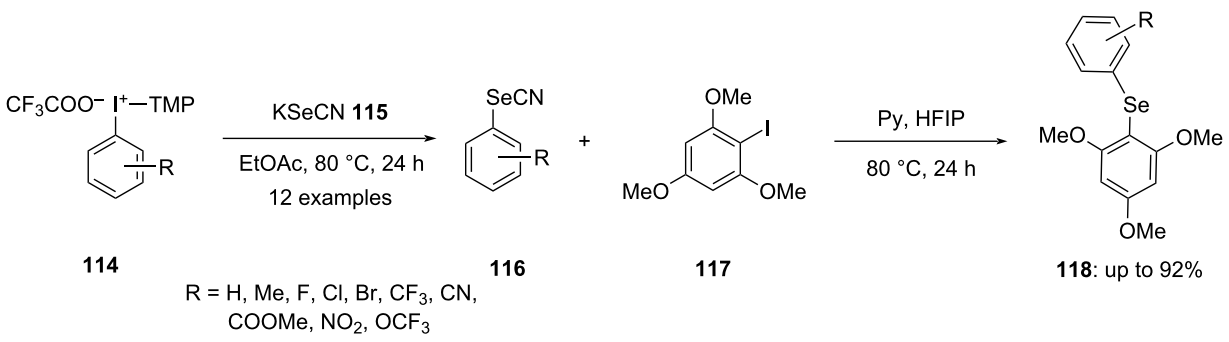

Scheme 45: Synthesis of diarylselenides **118** via diarylation of selenocyanate **115**.

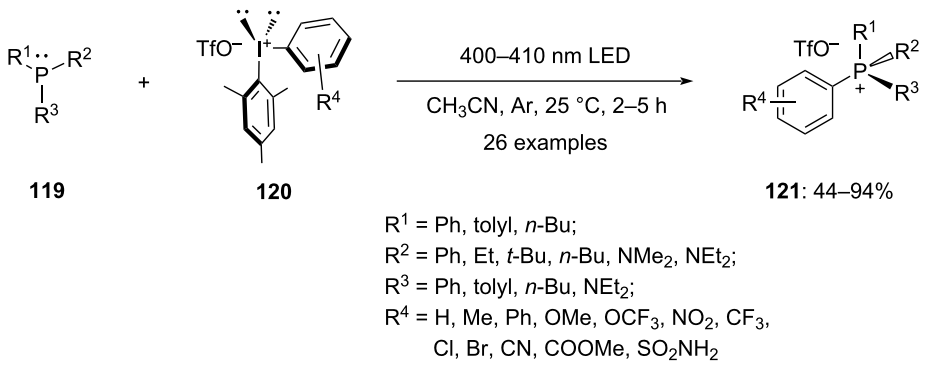

Scheme 46: Light-promoted arylation of tertiary phosphines **119** to quaternary phosphonium salts **121** using diaryliodonium salts **120**.

based on the observed chemoselectivity, it is recommended that the more electron-poor aryl group is transferred. Additionally, the scope of various tertiary phosphates concluded that changing the predetermined reaction conditions is not required to overcome the steric hindrances. Furthermore, with no indications of the N-quaternization products, the arylation of additional organophosphorus(III) compounds, including phosphinous and phosphonous amides, likewise proceeds fruitfully [99].

Karchava and team expanded the use of hypervalent iodine salts to the arylation of aminophosphorus compounds **122**, resulting in the formation of phosphine oxides **123** through oxidative P–N bond cleavages. This innovative method relies solely on light with wavelength of the visible region as the catalyst to achieve C–P bond formation and tolerates various functional groups.

It was observed that on irradiating 4-(diphenylphosphino)morpholine (**122**) dissolved in acetonitrile with blue LED of 400–410 nm wavelength and power of 6 W in the presence of aryl(mesityl)iodonium triflates **120** yielded aminophosphonium salts **123** within 4 h (Scheme 47). The reaction did not require any additive or high temperature and was highly selective as no products were obtained due to *N*-arylation or mesityl transfer. It was noticed that the steric effect had more influence on the selectivity of the aryl transfer in comparison to the electronic effect. The protocol was successful in synthesizing phosphine oxides even in the presence of a substituent at the *ortho* position, demonstrating that the protocol has excellent tolerance towards steric hindrance [100].

Rearrangement reactions

In 2022, Kepski demonstrated an unexpected arylation phenomenon when diphenyliodonium triflate (**16**) was heated in DMSO. It has been observed that diaryliodonium salts with substitution on phenyl and cyclic DAIS are less prone to react with DMSO. The reaction with DMSO is thought to follow a mechanism similar to the Pummerer and interrupted-Pummerer processes. The reaction starts with the arylation of the oxygen in DMSO yielding sulfonium ion **126**, which further deprotonates to give ylide **127**. Succeeding thia-Sommelet–Hauser rearrangement of ylide **127** affords compound **128**. Rearomatization then yields the product **129**, which immediately oxidizes to sulfoxide **125** in the presence of silica (Scheme 48). Since the 1,4-alkylated phenol is not obtained which indicates that the process involves rearrangement instead of elimination of phenol and subsequent addition [101].

Gao and group observed a similar rearrangement when diaryliodonium salts **131** were treated with arylhydroxylamines

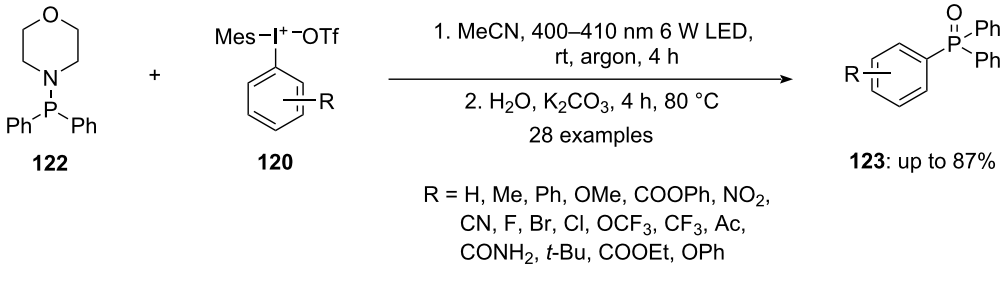

Scheme 47: Arylation of aminophosphorus substrate **122** to synthesize phosphine oxides **123** using aryl(mesityl)iodonium salts **120**.

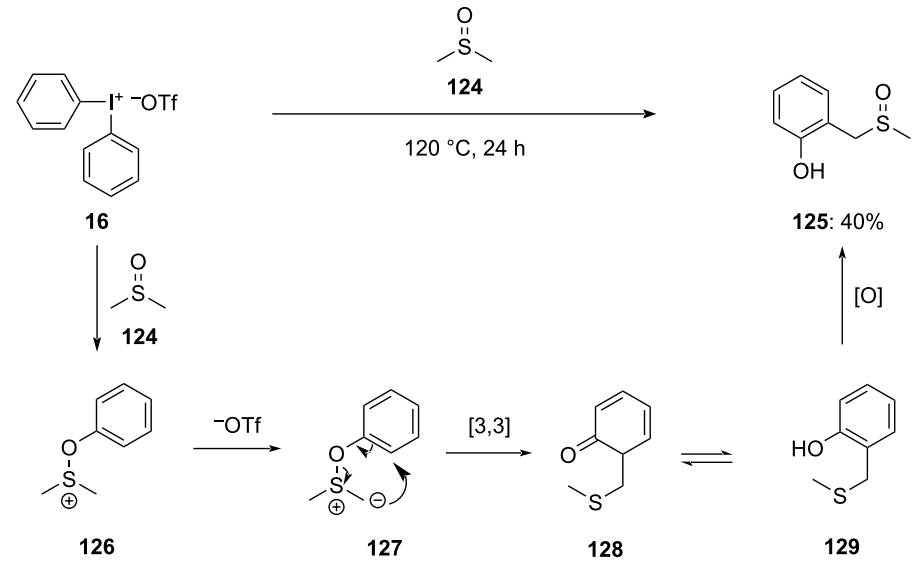

Scheme 48: Reaction of diphenyliodonium triflate (**16**) with DMSO (**124**) via thia-Sommelet–Hauser rearrangement.

130 in the presence of a base. After optimizing the reaction conditions, they investigated the scope and limitations of this transformation. They found that this transition-metal-free tandem approach could be applied to a wide range of arylhydroxylamines **130** and diaryliodonium salts **131**, yielding diverse highly functionalized biaryl amino alcohol motifs **132** (Scheme 49). They successfully obtained the desired racemic NOBIN-type products in decent to outstanding yields, showcasing excellent regioselectivity. Both the starting material compounds' **130** and the diaryliodonium salts' **131** substituents were effectively accommodated under the standard conditions. Notably, this methodology enabled the efficient preparation of biarylamino alcohols with multiple halogens or trifluoromethyl substitutions, which are challenging to access through conventional approaches. Furthermore, the protocol was also suitable for synthesis of naphthyl–phenyl non-C_2-symmetrical biaryls. The transformation was scalable, and the resulting biaryls could be further converted into new heterocycles and atropisomeric biaryl compounds [102].

Recently, Nie et al. approached a transition-metal-free diaryliodonium salt-mediated protocol to synthesize a series of functionalized *N*-(tetrahydrofuran-2-yl)-3-(2-hydroxyaryl)indazoles **135** and 3-(2-hydroxyaryl)indazoles **134** with moderate to good yields. The reported method encompasses a radical *O*-arylation followed by a sequential [3,3]-rearrangement cascade approach starting from *N*-hydroxyindazoles **133** and diaryliodonium salts **16** (Scheme 50). The quantity of diaryliodonium salts added to the reaction strongly influenced the structure of the expected products. The mechanistic study found that both *O*-arylation and N–O bond cleavage proceed via a [3,3]-rearrangement, which involves the transformation of

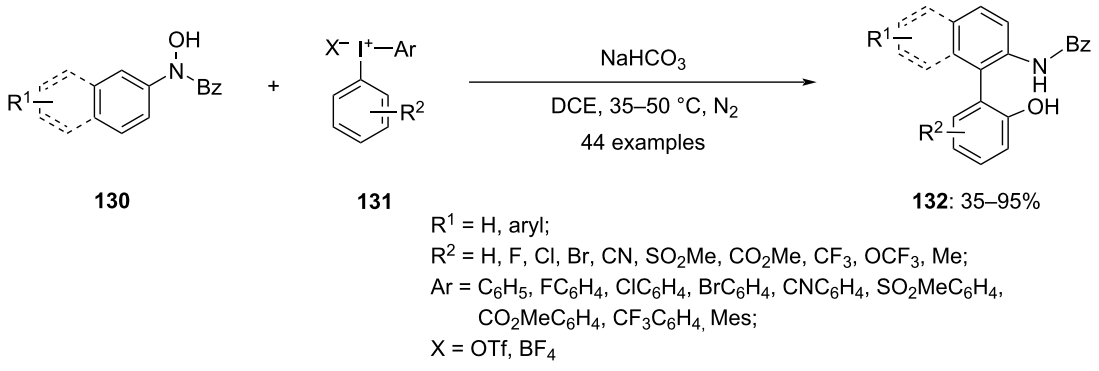

Scheme 49: Synthesis of biaryl compounds **132** by reacting diaryliodonium salts **131** with arylhydroxylamines **130** in the presence of a base.

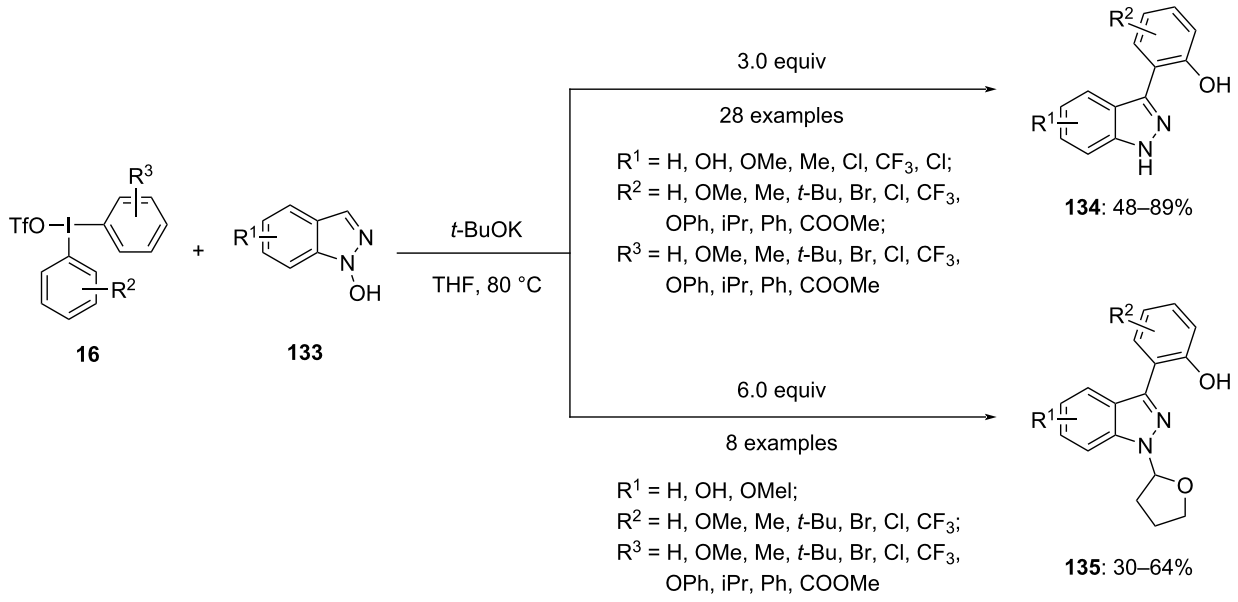

Scheme 50: Synthesis of substituted indazoles **134** and **135** from *N*-hydroxyindazoles **133**.

specific groups within the molecules. Furthermore, this rearrangement occurs through a process involving radicals formed between different molecules, known as an intermolecular radical process. The reaction confirmed tolerance towards a number of functional groups, as aldehydes, esters, and halides [103].

Conclusion

In conclusion, this review emphasises the exceptional selectivity and reactivity of DAIS that facilitate efficient arylation reactions with a diverse range of nucleophiles. This work includes recent advancements in practically simple and scalable methods for the arylation of carbon, nitrogen, sulfur, oxygen, and phosphorus in metal-free conditions. Both symmetrical and unsymmetrical diaryliodonium salts are employed to yield arylated products. Generally, it is observed that in unsymmetrical diaryliodonium salts, the transfer of the aryl group is influenced by its steric and electronic properties, favoring the transfer of the aryl group with lower electron density and less steric hindrance.

Acknowledgements

R.M., F.V.S. and K.S. are thankful to VIT Chennai for providing infrastructure for preparing the review article.

Funding

F.V.S. is also thankful to CSIR, New Delhi for providing the research grant [Grant No.: 02/(0330)/17-EMR].

Author Contributions

Ritu Mamgain: validation; writing – original draft. Kokila Sakthivel: writing – original draft. Fateh V. Singh: conceptualization; resources; supervision; writing – review & editing.

ORCID® iDs

Fateh V. Singh - https://orcid.org/0000-0002-6358-4408

Data Availability Statement

Data sharing is not applicable as no new data was generated or analyzed in this study.

References

1. Wirth, T. *Angew. Chem., Int. Ed.* **2005,** *44,* 3656–3665. doi:10.1002/anie.200500115
2. Richardson, R. D.; Wirth, T. *Angew. Chem., Int. Ed.* **2006,** *45,* 4402–4404. doi:10.1002/anie.200601817
3. Shetgaonkar, S. E.; Jothish, S.; Dohi, T.; Singh, F. V. *Molecules* **2023,** *28,* 5250. doi:10.3390/molecules28135250
4. Singh, F. V.; Wirth, T. *Synthesis* **2012,** *44,* 1171–1177. doi:10.1055/s-0031-1290588
5. Mangaonkar, S. R.; Kole, P. B.; Singh, F. V. *Synlett* **2018,** *29,* 199–202. doi:10.1055/s-0036-1588575
6. Singh, F. V.; Mangaonkar, S. R. *Synthesis* **2018,** *50,* 4940–4948. doi:10.1055/s-0037-1610650
7. Singh, F. V.; Wirth, T. *Org. Lett.* **2011,** *13,* 6504–6507. doi:10.1021/ol202800k
8. Mangaonkar, S. R.; Singh, F. V. *Synthesis* **2019,** *51,* 4473–4486. doi:10.1055/s-0039-1690621

9. Singh, F. V.; Wirth, T. *Synthesis* **2013,** *45,* 2499–2511. doi:10.1055/s-0033-1339679
10. Singh, F. V.; Rehbein, J.; Wirth, T. *ChemistryOpen* **2012,** *1,* 245–250. doi:10.1002/open.201200037
11. Kumar, R.; Singh, F. V.; Takenaga, N.; Dohi, T. *Chem. – Asian J.* **2022,** *17,* e202101115. doi:10.1002/asia.202101115
12. Shetgaonkar, S. E.; Singh, F. V. *Org. Biomol. Chem.* **2023,** *21,* 4163–4180. doi:10.1039/d3ob00057e
13. Shetgaonkar, S. E.; Raju, A.; China, H.; Takenaga, N.; Dohi, T.; Singh, F. V. *Front. Chem. (Lausanne, Switz.)* **2022,** *10,* 909250. doi:10.3389/fchem.2022.909250
14. Sakthivel, K.; Kole, P. B.; Mamgain, R.; Singh, F. V. *Curr. Org. Chem.* **2022,** *26,* 1917–1934. doi:10.2174/1385272827666230103110651
15. Mamgain, R.; Nagarkar, R.; Singh, F. V. *ARKIVOC* **2022,** No. vii, 57–107. doi:10.24820/ark.5550190.p011.768
16. Singh, F. V.; Shetgaonkar, S. E.; Krishnan, M.; Wirth, T. *Chem. Soc. Rev.* **2022,** *51,* 8102–8139. doi:10.1039/d2cs00206j
17. Singh, F. V.; Wirth, T. *Chem. – Asian J.* **2014,** *9,* 950–971. doi:10.1002/asia.201301582
18. Singh, F. V.; Kole, P. B.; Mangaonkar, S. R.; Shetgaonkar, S. E. *Beilstein J. Org. Chem.* **2018,** *14,* 1778–1805. doi:10.3762/bjoc.14.152
19. Shetgaonkar, S. E.; Singh, F. V. *Front. Chem. (Lausanne, Switz.)* **2020,** *8,* 705. doi:10.3389/fchem.2020.00705
20. Mangaonkar, S. R.; Singh, F. V. *Synthesis* **2019,** *51,* 4473–4486. doi:10.1055/s-0039-1690621
21. Shetgaonkar, S. E.; Singh, F. V. *ARKIVOC* **2020,** No. iv, 86–161. doi:10.24820/ark.5550190.p011.418
22. Singh, F. V.; Wirth, T. *ARKIVOC* **2021,** No. vii, 12–47. doi:10.24820/ark.5550190.p011.483
23. Shetgaonkar, S. E.; Mamgain, R.; Kikushima, K.; Dohi, T.; Singh, F. V. *Molecules* **2022,** *27,* 3900. doi:10.3390/molecules27123900
24. Shetgaonkar, S. E.; Singh, F. V. *ARKIVOC* **2020,** No. iv, 86–161. doi:10.24820/ark.5550190.p011.418
25. Singh, F. V.; Mangaonkar, S. R.; Kole, P. B. *Synth. Commun.* **2018,** *48,* 2169–2176. doi:10.1080/00397911.2018.1479760
26. Sakthivel, K.; J, S.; Raju, A.; Kumar, R.; Dohi, T.; Singh, F. V. *ARKIVOC* **2022,** No. vii, 138–165. doi:10.24820/ark.5550190.p011.996
27. Du, Y.; Banerjee, B., Eds. *Non-Metal Catalyzed Synthesis: Bioactive Heterocycles;* De Gruyter: Berlin, Boston, 2024; Vol. 3. doi:10.1515/9783110985474
28. Wirth, T. *Hypervalent Iodine Chemistry;* Topics in Current Chemistry, Vol. 373; Springer International Publishing: Cham, Switzerland, 2016. doi:10.1007/978-3-319-33733-3
29. Wang, M.; Chen, S.; Jiang, X. *Chem. – Asian J.* **2018,** *13,* 2195–2207. doi:10.1002/asia.201800609
30. Dohi, T.; Yamaoka, N.; Kita, Y. *Tetrahedron* **2010,** *66,* 5775–5785. doi:10.1016/j.tet.2010.04.116
31. Crivello, J. V. *J. Polym. Sci., Part A: Polym. Chem.* **1999,** *37,* 4241–4254. doi:10.1002/(sici)1099-0518(19991201)37:23<4241::aid-pola1>3.3.co;2-i
32. Lalevée, J.; Mokbel, H.; Fouassier, J.-P. *Molecules* **2015,** *20,* 7201–7221. doi:10.3390/molecules20047201
33. Lalevée, J.; Blanchard, N.; Tehfe, M.-A.; Morlet-Savary, F.; Fouassier, J. P. *Macromolecules* **2010,** *43,* 10191–10195. doi:10.1021/ma1023318
34. Zhang, Y.; Han, J.; Liu, Z.-J. *RSC Adv.* **2015,** *5,* 25485–25488. doi:10.1039/c5ra00209e
35. Lu, M.-Z.; Loh, T.-P. *Org. Lett.* **2014,** *16,* 4698–4701. doi:10.1021/ol502411c
36. Buslov, I.; Hu, X. *Adv. Synth. Catal.* **2014,** *356,* 3325–3330. doi:10.1002/adsc.201400646
37. Stang, P. J.; Zhdankin, V. V. *J. Am. Chem. Soc.* **1993,** *115,* 9808–9809. doi:10.1021/ja00074a061
38. Olenyuk, B.; Whiteford, J. A.; Stang, P. J. *J. Am. Chem. Soc.* **1996,** *118,* 8221–8230. doi:10.1021/ja961444r
39. Merritt, E. A.; Olofsson, B. *Angew. Chem., Int. Ed.* **2009,** *48,* 9052–9070. doi:10.1002/anie.200904689
40. Zhdankin, V. V.; Stang, P. J. *Chem. Rev.* **2008,** *108,* 5299–5358. doi:10.1021/cr800332c
41. Yamaoka, N. *Synlett* **2012,** *23,* 478–479. doi:10.1055/s-0031-1290133
42. Grushin, V. V. *Chem. Soc. Rev.* **2000,** *29,* 315–324. doi:10.1039/a909041j
43. Stuart, D. R. *Chem. – Eur. J.* **2017,** *23,* 15852–15863. doi:10.1002/chem.201702732
44. Olofsson, B. Arylation with Diaryliodonium Salts. *Hypervalent Iodine Chemistry;* Topics in Current Chemistry, Vol. 373; Springer International Publishing: Cham, Switzerland, 2016; pp 135–166. doi:10.1007/128_2015_661
45. Ledwith, A.; Al-Kass, S.; Sherrington, D. C.; Bonner, P. *Polymer* **1981,** *22,* 143–145. doi:10.1016/0032-3861(81)90188-9
46. Miyamoto, K.; Hirobe, M.; Saito, M.; Shiro, M.; Ochiai, M. *Org. Lett.* **2007,** *9,* 1995–1998. doi:10.1021/ol0706105
47. Chatterjee, N.; Goswami, A. *Eur. J. Org. Chem.* **2017,** 3023–3032. doi:10.1002/ejoc.201601651
48. Oae, S.; Uchida, Y. *Acc. Chem. Res.* **1991,** *24,* 202–208. doi:10.1021/ar00007a003
49. Liu, C.; Zhang, W.; Dai, L.-X.; You, S.-L. *Org. Lett.* **2012,** *14,* 4525–4527. doi:10.1021/ol301939w
50. Norrby, P.-O.; Petersen, T. B.; Bielawski, M.; Olofsson, B. *Chem. – Eur. J.* **2010,** *16,* 8251–8254. doi:10.1002/chem.201001110
51. Malmgren, J.; Santoro, S.; Jalalian, N.; Himo, F.; Olofsson, B. *Chem. – Eur. J.* **2013,** *19,* 10334–10342. doi:10.1002/chem.201300860
52. Kita, Y.; Dohi, T. *Chem. Rec.* **2015,** *15,* 886–906. doi:10.1002/tcr.201500020
53. Neufeldt, S. R.; Sanford, M. S. *Acc. Chem. Res.* **2012,** *45,* 936–946. doi:10.1021/ar300014f
54. Cahard, E.; Male, H. P. J.; Tissot, M.; Gaunt, M. J. *J. Am. Chem. Soc.* **2015,** *137,* 7986–7989. doi:10.1021/jacs.5b03937
55. Zaheer, M. K.; Vaishanv, N. K.; Kant, R.; Mohanan, K. *Chem. – Asian J.* **2020,** *15,* 4297–4301. doi:10.1002/asia.202001160
56. Zaheer, M. K.; Gupta, E.; Kant, R.; Mohanan, K. *Chem. Commun.* **2020,** *56,* 153–156. doi:10.1039/c9cc07859b
57. Zaheer, M. K.; Vaishanv, N. K.; Kumar, A.; Mishra, S.; Kant, R.; Mohanan, K. *Synthesis* **2023,** *55,* 3382–3392. doi:10.1055/a-2109-1419
58. Kikushima, K.; Yamada, K.; Umekawa, N.; Yoshio, N.; Kita, Y.; Dohi, T. *Green Chem.* **2023,** *25,* 1790–1796. doi:10.1039/d2gc04445e
59. Nilova, A.; Sibbald, P. A.; Valente, E. J.; González-Montiel, G. A.; Richardson, H. C.; Brown, K. S.; Cheong, P. H.-Y.; Stuart, D. R. *Chem. – Eur. J.* **2021,** *27,* 7168–7175. doi:10.1002/chem.202100201
60. Jiang, J.; Song, S.; Guo, J.; Zhou, J.; Li, J. *Tetrahedron Lett.* **2022,** *98,* 153820. doi:10.1016/j.tetlet.2022.153820
61. Ghosh, M. K.; Rzymkowski, J.; Kalek, M. *Chem. – Eur. J.* **2019,** *25,* 9619–9623. doi:10.1002/chem.201902204
62. Wu, C.; Zhao, C.; Zhou, J.; Hu, H.-S.; Li, J.; Wu, P.; Chen, C. *Commun. Chem.* **2020,** *3,* 92. doi:10.1038/s42004-020-00343-8

63. Li, D.; Liang, C.; Jiang, Z.; Zhang, J.; Zhuo, W.-T.; Zou, F.-Y.; Wang, W.-P.; Gao, G.-L.; Song, J. *J. Org. Chem.* **2020,** *85,* 2733–2742. doi:10.1021/acs.joc.9b02933
64. Meher, P.; Panda, S. P.; Mahapatra, S. K.; Thombare, K. R.; Roy, L.; Murarka, S. *Org. Lett.* **2023,** *25,* 8290–8295. doi:10.1021/acs.orglett.3c03365
65. Senapati, S.; Parida, S. K.; Karandikar, S. S.; Murarka, S. *Org. Lett.* **2023,** *25,* 7900–7905. doi:10.1021/acs.orglett.3c03146
66. Shaw, R.; Sihag, N.; Jain, S.; Sharma, R.; Yadav, M. R. *J. Org. Chem.* **2023,** *88,* 5652–5660. doi:10.1021/acs.joc.3c00141
67. Jiang, J.; Li, J. *ChemistrySelect* **2020,** *5,* 542–548. doi:10.1002/slct.201904188
68. Linde, E.; Bulfield, D.; Kervefors, G.; Purkait, N.; Olofsson, B. *Chem* **2022,** *8,* 850–865. doi:10.1016/j.chempr.2022.01.009
69. Linde, E.; Olofsson, B. *Angew. Chem., Int. Ed.* **2023,** *62,* 202310921. doi:10.1002/anie.202310921
70. Kervefors, G.; Kersting, L.; Olofsson, B. *Chem. – Eur. J.* **2021,** *27,* 5790–5795. doi:10.1002/chem.202005351
71. Roshandel, S.; Lunn, M. J.; Rasul, G.; Muthiah Ravinson, D. S.; Suri, S. C.; Prakash, G. K. S. *Org. Lett.* **2019,** *21,* 6255–6258. doi:10.1021/acs.orglett.9b02140
72. Saikia, R. A.; Dutta, A.; Sarma, B.; Thakur, A. J. *J. Org. Chem.* **2022,** *87,* 9782–9796. doi:10.1021/acs.joc.2c00848
73. Kuriyama, M.; Hanazawa, N.; Abe, Y.; Katagiri, K.; Ono, S.; Yamamoto, K.; Onomura, O. *Chem. Sci.* **2020,** *11,* 8295–8300. doi:10.1039/d0sc02516j
74. Linde, E.; Knippenberg, N.; Olofsson, B. *Chem. – Eur. J.* **2022,** *28,* e202202453. doi:10.1002/chem.202202453
75. Satkar, Y.; Wrobel, K.; Trujillo-González, D. E.; Ortiz-Alvarado, R.; Jiménez-Halla, J. O. C.; Solorio-Alvarado, C. R. *Front. Chem. (Lausanne, Switz.)* **2020,** *8,* 563470. doi:10.3389/fchem.2020.563470
76. Gallagher, R. T.; Basu, S.; Stuart, D. R. *Adv. Synth. Catal.* **2020,** *362,* 320–325. doi:10.1002/adsc.201901187
77. Kervefors, G.; Pal, K. B.; Tolnai, G. L.; Mahanti, M.; Leffler, H.; Nilsson, U. J.; Olofsson, B. *Helv. Chim. Acta* **2021,** *104,* e2000220. doi:10.1002/hlca.202000220
78. Zhou, J.; Bao, Z.; Wu, P.; Chen, C. *Molecules* **2021,** *26,* 3240. doi:10.3390/molecules26113240
79. Zhou, J.; Bao, Z.; Wu, P.; Chen, C. *Synthesis* **2022,** *54,* 1388–1394. doi:10.1055/a-1679-7753
80. Liu, M.; Jiang, H.; Tang, J.; Ye, Z.; Zhang, F.; Wu, Y. *Org. Lett.* **2023,** *25,* 2777–2781. doi:10.1021/acs.orglett.3c00600
81. Chen, H.; Han, J.; Wang, L. *Angew. Chem., Int. Ed.* **2018,** *57,* 12313–12317. doi:10.1002/anie.201806405
82. Wang, Y.; Zhang, Y.; Wang, L.; Han, J. *Asian J. Org. Chem.* **2022,** *11,* e202100669. doi:10.1002/ajoc.202100669
83. Liu, X.; Wang, L.; Wang, H.-Y.; Han, J. *J. Org. Chem.* **2023,** *88,* 13089–13101. doi:10.1021/acs.joc.3c01293
84. Kikushima, K.; Miyamoto, N.; Watanabe, K.; Koseki, D.; Kita, Y.; Dohi, T. *Org. Lett.* **2022,** *24,* 1924–1928. doi:10.1021/acs.orglett.2c00294
85. Elboray, E. E.; Bae, T.; Kikushima, K.; Kita, Y.; Dohi, T. *Adv. Synth. Catal.* **2023,** *365,* 2703–2710. doi:10.1002/adsc.202300406
86. Yoshimura, A.; Zhdankin, V. V. *Chem. Rev.* **2016,** *116,* 3328–3435. doi:10.1021/acs.chemrev.5b00547
87. Ghosh, M. K.; Rajkiewicz, A. A.; Kalek, M. *Synthesis* **2019,** *51,* 359–370. doi:10.1055/s-0037-1609639
88. Sarkar, S.; Wojciechowska, N.; Rajkiewicz, A. A.; Kalek, M. *Eur. J. Org. Chem.* **2022,** e202101408. doi:10.1002/ejoc.202101408
89. Wang, L.; Chen, M.; Zhang, J. *Org. Chem. Front.* **2019,** *6,* 32–35. doi:10.1039/c8qo00914g
90. Saikia, R. A.; Hazarika, N.; Biswakarma, N.; Chandra Deka, R.; Thakur, A. J. *Org. Biomol. Chem.* **2022,** *20,* 3890–3896. doi:10.1039/d2ob00406b
91. Byrne, S. A.; Bedding, M. J.; Corcilius, L.; Ford, D. J.; Zhong, Y.; Franck, C.; Larance, M.; Mackay, J. P.; Payne, R. J. *Chem. Sci.* **2021,** *12,* 14159–14166. doi:10.1039/d1sc03127a
92. Wu, X.; Li, Y.; Chen, M.; He, F.-S.; Wu, J. *J. Org. Chem.* **2023,** *88,* 9352–9359. doi:10.1021/acs.joc.3c00961
93. Zhou, Q.; Li, J.; Wang, T.; Yang, X. *Org. Lett.* **2023,** *25,* 4335–4339. doi:10.1021/acs.orglett.3c01436
94. Huang, G.; Lu, X.; Liang, F. *Org. Lett.* **2023,** *25,* 3179–3183. doi:10.1021/acs.orglett.3c01077
95. Bugaenko, D. I.; Volkov, A. A.; Andreychev, V. V.; Karchava, A. V. *Org. Lett.* **2023,** *25,* 272–276. doi:10.1021/acs.orglett.2c04143
96. Soldatova, N. S.; Postnikov, P. S.; Suslonov, V. V.; Kissler, T. Y.; Ivanov, D. M.; Yusubov, M. S.; Galmés, B.; Frontera, A.; Kukushkin, V. Y. *Org. Chem. Front.* **2020,** *7,* 2230–2242. doi:10.1039/d0qo00678e
97. Sarkar, S.; Kalek, M. *Org. Lett.* **2023,** *25,* 671–675. doi:10.1021/acs.orglett.2c04310
98. Radzhabov, A. D.; Soldatova, N. S.; Ivanov, D. M.; Yusubov, M. S.; Kukushkin, V. Y.; Postnikov, P. S. *Org. Biomol. Chem.* **2023,** *21,* 6743–6749. doi:10.1039/d3ob00833a
99. Bugaenko, D. I.; Volkov, A. A.; Livantsov, M. V.; Yurovskaya, M. A.; Karchava, A. V. *Chem. – Eur. J.* **2019,** *25,* 12502–12506. doi:10.1002/chem.201902955
100. Bugaenko, D. I.; Karchava, A. V. *Adv. Synth. Catal.* **2023,** *365,* 1893–1900. doi:10.1002/adsc.202300351
101. Kepski, K.; Moran, W. J. *Organics* **2022,** *3,* 275–280. doi:10.3390/org3030020
102. Yuan, H.; Du, Y.; Liu, F.; Guo, L.; Sun, Q.; Feng, L.; Gao, H. *Chem. Commun.* **2020,** *56,* 8226–8229. doi:10.1039/d0cc02919j
103. Nie, S.-M.; Zhang, X.; Wang, Z.-X.; Su, G.-F.; Pan, C.-X.; Mo, D.-L. *Adv. Synth. Catal.* **2022,** *364,* 3782–3788. doi:10.1002/adsc.202200569

BEILSTEIN JOURNAL OF ORGANIC CHEMISTRY

Structure and thermal stability of phosphorus-iodonium ylids

Andrew Greener, Stephen P. Argent, Coby J. Clarke* and Miriam L. O'Duill*

Full Research Paper

Open Access

Address:
School of Chemistry, University of Nottingham, University Park, Nottingham NG7 2RD, UK

Email:
Coby J. Clarke* - coby.clarke@nottingham.ac.uk; Miriam L. O'Duill* - miriam.oduill@nottingham.ac.uk

* Corresponding author

Keywords:
hypervalent iodine; reagent development; structural analysis; thermal stability; thermogravimetric analysis

Beilstein J. Org. Chem. **2024,** *20,* 2931–2939.
https://doi.org/10.3762/bjoc.20.245

Received: 09 August 2024
Accepted: 02 October 2024
Published: 14 November 2024

This article is part of the thematic issue "Hypervalent halogen chemistry".

Guest Editor: T. Gulder

Abstract

Hypervalent iodine(III) reagents have become indispensable tools in organic synthesis, but gaps remain in the functionalities they can transfer. In this study, a fundamental understanding of the thermal stability of phosphorus-iodonium ylids is obtained through X-ray diffraction, differential scanning calorimetry (DSC) and thermogravimetric analysis (TGA). Insights into the structural factors affecting thermal stability and potential decomposition pathways will enable the future design and development of new reagents.

Introduction

Hypervalent iodine(III) reagents have experienced a renaissance in synthetic organic chemistry, becoming indispensable tools in total synthesis, late-stage functionalisation and radiolabelling [1-9]. Due to their great mechanistic flexibility, including reactivity as oxidants, electrophiles, radical precursors and transmetalating agents, they often enable access to chemical motifs that are difficult to synthesise using traditional approaches. However, gaps remain in the functionality they can transfer. Specifically, unstabilised alkyl groups are still underrepresented. For the development of new hypervalent iodine reagents to bridge this gap, it is vital to gain a fundamental understanding of the structural factors affecting their stability and reactivity.

Previous reports have suggested a link between structural factors and thermal stability of hypervalent iodine compounds [10-16]. Iodine(III) compounds are generally trigonal bipyramidal (T-shaped) with the least electronegative group and the two nonbonding electron pairs occupying the equatorial positions, and the most electronegative substituents forming a hypervalent 3-centre-4-electron (3c-4e) bond in the axial position (Figure 1A) [17,18]. The LUMO of this bond is concentrated on iodine [19], making it highly electrophilic, while a nonbonding pair of electrons is mainly centred on the axial substituents, causing a build-up of electron density on these positions (Figure 1A) [1,20]. Stabilisation of this charge on the axial substituents by strong electron-withdrawing groups or delocalisation into a π-system results in crystalline, bench-stable reagents. In the absence of stabilising factors, rapid decomposition occurs [21-23].

In this study, we aim to gain a fundamental understanding of the factors that stabilise phosphorus-iodonium ylids **1** (Figure 1B) [24-27] and the mechanisms by which they decompose when

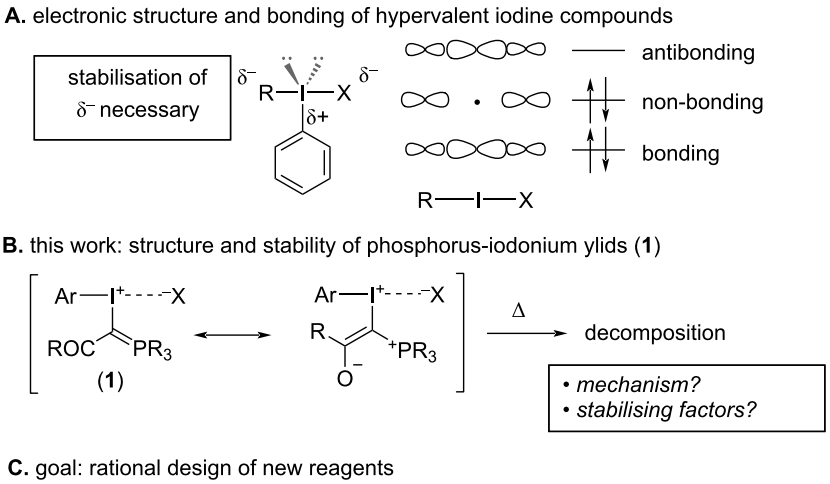

Figure 1: Structure and stability of hypervalent iodine compounds.

heated through a systematic investigation of structural data from X-ray diffraction (XRD) and thermal stability data from differential scanning calorimetry (DSC) and thermogravimetric analysis (TGA). The insights from this study will galvanise the rational design and synthesis of novel, unstabilised hypervalent iodine(III) compounds and expand the application of these powerful reagents in organic synthesis.

Results and Discussion

Structural data

Twelve phosphorus-iodonium ylids were synthesised (Figure 2). X-ray diffraction data (XRD) of compounds **1a–f** and **1i** were measured (see Supporting Information File 2), and data for compounds **2**–**4** were sourced from the literature [24,26,28]. A representative set of structural parameters obtained from XRD is presented in Table 1.

All compounds show a trigonal bipyramidal structure, in which the 3-centre-4-electron bond is slightly distorted from linear geometry by 5–20° (Table 1). The short C–P and C–C bonds (*d* and *e*) in the phosphorus ylid moiety confirm Moriarty and Zhdankin's observation that the ylid exists mainly in its enolate form (Figure 1B) [24,25] to stabilise the build-up of negative charge on this substituent in the hypervalent bond. The long I–X distances (*a* = 2.758–4.165 Å) are indicative of ionic compounds, with the exception of the cyclic benziodoxolone **2**, in which a covalent I–O bond is observed (*a* = 2.484 Å). We were unable to obtain a crystal structure of the *ortho*-nitro compound **1j**. However, a previously reported crystal structure of ylid **3**, which also contains an *ortho*-nitrobenzene substituent, suggests a pseudocyclic structure where the nitro group is coordinating to the iodine centre ($a_{(I–ON)}$ = 2.695 Å) [28], which we propose is likely to be the case in **1j** as well.

In the acyclic tetrafluoroborate (**1a**), triflate (**1b**), chloride (**1c**) and nitrate (**1d**), the anion X^- occupies the position *trans* to the arene substituent, with the ylid in the equatorial position. In tosylates **1e** and **1f**, as well as the cyclic and pseudocyclic structures **2** and **3**, the anion or coordinating ligand occupies the position *trans* to the ylid substituent, with the aryl substituent in the equatorial position. Substituents on hypervalent iodine compounds can interconvert via Barry pseudorotation [31] and, interestingly, the crystal structure for compound **1i** contains two isomers in its unit cell, with the tosylate *trans* to the arene in one (θ_2 = 177.8) and *trans* to the ylid in the other (θ_1 = 169.5), which suggests that this isomerisation is fast at room temperature and the position of the anion has no significant effect on the stability of these compounds. This hypothesis is further supported by the absence of a *trans* effect. While studies by Ochiai and Suresh found that strong sigma donors X cause a lengthening and weakening of the *trans* I–R bond in R–I(Ar)–X iodanes [32,33], little variation is observed in the I–C(ylid) (*b*) and I–C(arene) (*c*) bonds across the range of compounds investigated in our study (Table 1).

Thermal stability data

The phosphorus-iodonium ylids were analysed by differential scanning calorimetry (DSC) and thermogravimetric analysis (TGA) [34,35], and results have been summarised in Table 2 and Figure 3. (The full dataset is available in Supporting Information File 1.) All compounds show a multi-step mass loss behaviour with a range of TGA decomposition onset temperatures (T_{onset}) between 107–137 °C, with the exception of three compounds that are stable to higher temperatures (**1a**: T_{onset} = 176 °C, Δ*H* = 134 J/g; **1j**: 172 °C, 130 J/g; **2**: 225 °C, 274 J/g; Table 2) and two highly unstable compounds (**1d**: 88 °C, 671 J/g; **1k**: 74 °C, 70.2 J/g; Table 2).

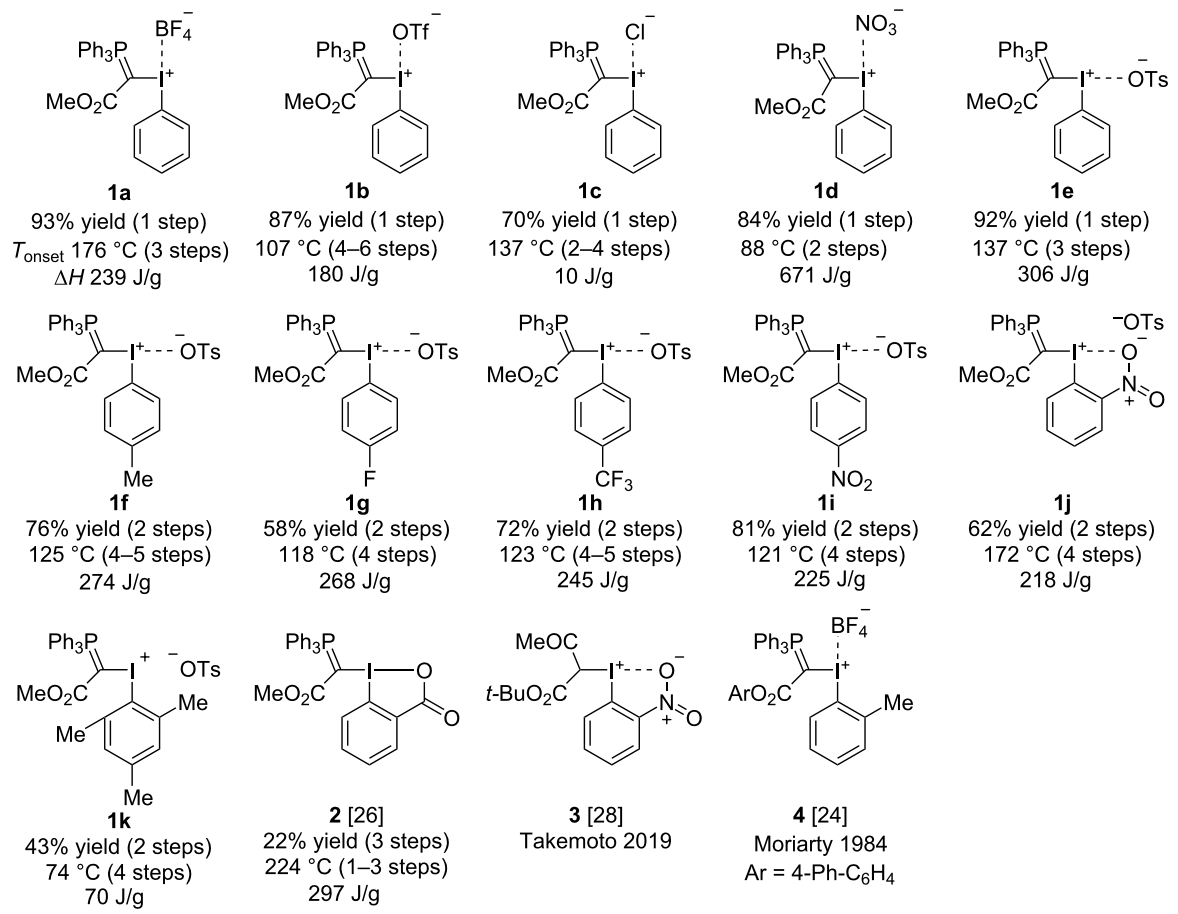

Figure 2: Phosphorus-iodonium ylids investigated in this study: Yields (for synthetic procedures, see Supporting Information File 1), structure and thermal data. The decomposition onset temperature, T_{onset}, and the number of decomposition steps (in brackets) were determined by TGA measurements, Δ*H* was obtained by DSC.

Table 1: XRD data.

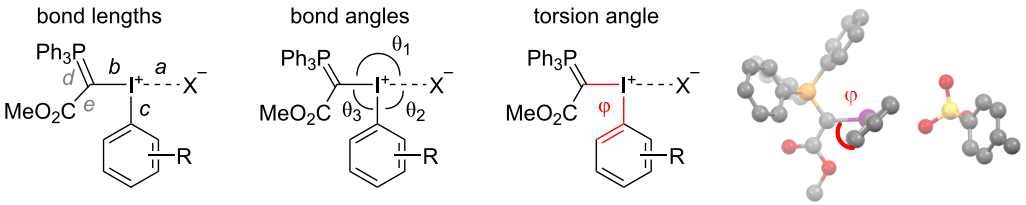

	Bond lengths [Å][a]					Bond angles [°]			Torsion angle [°]
	a	b	c	d	e	θ_1	θ_2	θ_3	φ
1a	4.165(2)	2.026(7)	2.108(7)	1.742(7)	1.421(9)	98.2(4)	158.85(5)	99.2(3)	29.5(7)
1b	3.069(3)	2.026(4)	2.129(4)	1.740(5)	1.454(7)	90.6(1)	160.6(2)	100.0(2)	38.3(5)
1c	3.1411(5)	2.051(2)	2.134(2)	1.736(2)	1.422(3)	89.40(6)	174.24(5)	95.92(8)	40.8(2)
1d[b]	3.16(1)[b]	2.07(2)	2.12(1)	1.72(1)	1.39(2)	101.6(5)[b]	157.7(5)[b]	97.0(6)	50.0(1)
1e	2.910(4)	2.048(5)	2.123(6)	1.736(6)	1.430(7)	169.1(2)	77.5(2)	97.2(2)	41.5(5)
1f-h1[c]	2.839(6)	2.050(7)	2.133(8)	1.736(7)	1.417(13)	170.0 (3)	84.25(3)	96.6(3)	46.2(7)

Table 1: XRD data. (continued)

1f-h2[c]	2.832(7)	2.042(7)	2.107(7)	1.726(7)	1.442(10)	171.6(3)	82.95(3)	96.6(3)	47.2(6)
1i[d]	2.803(4)	2.046(5)	2.112(3)	1.727(6)	1.429(8)	169.5(2)	76.6(2)	96.0(2)	58.7(5)
	2.758(3)	2.057(5)	2.119(3)	1.738(6)	1.432(8)	84.5(2)	177.8(2)	97.0(2)	44.0(5)
2 [26]	2.484(3)	2.056(3)	2.134(3)	1.736(3)	1.439(4)	169.2(1)	72.5(1)	97.0(1)	2.9(3)
3 [28]	2.695	2.050	2.119	N/A	1.449	168.0	68.8	99.9	4.8
4 [24]	4.062	2.056	2.094	1.709	1.457	92.6	168.4	96.8	42.9

[a]Standard bond lengths: P=C 1.66 Å, P–C 1.87 Å, C=C 1.34 Å, C–C 1.46 Å, C_{Ar}–I(I) 2.095 Å, C_{Ar}–I(III) 2.0–2.1 Å (diaryliodonium salts), C(sp^3)–I(I) 2.162 Å, C(sp^3)–I(III) 2.21–2.22 Å [22,29,30]. [b]The I–X bond length *a* is measured from I to the closest O in the nitrate anion. θ_1 and θ_2 are reported as the C–I–N bond angles. [c]Two different solvatomorphs were obtained (**1f-hydrate1** and **1f-hydrate2**, see Supporting Information File 1); bond length and angle data for both solvatomorphs are given in the table. [d]Two isomers exist in the unit cell of **1i**, with X^- axial (θ_1 = 169.5) in one of them and equatorial (θ_2 = 177.8) in the other; bond length and angle data for both isomers are given in Table 1.

Table 2: DSC and TGA data[a].

			DSC			TGA	
	Peaks[b]	Mass loss?[c]	T_{onset} [°C]	T_{peak} [°C]	Enthalpy ΔH [J/g]	T_{onset} [°C]	Steps
1a	1	N	151.39	159.42	104.61	175.68	3
	2	Y	182.30	186.56	134.15		
1b	u/r	Y	59.53	88.36	179.81	106.65	4–6
1c	1[d]		129.31	104.35	9.89	137.17	2–4
1d	1		79.51	84.66	671.31	88.23	2
1e	1	N	85.64	91.84	39.95	137.01	3
	2	Y	114.48	124.06	267.18		
1f	1	Y	115.16	121.31	273.83	124.93	4–5
1g	1	Y	101.98	110.95	268.36	118.07	4
1h	1	Y	106.21	118.93	167.70	122.81	4–5
	2	Y	121.95	131.75	78.30		
1i	1	Y	91.13	109.50	184.10	121.14	4
	2	Y	115.65	127.01	41.10		
1j[e]	1	Y	152.52	160.16	129.70	172.10	4
	2	Y	165.89	173.80	87.50		
1k[f]	1		52.68	71.92	70.18	73.62	4
2	1	N	100.41	101.88	22.88	224.08	1–3
	2	Y	214.56	220.84	273.90		

[a]Heating rates (DSC and TGA): 10 °C min^{-1}. [b]u/r = unresolved. [c]Mass loss is taken as <99% mass in the TGA at T_{peak} in the DSC. [d]The thermogram shows a range of complex peaks after this first peak. [e]A glass transition temperature of T_g = 32.24 °C was observed. [f]Heating rate (DSC and TGA): 5 °C min^{-1}.

We were interested to investigate whether we could identify structural features that could explain these outliers. We observed a quantifiable anion (X) effect, with acyclic tetrafluoroborate **1a** showing greater stability than the other acyclic phosphorus-iodonium ylids, while nitrate **1d** was highly thermally labile [36]. However, we were unable to rationalise or predict the anion effect with parameters such as the anion's donor ability σ_m, which has previously been used as a measure of its *trans* effect (Supporting Information File 1, Figure S6), the Kamlet–Taft hydrogen bond acceptor ability (β) (Supporting Information File 1, Figure S7) [37], the pK_a of the conjugate acid HX (Figure S8), or the anion's position (axial vs equatorial).

The main stabilising factor we identified was the torsion angle φ between the hypervalent R–I–X bond and the plane of the arene substituent (Figure 3c): When the plane of the arene ring was parallel to the R–I–X bond (φ < 5°), relatively stable com-

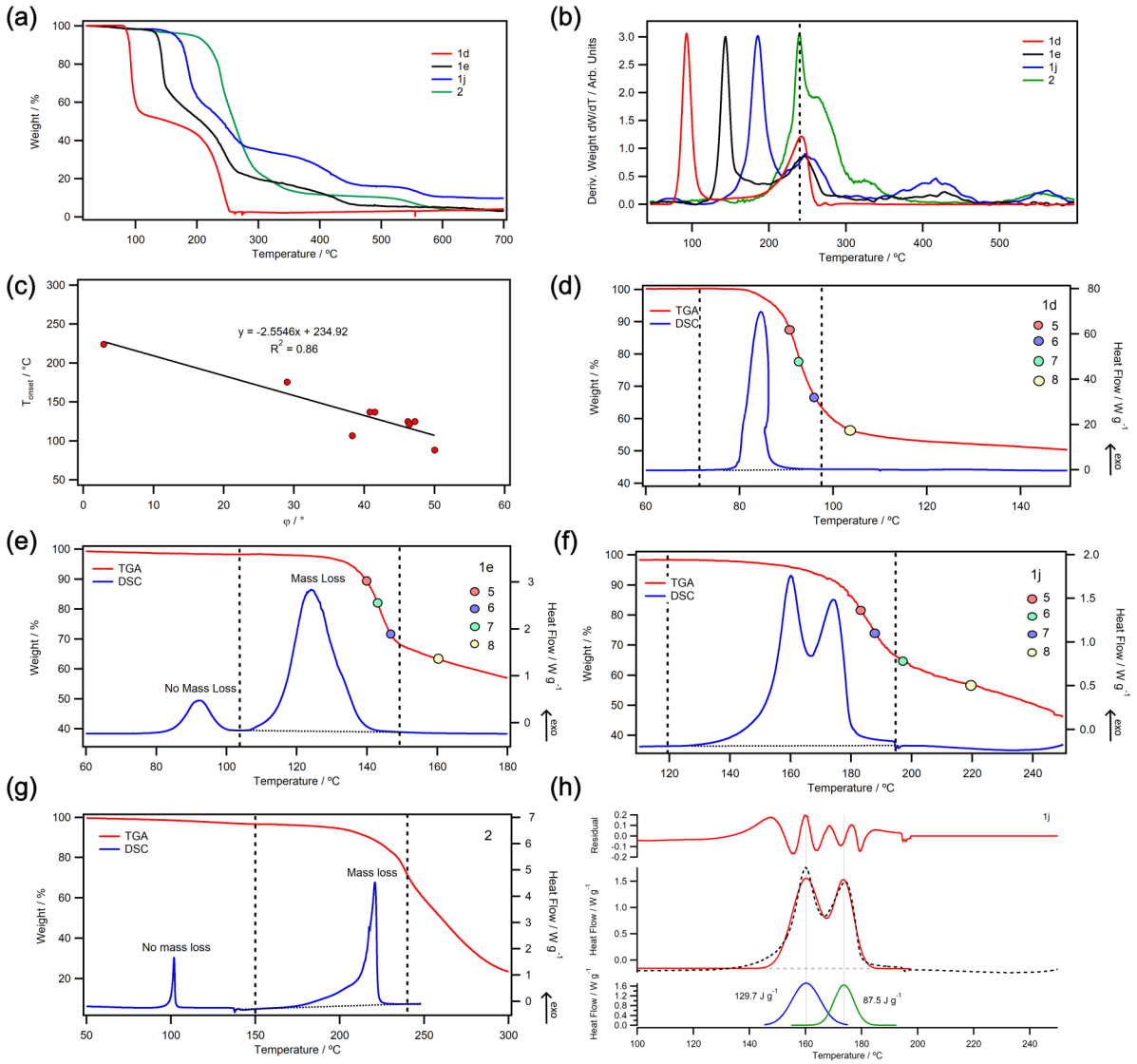

Figure 3: (a) Selected TGA thermograms of phosphorus-iodonium ylids at 10 °C min^{-1} in N_2 (full dataset in Supporting Information File 1). (b) First derivatives of TGA thermograms normalised to the intensity of the first peak. (c) Correlation of T_{onset} with the dihedral angle φ (between the R–I–X bond and the plane of the arene substituent). (d–g) DSC thermograms overlaid with TGA thermograms with integration windows (dashed lines). Points 5–8 on the TGA thermogram denote calculated weight % values for the decomposition products **5**–**8** shown in Figure 4a. (h) Enthalpy deconvolution in DSC data of **1j** by Gaussian fit.

pounds ensued, while a large twist away from planarity resulted in compounds that were destabilised towards thermal decomposition. For example, compound **1d**, which was extremely thermally labile, had the largest dihedral angle (φ = 50°), i.e., the strongest twist away from planarity, while **1a** had the smallest dihedral angle (φ = 29°) of the acyclic compounds and showed the highest stability. In benziodoxolone **2** (φ = 3°) and pseudocyclic **1j** (cf. φ (**3**) = 5°) [28], the arene ring is virtually in the same plane as the 3-centre-4-electron bond, giving rise to the most stable compounds in our series (T_{onset} (**2**) = 225 °C; T_{onset} (**1j**) = 172 °C). By contrast, mesityl phosphonium ylid **1k** showed very low thermal stability (T_{onset} = 74 °C, ΔH = 70 J/g). *Ortho*-methyl groups have been shown to destabilise iodonium species by inducing a larger hypervalent twist [31,38,39], and while we were unable to obtain a crystal structure of **1k**, a large dihedral angle (φ = 43°) was observed in Moriarty's *ortho*-methylbenzene phosphonium ylid **4** [24], which is structurally similar.

While most DSC thermograms of our phosphorus-iodonium ylids showed single exothermic peaks during the first step of thermal decomposition (Figure 3d), some samples (**1a**, **1e**, **2**) had exothermic peaks without mass loss (Figure 3e, 3g). It is possible that these peaks correspond to a geometric rearrange-

ment, e.g., Berry pseudorotation, which occurs prior to decomposition [31]. A large dihedral angle φ is thought to facilitate this rearrangement, thus accelerating decomposition [38,39].

Decomposition mechanism

Further analysis was carried out to gain a better understanding of the decomposition mechanism.

Despite large differences in T_{onset}, most samples showed relatively consistent second decomposition steps at ca. 225 °C (Figure 3b), which is indicative of a common decomposition intermediate for all compounds. To investigate this common intermediate, ex-situ mass spectrometry (MS) and NMR analysis were carried out on aborted TGA runs of compounds **1e**, **1i**, **1j** and **1k** that had been held at a constant temperature T_1 (50–140 °C, see Supporting Information File 1) under an N_2 atmosphere in open pans for 30 min or until a mass loss >5% of the original mass was observed, then heated to temperature T_2 (136–205 °C, see Supporting Information File 1) until 20–40% mass loss of original weight. Based on this data, the following decomposition mechanism is proposed (Figure 4a):

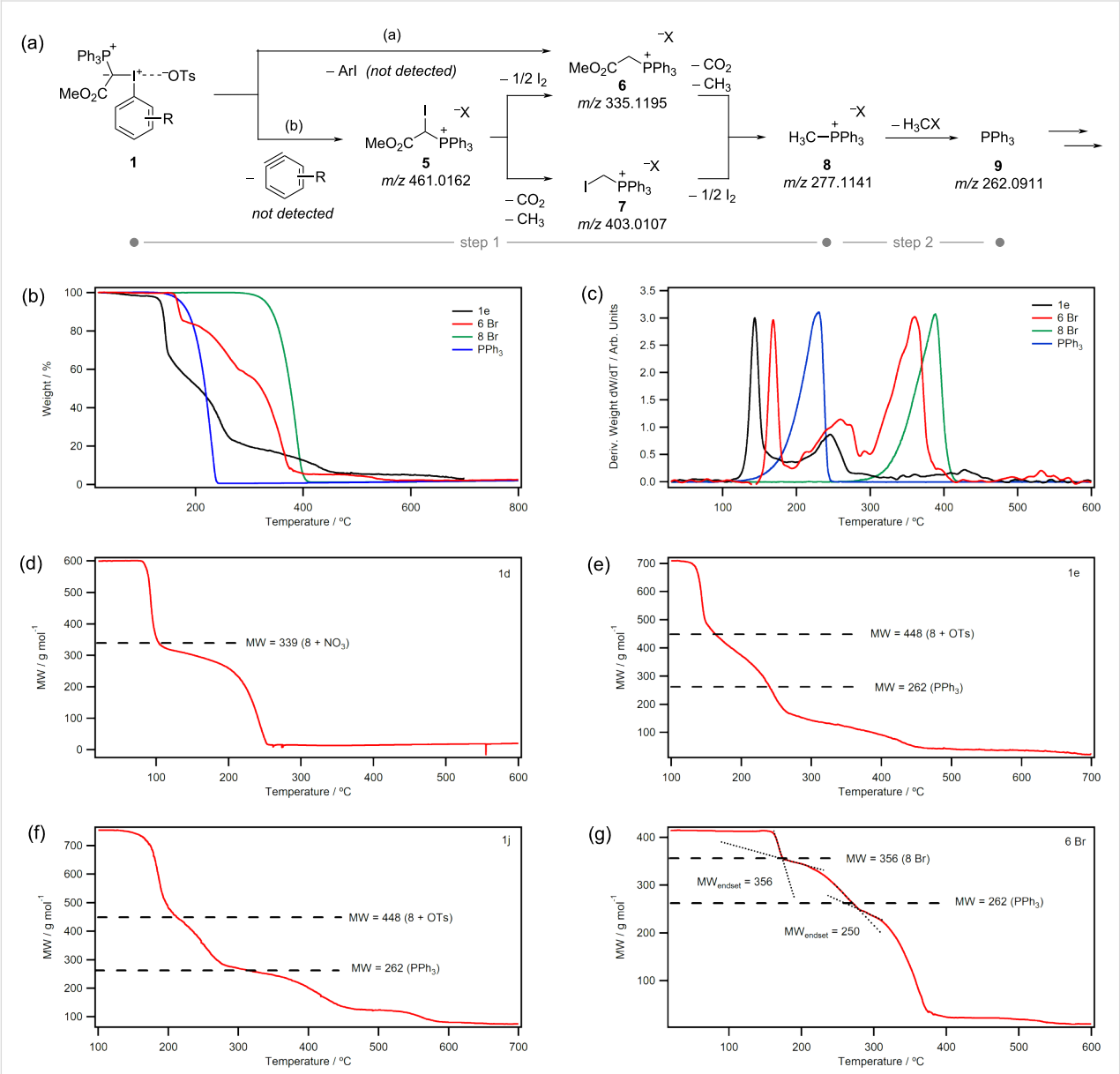

Figure 4: (a) Proposed decomposition mechanism based on ex situ analysis (^{1}H, ^{31}P NMR, ESI-MS) following aborted TGA experiments. (b–c) TGA and derivative plots for **1e** and commercial samples of decomposition products **6** (Br^- salt), **8** (Br^- salt) and PPh_3. (d–g) TGA thermograms replotted to show the molecular weight as a function of temperature assuming 100% conversion (i.e., constant moles) with decomposition product marked.

MS, ^{1}H and ^{31}P NMR analysis after heating to T_1 showed the presence of (methyloxycarbonylmethyl)triphenylphosphonium salt **6** and (iodomethyl)triphenyl-phosphonium salt **7**. Homolytic or heterolytic scission of the I–C(ylid) bond with loss of ArI (path a) would result in a carbene, though it is unclear how this would transform to compound **6**. Alternatively, scission of the I–C(Ar) bond with loss of benzyne (path b) results in (methoxycarbonyl(iodo)methyl)triphenylphosphonium salt **5** (observed by MS). Deiodination or decarboxylation from this intermediate afford **6** and **7**, respectively. After heating to T_2, (methyl)triphenylphosphonium salt **8** is observed, which may be formed from **6** and **7** by decarboxylation and loss of iodine, respectively. Decomposition products **5**–**8** have been marked on the TGA thermograms in Figure 3d–f. All points fall within the first mass loss step, suggesting that decomposition to compound **8** occurs in a single TGA step (labelled 'step 1' in Figure 4b–c). (Note that a single TGA step does not necessarily correspond to one elementary reaction [40].) This is further confirmed by Figure 4d–g, which show that calculated molecular weights of the (methyl)triphenylphosphonium salts **8** coincide with the end of the first TGA step. Compound **8** likely has compromised stability from other residual decomposition products and the second TGA step represents further decomposition of **8** to PPh_3 or a similar molecular weight salt (Figure 4a, step 2).

To confirm our mechanistic proposal for decomposition step 1, a commercial sample of (methyloxycarbonylmethyl)triphenylphosphonium bromide **6** was analysed by TGA (Figure 4b,c). The thermogram showed three decomposition steps, with a T_{onset} value of 164 °C. The molecular weight plot shows an endset value corresponding to the molecular weight of **8** after the first TGA step (Figure 4g), supporting the proposition that **6** decomposed to **8**.

Importantly, DSC data captures the enthalpy of decomposition for TGA step 1 only (decomposition of phosphorus-iodonium ylids **1** and **2** to (methyl)triphenylphosphonium salt **8**). This suggests that differences in the enthalpy of decomposition ΔH arise mainly due to difference in the aryl substituent and the anion.

When analysing *para*-substituted phosphoranyl(aryl)iodonium compounds **1f–i**, no direct correlation between the substituents' Hammett parameter σ_p and the decomposition onset temperature T_{onset} was observed (Supporting Information File 1, Figure S13). However, the DSC thermograms of iodonium ylids with electron-poor aryl substituents (**1h**,**i**) showed two exothermic peaks (Figure 3f), which suggests that two competing decomposition pathways may be occurring in these compounds, complicating the data and any correlations drawn from it. While DSC decomposition enthalpies of both steps can be deconvoluted (Figure 3h), further studies are necessary to fully understand the electronic effect of the arene substituent.

Conclusion

A systematic investigation of phosphorus-iodonium ylids was carried out, correlating structural data from X-ray crystallography with thermal stability data from DSC and TGA measurements.

A common decomposition mechanism involving scission of the C(ylid)–I bond or the C(Ar)–I bond was proposed based on ex situ MS and NMR analysis, resulting in the formation of (methyl)triphenylphosphonium intermediate **8**. The nature of the arene substituent (I–Ar) and anion (X) appear to play an important, yet currently unquantifiable, role in this decomposition, which will be elucidated with future computational studies.

It was, however, found that the torsion angle φ (or 'hypervalent twist') between the plane of the arene substituent and the hypervalent 3-centre-4-electron bond was instrumental: When the arene ring was locked in the same plane as the R–I–X bond through formation of a cyclic or pseudocyclic structure ($\varphi < 5°$), relatively stable compounds ensued, while a large twist away from planarity resulted in compounds that were destabilised towards thermal decomposition.

We envisage that the insights gained from this study will stimulate the design and synthesis of new hypervalent iodine compounds, expanding the functionalisation reactions currently available through these useful reagents in organic synthesis.

Supporting Information

Supporting Information File 1

Experimental procedures, analytical data (NMR spectra), thermal (DSC, TGA) and structural (XRD) data.
[https://www.beilstein-journals.org/bjoc/content/supplementary/1860-5397-20-245-S1.pdf]

Supporting Information File 2

X-ray structure data files.
[https://www.beilstein-journals.org/bjoc/content/supplementary/1860-5397-20-245-S2.cif]

Funding

The authors gratefully acknowledge financial support from UKRI / EPSRC (New Investigator Award EP/W00934X/1 to MOD), the Royal Society (research equipment grant

RGS\R2\212144 to MOD) and the University of Nottingham (Ph.D. studentship for AG).

ORCID® iDs

Andrew Greener - https://orcid.org/0000-0001-8098-6276
Stephen P. Argent - https://orcid.org/0000-0002-3461-9675
Miriam L. O'Duill - https://orcid.org/0000-0002-8312-824X

Data Availability Statement

All data that supports the findings of this study is available in the published article and/or the supporting information of this article.

References

1. Merritt, E. A.; Olofsson, B. *Angew. Chem., Int. Ed.* **2009,** *48,* 9052–9070. doi:10.1002/anie.200904689
2. Wirth, T., Ed. *Hypervalent Iodine Chemistry;* Topics in Current Chemistry, Vol. 373; Springer International Publishing: Cham, Switzerland, 2016. doi:10.1007/978-3-319-33733-3
3. Yoshimura, A.; Zhdankin, V. V. *Chem. Rev.* **2016,** *116,* 3328–3435. doi:10.1021/acs.chemrev.5b00547
4. Sihag, M.; Soni, R.; Rani, N.; Kinger, M.; Kumar Aneja, D. *Org. Prep. Proced. Int.* **2023,** *55,* 1–62. doi:10.1080/00304948.2022.2113964
5. Narobe, R.; König, B. *Org. Chem. Front.* **2023,** *10,* 1577–1586. doi:10.1039/d3qo00039g
6. Chassé, M.; Pees, A.; Lindberg, A.; Liang, S. H.; Vasdev, N. *Chem. Rec.* **2023,** *23,* e202300072. doi:10.1002/tcr.202300072
7. Mi, X.; Pi, C.; Feng, W.; Cui, X. *Org. Chem. Front.* **2022,** *9,* 6999–7015. doi:10.1039/d2qo01332k
8. Kumar, S.; Borkar, V.; Mujahid, M.; Nunewar, S.; Kanchupalli, V. *Org. Biomol. Chem.* **2023,** *21,* 24–38. doi:10.1039/d2ob01644c
9. Das, S.; McIvor, C.; Greener, A.; Suwita, C.; Argent, S. P.; O'Duill, M. L. *Angew. Chem., Int. Ed.* **2024,** *63,* e202410954. doi:10.1002/anie.202410954
10. Katsoulos, G. A.; Lalia-Kantouri, M.; Varvoglis, A. *Thermochim. Acta* **1992,** *197,* 285–294. doi:10.1016/0040-6031(92)85027-s
11. Verma, V.; Singh, K.; Kumar, A.; Kumar, D. *J. Therm. Anal. Calorim.* **2013,** *114,* 339–344. doi:10.1007/s10973-012-2894-1
12. Fiederling, N.; Haller, J.; Schramm, H. *Org. Process Res. Dev.* **2013,** *17,* 318–319. doi:10.1021/op400035b
13. Alazet, S.; Preindl, J.; Simonet-Davin, R.; Nicolai, S.; Nanchen, A.; Meyer, T.; Waser, J. *J. Org. Chem.* **2018,** *83,* 12334–12356. doi:10.1021/acs.joc.8b02068
14. Boelke, A.; Vlasenko, Y. A.; Yusubov, M. S.; Nachtsheim, B. J.; Postnikov, P. S. *Beilstein J. Org. Chem.* **2019,** *15,* 2311–2318. doi:10.3762/bjoc.15.223
15. Waser, J. Benziodoxoles Stability Data. https://www.epfl.ch/labs/lcso/research/bxstabilitydata/ (accessed Sept 18, 2024).
16. Obermüller, R.; Tobisch, H.; Stockhammer, L.; Waser, M. *Org. Process Res. Dev.* **2024,** *28,* 3735–3744. doi:10.1021/acs.oprd.4c00296
17. Amey, R. L.; Martin, J. C. *J. Org. Chem.* **1979,** *44,* 1779–1784. doi:10.1021/jo01325a007
18. Varvoglis, A. *The Organic Chemistry of Polycoordinate Iodine;* VCH: Weinheim, Germany, 1992.
19. Mylonas, V. E.; Sigalas, M. P.; Katsoulos, G. A.; Tsipis, C. A.; Varvoglis, A. G. *J. Chem. Soc., Perkin Trans. 2* **1994,** 1691–1696. doi:10.1039/p29940001691
20. Ochiai, M. Reactivities, Properties and Structures. In *Hypervalent Iodine Chemistry;* Wirth, T., Ed.; *Topics in current chemistry*, Vol. 224; Springer: Berlin, Germany, 2003; pp 5–68. doi:10.1007/3-540-46114-0_2
21. Ochiai, M.; Takaoka, Y.; Nagao, Y. *J. Am. Chem. Soc.* **1988,** *110,* 6565–6566. doi:10.1021/ja00227a048
22. Stang, P. J.; Zhdankin, V. V. *Chem. Rev.* **1996,** *96,* 1123–1178. doi:10.1021/cr940424+
23. Dasgupta, A.; Thiehoff, C.; Newman, P. D.; Wirth, T.; Melen, R. L. *Org. Biomol. Chem.* **2021,** *19,* 4852–4865. doi:10.1039/d1ob00740h
24. Moriarty, R. M.; Prakash, I.; Prakash, O.; Freeman, W. A. *J. Am. Chem. Soc.* **1984,** *106,* 6082–6084. doi:10.1021/ja00332a057
25. Zhdankin, V. V.; Callies, J. A.; Hanson, K. J.; Bruno, J. *Tetrahedron Lett.* **1999,** *40,* 1839–1842. doi:10.1016/s0040-4039(99)00082-9
26. Zhdankin, V. V.; Maydanovych, O.; Herschbach, J.; McDonald, R.; Tykwinski, R. R. *J. Am. Chem. Soc.* **2002,** *124,* 11614–11615. doi:10.1021/ja0277780
27. Zhdankin, V. V.; Maydanovych, O.; Herschbach, J.; Bruno, J.; Matveeva, E. D.; Zefirov, N. S. *J. Org. Chem.* **2003,** *68,* 1018–1023. doi:10.1021/jo026604y
28. Saito, M.; Kobayashi, Y.; Takemoto, Y. *Chem. – Eur. J.* **2019,** *25,* 10314–10318. doi:10.1002/chem.201902699
29. Allen, F. H.; Kennard, O.; Watson, D. G.; Brammer, L.; Orpen, A. G.; Taylor, R. *J. Chem. Soc., Perkin Trans. 2* **1987,** S1–S19. doi:10.1039/p298700000s1
30. Kayser, M. M.; Hatt, K. L.; Hooper, D. L. *Can. J. Chem.* **1991,** *69,* 1929–1939. doi:10.1139/v91-278
31. Parida, K. N.; Moorthy, J. N. *Chem. – Eur. J.* **2023,** *29,* e202203997. doi:10.1002/chem.202203997
32. Ochiai, M.; Sueda, T.; Miyamoto, K.; Kiprof, P.; Zhdankin, V. V. *Angew. Chem., Int. Ed.* **2006,** *45,* 8203–8206. doi:10.1002/anie.200603055
33. Sajith, P. K.; Suresh, C. H. *Inorg. Chem.* **2012,** *51,* 967–977. doi:10.1021/ic202047g
34. Clarke, C. J.; Bui-Le, L.; Hallett, J. P.; Licence, P. *ACS Sustainable Chem. Eng.* **2020,** *8,* 8762–8772. doi:10.1021/acssuschemeng.0c02473
35. Clarke, C. J.; Baaqel, H.; Matthews, R. P.; Chen, Y.; Lovelock, K. R. J.; Hallett, J. P.; Licence, P. *Green Chem.* **2022,** *24,* 5800–5812. doi:10.1039/d2gc01983c
36. Lin, W.-C.; Yu, W.-L.; Liu, S.-H.; Huang, S.-Y.; Hou, H.-Y.; Shu, C.-M. *J. Therm. Anal. Calorim.* **2018,** *133,* 683–693. doi:10.1007/s10973-018-7319-3
37. Spange, S.; Lungwitz, R.; Schade, A. *J. Mol. Liq.* **2014,** *192,* 137–143. doi:10.1016/j.molliq.2013.06.016
38. Su, J. T.; Goddard, W. A. *J. Am. Chem. Soc.* **2005,** *127,* 14146–14147. doi:10.1021/ja054446x
39. Guilbault, A.-A.; Legault, C. Y. *ACS Catal.* **2012,** *2,* 219–222. doi:10.1021/cs200612s
40. Koga, N.; Vyazovkin, S.; Burnham, A. K.; Favergeon, L.; Muravyev, N. V.; Pérez-Maqueda, L. A.; Saggese, C.; Sánchez-Jiménez, P. E. *Thermochim. Acta* **2023,** *719,* 179384. doi:10.1016/j.tca.2022.179384

BEILSTEIN JOURNAL OF ORGANIC CHEMISTRY

Hypervalent iodine-mediated intramolecular alkene halocyclisation

Charu Bansal, Oliver Ruggles, Albert C. Rowett and Alastair J. J. Lennox*

Review

Open Access

Address:
University of Bristol, School of Chemistry, Bristol, BS8 1TS, UK

Email:
Alastair J. J. Lennox* - a.lennox@bristol.ac.uk

* Corresponding author

Keywords:
cyclisation; halogenation; heterocycles; hypervalent iodine; oxidation

Beilstein J. Org. Chem. **2024,** *20,* 3113–3133.
https://doi.org/10.3762/bjoc.20.258

Received: 07 August 2024
Accepted: 13 November 2024
Published: 28 November 2024

This article is part of the thematic issue "Hypervalent halogen chemistry".

Guest Editor: T. Gulder

Abstract

The chemistry of hypervalent iodine (HVI) reagents has gathered increased attention towards the synthesis of a wide range of chemical structures. HVI reagents are characterized by their diverse reactivity as oxidants and electrophilic reagents. In addition, they are inexpensive, non-toxic and considered to be environmentally friendly. An important application of HVI reagents is the synthesis of halogenated cyclic compounds, in particular, the intramolecular HVI-mediated halocyclisation of alkenes using carbon, oxygen, nitrogen or sulfur nucleophiles. Herein, we describe the examples reported in the literature, which are organised by the different halogens involved and the internal nucleophiles.

Introduction

Halogenated carbocyclic and heterocyclic compounds are present in many active pharmaceutical ingredients [1,2]. The intramolecular halocyclisation of alkenes mediated by HVI(III) reagents allow access to a range of halogenated cyclic scaffolds in a cost effective and selective, one-pot transformation. Pharmaceutical uses for bio-active cyclic molecules accessible by I(III) reagents are plentiful; anticancer drugs can be formed from the basis of pyrrolo[2,3-*b*]indoles **1** [3,4], 2-oxazolines **2** [5,6], dihydrofuran **3** [7,8], and spirocyclic scaffolds **4** [9,10] (Figure 1). Halogenated cyclised structures have also been found to exhibit medicinal and pharmaceutical properties, including antibacterial [11], antibiotic [12], and enzyme inhibition [13] among others.

The general mechanism for the HVI-mediated halocyclisation of alkenes proceeds firstly through the coordination of an alkene by the HVI reagent, which activates it toward intramolecular attack by an internal nucleophile. Following this, substitution of the iodane(III) can occur from the nucleophilic halide in solution to reveal the halo-cyclised product (Figure 2).

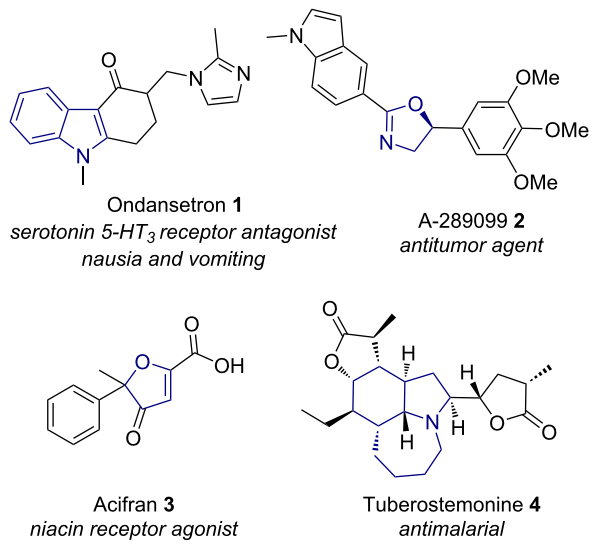

Figure 1: Example bioactive compounds containing cyclic scaffolds potentially accessible by HVI chemistry.

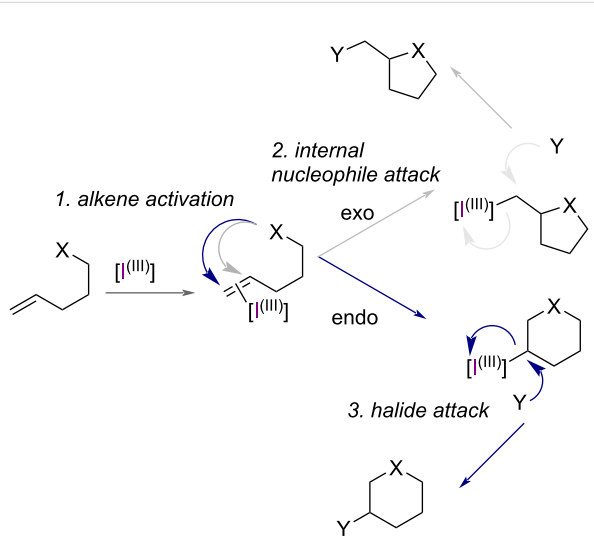

Figure 2: A general mechanism for HVI-mediated *endo*- or *exo*-halocyclisation.

In this review, we have collected and described the HVI-mediated halocyclisation reactions reported in the literature for each halide. We have organised the examples firstly by the halide nucleophile, and then secondly by the internal heteroatom nucleophile involved in the cyclisation. The selectivity (chemo-, regio-, stereo-) of the reaction, which is influenced by the type of HVI reagent, the nature of the substrates employed and the proposed mechanism from the authors are all described. The halocyclisation of alkenes to make halogenated carbo or heterocycles is yet to be covered by a review, which is the vacancy this review aims to fill. The synthetic uses of HVI reagents [14-16], their involvement in heterocycle synthesis [17-19], and alkene functionalisation [20,21], have each been well-reviewed elsewhere.

Review

Hypervalent iodine-mediated fluorocyclisation

Fluorine can substantially improve the activity of biologically relevant molecules [22], and compounds containing fluorine have seen huge success in medicine and agrochemicals, with over 30% of small molecule drugs [23,24] and 16% of pesticides [25] now containing fluorine atoms. A range of synthetically important fluorinated hetero- and carbocycles can be synthesized mildly and effectively using HVI reagents.

Nitrogen nucleophiles

A metal-free synthesis of β-fluorinated piperidines was reported in 2012 by Meng, Li and co-workers (Scheme 1) [26]. The authors describe a reaction using $PhI(OPiv)_2$ as oxidant with HF·pyridine as the source of fluoride and $BF_3{\cdot}OEt_2$ as activator. A range of unsaturated amines **5** were cyclised to racemic β-fluorinated piperidines **6**. Good yields were reported for all compounds except those with substituents present on the alkene. Homologation of the carbon chain from 5 to 6 carbons gave both 6- and 7-membered rings in poor yield with α preference for 7-membered rings **7** in a ratio of 1:9.3.

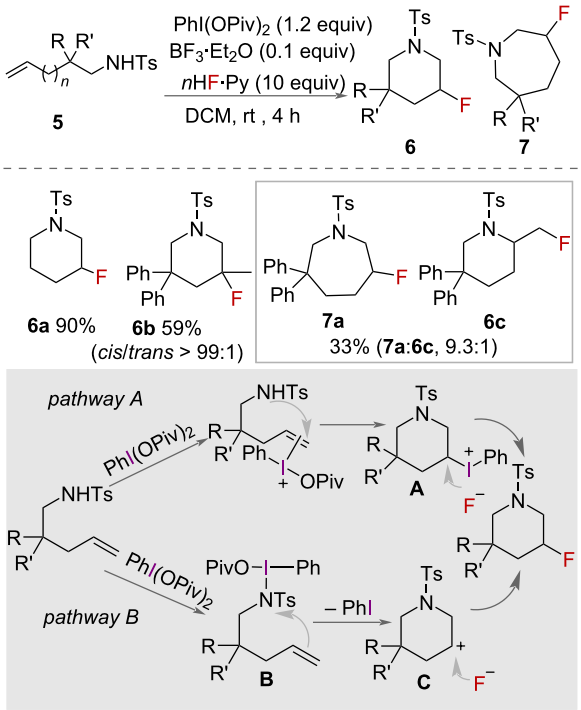

Scheme 1: Metal-free synthesis of β-fluorinated piperidines **6**. Ts = tosyl.

The authors proposed two mechanisms for the reaction (Scheme 1). In pathway A (top), the alkene-activated iodonium is formed, intramolecular attack of nitrogen forms the 6-membered ring **A** before an S_N2 reaction with the fluoride ion to displace PhI. In pathway B (bottom), the nitrogen is oxidised by the iodane, generating an electrophilic intermediate **B**. Nucleophilic attack by the double bond subsequently forms the 6-membered ring intermediate **C**, which is either immediately attacked by fluoride to form both *cis* and *trans* products or stabilised by the tosyl group and subsequently attacked to form only the *cis* product in an S_N2 reaction.

Liu and co-workers reported a palladium-catalysed intramolecular aminofluorination of unactivated alkenes [27] (Scheme 2) in the presence of $PhI(OPiv)_2$, AgF and $MgSO_4$ as an oxidant, source of fluorine and additive, respectively. Racemic β-fluorinated piperidines **6** were synthesised in excellent yields, under mild conditions. A small amount of amino carboxylation side-product was determined to have been additionally produced from the reaction. A range of other alkenes were cyclised in good yields, demonstrating the scope of the reaction. The authors proposed an alternative reaction mechanism to those already described, in which *trans*-aminopalladation of the alkene, mediated by Pd(II), occurs with intramolecular attack of the nitrogen on the terminal carbon, generating a 6-membered ring **A** (Scheme 2). The Pd(II) intermediate is oxidised by $PhI(OPiv)_2$/AgF, forming Pd(IV). Formation of the product can occur either by reductive elimination by Pd(IV) or S_N2 nucleophilic attack by fluorine with concomitant palladium reduction.

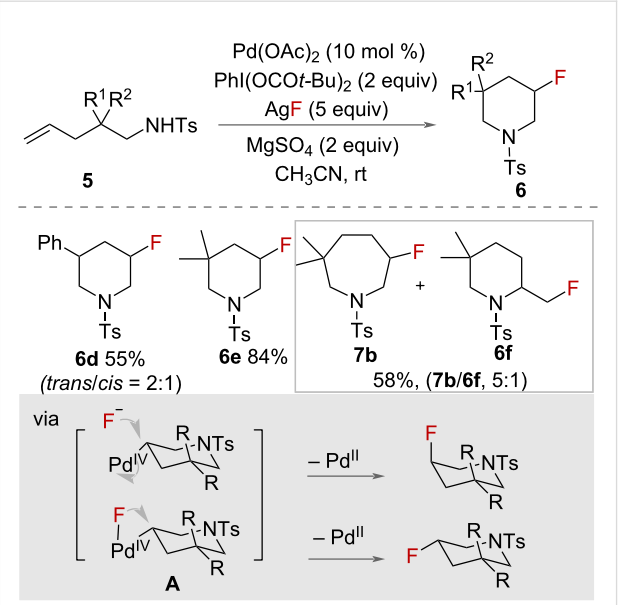

Scheme 2: Intramolecular aminofluorination of unactivated alkenes with a palladium catalyst.

Reductive elimination of the Pd(II) intermediate forms the C–F bond to give predominantly the *trans* product, but this pathway competes with a less favourable S_N2 nucleophilic attack by fluorine to form the *cis* product. However, a mechanism entirely mediated by the I(III) HVI reagent, with the $Pd(OAc)_2$ only acting as a Lewis acid to activate the HVI reagent, was not ruled out.

In 2013, Nevado and co-workers used (*R*,*R*)- and (*S*,*S*)-*tert*-butyl lactate iodotoluene difluoride (**8**) for the aminofluorination of alkenes toward the synthesis of enantiomerically pure β-fluorinated piperidines **6** (Scheme 3) [28]. A range of enantio-

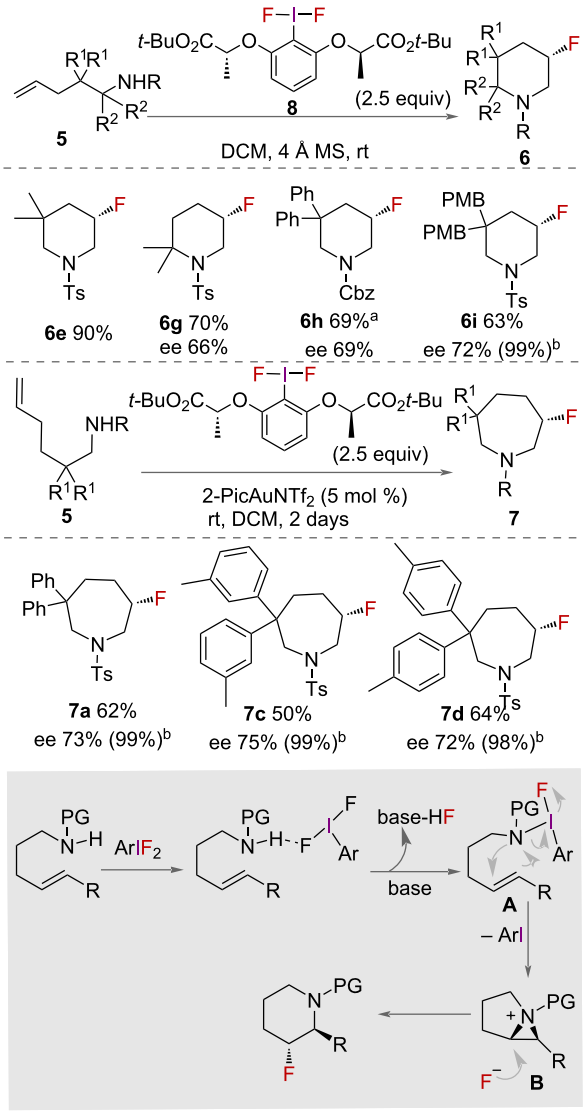

Scheme 3: Aminofluorination of alkenes in the synthesis of enantiomerically pure β-fluorinated piperidines. PMB = *para*-methoxybenzene, [a]the ee value was determined after Cbz group was replaced with tosyl group, [b]the value in brackets corresponds to the ee value after crystallization. PG = protecting group.

merically pure fluorinated piperidines were synthesised in moderate to excellent yields and enantiomeric excesses. In addition to the synthesis of 6-membered rings, 7-membered hexenamines **7** were synthesised. To the authors' surprise, reaction conditions for the synthesis of β-fluorinated piperidines **6** afforded no product. The reaction instead proceeded with addition of dichloro(pyridine-2-carboxylato)gold(III) complex in combination with silver triflimide, $AgNTf_2$. A range of β-fluoroazepanes **7** were successfully synthesised with high enantiomeric purity in good yields. A mechanism for the synthesis of β-fluorinated piperidines was proposed by the authors (Scheme 3). Activation of the HVI reagent by H-bonding leads to ligand exchange to give an aminofluoro iodonium intermediate **A**. Cyclisation occurs via nitrogen attack on the alkene to then give aziridinium intermediate **B**. Subsequent nucleophilic attack by fluoride on the more substituted carbon that is more cationic leads to the product.

Synthesis of β-fluorinated piperidines **6** with in situ-generated HVI reagent was reported in 2014 by Kita, Shibata and co-workers (Scheme 4) [29]. Using difluoroiodotoluene **10**, formed in situ from 4-iodotoluene, pyridine·HF and *m*-CPBA, intramolecular aminofluorination of a range of unsaturated amines formed β-fluorinated piperidines **6** and 3-fluoroazepanes **7** in good yields. Again, yields only significantly fell with substrates containing substituents on the alkene. Depending on the length of the alkyl chain, both 6- and 7-membered rings were formed. The use of a chiral aryl iodide was tested, which gave products with low enantiomeric excess. However, these preliminary trials represent the first example of a catalytic, enantioselective HVI-mediated fluorocyclisation.

The authors proposed a mechanism (Scheme 4) for this reaction that involved iodoarene difluoride **10** being generated from iodosylarene **9** (ArI=O) and HF, with iodosylarene itself generated by aryl iodide and *m*-CPBA. Ligand exchange of iodoarene

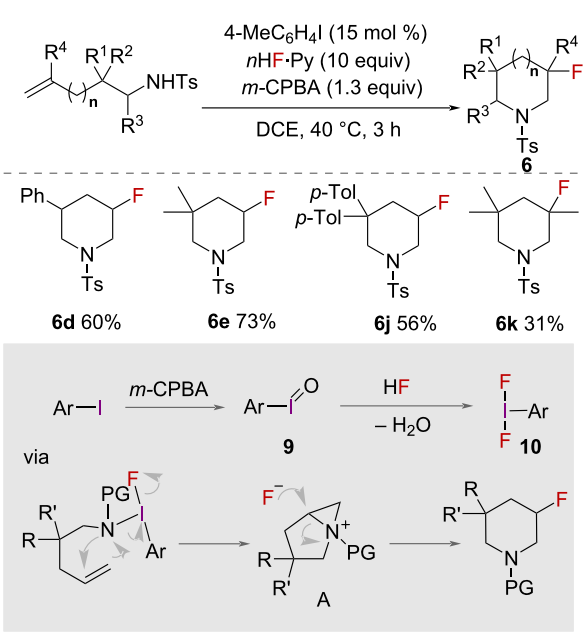

Scheme 4: Synthesis of β-fluorinated piperidines.

difluoride with nitrogen and reaction with the alkene forms aziridinium intermediate **A** which, after nucleophilic attack by fluoride, forms the product.

Li reported a haloamination of unsaturated amines in 2014 (Scheme 5) [30], to form fluorinated piperidines **6** using $PhI(OAc)_2$ as an oxidant and $BF_3{\cdot}OEt_2$ as the source of fluoride. Fluorocyclisations gave lower yields compared to other halocyclisations reported by the authors. Aminoacetylation of the alkene competed with the aminofluorination to form 3-acetoxypiperidines **11**. Other sources of fluoride were tested, with metal fluoride salts giving no or trace products. The authors reported that only 6-membered rings were formed, with a range of substituents on the β-carbon of the alkene. The

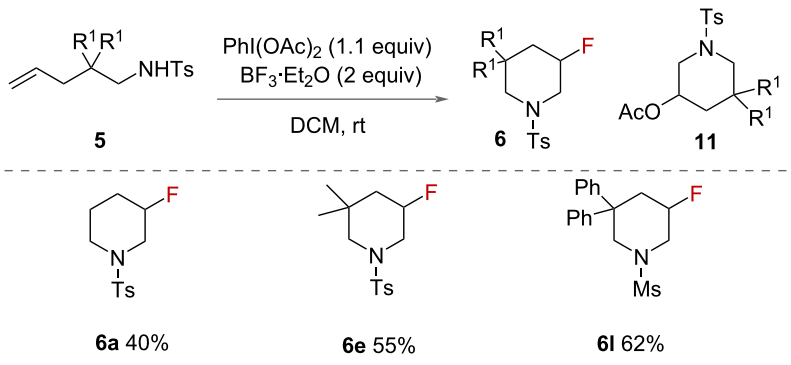

Scheme 5: Intramolecular fluoroaminations of unsaturated amines published by Li.

authors proposed a mechanism for the reaction, in which the alkene is activated by $PhI(OAc)_2$, followed by intramolecular nucleophilic attack of nitrogen and displacement of iodobenzene by fluoride.

The intramolecular aminofluorination of unsaturated amines using a structural analogue of Togni's reagent, 1-fluoro-3,3-dimethylbenziodoxole (**12**), was reported in 2015 by Szabó (Scheme 6) [31]. With catalytic $Zn(BF_4)_2$, 1-fluoro-3,3-dimethylbenziodoxole mediated the formation of fluorinated piperidines **6** and hexanamines **7** in high yields. A range of unsaturated amines with substituents on both carbons of the alkene were successfully cyclised in similarly good yields. However, increased substitution on the alkene resulted in an increased reaction time, with 9 hours required for disubstituted alkenes compared to 3 hours for non-substituted alkenes. With extended chain lengths, 5-, 6- and 7-membered aza-heterocycles were synthesised in good yields.

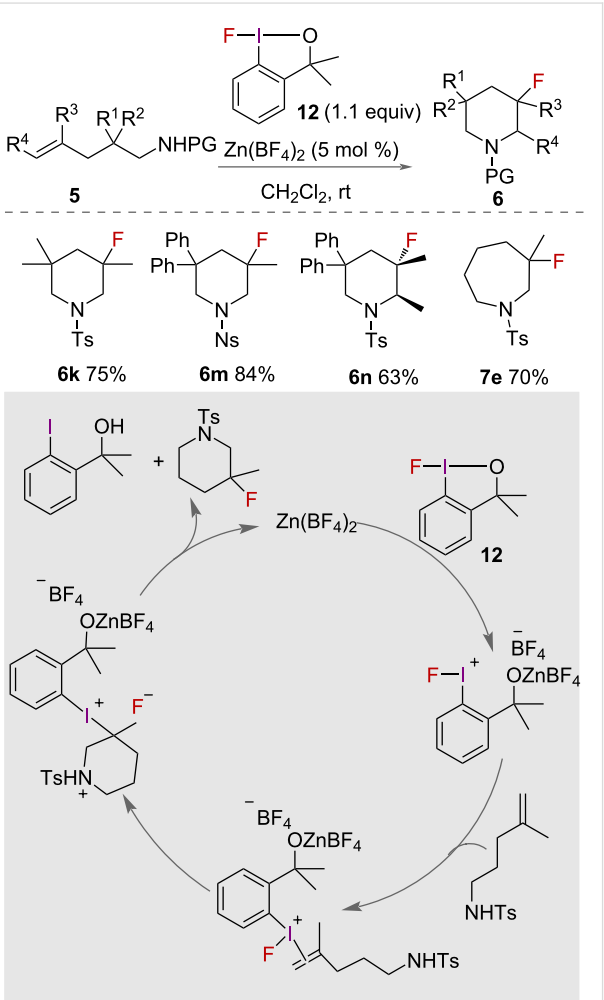

Scheme 6: Intramolecular aminofluorination of unsaturated amines using 1-fluoro-3,3-dimethylbenziodoxole (12). PG = protecting group.

The authors proposed a mechanism for the fluorocyclisation reactions (Scheme 6), which relies on the activation of the fluoro-iodane reagent **12** with the zinc catalyst. The activation enables better orbital overlap to occur with the π bond of the alkene to form an iodonium species. Nucleophilic attack occurs on the least hindered carbon of the iodonium, before displacement of the HVI by fluoride to give the product.

Zhang and co-workers reported the intramolecular aminofluorination of unsaturated amines using an HVI reagent generated in situ from iodosylbenzene **9** (Scheme 7) [32]. The authors reported the synthesis of 3-fluoropyrrolidines **14** with $BF_3{\cdot}OEt_2$ as a source of fluoride for the intramolecular aminofluorination of homoallylic amines **13**. The authors explored the reaction with various protecting groups on nitrogen and substituents on the alkene and alkyl chain. Substrates with *p*-tolylsulfonyl (Ts), *p*-nitrobenzenesulfonyl (Ns) and benzenesulfonyl (Bs) protecting groups were cyclised in high yields to the corresponding 3-fluoropyrrolidine derivatives **14**. A range of unsaturated amines were successfully cyclised. However, substrates with substituents on the alkene gave low yields of product. A mechanism was proposed involving the activation of iodosylbenzene **9** with $BF_3{\cdot}Et_2O$ to form an HVI intermediate that activates the alkene to form an iodonium species. Intramolecular nucleophilic attack of nitrogen, elimination of PhI and attack by fluoride then forms the product.

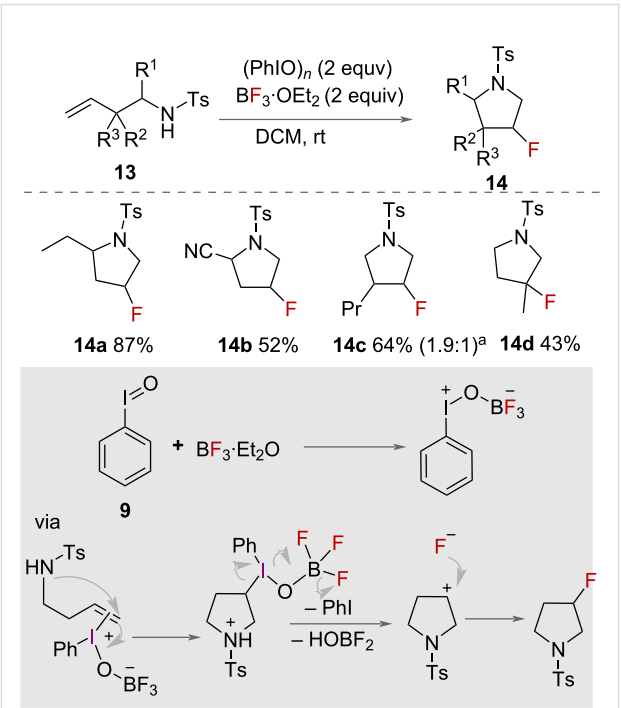

Scheme 7: 3-fluoropyrrolidine synthesis. [a]Diastereomeric ratio (*cis*/*trans*) determined by ^{19}F NMR analysis.

Kitamura and co-workers additionally reported a synthesis of 3-fluoropyrrolidines **14** in 2017 using an alternative source of fluoride (Scheme 8) [33]. The authors used either $PhI(OAc)_2$ or $PhI(OCOCF_3)_2$ as oxidants and pyridine·HF as a source of fluoride. This alternative reagent system was used due to concerns with the long-term stability of iodosylbenzene and unwanted reactions of $BF_3{\cdot}Et_2O$ with other reagents. In addition, a catalytic system was reported that employed 20 mol % iodotoluene with 1 equivalent of *m*-CPBA as terminal oxidant. The authors proposed that difluoroiodobenzene **10** is formed in situ, which is activated by HF. Two possible mechanisms were given for the synthesis of pyrrolidines **14**, which are the same two proposed for the synthesis of piperidines **6** (Scheme 1). Either an alkene-activated iodonium is formed or an activated electrophilic nitrogen is generated from interaction with the HVI, that is then attacked by the alkene.

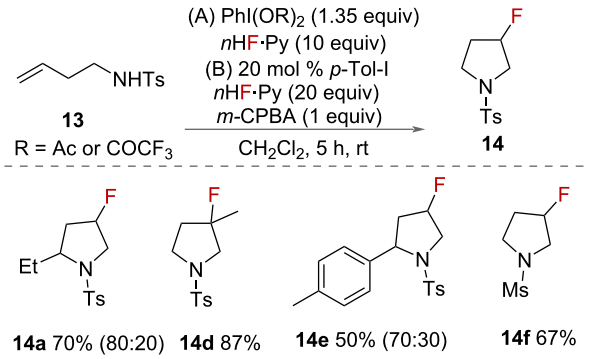

Scheme 8: Kitamura's synthesis of 3-fluoropyrrolidines. Values in parentheses represent the *cis*:*trans* ratio.

While the fluoroamination of alkenes to form 4-membered azetidines has not been reported, an *exo* fluorocyclisation to form 3-membered aziridines with an adjacent fluorine was reported by Jacobsen in 2018 (Scheme 9) [34]. The synthesis from the styrenyl starting materials is stereoselective, giving the *syn*-diasteroisomer in high yields. A chiral iodoarene catalyst **16** was employed, along with a stoichiometric sacrificial oxidant, to give good to excellent levels of enantioselectivity. This elegant strategy led to a variety of β-fluorinated tosylated aziridines **15** with good tolerance to styrenyl arenes with electron-withdrawing groups on them. The yields of product dropped off significantly when the ring did not contain an electron-withdrawing group on it.

In 2023, Šmit and co-workers conducted an in-depth mechanistic study on the cyclisation of alkenyl *N*-tosylamides using BF_3-activated aryl iodane(III) carboxylates to create 3-fluoropiperidines [35]. The challenges faced relate to selectivity due

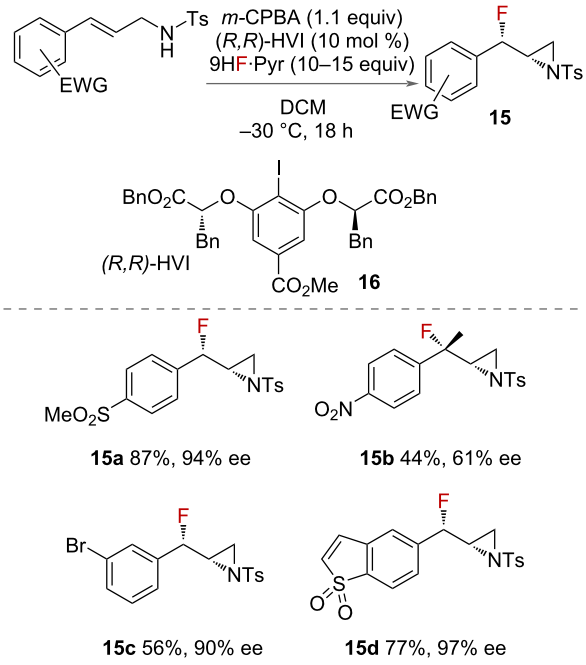

Scheme 9: Jacobsen's enantio- and diastereoselective protocol for the synthesis of *syn*-β-fluoroaziridines **15**.

to competing carboxyaminations (**18**, **18'**), rather than fluoroamination (**17**, **17'**), and difficulties in controlling the diastereoselectivity. The authors studied the stereo-, regio, and chemoselectivity in both cyclic and acyclic substrates. It was observed that the use of acyclic iodane reagents **19** and **20** predominantly led to products with β-stereochemistry, whereas the cyclic iodanes **21** and **22** favour pathways leading to α-stereochemistry (Scheme 10). The selectivity of the reaction was also found to be influenced by the presence of electrolytes like $TBABF_4$, and the ligand attached to I(III). Carboxyfluorination was observed, in which a ligand from the iodane, e.g., OAc, OPiv or *o*-I-OBz, adds and was found to compete with fluoroamination. The level of this chemoselectivity was dependent on the iodane ligand: OPiv was more selective for aminofluorination than OAc, which was proposed to be due to differences in basicity and nucleophilicity (Scheme 10).

Detailed mechanistic studies were carried out using multinuclear NMR spectroscopy, deuterium labelling, rearrangements on stereodefined substrates, and structural analyses (NMR and X-ray) of the reaction products. RT-NMR-derived data strongly supported a pathway of alkene activation by the iodane, as opposed to the formation of an N-I(III) adduct. The presence of 5-*exo*-products, with support of a deuterium labelling experiment, also ruled out the possibility of an *N*-activation pathway. Therefore, the proposed mechanism involves BF_3-coordinated

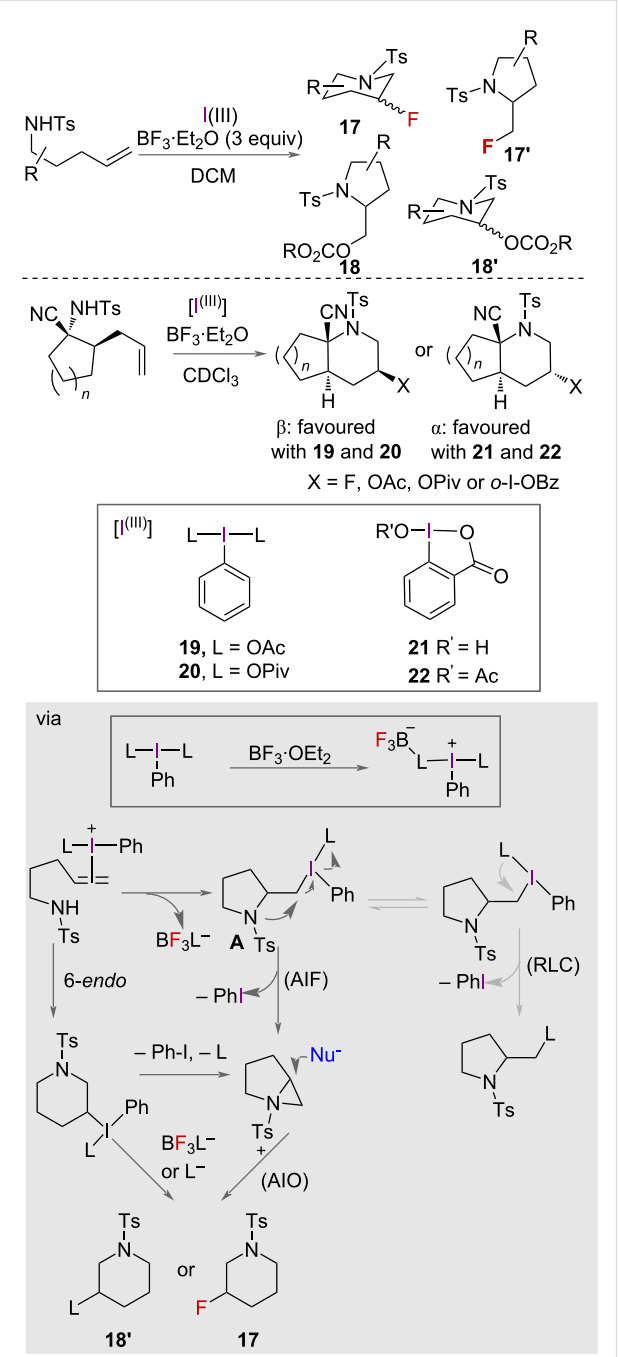

Scheme 10: Different HVI reagents lead to different diastereoselectivity in aminofluorination competing with carboxyfluorination products. Mechanistic studies of the fluoroamination of acyclic substrates showing the competing carboxyfluorination products. AIF = aziridinium ion formation, AIO = aziridinium ion opening, RLC = reductive ligand coupling.

I(III) iodane forming iodiranium(III) ions with the alkene, followed by diastereo-determining 5-*exo*-cyclisation. These transiently formed pyrrolidine intermediates **A** can undergo further transformations (Scheme 10), depending on their structure and the iodane reagent being used. For example, higher yields of 3-fluoropiperidine products **6** were observed when using cyclic iodane reagents **21** and **22** (Scheme 10), which was suggested to be because a reductive ligand coupling (RLC) pathway would be suppressed due to reduced fluxionality of the carboxylate ligand on I(III). These important findings are expected to enhance the use of aryl iodane(III)-dicarboxylates for constructing fluorinated azaheterocycles with improved selectivity and control.

Oxygen nucleophiles

In 2000, Hara and co-workers reported the fluorocyclisation of unsaturated alcohols and carboxylic acids promoted by HVI reagents (Scheme 11) [36]. Using 4-tolyl difluoroiodane **10** as the reaction promoter, and pyridine·6HF as a source of fluoride, a range of unsaturated alcohols **23** to fluorinated tetrahydrofurans **25** and tetrahydropyrans **26**. Unsaturated carboxylic acids **24** was also cyclised to form 5-membered fluorinated lactones **27**.

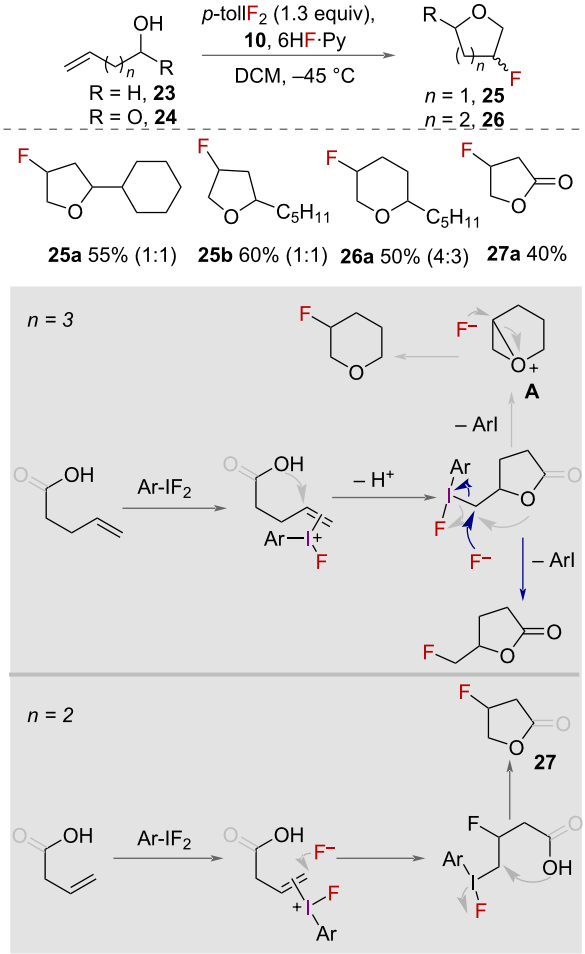

Scheme 11: Fluorocyclisation of unsaturated alcohols and carboxylic acids to make tetrahydrofurans, fluoromethyl-γ-lactones and tetrahydropyrans. The ratio of stereoisomers is shown in parentheses.

The mechanisms proposed for the cyclisation of unsaturated alcohols and carboxylic acids both proceed first through the activation of the alkene by the iodane (Scheme 11). The internal oxygen nucleophile and fluoride then sequentially attack the activated alkene, to either form 5- or 6-membered furan or pyran heterocycles depending on the chain length in the substrate. The pyran ring is only formed from the alcohol starting material, presumably because the oxygen is reactive enough to displace the iodane to form the oxonium species **A**. When the carboxylic acid is used, the oxygen in the lactone intermediate is less reactive and so substitution of the iodane by fluoride is more favourable and the branched product is formed.

In addition to aminofluorination, Szabó also reported the oxyfluorination of alkenes in 2015 [31]. Under identical conditions to the aminofluorination using 1-fluoro-3,3-dimethylbenziodoxole (**12**) with $Zn(BF_4)_2$ catalyst, unsaturated alcohols were cyclised to fluorinated tetrahydropyrans **26** and oxepanes **28** (Scheme 12) in 1–2 hours in good yields.

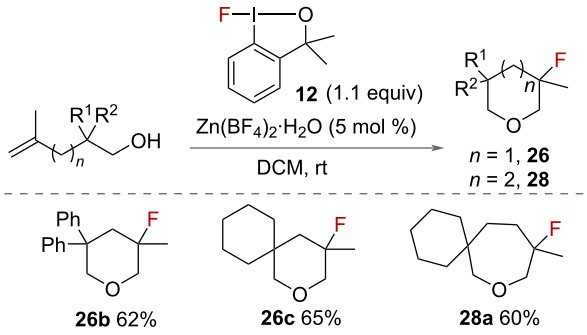

Scheme 12: Oxyfluorination of unsaturated alcohols.

Gulder and co-workers reported a mild, metal free-synthesis of fluorobenzoxazepines **30** in 2016 (Scheme 13) [37]. Using 1-fluoro-3,3-dimethylbenziodoxole (**12**) and 4 Å molecular sieves, a range of benzamides **29** were successfully cyclised in good yields. The sustainability of the reaction was improved by regeneration of 1-fluoro-3,3- dimethylbenziodoxole (**12**) in 91% yield from isolated benzyl alcohol after the fluorination reaction. A mechanism of the reaction was proposed (Scheme 13) in which the iodane-activated alkene is attacked by fluoride and the aromatic ring, to form a fluorinated phenonium intermediate **A**. The product is formed following a 6-*endo* cyclisation with nucleophilic attack from oxygen to provide the fluorobenzoxazepines **30**.

In 2015, Stuart and co-workers reported an intramolecular fluorocyclisation of unsaturated carboxylic acids **24** (Scheme 14) [38]. Using 1-fluoro-3,3-dimethylbenziodoxole (**12**) as an oxidant with $AgBF_4$ and 4 Å molecular sieves to prevent water

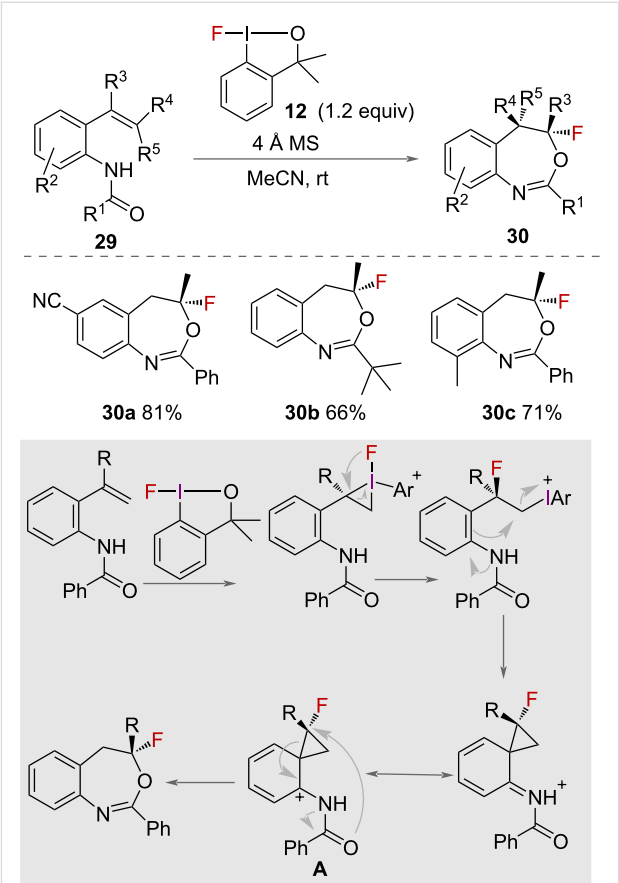

Scheme 13: Synthesis and mechanism of fluoro-benzoxazepines.

competing with fluoride as the nucleophile, a range of unsaturated carboxylic acids were successfully cyclised to fluorinated lactones **27** in good yields. The authors proposed a mechanism for fluorolactonization (Scheme 14) whereby $AgBF_4$ first activates the fluoroiodane **12** for alkene coordination. Intramolecular nucleophilic attack of oxygen on the more substituted carbon forms the cyclised intermediate **A** and eliminates fluoride. Phenonium intermediate **B** is formed with elimination of the iodoarene and subsequent attack of fluoride forms the product.

In 2017, Kitamura and co-workers reported the synthesis of fluorinated tetrahydrofurans **25** and butyrolactone **27** (Scheme 15) [33]. Unsaturated alcohols **23** and 3-butenoic acid (**24**) were competent starting materials, using $PhI(OPiv)_2$ as an oxidant and pyridine·HF as a source of fluoride. Unsaturated alcohols gave moderate yields of racemic fluorinated tetrahydrofurans **26**. Moderate yields were also reported for the fluorocyclisation of 3-butenoic acid (**24**) to form the fluorinated butyrolactone **28**.

The preparation of fluorinated oxazolines was reported in 2018 by Gilmour and co-workers (Scheme 16) [39]. *p*-$TolIF_2$ is

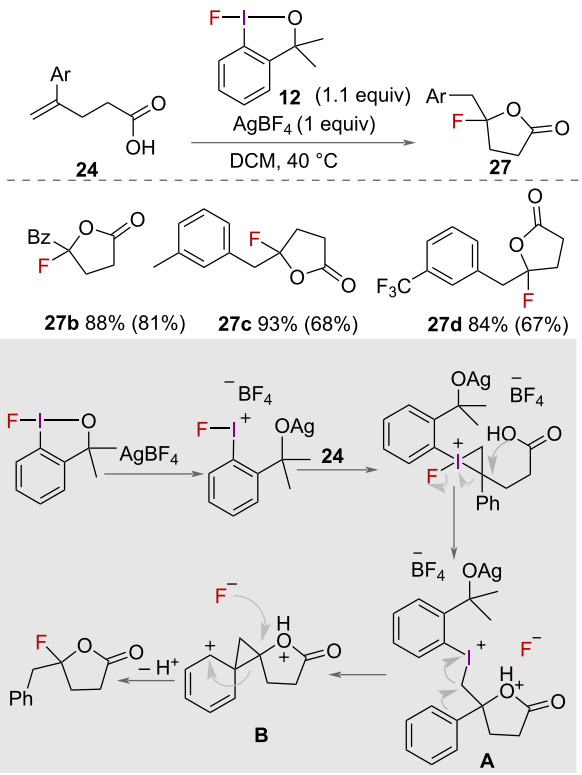

Scheme 14: Intramolecular fluorocyclisation of unsaturated carboxylic acids. Yield of isolated product within parentheses.

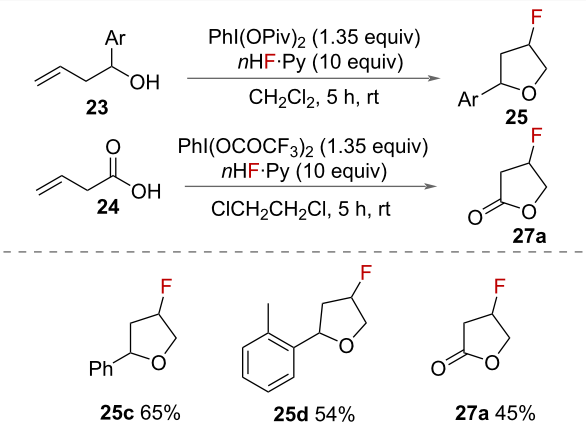

Scheme 15: Synthesis of fluorinated tetrahydrofurans and butyrolactone.

formed in situ from *p*-iodotoluene and Selectfluor in a 4.5:1 HF:amine solution, which is obtained by combining $Et_3N{\cdot}3HF$ and pyridine·HF. A range of *N*-allyl carboxamides **31** were successfully cyclised forming fluoromethyl-2-oxazolines **32** in good yields.

The synthesis of fluorinated oxazolines **32** was also reported using an electrochemical approach in 2019 by Waldvogel and co-workers (Scheme 17) [40]. The authors used electrochemical oxidation to form *p*-tolyl-difluoro-λ^3-iodane **10** on the anode using an undivided cell with platinium electrodes in a 1:1 solution of CH_2Cl_2 and $Et_3N{\cdot}5HF$. The in situ formation of this unstable HVI reagent avoided the requirement for it to be isolated. It was used either in a 1-step in-cell procedure with alkene, or in a 2-step, ex-cell approach [41], in which the substrate was added after the electrolysis, thereby avoiding any competing electrochemical oxidation of the substrate. A range of *N*-allyl-carboxamides **31** were cyclised to fluorinated oxazolines **32** in moderate to very good yields. Poor yields, however, were reported with electron-withdrawing aryl groups on the substrate. Intramolecular nucleophilic attack from oxygen onto the activated alkene forms the oxazoline **A**, and S_N2 substitution with the fluoride ion displaces iodotoluene to form the product.

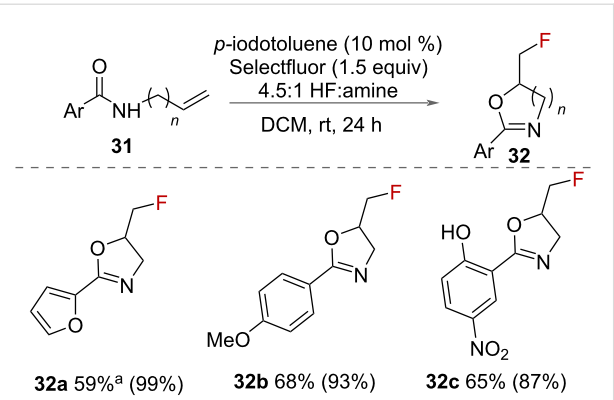

Scheme 16: Synthesis of fluorinated oxazolines **32.** [a]Reaction time increased to 40 hours. Yields refer to isolated values whilst NMR yields are given in parentheses (^{19}F NMR using ethyl fluoroacetate as an internal standard).

An electrochemical approach was also reported by Lennox and co-workers for the synthesis of chromanes **34** (Scheme 18) [42]. The authors reported using *p*-tolyl-difluoro-λ^3-iodane **10**, formed via electrochemical oxidation of 4-iodotoluene at the anode, in a 5:6 HF:amine mixture to cyclise a range of phenolic ethers **33**. Tolerance for substituents on both the aromatic ring and the alkene were shown, although the electronic requirements were quite narrow for reaction success. As the arene ring attacks the activated alkene, if it is too electron-poor then it is not reactive enough. Moreover, if it is too electron-rich, then it preferentially oxidises via a single electron transfer mechanism which deactivates the ring as a nucleophile.

The synthesis of fluorinated oxazepanes **36** was reported by Ding and co-workers in 2021 (Scheme 19) [43]. Using fluoro benziodoxole **12** as oxidant and $Zn(BF_4)_2$ as a catalytic activator, a range of fluorinated oxazepanes were synthesised from allylamino ethanols **35** in good yields.

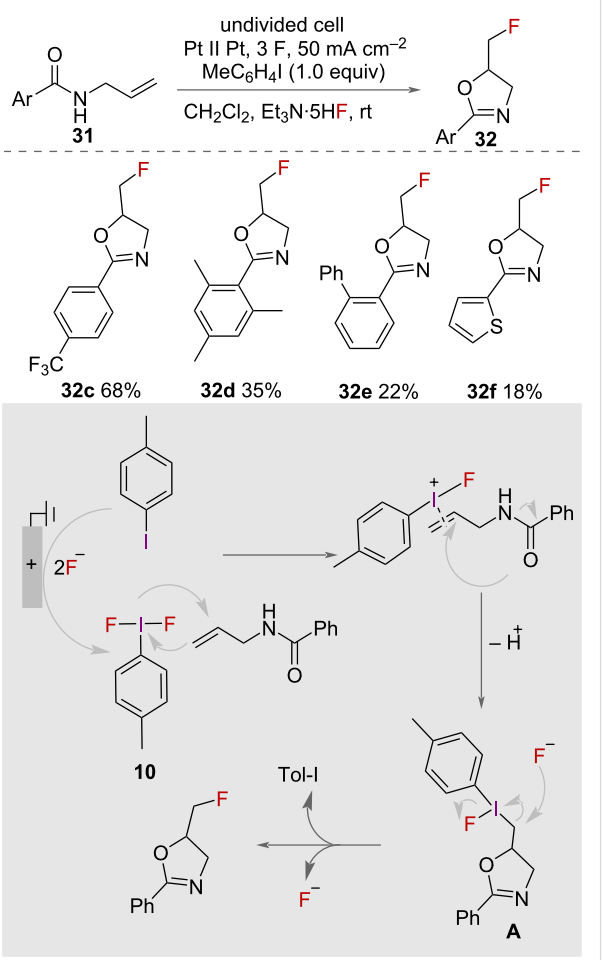

Scheme 17: Electrochemical synthesis of fluorinated oxazolines.

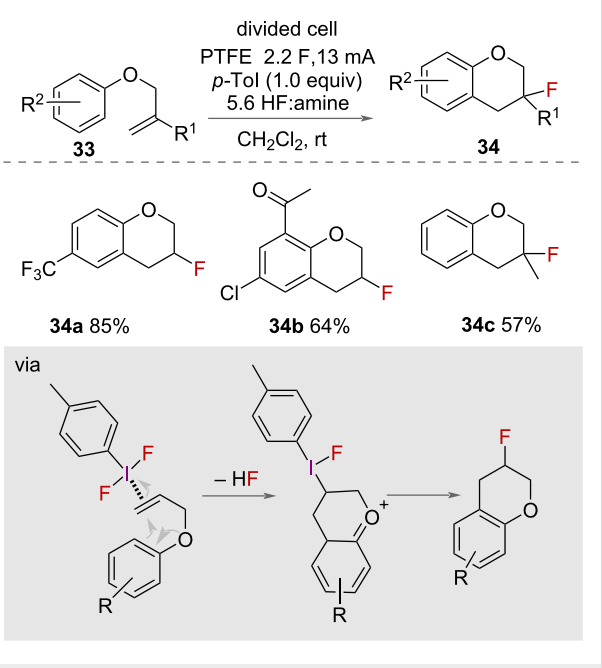

Scheme 18: Electrochemical synthesis of chromanes.

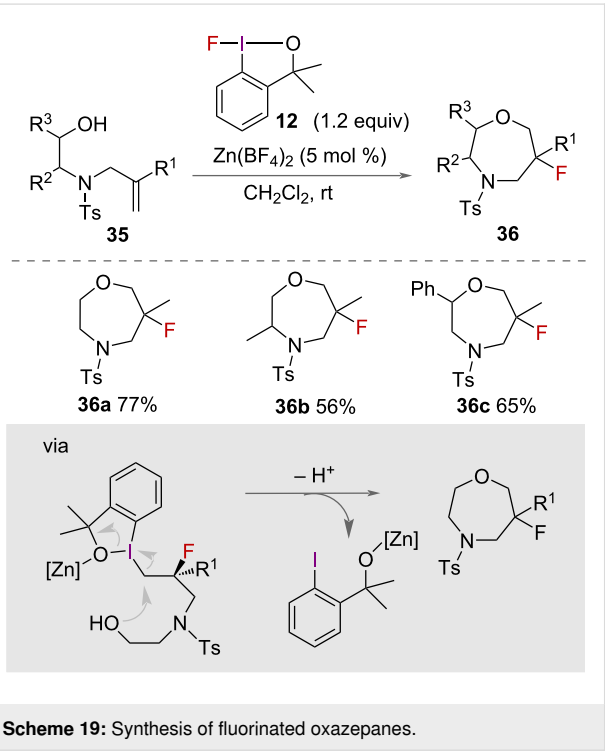

Scheme 19: Synthesis of fluorinated oxazepanes.

In 2021, Jiang and co-workers reported catalytic asymmetric aminofluorination using $BF_3{\cdot}Et_2O$ with a chiral aryliodide **16** catalyst (Scheme 20) [44]. The study successfully obtained various chiral fluorinated oxazine products **38** with high enantioselectivity (up to >99% ee) and diastereoselectivity (up to >20:1 dr). Control experiments showed that using Py·9HF or $Et_3N{\cdot}3HF$ as the fluoride source did not yield the desired fluorooxazines, highlighting the role of $BF_3{\cdot}Et_2O$ as both a fluoride reagent and an activating reagent of iodosylbenzene. Different chiral iodide catalysts were studied, revealing that the substituents of the catalysts significantly influenced the stereochemistry of the reaction. Linear chiral catalysts were found to offer higher stereoselectivity compared to spiro-catalysts. Under optimized conditions, the asymmetric aminofluorination of *N*-cinnamylbenzamides **37** using $BF_3{\cdot}Et_2O$ as the fluorine reagent demonstrated good yields and high stereoselectivity (Scheme 20). The scope of the reaction was probed, showcasing the versatility and applicability of the method in synthesizing chiral fluorinated oxazines. The authors proposed the mechanism of the catalytic asymmetric nucleophilic fluorination to involve the activation of iodosylbenzene by $BF_3{\cdot}Et_2O$ which is then attacked by a nucleophile. The use of chiral iodine catalysts is essential for controlling the stereochemistry of the reaction. The specific arrangement of the catalyst influences the orientation of this nucleophilic attack as supported by density functional theory (DFT) calculations.

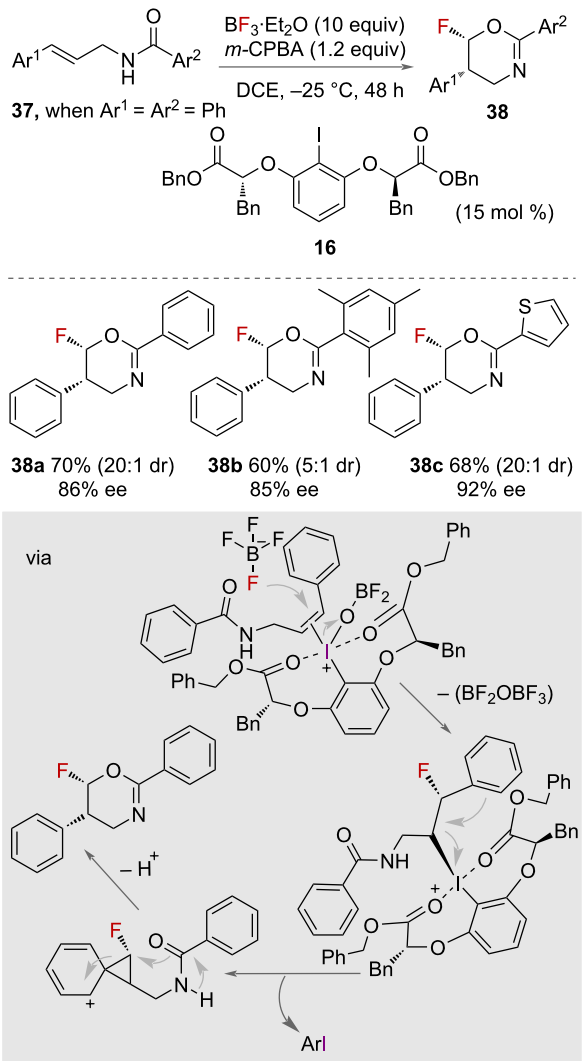

Scheme 20: Enantioselective oxy-fluorination with a chiral aryliodide catayst.

In 2022, Xu, Zhang, Zhu and co-workers reported a method to catalytically synthesise 5-fluoro-2-aryloxazolines **39** by utilising $BF_3{\cdot}Et_2O$ as the fluoride source and activating reagent (Scheme 21) [6]. The synthesis of these derivatives was achieved with high efficiency, resulting in good to excellent yields of up to 95% within a short time-frame of 10 minutes. Treatment of *N*-(2-phenylallyl)benzamides with 10 equivalents of $BF_3{\cdot}Et_2O$, iodobenzene, *m*-CPBA in dichloromethane (DCM) at 0 °C resulted in the formation of the oxazoline product (Scheme 21). DFT calculations indicated several steps in the mechanism, including ligand coupling, oxidative addition, intermolecular nucleophilic attack, 1,2-aryl migration, reductive elimination, and intramolecular nucleophilic attack. This approach offers a rapid and effective way to produce 5-fluoro-2-aryloxazoline compounds, which are valuable building blocks in organic synthesis.

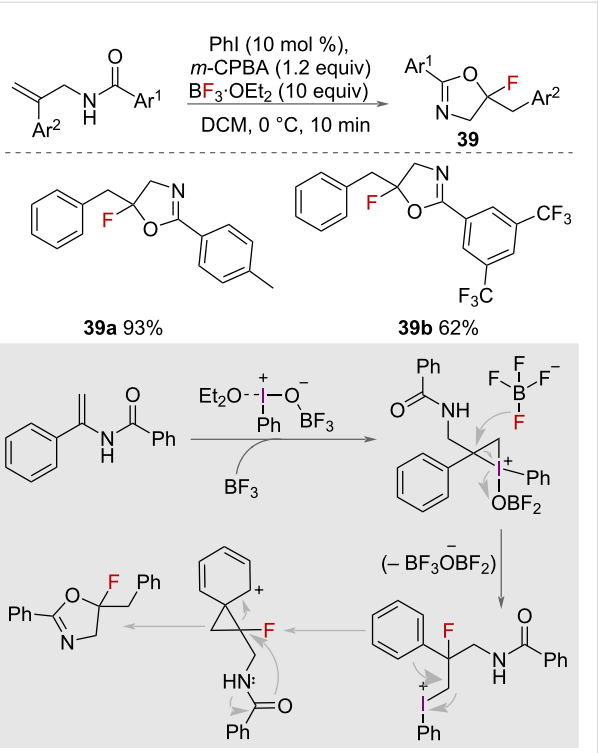

Scheme 21: Catalytic synthesis of 5-fluoro-2-aryloxazolines using $BF_3{\cdot}Et_2O$ as a source of fluoride and an activating reagent.

Carbon nucleophiles

In addition to intramolecular aminofluorination and oxyfluorination, Szabó and co-workers reported alkene carbofluorination in 2015 (Scheme 22) [31]. Using 1-fluoro-3,3-dimethylbenziodoxole (**12**) and $[Cu(MeCN)_4]BF_4$ as a catalyst to activate it, the authors reported the synthesis of fluorinated cyclopentane products **41** from alkenyl malonate derivatives **40**. The malonate nucleophile required longer reaction times of 8 hours compared to 1–3 hours for aminofluorination and oxyfluorination, however good yields were reported.

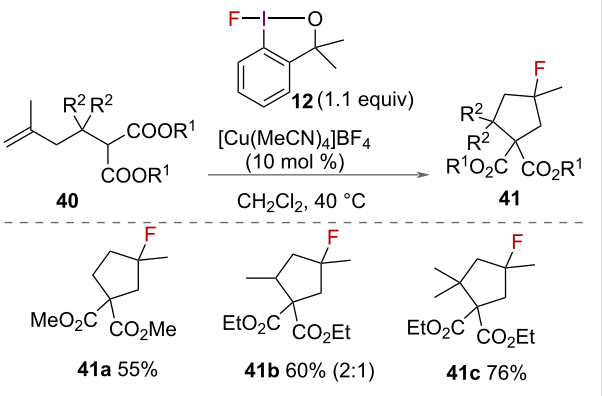

Scheme 22: Intramolecular carbofluorination of alkenes.

Hypervalent iodine-mediated chlorocyclisation

Although less common than fluorine in biologically active compounds, chlorine-containing molecules have interest in drug discovery, with over 250 chloro-containing drugs presently available [43]. The introduction of a chlorine atom into biologically active compounds for use in pharmaceuticals and agrochemicals has been shown to greatly increase the potency of a compound [45,46] and can be considered a bioisostere for a methyl group. Chlorination through HVI approaches provides a safe and mild approach to chlorinated cyclic compounds.

Nitrogen nucleophiles

Intramolecular chlorocyclisation promoted by $PhI(OAc)_2$ was reported by Liu and Li in 2014 alongside their intramolecular fluorocyclisation (Scheme 23) [30]. The authors reported the formation of 5- and 6-membered chlorinated azaheterocycles **42** from unsaturated amines, using $PhI(OAc)_2$ as an oxidant and pyridinium chloride as a chlorine source. Substrates with a range of substituents on the alkyl chain were cyclised in good yields, yet introduction of substituents on the alkene led to a reduction of yield. The authors proposed a standard mechanism for the reaction (Scheme 23) in which $PhI(OAc)_2$ activates the alkene, intramolecular attack of nitrogen forms the cyclised intermediate and a chloride ion displaces iodobenzene.

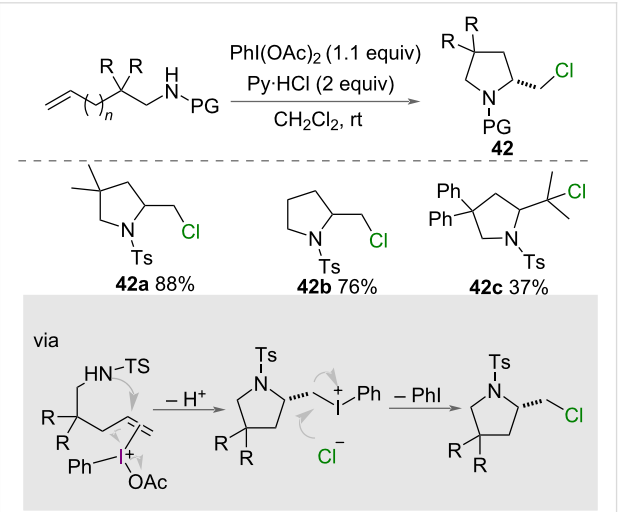

Scheme 23: Intramolecular chlorocyclisation of unsaturated amines.

In 2015, Cariou, Dodd and co-workers reported the synthesis of chlorinated cyclic guanidines **44** (Scheme 24) [47]. Using Koser's reagent as an oxidant with LiCl as a source of chloride, a range of unsaturated guanidines **43** were cyclised forming 5- or 6-membered rings in good yields. The change in ring size was proposed to be due to the position of the positive charge on the activated alkene. The carbon with the higher substitution has the greater positive charge and therefore undergoes nucleophilic attack by nitrogen. The authors proposed two possible mechanisms for the reaction (Scheme 24). Firstly, a chloronium ion is generated by HVI and LiCl followed by intramolecular nucleophilic attack by nitrogen to form the heterocycle. Secondly, oxidation of the unsaturated guanidine forms an intermediate aziridinium **A** with subsequent nucleophilic attack by chloride to form the product.

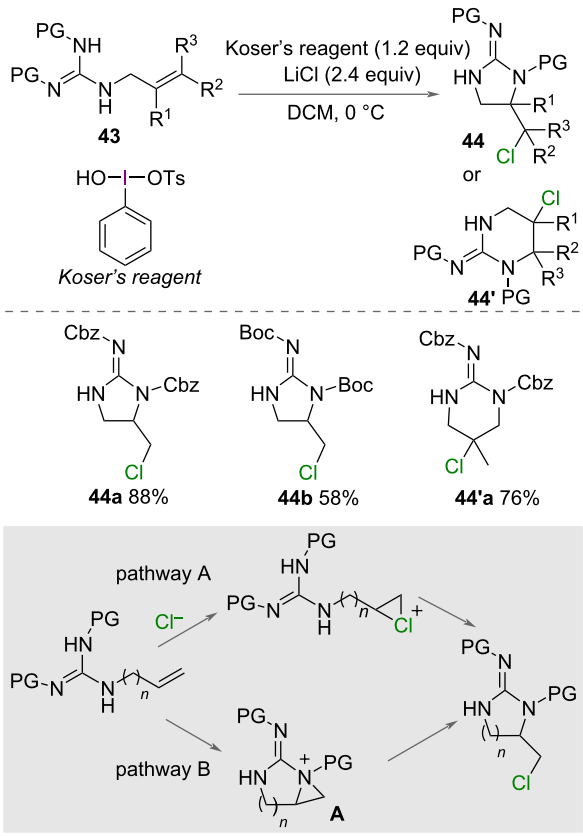

Scheme 24: Synthesis of chlorinated cyclic guanidines **44**.

A metal-free chlorocyclisation of indole derivatives was reported by Yu and co-workers in 2019 (Scheme 25) [45]. The authors reported the use of 1-chloro-1,2-benziodoxol-3-one (**45**) as a single reagent to form 6- or 7-membered rings under mild conditions in DCM at room temperature. A range of substituents on the aromatic ring were tested with electron-withdrawing groups resulting in lower yields compared to electron-donating groups. The proposed mechanism for the reaction involved formation of a chloronium ion and nucleophilic attack from nitrogen on the less sterically-hindered carbon, forming a cyclic intermediate **A** (Scheme 25). Chloride is subsequently eliminated with formation of an enamine **B** that reacts with a second equivalent of 1-chloro-1,2-benziodoxol-3-one (**45**) to afford the product **46**.

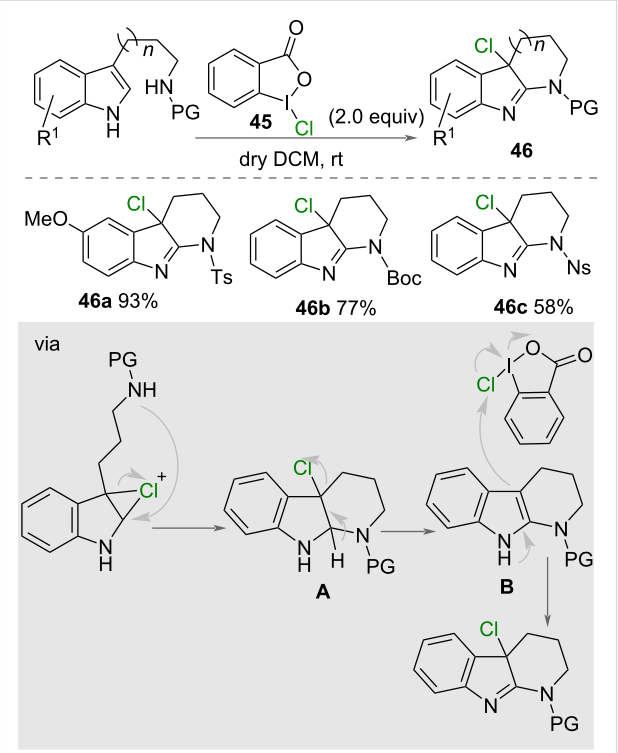

Scheme 25: Synthesis of chlorinated pyrido[2,3-b]indoles **46**.

Oxygen nucleophiles

Liu and Li reported the chlorolactonization and chloroetherification (Scheme 26) of 2,2-diphenylpent-4-enoic acid (**47'**) and 2,2-diphenyl-4-penten-1-ol (**47**), respectively, using $PhI(OAc)_2$ as an oxidant and pyridinium chloride as a chlorine source. This was an expansion of their scope that used nitrogen nucleophiles [30].

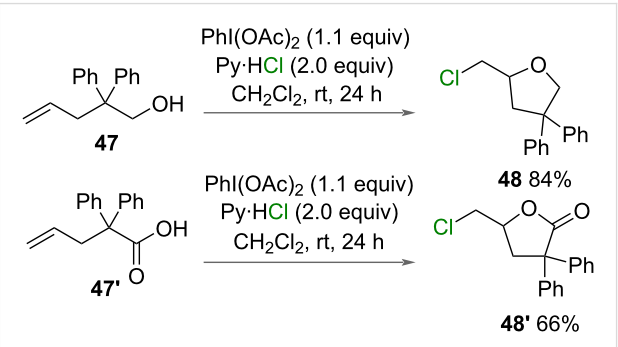

Scheme 26: Chlorolactonization and chloroetherification reactions.

In 2015, Li and co-workers reported the synthesis of chloromethyloxazolines **49** [48] (Scheme 27). Using $PhI(OAc)_2$ as an oxidant and TMSCl as a source of chloride and activator, a range of *N*-allyl carboxamides **31** were successfully cyclised, forming 5-chloromethyl-2-aryloxazolines **49** in good yields. A mechanism for the reaction was proposed by the authors (Scheme 27), whereby a TMS-adduct **A** of the amide is formed, alkene activation and cyclisation from oxygen forms the cyclised intermediate **B**, then displacement of PhI by chloride gives the product.

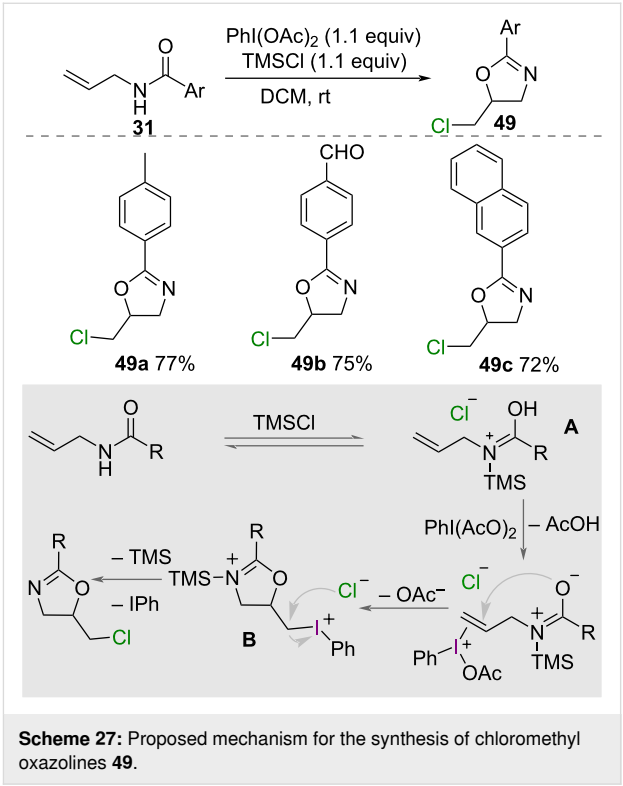

Scheme 27: Proposed mechanism for the synthesis of chloromethyl oxazolines **49**.

Chai, Jiang, Zhu and co-workers reported the synthesis of various halogenated 1,3-oxazine **50** and 2-oxazoline derivatives **51** using boron trihalides as the halogen source [6,49]. They found that the choice of halogen source influences the reaction outcomes. With the use of BCl_3 (Scheme 28), *N*-cinnamylbenzamides **52** were transformed to give the corresponding chlorinated dihydro-[1,3]-oxazines **50** in good to excellent isolated yields [49]. When various substituted *N*-(2-phenylallyl)benzamides (**52**) were tolerated, it led to the formation of chlorinated 2-oxazolines **51** in good to excellent yields. When BF_3 was used as the halogen source in the author's previous work (Scheme 21) [6], it led to the formation of different products compared to when BCl_3 was utilized, suggesting a different mechanism is operative.

Hypervalent iodine-mediated bromocyclisation

Bromocyclisation promoted by HVI reagents allows for a mild, metal-free synthesis of various cyclic functional groups and avoids the use of highly toxic and corrosive bromine. Approaches using this approach are outlined below.

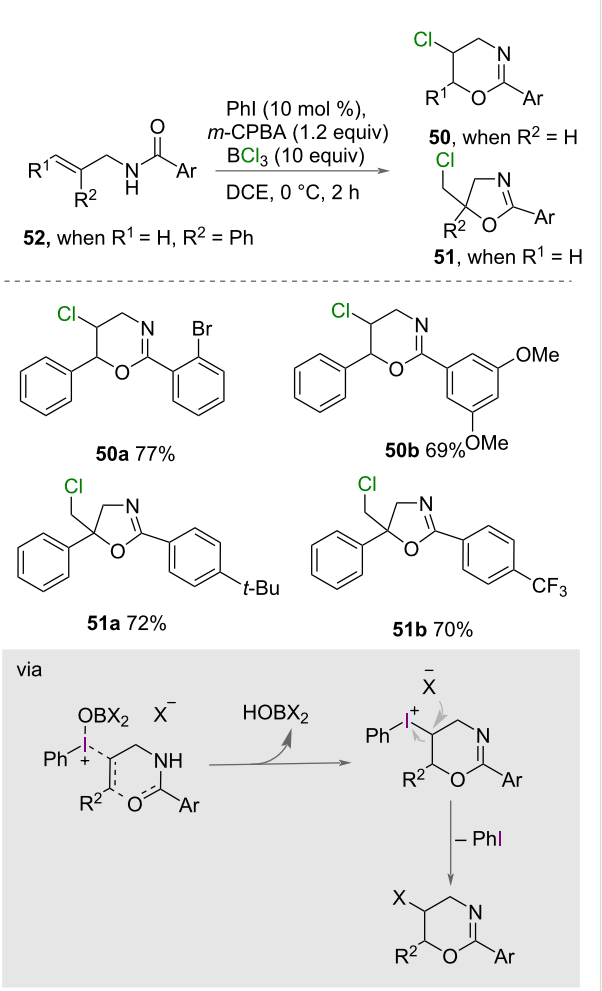

Scheme 28: Oxychlorination to form oxazine and oxazoline heterocycles promoted by BCl_3.

Nitrogen nucleophiles

In 2007, aminobromocyclisation of homoallylic sulfonamides **53** was reported by Fan, Wang and co-workers (Scheme 29) [50]. Using $PhI(OAc)_2$ as an oxidant with KBr as the bromine source and Bu_4NBr as a reaction promoter, racemic brominated pyrrolidines **54** were synthesised from a range of homoallylic sulfonamides **53** in excellent yields under mild conditions at room temperature. A mechanism was suggested by the authors (Scheme 29), whereby ligand exchange on $PhI(OAc)_2$ with a bromide ion forms unstable PhIOAcBr. Elimination of bromoacetate then gives a reactive electrophilic bromine source, which forms a bromonium intermediate **A** after reaction with the alkene. Intramolecular nucleophilic attack from nitrogen forms the product **54**.

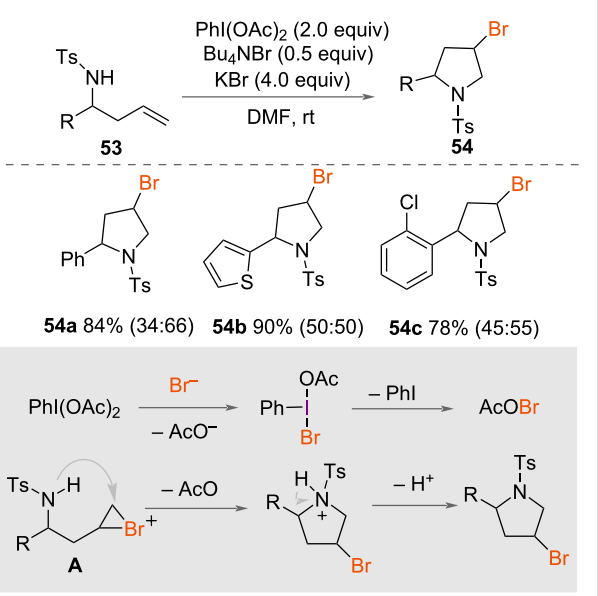

Scheme 29: Aminobromocyclisation of homoallylic sulfonamides **53**. The *cis*:*trans* ratios based on the ^1H NMR of the corresponding products are given in parentheses.

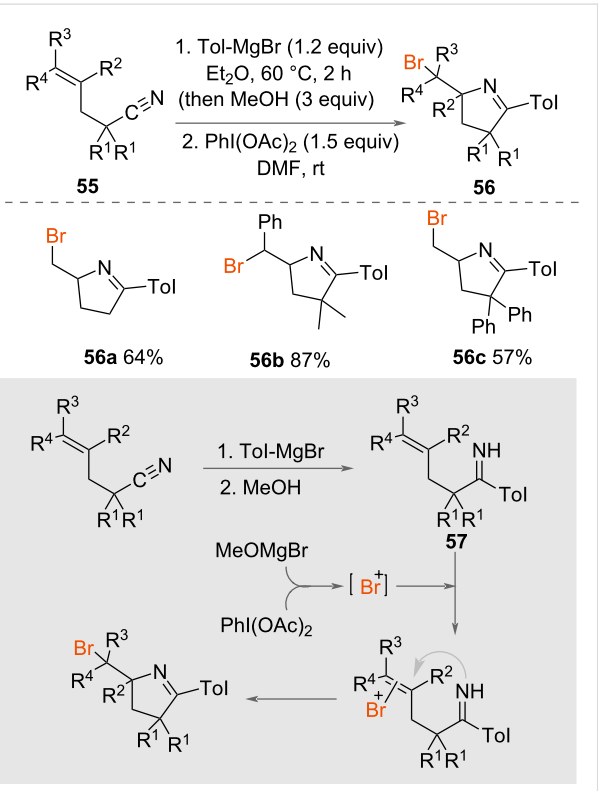

Scheme 30: Synthesis of cyclic imines **45**.

Chiba and co-worker reported the synthesis of cyclic imines using a one-pot protocol involving Grignard addition to a cyano group followed by $PhI(OAc)_2$ (Scheme 30) [51]. The authors used *p*-tolylmagnesium bromide for both the arylation of the unsaturated carbonitriles **55** and as a bromide source. Bromocyclisation was achieved using $PhI(OAc)_2$, which formed a range

of 5- and 6-membered bromomethyl cyclic imines **56** in good yields from unsaturated imines **57**.

Xia and co-workers reported the bromocyclisation of indole derivatives **58** (Scheme 31) using PIDA and $CuBr_2$ as the oxidant and bromide source, respectively [52]. Racemic pyrrolo[2,3-*b*]indoles **59** were synthesised in up to quantitative yields under mild reaction conditions at room temperature. A range of other indole derivatives were cyclised in similarly good yields demonstrating the scope of the reaction.

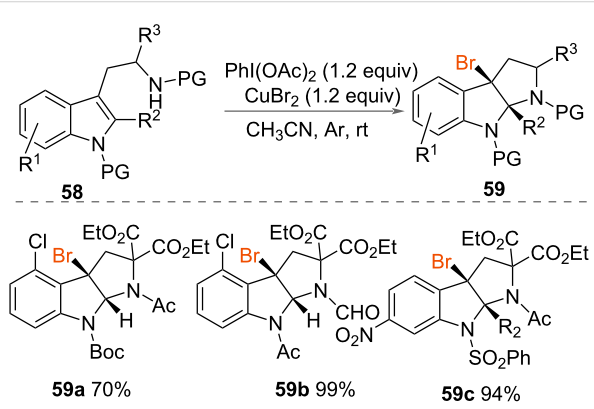

Scheme 31: Synthesis of brominated pyrrolo[2,3-*b*]indoles **59**.

Li and Liu reported the bromoamidation of alkenes in 2014 (Scheme 32) [30]. Using $PhI(OAc)_2$ as an oxidant and LiBr as a source of bromine, a range of unsaturated amines were successfully cyclised to from 5- and 6-membered aza-heterocycles **60** under mild conditions at room temperature.

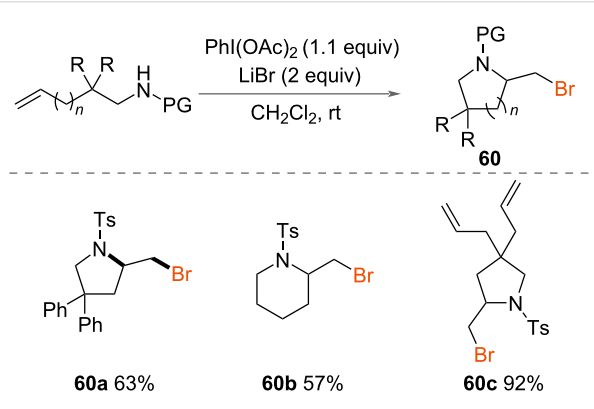

Scheme 32: Bromoamidation of alkenes.

Cariou, Dodd and co-workers reported in 2015 the synthesis of brominated cyclic guanidines **61** (Scheme 33) alongside their chlorinated cyclic guanidines **44** (vide supra) [47]. Koser's reagent was employed with LiBr to form 5- and 6-membered brominated cyclic guanidines **61** and **61'** in good yields from allylic guanidines **43**. A range of substrates with substituents on the terminal alkene were investigated, which were successfully cyclised to brominated 5- or 6-membered rings in good yields.

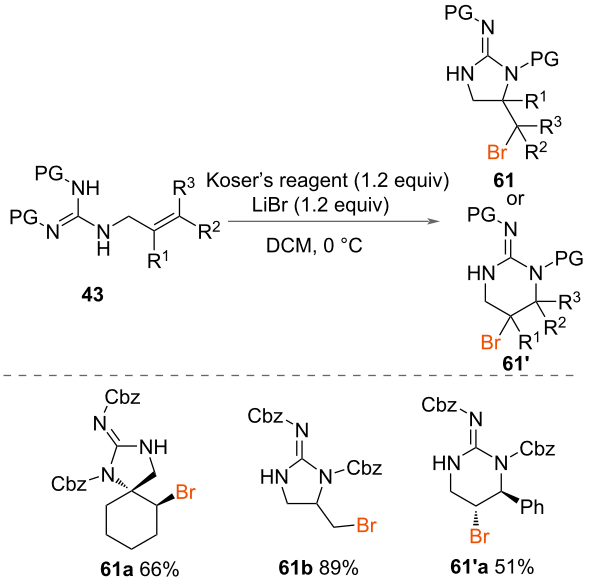

Scheme 33: Synthesis of brominated cyclic guanidines **61** and **61'**.

The intramolecular bromocyclisation of *N*-oxyureas was also reported by Cariou and co-workers in 2019 (Scheme 34) [53]. From the same starting material, the authors reported the synthesis of both oxazolidinone oximes **63** and *N*-hydroxylated ureas **64** depending on the reagent system used. Formation of oxazolidinone oximes **63** occurred using $PhI(OCOCF_3)_2$ (PIFA) as an oxidant with pyridine·HBr and the MgO additive. The oxybromocyclisation of a range of unsaturated *N*-alkoxyureas **62** occurred rapidly in 10 minutes at room temperature in acetonitrile with good yields. Formation of the *N*-hydroxylated ureas **64** occurred using $PhI(OPiv)_2$ and TBABr, with MgO as an additive to trap acetic acid. Aminobromocylization of a range of unsaturated *N*-alkoxyureas **62** was less successful with longer reactions times up to 1 hours required and poorer yields afforded. The rationale for the difference in mechanism was attributed to the oxycyclisation to yield oxazolidinone oximes **63** occurring through an ionic mechanism, whereas the aminocyclisation takes place through a radical manifold, a difference that is triggered by the difference in HVI reagent used.

In 2023, Du and co-workers reported a method for synthesizing 3-bromoindoles via a cascade oxidative cyclisation–halogenation encompassing oxidative C–N/C–Br bond formation, and utilising phenyliodine(III) diacetate (PIDA) in combination with LiBr in HFIP (Scheme 35) [54]. The reaction of 2-alkenylani-

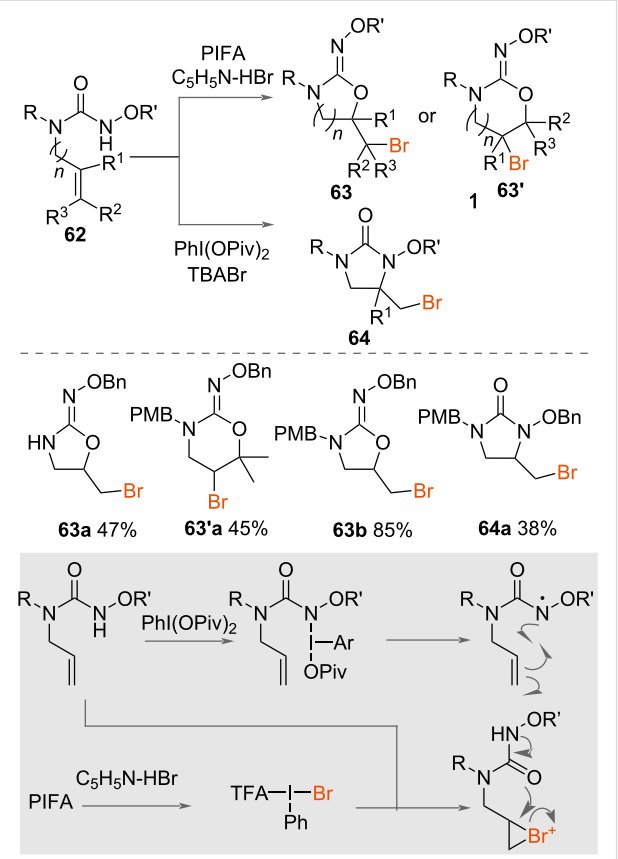

Scheme 34: Intramolecular bromocyclisation of *N*-oxyureas.

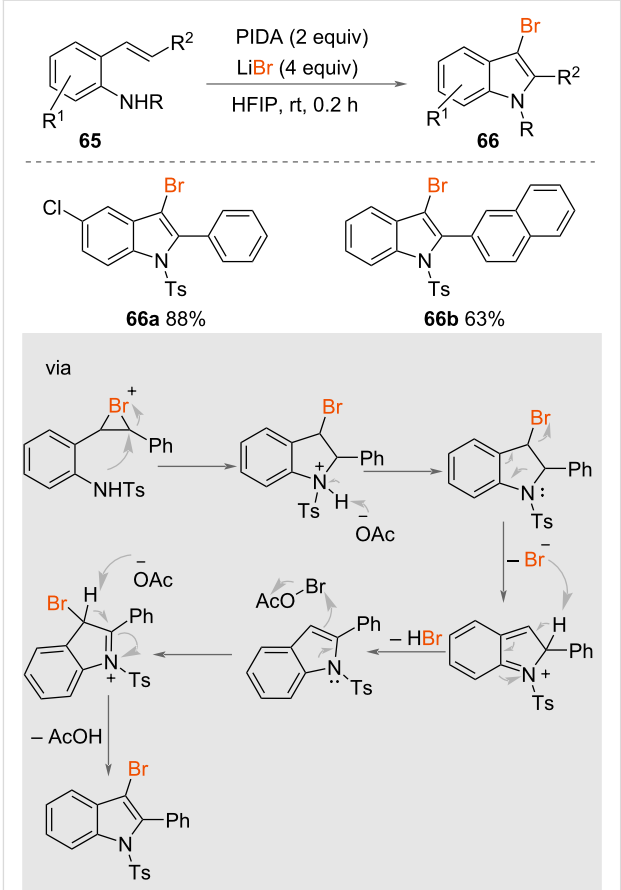

Scheme 35: The formation of 3-bromoindoles.

lines **65** with PIDA and LiBr resulted in the successful synthesis of various 3-bromoindoles **66** in high yields obtained under the optimised reaction conditions, highlighting the efficiency of the synthetic protocol. The proposed mechanism suggests that the reactive AcO–Br species is formed in situ from the reaction of PIDA and LiBr.

Oxygen nucleophiles

A novel use of HVI reagents that promotes bromocyclization was reported by Braddock and co-workers in 2006 (Scheme 36) [55]. The authors reported the use of a bromoiodinane, formed in situ from *ortho*-substituted amidine iodobenzene **67** and *N*-bromosuccinimide (NBS), which promoted the intramolecular bromolactonisation of unsaturated acids **68**. The authors investigated the oxidation using a variety of *ortho*-substituted iodobenzenes. Increasing the nucleophilicity of the groups at the *ortho*-substituted positions of iodobenzene gave increased yields of cyclised product. Both 5- and 6-membered bromolactone products **69** and **70** were formed with 5-*exo* ring closure preferred.

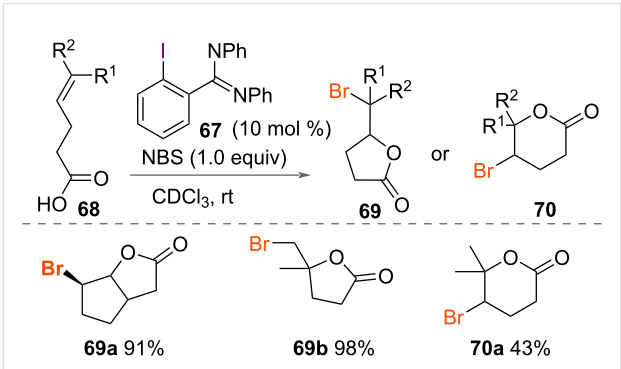

Scheme 36: Bromolactonisation of unsaturated acids **68**.

In addition to the synthesis of 5-chloromethyl-2-oxazolines **49**, Li and co-workers reported the preparation of 5-bromomethyl-2-oxazolines **71** (Scheme 37) [48]. Treatment of a range of *N*-allyl carboxamides **31** with $PhI(OAc)_2$ and TMSBr formed 5-bromomethyl-2-oxazolines **71** in excellent yields.

In 2015, Wang and co-workers reported the bromocyclisation of allylamino alcohols **72** to give chiral morpholines **73** (Scheme 38) [56]. Using an amino acid-derived chiral HVI reagent with KBr and NaOAc, a range of chiral 2,3,6-trisubsti-

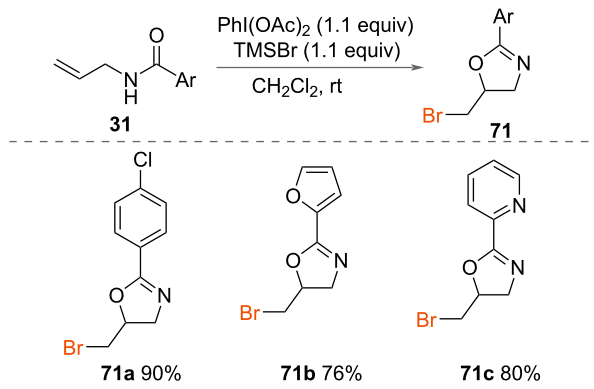

Scheme 37: Synthesis of 5-bromomethyl-2-oxazolines.

tuted bromomethylmorpholines **73** were synthesised in excellent yields and diastereoselectivities that ranged from nothing to excellent depending on the substrate. The enantioselectivity of the reaction was not measured. The authors suggested a mechanism for the reaction (Scheme 38) in which activation of the alkene and intramolecular attack of oxygen through a 6-*exo*-*trig* mechanism followed by S_N2 reaction with bromide eliminates the chiral aryliodide to form the product **73**.

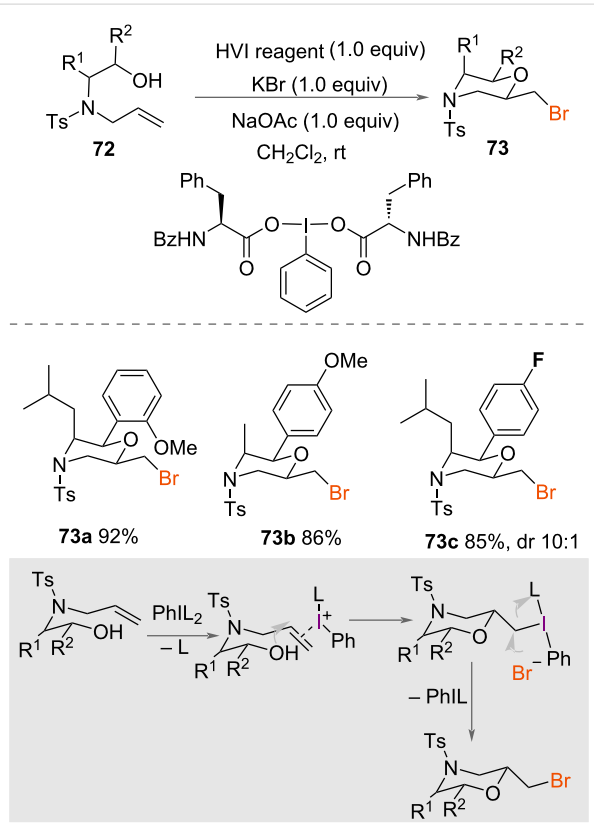

Scheme 38: Synthesis of brominated chiral morpholines.

In 2018, Liu, Ling and co-workers reported bromoenol-cyclisation of unsaturated dicarbonyls **74** (Scheme 39) [57]. Using $PhI(OAc)_2$ as an oxidant and TMSBr as a source of bromine and reaction promoter, a range of bromomethyldihydrofurans **75** were cyclised in good yields. Both 5- and 6-membered rings were formed, with homologation of the unsaturated chain. The authors initially proposed two alternative mechanisms for the reaction (Scheme 39). Either the reaction of $PhI(OAc)_2$ (PIDA) with TMSBr generates BrOAc, which forms a bromonium ion **A** with the alkene, followed by intramolecular nucleophilic attack of oxygen to form the cyclic product **75**. Alternatively, the alkene could be activated after coordination to $PhI(OAc)_2$, then intramolecular nucleophilic attack from oxygen and nucleophilic attack by bromide forms the final product. NMR studies of PIDA and the substrate indicated that there was no interaction between them, thereby discounting this second pathway and thereby providing support for the former pathway (Scheme 39).

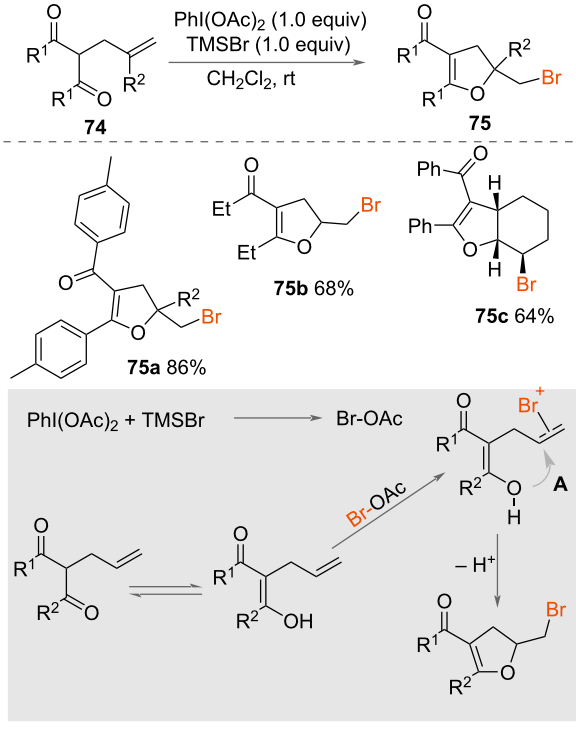

Scheme 39: Bromoenolcyclisation of unsaturated dicarbonyl groups.

In 2023, Chai, Jiang, Zhu and co-workers included the oxybromination of alkenes to form brominated dihydro-[1,3]-oxazines **76** and 2-oxazoline **77** derivative (Scheme 40) [6,49], alongside their chlorination examples. Optimized reaction conditions were developed with BBr_3 as bromide source and activating reagent, which led to the formation of the brominated oxazines **76** and 2-oxazoline **77** in very good to excellent

yields. The authors found that when substituted *N*-(2-phenylallyl)benzamides **52** were tolerated, it led to the formation of brominated 2-oxazolines in excellent yields. The structures were also assigned by X-ray crystallography.

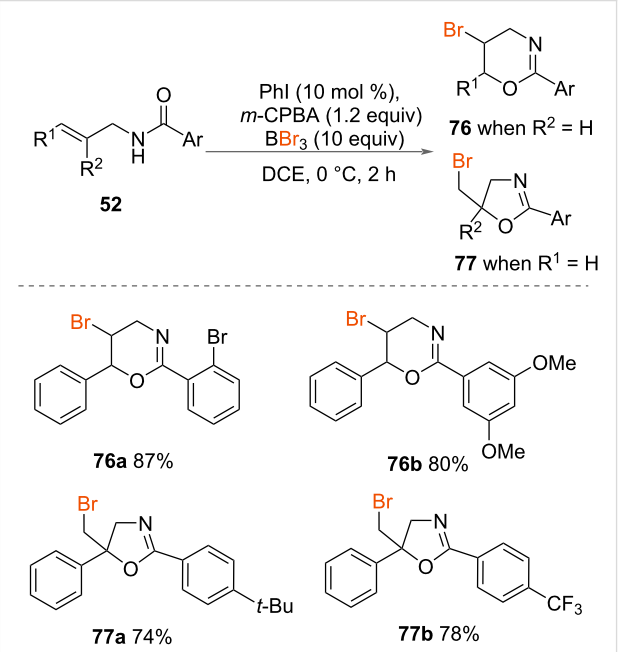

Scheme 40: Brominated oxazines and oxazolines with BBr_3.

Sulfur nucleophiles

In 2015, Li and co-workers reported the synthesis of 5-bromomethyl-2-phenylthiazoline (**79**, Scheme 41) [48]. Sulfur was used as the internal nucleophile instead of nitrogen, as previously reported by the authors in the formation of oxazolines. Using $PhI(OAc)_2$ with TMSBr as an oxidant and source of bromine respectively, *N*-allylbenzothioamide (**78**) was cyclised to form 5-bromomethtyl-2-phenylthiazoline (**79**) in a good yield.

Scheme 41: Synthesis of 5-bromomethtyl-2-phenylthiazoline.

Hypervalent iodine-mediated iodocyclisation

Reactions involving iodocyclisation mediated by HVI compounds are less prevalent compared to other halocyclisations. The use of $PhI(OAc)_2$ with KI or TMSI as the iodide source has been reported to promote iodocyclisation in unsaturated compounds with internal nucleophiles.

Nitrogen nucleophiles

In addition to both chloro- and bromoaminations, Liu and Li reported intramolecular iodoamidiation of unsaturated amines in 2014 (Scheme 42) [30]. Using PIDA as an oxidant and KI as a source of iodide, iodinated pyrrolidines **80** were synthesized in excellent yields under mild conditions of CH_2Cl_2 at room temperature. A range of unsaturated amines were successfully cyclised to form 5-membered rings. Lower yields were observed with substituted alkenes. A mechanism was proposed by the authors identical to both chloro- and bromoaminations previously reported.

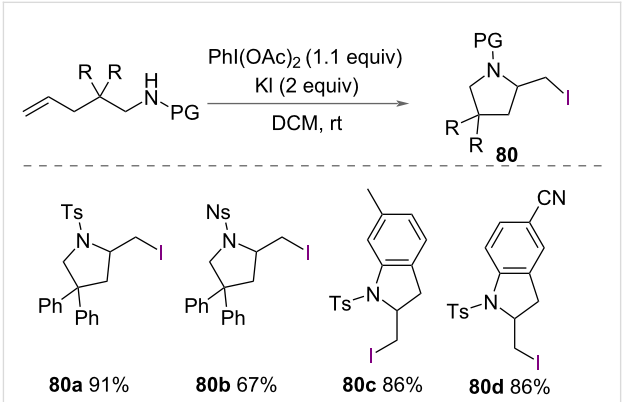

Scheme 42: Intramolecular iodoamination of unsaturated amines.

Du and co-workers described the formation of 3-iodoindoles **81** in their 2023 report that also demonstrated the formation of 3-bromoindoles **66** (Scheme 43) [54]. In this instance, KI was used as the iodide source with PIDA in HFIP. The mechanism proposed was the same as that for the bromoindoles (Scheme 35).

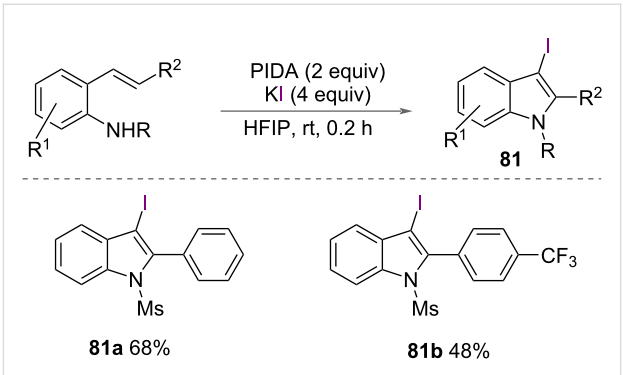

Scheme 43: Formation of 3-iodoindoles.

Oxygen nucleophiles

In addition to chloroamidation and chlorolactonization, iodoetherification of 2,2-diphenyl-4-penten-1-carboxylic acid

(**47'**) and 2,2-diphenyl-4-penten-1-ol (**47**) was reported by Liu and Li in 2014 (Scheme 26) [30]. The authors reported using $PhI(OAc)_2$ and KI in the synthesis of iodonated γ-butyrolactone **83** and iodomethyltetrahydrofuran **82** in excellent yields (Scheme 44).

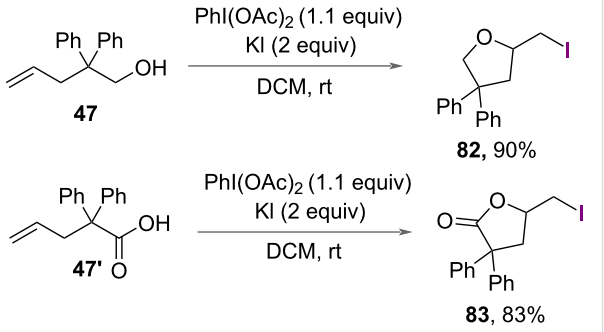

Scheme 44: Iodoetherification of 2,2-diphenyl-4-penten-1-carboxylic acid (**47'**) and 2,2-diphenyl-4-penten-1-ol (**47**).

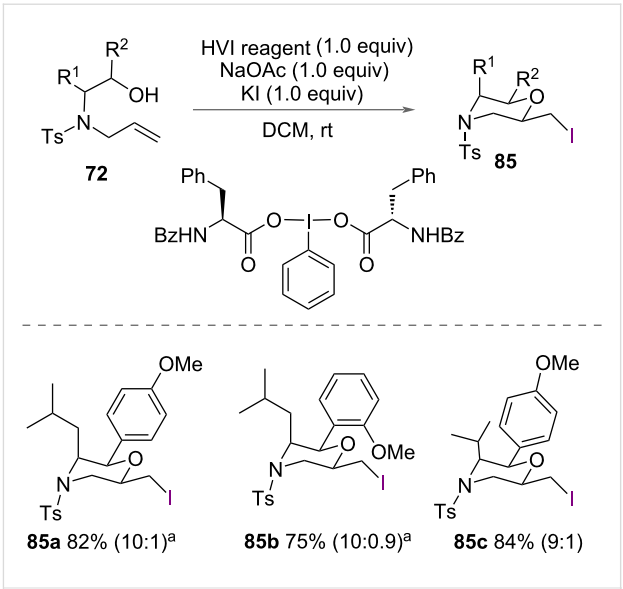

Scheme 46: Synthesis of chiral iodinated morpholines. [a]From the L-form of the amino acid starting material. The dr values were determined by ^1H NMR given in parentheses.

Li and co-workers reported the synthesis of 5-iodomethyl-2-aryloxazolines **84** in addition to the synthesis of 5-chloromethyl-2-aryloxazolines **49** and 5-bromomethyl-2-aryloxzaolines **71** (Scheme 27) [48]. Treatment of a *N*-allyl carboxamides **31** with $PhI(OCOCH_3)_2$ as an oxidant and TMSI as a source of iodide formed a range of 5-iodomethyl-2-aryloxazolines **84** in good yields (Scheme 45).

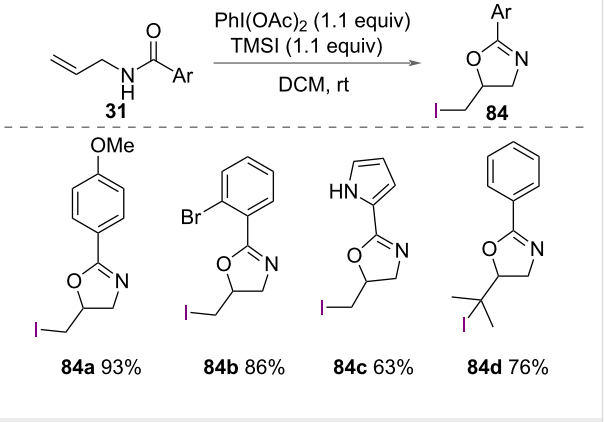

Scheme 45: Synthesis of 5-iodomethyl-2-oxazolines.

In addition to the synthesis of brominated morpholines, Wang and co-workers reported the synthesis of chiral iodinated morpholines **85** (Scheme 46) [56]. Using an amino acid-derived chiral iodine(III) reagent with KI and NaOAc, a range of allylamino alcohols **72** were cyclised in excellent yields, again without reporting the enantioselectivity of the reaction.

As well as bromoenol cyclisation (Scheme 39), Liu, Ling and co-workers reported iodoenolcyclisation of unsaturated dicarbonyl compounds **74** in 2018 (Scheme 47) [57]. Using $PhI(OAc)_2$ and TMSI, a range of polysubstituted iodomethyldihydrofurans **86** were successfully synthesised in good yields. From NMR measurements, the authors proposed the formation of an iodonium intermediate.

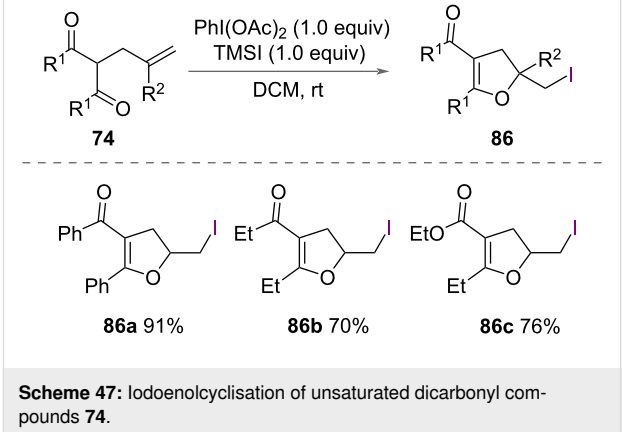

Scheme 47: Iodoenolcyclisation of unsaturated dicarbonyl compounds **74**.

Sulphur nucleophiles

Li and co-workers reported the synthesis of 5-iodomethyl-2-phenylthiazoline (**87**) in 2015 in addition to the synthesis of 5-bromomethtyl-2-thiazoline (Scheme 41), using sulfur as an internal nucleophile (Scheme 48) [48]. Using $PhI(OAc)_2$ with TMSI, *N*-allylbenzothioamide (**78**) was cyclised to form **87** in excellent yield.

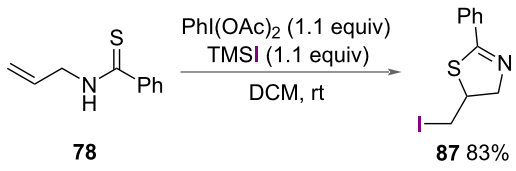

Scheme 48: Synthesis of 5-iodomethtyl-2-phenylthiazoline (**87**).

Conclusion

The HVI-mediated halocyclization of alkenes is an important approach that yields a broad variety of heterocycles under mild and efficient oxidative conditions. The internal nucleophile, length of the carbon chain and halide can be designed such that a very broad range of 5-, 6- and 7-membered heterocycles can be accessed. The identity of the HVI reagent has also shown to dictate the regioselectivity of the reaction. Future research efforts should focus on further developing access to new heterocycles, as well as designing better systems to incorporate high levels of diastereoselectivity and enantioselectivity into chiral halogenated heterocycles.

Acknowledgements

We would like to thank Dr Anna Chiara Vicini (Pfizer) for helpful discussion on the topic of the review, and Sultan Abu A Aeash (University of Bristol) for proof-reading and preliminary edits.

Funding

We would like to acknowledge the Royal Society (University Research Fellowship and Enhancement Awards to AJJL), the European Research Council (StG 949821), the EPSRC (EP/L016443/1), the University of Bristol and Pfizer for funding.

Author Contributions

Charu Bansal: writing – original draft. Oliver Ruggles: writing – original draft. Albert C. Rowett: writing – review & editing. Alastair J. J. Lennox: supervision; writing – review & editing.

ORCID® iDs

Albert C. Rowett - https://orcid.org/0000-0001-5546-9488
Alastair J. J. Lennox - https://orcid.org/0000-0003-2019-7421

Data Availability Statement

Data sharing is not applicable as no new data was generated or analyzed in this study.

References

1. Gerebtzoff, G.; Li-Blatter, X.; Fischer, H.; Frentzel, A.; Seelig, A. *ChemBioChem* **2004,** *5,* 676–684. doi:10.1002/cbic.200400017
2. Hernandes, M. Z.; Cavalcanti, S. M. T.; Moreira, D. R. M.; de Azevedo Junior, W. F.; Leite, A. C. L. *Curr. Drug Targets* **2010,** *11,* 303–314. doi:10.2174/138945010790711996
3. Depew, K. M.; Marsden, S. P.; Zatorska, D.; Zatorski, A.; Bornmann, W. G.; Danishefsky, S. J. *J. Am. Chem. Soc.* **1999,** *121,* 11953–11963. doi:10.1021/ja991558d
4. Li Petri, G.; Spanò, V.; Spatola, R.; Holl, R.; Raimondi, M. V.; Barraja, P.; Montalbano, A. *Eur. J. Med. Chem.* **2020,** *208,* 112783. doi:10.1016/j.ejmech.2020.112783
5. Li, Q.; Woods, K. W.; Claiborne, A.; Gwaltney, II, S. L.; Barr, K. J.; Liu, G.; Gehrke, L.; Credo, R. B.; Hui, Y. H.; Lee, J.; Warner, R. B.; Kovar, P.; Nukkala, M. A.; Zielinski, N. A.; Tahir, S. K.; Fitzgerald, M.; Kim, K. H.; Marsh, K.; Frost, D.; Ng, S.-C.; Rosenberg, S.; Sham, H. L. *Bioorg. Med. Chem. Lett.* **2002,** *12,* 465–469. doi:10.1016/s0960-894x(01)00759-4
6. Chai, H.; Zhen, X.; Wang, X.; Qi, L.; Qin, Y.; Xue, J.; Xu, Z.; Zhang, H.; Zhu, W. *ACS Omega* **2022,** *7,* 19988–19996. doi:10.1021/acsomega.2c01791
7. Zhang, Y.; Zhong, H.; Wang, T.; Geng, D.; Zhang, M.; Li, K. *Eur. J. Med. Chem.* **2012,** *48,* 69–80. doi:10.1016/j.ejmech.2011.11.036
8. Nangunuri, B. G.; Shirke, R. P.; Kim, M.-h. *Org. Biomol. Chem.* **2023,** *21,* 960–965. doi:10.1039/d2ob02077g
9. Singh, F. V.; Kole, P. B.; Mangaonkar, S. R.; Shetgaonkar, S. E. *Beilstein J. Org. Chem.* **2018,** *14,* 1778–1805. doi:10.3762/bjoc.14.152
10. Bora, D.; Kaushal, A.; Shankaraiah, N. *Eur. J. Med. Chem.* **2021,** *215,* 113263. doi:10.1016/j.ejmech.2021.113263
11. Bahrin, L. G.; Hopf, H.; Jones, P. G.; Sarbu, L. G.; Babii, C.; Mihai, A. C.; Stefan, M.; Birsa, L. M. *Beilstein J. Org. Chem.* **2016,** *12,* 1065–1071. doi:10.3762/bjoc.12.100
12. Pirrung, M. C.; Tumey, L. N.; McClerren, A. L.; Raetz, C. R. H. *J. Am. Chem. Soc.* **2003,** *125,* 1575–1586. doi:10.1021/ja0209114
13. Goossens, F.; Vanhoof, G.; De Meester, I.; Augustyns, K.; Borloo, M.; Tourwe, D.; Haemers, A.; Scharpé, S. *Eur. J. Biochem.* **1997,** *250,* 177–183. doi:10.1111/j.1432-1033.1997.00177.x
14. Wang, X.; Studer, A. *Acc. Chem. Res.* **2017,** *50,* 1712–1724. doi:10.1021/acs.accounts.7b00148
15. Singh, F. V.; Shetgaonkar, S. E.; Krishnan, M.; Wirth, T. *Chem. Soc. Rev.* **2022,** *51,* 8102–8139. doi:10.1039/d2cs00206j
16. Yoshimura, A.; Zhdankin, V. V. *Chem. Rev.* **2016,** *116,* 3328–3435. doi:10.1021/acs.chemrev.5b00547
17. Sun, J.; Zhang-Negrerie, D.; Du, Y.; Zhao, K. *Rep. Org. Chem.* **2016,** *6,* 25–45. doi:10.2147/roc.s84894
18. Alam, M. M.; Hussien, M.; Bollikolla, H. B.; Seema, V.; Dubasi, N.; Amanullah, M.; Varala, R. *J. Heterocycl. Chem.* **2023,** *60,* 1326–1355. doi:10.1002/jhet.4627
19. Reddy Kandimalla, S.; Prathima Parvathaneni, S.; Sabitha, G.; Subba Reddy, B. V. *Eur. J. Org. Chem.* **2019,** 1687–1714. doi:10.1002/ejoc.201801469
20. Li, X.; Chen, P.; Liu, G. *Beilstein J. Org. Chem.* **2018,** *14,* 1813–1825. doi:10.3762/bjoc.14.154
21. Lee, J. H.; Choi, S.; Hong, K. B. *Molecules* **2019,** *24,* 2634. doi:10.3390/molecules24142634
22. Smart, B. E. *J. Fluorine Chem.* **2001,** *109,* 3–11. doi:10.1016/s0022-1139(01)00375-x
23. Xu, Z.; Yang, Z.; Liu, Y.; Lu, Y.; Chen, K.; Zhu, W. *J. Chem. Inf. Model.* **2014,** *54,* 69–78. doi:10.1021/ci400539q
24. Marshall, C. M.; Federice, J. G.; Bell, C. N.; Cox, P. B.; Njardarson, J. T. *J. Med. Chem.* **2024,** *67,* 11622–11655. doi:10.1021/acs.jmedchem.4c01122

25. Ogawa, Y.; Tokunaga, E.; Kobayashi, O.; Hirai, K.; Shibata, N. *iScience* **2020,** *23,* 101467. doi:10.1016/j.isci.2020.101467
26. Wang, Q.; Zhong, W.; Wei, X.; Ning, M.; Meng, X.; Li, Z. *Org. Biomol. Chem.* **2012,** *10,* 8566–8569. doi:10.1039/c2ob26664d
27. Wu, T.; Yin, G.; Liu, G. *J. Am. Chem. Soc.* **2009,** *131,* 16354–16355. doi:10.1021/ja9076588
28. Kong, W.; Feige, P.; de Haro, T.; Nevado, C. *Angew. Chem., Int. Ed.* **2013,** *52,* 2469–2473. doi:10.1002/anie.201208471
29. Suzuki, S.; Kamo, T.; Fukushi, K.; Hiramatsu, T.; Tokunaga, E.; Dohi, T.; Kita, Y.; Shibata, N. *Chem. Sci.* **2014,** *5,* 2754–2760. doi:10.1039/c3sc53107d
30. Liu, G.-Q.; Li, Y.-M. *J. Org. Chem.* **2014,** *79,* 10094–10109. doi:10.1021/jo501739j
31. Yuan, W.; Szabó, K. J. *Angew. Chem.* **2015,** *127,* 8653–8657. doi:10.1002/ange.201503373
32. Cui, J.; Jia, Q.; Feng, R.-Z.; Liu, S.-S.; He, T.; Zhang, C. *Org. Lett.* **2014,** *16,* 1442–1445. doi:10.1021/ol500238k
33. Kitamura, T.; Miyake, A.; Muta, K.; Oyamada, J. *J. Org. Chem.* **2017,** *82,* 11721–11726. doi:10.1021/acs.joc.7b01266
34. Mennie, K. M.; Banik, S. M.; Reichert, E. C.; Jacobsen, E. N. *J. Am. Chem. Soc.* **2018,** *140,* 4797–4802. doi:10.1021/jacs.8b02143
35. Pavlović, R. Z.; Kop, T. J.; Nešić, M.; Stepanović, O.; Wang, X.; Todorović, N.; Rodić, M. V.; Šmit, B. M. *J. Org. Chem.* **2023,** *88,* 10946–10959. doi:10.1021/acs.joc.3c00944
36. Sawaguchi, M.; Hara, S.; Fukuhara, T.; Yoneda, N. *J. Fluorine Chem.* **2000,** *104,* 277–280. doi:10.1016/s0022-1139(00)00241-4
37. Ulmer, A.; Brunner, C.; Arnold, A. M.; Pöthig, A.; Gulder, T. *Chem. – Eur. J.* **2016,** *22,* 3660–3664. doi:10.1002/chem.201504749
38. Geary, G. C.; Hope, E. G.; Stuart, A. M. *Angew. Chem., Int. Ed.* **2015,** *54,* 14911–14914. doi:10.1002/anie.201507790
39. Scheidt, F.; Thiehoff, C.; Yilmaz, G.; Meyer, S.; Daniliuc, C. G.; Kehr, G.; Gilmour, R. *Beilstein J. Org. Chem.* **2018,** *14,* 1021–1027. doi:10.3762/bjoc.14.88
40. Haupt, J. D.; Berger, M.; Waldvogel, S. R. *Org. Lett.* **2019,** *21,* 242–245. doi:10.1021/acs.orglett.8b03682
41. Coppock, S. B.; Lennox, A. J. J. *Curr. Opin. Electrochem.* **2022,** *35,* 101069. doi:10.1016/j.coelec.2022.101069
42. Doobary, S.; Poole, D. L.; Lennox, A. J. J. *J. Org. Chem.* **2021,** *86,* 16095–16103. doi:10.1021/acs.joc.1c01946
43. Yang, S.; Shi, S.; Chen, Y.; Ding, Z. *J. Org. Chem.* **2021,** *86,* 14004–14010. doi:10.1021/acs.joc.1c00159
44. Zhu, W.; Zhen, X.; Wu, J.; Cheng, Y.; An, J.; Ma, X.; Liu, J.; Qin, Y.; Zhu, H.; Xue, J.; Jiang, X. *Nat. Commun.* **2021,** *12,* 3957. doi:10.1038/s41467-021-24278-3
45. Jiang, X.; Zhu, W.; Yang, L.; Zheng, Z.; Yu, C. *Eur. J. Org. Chem.* **2019,** 2268–2274. doi:10.1002/ejoc.201801842
46. Chiodi, D.; Ishihara, Y. *J. Med. Chem.* **2023,** *66,* 5305–5331. doi:10.1021/acs.jmedchem.2c02015
47. Daniel, M.; Blanchard, F.; Nocquet-Thibault, S.; Cariou, K.; Dodd, R. H. *J. Org. Chem.* **2015,** *80,* 10624–10633. doi:10.1021/acs.joc.5b01750
48. Liu, G.-Q.; Yang, C.-H.; Li, Y.-M. *J. Org. Chem.* **2015,** *80,* 11339–11350. doi:10.1021/acs.joc.5b01832
49. Qin, Y.; Qi, L.; Zhen, X.; Wang, X.; Chai, H.; Ma, X.; Jiang, X.; Cai, X.; Zhu, W. *J. Org. Chem.* **2023,** *88,* 4359–4371. doi:10.1021/acs.joc.2c02967
50. Fan, R.; Wen, F.; Qin, L.; Pu, D.; Wang, B. *Tetrahedron Lett.* **2007,** *48,* 7444–7447. doi:10.1016/j.tetlet.2007.08.085
51. Sanjaya, S.; Chiba, S. *Tetrahedron* **2011,** *67,* 590–596. doi:10.1016/j.tet.2010.11.060
52. Tu, D.; Ma, L.; Tong, X.; Deng, X.; Xia, C. *Org. Lett.* **2012,** *14,* 4830–4833. doi:10.1021/ol302158h
53. Peilleron, L.; Retailleau, P.; Cariou, K. *Adv. Synth. Catal.* **2019,** *361,* 5160–5169. doi:10.1002/adsc.201901135
54. Zhao, B.; Li, X.; Wang, X.; Jiang, L.; Li, Z.; Du, Y. *J. Org. Chem.* **2023,** *88,* 1493–1503. doi:10.1021/acs.joc.2c02480
55. Braddock, D. C.; Cansell, G.; Hermitage, S. A. *Chem. Commun.* **2006,** 2483–2485. doi:10.1039/b604130b
56. Kishore Vandavasi, J.; Hu, W.-P.; Chandru Senadi, G.; Chen, H.-T.; Chen, H.-Y.; Hsieh, K.-C.; Wang, J.-J. *Adv. Synth. Catal.* **2015,** *357,* 2788–2794. doi:10.1002/adsc.201500177
57. Liu, J.; Liu, Q.-Y.; Fang, X.-X.; Liu, G.-Q.; Ling, Y. *Org. Biomol. Chem.* **2018,** *16,* 7454–7460. doi:10.1039/c8ob02161a

License and Terms

BEILSTEIN JOURNAL OF ORGANIC CHEMISTRY

Direct trifluoroethylation of carbonyl sulfoxonium ylides using hypervalent iodine compounds

Radell Echemendía[1,2], Carlee A. Montgomery[2], Fabio Cuzzucoli[2], Antonio C. B. Burtoloso[*1] and Graham K. Murphy[*2]

Full Research Paper

Open Access

Address:
[1]São Carlos Institute of Chemistry, University of São Paulo, 13560-970, São Carlos, SP, Brazil and [2]Department of Chemistry, University of Waterloo, 200 University Ave W., Waterloo, Ontario, Canada

Email:
Antonio C. B. Burtoloso[*] - antonio@iqsc.usp.br; Graham K. Murphy[*] - graham.murphy@uwaterloo.ca

* Corresponding author

Keywords:
alkylation; DFT calculations; fluorine chemistry; hypervalent iodine; sulfoxonium ylide; sulphur ylides

Beilstein J. Org. Chem. **2024,** *20,* 3182–3190.
https://doi.org/10.3762/bjoc.20.263

Received: 20 August 2024
Accepted: 20 November 2024
Published: 04 December 2024

This article is part of the thematic issue "Hypervalent halogen chemistry".

Guest Editor: T. Gulder

Abstract

A novel study on the hypervalent iodine-mediated polyfluoroalkylation of sulfoxonium ylides was developed. Sulfoxonium ylides, known for their versatility and stability, are promising substrates for numerous transformations in synthetic chemistry. This report demonstrates the successful derivatization of sulfoxonium ylides with trifluoroethyl or tetrafluoropropyl groups, and provides valuable insights into the scope and limitations of this approach. Nineteen examples have been prepared (45–92% yields), with structural diversity modified at two key sites on the sulfoxonium ylide reactants. Finally, DFT calculations provided insights about the mechanism of this transformation, which strongly suggest that an S_N2 reaction is operative.

Introduction

Introducing fluorine or fluoroalkyl motifs into organic molecules or key frameworks stands out as a crucial and appealing approach in uncovering and crafting innovative drugs, agrochemicals, and functional materials (Figure 1) [1-4]. Fluorinated functional groups can positively alter the electronic characteristics of compounds, increase their metabolic stability, and boost their lipophilicity [5-7]. Consequently, developing new synthetic techniques that incorporate fluorine and fluorinated groups represents a significant area of research in synthetic organic chemistry [8,9].

Among the various fluorine-containing functional groups, the 2,2,2-trifluoroethyl group (CF_3CH_2), is gaining significant interest from synthetic chemists. This is due to its reduced electron-withdrawing aspect compared to the CF_3 group, its larger steric bulk and increased polarity. This moiety is also consid-

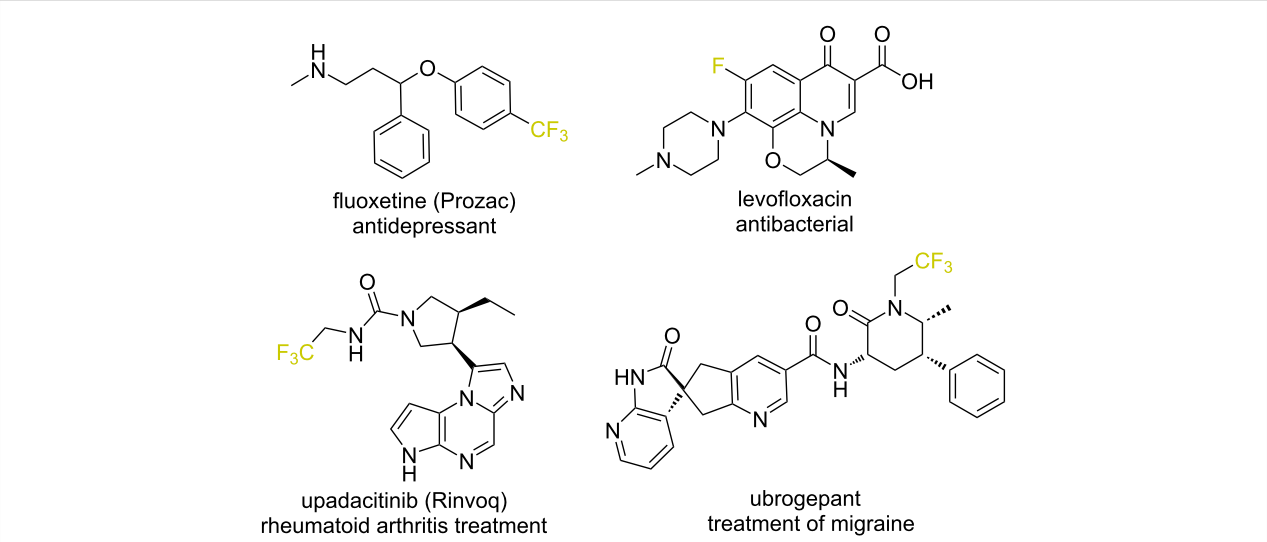

Figure 1: Representative examples of fluorine containing, biologically active compounds.

ered as a bioisostere of the ethyl or ethoxy groups and therefore it is very attractive for applications in medicinal chemistry and related areas [10-13].

α-Carbonyl sulfoxonium ylides are well recognized as more stable and more easily handled surrogates of diazo compounds [14,15]. They have also emerged as versatile intermediates in organic synthesis due to their unique reactivity and ability to participate in a wide range of chemical transformations. In this scenario, sulfoxonium ylides are excellent substrates for bifunctionalization reactions, due to the ambiphilic character in their ylidic carbon [16]. This synthetic potential has been demonstrated in a range of insertions into polar bonds [17-20], C–H activation transformations [21-23], and geminal difunctionalizations [24,25].

Within the literature, a broad array of classical methods describes the synthesis of sulfoxonium ylides [26]. The most frequently used involves deprotonating the corresponding sulfoxonium salt with strong base, followed by the addition of an acylating agent (usually an acid chloride or chloroformate). Nevertheless, achieving a wide range of structural variations in sulfoxonium salts or ylides, particularly those that lead to α-alkyl-substituted compounds, is still challenging [27]. For example, in the S_N2 reaction of alkyl halides with sulfoxonium ylides, the initially formed α-alkyl-substituted ylide reacts further with the halide to expel the sulfoxide and ultimately generate an α-halogenated product [28]. In 2017, the Aïssa group described a procedure to better synthesize such α-alkyl-substituted carbonyl sulfoxonium ylides [29]. This protocol involved the alkylation of a dialkyl thioether, counterion exchange, oxidation, and eventual acylation (Scheme 1a). More recently, the Burtoloso group reported the α-alkylation of carbonyl sulfoxonium ylides via a Michael addition approach that occurred without any competition from cyclopropanation [30]. While this reaction represented the first direct alkylation of sulfoxonium ylides, it was nonetheless limited to the more reactive ester ylide variants (Scheme 1b). As far as we know, aside from the methodologies mentioned above, there are no other reports on the direct alkylation or fluoroalkylation of these ylide compounds.

In line with our ongoing interest in the chemistry of sulfoxonium ylides, we aimed to develop a new alkylation methodology using fluoroalkyliodonium salts as sources of electrophilic trifluoroethyl synthon. Given the non-nucleophilic nature of the iodoarene byproduct, this protocol should not suffer from further reactivity that decomposes the ylide. We describe here the coupling of α-carbonyl sulfoxonium ylides with polyfluoroalkyl(aryl) hypervalent iodonium salts, for the efficient synthesis of fluorinated sulfoxonium ylides (Scheme 1c).

Results and Discussion

Since the introduction of hypervalent iodonium salts in organic chemistry, these valuable reagents have led to many new strategies for carbon–carbon bond formation [31,32]. Our research groups recently reported the α-arylation between sulfoxonium ylides and diaryliodonium salts [33], and encouraged by this precedent, we envisioned that the chemistry between sulfoxonium ylides and hypervalent iodine compounds might be ripe for further exploitation. The trifluoroethyliodonium salt discovered by Umemoto has proven an effective electrophilic trifluoroethyl transfer reagent [34,35], and to further explore the potential of fluoroalkyliodonium salts we evaluated the reactivi-

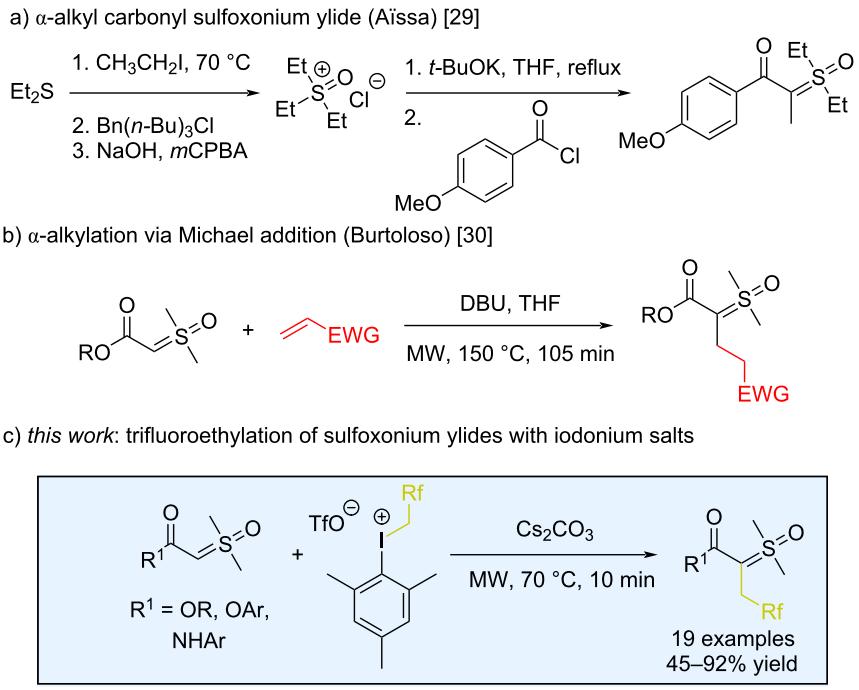

Scheme 1: Strategies for the synthesis of α-alkyl sulfoxonium ylides.

ty of such compounds in the context of sulfoxonium ylide derivatization.

As depicted in Table 1, we began our studies using methyl ester sulfoxonium ylide **1a** and 2,2,2-trifuoroethyl(mesityl)iodonium triflate salt (**2a**), as model substrates (see also Table S1 in Supporting Information File 1). Combining these at room temperature in acetonitrile produced **3a** in 8% ^{1}H NMR yield (Table 1, entry 1). Repeating the reaction with Cs_2CO_3 (1.3 equiv) produced **3a** in a much improved 60% yield (Table 1, entry 2). We screened other solvents and tested the impact of other inorganic bases but none of these changes improved the formation of the ylide **3a** (Table 1, entries 3–6). And while increasing the reaction concentration was also not effective (Table 1, entry 7; 56% yield), extending the reaction time to 24 hours at room temperature gave **3a** in 69% yield (Table 1, entry 8). Other chlorinated, ethereal or polar solvents were also tested under this prolonged reaction time, but none proved better than acetonitrile (Table 1, entries 9–12). We attempted to decrease the reaction time by increasing the temperature, but these changes resulted in decreased yields of **3a** (Table 1, entries 13 and 14). Surprisingly, when using microwave (MW) heating at 70 °C for 10 min in ACN, product **3a** was formed in 74% yield (Table 1, entry 15). An additional solvent screen under microwave conditions offered no improvement (Table 1, entries 16–18). Finally, multivariate screening ultimately showed that **3a** could be obtained in 79% ^{1}H NMR yield (75% isolated yield, Table 1, entry 19) when using **1a** (1.0 equiv), **2a** (2.0 equiv) in ACN (1 M) with Cs_2CO_3 (1.0 equiv) under microwave irradiation at 70 °C for 10 min. Though the yield only improved by 5% compared with using 1.3 equiv of **2a**, these were nonetheless adopted as the optimal reaction conditions.

Once the optimal reaction conditions were established, we then investigated the scope and limitations of this novel transformation (Scheme 2). Initially, we investigated the effects of introducing various substituents around the ester group of the carbonyl sulfoxonium ylide. We discovered that the reaction worked very well for various alkyl ester derived substrates (**3b–g**). For instance, when the bulky *tert*-butyl ester sulfoxonium ylide was used, the fluoroalkyl product **3f** was obtained in 82% yield. A 60% yield was obtained for **3g** when the reaction was carried out with the cyclopentyl ester ylide derivative. The allyl sulfoxonium ylide reacted to produce **3h** in an excellent 92% yield, however, the related benzyl derived ylides gave **3i** and **3j** in 73% and 61% yields, respectively. Phenyl esters performed well with this methodology (**3k,l**), but switching to anilide-derived ylides were consistently poorer performing. The *N*-phenyl ylide derivative reacted to produce **3m** in only 50% yield, and comparable yields were observed for the *p*-tolyl and *p*-chlorophenyl derivatives **3n** and **3o**. A slight increase in yield was found with the *p*-anisyl derivative (**3p**, 61% yield), whereas the yield decreased when the arene was appended with an electron-withdrawing CF_3 group (**3q**, 45% yield). Though we

Table 1: Optimization of reaction conditions.

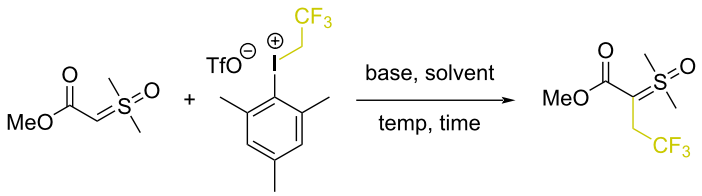

1a **2a** **3a**

Entry[a]	Temperature	Time	Solvent	Base	Yield **3a** (%)[b]
1	rt	6 h	ACN	–	8
2	rt	6 h	ACN	Cs_2CO_3	60
3	rt	6 h	dioxane	Cs_2CO_3	NR
4	rt	6 h	Et_2O	Cs_2CO_3	22
5	rt	6 h	ACN	Na_2CO_3	27
6	rt	6 h	ACN	K_3PO_4	48
7[c]	rt	6 h	ACN	Cs_2CO_3	56
8	rt	24 h	ACN	Cs_2CO_3	69
9	rt	24 h	DCM	Cs_2CO_3	7
10	rt	24 h	DCE	Cs_2CO_3	2
11	rt	24 h	THF	Cs_2CO_3	NR
12	rt	24 h	AcOEt	Cs_2CO_3	9
13	50 °C	1 h	ACN	Cs_2CO_3	46
14	60 °C	30 min	ACN	Cs_2CO_3	49
15	70 °C (MW)	10 min	ACN	Cs_2CO_3	74
16	70 °C (MW)	10 min	DCE	Cs_2CO_3	62
17	70 °C (MW)	10 min	AcOEt	Cs_2CO_3	70
18	70 °C (MW)	10 min	TFE	Cs_2CO_3	2
19[c,d]	**70 °C (MW)**	**10 min**	**ACN**	**Cs_2CO_3**	**79 (75[e])**

[a]Reaction performed with **1a** (0.2 mmol, 1.0 equiv), **2a** (0.26 mmol, 1.3 equiv), solvent (0.4 mL) and base (0.26 mmol, 1.3 equiv). [b]^{1}H NMR yield using (trifluoromethyl)benzene as internal standard. [c]Reaction performed with 0.2 mL of solvent. [d]Using 2.0 equiv of **2a** and 1.0 equiv Cs_2CO_3. [e]Isolated yield.

were unable to isolate any N-alkylated products, it is possible that competing C-alkylation and N-alkylation processes were responsible for the decreased yields observed with the anilides (compared to the ester-derived precursors). Finally, the bis-sulfonyl ylide reacted to produce **3r** in good yield (64%), and the methyl ester-derived sulfoxonium ylide could be reacted with a tetrafluoropropyl(mesityl)iodonium salt to produce tetrafluoropropyl ylide **3s** in 68% yield. These results show that a wide range of sulfoxonium ylides can be efficiently transformed to their corresponding polyfluoroalkylated derivatives in moderate to very good (45–92%) yields. It is nonetheless crucial to underscore that the reaction developed herein was ineffective with aromatic and aliphatic variants of both keto and imino sulfoxonium ylides, and no reaction was observed in any of the attempts (see Supporting Information File 1 for details). This limitation is attributed to the diminished reactivity of these ylides compared to ester and amide-derived sulfoxonium ylides.

Having established this new methodology, we then turned our attention to demonstrate additional synthetic applications of this procedure. The reaction could be easily performed on a 1 mmol scale, which gave the desired product **3a** in 71% yield (Scheme 3a). Lastly, product **3a** was subjected to our previously developed S–H insertion reaction protocol with sulfoxonium ylides [36], which generated a new 2,2,2-trifluoroethyl-coumarine-based compound **4** in 87% yield (Scheme 3b).

To gain insight into the mechanism, we modelled two reaction pathways commonly suggested for the 2,2,2-trifluoroethyl(mesityl)iodonium triflate salt, and for related diaryliodonium salts (Figure 2). The first mechanism explored was the associative pathway that terminates via reductive elimination (path 1) [37-39]. This pathway initiates by formation of a halogen bond complex between **1a** and the trifluoroethyl(mesityl)iodonium ion **2a'**, where adduct **XB-1** is presum-

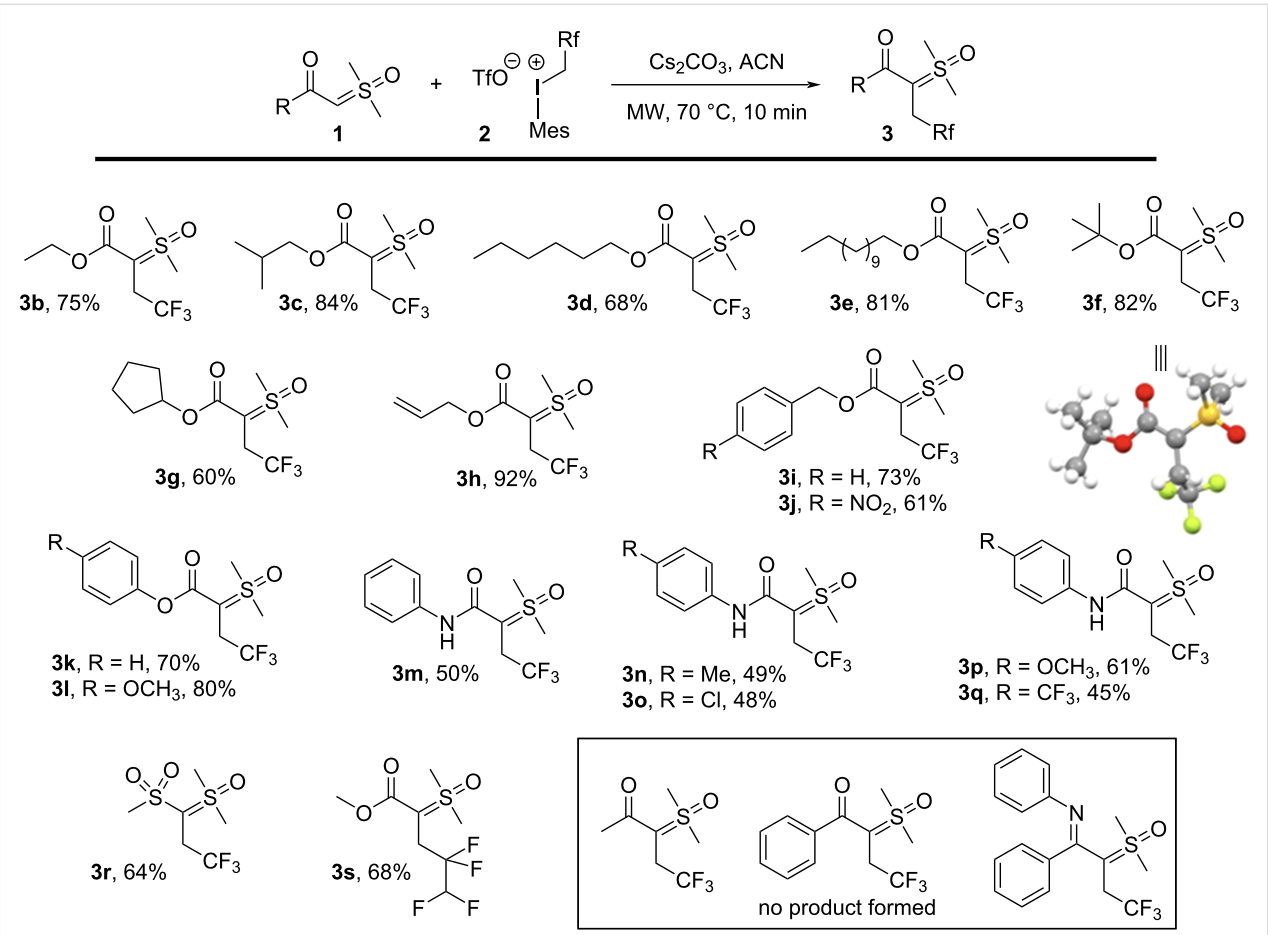

Scheme 2: Exploring substrate scope in the direct α-fluoroalkylation of sulfoxonium ylides.

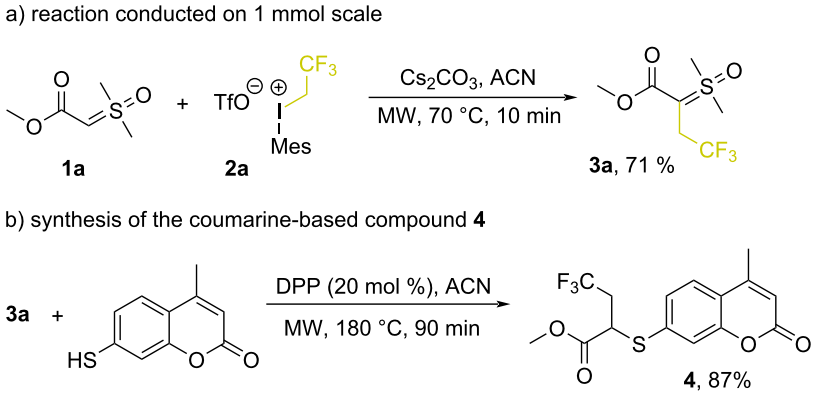

Scheme 3: Synthetic applications of fluoroalkylated sulfoxonium ylides.

ably in equilibrium with isomeric **XB-2**. Reductive elimination of the iodoarene from **XB-2** would furnish **B**, whose deprotonation would complete the pathway. The alternative mechanistic proposal is an S_N2 reaction [40-42] between **1a** and the iodonium ion **2a'**, which directly furnishes **B** without invoking halogen bonded adducts.

To assess which of these mechanistic possibilities was more probable, we turned to computational analysis. The geometries of starting materials **1a** and **2a'** were pre-optimized in the solvated phase using Gaussian 16 at the PBE0/def2-TZVP/def2-TZVPD level of theory, after a conformation search using Crest [43-49]. Next, the electrostatic potential map of the iodonium

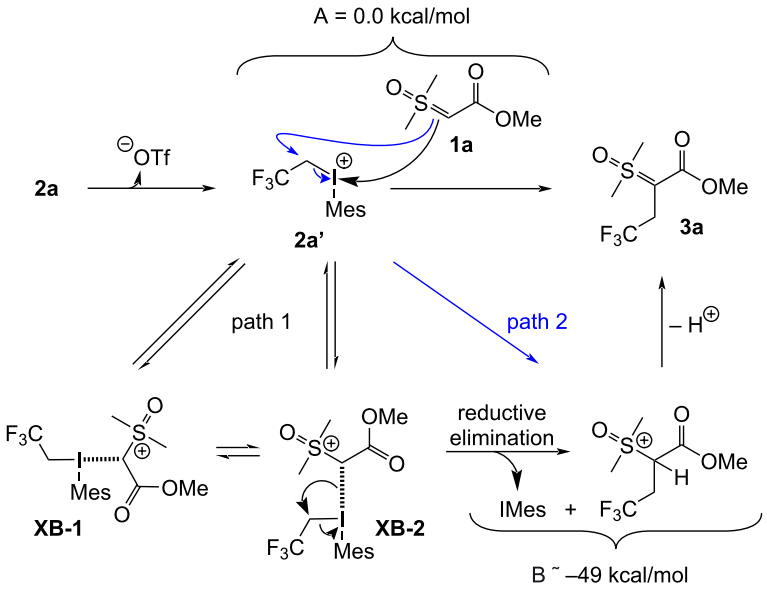

Figure 2: Possible mechanisms for the reaction of **1a** and **2a** leading to **3a** (via **B**), proceeding via either halogen-bonded adducts and reductive elimination (path 1) or directly via an S_N2 reaction (path 2).

ion **2a'** was generated using an isodensity surface of 0.001 a.u. [50]. This showed two sigma holes of different potentials, with the stronger (0.21 *e*) residing opposite the arene, and the slightly weaker (0.20 *e*) hole residing opposite the trifluoroethyl motif (Figure 3, left). These sigma-hole potentials are consistent with them being viable electrophilic sites for halogen bond formation with **1a**, supporting the mechanism in path 1. We also expressed the LUMO and LUMO+1 molecular orbitals of **2a'** (Figure 3, middle and right, respectively), which showed lobes centered on the I–C bonds to both the trifluoroethyl and arene moieties. These observations confirmed the LUMO as an appropriate lobe for nucleophilic attack via the S_N2 pathway (path 2), and confirmed the LUMO+1 as an appropriate lobe for substitution via reductive elimination (path 1). As such, neither mechanism could be immediately discarded, and we were encouraged to further explore these computationally.

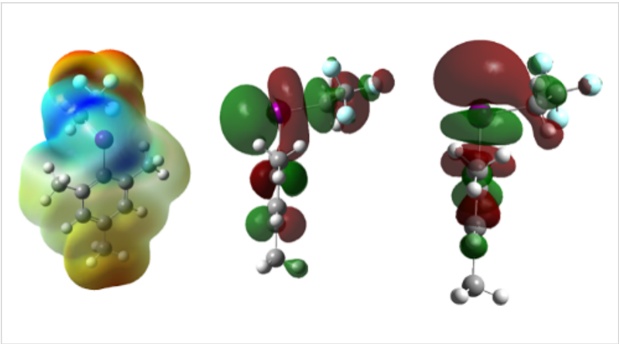

Figure 3: Electrostatic potential of **2a'** from 0.075 *e* to 0.21 *e*, showing two sigma holes of potentials 0.20 and 0.21 *e* (left). LUMO (middle) and LUMO+1 (right) of **2a'**.

For both pathways, a potential energy surface (PES) was used to generate an 'initial guess' for stationary and saddle point geometries (see also section 4.1 in Supporting Information File 1). The PES scan strongly indicated that the S_N2 mechanistic proposal was operative, owing to its lower-energy barrier; however, the saddle point geometries identified at this low level of theory were not close enough to the true transition state geometries to meet convergence criteria. Thus, using the guidance of the PES scans, **A**, **XB-2**, and **B** were subjected to the nudged elastic band climbing image (NEB-CI) method using Orca 5.0.1 at the PBE/def2-SVP D4 level of theory in the CPCM solvation model (see also section 4.2 in Supporting Information File 1) [51-56].

Both climbing images were subjected to transition state optimization and successfully met convergence criteria. Consistent with the PES scan outcome, the NEB-CI approach also indicated that the S_N2 mechanistic proposal (Figure 2, path 2) dominates.

Finally, for both mechanistic pathways, all intermediates and transition states were subjected to optimization and frequency calculations using Orca 5.0.1 at the PBE0/def2-TZVPD [57] level of theory, to generate reaction coordinate diagrams for both pathways (Figure 4). Both barrier steps were confirmed

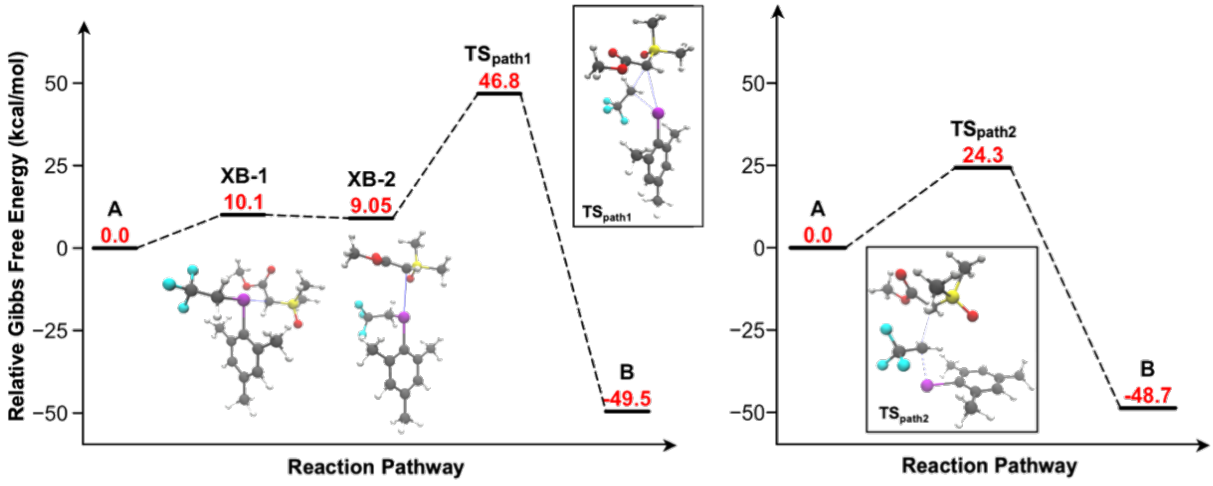

Figure 4: The optimized reaction coordinate diagrams for the halogen bond-mediated mechanism (path 1, left) and the S_N2 mechanism (path 2, right).

using the intrinsic reaction coordinate (IRC) method. Ion **2a'** was found to have an initial bond length of 2.1 Å. The transition to **XB-1** was found at a relative energy of 10.1 kcal/mol, where the C–I–C bond angle is 178° with C–I bond lengths of 2.2 Å (I–CH_2CF_3) and 2.9 Å. The reaction coordinate diagram for path 1 showed a near barrierless equilibrium between halogen bond adducts **XB-1** and **XB-2**, where **XB-2** has a C–I–C bond angle of 86° and C–I bond lengths of 2.1 Å (I–CH_2CF_3) and 3.2 Å. Finally, a 37.8 kcal/mol activation energy between **XB-2** and **B** for path 1 was calculated. On the other hand, path 2 had a much lower Gibbs free energy of activation of 24.3 kcal/mol, where the angle of attack from **1a** to **2a'** was found at approximately 160° with equal C–I bond lengths of 2.5 Å in the transition state. The significantly lower activation energy allowed us to conclude that the S_N2 mechanism was the more favourable pathway.

Conclusion

In conclusion, we have developed a direct polyfluoroalkylation reaction of sulfoxonium ylides. The easily available 2,2,2-trifluoroethyl(mesityl)iodonium triflate reagent enabled the straightforward trifluoroethylation of diverse sulfoxonium ylides under mild conditions and short reaction times. Various computational strategies were also employed to differentiate between competing halogen bond-mediated and S_N2 reaction mechanisms. Ultimately, the nudged elastic band climbing image (NEB-CI) method predicted the S_N2 pathway to be favoured, and transition state optimization showed this to possess a Gibbs free energy of activation of 24.3 kcal/mol. This report shows the ease with which sulfoxonium ylides can be derivatized using hypervalent iodine reagents, and our continued efforts towards this will be reported in due course.

Experimental

Representative procedure for 2,2,2-trifluoroethylation of sulfoxonium ylides

An oven dried 5 mL microwave flask containing a magnetic stirrer was charged with Cs_2CO_3 (70.5 mg, 0.2 mmol, 1.0 equiv), sulfoxonium ylide (0.2 mmol, 1.0 equiv) and the corresponding fluoroethyliodonium salt (0.40 mmol, 2.0 equiv). The reaction vessel was capped with a rubber septum and filled with nitrogen. Then ACN (0.2 mL) was added. The rubber septum was removed and the microwave vial was quickly capped with a Teflon microwave cap. The reaction was heated to 70 ºC for 10 min. The crude mixture was dissolved with DCM (3 mL), the solvent was removed under reduced pressure to furnish a crude product that was purified by flash column chromatography, using silica gel 60 (200–400 mesh) as a stationary phase (eluent *n*-hex/AcOEt 5:95%).

Supporting Information

Supporting Information File 1

Experimental part, NMR spectra, computational details and crystallgraphic data.
[https://www.beilstein-journals.org/bjoc/content/supplementary/1860-5397-20-263-S1.pdf]

Acknowledgements

We would like to acknowledge the Schipper lab at the University of Waterloo for providing access to the microwave reactor used in this study. We would also like to acknowledge Boris

Ragula from the University of Waterloo (Department of Applied Math) for assisting in the preparation of the Julia script used to generate the reaction coordinate diagrams.

Funding

We would like to thank the São Paulo Research Foundation (FAPESP) for financial support (2023/02675-7) and in the form of fellowship grants to RE (2019/12300-5; 2022/09140-9). We also thank the Natural Sciences and Engineering Research Council (NSERC) of Canada for funding (DG 2019-04086, 2024-04404). FC acknowledges NSERC for a doctoral scholarship, and CAM acknowledges OGS and NSERC for graduate scholarships.

Conflict of Interest

The authors declare no conflict of interest.

ORCID® iDs

Radell Echemendía - https://orcid.org/0000-0001-5310-2068
Carlee A. Montgomery - https://orcid.org/0000-0003-3708-2997
Fabio Cuzzucoli - https://orcid.org/0000-0002-2296-3268
Antonio C. B. Burtoloso - https://orcid.org/0000-0003-2203-1556
Graham K. Murphy - https://orcid.org/0000-0002-8795-2404

Data Availability Statement

All data that supports the findings of this study is available in the published article and/or the supporting information to this article.

References

1. Zhou, Y.; Wang, J.; Gu, Z.; Wang, S.; Zhu, W.; Aceña, J. L.; Soloshonok, V. A.; Izawa, K.; Liu, H. *Chem. Rev.* **2016,** *116,* 422–518. doi:10.1021/acs.chemrev.5b00392
2. Ni, C.; Hu, M.; Hu, J. *Chem. Rev.* **2015,** *115,* 765–825. doi:10.1021/cr5002386
3. Vitale, A.; Bongiovanni, R.; Ameduri, B. *Chem. Rev.* **2015,** *115,* 8835–8866. doi:10.1021/acs.chemrev.5b00120
4. Jeschke, P. *ChemBioChem* **2004,** *5,* 570–589. doi:10.1002/cbic.200300833
5. Tang, Y.; Ghirlanda, G.; Vaidehi, N.; Kua, J.; Mainz, D. T.; Goddard, W. A.; DeGrado, W. F.; Tirrell, D. A. *Biochemistry* **2001,** *40,* 2790–2796. doi:10.1021/bi0022588
6. Tang, Y.; Ghirlanda, G.; Petka, W. A.; Nakajima, T.; DeGrado, W. F.; Tirrell, D. A. *Angew. Chem., Int. Ed.* **2001,** *40,* 1494–1496. doi:10.1002/1521-3773(20010417)40:8<1494::aid-anie1494>3.0.co;2-x
7. O'Hagan, D. *Chem. Soc. Rev.* **2008,** *37,* 308–319. doi:10.1039/b711844a
8. Wang, J.; Sánchez-Roselló, M.; Aceña, J. L.; del Pozo, C.; Sorochinsky, A. E.; Fustero, S.; Soloshonok, V. A.; Liu, H. *Chem. Rev.* **2014,** *114,* 2432–2506. doi:10.1021/cr4002879
9. Inoue, M.; Sumii, Y.; Shibata, N. *ACS Omega* **2020,** *5,* 10633–10640. doi:10.1021/acsomega.0c00830
10. Uneyama, K.; Yamazaki, T. *J. Fluorine Chem.* **2017,** *203,* 3–30. doi:10.1016/j.jfluchem.2017.07.010
11. Shi, G. Q.; Dropinski, J. F.; Zhang, Y.; Santini, C.; Sahoo, S. P.; Berger, J. P.; MacNaul, K. L.; Zhou, G.; Agrawal, A.; Alvaro, R.; Cai, T.-q.; Hernandez, M.; Wright, S. D.; Moller, D. E.; Heck, J. V.; Meinke, P. T. *J. Med. Chem.* **2005,** *48,* 5589–5599. doi:10.1021/jm050373g
12. van Oeveren, A.; Motamedi, M.; Mani, N. S.; Marschke, K. B.; López, F. J.; Schrader, W. T.; Negro-Vilar, A.; Zhi, L. *J. Med. Chem.* **2006,** *49,* 6143–6146. doi:10.1021/jm060792t
13. Gujjar, R.; El Mazouni, F.; White, K. L.; White, J.; Creason, S.; Shackleford, D. M.; Deng, X.; Charman, W. N.; Bathurst, I.; Burrows, J.; Floyd, D. M.; Matthews, D.; Buckner, F. S.; Charman, S. A.; Phillips, M. A.; Rathod, P. K. *J. Med. Chem.* **2011,** *54,* 3935–3949. doi:10.1021/jm200265b
14. Burtoloso, A. C. B.; Dias, R. M. P.; Leonarczyk, I. A. *Eur. J. Org. Chem.* **2013,** 5005–5016. doi:10.1002/ejoc.201300581
15. Bisag, G. D.; Ruggieri, S.; Fochi, M.; Bernardi, L. *Org. Biomol. Chem.* **2020,** *18,* 8793–8809. doi:10.1039/d0ob01822h
16. Caiuby, C. A. D.; Furniel, L. G.; Burtoloso, A. C. B. *Chem. Sci.* **2022,** *13,* 1192–1209. doi:10.1039/d1sc05708a
17. Liu, X.; Shao, Y.; Sun, J. *Org. Lett.* **2021,** *23,* 1038–1043. doi:10.1021/acs.orglett.0c04229
18. Furniel, L. G.; Echemendía, R.; Burtoloso, A. C. B. *Chem. Sci.* **2021,** *12,* 7453–7459. doi:10.1039/d1sc00979f
19. Li, J.; He, H.; Huang, M.; Chen, Y.; Luo, Y.; Yan, K.; Wang, Q.; Wu, Y. *Org. Lett.* **2019,** *21,* 9005–9008. doi:10.1021/acs.orglett.9b03410
20. Denisa Bisag, G.; Ruggieri, S.; Fochi, M.; Bernardi, L. *Adv. Synth. Catal.* **2021,** *363,* 3053–3059. doi:10.1002/adsc.202100124
21. Wu, X.; Sun, S.; Yu, J.-T.; Cheng, J. *Synlett* **2019,** *30,* 21–29. doi:10.1055/s-0037-1610263
22. Kumar, A.; Sherikar, M. S.; Hanchate, V.; Prabhu, K. R. *Tetrahedron* **2021,** *101,* 132478. doi:10.1016/j.tet.2021.132478
23. Leveille, A. N.; Echemendía, R.; Mattson, A. E.; Burtoloso, A. C. B. *Org. Lett.* **2021,** *23,* 9446–9450. doi:10.1021/acs.orglett.1c03627
24. Gallo, R. D. C.; Ahmad, A.; Metzker, G.; Burtoloso, A. C. B. *Chem. – Eur. J.* **2017,** *23,* 16980–16984. doi:10.1002/chem.201704609
25. Day, D. P.; Mora Vargas, J. A.; Burtoloso, A. C. B. *J. Org. Chem.* **2021,** *86,* 12427–12435. doi:10.1021/acs.joc.1c01441
26. Corey, E. J.; Chaykovsky, M. *J. Am. Chem. Soc.* **1962,** *84,* 867–868. doi:10.1021/ja00864a040
27. Johnson, A. W.; LaCount, R. B. *J. Am. Chem. Soc.* **1961,** *83,* 417–423. doi:10.1021/ja01463a040
28. Onuki, Y.; Nambu, H.; Yakura, T. *Chem. Pharm. Bull.* **2020,** *68,* 479–486. doi:10.1248/cpb.c20-00132
29. Barday, M.; Janot, C.; Halcovitch, N. R.; Muir, J.; Aïssa, C. *Angew. Chem., Int. Ed.* **2017,** *56,* 13117–13121. doi:10.1002/anie.201706804
30. de Jesus, M. P.; Echemendía, R.; Burtoloso, A. C. B. *Org. Chem. Front.* **2023,** *10,* 3577–3584. doi:10.1039/d3qo00688c
31. Zhdankin, V. V.; Stang, P. J. *Chem. Rev.* **2008,** *108,* 5299–5358. doi:10.1021/cr800332c
32. Merritt, E. A.; Olofsson, B. *Angew. Chem., Int. Ed.* **2009,** *48,* 9052–9070. doi:10.1002/anie.200904689
33. Echemendía, R.; To, A. J.; Murphy, G. K.; Burtoloso, A. C. B. *Adv. Synth. Catal.* **2024,** *366,* 396–401. doi:10.1002/adsc.202301061
34. Umemoto, T.; Gotoh, Y. *J. Fluorine Chem.* **1986,** *31,* 231–236. doi:10.1016/s0022-1139(00)80536-9
35. Béke, F.; Csenki, J. T.; Novák, Z. *Chem. Rec.* **2023,** *23,* e202300083. doi:10.1002/tcr.202300083

36. Dias, R. M. P.; Burtoloso, A. C. B. *Org. Lett.* **2016,** *18,* 3034–3037. doi:10.1021/acs.orglett.6b01470
37. Rotstein, B. H.; Wang, L.; Liu, R. Y.; Patteson, J.; Kwan, E. E.; Vasdev, N.; Liang, S. H. *Chem. Sci.* **2016,** *7,* 4407–4417. doi:10.1039/c6sc00197a
38. Han, Z.-Z.; Zhang, C.-P. *Tetrahedron Lett.* **2021,** *73,* 153146. doi:10.1016/j.tetlet.2021.153146
39. Wang, B.; Graskemper, J. W.; Qin, L.; DiMagno, S. G. *Angew. Chem., Int. Ed.* **2010,** *49,* 4079–4083. doi:10.1002/anie.201000695
40. Tolnai, G. L.; Székely, A.; Makó, Z.; Gáti, T.; Daru, J.; Bihari, T.; Stirling, A.; Novák, Z. *Chem. Commun.* **2015,** *51,* 4488–4491. doi:10.1039/c5cc00519a
41. Zhao, C.-L.; Shi, J.; Lu, X.; Wu, X.; Zhang, C.-P. *J. Fluorine Chem.* **2019,** *226,* 109360. doi:10.1016/j.jfluchem.2019.109360
42. Csenki, J. T.; Novák, Z. *Chem. Commun.* **2024,** *60,* 726–729. doi:10.1039/d3cc04985j
43. Pracht, P.; Bohle, F.; Grimme, S. *Phys. Chem. Chem. Phys.* **2020,** *22,* 7169–7192. doi:10.1039/c9cp06869d
44. *Gaussian 16,* Revision C.01; Gaussian, Inc.: Wallingford, CT, 2016.
45. Perdew, J. P.; Burke, K.; Ernzerhof, M. *Phys. Rev. Lett.* **1996,** *77,* 3865–3868. doi:10.1103/physrevlett.77.3865
46. Adamo, C.; Barone, V. *J. Chem. Phys.* **1999,** *110,* 6158–6170. doi:10.1063/1.478522
47. Weigend, F.; Ahlrichs, R. *Phys. Chem. Chem. Phys.* **2005,** *7,* 3297–3305. doi:10.1039/b508541a
48. Rappoport, D.; Furche, F. *J. Chem. Phys.* **2010,** *133,* 134105. doi:10.1063/1.3484283
49. Robidas, R.; Legault, C. Y. *Int. J. Quantum Chem.* **2024,** *124,* e27277. doi:10.1002/qua.27277
    See for a selected method based on its favourable results in modelling halogen bonding for monovalent iodine.
50. Bader, R. F. W.; Carroll, M. T.; Cheeseman, J. R.; Chang, C. *J. Am. Chem. Soc.* **1987,** *109,* 7968–7979. doi:10.1021/ja00260a006
51. Ásgeirsson, V.; Birgisson, B. O.; Bjornsson, R.; Becker, U.; Neese, F.; Riplinger, C.; Jónsson, H. *J. Chem. Theory Comput.* **2021,** *17,* 4929–4945. doi:10.1021/acs.jctc.1c00462
52. Stoychev, G. L.; Auer, A. A.; Neese, F. *J. Chem. Theory Comput.* **2017,** *13,* 554–562. doi:10.1021/acs.jctc.6b01041
53. Neese, F. *Wiley Interdiscip. Rev.: Comput. Mol. Sci.* **2012,** *2,* 73–78. doi:10.1002/wcms.81
54. Neese, F. *Wiley Interdiscip. Rev.: Comput. Mol. Sci.* **2022,** *12,* e1606. doi:10.1002/wcms.1606
55. Marenich, A. V.; Cramer, C. J.; Truhlar, D. G. *J. Phys. Chem. B* **2009,** *113,* 6378–6396. doi:10.1021/jp810292n
56. Caldeweyher, E.; Bannwarth, C.; Grimme, S. *J. Chem. Phys.* **2017,** *147,* 034112. doi:10.1063/1.4993215
57. Peterson, K. A.; Figgen, D.; Goll, E.; Stoll, H.; Dolg, M. *J. Chem. Phys.* **2003,** *119,* 11113–11123. doi:10.1063/1.1622924

License and Terms

BEILSTEIN JOURNAL OF ORGANIC CHEMISTRY

Reactivity of hypervalent iodine(III) reagents bearing a benzylamine with sulfenate salts

Beatriz Dedeiras, Catarina S. Caldeira‡, José C. Cunha‡, Clara S. B. Gomes and M. Manuel B. Marques*

Full Research Paper

Open Access

Address:
LAQV-REQUIMTE, Department of Chemistry, NOVA School of Science and Technology, NOVA FCT , 2829-516 Caparica, Portugal

Email:
M. Manuel B. Marques* - msbm@fct.unl.pt

* Corresponding author ‡ Equal contributors

Keywords:
electrophilic amination; hypervalent iodine reagents; sulfinamide; sulfonamide

Beilstein J. Org. Chem. **2024,** *20,* 3281–3289.
https://doi.org/10.3762/bjoc.20.272

Received: 25 July 2024
Accepted: 13 December 2024
Published: 19 December 2024

This article is part of the thematic issue "Hypervalent halogen chemistry".

Guest Editor: J. Wencel-Delord

Abstract

The reactivity of our recently disclosed hypervalent iodine reagents (HIRs) bearing a benzylamine with in situ-generated sulfenate salts was investigated. Under the studied conditions sulfonamides have been obtained in up to 52% yield. This reaction has been extended to a variety of HIRs and sulfenate salts to explore the different reactivity of these new reagents. A plausible mechanism is proposed, suggesting a possible radical pathway.

Introduction

Iodine(III) compounds, known as λ^3-iodanes, have been extensively applied in organic synthesis. Although initially used as strong oxidizing agents [1], during the last decades HIRs have been investigated as group-transfer reagents, useful in several bond-forming reactions, such as in C–C, C–N, and C–O [2-5].

The benziodoxol(on)e family, cyclic iodine(III) reagents, stands out for their thermal stability and reactivity, yielding numerous derivatives with wide applications [2-4,6-8]. Their enhanced stability, compared to other HIRs, is due to: (i) the molecular geometry, which allows better overlap between the non-bonding electrons of the central iodine atom and the π-orbitals of the aromatic ring [2,9]; (ii) the incorporation of the iodine atom in the 5-membered heterocycle [10]; and (iii) the *trans* effect, due to the interaction of the hypervalent bonds established by the axial ligands, where iodine orbitals are shared with both heteroatoms [11]. As a result, benziodoxol(on)es have found application in electrophilic transfer reactions, with emphasis on umpolung reactivity of usually nucleophilic functional groups. Thus constituting a powerful synthetic tool, opening room for new synthetic disconnections [10].

Within the benziodoxol(on)e class, a range of HIRs featuring nitrogen-containing groups have been reported [12]. These

reagents have proven effective in delivering azides (**I**) [13], amides (**II**) [14], aliphatic cyclic amines (**III**) [15], phthalimidates (**IV**) [16], imines (**V**) [17], sulfoximides (**VI**) [18], carbazoles (**VII**) [19], secondary (**VIII**) [4] and primary (**IX**) [20] amines (Figure 1).

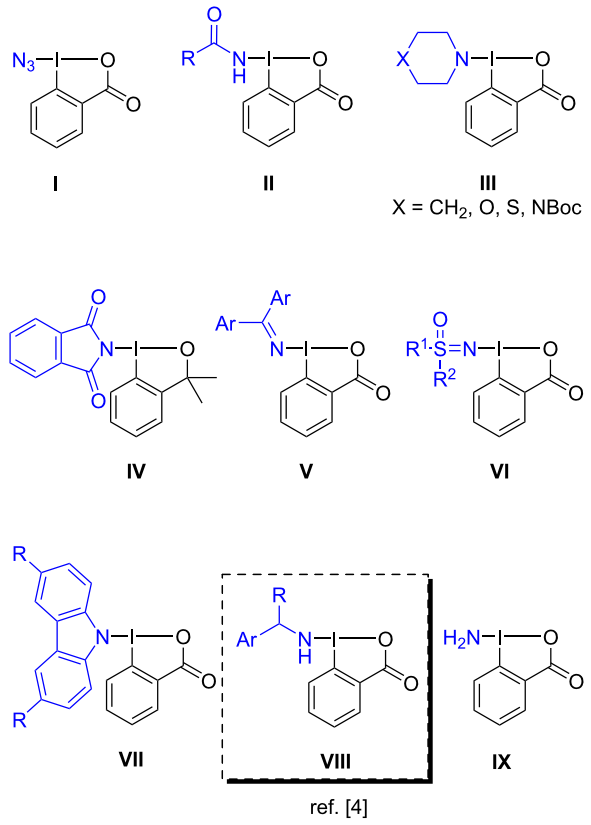

Figure 1: Examples of cyclic HIRs with a nitrogen-based group transfer [4,10,13-20].

The first report from Zhdankin and co-workers in 1994, described the preparation of azidobenziodoxolone, ABX (**I**), a reagent widely used in oxidative azide transfer reactions [21]. Years later, Zhdankin's group also reported the synthesis of amidobenziodoxolone (**II**) [14]. Other examples of N-containing benziodoxol(on)es can be found in the literature, including reagents featuring cyclic aliphatic amine moieties (**III**) [15], phthalimidates (**IV**) [16], and carbazoles (**VII**) [19]. Minakata and co-workers proposed an innovative approach for transferring imine groups using iodane-containing (diarylmethylene)amino groups (**V**), which proved to be useful in the transfer of imine radicals [17]. Bolm et al. contributed also to this topic by introducing a sulfoximidoyl-containing benziodoxolone (**VI**) [18]. Recently, our group disclosed the first HIRs bearing a primary amine moiety, the benzylamine benziodoxolone reagent **VIII** (named BBX), and investigated its reactivity on the α-amination of indanone-based β-ketoesters (Scheme 1) [4]. Very recently, Minakata's group also reported iodine(III) reagents with transferable amino groups, particularly a benziodoxolone bearing a transferable NH_2 group (**IX**) [20].

HIRs have been a central theme of the work carried out by our research group in recent years, focusing on the formation of the S–N bond by applying the umpolung reactivity of HIRs, in particular in the preparation of sulfonamides and sulfonyl hydrazides [22,23]. In both approaches, a sulfonyl-containing benziodoxolone was generated in situ, via a reaction of chlorobenziodoxolone with sulfinate salts, followed by the addition of amines or hydrazines, respectively.

On the follow-up on our research, we envisaged to extend the diversity of BBX reagents as electrophilic amine reagents and investigated their reactivity with in situ-generated sulfenate anions, from β-sulfinyl esters, to achieve S–N bond formation. The importance of establishing this S–N bond results from the widespread presence of sulfonyl-containing bioactive compounds, such as the sulfonamide group which can be found in many pharmaceuticals, commonly referred to as sulfa drugs. These include top seller drugs, e.g., antimicrobials, anti-inflammatories, antihypertensives, and antitumor agents [24-26]. Particularly, the sulfonamide motif can act as a bioisostere of carboxylic acids, establishing a set of hydrogen bonds similar to those formed by carboxylic acids, enhancing its versatility and effectiveness in drug design [27].

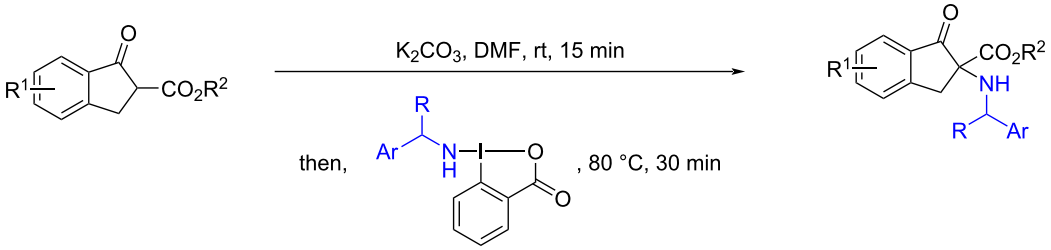

Scheme 1: Electrophilic α-amination of indanone-based β-ketoesters [4].

Traditional sulfonamide preparation involves combining sulfonyl chlorides and amines [25,28,29]. Despite the efficiency of traditional methods, challenges still remain, e.g., use of harsh conditions, like oxidative chlorination with aqueous chlorine [30], or treatment with toxic sulfur dioxide. Thus, we envisaged to further investigate BBX reactivity to address the S–N-bond formation, as an alternative method towards sulfur-containing compounds [22].

Results and Discussion

We initiated our study by extending the functionalization of BBX reagents. (Benzylamino)benziodoxolones, BBXs **2**, were prepared according to our reported procedure, via reaction with previously silylated benzylamines (Scheme 2) [4]. Using this methodology, a total of four benziodoxolones (including the new *p*-fluorobenzylamine benziodoxolone, **2d**) were obtained with quantitative yields, as white solids on the gram-scale, easy to manipulate and long-term stable below 0 °C.

Crystals of compound **2d** were successfully obtained and its molecular structure was confirmed through single-crystal X-ray diffraction. The X-ray analysis revealed a distorted T-shaped geometry, consistent with previously reported N–bound hypervalent iodine reagents. Additionally, the N–I bond distance is 2.0454(5) Å, which aligns with our previously reported values [4]. The two aromatic rings are nearly coplanar, exhibiting a dihedral angle of 0.7(3)°. All other bond lengths and angles fall within the expected range for similar compounds [31].

Later, the β-sulfinyl esters **4** were prepared by Michael addition reaction of thiols and α,β-unsaturated esters [32], followed by oxidation of the corresponding sulfides **3** using two different oxidizing agents (oxone and *m*-CPBA) [32,33]. To investigate the reactivity of the BBXs in this electrophilic amination reaction, the generated compound **4** was subjected to a retro-Michael addition to produce the sulfenate anion intermediate, followed by the addition of BBX **2**. Based on our experience with HIRs, the reaction of **2** with nucleophiles is more effective when a pre-formed nucleophile is used [4]. Thus, HIR **2** was added to the reaction mixture after the in situ formation of the sulfenate anion (by retro-Michael addition).

First experiments were carried out under the previously described conditions for BBX electrophilic amination reaction (Table 1, entry 1) [4]. In the presence of potassium carbonate, only starting material **4a** was detected. A stronger base to generate the nucleophilic intermediate was tested, and sulfonamide **5aa** was detected in trace amounts (Table 1, entry 2).

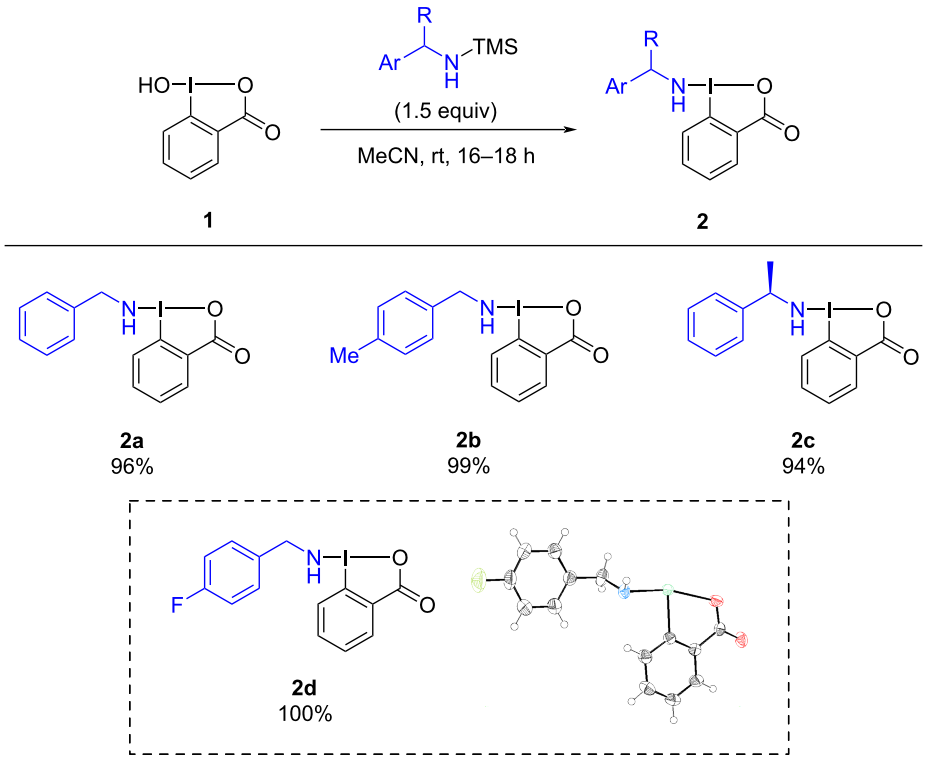

Scheme 2: Scope of the different (benzylamino)benziodoxolones (BBXs) **2** with ORTEP-3 diagram of compound **2d**, using 50% probability level ellipsoids. One co-crystallized water molecule was omitted for clarity. CCDC 2368436 contains the supporting crystallographic data for this paper.

Table 1: Optimization of the electrophilic amination of *tert*-butyl 3-(*p*-tolylsulfinyl)propanoate (**4a**) with BBX **2a** (0.23 mmol of limitant in 2 mL of solvent).

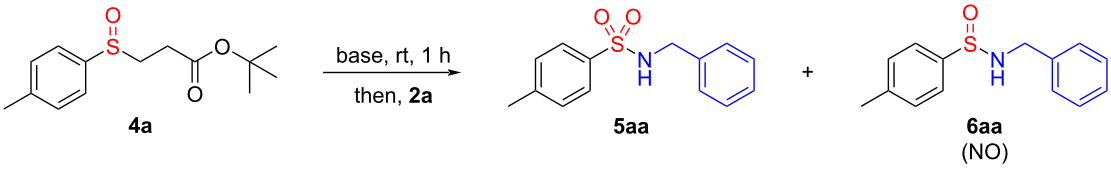

Entry	**4a** (equiv)	**2a** (equiv)	Base (equiv)	Solvent	*T* (°C)	Time (h)	**5aa** (yield %)[a]
1	1	1.5	K_2CO_3 1	DMF	50	3	NO
2	1	2	NaH 1	DMF	50	20	trace
3	1	2	NaH 1.2	PhMe	50	20	NO
4	1	2	NaH 1.2	DMF[b]	50	3	29
5	1	2	NaH 1.2	DMF[b]	rt	20	9
6	2	1	NaH 2.4	DMF[b]	50	6	38
7	**2**	**1**	**NaH 2.4**	**DMF[b]**	**50**	**20**	**52**
8	2	1	NaH 2.4	DMF[b]	50	72	48

[a]Isolated yields; [b]degassed solvent; rt – room temperature; NO – not observed.

Considering the low solubility of the hypervalent reagent **2a** in most organic solvents, an alternative solvent was tested; nevertheless, BBX **2a** showed to be insoluble when using toluene (Table 1, entry 3).

To have further insights on the formation of sulfonamide **5aa**, an experiment was conducted under the same stoichiometric conditions that yielded product **5aa** (Table 1, entry 2) but with prior degassed solvent (DMF), to prevent potential oxidation of the sulfenate to sulfinate anions. Indeed, the oxidation of the unstable sulfenate intermediates has been previously reported by Waser when using EBX – an HIR applied in the transfer of alkynes to sulfenate salts [34]. Under these conditions, *N*-benzyl-4-methylbenzenesulfinamide (**6aa**) was not observed, and *N*-benzyl-*p*-toluenesulfonamide (**5aa**) was isolated in 29% yield (Table 1, entry 4).

To prevent the regeneration of *tert*-butyl 3-(*p*-tolylsulfinyl)propanoate (**4a**) and employ milder conditions, a study was conducted at room temperature for 20 hours, which resulted in a reduction of the yield for **5aa** to 9% (Table 1, entry 5). This result might be due to the reactivity of this hypervalent iodine reagent. Indeed, we have previously observed that the transfer of the benzylamine moiety to carbon-based nucleophiles is more favorable at higher temperatures [4].

Due to the reversibility of the retro-Michael addition, an experiment was carried out using an excess of *tert*-butyl 3-(*p*-tolylsulfinyl)propanoate (**4a**) leading to an increase in the yield of the corresponding sulfonamide **5aa** by 38% (Table 1, entry 6). A longer reaction time was tested, with the reaction running overnight, which led to an increase of 52% in the reaction yield (Table 1, entry 7), consisting of the best conditions achieved for this electrophilic amination. The reaction time was extended to 72 hours in an attempt to promote the transfer reaction; however, the corresponding sulfonamide **5aa** was obtained in 48% yield (Table 1, entry 8), thus proving that beyond 20 hours, the reaction does not develop any further.

The experiment carried out with degassed solvent (Table 1, entry 4) eliminated the hypothesis of sulfonamide **5aa** formation via oxidation of sulfinamide **6aa** by dissolved oxygen molecules in the media. Therefore, an additional experiment was conducted using sodium benzenesulfinate to simulate the potential in situ oxidation of the sulfenate anion before the addition of BBX **2a**, but only trace amounts of sulfonamide **5ea** were observed.

A deeper analysis of the composition of the crude mixture revealed the presence of sulfide **3a** and disulfide **7a**, which formation might probably result from an oxidative reaction involv-

ing species generated from 2 sulfenate molecules. A further experiment was carried out in the absence of light. Under these conditions, no amine-transfer products **5aa** (sulfonamide) or **6aa** (sulfinamide) were observed.

Next, and with the optimized conditions in hand (Table 1, entry 7), we studied the scope of the reaction by varying both the β-sulfinyl esters **4** and the electrophilic amines **2**. Thus, a variety of functionalized thiols (aromatic, aliphatic, and heterocyclic) were chosen to produce the β-sulfinyl esters **4** (Scheme 3).

We next investigated the electrophilic amination reaction (Scheme 4). First, different functionalized β-sulfinyl esters were reacted with BBX **2a**. For the aromatic and pyridine moieties, the electrophilic amination reaction afforded sulfonamides **5aa**, **5ba**, **5da**, and **5ea** with moderate yields. However, no amination product was detected with *tert*-butyl 3-(benzylsulfinyl)propanoate (**4c**). This result suggests that aliphatic β-sulfinyl esters may not possess sufficient nucleophilicity to react with the primary amine-containing HIRs, or it might be due to the inability of the benzyl moiety to stabilize the sulfenate ion during the reaction.

For *tert*-butyl 3-(*p*-tolylsulfinyl)propanoate (**4a**), and similarly to the outcome obtained for BBX **2a**, sulfonamides **5ab** and **5ac** were obtained with moderate yields. The slight decrease observed for **5ac**, with chiral (*R*)-1-((1-phenylethyl)amino)-1,2-benziodoxol-3-(1*H*)-one (**2c**), can be attributed to potential steric hindrance induced by the methyl group attached to the benzylic carbon, which may hinder the nucleophile's access to the electrophilic center of the HIR.

The new hypervalent reagent 1-(4-fluorobenzyl)amino-1,2-benziodoxol-3-(1*H*)-one (**2d**) was also tested in the amination reaction, leading to the formation of sulfonamides **5ad**, **5dd**, and **5ed** (25%, 28%, and trace amount, respectively). In the last example, the low amount of sulfonamide **5ed** obtained may result from the simultaneous formation of sulfinamide **6ea** also isolated in this reaction for the first time (both in trace amounts).

Reaction mechanism

The inability to detect sulfinamide **6** and the isolation of sulfonamide **5**, along with other byproducts (**3**, **4**, and **7**), stimulated us to propose a plausible reaction mechanism that would support both the obtained yields and the formation of unexpected species.

As mentioned above, the presence of light influences the reaction outcome. When the reaction was carried out in the absence of light, only **4a**, **3a**, and **7a** were isolated (under these conditions, there was a high decrease in the isolated amount of **3a**, compared to the same experiment carried out in the presence of

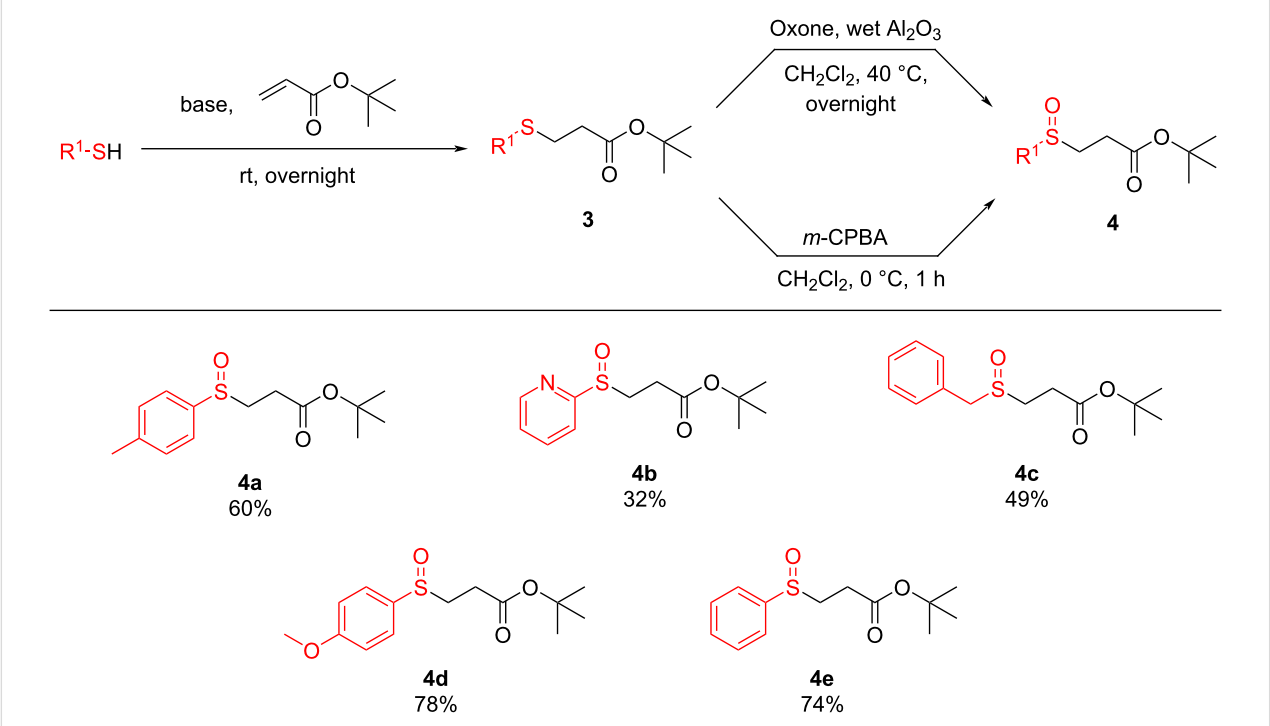

Scheme 3: Scope of the different β-sulfinyl esters **4** [32,33]. Isolated yields. rt – room temperature.

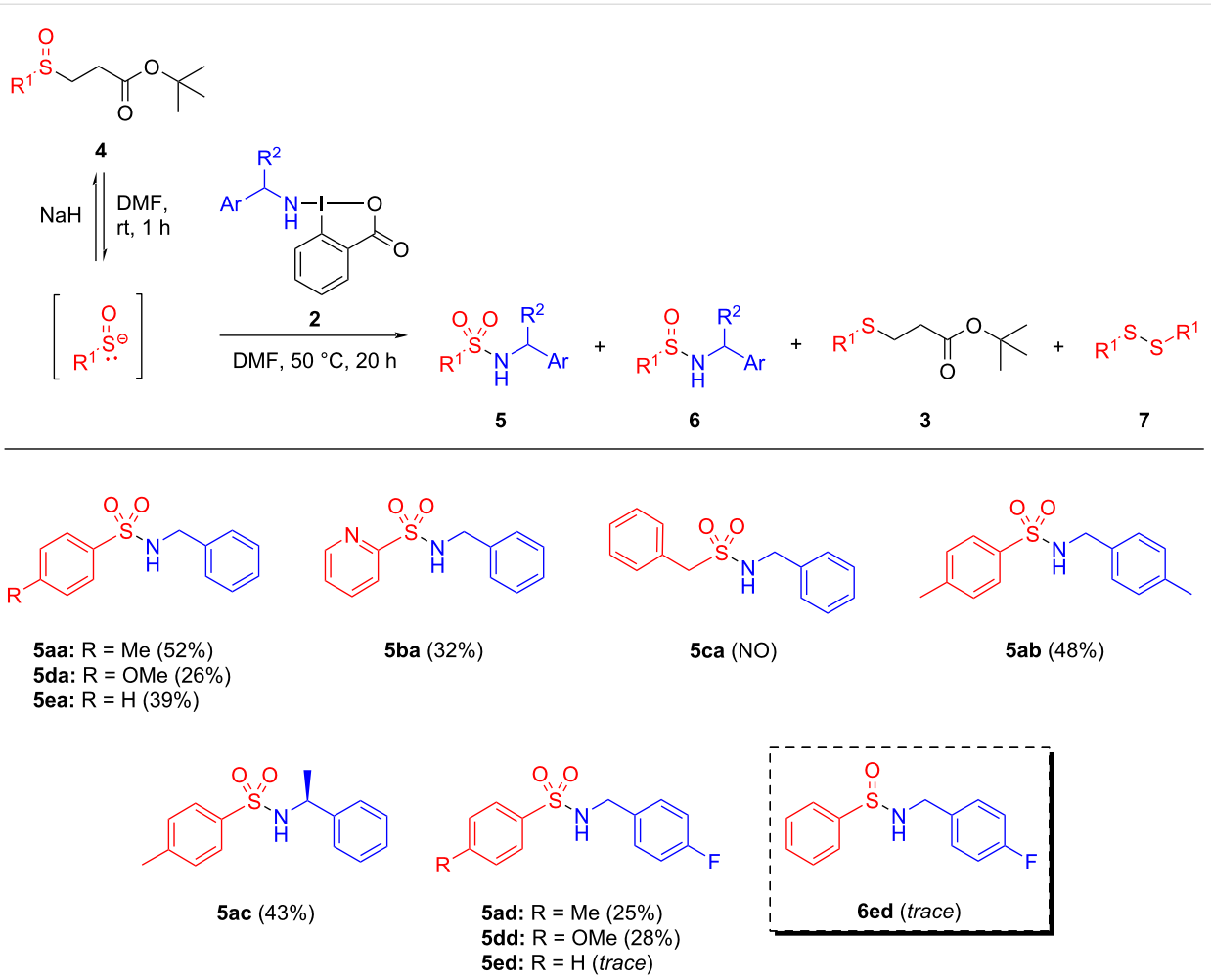

Scheme 4: Scope of the primary amine electrophilic reaction of sulfenate salts. Reaction conditions: **4** (2 equiv), NaH (2.4 equiv), **2**, degassed DMF (0.055 M). Isolated yields. rt – room temperature; NO – not observed.

light, from 20% to 2% yield). Considering the potential occurrence of a radical pathway, additional experiments were conducted in the presence of galvinoxyl and TEMPO, powerful radical scavengers capable of abstracting the radical species that could emerge in the reaction media. The use of galvinoxyl proved to be insufficient to conclude since a control experiment showed that HIRs **2** decompose in the presence of galvinoxyl. When using TEMPO (Scheme 5), sulfinamide **6aa** was not detected, but a drastic decrease in the yield of sulfonamide **5aa** was observed, suggesting that the benzylamine-transfer reaction might occur via a radical mechanism. This finding supports the hypothesis that, beyond the ionic mechanism previously

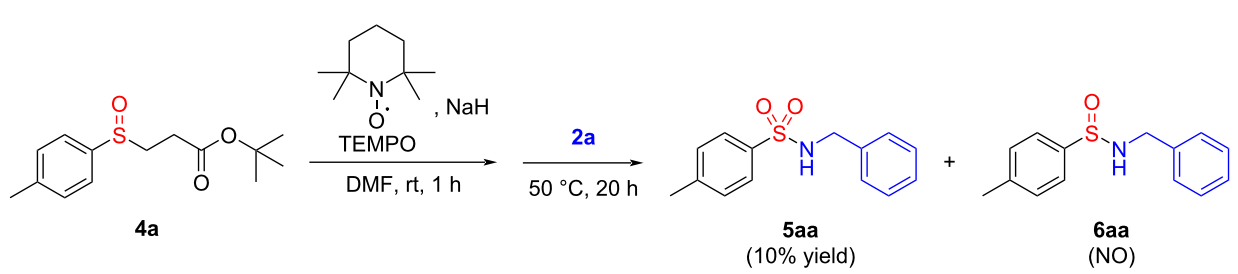

Scheme 5: Electrophilic amination reaction in the presence of TEMPO. Reaction conditions: **4a** (2 equiv), NaH (2.4 equiv), **2a**, TEMPO (10 mol %), degassed DMF (0.055 M). NO – not observed.

explored for our electrophilic primary amine transfer reagent [4], HIR **2a** might also be engaged in a radical mechanism contingent upon the medium or the species present.

Analysis of data from optimization and scope experiments provided valuable insights into the reaction, leading to a plausible mechanistic proposal (Scheme 6). This suggestion is based on the recognized ionic character of the sulfenate ion generated in the retro-Michael addition, on the results obtained with TEMPO (Scheme 5), and also on the results obtained when the reaction was carried out in the absence and presence of light, as well as the control experiments in the absence of BBX (see Supporting Information File 1).

We propose a mechanism pathway involving the retro-Michael addition of **4**, releasing acrylate and hydrogen (H_2). The charge

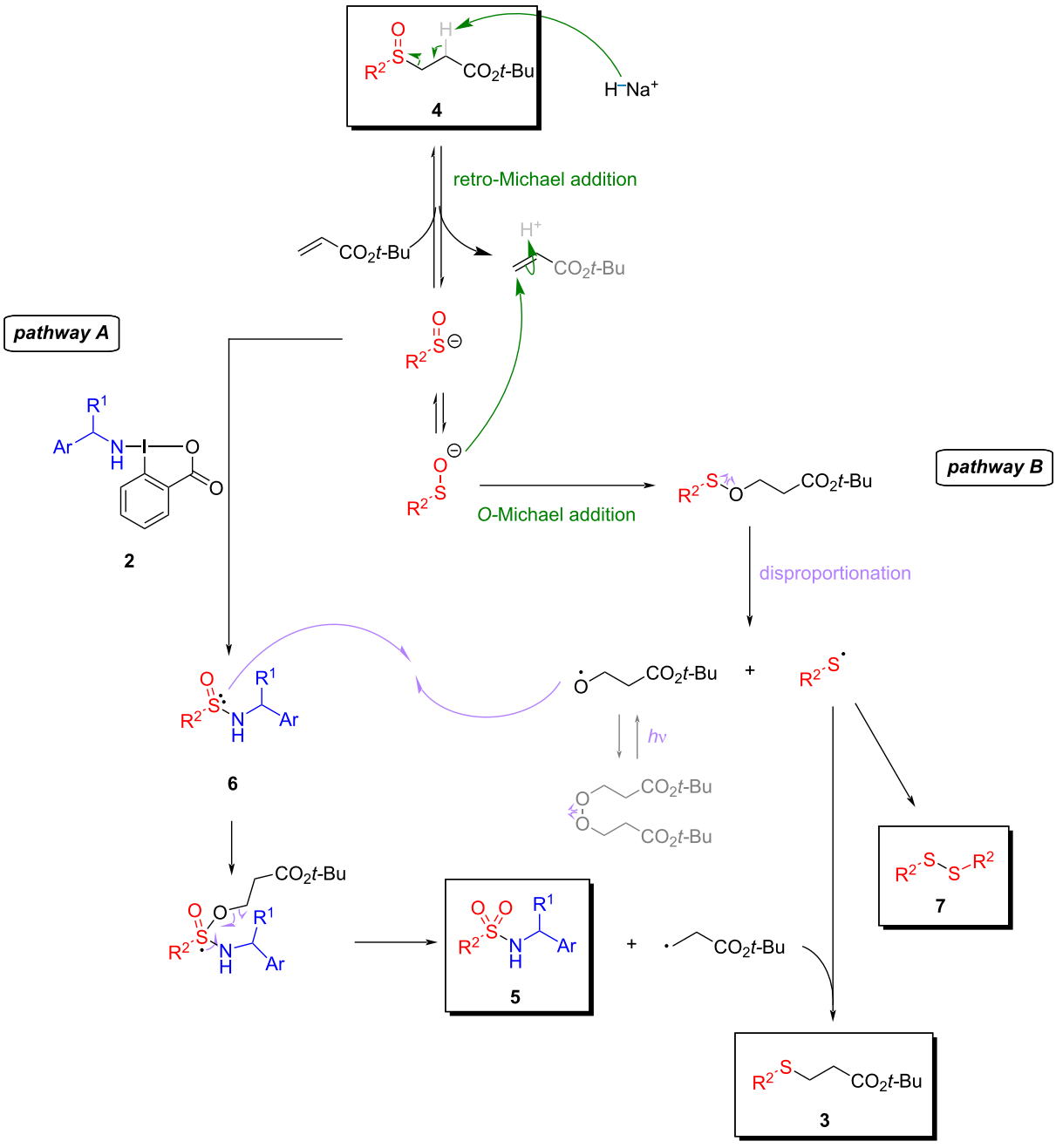

Scheme 6: Mechanism proposed for sulfonamide **5**, β-sulfinyl ester **4**, disulfide **7**, and sulfide **3** formations. The ionic steps are illustrated in green, whereas the radical steps appear in purple [35].

of the sulfenate anion may shift between sulfur and oxygen atoms, possibly leading to an *O*-Michael addition (pathway B) [35]. The intermediate of these reactions could undergo disproportionation, a radical process resulting in the homolytic cleavage of the S–O bond [35]. The formation of disulfide **7** isolated in the experiments can be explained by combining two radical sulfur species. Furthermore, the oxygen species generated in this radical reaction may dimerize to yield peroxide. However, the instability of peroxide favors the predominance of radical oxygen species, which can react with the sulfur atom from sulfinamide **6** previously formed in the reaction medium (pathway A). Following the establishment of the new S–O bond, a radical reaction akin to retro-Michael is expected, yielding sulfonamide **5** and a *C*-radical derivative from acrylate. This derivative may then combine with sulfur radical molecules to produce sulfide **3**, the final byproduct of this reaction.

Conclusion

As mentioned above, HIRs have emerged as alternative reagents for conducting various transformations. The umpolung reactivity provided by these iodine reagents enables chemical transformations that would typically demand less environmentally friendly conditions. The investigations conducted in this work confirmed the ability of the novel hypervalent iodine(III) reagents **2** to transfer their amine moieties to various β-sulfinyl esters via an umpolung mechanism, generating the corresponding sulfonamides.

Supporting Information

Supporting Information File 1

Experimental procedures, characterization data, NMR spectra, and X-ray diffraction data.
[https://www.beilstein-journals.org/bjoc/content/supplementary/1860-5397-20-272-S1.pdf]

Funding

The authors thank the Fundação para a Ciência e Tecnologia (FCT, project 2022.04623.PTDC, fellowship 2022.11629.BD (J.C.). The authors also thank the support by the Associate Laboratory for Green Chemistry – LAQV which is financed by national funds from FCT/MCTES (UIDB/50006/2020 DOI 10.54499/UIDB/50006/2020, UIDP/50006/2020 DOI 10.54499/UIDP/50006/2020, and LA/P/0008/2020 DOI 10.54499/LA/P/0008/2020). FCT/MCTES is also acknowledged for supporting the National NMR Facility (ROTEIRO/0031/2013 − PINFRA/22161/2016, cofinanced by FEDER through COMPETE 2020, POCI, and PORL and FCT through PIDDAC), and RECI/BBB-BEP/0124/2012 (X-ray Infrastructure), which was cofinanced by the ERDF under the PT2020 Partnership Agreement (POCI-01-0145-FEDER - 007265).

Author Contributions

Beatriz Dedeiras: formal analysis; investigation; validation; writing – original draft. Catarina S. Caldeira: formal analysis; investigation. José C. Cunha: formal analysis; investigation; validation; writing – original draft. Clara S. B. Gomes: formal analysis. M. Manuel B. Marques: conceptualization; funding acquisition; investigation; methodology; project administration; supervision; writing – original draft; writing – review & editing.

ORCID® iDs

Beatriz Dedeiras - https://orcid.org/0009-0006-2527-101X
José C. Cunha - https://orcid.org/0000-0002-6957-0330
Clara S. B. Gomes - https://orcid.org/0000-0003-3672-0045
M. Manuel B. Marques - https://orcid.org/0000-0002-6712-752X

Data Availability Statement

All data that supports the findings of this study is available in the published article and/or the supporting information to this article.

References

1. Kiyokawa, K.; Minakata, S. *Synlett* **2020,** *31,* 845–855. doi:10.1055/s-0039-1690827
2. Yoshimura, A.; Zhdankin, V. V. *Chem. Rev.* **2016,** *116,* 3328–3435. doi:10.1021/acs.chemrev.5b00547
3. Li, Y.; Hari, D. P.; Vita, M. V.; Waser, J. *Angew. Chem., Int. Ed.* **2016,** *55,* 4436–4454. doi:10.1002/anie.201509073
4. Poeira, D. L.; Negrão, A. C. R.; Faustino, H.; Coelho, J. A. S.; Gomes, C. S. B.; Gois, P. M. P.; Marques, M. M. B. *Org. Lett.* **2022,** *24,* 776–781. doi:10.1021/acs.orglett.1c04312
5. Makitalo, C. L.; Yoshimura, A.; Rohde, G. T.; Mironova, I. A.; Yusubova, R. Y.; Yusubov, M. S.; Zhdankin, V. V.; Saito, A. *Eur. J. Org. Chem.* **2020,** 6433–6439. doi:10.1002/ejoc.202000961
6. Ishihara, K.; Muñiz, K., Eds. *Iodine Catalysis in Organic Synthesis;* Wiley-VCH: Weinheim, Germany, 2022.
7. Olofsson, B.; Marek, I.; Rappoport, Z. *Patai's Chemistry of Functional Groups: The Chemistry of Hypervalent Halogen Compounds;* Wiley-VCH: Weinheim, Germany, 2019.
8. Wirth, T. *Hypervalent Iodine Chemistry: Modern Developments in Organic Synthesis;* Springer International Publishing: Cham, Switzerland, 2016.
9. Sajith, P. K.; Suresh, C. H. *Inorg. Chem.* **2013,** *52,* 6046–6054. doi:10.1021/ic400399v
10. Hari, D. P.; Caramenti, P.; Waser, J. *Acc. Chem. Res.* **2018,** *51,* 3212–3225. doi:10.1021/acs.accounts.8b00468
11. Kiprof, P. *ARKIVOC* **2005,** No. 4, 19–25. doi:10.3998/ark.5550190.0006.403
12. Macara, J.; Caldeira, C.; Poeira, D. L.; Marques, M. M. B. *Eur. J. Org. Chem.* **2023,** *26,* e202300109. doi:10.1002/ejoc.202300109
13. Zhdankin, V. V.; Kuehl, C. J.; Bolz, J. T.; Formaneck, M. S.; Simonsen, A. J. *Tetrahedron Lett.* **1994,** *35,* 7323–7326. doi:10.1016/0040-4039(94)85304-5

14. Zhdankin, V. V.; McSherry, M.; Mismash, B.; Bolz, J. T.; Woodward, J. K.; Arbit, R. M.; Erickson, S. *Tetrahedron Lett.* **1997,** *38,* 21–24. doi:10.1016/s0040-4039(96)02245-9
15. Zhang, Y.; Lu, J.; Lan, T.; Cheng, S.; Liu, W.; Chen, C. *Eur. J. Org. Chem.* **2021,** 436–442. doi:10.1002/ejoc.202001373
16. Kiyokawa, K.; Kosaka, T.; Kojima, T.; Minakata, S. *Angew. Chem., Int. Ed.* **2015,** *54,* 13719–13723. doi:10.1002/anie.201506805
17. Okumatsu, D.; Kawanaka, K.; Kainuma, S.; Kiyokawa, K.; Minakata, S. *Chem. – Eur. J.* **2023,** *29,* e202203722. doi:10.1002/chem.202203722
18. Wang, H.; Zhang, D.; Sheng, H.; Bolm, C. *J. Org. Chem.* **2017,** *82,* 11854–11858. doi:10.1021/acs.joc.7b01535
19. Lan, T.; Qin, H.; Chen, W.; Liu, W.; Chen, C. *Chin. Chem. Lett.* **2020,** *31,* 357–360. doi:10.1016/j.cclet.2019.07.031
20. Kiyokawa, K.; Kawanaka, K.; Minakata, S. *Angew. Chem., Int. Ed.* **2024,** *63,* e202319048. doi:10.1002/anie.202319048
21. Zhdankin, V. V.; Kuehl, C. J.; Krasutsky, A. P.; Formaneck, M. S.; Bolz, J. T. *Tetrahedron Lett.* **1994,** *35,* 9677–9680. doi:10.1016/0040-4039(94)88357-2
22. Poeira, D. L.; Macara, J.; Faustino, H.; Coelho, J. A. S.; Gois, P. M. P.; Marques, M. M. B. *Eur. J. Org. Chem.* **2019,** 2695–2701. doi:10.1002/ejoc.201900259
23. Macara, J.; Caldeira, C.; Cunha, J.; Coelho, J. A. S.; Silva, M. J. S. A.; Krämer, K.; Grathwol, C. W.; Bräse, S.; Marques, M. M. B. *Org. Biomol. Chem.* **2023,** *21,* 2118–2126. doi:10.1039/d2ob02160a
24. Drews, J. *Science* **2000,** *287,* 1960–1964. doi:10.1126/science.287.5460.1960
25. Mondal, S.; Malakar, S. *Tetrahedron* **2020,** *76,* 131662. doi:10.1016/j.tet.2020.131662
26. Ovung, A.; Bhattacharyya, J. *Biophys. Rev.* **2021,** *13,* 259–272. doi:10.1007/s12551-021-00795-9
27. Wan, Y.; Fang, G.; Chen, H.; Deng, X.; Tang, Z. *Eur. J. Med. Chem.* **2021,** *226,* 113837. doi:10.1016/j.ejmech.2021.113837
28. De Luca, L.; Giacomelli, G. *J. Org. Chem.* **2008,** *73,* 3967–3969. doi:10.1021/jo800424g
29. Wright, S. W.; Hallstrom, K. N. *J. Org. Chem.* **2006,** *71,* 1080–1084. doi:10.1021/jo052164+
30. Bahrami, K.; Khodaei, M. M.; Soheilizad, M. *J. Org. Chem.* **2009,** *74,* 9287–9291. doi:10.1021/jo901924m
31. Groom, C. R.; Bruno, I. J.; Lightfoot, M. P.; Ward, S. C. *Acta Crystallogr., Sect. B: Struct. Sci., Cryst. Eng. Mater.* **2016,** *72,* 171–179. doi:10.1107/s2052520616003954
32. Maitro, G.; Prestat, G.; Madec, D.; Poli, G. *J. Org. Chem.* **2006,** *71,* 7449–7454. doi:10.1021/jo061359u
33. Wang, L.; Chen, M.; Zhang, P.; Li, W.; Zhang, J. *J. Am. Chem. Soc.* **2018,** *140,* 3467–3473. doi:10.1021/jacs.8b00178
34. Amos, S. G. E.; Nicolai, S.; Gagnebin, A.; Le Vaillant, F.; Waser, J. *J. Org. Chem.* **2019,** *84,* 3687–3701. doi:10.1021/acs.joc.9b00050
35. Zhang, Q.; Feng, H.; Chen, F.; He, Z.; Zeng, Q. *J. Org. Chem.* **2021,** *86,* 7806–7812. doi:10.1021/acs.joc.1c00615

License and Terms

BEILSTEIN JOURNAL OF ORGANIC CHEMISTRY

Electrochemical synthesis of cyclic biaryl λ^3-bromanes from 2,2'-dibromobiphenyls

Andrejs Savkins[1,2] and Igors Sokolovs[*1]

Letter

Open Access

Address:
[1]Latvian Institute of Organic Synthesis, Aizkraukles 21, 1006 Riga, Latvia and [2]Faculty of Medicine and Life Sciences, University of Latvia, Jelgavas 1, 1004 Riga, Latvia

Email:
Igors Sokolovs[*] - igorss@osi.lv

* Corresponding author

Keywords:
anodic oxidation; cyclic biaryl λ^3-bromane; cyclic voltammetry; electrochemistry; hypervalent bromine

Beilstein J. Org. Chem. **2025,** *21,* 451–457.
https://doi.org/10.3762/bjoc.21.32

Received: 21 November 2024
Accepted: 12 February 2025
Published: 27 February 2025

This article is part of the thematic issue "Hypervalent halogen chemistry".

Guest Editor: J. Wencel-Delord

Abstract

The remarkable nucleofugality of bromoarenes in diarylbromonium species renders them particularly suitable for the generation of arynes for subsequent use in a wide range of synthetic applications. The common approach to generate cyclic biaryl λ^3-bromanes is based on thermal decomposition of hazardous diazonium salts. Herein, we disclose a mild and straightforward approach to diarylbromonium species by direct anodic oxidation of 2,2'-dibromo-1,1'-biphenyl. The electrochemical method provides access to a range of symmetrically and non-symmetrically substituted cyclic biaryl λ^3-bromanes in moderate yields.

Introduction

Chemistry of hypervalent bromine(III) species has experienced rapid advancements during the recent years [1,2]. The remarkable nucleofugality of aryl bromides in hypervalent bromine(III) compounds has been exploited in the generation of arynes from cyclic diaryl λ^3-bromanes under remarkably mild conditions with subsequent applications of the in situ-generated arynes in cycloaddition reactions [3], *meta*-selective reactions with oxygen and nitrogen nucleophiles [4,5], regiodivergent *meta* or *ortho*-alkynylations [6], and regioselective (di)halogenation [7]. In addition, cyclic diaryl λ^3-bromanes have been successfully employed as halogen-bonding organocatalysts in Michael addition [8] and their chiral variants were efficient in catalyzing enantioselective Mannich reactions of ketimines with cyanomethyl coumarins [9] and malonic esters [10]. These notable examples underscore the remarkable potential of cyclic diaryl λ^3-bromanes in the development of efficient synthetic transformations.

Cyclic diaryl λ^3-bromanes **1** are typically synthesized using a method developed by Sandin and Hay in 1952 [11] that relies on the excellent nucleofugality of molecular nitrogen in diazonium compounds. Accordingly, pre-formed [12] or in situ-generated 2,2'-bromodiazonium salts **2** [11,13,14] furnish cyclic bromine(III) species **1** under thermal decomposition

conditions (Scheme 1, reaction 1). The diazonium intermediates **2** are obtained by diazotation of 2'-bromo-[1,1'-biphenyl]-2-amines **3** with sodium nitrite and an acid under aqueous conditions. Recently, Wencel-Delord and co-workers disclosed an improved protocol toward diazonium intermediates **2** under non-aqueous conditions (*t*-BuONO and MsOH in acetonitrile) [4]. Nevertheless, the improved method still required thermal decomposition of the diazonium salt to effect the cyclization. In the quest for mild (room temperature) and scalable conditions toward cyclic diaryl λ^3-bromanes **1** we realized that bromanyl units possess leaving group abilities comparable to the diazonium moiety [1,15]. Hence, the oxidation of 2,2'-dibromo-[1,1'-biphenyl] into mono-λ^3-bromane **5** would set the stage for the key cyclization event (Scheme 1, reaction 2). We also reasoned that an anodic oxidation of the aryl bromide is perfectly suited for the generation of mono-λ^3-bromane **5** under mild conditions [16-18]. This approach would conceptually differ from previously reported anodic syntheses of cyclic diaryl iodonium compounds, where an electrochemically generated acyclic iodine(III) intermediate undergoes an intramolecular S_EAr-type reaction to form the cyclic product [19,20]. Herein, we report on the development of an electrochemical synthesis of cyclic diaryl λ^3-bromanes under anodic oxidation conditions.

Results and Discussion

Symmetric 2,2'-dibromo-1,1'-biphenyl **4a** possessing ethoxycarbonyl groups *ortho* to the bromine was chosen as a model compound for our study. We anticipated that the presence of the ester moiety would help to stabilize the key λ^3-bromane(III) intermediate **5**, as demonstrated in the work of Miyamoto et al. [21], thus facilitating its formation in anodic oxidation. The anodic oxidation of **4a** under previously published conditions for the synthesis of Br(III) species [16,18] (GC as working electrode, Pt foil as counter electrode, 0.1 M tetrabutylammonium tetrafluoroborate (TBA-BF_4) in HFIP electrolyte and 2 F passed charge at a current density of 10 mA·cm^{-2}) afforded the desired Br(III) product **1a** in poor 14% NMR yield (Table 1, entry 1). The cyclic diarylbromonium salt **1a** was isolated by extractive workup followed by reversed-phase chromatography and its structure was unambiguously confirmed by X-ray crystallography (Table 1, graphic). Gratifyingly, a two-fold increase in the yield was achieved by a slight reduction of the current density to j = 8 mA·cm^{-2} (entry 2 vs entry 1 in Table 1). A further increase in the yield of **1a** to 45% was possible by increasing the amount of passing charge (6.0 F; Table 1, entry 3). Tetraethylammonium tetrafluoroborate (TEA-BF_4) appeared to be somewhat superior as the electrolyte to TBA-BF_4 and tetramethylammonium tetrafluoroborate (TMA-BF_4) (entry 4 vs entries 3 and 5, Table 1). In all experiments with a passed charge of 6.0 F (Table 1, entries 3–5), nearly complete conversion of starting **4a** and moderate yield of the desired product **1a** was observed pointing at a possible degradation of either starting material or product. Linear sweep voltammetry (LVS) experiments (0.1 M TBA-BF_4 in HFIP on a Pt disk electrode) revealed that the reduction current increases almost 4 times upon the addition of 5 mM **1a** to the electrolyte (see Supporting Information File 1, Figure S1). At the same time, passing 6.0 F through a solution of **1a** in 50 mM TBA-BF_4/HFIP at j = 8 mA·cm^{-2} led to 60% λ^3-bromane **1a** degradation, suggesting that cationic **1a**, formed on the anode, decomposes on the cathode. To avoid the undesired cathodic decomposition of **1a**, the cathode and anode chambers were separated, and further experiments were performed in a divided cell. Gratifyingly, the change of the cell type allowed for more than a two-fold increase in the yield of product **1a** from 28% (entry 2, undivided cell, Table 1) to 60% (entry 6, divided cell). Interestingly, higher amounts of passed charge did not improve the

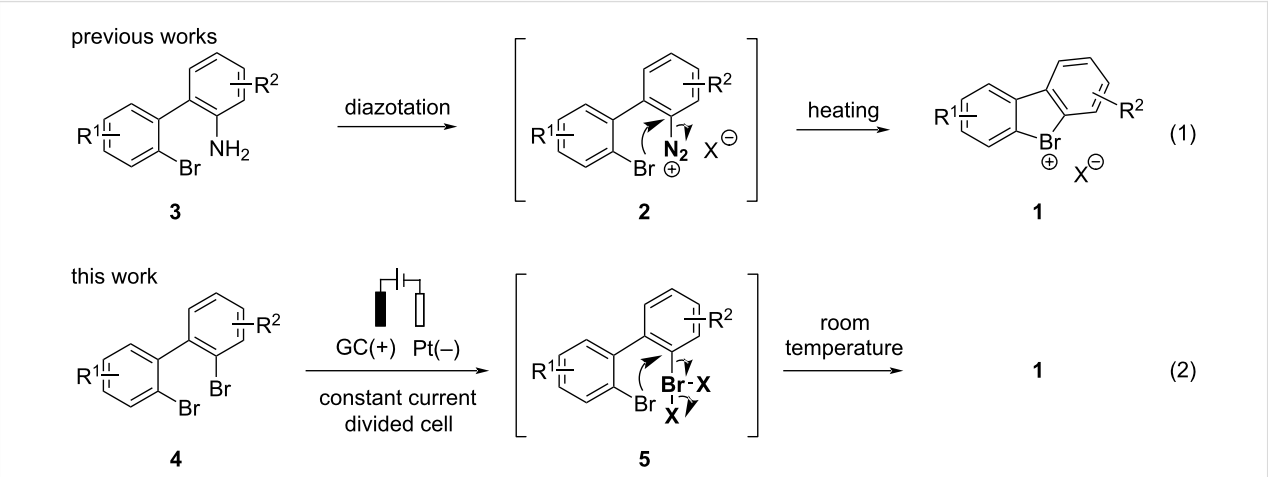

Scheme 1: Synthesis of cyclic diarylbromonium compounds.

Table 1: Optimization of electrochemical oxidation/cyclization conditions.[a]

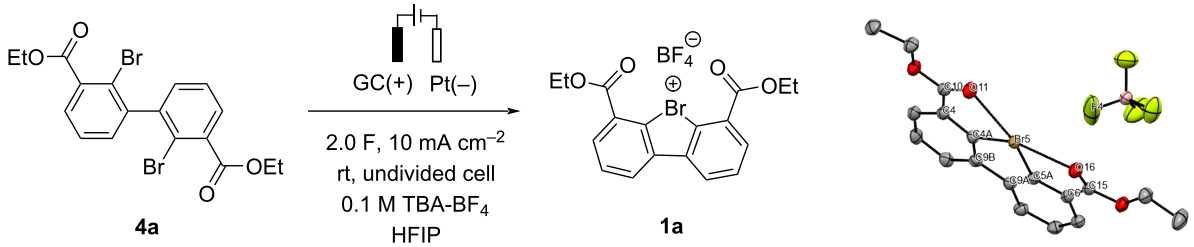

Entry	Deviation from starting conditions	**1a** [%]	**4a** [%]	Mass balance [%]
1	none	14	61	75
2	j = 8 mA cm^{-2}	28	49	77
3	j = 8 mA cm^{-2}, q/mol = 6.0 F	45	5	50
4	TEA-BF_4, j = 8 mA cm^{-2}, q/mol = 6.0 F	48	5	53
5	TMA -BF_4, j = 8 mA cm^{-2}, q/mol = 6.0 F	42	6	48
6	**divided cell, 0.25 M TEA-BF_4, j = 8 mA cm^{-2}**	**60**	**24**	**84**
7	divided cell, 0.25 M TEA-BF_4, j = 8 mA cm^{-2}, q/mol = 3.0 F	41	19	60
8	divided cell, RVC, 0.25 M TEA-BF_4, j = 8 mA cm^{-2}	62	0	62
9	divided cell, BDD, 0.25 M TEA-BF_4, j = 8 mA cm^{-2}	57	10	67
10	divided cell, 0.20 M TEA-BF_4, j = 8 mA cm^{-2}	15	55	70
11	divided cell, 0.30 M TEA-BF_4, j = 8 mA cm^{-2}	15	63	78
12	divided cell, 0.25 M TEA-ClO_4, j = 8 mA cm^{-2}	31	26	57
13	divided cell, 0.25 M TEA-PF_6, j = 8 mA cm^{-2}	46	19	65

[a]Reactions were performed on a 0.15 mmol scale. Yields and mass balance were determined by ^{1}H NMR in the crude reaction mixture using 1,2,3,4-tetrafluorobenzene as an internal standard. [b]Ellipsoids are shown at 50% probability, with hydrogen atoms omitted for clarity. Selected bond distances (Å) and angles (deg) for **1a**: Br5–O11, 2.657(2); Br5–O16, 2.647(2); Br5–C4A, 1.917(3); Br5–C5A, 1.915(2); Br5–F4, 3.081(5); C4A–Br5–C5A, 86.6(1); C4A–C9B–C9A-C5A, 1.0(3); C4A–C4–C10–O11, 0.1(4), and C5A–C6–C15–O16, 7.8(4).

reaction outcome (Table 1, entry 7). Neither successful was also a change of the anode material from GC to RVC or BDD (entries 8 and 9, Table 1), variation of electrolyte amount (entries 10 and 11) or altering of counter anions in the supporting electrolyte (entries 12 and 13; for complete optimization results, see Supporting Information File 1, Table S1).

With the optimized reaction conditions in hand, next, the substrate scope was evaluated (Scheme 2). Symmetrical biaryls with electron-deficient substituents such as Cl (**4b**) or CF_3 (**4c**) afforded the respective Br(III) products **1b**,**c** in slightly reduced yields as compared to that of **1a**. Gratifyingly, electron-rich MeO-substituted **1d** could be also obtained under the developed conditions. Unsymmetrically substituted **4e** and mono-substituted dibromides **4f**,**g** demonstrated reactivity similar to that of their symmetrical analogues **4b**,**c** with exception of the mono-MeO-substituted dibromide **4h**. Notably, the presence of two stabilizing ester moieties is critical for the synthesis of Br(III) species: the removal of one ester group (**4i**–**k**), or its replacement by NO_2 (**4l**) or SO_2t-Bu (**4m**) substituents in 2,2'-dibromo-1,1'-biphenyls resulted in starting material degradation with no formation of the desired product (for a complete list of substrates that do not form the desired electrochemical oxidation product see Supporting Information File 1, Scheme S1).

A series of control experiments was performed to rationalize the observed reactivity trends (Scheme 2). The measured redox potentials $E_{P/2}$ for 2,2'-dibromo-1,1'-biphenyls **4a**–**g** (from 1.77 V to 2.88 V) and unsuccessful substrates **4i**–**m**, **S9a**, **S9b** (from 1.73 V to 2.54 V) (Table S2 in Supporting Information File 1) span similar potential regimes suggesting that the success of the anodic oxidation likely depends on the structural rather than the electrochemical properties of the starting 2,2'-dibromo-1,1'-biphenyls **4a**–**m**. A closer inspection of the electrochemical behaviour of compound **4a** revealed an irreversible electron transfer at scan rates up to 1 V s^{-1} (Scheme 3A) indicating that one or more rapid chemical steps are following the electrochemical step [22,23]. Besides, the observed linear correlation between E_p of the redox event and the square root of the scan rate (Scheme 3B) suggested that compound **4a** is not significantly adsorbed on the electrode surface [23]. Comparison

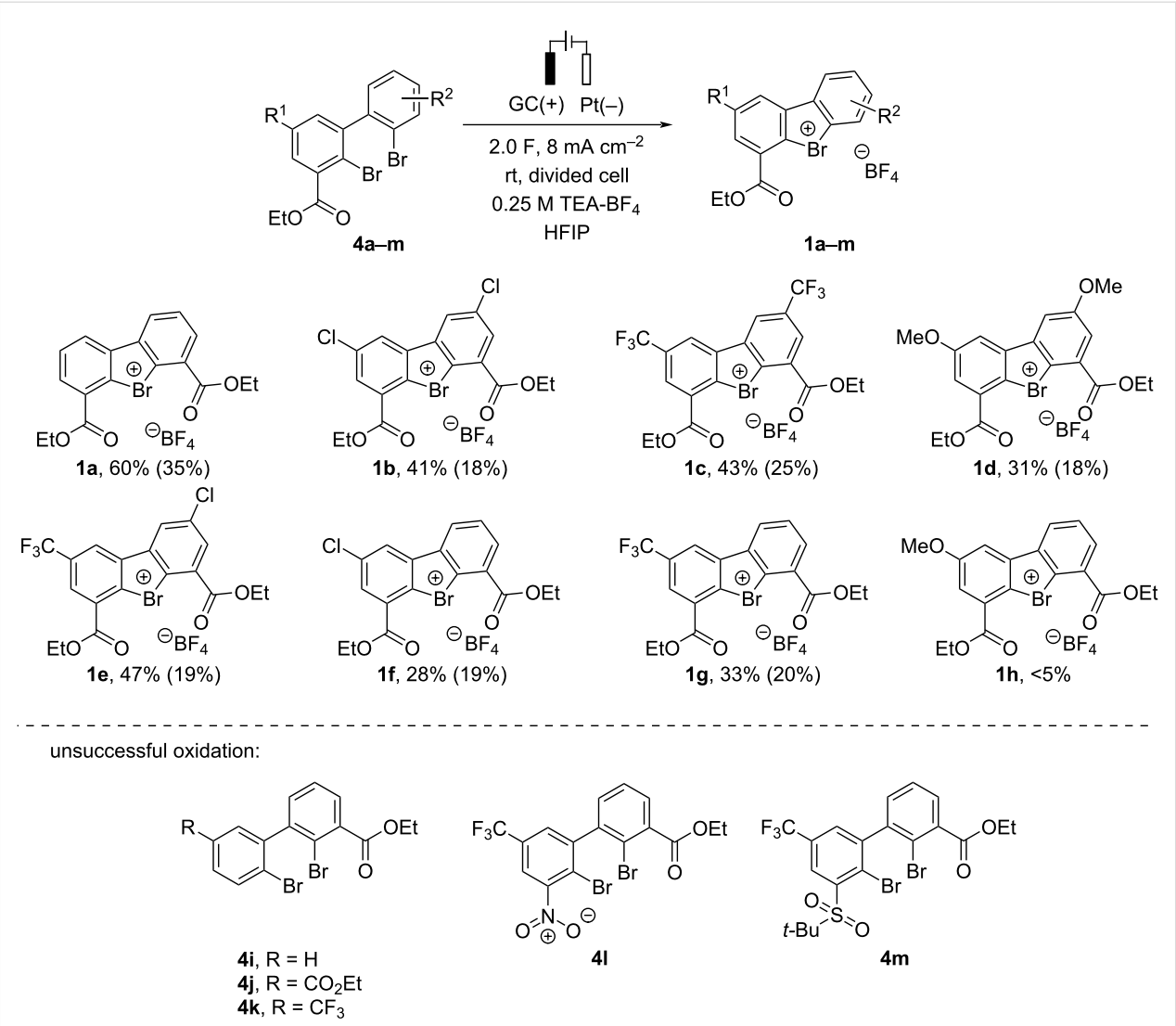

Scheme 2: Substrate scope. Reactions were performed on a 0.15 mmol scale. Yields were determined by ^{1}H NMR spectroscopy of the reaction mixture using 1,2,3,4-tetrafluorobenzene as an internal standard. Isolated yields are given in parentheses.

of the j_p vs $v^{0.5}$ slope with our previously obtained results for the anodic oxidation of aryl bromides **6a** (two-electron oxidation) and **6b** (one-electron oxidation) into the respective bromine(III) species (Scheme 3C) [17] demonstrated a more similar behaviour to **6b** suggesting that revealed oxidation is a single-electron-transfer process. It is important to note that this comparison assumes that the diffusion coefficients of **4a** and **6**, parameters that influence the j_p vs $v^{0.5}$ slope, are similar. On the other hand, anodic oxidation of **4a** under optimized conditions (entry 6, Table 1) using 1 F returned only 35% of **1a** (NMR yield), whereas passing 2 F charge delivered **1a** in 60% yield. The latter data provides an evidence that the overall oxidation of **4a** to **1a** likely is a two-electron process, suggesting that the second oxidation step may involve disproportionation of putative Br(II) species (see Scheme 3D).

Based on the control experiments described above we propose a plausible mechanism as shown in Scheme 3D. The reaction starts with a single-electron oxidation of **4a** on the electrode surface to form cation radical **A**, in which Br(II) is chelation-stabilized by the carboxyl group [21] and the neighbouring Br substituent [24]. Intermediate **A** rapidly undergoes irreversible chemical reaction by HFIP coordination to transient Br(II) followed by subsequent deprotonation to generate radical **B**. A following disproportionation of radical **B** would lead to the formation of Br(III) species **C** (anodic oxidation cannot be fully excluded), which undergoes intramolecular S_NAr-type substitution to form cyclic λ^3-bromane **1a** and hypobromite **D**. The latter decomposes into bromide and hexafluoroacetone, with the latter observed by ^{19}F NMR [25]. Assuming that intermediate **B** is sufficiently stable to leave the diffusion layer and undergoes

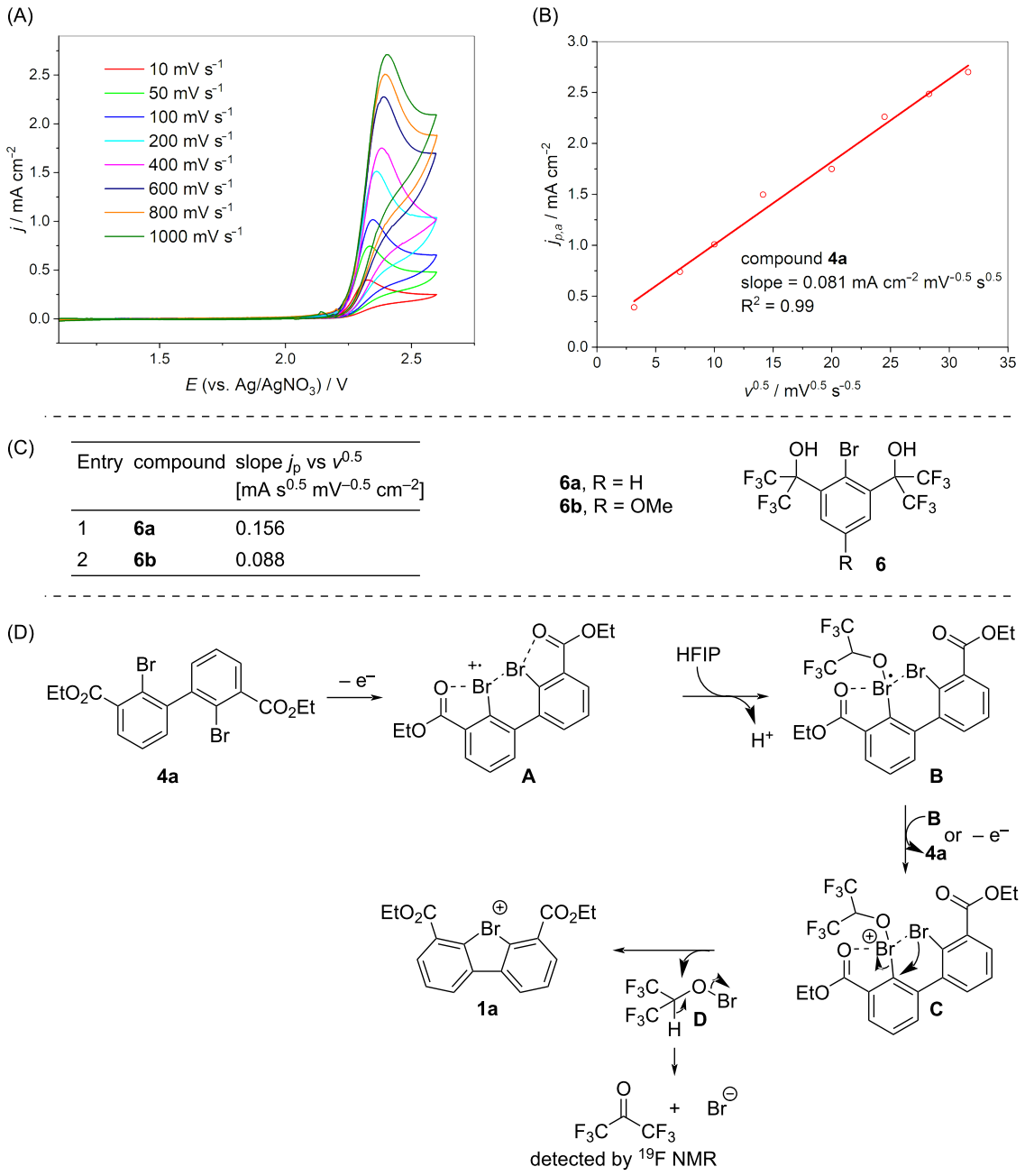

Scheme 3: A: Background and *iR* drop-corrected CVs of 5 mM **4a** at different scan rates (solvent: HFIP, working electrode: glassy carbon, supporting electrolyte: 0.1 M TBA-BF_4). B: Plot of the peak current densities (j_p) vs $v^{0.5}$. C: Representative j_p vs $v^{0.5}$ slope values for oxidation of Martin's bromane precursor **6** (ref. [17]). D: Plausible reaction mechanism.

disproportionation to the species **C** in the bulk electrolyte provides a reasonable explanation for why the reaction appears as a one-electron oxidation in CV experiments, but still as a two-electron oxidation in electrolysis.

Conclusion

In conclusion, we have demonstrated a conceptual approach to cyclic diaryl λ^3-bromanes by electrochemical oxidative cyclization of 2,2'-dibromo-1,1'-biphenyls. The developed method represents a safe and inexpensive alternative to the commonly used thermal decomposition of potentially explosive diazonium salts. The successful electrochemical oxidation requires the presence of two chelating ester groups that stabilize the formed Br(III) species. Further work towards improving the substrate scope and understanding the reaction mechanism are in progress in our laboratory.

Supporting Information

Crystallographic data for the structure reported in this paper have been deposited with the Cambridge Crystallographic Data Centre and allocated the deposition number CCDC 2404146.

Supporting Information File 1

Experimental procedures, analytical and spectroscopic data for new compounds, copies of NMR spectra, and X-ray crystallographic data.
[https://www.beilstein-journals.org/bjoc/content/supplementary/1860-5397-21-32-S1.pdf]

Acknowledgements

The authors thank Dr. Sergey Belyakov from the Latvian Institute of Organic Synthesis (LIOS) for X-ray crystallographic analysis. We also thank Prof. Edgars Suna (LIOS) for helpful discussions and assistance in preparing the manuscript.

Funding

This work was financially supported by Latvian Science Council grant LZP-2021/1-0595.

ORCID® iDs

Andrejs Savkins - https://orcid.org/0009-0008-0014-0843
Igors Sokolovs - https://orcid.org/0000-0002-5424-0451

Data Availability Statement

All data that supports the findings of this study is available in the published article and/or the supporting information of this article.

Preprint

A non-peer-reviewed version of this article has been previously published as a preprint: https://doi.org/10.3762/bxiv.2024.68.v1

References

1. Lanzi, M.; Wencel-Delord, J. *Chem. Sci.* **2024,** *15,* 1557–1569. doi:10.1039/d3sc05382b
2. Winterson, B.; Patra, T.; Wirth, T. *Synthesis* **2022,** *54,* 1261–1271. doi:10.1055/a-1675-8404
3. Lanzi, M.; Ali Abdine, R. A.; De Abreu, M.; Wencel-Delord, J. *Org. Lett.* **2021,** *23,* 9047–9052. doi:10.1021/acs.orglett.1c03278
4. Lanzi, M.; Dherbassy, Q.; Wencel-Delord, J. *Angew. Chem., Int. Ed.* **2021,** *60,* 14852–14857. doi:10.1002/anie.202103625
5. Wang, Y.; Tian, Y.-N.; Ren, S.; Zhu, R.; Huang, B.; Wen, Y.; Li, S. *Org. Chem. Front.* **2023,** *10,* 793–798. doi:10.1039/d2qo01406h
6. De Abreu, M.; Rogge, T.; Lanzi, M.; Saiegh, T. J.; Houk, K. N.; Wencel-Delord, J. *Angew. Chem., Int. Ed.* **2024,** *63,* e202319960. doi:10.1002/anie.202319960
7. Carter Martos, D.; de Abreu, M.; Hauk, P.; Fackler, P.; Wencel-Delord, J. *Chem. Sci.* **2024,** *15,* 6770–6776. doi:10.1039/d4sc01234h
8. Yoshida, Y.; Ishikawa, S.; Mino, T.; Sakamoto, M. *Chem. Commun.* **2021,** *57,* 2519–2522. doi:10.1039/d0cc07733j
9. Yoshida, Y.; Mino, T.; Sakamoto, M. *ACS Catal.* **2021,** *11,* 13028–13033. doi:10.1021/acscatal.1c04070
10. Yoshida, Y.; Ao, T.; Mino, T.; Sakamoto, M. *Molecules* **2023,** *28,* 384. doi:10.3390/molecules28010384
11. Sandin, R. B.; Hay, A. S. *J. Am. Chem. Soc.* **1952,** *74,* 274–275. doi:10.1021/ja01121a524
12. Heaney, H.; Lees, P. *Tetrahedron* **1968,** *24,* 3717–3723. doi:10.1016/s0040-4020(01)92003-4
13. Riedmüller, S.; Nachtsheim, B. J. *Beilstein J. Org. Chem.* **2013,** *9,* 1202–1209. doi:10.3762/bjoc.9.136
14. Huss, C. D.; Yoshimura, A.; Rohde, G. T.; Mironova, I. A.; Postnikov, P. S.; Yusubov, M. S.; Saito, A.; Zhdankin, V. V. *ACS Omega* **2024,** *9,* 2664–2673. doi:10.1021/acsomega.3c07512
15. Nakajima, M.; Miyamoto, K.; Hirano, K.; Uchiyama, M. *J. Am. Chem. Soc.* **2019,** *141,* 6499–6503. doi:10.1021/jacs.9b02436
16. Sokolovs, I.; Mohebbati, N.; Francke, R.; Suna, E. *Angew. Chem., Int. Ed.* **2021,** *60,* 15832–15837. doi:10.1002/anie.202104677
17. Mohebbati, N.; Sokolovs, I.; Woite, P.; Lõkov, M.; Parman, E.; Ugandi, M.; Leito, I.; Roemelt, M.; Suna, E.; Francke, R. *Chem. – Eur. J.* **2022,** *28,* e202200974. doi:10.1002/chem.202200974
18. Sokolovs, I.; Suna, E. *Org. Lett.* **2023,** *25,* 2047–2052. doi:10.1021/acs.orglett.3c00405
19. Scherkus, A.; Gudkova, A.; Čada, J.; Müller, B. H.; Bystron, T.; Francke, R. *J. Org. Chem.* **2024,** *89,* 14129–14134. doi:10.1021/acs.joc.4c01521
20. Elsherbini, M.; Moran, W. J. *Org. Biomol. Chem.* **2021,** *19,* 4706–4711. doi:10.1039/d1ob00457c
21. Miyamoto, K.; Saito, M.; Tsuji, S.; Takagi, T.; Shiro, M.; Uchiyama, M.; Ochiai, M. *J. Am. Chem. Soc.* **2021,** *143,* 9327–9331. doi:10.1021/jacs.1c04536
22. Heinze, J. *Angew. Chem., Int. Ed. Engl.* **1984,** *23,* 831–847. doi:10.1002/anie.198408313
23. Sandford, C.; Edwards, M. A.; Klunder, K. J.; Hickey, D. P.; Li, M.; Barman, K.; Sigman, M. S.; White, H. S.; Minteer, S. D. *Chem. Sci.* **2019,** *10,* 6404–6422. doi:10.1039/c9sc01545k
24. Frey, B. L.; Figgins, M. T.; Van Trieste, G. P., III; Carmieli, R.; Powers, D. C. *J. Am. Chem. Soc.* **2022,** *144,* 13913–13919. doi:10.1021/jacs.2c05562
25. Anderson, J. D. O.; DesMarteau, D. D. *J. Fluorine Chem.* **1996,** *77,* 147–152. doi:10.1016/0022-1139(96)03400-8

License and Terms

BEILSTEIN JOURNAL OF ORGANIC CHEMISTRY

Asymmetric synthesis of β-amino cyanoesters with contiguous tetrasubstituted carbon centers by halogen-bonding catalysis with chiral halonium salt

Yasushi Yoshida*[1,2], Maho Aono[2], Takashi Mino[2] and Masami Sakamoto[2]

Letter

Open Access

Address:
[1]Institute for Advanced Academic Research (IAAR), Chiba University, 1-33, Yayoi-cho, Inage-ku, Chiba 263-8522, Japan and [2]Molecular Chirality Research Center, Graduate School of Engineering, Chiba University, 1-33, Yayoi-cho, Inage-ku, Chiba-shi, Chiba 263-8522, Japan

Email:
Yasushi Yoshida* - yoshiday@chiba-u.jp

* Corresponding author

Keywords:
asymmetric catalysis; chiral halonium salt; contiguous stereocenters; halogen bonding; Mannich reaction

Beilstein J. Org. Chem. **2025,** *21,* 547–555.
https://doi.org/10.3762/bjoc.21.43

Received: 07 September 2024
Accepted: 26 February 2025
Published: 12 March 2025

This article is part of the thematic issue "Hypervalent halogen chemistry".

Guest Editor: J. Wencel-Delord

Abstract

β-Amino cyanoesters are important scaffolds because they can be transformed into useful chiral amines, amino acids, and amino alcohols. Halogen bonding, which can be formed between halogen atoms and electron-rich chemical species, is attractive because of its unique interaction in organic synthesis. Chiral halonium salts have been found to have strong halogen-bonding-donor abilities and work as powerful asymmetric catalysts. Recently, we have developed binaphthyl-based chiral halonium salts and applied them in several enantioselective reactions, which formed the corresponding products in high to excellent enantioselectivities. In this paper, the asymmetric synthesis of β-amino cyanoesters with contiguous tetrasubstituted carbon stereogenic centers by the Mannich reaction through chiral halonium salt catalysis is presented, which provided the corresponding products in excellent yields with up to 86% ee. To the best of our knowledge, the present paper is the first to report the asymmetric construction of β-amino cyanoesters with contiguous tetrasubstituted carbon stereogenic centers by the catalytic Mannich reaction.

Introduction

Halogen bonding (XB) has attracted intense research attention for its unique interaction between halogen atoms and electron-rich substituents [1]. XB has been applied to various fields of chemistry, such as organic chemistry [2-5], organocatalysis [6,7], metal catalysis [8,9], biochemistry [10,11], materials science [12,13], and supramolecular chemistry [14,15], although its successful application to asymmetric catalysis has been limited (Figure 1) [16-20]. In 2018, Arai and co-workers developed chiral amine **1** with an electron-deficient iodine atom, which catalyzed the Mannich reaction in excellent yields and enantioselectivities [17]. In 2020, Huber and co-workers reported the bis(iodoimidazolium) **2**-catalyzed Mukaiyama–aldol

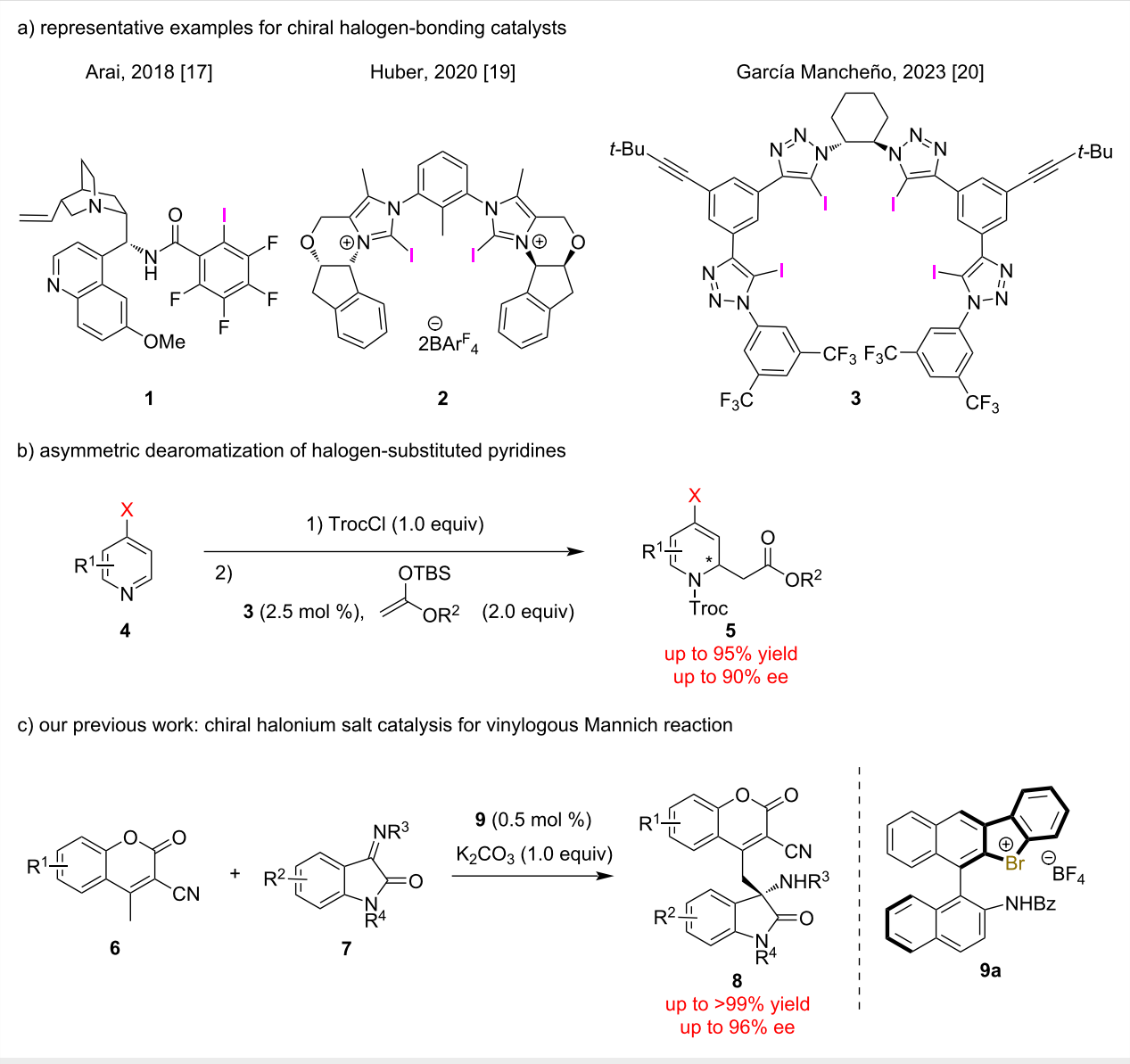

Figure 1: Selected examples and applications of chiral halogen-bonding catalysts.

reaction of carbonyl compounds with enol silyl ethers, which provided the products in high yields with up to 33% ee [19]. In 2023, García Mancheño and co-workers reported the tetrakis(iodotriazole) **3**-catalyzed dearomatization of halogen-substituted pyridines **4**, which formed the corresponding products **5** in high yields with up to 90% ee (Figure 1b) [20]. Hypervalent halogen compounds have been utilized as highly reactive substrates [21-27] and have recently been reported to work as halogen-bonding catalysts [28-31]. Previously, chiral halonium salts have been utilized in asymmetric catalysis [32-35], and we have developed chiral halonium salts and applied them to asymmetric reactions such as vinylogous Mannich reactions of cyanomethylcoumarins **6** with isatin-derived ketimines **7** [33,35] and 1,2-addition reaction of thiols to ketimine [34], which formed the corresponding products **8** in high yields with high to excellent enantioselectivities (Figure 1c). Despite these successful examples, the construction of only one stereocenter has been reported to date.

The Mannich reaction has great importance because of its utility in the preparation of useful chiral molecules such as amines [36], amino acids [37], and amino alcohols [38]. In this context, their asymmetric syntheses are important and have also been researched mainly using chiral catalysts [39,40]. Previously, the Mannich reaction has been applied in the construction of contiguous stereogenic centers (Figure 2). In 2005, Jørgensen and co-workers reported the enantio- and diastereoselective Mannich reaction of α-cyanoesters with aldimines catalyzed by

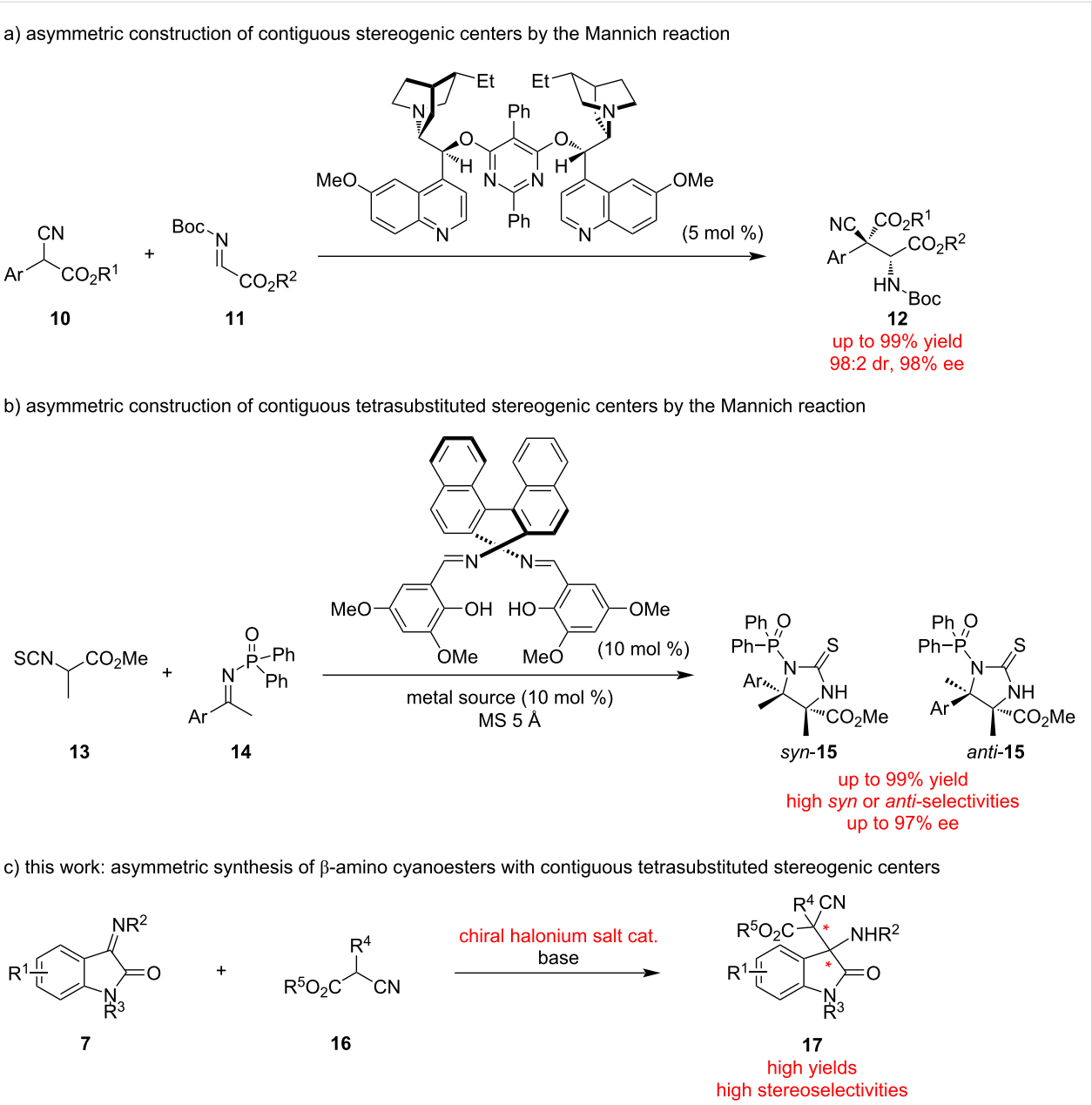

Figure 2: Selected examples for the construction of contiguous tetrasubstituted carbon centers via the Mannich reaction and this work.

chiral amines, which provided β-amino cyanoesters in excellent yield and diastereoselectivities with up to 98% ee (Figure 2a) [41]. The Mannich reaction has been also applied in the construction of contiguous tetrasubstituted carbon stereogenic centers [42-46]. In 2011, Shibasaki, Matsunaga and co-workers reported strontium or magnesium-catalyzed stereodivergent asymmetric Mannich reactions of an α-isothiocyanato ester with ketimines, which provided the products in excellent yields and diastereoselectivities with up to 97% ee (Figure 2b) [42]. To the best of our knowledge, the present paper is the first to report the asymmetric construction of β-amino cyanoesters with contiguous tetrasubstituted carbon stereogenic centers by the Mannich reaction, using our originally developed chiral halonium salt catalysis (Figure 2c).

Results and Discussion

Chiral halonium salts **9a–c** were prepared according to our previously reported methods [33]. The Mannich reaction of ketimine **7a** and cyanoester **16a** was selected as a benchmark, and catalyst screening was conducted (Scheme 1). The reaction was carried out with 1.0 equivalent of **7a** and 5.0 equivalents of **16a** in the presence of stoichiometric potassium carbonate and

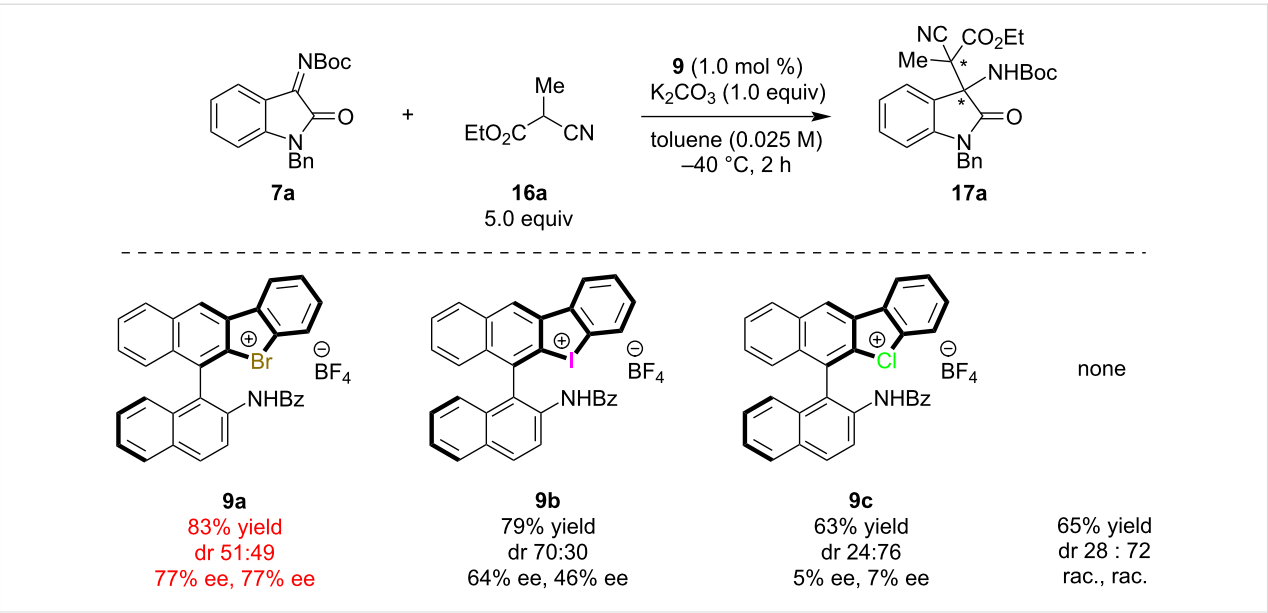

Scheme 1: Catalyst screening for the asymmetric Mannich reaction. All yields were determined by ^{1}H NMR spectroscopy using 1,3,5-trimethoxybenzene as an internal standard.

1.0 mol % of **9**. When bromonium salt **9a** was applied to the reaction, the desired product was obtained in 83% yield with 77% ee but almost no diastereoselectivity. The iodonium salt **9b** also worked well and the product was obtained in moderate diastereo- and enantioselectivity, however, chloronium salt **9c** did not show significant catalytic activity, and the product was formed in nearly the same yield as that obtained without a catalyst with low stereoselectivity. From these observations, bromonium salt **9a** was found to be optimal in enantioselectivity, and iodonium salt **9b** was superior in terms of diastereoselectivity. These results can be explained by the strength of halogen bonding: generally, iodo-substituted compounds form stronger halogen bonding with Lewis bases than chloro-substituted ones [1]. Notably, the reaction catalyzed by only 1 mol % of iodonium salt **9b** provided the opposite diastereomer of **17a** as the major product compared with that without a catalyst, which revealed the high catalytic activity of our catalyst. Further reaction conditions optimization was conducted using **9a** as a catalyst (Table 1). Solvent screening was carried out, and it was found to strongly affect the product's stereoselectivity. Nonpolar solvents yielded better results, and toluene was found to be optimal (Table 1, entries 1–6). Polar solvents such as acetonitrile prohibited halogen bonding between **9a** and the chiral halonium salt. Next, the reaction temperature was optimized, and −40 °C was found to be optimal (Table 1, entries 7–9). Further optimization of the reaction conditions (amounts of potassium carbonate and pre-nucleophile, catalyst loading, and concentration) were conducted, and the reaction with 5.0 equivalents of pre-nucleophile and 1.0 equivalent of potassium carbonate in the presence of 1.0 mol % of **9** at 0.025 M of toluene and −40 °C was found to be optimal (Table 1, entries 10–13). Five equivalents of pre-nucleophile are required to obtain higher yields and enantioselectivities.

Next, the optimization of the substituent on the 1-position of imines was conducted (Scheme 2). In most cases, the products were obtained in high yields with moderate to high enantioselectivities; the sterically less-hindered methyl-substituted substrate **7b** was found to be better than the other substrates. The bulky phenyl- or trityl-substituted **7c** and **7d** yielded products with decreased enantioselectivities, likely due to the inhibition of the interaction between the imines and the chiral catalyst by hydrogen and/or halogen bonding. From these observations, the substituent on the 1-position strongly affected the product's enantioselectivities. Therefore, catalyst screening was conducted again with **7b** as a substrate (Scheme 3). In this case, iodonium salt **9b** showed the best performance, and the product **17b** was formed in 98% yield with a 67 (85% ee):33 (58% ee) diastereomeric ratio. In order to demonstrate the importance of halogen bonding in the catalyst for the present reaction, chiral amide **9d** and tetrabutylammonium bromide (**9e**) were applied as catalysts. The results indicate that **9d** with only hydrogen bonding provided **17b** in a lower yield than without catalyst maybe due to the deactivation of base by acidic amide moiety and with almost no enantioselectivity. Although the addition of a catalytic amount of **9e** accelerated the reaction, the same diastereomer of **17b** as the major product was obtained as for the reaction without a catalyst, which shows the importance of halonium salt moieties in our catalysts. From these results, the substrate scope was conducted using **9b** as a catalyst.

Table 1: Optimization of reaction conditions.[a]

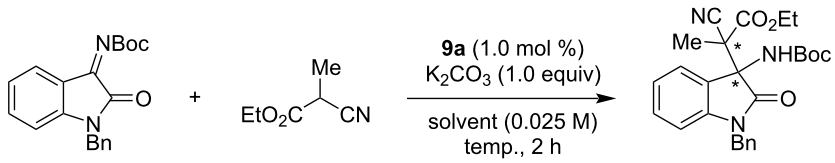

7a **16a** 5.0 equiv **17a**

Entry	Solvent	Temp. (°C)	Yield (%)[b]	dr (ee (%))
1	toluene	–40	83	51 (77% ee):49 (77% ee)
2	Et_2O	–40	76	57 (70% ee):43 (65% ee)
3	CH_2Cl_2	–40	76	58 (51% ee):42 (53% ee)
4	THF	–40	77	58 (32% ee):42 (40% ee)
5	$CHCl_3$	–40	68	60 (33% ee):40 (35% ee)
6	CH_3CN	–40	90	70 (6% ee):30 (14% ee)
7	toluene	0	84	25 (rac.):75 (rac.)
8	toluene	–20	90	52 (70% ee):48 (63% ee)
9[c]	toluene	–80	57	40 (70% ee):60 (75% ee)
10[d]	toluene	–40	87	51 (70% ee):49 (75% ee)
11[e]	toluene	–40	82	51 (73% ee):49 (74% ee)
12[f]	toluene	–40	68	54 (74% ee):46 (73% ee)
13[g]	toluene	–40	74	50 (63% ee):50 (72% ee)

[a]Reactions were conducted using **7a** (1.0 equiv), **16a** (5.0 equiv) and K_2CO_3 (1.0 equiv) at the appropriate solvent and temperature for 2 h. [b]Determined by ^{1}H NMR spectroscopy using 1,3,5-trimethoxybenzene as an internal standard. [c]Reaction conducted for 96 h. [d]With 10 mol % of K_2CO_3. [e]With 5 mol % of **9a**. [f]With 1.5 equivalents of **16a**. [g]Toluene (0.1 M).

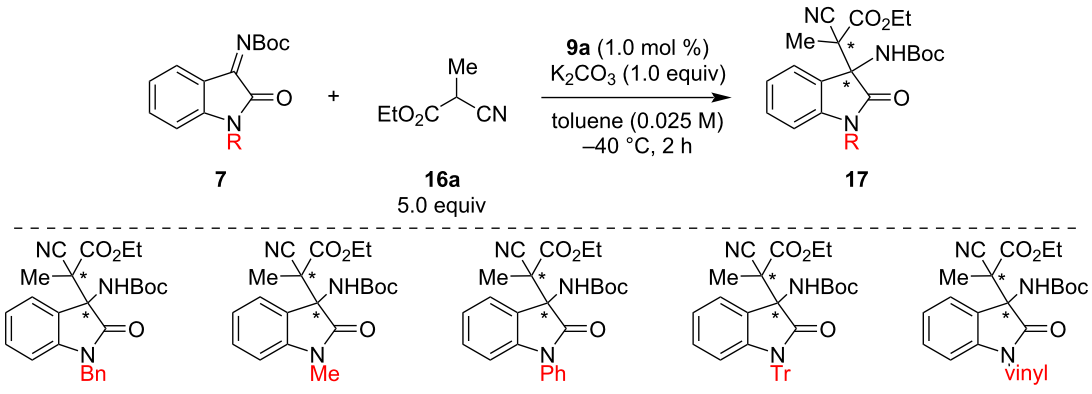

17a 83% yield dr 51:49 77% ee, 77% ee

17b 81% yield dr 59:41 82% ee, 72% ee

17c 85% yield dr 50:50 49% ee, 54% ee

17d[a] 46% yield dr 78:22 54% ee, 73% ee

17e 62% yield dr 44:56 71% ee, 79% ee

Scheme 2: *N*-Protecting group optimization for the asymmetric Mannich reaction. All yields were determined by ^{1}H NMR spectroscopy using 1,3,5-trimethoxybenzene as an internal standard. [a]Reaction conducted for 24 h.

First, the scope for the imines was carried out (Scheme 4). 5-Methyl-substituted **7f** provided the corresponding product **17f** in 87% yield and 65:35 diastereomeric ratio with 85% ee and 58% ee for each. 5-Chloro-substituted **7g** formed **17g** in good yield and diastereoselectivity with decreased enantioselectivity, likely due to electronic effects. 6-Bromo- and 7-chloro-substi-

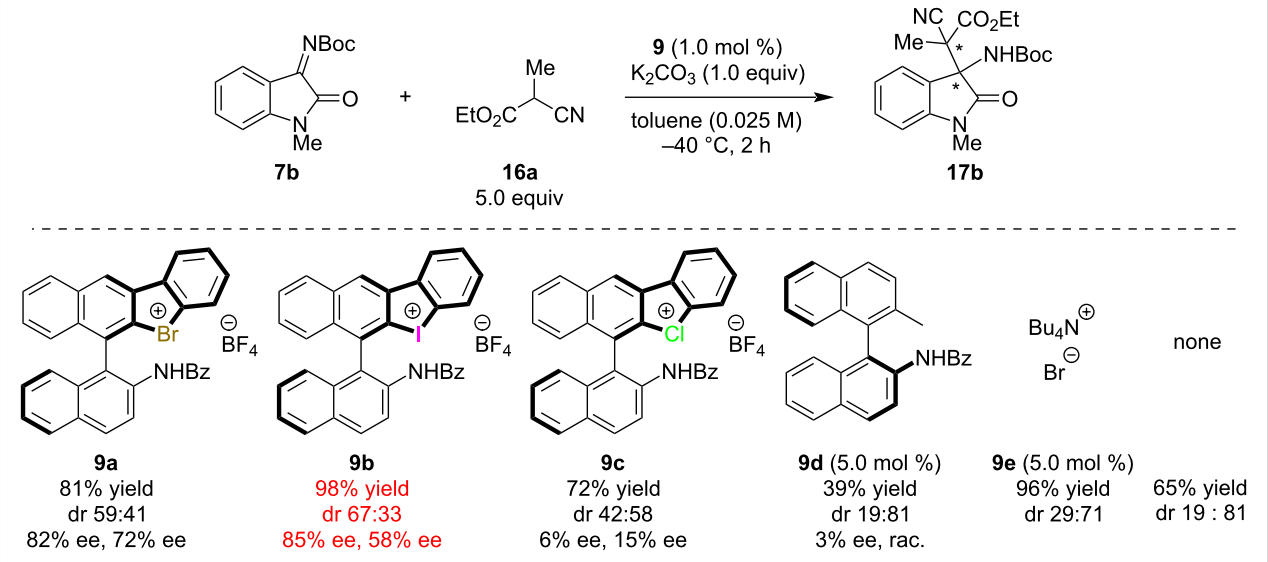

Scheme 3: Catalyst screening using **7b** as a substrate. All yields were determined by ^{1}H NMR spectroscopy using 1,3,5-trimethoxybenzene as an internal standard.

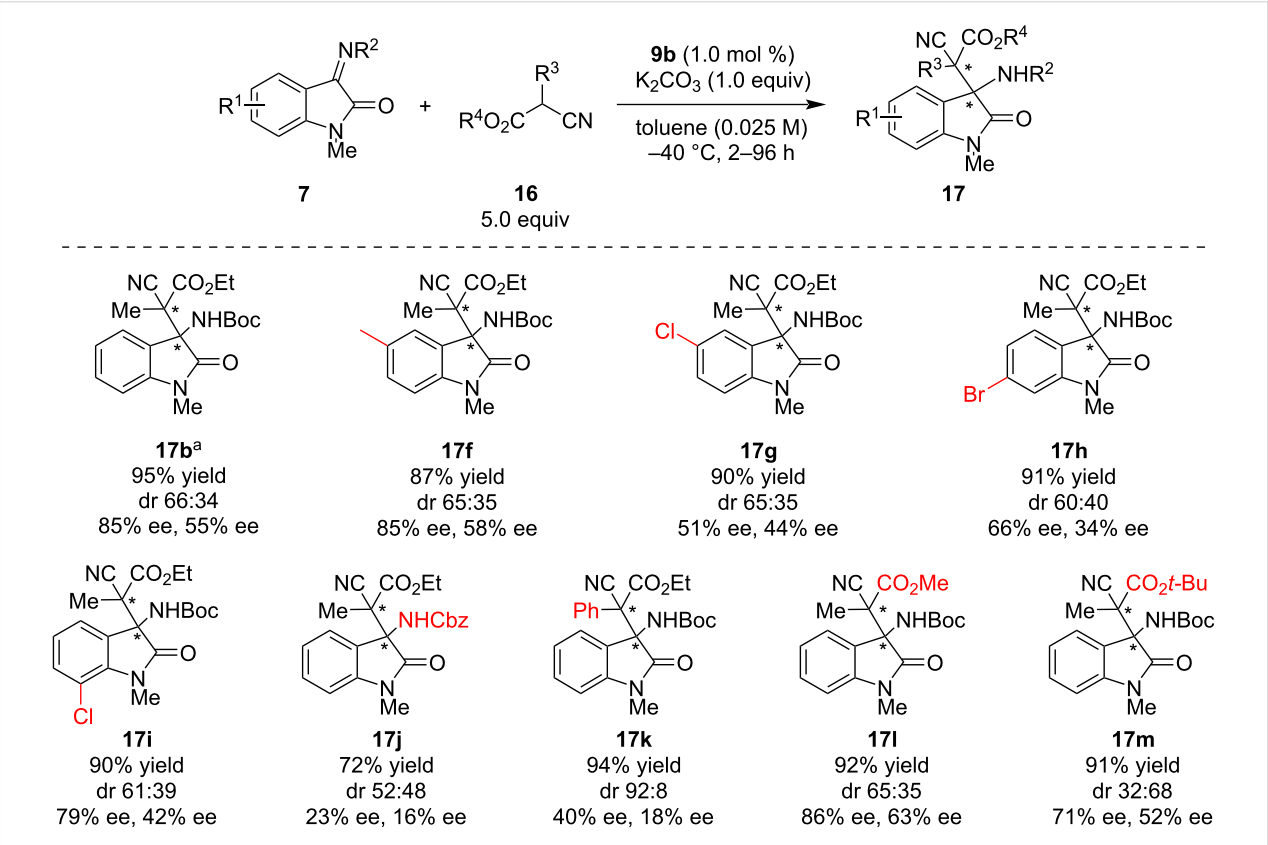

Scheme 4: Substrate scope for the asymmetric Mannich reaction using 0.06 mmol of **7**. Isolated product yields are shown. [a]The result of the reaction using 100.0 mg (0.34 mmol) of **7b**.

tuted substrates also provided **17h** and **17i** in good yields with moderate to good stereoselectivities. Next, Cbz-protected imine **7j** was employed in the present reaction; the stereoselectivity of product **17j** drastically dropped. The scope for the pre-nucleophile showed that phenyl-substituted **16b** provided **17k** in 94% yield with high diastereoselectivity, albeit with decreased enan-

tioselectivities. Methyl ester **16c** and *tert*-butyl ester **16d** were also applied to the present reaction, and products **17l** and **17m** were isolated in high yields with moderate to high stereoselectivities.

The plausible reaction mechanism is shown in Figure 3. First, the removal of the acidic proton of the pre-nucleophile by potassium carbonate to form intermediate **I**, which undergoes cation exchange from tetrafluoroborate to the halonium moiety to form chiral ion pair **II**. Attack of the chiral nucleophilic intermediate **II** to imine **7** leads to intermediate **III**. The latter is protonated by in the situ-formed potassium bicarbonate to form the desired product **17**, together with the regenerated chiral halonium salt.

Conclusion

In conclusion, the enantio- and diastereoselective Mannich reaction was developed by chiral halonium salt catalysis, which provided the corresponding products with contiguous chiral tetrasubstituted carbon centers in excellent yields with up to 86% ee using only 1 mol % catalyst loading. Although the diastereoselectivity of the products were moderate in most cases, the opposite diastereomer was obtained as the major product compared with reactions without a catalyst. To the best of our knowledge, the present paper is the first to report the asymmetric construction of β-amino cyanoesters with contiguous tetrasubstituted carbon stereogenic centers by the catalytic Mannich reaction. Further investigations into the reaction mechanism and product applications are ongoing in our group.

Supporting Information

Supporting Information File 1

Experimental procedures, characterization data, NMR spectra, and HPLC chromatograms.
[https://www.beilstein-journals.org/bjoc/content/supplementary/1860-5397-21-43-S1.pdf]

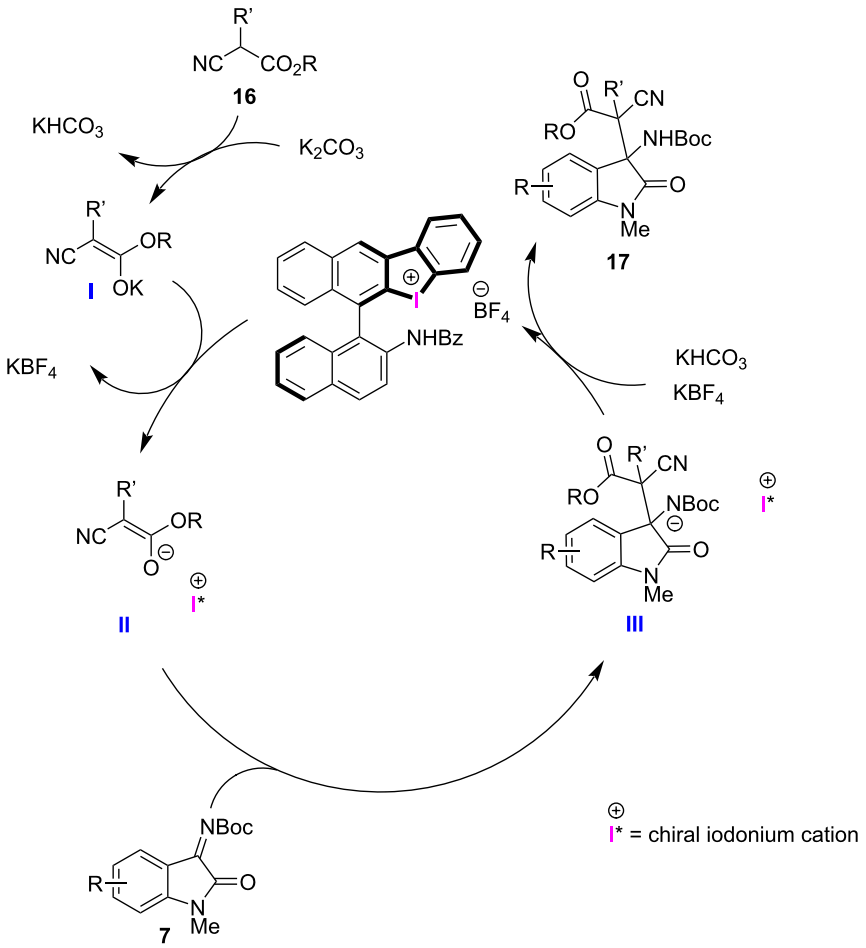

Figure 3: Plausible reaction mechanism.

Funding

This research was funded by an IAAR Research Support Program (Chiba Halogen Science: Halogen-Linkage of Molecular Functions); Chiba University Open Recruitment for International Exchange Program, Chiba University, Japan; Grant-in-Aid for Early-Career Scientists (No. 22K14674) and Scientific Research (C) (No. 24K08424) from the Japan Society for the Promotion of Science; and the Leading Research Promotion Program "Soft Molecular Activation" of Chiba University, Japan.

Author Contributions

Yasushi Yoshida: conceptualization; formal analysis; funding acquisition; investigation; methodology; project administration; resources; supervision; validation; writing – original draft; writing – review & editing. Maho Aono: data curation; formal analysis; investigation; writing – review & editing. Takashi Mino: funding acquisition; writing – review & editing. Masami Sakamoto: funding acquisition; writing – review & editing.

ORCID® iDs

Yasushi Yoshida - https://orcid.org/0000-0002-3498-3696

Data Availability Statement

All data that supports the findings of this study is available in the published article and/or the supporting information of this article.

References

1. Cavallo, G.; Metrangolo, P.; Milani, R.; Pilati, T.; Priimagi, A.; Resnati, G.; Terraneo, G. *Chem. Rev.* **2016,** *116,* 2478–2601. doi:10.1021/acs.chemrev.5b00484
2. Lu, Y.; Nakatsuji, H.; Okumura, Y.; Yao, L.; Ishihara, K. *J. Am. Chem. Soc.* **2018,** *140,* 6039–6043. doi:10.1021/jacs.8b02607
3. Lindblad, S.; Mehmeti, K.; Veiga, A. X.; Nekoueishahraki, B.; Gräfenstein, J.; Erdélyi, M. *J. Am. Chem. Soc.* **2018,** *140,* 13503–13513. doi:10.1021/jacs.8b09467
4. Zhang, X.; Ren, J.; Tan, S. M.; Tan, D.; Lee, R.; Tan, C.-H. *Science* **2019,** *363,* 400–404. doi:10.1126/science.aau7797
5. Jovanovic, D.; Poliyodath Mohanan, M.; Huber, S. M. *Angew. Chem., Int. Ed.* **2024,** *63,* e202404823. doi:10.1002/anie.202404823
6. Chan, Y.-C.; Yeung, Y.-Y. *Org. Lett.* **2019,** *21,* 5665–5669. doi:10.1021/acs.orglett.9b02006
7. Oishi, S.; Fujinami, T.; Masui, Y.; Suzuki, T.; Kato, M.; Ohtsuka, N.; Momiyama, N. *iScience* **2022,** *25,* 105220. doi:10.1016/j.isci.2022.105220
8. Wolf, J.; Huber, F.; Erochok, N.; Heinen, F.; Guérin, V.; Legault, C. Y.; Kirsch, S. F.; Huber, S. M. *Angew. Chem., Int. Ed.* **2020,** *59,* 16496–16500. doi:10.1002/anie.202005214
9. Jónsson, H. F.; Sethio, D.; Wolf, J.; Huber, S. M.; Fiksdahl, A.; Erdelyi, M. *ACS Catal.* **2022,** *12,* 7210–7220. doi:10.1021/acscatal.2c01864
10. Auffinger, P.; Hays, F. A.; Westhof, E.; Ho, P. S. *Proc. Natl. Acad. Sci. U. S. A.* **2004,** *101,* 16789–16794. doi:10.1073/pnas.0407607101
11. Li, J.; Zhou, L.; Han, Z.; Wu, L.; Zhang, J.; Zhu, W.; Xu, Z. *J. Med. Chem.* **2024,** *67,* 4782–4792. doi:10.1021/acs.jmedchem.3c02359
12. Berger, G.; Frangville, P.; Meyer, F. *Chem. Commun.* **2020,** *56,* 4970–4981. doi:10.1039/d0cc00841a
13. Kampes, R.; Zechel, S.; Hager, M. D.; Schubert, U. S. *Chem. Sci.* **2021,** *12,* 9275–9286. doi:10.1039/d1sc02608a
14. Nieland, E.; Komisarek, D.; Hohloch, S.; Wurst, K.; Vasylyeva, V.; Weingart, O.; Schmidt, B. M. *Chem. Commun.* **2022,** *58,* 5233–5236. doi:10.1039/d2cc00799a
15. Meazza, L.; Foster, J. A.; Fucke, K.; Metrangolo, P.; Resnati, G.; Steed, J. W. *Nat. Chem.* **2013,** *5,* 42–47. doi:10.1038/nchem.1496
16. Zong, L.; Ban, X.; Kee, C. W.; Tan, C.-H. *Angew. Chem., Int. Ed.* **2014,** *53,* 11849–11853. doi:10.1002/anie.201407512
17. Kuwano, S.; Suzuki, T.; Hosaka, Y.; Arai, T. *Chem. Commun.* **2018,** *54,* 3847–3850. doi:10.1039/c8cc00865e
18. Sutar, R. L.; Huber, S. M. *ACS Catal.* **2019,** *9,* 9622–9639. doi:10.1021/acscatal.9b02894
19. Sutar, R. L.; Engelage, E.; Stoll, R.; Huber, S. M. *Angew. Chem., Int. Ed.* **2020,** *59,* 6806–6810. doi:10.1002/anie.201915931
20. Keuper, A. C.; Fengler, K.; Ostler, F.; Danelzik, T.; Piekarski, D. G.; García Mancheño, O. *Angew. Chem., Int. Ed.* **2023,** *62,* e202304781. doi:10.1002/anie.202304781
21. Ochiai, M.; Miyamoto, K.; Kaneaki, T.; Hayashi, S.; Nakanishi, W. *Science* **2011,** *332,* 448–451. doi:10.1126/science.1201686
22. Yoshimura, A.; Zhdankin, V. V. *Chem. Rev.* **2016,** *116,* 3328–3435. doi:10.1021/acs.chemrev.5b00547
23. Mayer, R. J.; Ofial, A. R.; Mayr, H.; Legault, C. Y. *J. Am. Chem. Soc.* **2020,** *142,* 5221–5233. doi:10.1021/jacs.9b12998
24. Lanzi, M.; Dherbassy, Q.; Wencel-Delord, J. *Angew. Chem., Int. Ed.* **2021,** *60,* 14852–14857. doi:10.1002/anie.202103625
25. Miyamoto, K.; Saito, M.; Tsuji, S.; Takagi, T.; Shiro, M.; Uchiyama, M.; Ochiai, M. *J. Am. Chem. Soc.* **2021,** *143,* 9327–9331. doi:10.1021/jacs.1c04536
26. Lanzi, M.; Rogge, T.; Truong, T. S.; Houk, K. N.; Wencel-Delord, J. *J. Am. Chem. Soc.* **2023,** *145,* 345–358. doi:10.1021/jacs.2c10090
27. Chen, W. W.; Artigues, M.; Font-Bardia, M.; Cuenca, A. B.; Shafir, A. *J. Am. Chem. Soc.* **2023,** *145,* 13796–13804. doi:10.1021/jacs.3c02406
28. Heinen, F.; Engelage, E.; Dreger, A.; Weiss, R.; Huber, S. M. *Angew. Chem., Int. Ed.* **2018,** *57,* 3830–3833. doi:10.1002/anie.201713012
29. Yoshida, Y.; Ishikawa, S.; Mino, T.; Sakamoto, M. *Chem. Commun.* **2021,** *57,* 2519–2522. doi:10.1039/d0cc07733j
30. Robidas, R.; Reinhard, D. L.; Legault, C. Y.; Huber, S. M. *Chem. Rec.* **2021,** *21,* 1912–1927. doi:10.1002/tcr.202100119
31. Il'in, M. V.; Sysoeva, A. A.; Novikov, A. S.; Bolotin, D. S. *J. Org. Chem.* **2022,** *87,* 4569–4579. doi:10.1021/acs.joc.1c02885
32. Zhang, Y.; Han, J.; Liu, Z.-J. *RSC Adv.* **2015,** *5,* 25485–25488. doi:10.1039/c5ra00209e
33. Yoshida, Y.; Mino, T.; Sakamoto, M. *ACS Catal.* **2021,** *11,* 13028–13033. doi:10.1021/acscatal.1c04070
34. Yoshida, Y.; Fujimura, T.; Mino, T.; Sakamoto, M. *Adv. Synth. Catal.* **2022,** *364,* 1091–1098. doi:10.1002/adsc.202101380
35. Yoshida, Y.; Ao, T.; Mino, T.; Sakamoto, M. *Molecules* **2023,** *28,* 384. doi:10.3390/molecules28010384
36. France, S.; Guerin, D. J.; Miller, S. J.; Lectka, T. *Chem. Rev.* **2003,** *103,* 2985–3012. doi:10.1021/cr020061a

37. Seebach, D.; Beck, A. K.; Bierbaum, D. J. *Chem. Biodiversity* **2004,** *1,* 1111–1239. doi:10.1002/cbdv.200490087
38. Pruett, S. T.; Bushnev, A.; Hagedorn, K.; Adiga, M.; Haynes, C. A.; Sullards, M. C.; Liotta, D. C.; Merrill, A. H., Jr. *J. Lipid Res.* **2008,** *49,* 1621–1639. doi:10.1194/jlr.r800012-jlr200
39. Bagheri, I.; Mohammadi, L.; Zadsirjan, V.; Heravi, M. M. *ChemistrySelect* **2021,** *6,* 1008–1066. doi:10.1002/slct.202003034
40. Arrayás, R. G.; Carretero, J. C. *Chem. Soc. Rev.* **2009,** *38,* 1940–1948. doi:10.1039/b820303b
41. Poulsen, T. B.; Alemparte, C.; Saaby, S.; Bella, M.; Jørgensen, K. A. *Angew. Chem., Int. Ed.* **2005,** *44,* 2896–2899. doi:10.1002/anie.200500144
42. Lu, G.; Yoshino, T.; Morimoto, H.; Matsunaga, S.; Shibasaki, M. *Angew. Chem., Int. Ed.* **2011,** *50,* 4382–4385. doi:10.1002/anie.201101034
43. Takeda, T.; Kondoh, A.; Terada, M. *Angew. Chem., Int. Ed.* **2016,** *55,* 4734–4737. doi:10.1002/anie.201601352
44. Trost, B. M.; Hung, C.-I. (Joey).; Scharf, M. J. *Angew. Chem., Int. Ed.* **2018,** *57,* 11408–11412. doi:10.1002/anie.201806249
45. Zhang, H.-J.; Xie, Y.-C.; Yin, L. *Nat. Commun.* **2019,** *10,* 1699. doi:10.1038/s41467-019-09750-5
46. Ding, R.; De los Santos, Z. A.; Wolf, C. *ACS Catal.* **2019,** *9,* 2169–2176. doi:10.1021/acscatal.8b05164

License and Terms